frontiers | Research Topics

Innate immune responses to SARS-CoV-2 in infected and vaccinated individuals

Edited by
Srinivasa Reddy Bonam, Nicasio Mancini, Nitin Saksena and Pedro A. Reche

Published in
Frontiers in Immunology

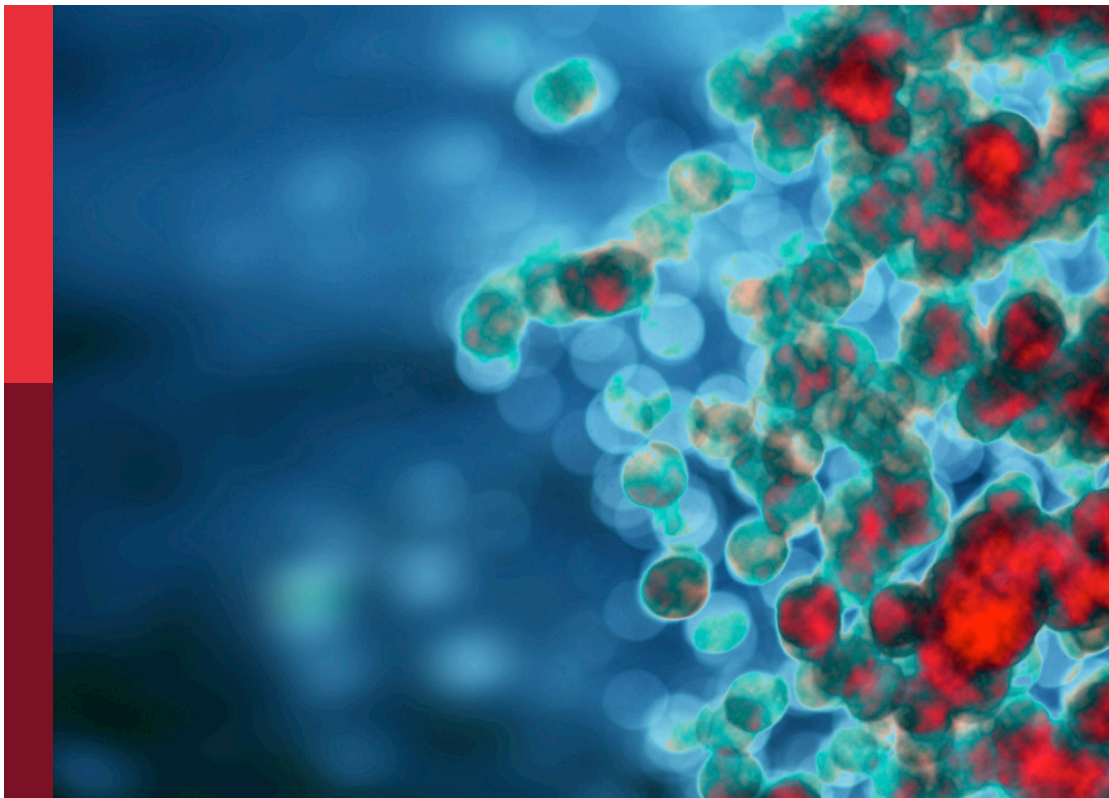

ISSN 1664-8714
ISBN 978-2-83251-744-4
DOI 10.3389/978-2-83251-744-4

About Frontiers

Frontiers is more than just an open access publisher of scholarly articles: it is a pioneering approach to the world of academia, radically improving the way scholarly research is managed. The grand vision of Frontiers is a world where all people have an equal opportunity to seek, share and generate knowledge. Frontiers provides immediate and permanent online open access to all its publications, but this alone is not enough to realize our grand goals.

Frontiers journal series

The Frontiers journal series is a multi-tier and interdisciplinary set of open-access, online journals, promising a paradigm shift from the current review, selection and dissemination processes in academic publishing. All Frontiers journals are driven by researchers for researchers; therefore, they constitute a service to the scholarly community. At the same time, the *Frontiers journal series* operates on a revolutionary invention, the tiered publishing system, initially addressing specific communities of scholars, and gradually climbing up to broader public understanding, thus serving the interests of the lay society, too.

Dedication to quality

Each Frontiers article is a landmark of the highest quality, thanks to genuinely collaborative interactions between authors and review editors, who include some of the world's best academicians. Research must be certified by peers before entering a stream of knowledge that may eventually reach the public - and shape society; therefore, Frontiers only applies the most rigorous and unbiased reviews. Frontiers revolutionizes research publishing by freely delivering the most outstanding research, evaluated with no bias from both the academic and social point of view. By applying the most advanced information technologies, Frontiers is catapulting scholarly publishing into a new generation.

What are Frontiers Research Topics?

Frontiers Research Topics are very popular trademarks of the *Frontiers journals series*: they are collections of at least ten articles, all centered on a particular subject. With their unique mix of varied contributions from Original Research to Review Articles, Frontiers Research Topics unify the most influential researchers, the latest key findings and historical advances in a hot research area.

Find out more on how to host your own Frontiers Research Topic or contribute to one as an author by contacting the Frontiers editorial office: frontiersin.org/about/contact

Innate immune responses to SARS-CoV-2 in infected and vaccinated individuals

Topic editors

Srinivasa Reddy Bonam — University of Texas Medical Branch at Galveston, United States

Nicasio Mancini — Vita-Salute San Raffaele University, Italy

Nitin Saksena — Victoria University, Australia

Pedro A. Reche — Complutense University of Madrid, Spain

Citation

Bonam, S. R., Mancini, N., Saksena, N., Reche, P. A., eds. (2023). *Innate immune responses to SARS-CoV-2 in infected and vaccinated individuals*. Lausanne: Frontiers Media SA. doi: 10.3389/978-2-83251-744-4

Table of contents

frontiers | Frontiers in Immunology

TYPE Editorial
PUBLISHED 08 February 2023
DOI 10.3389/fimmu.2023.1141405

OPEN ACCESS

EDITED AND REVIEWED BY
Ralf Kircheis,
Syntacoll GmbH, Germany

*CORRESPONDENCE
Nitin K. Saksena
nitin.saksena@bigpond.com
Pedro A. Reche
parecheg@med.ucm.es
Srinivasa Reddy Bonam
bsrpharmacy90@gmail.com
Nicasio Mancini
mancini.nicasio@hsr.it

SPECIALTY SECTION
This article was submitted to Vaccines and Molecular Therapeutics, a section of the journal Frontiers in Immunology

RECEIVED 10 January 2023
ACCEPTED 30 January 2023
PUBLISHED 08 February 2023

CITATION
Saksena NK, Reche PA, Bonam SR and Mancini N (2023) Editorial: Innate immune responses to SARS-CoV-2 in infected and vaccinated individuals. *Front. Immunol.* 14:1141405. doi: 10.3389/fimmu.2023.1141405

Editorial: Innate immune responses to SARS-CoV-2 in infected and vaccinated individuals

Nitin K. Saksena[1,2*], Pedro A. Reche[3*], Srinivasa Reddy Bonam[4*] and Nicasio Mancini[5*]

[1]Institute for health and Sports (IHES), Victoria University, Melbourne, VIC, Australia, [2]Research & Development (R&D), Aegros Therapeutics, Sydney, NSW, Australia, [3]Department of Immunology, School of Medicine, Complutense University of Madrid, Madrid, Spain, [4]Department of Microbiology and Immunology, University of Texas Medical Branch, Galveston, TX, United States, [5]Laboratory of Medical Microbiology and Virology, University Vita-Salute San Raffaele, IRCCS San Raffaele Hospital, Milan, Italy

KEYWORDS

SARS-CoV-2, acute respiratory disease, vaccines, mRNA vaccines, neutralization, viral variants

Editorial on the Research Topic
Innate immune responses to SARS-CoV-2 in infected and vaccinated individuals

The COVID-19 pandemic triggered the intensity of the pursuit of vaccines that had not been seen before and were developed at an unprecedented speed, approved, and delivered for human use globally. During the pandemic, the first mRNA vaccine, a new paradigm in vaccinology for SARS-CoV-2, was also developed by Pfizer-BioNTech and Moderna. Most current vaccines in use have aimed to induce specific adaptive immunity by taking advantage of host T-cell responses and virus-neutralizing antibodies (nAbs). Innate immunity, critical to host defense against infections, is triggered by a family of pattern recognition receptors, which in turn induce interferons and cytokines, activating myeloid and lymphoid cells to provide immune protection against a range of viral and bacterial infections. Through thematic convergence, the assemblage of 18 original articles and reviews presented in this special issue, entitled "Innate immune responses to SARS-CoV-2 in infected and vaccinated individuals," discusses various perspectives and provides a profound and multidisciplinary understanding of SARS-CoV-2 vaccines and innate immune responses. This information provided in the special issue is critical to defining the limitations of current approaches and facilitating greater understanding and refinement of current and future vaccine design.

While the COVID-19-approved vaccines are generally safe, serious side effects have remained an issue with both mRNA and non-mRNA vaccines, and more time is needed to assess their potential long-term effects. The limited production of heterogeneous neutralizing antibodies and their short durability *in vivo* remain unsolved and need to be addressed. Nonetheless, even though the current COVID-19 vaccines have not always been used in concert with the circulating strain, they have been shown to protect against severe disease, which is usually typified by pneumonia, cytokine storm, acute respiratory distress syndrome (ARDS), multiorgan failure, and death. Most current vaccines also lack variant-specificity; therefore, the newly emerging viral variants have been seen to breach host immunity through mutations during the COVID-19 pandemic. As a result, we have seen millions of re-

infections globally post-vaccination and post-booster vaccination, with varying recovery rates depending on the host immunology and circulating mutations in the viral strains (Kumar et al.). For instance, patients infected with the Delta variant of SARS-CoV-2 were found to have a slower recovery rate than their counterparts infected with Alpha or Omicron variants. This trend was consistent in both vaccinated and unvaccinated patients. Omicron causes less severe disease than Delta, which could be attributed to Omicron being less able to infect the lungs as it does in the upper airways, thereby resulting in less severe disease than Delta, coupled with a lower risk of hospitalization and ICU admissions (40–80% and lower than that of Delta) and death (60% less death rate than Delta) (1). Möhlendick et al determined that the risk of developing an Omicron breakthrough infection was independent of vaccination scheme sex, body mass index, smoking status or pre-existing conditions, but it correlated with lower antibody responses induced after booster immunization.

Overall, such observations are significant in defining vaccine efficacy, as viral mutations that define viral infectivity and transmissibility work together to evade the host-and vaccine-induced immunity, and require further investigation to create specific and durable SARS-CoV-2 vaccines. Furthermore, unless SARS-CoV-2 vaccines can provide long-term sterilizing immunity, they will most likely become seasonal and will require yearly immunizations, as is known for the influenza virus. To develop a vaccine of this kind, a clear understanding of the mechanism of interaction of the virus with the host and the host's response to the vaccine is urgently needed. More insights are needed into the innate immune system components, including monocytes, macrophages, dendritic cells, and granulocytes (Bonam et al.; Sonaglioni et al.; Beirag et al.).

There is a big focus on finding epigenomic modalities for treating SARS-CoV-2, as the virus uses the host epigenetic machinery to subdue antiviral components and complete its life cycle within the host (2). Gianella et al. show that severe COVID-19, compared to mild/moderate disease, was characterized by miRNA (non-coding RNAs that regulate gene expression) signatures showing of a profound impairment of innate and adaptive immune responses, inflammation, lung fibrosis, heart failure, and mortality. A combination of high serum miR-22-3p and miR-21-5p, which target antiviral response genes, and low miR-224-5p and miR-155-5p, targeting pro-inflammatory factors, discriminated between severe and mild/moderate COVID-19. Simultaneously, a high leukocyte count and low levels of miR-1-3p, miR-23b-3p, miR-141-3p, miR-155-5p and miR-4433b-5p predicted mortality. Some differentially expressed miRNAs that were modulated directly by SARS-CoV-2 infection in permissive lung epithelial cells could have immense value in defining prognostic biomarkers in stratifying clinical outcomes and preponderance to disease severity for treating the infection earlier.

Given that the different approaches and strategies have been used in designing SARS-CoV-2 vaccines, it is thus important to have comparative analyses between them. To carry out such comparative analyses it is equally important to have high-throughput technologies that can systematically evaluate vaccine attributes in a clinical context, providing gold standards to asses vaccine efficacy. Before the broader deployment of a vaccine, it is crucial to understand the molecular, immunological, genomic, and proteomic bases of the immune responses and their evaluation. This was demonstrated through peptidome analysis of vaccinated individuals by Zhang et al., demonstrating the utility of MALDI-TOF MS in evaluating immune responses after vaccination with CoronaVac along with the discovery of new biomarkers for vaccination and neutralizing antibody generation. Furthermore, Kaznadzey et al., through a simultaneous comparison of Pfizer-BNT162b2, Moderna-mRNA1273, and Sputnik V vaccines, provided the first parallel comparison of immune responses of mRNA and non-mRNA vaccines, with no significant differences after the second challenge in vaccinated individuals who also had COVID-19 before being vaccinated, confirmed by antibodies against the nucleocapsid (N) protein and RBD of SARS-CoV-2 using a Unified ELISA-based assay previously developed in the laboratory. Concurrently, Jochum et al. also demonstrated the value of the high automated throughput Roche Elecsys® Anti-SARS-CoV-2 S assay (referred to as ACOV2S) to detect and quantify the antibody response against the RBD of the S protein in delineating humoral immune responses in mRNA-1273-vaccinated individuals. Therefore, the Elecsys Anti-SARS-CoV-2 S assay (ACOV2S) can be valuable in assessing and quantifying the presence of RBD-directed antibodies against SARS-CoV-2 following vaccination and in the assessment of vaccine-induced humoral immune responses. Similarly, Hosseinian et al. quantified the persistence of humoral immunity (SARS-CoV-2 IgG levels) following vaccination using a coronavirus antigen microarray, which included 10 SARS-CoV-2 antigens. Overall, these aspects have a strong potential to define immune responses in infected and vaccinated individuals and the post-market evaluation of SARS-CoV-2 vaccines in a high throughput manner.

In the context of an effective vaccine, it is also important to identify how the vaccines generate immune response with and without prior exposure to SARS-CoV-2. This knowledge is also valuable in defining the relevance of booster regimens, which have been arbitrarily introduced without a proper definition of timing and consideration of circulating strain at the time. Kaznadzey et al. further showed that vaccinated individuals with Sputnik V with prior SARS-CoV-2 infection showed high levels of antibodies with the ability to effectively neutralize the interaction of RBD with ACE2 following the first dose of Sputnik V, which was consistent with Moderna and Pfizer vaccines, suggesting that anti-RBD signals were comparable among the three vaccines (3, 4). What value do booster doses have in the context of naive and previously infected SARS-CoV-2 individuals? This study also shows that a single administration of Sputnik V (Sputnik Light) could be a sufficient boost to the immune system for those who have had a prior exposure to SARS-CoV-2 infection, but this was not the case with naïve patients who had a two-dose regime, which is in line with other studies on Sputnik Light (6). This, along with the study by Ogric et al., which assessed the humoral immune response after the first, second, and third (booster) doses of BNT162b2 vaccine in SARS-CoV-2 naïve and previously infected healthcare professionals, showed no efficacy of booster shots in individuals with prior exposure to SARS-CoV-2, which is highly relevant in making clinical decisions on booster regimens. A concurrent study by Busa et al., using the same BNT162b2 vaccine, found a potential benefit of the third dose of mRNA vaccine on the lifespan of memory B and T cells, suggesting that booster doses could increase protection against SARS-CoV-2 infection. In contrast, Seidel et al. used another approach in assessing the value of booster using

heterologous ChAdOx1 nCoV-19 BNT162b2 prime-boost vaccination in young adults and showed that booster after heterologous vaccination results in adequate immune maturation and potent protection against the Omicron BA.1 variant in young adults, concurring with a study by Dowell et al., which analyzed antibody and cellular responses in adolescents who received COVID-19 vaccination with either ChAdOx1 or an mRNA vaccine (mRNA-1273, BNT162b2). Together, these studies provide a platform for vigorous and tantalizing discussion on the actual value of booster shots in naïve and previously-infected individuals, and also in the context of newly emerging SARS-CoV-2 variants as Omicron can breach immune protection in individuals with weak antibody response despite boosting, as shown by Mohlendick et al., which also underscores the establishment of thresholds for SARS-CoV-2 IgG antibody levels identifying "non"-, "low" and "high"-responders that can be used as an indication for re-vaccination.

Ideally, a robust vaccine must serve to all but that is not always the case, and difficult to achieve. Indeed, we have learnt that the immune response and efficacy of current SARS-CoV-2 vaccines is often conditioned by sex and age (5). Shen et al., who analyzed the innate immune responses to the ChAdOx1 nCoV-19 (AZD1222) adeno-virus-based vaccine in the 25-35, and 60-70-years old age groups, showed that the innate immune response after the first vaccination correlated with neutralizing antibody production and that older people displayed weakened innate immune responses by TLR stimulation and weak or delayed innate immune activation profiles after vaccination compared to young people. Thus, age is an important consideration for vaccine design and efficacy because aging is associated with alterations in the number and quality of innate and adaptive immune cells and mounting of immune responses to immune stimulation. This process is termed immune senescence (6; Pietrobon et al.), which is accompanied by reduced chemotaxis, defective cytokine production, and poor TLR signalling (7), thereby affecting and impairing antigen processing and presentation to T cells and activation of B cells, hence weakening adaptive immunity in older age groups. This was the reason, which could be attributed to the high mortality with SARS-CoV-2 infection observed in the older age group with SARS-CoV-2 infection during the earlier part of COVID-19 pandemic, and subsequently.

In case of Influenza, we have already seen that age is associated with decrease in TLR function in human dendritic cells and with poor antibody response to influenza immunization, further underpinning the importance immune-senescence of the innate immune system in vaccine response as a result of aging (8); and, that immuno-senescence can lead to no or suboptimal response to vaccination, posing a potential risk of breakthrough infection with newly emerging SARS-CoV2 variants. Lopera et al. underpins this aspect and show that the decaying of serum neutralizing activity, both over time and across SARS-CoV-2 variants (using the Pfizer-BioNTechvaccine), is more significant in older men- an essential attribute in vaccine considerations in addition to approaches that can boost the immune response in the elderly, either by adding potent adjuvants or by bringing changes to the route of vaccine administration, augmenting the dose of immunogen, and altering the vaccine design and compositions, allowing more immunogenic targets, must be made (9; Pereira et al.). The current trend in vaccine design seen in most COVID-19 vaccines is the antigenic simplicity, aimed to focus the immune response in those antigens that are likely to induce protective responses. In this context, Pratesi et al took a step further showing that 72 aa long-peptide from SARS-CoV-2 spike protein corresponding to the receptor binding motif (RBM436-507) could generate neutralizing antibodies in mice and was recognized by sera from humans exposed to the infection. Hence, this peptide could be used rather than the entire Spike protein in next-generation of COVID-19 vaccines as an immunogen. This also makes a case for identifying immunogenic peptides from regions other than the spike protein, which can be incorporated in future multi-subunit-vaccines for a broader immune response.

In summary, this special issue encapsulates and provides vigorous discussions on the current and evolving state of SARS-CoV-2 vaccines, their design (Pratesi et al.), and development (Prasad et al.) in the context of innovative strategies that will provide better immune protection, robust responses, variant-specificity, broader coverage, better evaluation and assessment, and improvement in the effectiveness of vaccines in the general population and the elderly.

Together, these articles highlight current and future challenges, and possible strategies to overcome them. Because all SARS-CoV-2 vaccines were rolled out due to urgency, there is a urgent need for an increased understanding of the level of immune response variability; adjuvant in boosting effectiveness; the mechanistic basis, genomic, and proteomic bases of mRNA and non-mRNA vaccines; strain specificity; live attenuated viral vaccine development for better durability; and mode of action of the current and future vaccines that can also integrate how vaccines can be made effective when dealing with factors including age, sex, and health status. Live-attenuated vaccines (LAV), which have been used for targeting measles, Mycobacterium tuberculosis, and polio to induce innate protective immunity, have not been tested for SARS-CoV-2 because of the risks involved, coupled with the paucity of immunological knowledge. LAVs offer better and broader protection against viruses. It may be essential to bend the pandemic curve by providing better therapeutic outcomes through training of the innate immune system.

Author contributions

All authors contributed to the article and approved the submitted version.

Conflict of interest

Author NS was employed by company Aegros Therapeutics.

The remaining authors declare that the research was conducted in the absence of any commercial or financial relationships that could be construed as a potential conflict of interest.

Publisher's note

References

1. Wrenn JO, Pakala SB, Vestal G, Shilts MH, Brown HM, Bowen SM, et al. COVID-19 severity from Omicron and Delta SARS-CoV-2 variants. *Influenza Other Respir Viruses* (2022) 16(5):832–836. doi: 10.1111/irv.12982

2. Saksena N, Reddy Bonam S, Miranda-Saksena M. Epigenetic lens to visualize the severe acute respiratory syndrome coronavirus-2 (SARS-CoV-2) infection in COVID-19 pandemic. *Front Genet* (2021) 12:581726.3. doi: 10.3389/fgene.2021.581726.3

3. Mulligan MJ, Lyke KE, Kitchin N, Absalon J, Gurtman A, Lockhart S, et al. Phase I/II study of COVID-19 RNA vaccine BNT162b1 in adults. *Nature* (2020) 586:589–93. doi: 10.1038/s41586-020-2639-4

4. Wang Z, Schmidt F, Weisblum Y, Muecksch F, Barnes CO, Finkin S, et al. mRNA vaccine-elicited antibodies to SARS-CoV-2 and circulating variants. *Nature* (2021) 592:616–22. doi: 10.1038/s41586-021-03324-6

5. Potluri T, Fink AL, Sylvia KE, Dhakal S, Vermillion MS, Vom Steeg L, et al. Age-associated changes in the impact of sex steroids on influenza vaccine responses in males and females. *NPJ Vaccines* (2019) 4:29. doi: 10.1038/s41541-019-0124-6

6. Connors J, Bell MR, Marcy J, Kutzler M, Haddad EK. The impact of immuno-aging on SARS-CoV-2 vaccine development. *Geroscience* (2021) 43(1):31–51. doi: 10.1007/s11357-021-00323-3

7. Panda A, Qian F, Mohanty S, van Duin D, Newman FK, Zhang L, et al. Age-associated decrease in TLR function in primary human dendritic cells predicts influenza vaccine response. *J Immunol* (2010) 184(5):2518–27. doi: 10.4049/jimmunol.0901022

8. Lefebvre JS, Haynes L. Vaccine strategies to enhance immune responses in the aged. *Curr Opin Immunol* (2013) 25(4):523–8. doi: 10.1016/j.coi.2013.05.014

9. Krammer F, Srivastava K, Alshammary H, Amoako AA, Awawda MH, Beach KF, et al. Antibody responses in seropositive persons after a single dose of SARS-CoV-2 mRNA vaccine. *N Engl J Med* (2021) 384:1372–4. doi: 10.1056/NEJMc2101667

frontiers in Immunology

ORIGINAL RESEARCH
published: 19 January 2022
doi: 10.3389/fimmu.2021.798117

Clinical Utility of Elecsys Anti-SARS-CoV-2 S Assay in COVID-19 Vaccination: An Exploratory Analysis of the mRNA-1273 Phase 1 Trial

Simon Jochum[1], Imke Kirste[2], Sayuri Hortsch[3], Veit Peter Grunert[3], Holly Legault[4], Udo Eichenlaub[2], Basel Kashlan[5] and Rolando Pajon[4]**

[1] Research and Development Immunoassays, Roche Diagnostics GmbH, Penzberg, Germany, [2] Clinical Development & Medical Affairs, Roche Diagnostics Operations, Indianapolis, IN, United States, [3] Biostatistics and Data Science, Roche Diagnostics GmbH, Penzberg, Germany, [4] Clinical Biomarkers, Moderna, Cambridge, MA, United States, [5] Lab Operations, PPD, part of Thermo Fisher Scientific, Highland Heights, KY, United States

OPEN ACCESS

Edited by:
Nicasio Mancini,
Vita-Salute San Raffaele University, Italy

Reviewed by:
Jakob Nilsson,
University Hospital Zürich, Switzerland
Tengchuan Jin,
University of Science and Technology of China, China

***Correspondence:**
Simon Jochum
simon.jochum@roche.com
Rolando Pajon
rolando.pajon@modernatx.com

Specialty section:
This article was submitted to Vaccines and Molecular Therapeutics, a section of the journal Frontiers in Immunology

Received: 19 October 2021
Accepted: 23 December 2021
Published: 19 January 2022

Citation:
Jochum S, Kirste I, Hortsch S, Grunert VP, Legault H, Eichenlaub U, Kashlan B and Pajon R (2022) Clinical Utility of Elecsys Anti-SARS-CoV-2 S Assay in COVID-19 Vaccination: An Exploratory Analysis of the mRNA-1273 Phase 1 Trial. Front. Immunol. 12:798117. doi: 10.3389/fimmu.2021.798117

Background: The ability to quantify an immune response after vaccination against severe acute respiratory syndrome coronavirus 2 (SARS-CoV-2) is essential. This study assessed the clinical utility of the quantitative Roche Elecsys® Anti-SARS-CoV-2 S assay (ACOV2S) using samples from the 2019-nCoV vaccine (mRNA-1273) phase 1 trial (NCT04283461).

Methods: Samples from 30 healthy participants, aged 18–55 years, who received two injections with mRNA-1273 at a dose of 25 µg (n=15) or 100 µg (n=15), were collected at Days 1 (first vaccination), 15, 29 (second vaccination), 43 and 57. ACOV2S results (shown in U/mL – equivalent to BAU/mL per the first WHO international standard) were compared with results from ELISAs specific to antibodies against the Spike protein (S-2P) and the receptor binding domain (RBD) as well as neutralization tests including nanoluciferase (nLUC80), live-virus (PRNT80), and a pseudovirus neutralizing antibody assay (PsVNA50).

Results: RBD-specific antibodies were already detectable by ACOV2S at the first time point of assessment (d15 after first vaccination), with seroconversion before in all but two participants (25 µg dose group); all had seroconverted by Day 29. Across all post-baseline visits, geometric mean concentration of antibody levels was 3.27–7.48-fold higher in the 100 µg compared with the 25 µg dose group. ACOV2S measurements were highly correlated with those from RBD ELISA (Pearson's r=0.938; p<0.0001) and S-2P ELISA (r=0.918; p<0.0001). For both ELISAs, heterogeneous baseline results and smaller increases in antibody levels following the second *vs* first vaccination compared with ACOV2S were observed. ACOV2S showed absence of any baseline noise indicating high specificity detecting vaccine-induced antibody response. Moderate–strong correlations were observed between ACOV2S and neutralization tests (nLUC80 r=0.933; PsVNA50, r=0.771; PRNT80, r=0.672; all $p \leq 0.0001$).

Conclusion: The Elecsys Anti-SARS-CoV-2 S assay (ACOV2S) can be regarded as a highly valuable method to assess and quantify the presence of RBD-directed antibodies against SARS-CoV-2 following vaccination and may indicate the presence of neutralizing antibodies. As a fully automated and standardized method, ACOV2S could qualify as the method of choice for consistent quantification of vaccine-induced humoral response.

Keywords: SARS-CoV-2, COVID-19, quantitative serology, vaccination, ELISA

1 INTRODUCTION

First recognized in Wuhan, China in late 2019, the severe acute respiratory syndrome coronavirus 2 (SARS-CoV-2) has since spread rapidly and infected millions of people globally (1). The prompt development and approval of vaccines against the virus has been crucial. With over 100 vaccine candidates currently in clinical development (2), there is a high need for sensitive and specific assays that can reliably quantify immune responses following vaccination (3).

SARS-CoV-2 is an enveloped positive-sense single-stranded RNA virus containing four structural proteins: spike (S), envelope, membrane, and nucleocapsid (N) protein. The S glycoprotein is proteolytically cleaved into two subunits: S1 containing the host receptor binding domain (RBD) which facilitates entry to host cell through binding to membrane bound angiotensin-converting enzyme 2 (ACE 2), and S2, a membrane-proximal domain (4). Seroconversion often starts 5–7 days after symptom onset and the antibodies, immunoglobulin M (IgM), IgG and IgA, can be observed after approximately two weeks (3, 5, 6). While antibody response can be directed against all viral proteins, S and N are considered the main targets of humoral response (6, 7). Based on the potential for antibodies targeting the spike antigen to inhibit viral entry into the target cells, the majority of vaccine candidates have been designed to induce humoral immune responses against the S antigen (8).

Neutralizing antibodies are important contributors to protective immunity (3). *In vitro* neutralization testing is a widely applied test to assess the presence of neutralizing antibodies and to titrate them to limiting dilution. A variety of neutralization tests are available, including direct neutralization, which requires biosafety level 3 handling, and pseudotyped-virus assays (9–11). In convalescent plasma, Ig antibodies towards the SARS-CoV-2 S protein, in particular when directed against the RBD, have been shown to correlate with virus neutralizing titers, suggesting that immunoglobulin levels may predict levels of neutralization (12, 13). Thus, the potential use of antibody concentrations, quantified by commercially-available immunoassays, as a surrogate for neutralizing titers is currently being explored (14–16).

The automated, high throughput Roche Elecsys® Anti-SARS-CoV-2 S assay (hereby referred to as ACOV2S) detects and quantifies antibodies against the RBD of the S protein. A previous study showed that the presence of antibodies detected with ACOV2S correlated with the presence of neutralizing antibodies, as detected with direct virus neutralization and surrogate neutralization tests among individuals with minor or no symptoms (17). In order to generate further supporting evidence for the clinical utility of ACOV2S, in addition to existing studies (18, 19), we studied the antibody concentration, as measured by ACOV2S, over time in a phase 1 trial of the widely approved, highly effective mRNA-based 2019-nCoV vaccine (mRNA-1273; Moderna, Cambridge, MA) which encodes the stabilized prefusion S trimer, S-2P (20). We also performed an exploratory analysis comparing ACOV2S results with those from enzyme-linked immunosorbent assays (ELISA) and neutralization tests, based on data from the phase 1 trial.

2 METHODS

2.1 Study Design and Participants

We used stored samples from participants enrolled in the phase 1 trial of mRNA-1273 (NCT04283461); full methodological details have previously been described (20). In this retrospective exploratory analysis, samples from healthy participants aged 18–55 years who received two injections of trial vaccine 28 days apart at a dose of 25 μg or 100 μg were included for assessment. All participants received their first vaccination between March 16 and April 14, 2020.

Blood samples were collected as previously described (20). Samples collected at baseline (Day 1, first vaccination), and Days 15, 29 (second vaccination), 43 and 57, were analyzed.

Informed written consent was originally obtained from all study participants in the context of the associated vaccine phase I study and the study was conducted in accordance with the principles of the Declaration of Helsinki and Good Clinical Practice Guidelines. Approval was granted by the Advarra institutional review board for the phase 1 trial (20) and the diagnostic protocol under which the existing samples were tested.

For comparison of antibody responses induced by vaccination to antibody response to natural SARS-CoV-2 infection, anonymized cross-sectional samples from individuals with polymerase chain reaction (PCR)-confirmed SARS-CoV-2 infection were taken 0–15 days and 16-35 days post-PCR diagnosis and analyzed for presence of SARS-CoV-2 specific antibodies using ACOV2S. These samples were derived from individuals with mild course of disease that underwent quarantine at home or from individuals with more severe course of disease that required hospitalization. In contrast to the samples from the vaccination trial, the sample collection from natively-infected individuals was not balanced for representative reflection of the population demographics. The age distribution for donors with mild disease ranged from 17 to 68 years (median 35 years), for donors with severe disease ranged

from 21 to 85 years (median 53 years). Detailed clinical information, e.g. on putative medication or treatment, was not available for data privacy reasons. All samples were collected between March and July 2020 in Switzerland, Germany, and Ukraine.

2.2 Laboratory Assays

2.2.1 Elecsys Anti-SARS-CoV-2-S Immunoassay (ACOV2S)

The ACOV2S results were measured on a cobas e 602 module (performed at PPD Central Laboratory, Highland Heights, KY, USA for all samples provided by Moderna and Roche, Mannheim, Germany for samples from SARS-CoV-2-infected subjects). All samples were processed according to the manufacturer's instructions. The ACOV2S assay quantitatively determines RBD-specific antibodies (21). Standardization of each manufactured batch of ACOV2S towards an unchanged internal reference material ensures consistent quantification of antibody titers with each assay batch and all available analyzers. Development and manufacturing fulfill requirements for a medical device and ACOV2S is a registered *in vitro* diagnostic with CE marking for use as an aid to assess the adaptive humoral immune response, including neutralizing antibodies, to the SARS−CoV−2 S protein after natural infection with SARS−CoV−2 or in vaccine recipients. Additionally, ACOV2S has been granted US Food and Drug Administration emergency use approval.

The ACOV2S assay applies the double antigen sandwich format for detection of antibodies and can thereby theoretically detect any class of immunoglobulin. The reaction conditions of the assay (use of monomeric antigen and application of relatively stringent buffer conditions) however strongly favor binding of IgG. Measurement results are shown in U/mL, with a medical decision point at 0.80 U/mL to differentiate samples as reactive (≥ 0.80 U/mL) and non-reactive (< 0.80 U/mL) for SARS-CoV-2 RBD-specific antibodies. Values between 0.40–250 U/mL represent the primary measuring range. Results below this range were set to 0.4 U/mL and qualified non-reactive. Samples above 250 U/mL were automatically diluted into the linear range of the assay (realized dilutions in this study: 1:10 or 1:100) with Diluent Universal (Roche Diagnostics, Rotkreuz, Switzerland). The analyzer automatically multiplies diluted results with the dilution factor, which in the applied setting enabled an upper limit of quantification of 25000 U/mL for the analyses in this study.

2.2.2 Traceability of Results to International BAU/mL

Of note, the assigned U/mL are equivalent to Binding Antibody Units (BAU)/mL as defined by the first World Health Organization (WHO) International Standard for anti-SARS-CoV-2 immunoglobulin (NIBSC code 20/136). No conversion of units is required and reported results in U/mL can be directly compared to other studies or results in BAU/mL.

2.2.3 Serologic Monitoring for Breakthrough Infections

In addition to the quantification of RBD-specific antibody titers induced by mRNA-1273 vaccination, all samples were also assessed on the same cobas e 602 module with the previously described Elecsys Anti-SARS-CoV-2 immunoassay detecting antibodies to the N protein (22). As natural infection with SARS-CoV-2 and not vaccination with mRNA-1273 can trigger a positive result in the context of the mRNA-1273 vaccine, this assay was used to determine whether participants were naïve for prior COVID-19 infection or acquired a putative breakthrough infection despite vaccination throughout the period of investigation.

2.2.4 Comparator Assays

Further assay results were generated under the phase 1 study protocol (20) and the results were transferred to Roche for analysis. Details of the comparator assay methods have been published (20, 23).

Serum antibody levels against SARS-CoV-2 were measured by ELISA specific to the S protein [stabilized containing 2 Proline mutations and thus referred to as S-2P protein (hereby referred to as S-2P ELISA [and described in detail in the **Supplementary Appendix** in (20)] and the isolated RBD of the viral S protein (hereby referred to as RBD ELISA). ELISA assay results were expressed as reciprocal endpoint dilution titer. Notably, no reactivity cut-offs or lower limit of quantification were defined, and no standardization was applied for either ELISA. The ELISA methods applied an indirect solid phase format with IgG-specific detection by a secondary staining step.

Results from assays that target neutralizing antibodies, providing an estimate of vaccine-induced, antibody-mediated neutralizing activity, were also assessed. These included: 1) a nanoluciferase assay (nLUC) with titers reported as the dilution required to achieve 80% neutralization (80% inhibitory dilution; hereby referred to as nLUC80); 2) a live wild-type SARS-CoV-2 plaque reduction neutralization assay (PRNT) with titers expressed as reciprocal of dilution needed for 80% reduction in virus infectivity (hereby referred to as PRNT80); and 3) a pseudovirus neutralizing antibody assay (PsVNA) with titers reported as dilution required for 50% neutralization (50% inhibitory dilution; hereby referred to as PsVNA50, respectively). Because of the labor-intense nature of the nLUC80 and PRNT80 assays involving several manual handling steps and cell culture,(20 results were available only for the time points, Day 1, Day 29 (nLUC80 only) and Day 43.

In case no significant inhibition of infection was observed (i.e. < 50% or <80% neutralization) even with the highest sample concentration (i.e. the starting dilution titer), the numerical result of the assay was set to the starting dilution titer and the assay result was interpreted as negative for neutralizing activity in all qualitative concordance analyses. Samples showing significant inhibition (i.e. ≥ 50% or ≥80% neutralization) at any of the applied concentrations were interpreted as positive for neutralizing activity in all qualitative concordance analyses.

2.3 Statistical Analysis

For each trial population and dosage group, ACOV2S-measured anti-RBD antibody levels are shown as boxplots (log-scale) for every measurement time point, with values outside the measuring range censored. Comparison of ACOV2S-measured antibody levels per dose group and time point were conducted

using reverse cumulative distribution curves. For ACOV2S, geometric mean concentrations (GMCs) and, for ELISA, geometric mean titers (GMTs) were calculated for each time point and stratified by dose group, and 95% confidence intervals (CIs) were calculated by Student's t distribution on log-transformed data and subsequent back-transformation to original scale.

For the assessment of seroconversion, as measured by ACOV2S, the percentage of subjects who crossed the reactivity cut-off at 0.8 U/mL at or before a given time point was evaluated. A seropositive status was carried forward to later time points.

Pairwise method comparison across all available data points using Passing-Bablok (log-scale) regression analyses (24) with 95% bootstrap CIs were provided for all comparator assays, excluding values outside the measuring range, and Pearson's correlation coefficients (r) with 95% CIs were calculated.

Qualitative agreement between ACOV2S and neutralization assays was analyzed by positive percentage agreement (PPA), negative percentage agreement (NPA), and overall percentage agreement (OPA), positive and negative predictive value (PPV and NPV) with exact 95% binomial CIs and the positive and negative likelihood ratio with 95% CIs calculated [per Simel et al. approximation (25)]. The software R, version 3.4.0, was used for statistical analysis and visualization (26).

3 RESULTS

The analyses included longitudinal sample panels from in total 30 mRNA-1273-vaccinated participants. Of those, 15 participants had received 25 μg dose and the other 15 had received 100 μg dose (both administered as two injections of the indicated dose with a delay of 28 days). Demographics and baseline characteristics of participants have been previously described (20). In brief, in the 25 μg and 100 μg dose groups, mean ages (± SD) were 36.7 (± 7.9) and 31.3 (± 8.7) years, 60% and 47% were males, respectively, and the majority were of white ethnicity across both cohorts. All participants were naïve for natural SARS-CoV-2 infection at study start and throughout the investigated timeframe as determined with the Elecsys Anti-SARS-CoV-2 (anti-N) assay (**Supplementary Figure 1**).

3.1 Humoral Response After Vaccination With mRNA-1273 Assessed by Elecsys Anti-SARS-CoV-2 S Assay

Anti-RBD antibody levels as measured by ACOV2S, increased over time for both dose groups (**Table 1**). All participants were non-reactive in ACOV2S at baseline (< 0.4 U/mL), confirming the naïve antibody status for SARS-CoV-2. RBD-specific antibodies were readily detectable by ACOV2S at the first sampling time point (Day 15) and determined high antibody levels indicated that seroconversion had apparently occurred earlier than Day 15 for almost all participants (25 μg: 13/15; 100 μg: 15/15). At Day 29, i.e. day of second vaccination, the remaining two participants of the 25 μg group had seroconverted and developed significant antibody concentrations. The determined antibody concentrations correlated with the applied vaccine dose (**Figure 1A**), with 3.27–7.48-fold higher GMCs observed in the 100 μg group compared with the 25 μg group at all follow up visits (**Table 1**). The 100 μg dose group showed a more homogenous anti-RBD response, as reflected by the smaller geometric standard deviations, indicating reduced inter-individual spread in response to the vaccine at higher dose. In both groups, antibody levels tended to increase until Day 43 and remained high through Day 57 (**Figure 1B**). None of the measured antibody levels exceeded the selected upper limit of quantitation of 25000 U/mL of ACOV2S that resulted from maximally applied 1:100 dilution in this study.

ACOV2S-measured antibody levels over time in vaccinated samples compared with those in post-PCR confirmed SARS-CoV-2 infection are shown in **Figure 2**. Natively-

TABLE 1 | ACOV2S summary statistics and GMR, comparing the 100 μg group to the 25 μg group.

	Day 1	Day 15	Day 29	Day 43	Day 57
25 μg	**n = 15**	**n = 15**	**n = 15**	**n = 15**	**n = 15**
Median	0.400	6.47	79.2	2714	2176
Q1–Q3	0.400–0.400	1.73–30.2	21.0–120	1156–10918	1112–7865
Min–Max	0.400–0.400	0.400–147	7.49–226	45.4–14492	62.8–11738
GMC	0.400	6.86	55.0	2123	1709
(95% CI)	(0.400–0.400)	(2.75–17.1)	(30.2–100)	(860–5237)	(745–3920)
GSD	1.00	5.20	2.96	5.11	4.48
100 μg	**n = 15**	**n = 15**	**n = 15**	**n = 14**	**n = 14**
Median	0.400	44.7	209	8476	6044
Q1–Q3	0.400–0.400	26.9–182	135–238	6407–9237	4637–6998
Min–Max	0.400–0.400	2.08–629	25.9–726	4050–13205	2637–9827
GMC	0.400	51.3	182	7803	5596
(95% CI)	(0.400–0.400)	(23.1–114)	(125–264)	(6259–9727)	(4538–6901)
GSD	1.00	4.21	1.97	1.46	1.44
GMR (100 *vs* 25 μg)	1.00	7.48	3.30	3.68	3.27
(95% CI)	(1.00–1.00)	(2.35–23.8)	(1.68–6.49)	(1.47–9.20)	(1.41–7.62)

All values below the lower limit of the measuring range were substituted by this lower limit at 0.4 U/mL. Of note, all ACOV2S levels measured at baseline Day 1 were actually below 0.4 U/mL. GMC, geometric mean concentrations; GMR, geometric mean ratio; GSD, geometric standard deviation; Q1, first quartile; Q3, third quartile.

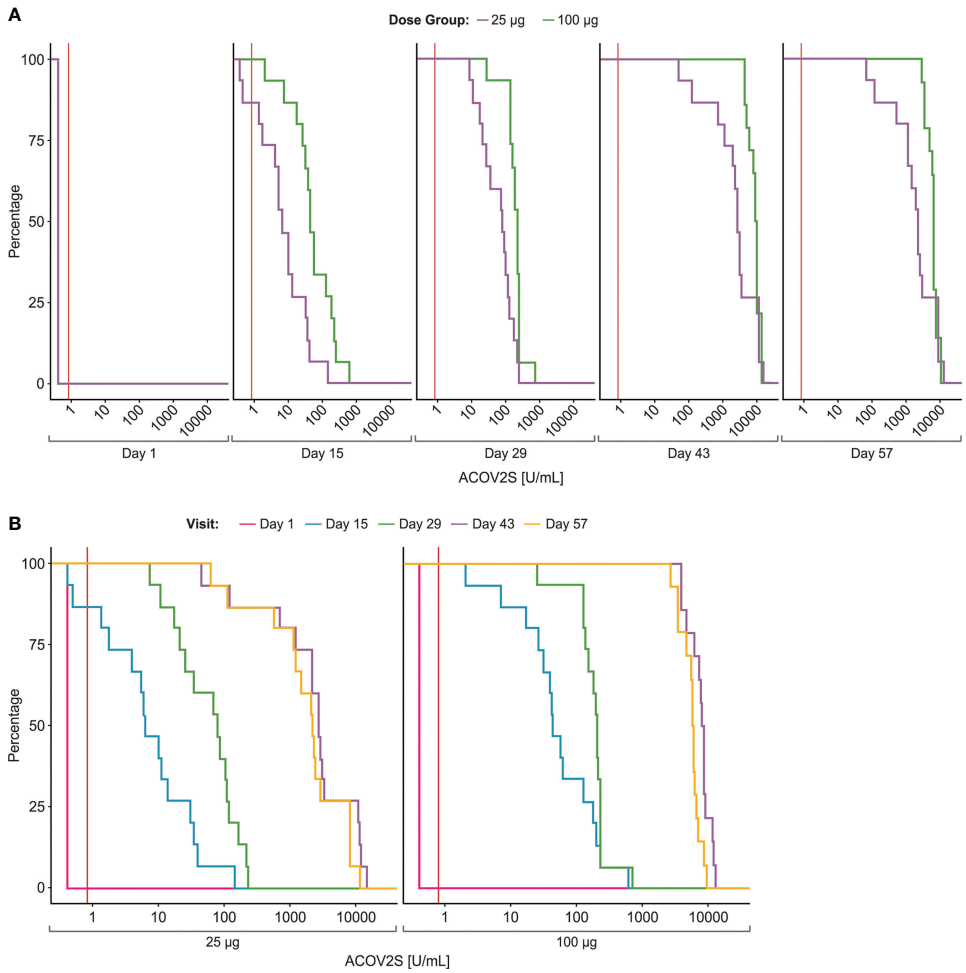

FIGURE 1 | Time-dependent antibody responses as measured by the ACOV2S. Reverse cumulative distribution curves allow for comparison of ACOV2S-measured antibody level distributions between dose groups **(A)** and visit days **(B)**. Red vertical line indicates reactivity cut-off (0.8 U/mL).

infected individuals developed a more heterogeneous antibody response to SARS-CoV-2 infection compared with vaccination, likely due to differences in viral load and the course of disease. ACOV2S-measured anti-RBD antibody levels after the first vaccination were within the range developed upon native infection, with levels following the 25 µg dose more aligned with those induced by mild disease (**Figures 2A, C**) and the 100 µg dose with severe disease (**Figures 2B, D**). After the second vaccination, it can be construed that ACOV2S-measured antibody levels exceeded those induced by native SARS-CoV-2 infection by approximately 10-100 fold.

3.2 Concordance of ACOV2S With RBD and S-2P ELISA Assays

In total, 113 samples were available for comparative analysis with both ELISA assays across various time points. Measurements by ACOV2S were highly correlated with both RBD ELISA (r=0.938 [95% CI 0.911–0.957]; p<0.0001; **Figure 3A**) and S-2P ELISA (r=0.918 [95% CI 0.883–0.943]; p<0.0001; **Figure 3B**) measurements. Notably, there was distinct heterogeneity of both ELISA results at baseline in contrast to ACOV2S which showed all samples as non-reactive.

Antibody levels measured with ACOV2S and the RBD or S-2P ELISA showed similar time courses following first and second vaccinations (**Figures 3C, D**, respectively). A transient difference became apparent in the 25 µg dose group in which the S-2P ELISA already determined seroconversion for all participants 15 days after first vaccination, whereas ACOV2S did not detect samples from two donors at this time point. A more continuous antibody level development over time and dose groups was observed with the ACOV2S. The obtained results are additionally plotted as GMCs of ACOV2S-measured antibody levels and GMTs of the ELISA-endpoint dilution titers over time in **Figures 3E, F**, respectively, to facilitate relative result comparisons. The ELISA methods showed strong signal increase early after first vaccination followed by a plateau of antibody levels between Day 15 and Day 29, more frequently observed with the S-2P ELISA, and a smaller increase after

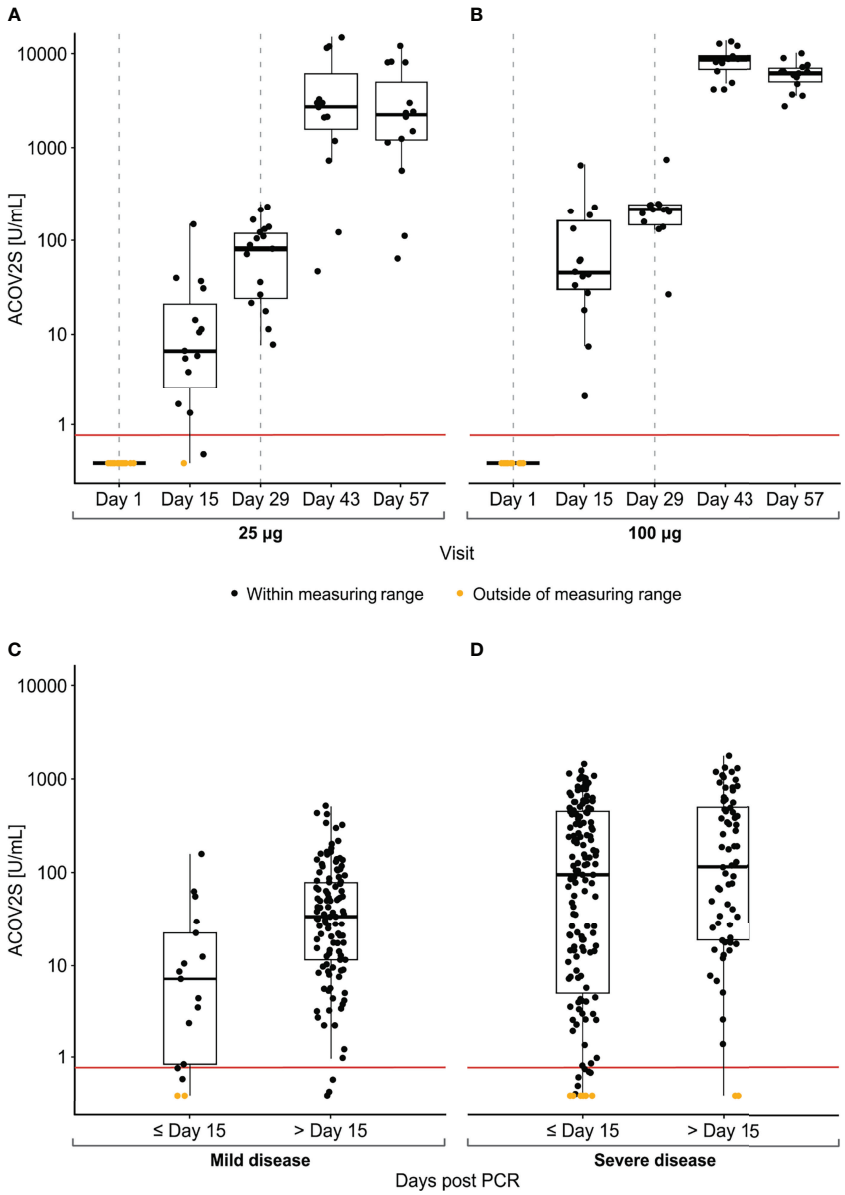

FIGURE 2 | Time course of ACOV2S-measured antibody levels following mRNA-1273 vaccination and native infection. Antibody levels following vaccination are shown in **(A, B)**; dotted grey vertical lines indicate time of vaccination, administered at Days 1 and 29. Antibody levels in samples post PCR-confirmed SARS-CoV-2 infection are shown in **(C, D)**. Box plots show the individual readouts (black dots) and, 25th, 50th, and 75th percentiles (black box). Red horizontal line indicates reactivity cut-off (0.8 U/mL).

second vaccination compared with the ACOV2S. This infers that the ELISA methods detect the antibody titer development over time in a more stepwise manner compared to a more continuous antibody titer development as determined with ACOV2S. Also, by making use of the automated onboard dilution, ACOV2S can resolve very high titers while ELISAs appear to approach saturation. This is evident by the more prominent geometric fold-rise after the second vaccination versus the first vaccination for the ACOV2S compared with the ELISA methods (**Supplementary Table 1**).

3.3 Concordance of ACOV2S With Neutralization Assays

Figure 4 visualizes concordance of ACOV2S with comparative assays assessing neutralization. For comparison with nLUC80, 47 samples had quantifiable results. Numerical correlation with nLUC80 measurements was very strong (Pearson's r=0.933 [95% CI 0.882–0.962]; p<0.0001) and all samples with a positive nLUC80 had a positive ACOV2S measurement (**Figure 4A**). At Day 29, there were 8 samples with a positive ACOV2S result whose nLUC80 result was negative,

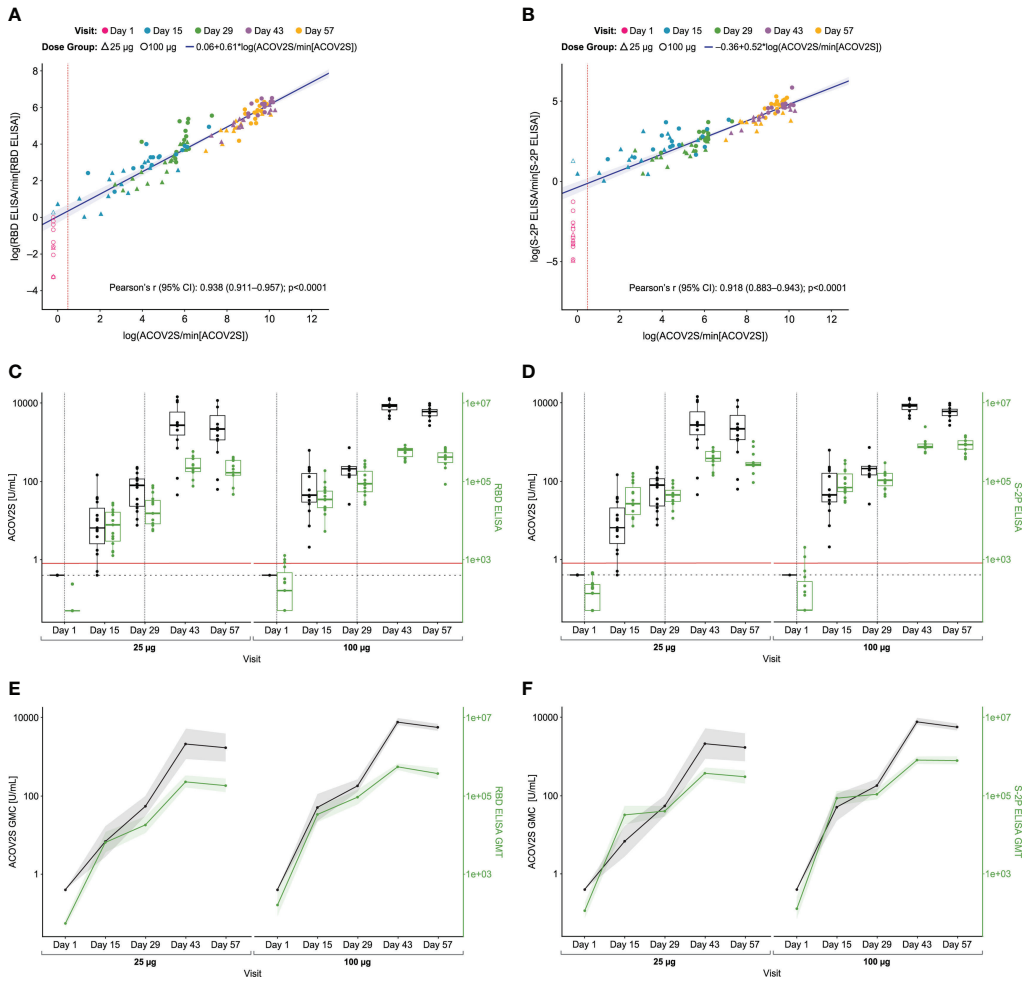

FIGURE 3 | Comparison of ACOV2S and ELISA. Passing–Bablok regression fit (log-scale) for the comparison with RBD ELISA is shown in **(A)**, and with S-2P ELISA in **(B)** Red dotted line shows ACOV2S reactivity cut-off. The shaded area represents the 95% confidence interval for the fitted curve. Dots and triangles represent individual samples; filled dots or triangles represent samples within the measuring range for the ACOV2S assay. Time courses of antibody responses measured by RBD ELISA and S-2P ELISA compared to ACOV2S are shown in **(C, D)**, respectively. Dotted grey vertical lines show when vaccination injections were administered at Days 1 and 29. Red horizontal line shows ACOV2S reactivity cutoff, and the black dashed horizontal line represents the lower end of the ACOV2S measuring range. Box plots show the individual readouts (dots) and, 25th, 50th, and 75th percentiles (box). Time-dependent geometric mean concentrations and geometric mean titers across vaccine dose groups of ACOV2S levels *vs* RBD ELISA and S-2P ELISA are shown in **(E, F)**, respectively. Shaded areas indicate 95% confidence intervals.

predominantly occurring in 25 µg dose group. A total of 79 samples across all time points had quantifiable PsVNA50 results. Strong correlation was observed between ACOV2S and PsVNA50 (r=0.771 [0.663–0.848]; p<0.0001) results and all samples with a positive PsVNA50 result had a positive ACOV2S measurement. A proportion of samples had a negative PsVNA50 result but a positive result with ACOV2S (**Figure 4B**). Analysis with 27 available samples obtained two weeks after the second vaccination (Day 43) showed ACOV2S levels moderately correlated with PRNT80 results [r=0.672 (0.392–0.838); p=0.0001 (**Figure 4C**)].

Qualitative agreement between ACOV2S and neutralizing test results is presented in **Supplementary Table 2**. The PPA and NPV for all neutralization assays was 100%, highlighting that no samples were negative for ACOV2S while positive for neutralization.

4 DISCUSSION

Immune responses to SARS-CoV-2 infection and vaccination can significantly vary with each individual (27–29) and longevity of the humoral immune response to SARS-CoV-2 has repeatedly been a matter of investigation (30). Correlation of protection from symptomatic disease with determined antibody titers is also being explored (31). Here, reliable correlation requires evaluation of large cohorts and multi-centric datasets and determination of titers with a standardized and globally

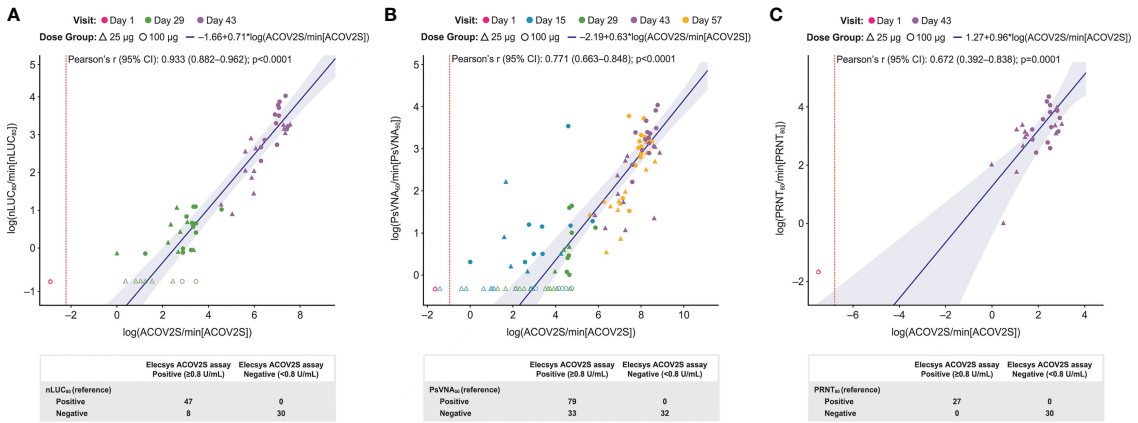

FIGURE 4 | Comparison of ACOV2S and neutralization assays. Passing–Bablok regression fit (log-scale) of ACOV2S with $nLUC_{80}$ is shown in **(A)**, $PsVNA_{50}$ in **(B)** and $PRNT_{80}$ in **(C)**. Red dotted line shows ACOV2S reactivity cut-off. The shaded area represents the 95% confidence interval for the fitted curve. Dots or crosses show individual sample readouts. Filled dots or triangles represent samples within the measuring range for both ACOV2S and respective comparator assay. Overlaid table shows the qualitative agreement between Elecsys ACOV2S and comparator assays.

available method. The reported high efficacy of the mRNA1273 vaccine renders breakthrough infections rare and non-responders unlikely (20, 32, 33). Together with the rapidly growing number of SARS-CoV-2 vaccines in development, these aspects further emphasize the need for automated, high-throughput methods to reliably quantify immune response in a standardized manner to enable large dataset comparisons, confirm seroconversion in all targeted individuals, independent of pre-existing conditions or medications (34), as well as long-term monitoring.

In this exploratory analysis of mRNA-1273-vaccinated human samples from the phase 1 trial (20), the quantification of the anti-RBD antibodies through ACOV2S allowed the monitoring of changes between visits and resolution of differences between dosage groups, with antibody concentrations increasing in a time- and dose-dependent manner. Primary vaccination resulted in seroconversion in all participants early after the first injection. Seroconversion after initial vaccination and overall anti-RBD concentration development after application of 100 µg per injection was stronger than 25 µg. Antibody levels present two weeks after second vaccination with mRNA-1273 were seen to exceed those induced by natural SARS-CoV-2 infection, both of which provide protection against symptomatic infection with higher antibody levels expected to be synonymous with longevity (32, 35, 36).

Although the design of the methods differs, results from ACOV2S compared well and closely correlated with those obtained with two ELISA methods, one targeting antibodies against the S-2P protein of the virus and the other specifically against the RBD domain (both $r>0.9$; $p<0.0001$). However, there was high heterogeneity in ELISA baseline values, potentially due to less specific signals. The lower end of the measuring range is not defined for either ELISA. Additionally, no validated reactivity cut-off was available, hence it was not possible to formally assess the qualitative agreement between the ACOV2S and ELISA methods. A more continuous increase of titer up to peak was observed with the ACOV2S, while the ELISA measurements seemed to approach a saturation limit. Of note, the linear range and thus the upper limit of quantitation has not been established for either ELISA. Despite our findings and previous studies suggesting that S-focused ELISAs may offer greater sensitivity (37), antibody responses measured with the RBD ELISA were similar to the S-2P ELISA, with better signal dynamics illustrated by the more homogenous increase in GMT. Additionally, the high S-2P ELISA titers detected soon after the first vaccination, even with the low 25 µg dose, could misleadingly be interpreted as suggestive of strong immune response from early on, while efficient immunity has been reported to occur only later after vaccination (33). In contrast, dynamic increase of antibody levels accompanying vaccination enable better characterization of the developing immune response than plateau reactivity. Less variation in baseline titer was also observed with the RBD ELISA, potentially due to lower cross-reactivity with antibodies to previously endemic and highly abundant coronavirus strains, which show structural similarities in the S2 subunit (38). Taking into consideration that the RBD is poorly conserved among them (7), antibody-detection assays specifically targeting antibodies directed against the RBD appear highly suitable for quantifying the humoral immune response to SARS-CoV-2.

In this study, good correlation was observed with ACOV2S and the established surrogate neutralization tests, nLUC80, and PsVNA50. Disagreement was observed only with earlier samples where some positive, but relatively low ACOV2S results coincided with non-reactive neutralizing antibody test results. This was possibly due to insufficient antibody concentrations to prevent infection in the *in vitro* setting of a neutralization test, supporting the clinical finding that single dose vaccination does not convey optimal protection from infection and that two-step vaccination inducing higher antibody titers is required. With an

apparent more continuous resolution of antibody development, these observations suggest ACOV2S might allow for more precise timing of reaching putatively protective levels than methods with rapidly developing plateaus. Although limited to samples from a singular visit (Day 43), we found ACOV2S levels also correlated with live-virus neutralization test PRNT80 titers. For all three neutralization tests, appearance of neutralizing effects was suggested within two weeks of the second vaccination, further supporting the need for a two-dose schedule. Also, it has been described manifold that RBD is not necessarily the exclusive, yet the dominant target for antibody-mediated virus neutralization, meaning that RBD-directed antibodies contribute to virus neutralization. Together with the observed rapid development of very high anti-RBD titers illustrating the strong immunogenic potential of the mRNA-1273 vaccine especially with the clinically-selected 100 μg dose (32), these findings render anti-RBD levels a suitable and convenient surrogate marker for the presence of neutralizing antibodies during vaccination monitoring, with high levels suggestive of greater protective immunity.

Live virus neutralization using wild type virus requires handling of live SARS-CoV-2 in a specialized biosafety level 3 containment facility and is time-consuming, deeming it unsuitable for large scale use. Neutralization test methods using replication-defective pseudotyped viral particles have been developed; however, these still require live-cell culture, considerable manual handling steps and, consequently, inevitable variance in neutralization results. Although surrogate neutralization assays have been developed and validated (10, 39), their applied competitive assay principle goes along with a rather small dynamic range, which limits resolution of change in high titer vaccination samples. In addition, challenges of semi-automatable methods and costs remain. Also, neutralization tests are potentially limited in that they only address static antibody levels at a given time point and do not take into account antibody avidity, maturation or the immediate re-stimulation of the immune memory by a recurring infection *in vivo*. Poor signal resolution at the lower end of the measuring range of neutralization tests is also a concern. The ACOV2S assay has been developed to detect the presence of low levels of RBD-directed antibodies with a high sensitivity (97.92%; 95% CI: 95.21–99.32) and specificity (99.95%; 95% CI: 99.87–99.99) (40), and a medical decision point at 0.8 U/mL as an indicator of infection or vaccination, i.e. the lowest quantity of antibody that determines reactivity for SARS-CoV-2 RBD-specific antibodies. The quantitative setup of the assay however allows for definition of additional medical decision points that might best suit other purposes, like protective levels of antibody or high titer plasma for therapeutic use (41). In addition, ACOV2S is standardized congruently to the first WHO international standard and assigned units can be used interchangeably to BAU/mL, making it suitable for long-term monitoring and referencing of results to the international standard. At present, the assay is approved for use in multiple regulatory markets including CE mark and FDA. It is accessible in more than 100 countries across the globe, including developing and underdeveloped countries in South America, Africa and Asia. Thus, ACOV2S fulfils the requirements of a standardized and widely available method with consistent results to allow reliable detection and monitoring of anti-RBD titers over time.

Altogether, these findings suggest that ACOV2S levels may predict the presence of neutralizing antibodies (17), especially at later time points after vaccination, and therefore, potentially provide a more accessible method for enumerating immune response in vaccinated individuals. However, further ongoing research is required to elucidate if protective anti-RBD thresholds can be defined that are indicative of, for example, sterile immunity or of preventing symptomatic infection.

Limitations of our study include the small sample size of the vaccination samples as well as the lack of variation in time points available for analysis for some of the neutralization assays. The comparison to titers observed in native infection might be biased by an unbalanced representation of natively-infected samples. The relatively short follow-up mitigates analysis of the ability of ACOV2S assay to determine the sustainability of antibody response. Further comparison studies using longer term follow-up and bigger samples sizes are warranted.

5 CONCLUSION

Assessing the longevity of antibody titers over time together with monitoring for symptomatic re-infection is essential to determine long-term immune protection and define antibody levels as a reliable and conveniently accessible surrogate marker of protection. These data indicate that the ACOV2S immunoassay can be regarded as a highly valuable, convenient and widely accessible method to assess and quantify the presence of antibodies directed at the RBD of SARS-CoV-2, conducive to immune response. ACOV2S sensitively detects and reliably quantifies the vaccination-induced humoral response over a dynamic range that can be conveniently scaled by automated onboard dilution. Our results support the potential for RBD-based immunoassays to replace neutralization tests in the assessment of immune response after vaccination against SARS-CoV-2. These findings also support the use of ACOV2S for longitudinal response monitoring of the RBD-specific antibody response to vaccination and, ultimately, the investigation of an antibody-based correlate of protection from symptomatic COVID-19.

DATA AVAILABILITY STATEMENT

The datasets presented in this article are not readily available because the authors are committed to sharing data supporting the findings of eligible studies. Access to de-identified patient-level data and supporting clinical documents with qualified external researchers may be available upon request once the trial is complete. Requests to access the datasets should be directed to simon.jochum@roche.com; rolando.pajon@modernatx.com.

ETHICS STATEMENT

Approval was granted by the Advarra institutional review board for the phase 1 trial and the diagnostic protocol under which the existing samples were tested. The patients/participants provided their written informed consent to participate in this study.

AUTHOR CONTRIBUTIONS

Study concept/design: IK, UE, SJ, and SH. Data acquisition: IK and BK. Data analysis and interpretation: SH, VG, SJ, and IK. Review and final approval of the manuscript: SJ, IK, SH, HL, UE, VG, BK, and RP. All authors contributed to the article and approved the submitted version.

FUNDING

This study utilized samples obtained under NCT04283461 funded by NIAID, National Institutes of Health (NIH), Bethesda MD USA. Moderna provided mRNA-1273 samples from their phase 1 trial for this study but did not provide any financial support. The phase 1 trial was supported by the NIAID, National Institutes of Health (NIH), Bethesda MD USA, under award numbers UM1AI148373 (Kaiser Washington), UM1AI148576 (Emory University), UM1AI148684 (Emory University), UM1Al148684-01S1 (Vanderbilt University Medical Center), and HHSN272201500002C (Emmes); by the National Center for Advancing Translational Sciences, NIH, under award number UL1 TR002243 (Vanderbilt University Medical Center); and by the Dolly Parton COVID-19 Research Fund (Vanderbilt University Medical Center).This analysis was funded by Roche Diagnostics GmbH (Penzberg, Germany).

ACKNOWLEDGMENTS

We would like to thank the associated mRNA-1273 Study Team for their contribution to data collection as part of the associated Phase I study (NCT04283461). Additionally, we would like to thank Micah Taylor, Kristin Lucas, and the lab operators at PPD Central Labs (Kentucky, USA) for their contribution to data collection and study execution. We would also like to acknowledge and thank Celine Leroy, Tara Pigg, Emma Tao, Yuli Sun, Walter Stoettner (Roche Diagnostics) and Maha Maglinao (Moderna) for their individual contributions to study execution. Additional gratitude goes to Laura Schlieker (Staburo GmbH) for the validation of the analysis. ELECSYS and COBAS are trademarks of Roche. All other product names and trademarks are the property of their respective owners. The Elecsys Anti-SARS-CoV-2 S assay is approved under an Emergency Use Authorisation in the US. Editorial support was provided by Jade Drummond of inScience Communications, Springer Healthcare Ltd, UK, and was funded by Roche Diagnostics International Ltd (Rotkreuz, Switzerland).

SUPPLEMENTARY MATERIAL

The Supplementary Material for this article can be found online at: https://www.frontiersin.org/articles/10.3389/fimmu.2021.798117/full#supplementary-material

REFERENCES

1. Center JHUCR. *COVID-19 Dashboard by the Center for Systems Science and Engineering (CSSE) at Johns Hopkins University* (2021). Available at: https://coronavirus.jhu.edu/map.html.
2. COVID-19 W. *COVID-19 Vaccine Tracker and Landscape 2021*. Available at: https://www.who.int/publications/m/item/draft-landscape-of-covid-19-candidate-vaccines.
3. Carrillo J, Izquierdo-Useros N, Avila-Nieto C, Pradenas E, Clotet B, Blanco J. Humoral Immune Responses and Neutralizing Antibodies Against SARS-Cov-2; Implications in Pathogenesis and Protective Immunity. *Biochem Biophys Res Commun* (2021) 538:187–91. doi: 10.1016/j.bbrc.2020.10.108
4. Walls AC, Park YJ, Tortorici MA, Wall A, McGuire AT, Veesler D. Structure, Function, and Antigenicity of the SARS-Cov-2 Spike Glycoprotein. *Cell* (2020) 183(6):1735. doi: 10.1016/j.cell.2020.11.032
5. Lou B, Li TD, Zheng SF, Su YY, Li ZY, Liu W, et al. Serology Characteristics of SARS-Cov-2 Infection After Exposure and Post-Symptom Onset. *Eur Respir J* (2020) 56(2):2000763. doi: 10.1183/13993003.00763-2020
6. Zhao J, Yuan Q, Wang H, Liu W, Liao X, Su Y, et al. Antibody Responses to SARS-Cov-2 in Patients With Novel Coronavirus Disease 2019. *Clin Infect Dis* (2020) 71(16):2027–34. doi: 10.1093/cid/ciaa344
7. Premkumar L, Segovia-Chumbez B, Jadi R, Martinez DR, Raut R, Markmann A, et al. The Receptor Binding Domain of the Viral Spike Protein is an Immunodominant and Highly Specific Target of Antibodies in SARS-Cov-2 Patients. *Sci Immunol* (2020) 5(48):eabc8413. doi: 10.1126/sciimmunol.abc8413
8. Dai L, Gao GF. Viral Targets for Vaccines Against COVID-19. *Nat Rev Immunol* (2021) 21(2):73–82. doi: 10.1038/s41577-020-00480-0
9. Bewley KR, Coombes NS, Gagnon L, McInroy L, Baker N, Shaik I, et al. Quantification of SARS-Cov-2 Neutralizing Antibody by Wild-Type Plaque Reduction Neutralization, Microneutralization and Pseudotyped Virus Neutralization Assays. *Nat Protoc* (2021) 16(6):3114–40. doi: 10.1038/s41596-021-00536-y
10. Tan CW, Chia WN, Qin X, Liu P, Chen MI, Tiu C, et al. A SARS-Cov-2 Surrogate Virus Neutralization Test Based on Antibody-Mediated Blockage of ACE2-Spike Protein-Protein Interaction. *Nat Biotechnol* (2020) 38(9):1073–8. doi: 10.1038/s41587-020-0631-z
11. Riepler L, Rossler A, Falch A, Volland A, Borena W, von Laer D, et al. Comparison of Four SARS-Cov-2 Neutralization Assays. *Vaccines (Basel)* (2020) 9(1):13. doi: 10.3390/vaccines9010013
12. Legros V, Denolly S, Vogrig M, Boson B, Siret E, Rigaill J, et al. A Longitudinal Study of SARS-Cov-2-Infected Patients Reveals a High Correlation Between Neutralizing Antibodies and COVID-19 Severity. *Cell Mol Immunol* (2021) 18 (2):318–27. doi: 10.1038/s41423-020-00588-2
13. Salazar E, Kuchipudi SV, Christensen PA, Eagar T, Yi X, Zhao P, et al. Convalescent Plasma Anti-SARS-Cov-2 Spike Protein Ectodomain and Receptor-Binding Domain Igg Correlate With Virus Neutralization. *J Clin Invest* (2020) 130(12):6728–38. doi: 10.1172/JCI141206
14. Bal A, Pozzetto B, Trabaud MA, Escuret V, Rabilloud M, Langlois-Jacques C, et al. Evaluation of High-Throughput SARS-Cov-2 Serological Assays in a Longitudinal Cohort of Patients With Mild COVID-19: Clinical Sensitivity, Specificity, and Association With Virus Neutralization Test. *Clin Chem* (2021) 67(5):742–52. doi: 10.1093/clinchem/hvaa336
15. Irsara C, Egger AE, Prokop W, Nairz M, Loacker L, Sahanic S, et al. Clinical Validation of the Siemens Quantitative SARS-Cov-2 Spike Igg Assay (Scovg)

Reveals Improved Sensitivity and a Good Correlation With Virus Neutralization Titers. *Clin Chem Lab Med* (2021) 59(8):1453–62. doi: 10.1515/cclm-2021-0214
16. Padoan A, Bonfante F, Pagliari M, Bortolami A, Negrini D, Zuin S, et al. Analytical and Clinical Performances of Five Immunoassays for the Detection of SARS-Cov-2 Antibodies in Comparison With Neutralization Activity. *EbioMedicine* (2020) 62:103101. doi: 10.1016/j.ebiom.2020.103101
17. Rubio-Acero R, Castelletti N, Fingerle V, Olbrich L, Bakuli A, Wolfel R, et al. In Search of the SARS-Cov-2 Protection Correlate: Head-to-Head Comparison of Two Quantitative S1 Assays in Pre-Characterized Oligo-/Asymptomatic Patients. *Infect Dis Ther* (2021) 10:1–14. doi: 10.1007/s40121-021-00475-x
18. Salvagno GL, Henry BM, di Piazza G, Pighi L, De Nitto S, Bragantini D, et al. Anti-SARS-Cov-2 Receptor-Binding Domain Total Antibodies Response in Seropositive and Seronegative Healthcare Workers Undergoing COVID-19 mRNA BNT162b2 Vaccination. *Diagn (Basel)* (2021) 11(5):832. doi: 10.3390/diagnostics11050832
19. Seyahi E, Bakhdiyarli G, Oztas M, Kuskucu MA, Tok Y, Sut N, et al. Antibody Response to Inactivated COVID-19 Vaccine (Coronavac) in Immune-Mediated Diseases: A Controlled Study Among Hospital Workers and Elderly. *Rheumatol Int* (2021) 41(8):1429–40. doi: 10.1007/s00296-021-04910-7
20. Jackson LA, Anderson EJ, Rouphael NG, Roberts PC, Makhene M, Coler RN, et al. An mRNA Vaccine Against SARS-Cov-2 – Preliminary Report. *N Engl J Med* (2020) 383(20):1920–31. doi: 10.1056/NEJMoa2022483
21. Roche Diagnostics GmbH. *Elecsys® Anti-SARS-Cov-2 s, Instructions for Use*. (2021).
22. Muench P, Jochum S, Wenderoth V, Ofenloch-Haehnle B, Hombach M, Strobl M, et al. Development and Validation of the Elecsys Anti-SARS-Cov-2 Immunoassay as a Highly Specific Tool for Determining Past Exposure to SARS-Cov-2. *J Clin Microbiol* (2020) 58(10):e01694-20. doi: 10.1128/JCM.01694-20
23. Anderson EJ, Rouphael NG, Widge AT, Jackson LA, Roberts PC, Makhene M, et al. Safety and Immunogenicity of SARS-Cov-2 mRNA-1273 Vaccine in Older Adults. *N Engl J Med* (2020) 383(25):2427–38. doi: 10.1056/NEJMoa2028436
24. Passing H, Bablok. A New Biometrical Procedure for Testing the Equality of Measurements From Two Different Analytical Methods. Application of Linear Regression Procedures for Method Comparison Studies in Clinical Chemistry, Part I. *J Clin Chem Clin Biochem* (1983) 21(11):709–20. doi: 10.1515/cclm.1983.21.11.709
25. Simel DL, Samsa GP, Matchar DB. Likelihood Ratios With Confidence: Sample Size Estimation for Diagnostic Test Studies. *J Clin Epidemiol* (1991) 44(8):763–70. doi: 10.1016/0895-4356(91)90128-V
26. Team RC. R: A Language and Environment for Statistical Computing. In: *R Foundation for Statistical Computing*. Vienna, Austria (2020). Available at: https://www.R-project.org/.
27. Brodin P, Jojic V, Gao T, Bhattacharya S, Angel CJ, Furman D, et al. Variation in the Human Immune System is Largely Driven by non-Heritable Influences. *Cell* (2015) 160(1-2):37–47. doi: 10.1016/j.cell.2014.12.020
28. Castro Dopico X, Ols S, Lore K, Karlsson Hedestam GB. Immunity to SARS-Cov-2 Induced by Infection or Vaccination. *J Intern Med* (2021) 291(1):32–50. doi: 10.1111/joim.13372
29. Jonsson S, Sveinbjornsson G, de Lapuente Portilla AL, Swaminathan B, Plomp R, Dekkers G, et al. Identification of Sequence Variants Influencing Immunoglobulin Levels. *Nat Genet* (2017) 49(8):1182–91. doi: 10.1038/ng.3897
30. Turner JS, Kim W, Kalaidina E, Goss CW, Rauseo AM, Schmitz AJ, et al. SARS-Cov-2 Infection Induces Long-Lived Bone Marrow Plasma Cells in Humans. *Nature* (2021) 595(7867):421–5. doi: 10.1038/s41586-021-03647-4
31. Gaebler C, Wang Z, Lorenzi JCC, Muecksch F, Finkin S, Tokuyama M, et al. Evolution of Antibody Immunity to SARS-Cov-2. *Nature* (2021) 591(7851):639–44. doi: 10.1038/s41586-021-03207-w
32. Baden LR, El Sahly HM, Essink B, Kotloff K, Frey S, Novak R, et al. Efficacy and Safety of the mRNA-1273 SARS-Cov-2 Vaccine. *N Engl J Med* (2021) 384(5):403–16. doi: 10.1056/NEJMoa2035389
33. Chu L, McPhee R, Huang W, Bennett H, Pajon R, Nestorova B, et al. A Preliminary Report of a Randomized Controlled Phase 2 Trial of the Safety and Immunogenicity of mRNA-1273 SARS-Cov-2 Vaccine. *Vaccine* (2021) 39(20):2791–9. doi: 10.1016/j.vaccine.2021.02.007
34. Rubbert-Roth A, Vuilleumier N, Ludewig B, Schmiedeberg K, Haller C, von Kempis J. Anti-SARS-Cov-2 mRNA Vaccine in Patients With Rheumatoid Arthritis. *Lancet Rheumatol* (2021) 3(7):e470–e2. doi: 10.1016/S2665-9913(21)00186-7
35. Feng C, Shi J, Fan Q, Wang Y, Huang H, Chen F, et al. Protective Humoral and Cellular Immune Responses to SARS-Cov-2 Persist Up to 1 Year After Recovery. *Nat Commun* (2021) 12(1):4984. doi: 10.1038/s41467-021-25312-0
36. Figueiredo-Campos P, Blankenhaus B, Mota C, Gomes A, Serrano M, Ariotti S, et al. Seroprevalence of Anti-SARS-Cov-2 Antibodies in COVID-19 Patients and Healthy Volunteers Up to 6 Months Post Disease Onset. *Eur J Immunol* (2020) 50(12):2025–40. doi: 10.1002/eji.202048970
37. Tian Y, Lian C, Chen Y, Wei D, Zhang X, Ling Y, et al. Sensitivity and Specificity of SARS-Cov-2 S1 Subunit in COVID-19 Serology Assays. *Cell Discov* (2020) 6:75. doi: 10.1038/s41421-020-00224-3
38. Ladner JT, Henson SN, Boyle AS, Engelbrektson AL, Fink ZW, Rahee F, et al. Epitope-Resolved Profiling of the SARS-Cov-2 Antibody Response Identifies Cross-Reactivity With Endemic Human Coronaviruses. *Cell Rep Med* (2021) 2(1):100189. doi: 10.1016/j.xcrm.2020.100189
39. Marien J, Michiels J, Heyndrickx L, Nkuba-Ndaye A, Ceulemans A, Bartholomeeusen K, et al. Evaluation of a Surrogate Virus Neutralization Test for High-Throughput Serosurveillance of SARS-Cov-2. *J Virol Methods* (2021) 114228:114228. doi: 10.1016/j.jviromet.2021.114228
40. Riester E, Findeisen J, Hegel K, Kabesch M, Ambrosch A, Rank CM, et al. *Performance Evaluation of the Roche Elecsys Anti-SARS-Cov-2 s Immunoassay Medrxiv2021* . Available at: https://www.medrxiv.org/content/10.1101/2021.03.02.21252203v1.
41. Hinton DM. *Convelescent Plasma EUA Letter of Authorization: FDA* (2021). Available at: https://www.fda.gov/media/141477/download.

Conflict of Interest: SJ, IK, SH, VPG and UE are employees of Roche Diagnostics. BK is an employee of PPD, Inc. HL and RP are employees of Moderna, Inc.

The authors declare that this study received funding from Roche Diagnostics GmbH. The funder was involved in the study design, analysis, interpretation of data, the writing of this article and the decision to submit it for publication.

frontiers in Immunology

ORIGINAL RESEARCH
published: 25 January 2022
doi: 10.3389/fimmu.2022.807454

Innate Immune Responses of Vaccinees Determine Early Neutralizing Antibody Production After ChAdOx1nCoV-19 Vaccination

Ching-Fen Shen[1,2†], Chia-Liang Yen[1†], Yi-Chen Fu[3], Chao-Min Cheng[3], Tzu-Chi Shen[1], Pei-De Chang[1], Kuang-Hsiung Cheng[4], Ching-Chuan Liu[2], Yu-Tzu Chang[5], Po-Lin Chen[5], Wen-Chien Ko[5] and Chi-Chang Shieh[1,2]*

[1] Institute of Clinical Medicine, College of Medicine, National Cheng Kung University, Tainan City, Taiwan, [2] Department of Pediatrics, National Cheng Kung University Hospital, College of Medicine, National Cheng Kung University, Tainan City, Taiwan, [3] Institute of Biomedical Engineering, National Tsing Hua University, Hsinchu City, Taiwan, [4] Department of Pathology, National Cheng Kung University Hospital, College of Medicine, National Cheng Kung University, Tainan City, Taiwan, [5] Department of Internal Medicine, National Cheng Kung University Hospital, College of Medicine, National Cheng Kung University, Tainan City, Taiwan

OPEN ACCESS

Edited by:
Srinivasa Reddy Bonam, Institut National de la Santé et de la Recherche Médicale (INSERM), France

Reviewed by:
Gunnveig Grødeland, University of Oslo, Norway
Nitin Saksena, Victoria University, Australia, Australia

***Correspondence:**
Chi-Chang Shieh
cshieh@mail.ncku.edu.tw

[†]These authors have contributed equally to this work

Specialty section:
This article was submitted to Vaccines and Molecular Therapeutics, a section of the journal Frontiers in Immunology

Received: 02 November 2021
Accepted: 06 January 2022
Published: 25 January 2022

Citation:
Shen C-F, Yen C-L, Fu Y-C, Cheng C-M, Shen T-C, Chang P-D, Cheng K-H, Liu C-C, Chang Y-T, Chen P-L, Ko W-C and Shieh C-C (2022) Innate Immune Responses of Vaccinees Determine Early Neutralizing Antibody Production After ChAdOx1nCoV-19 Vaccination. Front. Immunol. 13:807454. doi: 10.3389/fimmu.2022.807454

Background: Innate immunity, armed with pattern recognition receptors including Toll-like receptors (TLR), is critical for immune cell activation and the connection to anti-microbial adaptive immunity. However, information regarding the impact of age on the innate immunity in response to SARS-CoV2 adenovirus vector vaccines and its association with specific immune responses remains scarce.

Methods: Fifteen subjects between 25-35 years (the young group) and five subjects between 60-70 years (the older adult group) were enrolled before ChAdOx1 nCoV-19 (AZD1222) vaccination. We determined activation markers and cytokine production of monocyte, natural killer (NK) cells and B cells *ex vivo* stimulated with TLR agonist (poly (I:C) for TLR3; LPS for TLR4; imiquimod for TLR7; CpG for TLR9) before vaccination and 3-5 days after each jab with flow cytometry. Anti-SARS-CoV2 neutralization antibody titers (surrogate virus neutralization tests, sVNTs) were measured using serum collected 2 months after the first jab and one month after full vaccination.

Results: The older adult vaccinees had weaker vaccine-induced sVNTs than young vaccinees after 1st jab (47.2±19.3% vs. 21.2±22.2%, p value<0.05), but this difference became insignificant after the 2nd jab. Imiquimod, LPS and CpG strongly induced CD86 expression in IgD^{+}CD27^{-} naïve and IgD^{-}CD27^{+} memory B cells in the young group. In contrast, only the IgD^{+} CD27^{-} naïve B cells responded to these TLR agonists in the older adult group. Imiquimode strongly induced the CD86 expression in CD14^{+} monocytes in the young group but not in the older adult group. After vaccination, the young group had significantly higher IFN-γ expression in CD3^{-} CD56^{dim} NK cells after the 1st jab, whilst the older adult group had significantly higher IFN-γ and granzyme B expression in CD56^{bright} NK cells after the 2nd jab (all p value <0.05). The IFN-γ expression in CD56^{dim} and CD56^{bright} NK cells after the first vaccination and CD86 expression in CD14^{+} monocyte

and $IgD^{-}CD27^{-}$double-negative B cells after LPS and imiquimod stimulation correlated with vaccine-induced antibody responses.

Conclusions: The innate immune responses after the first vaccination correlated with the neutralizing antibody production. Older people may have defective innate immune responses by TLR stimulation and weak or delayed innate immune activation profile after vaccination compared with young people.

Keywords: innate immune, neutralizing antibodies, SARS-CoV-2 vaccines, adenoviral vector vaccine, immunosenescence

BACKGROUND

With global spreading of SARS-CoV-2, COVID-19 pandemic has caused tremendous impact on the entire world with fast-transmitted illness and huge loss of lives. Rapid surge of severe COVID-19 infections not only threatened infected people, but also overloaded medical resources and led to collapse of healthcare system in many countries. The destructive impact of this pandemic on economic, sociological, and psychological aspect is overwhelming. Vaccines for the prevention of SARS-CoV-2 infection promise to be the fastest and most effective way to control this pandemic. Up to now, there are several COVID-19 vaccines available for clinical use and more are under developments. Among them, the chimpanzee non-replicating adenovirus vector vaccine, ChAdOx1 nCoV-19 (AZD1222) developed at Oxford University and produced by AstraZeneca is one of the most widespread used vaccines around the world (1). This AstraZeneca (AZ) vaccine was reported to have an overall 70.4% vaccine efficacy against symptomatic disease after two does and 100% of vaccine efficacy against severe COVID-19 infection and hospitalization in an early clinical study (2). Even with this high overall protective effect, the protection efficiency in different individuals may vary significantly. Importantly, the efficacy of COVID-19 vaccine in people of different age groups is not well studied, even though older adults is the most important risk factor for developing severe COVID-19 disease (3, 4).

To generate adequate immunity after vaccination, early innate immune responses are crucial for subsequent signaling for T cell activation and adaptive immune development. Innate immunity is triggered *via* different pathways in the different formulations of novel vaccines to induce immunity against SARS-CoV-2 infection. For mRNA vaccine, the endosomal Toll-like receptor (TLR3 and TLR7) bind to single-strand RNA (ssRNA) in the endosome, while component in the inflammasome including MDA5, RIG-1, NOD2 and PKR binds to ssRNA and double-stranded RNA (dsRNA) in the cytosol, all together leading to cellar activation and production of inflammatory mediators (5). For the adenovirus vector vaccine (AdV), it contains self-adjuvanticity properties because the vector's hexon protein itself is an intrinsic adjuvant to stimulate innate immune responses (6). Following injection, the innate immune recognition by AdV particles involved multiple pattern-recognition receptors, such as Toll-like receptor 3 (TLR3), TLR7/8, and in particular TLR9 to recognize dsDNA, ssRNA and ssDNA of the viral vector. In antigen presenting cells including dendritic cells (DCs) and macrophages, these innate immune stimulations subsequently trigger the production of type I interferon (IFN), multiple proinflammatory cytokine and chemokines. These stimulated immune cells may express high levels of co-stimulatory molecules to stimulate T cells in draining lymph nodes where further activation of adaptive immune cells including B cells occurs (7).

Aging is often associated with important immunological alterations including changes in number of innate and adaptive immune cells and different responses to immune stimulations, leading to different of immune functions, termed immunosenescence (8, 9). Changes in innate immunity with aging includes reduced chemotaxis, aberrant cytokine production, and weakened TLR signaling (10). This impairment in innate immunity then affects the capacity to process and present antigen to T cells and activate B cells, hence weakens adaptive immunity. Immunosenescence has been increasingly considered a major drawback for vaccine-induced immune response. The age-associated decrease in TLR function in human DCs has been linked with poor antibody response to influenza immunization, showing the importance of innate immune system in vaccine response and the influence of aging (11). It's very likely that the immunosenescence of the older adults will lead to no response or sub-optimal response to vaccination, a potential risk for breakthrough infection when encountering the defense against new SARS-CoV2 variants. Recently, the emergence of two major variants of concern (VOCs), the Delta (B.1.617.2) and Omicron (B.1.1.529) variants have raised the concern that antibody generated by two doses of COVID-19 vaccines are insufficient for protection against infection. The neutralization activity after two doses of COVID-19 vaccine were found to be lower against these two VOCs in comparison with previous strains. In the real world, the vaccine effectiveness also decreased greatly. The effectiveness of AZ vaccine decreased from 74.5% for Alpha variant to 67.0% for Delta variant while the effectiveness of BNT162b2 vaccine lowered from 93.7% for Alpha variant to 88.0% for Delta variant (12). For Omicron variants, the decrease of protection was even more obvious (13).

Several approaches had been adapted to boost immune response in the elderly, including adding more potent adjuvants, changing the route of administration, increasing the dose of immunogen, or changing the vaccine composition with more immunogenic target (14). High-dose inactivated influenza vaccine which contains four-times hemagglutinin antigen than the standard influenza vaccine is available for people older than 65 years old (15). In addition, vaccine adjuvants, including TLR agonists or oil-in-water emulsion (MF59 and AS03 in influenza vaccine, and AS02 in recombinant herpes

zoster vaccine), which evoke stronger antigen presenting cells activation and proinflammatory cytokines production, have been used in vaccines for older people (16, 17). Recently, scientists had proposed a new concept of system vaccinology incorporating the concepts of immunobiography integrated with clinical, immunological and "omics" data to identify biomarkers to guide the precise development of vaccines for different population groups (18). Therefore, there is an urgent need to elucidate the innate immune response among vaccinees of different age populations and the relationship between innate immune responses and the protection effect after vaccination. In the current study, we investigated peripheral blood immune cell activation and cytokine secretion induced by TLR stimulation or AZ vaccine in older and young age groups and measured the anti-SARS-CoV-2 spike protein RBD antibody and neutralization antibody after vaccination to identify the role of innate immunity in vaccine-induced protection.

METHODS

Volunteer Vaccination Study Design

Healthy adults within two age groups (25-35 years and 60-70 years) without any contra-indications for vaccine and pre-existing immunocompromised conditions were eligible for this study. Participants provided written informed consent upon recruitment. The protocol of this study was reviewed and approved by the Institutional Review Board (IRB) of National Cheng Kung University Hospital (NCKU) (IRB no. A-BR-110-051). Participants with preceding immunocompromised status, receiving cytotoxic treatment, or immunosuppressants were excluded. All participants received two doses of AstraZeneca (AZ) SARS-CoV-2 vaccines with 8 to 12 weeks apart. Blood samples were taken at 4 time points (before vaccination, 3-5 days after both jabs and 1 month after full vaccination). Participants' demographic data, clinical response after vaccination were recorded for further analysis.

Innate Immune Cell Activation

Sample Processing

Peripheral blood mononuclear cells (PBMCs) were isolated with Ficoll-Paque from heparinized whole blood samples collected from young and older adult subjects before and 3 days after vaccination. Isolated PBMCs were suspended with RPMI1640+10% FBS. Cells isolated from subjects before first vaccination were stimulated with TLR agonists including poly(I:C) (20 μg/ml, for TLR3), lipopolysaccharides (LPS, 10 μg/ml, for TLR4), imiquimod (10 μg/ml, for TLR7) and CpG (20 ng/ml, for TLR9). All the TLR agonists were from InvivoGen (San Diego, CA, USA, product information in **Supplementary Table 1**). Stimulated cells were cultured at 37°C for 3 days. On day 2, stimulated cells were treated with protein transport inhibitor brefeldin A (BFA). Cells isolated from vaccinated subjects were treated with brefeldin A (BFA) immediately. Cells isolated from vaccinated subjects after vaccination were treated with brefeldin A (BFA) immediately without TLR-agonist stimulations then harvested one day after.

Surface Markers and Intracellular Cytokines Analysis With Flow Cytometry

BFA-treated PBMCs were washed twice with iced cold phosphate-buffered saline (PBS). Cells were incubated with 10% of fetal bovine serum (FBS) for 30 minutes. After blocking with 10% FBS, antibodies against surface markers of NK, B cells, and monocytes were used. For detecting NK cells, anti-CD3 APC, anti-CD56 FITC, and anti- CD16 APC/Cy7 were used. $CD56^{dim}$ NK is $CD3^-$, $CD16^+$ and $CD56^{low}$ and $CD56^{bright}$ NK is $CD3^-$, $CD16^-$ and $CD56^{high}$ in lymphocyte region. For detecting B cells, anti-CD19 FITC, anti-IgD PE/Cy7, and anti-CD27 APC/Cy7 were used. Naïve B cell is $CD19^+$, IgD^+ and $CD27^-$, double negative B cell is $CD19^+$, IgD^- and $CD27^-$, Unswitched memory cell is $CD19^+$, IgD^+ and $CD27^+$, switched memory B cell is $CD19^+$, IgD^- and $CD27^+$. For detecting monocytes, anti-CD14 APC/Cy7, anti-CD68 PE/Cy7, anti-CD86 BB700 and anti-CD204 BV421 were used. All the staining monoclonal antibody were from BD Biosciences (San Jose, CA, USA, product information in **Supplementary Table 1**). After incubating with antibodies on ice for 30 minutes, cells were washed twice with staining buffer containing 2% FBS in PBS. Cells were fixed with 4% paraformaldehyde for 15 minutes and washed twice with iced cold PBS. Cell permeabilization were performed with a BD permeabilization kit. In brief, fixed cells were incubated with 1x BD Perm/Wash solution on ice for 15 minutes. After being washed with Perm/Wash solution, the cells were incubated with antibodies against intracellular proteins including anti-IFN-γ PE/Cy7, anti-IFN-α PE, anti-IL-10 APC anti-IL-6 PE, and anti-granzyme B BB700 on ice for 30 minutes. After wash twice with 1x BD Perm/Wash solution, stained cells were analyzed with FACS Canto II flow cytometry. Data was analyzed with FlowJo™ v10 software (TreeStar).

SARS-CoV-2 Antibody Assay

Surrogate SARS-CoV-2 Neutralization Test (sVNT)

The cPass SARS-CoV-2 Neutralization Antibody Detection Kit (GenScript, Piscataway, NJ) was performed according to the manufacturer's instructions (19). Briefly, patient sera were mixed with sample dilution buffer (1:10) and horseradish peroxidase conjugated recombinant SARS-CoV-2 receptor binding domain (HRP-RBD) fragments. The pre-incubation step allows for the binding of circulating neutralizing to the HRP-RBD. After 30 minutes at 37°C, the mixture will be added to a capture plate which had been precoated with the ACE2 protein. Any unbound HRP-RBD or HRP-RBD bound to non-neutralization antibodies was bound to the plate while the circulating neutralization antibody HRP-RBD complexes remained in the supernatant and was removed during the wash step. After washing, tetramethyl benzidine substrate solution was added followed by the Stop Solution which quenched the reaction, turning the well color yellow. The plates were immediately read at 450 nm on a microtiter plate reader.

Signal inhibition was calculated as follows: Percent Signal Inhibition= (1-average optical density value of a sample/average optic density value of negative control)*100%

The test results were interpreted as positive when the percent signal inhibition was ≥30%, which is the cut-off for signal inhibition claimed by the manufacturer.

Anti-SARS-CoV-2 Total Antibody (Roche Elecsys)

Roche Elecsys anti-SARS-CoV-2 S (Roche Diagnostics; hereafter called Roche S), an automated electrochemiluminescence immunoassay for the quantitative determination of pan-immunoglobulin to RBD of the spike protein of SARS-CoV-2 was used. The assay was performed on Roche cobas e601 system (Roche Diagnostics) as described before and used plasma or serum from vaccinated volunteers for measurement (20).

Statistical Analysis

Descriptive analyses of numerical variables were presented as mean and standardized deviation (Mean ± SD), and categorical variables were presented as frequency and percentage. Means of continuous variables were assessed with the Student's t test, Wilcoxon signed-rank and 1-way ANOVA. A *P*-value of< 0.05 was considered statistical significance. All statistical analyses were performed using Prism software (GraphPad Software).

RESULTS

Older Adult Vaccinees Had Distinct Immune Cell Composition Proportions and Weakened First-Dose Antibody Response

A total of 15 young and 5 older adult people were recruited into this study with mean ages of 29.9 and 66.4 years, respectively. Before vaccination, these two groups did not differ in baseline hemogragm, including total white blood cells, platelet counts, or hemoglobin level (**Table 1**). However, the older adult vaccinees had less neutrophils, higher lymphocytes, higher $CD56^+$ NK cell, and $CD19^+$ B cells compared to young vaccines (**Table 1**, all p value < 0.05). The older adult vaccinees had weaker 1st dose antibody response than young vaccinees (sVNT: 21.2 ± 22.2% vs. 47.2 ± 19.3%, p value <0.05). However, both groups demonstrated good booster response after the 2nd jab and had no statistically different antibody levels even though some vaccinees in the older adult group still had low antibody levels (**Figure 1**).

Aberrant TLR-Induced Monocyte and B Cell Activations in PBMCs of Older Adult Subjects

We collected blood samples before and 3 days after the first and second ChAdOx1 nCoV-19 vaccination. Before the vaccination, their PBMCs were first stimulated with TLR agonists and analyzed with flow cytometry. There were no significant differences in the percentages of cytokine-expressing cells after TLR-agonists stimulation in young and older adult groups (data not shown). Among the parameters we examined, no significant differences in the induced expression of IFN-γ and granzyme B levels in NK cells between young and older adult subjects were found (**Figures 2A, B**). However, we found that imiquimod-induced CD86 expression on monocytes was higher in young subjects when compared with that in older adult subjects. (**Figure 2C**). Poly(I:C)-induced IL-6 and CpG-induced IL-10 expressions in monocytes, however, were stronger in the older adult group. (**Figure 2C**). Moreover, all the TLR agonists except poly (I:C) induced significantly higher IFN-α production and CD86 cell-surface expression in IgD^+CD27^- naïve B cells in young and older adult vaccinees but there were no significant differences in TLR-induced CD86 expression in IgD^+ $CD27^-$ naïve B cells and IgD^+CD27^+ unswitched memory B cells between young and older adult subjects (**Figure 2D**). TLR-induced CD86 and IFN-α expression levels from IgD^-CD27^- double-negative (DN) B cells and IgD^-CD27^+ switched memory B cells were significantly lower in older adult subjects when compared with young subjects (**Figure 2E**). These findings indicated that there are aberrant TLR-induced monocyte and B cell activation in the older adult subjects.

TABLE 1 | Demographic information, baseline hemogram, immune cells distribution and antibody response post vaccination of the vaccinees by age group.

Group	Young vaccinees (n=15)	Older adult vaccinees (n=5)	*p* value
Age	29.9 ± 7.3	66.4 ± 1.9	**<0.001**
Male/Female ratio	1.5	4	0.786
Baseline hemogram			
WBC (x k/cmm)	6720 ± 2144	5540 ± 720	0.29
Hb (g/dl)	13.9 ± 0.9	14.1 ± 0.9	.66
Platelet (x k/cmm)	239.3 ± 71.9	225.4 ± 55.4	.74
Neutrophil (%)	63.9 ± 5.7	50.6 ± 5.5	**< 0.01**
Lymphocyte (%)	26.02 ± 4.4	37.5 ± 5.3	**< 0.01**
NK cells/lymphocytes (%)	12.1 ± 5.8	22.1 ± 8.1	**0.0073**
Monocyte (%)	7.2 ± 1.3	8.0 ± 1.5	.37
Post-vaccination antibody			
2 months after 1nd dose			
Anti-SARS-CoV-2 Ab (Roche, cutoff index, COI)	125.0 ± 66.3	54.1 ± 55.9	**0.046**
Anti-SARS-CoV-2 sVNT (%)	47.2 ± 19.3	21.2 ± 22.2	**0.02**
1 month after 2nd dose			
Anti-SARS-CoV-2 Ab (Roche, cutoff index, COI)	641.2 ± 258.3	657.0 ± 582.6	0.956
Anti-SARS-CoV2 sVNT (%)	78.0 ± 13.7	61.3 ± 42.2	0.181

Data are shown as mean ± standard deviation.
Numbers in bold indicates statistical significance (p value < 0.05).

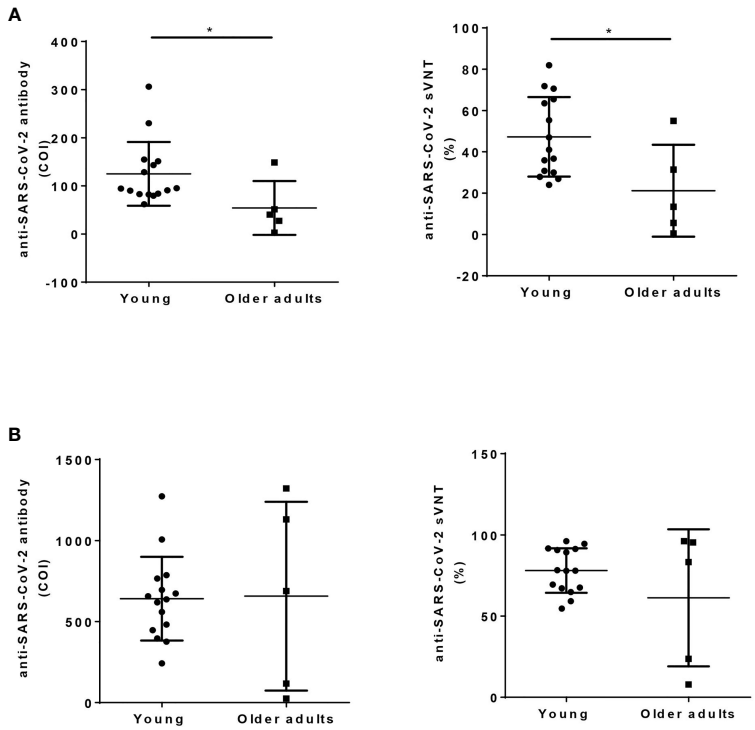

FIGURE 1 | Humoral response after ChAdOx1 nCoV-19 vaccination in young and older adult groups. Anti-SARS-CoV-2 total antibody (left panel, Roche Elecsys), and sVNT (right panel, cPass) were measured using serum collected 2 months after the first dose of vaccination **(A)**, and 1 month after the 2nd dose of vaccination **(B)** in young and older adult groups. Statistical significance was determined using t-test between 2 groups. (*p value < 0.05).

Delayed NK and Monocyte Activation in the Older Adult Subjects After ChAdOx1 nCoV-19 Vaccination

We then investigated the phenotypes of NK and monocyte activation 3 days after vaccinations in the young and older adult groups. We found that the expressions of IFN-γ in $CD56^{dim}$ and $CD56^{bright}$ NK cells were enhanced after the first vaccination in the young group but not in the older adult group (**Figures 3A, B**). However, the expressions of IFN-γ in $CD56^{dim}$ and $CD56^{bright}$ NK cells and granzyme B expression in $CD56^{bright}$ NK cells were enhanced after the second vaccination in the older adult group. We also found that in the older adult group, the percentages of IFN-γ- and granzyme B-producing NKs were reduced after the first vaccination and the percentages restored after the second vaccination (**Supplementary Figures 1A, B**). In monocytes, we found that the cells isolated from the older adult subjects produced significantly lower levels of CD86 when compared with young subjects, who had higher and increasing CD86 expression levels after the 1st and the 2nd vaccinations. (**Figure 3C**). Moreover, the IL-6 and IFN-α levels in monocytes and the percentage of IL-6-producing monocytes were significantly higher in the older adult group before vaccination but decreased after the 1st and 2nd vaccination. However, there were no significant changes in the percentages of IFN-α-expressing monocytes between young and older adult groups after vaccinations (**Supplementary Figure 1C**). We also found that the IL-10 levels in monocytes were enhanced after the first vaccination in both young and older adult groups. The percentages of IL-10-expressing monocytes in young subjects were enhanced after the first and second vaccination. However, the percentage of IL-10-expressing monocytes was lowered in the older adults after the second vaccination. There were no significant differences between young and older adult groups regarding the expression of CD86 and IFN-α 3 days after the 1st and 2nd jabs on B cells. (data not shown).

Stronger NK and Monocyte Activation After the First Vaccination and TLR-Induced DN B Cell Activation in Subjects With Higher Early Antibody Levels

We next investigated whether the innate immune activation correlated with neutralization antibody titers induced by ChAdOx1 nCoV-19 vaccination. We compared the sVNT 2 months after the 1st vaccination and 1 month after the second vaccination from the whole cohort simultaneously. We found that subjects whose early levels of sVNT were higher tended to have higher sVNT 1 month after the second vaccination (**Figure 4**). Therefore, we divided the young subjects into high (black) and low groups (blue) according to the sVNT. The high sVNT, low

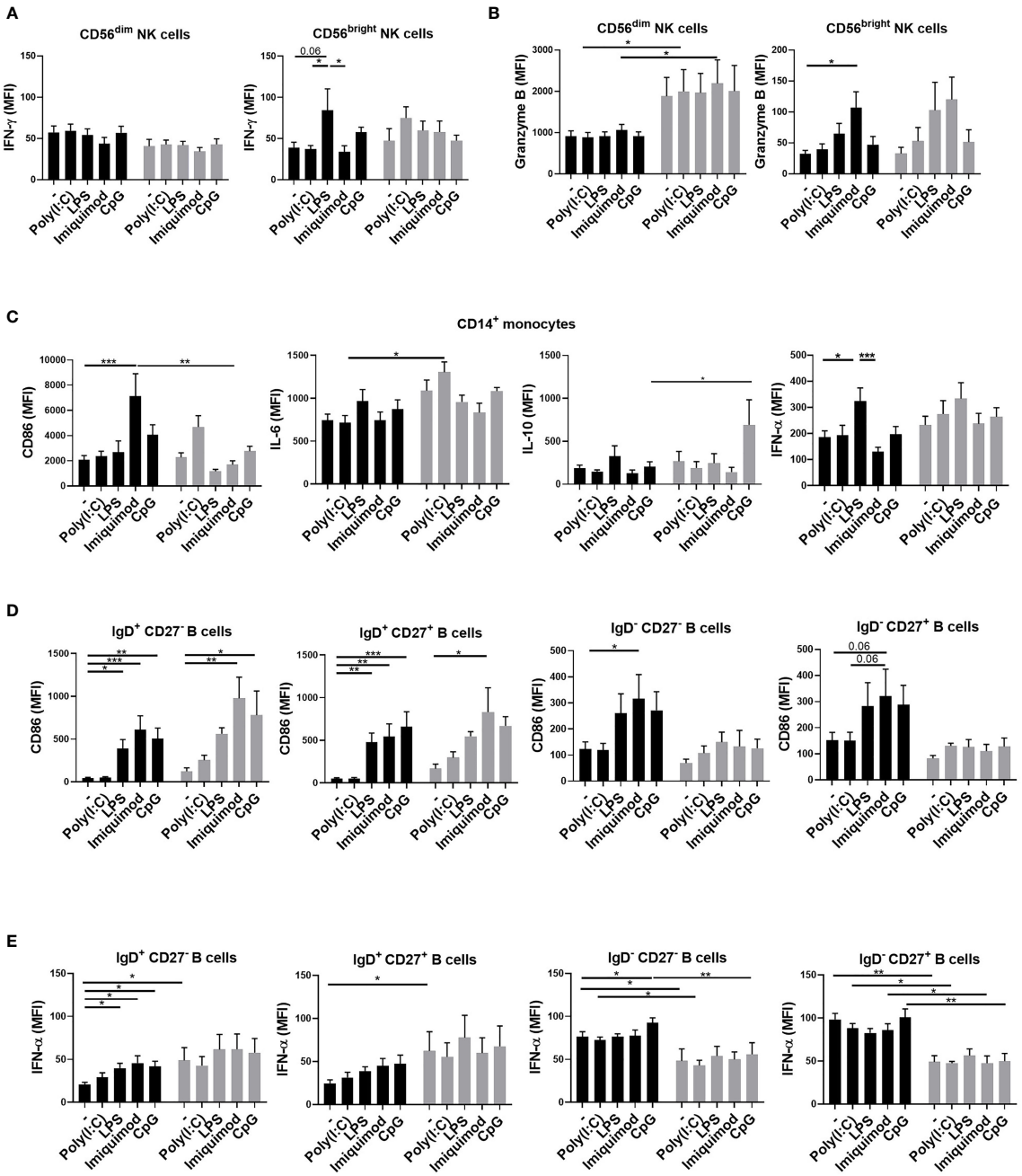

FIGURE 2 | Aberrant TLR-induced monocyte and B cell activation in the older adult subjects. PBMCs were isolated from young (black bars) and older adult subjects (gray bars) before vaccination. TLR-induced IFN-γ **(A)** and granzyme B **(B)** expression in $CD3^{-}CD56^{dim}$ or $CD3^{-}CD56^{bright}$NK cells; CD86, IL-6, IL-10, and IFN-α in monocytes **(C)**; CD86 **(D)** and IFN-α **(E)** in B cells of the young and older adult vaccinees were detected after 3 days of stimulation. Statistical significance was determined using ANOVA with Tukey's multiple-comparisons testing between all groups. (Black: young vaccinees; Grey: older adult vaccinees) (*p value < 0.05; **p value <0.01; ***p value < 0.001).

sVNT and older adult group all demonstrated significant booster effect and had higher sVNT one month after full vaccination than two months after 1st jab (all p value < 0.05). Next, we compared the innate immune activation between high and low sVNT groups and the older adult subjects. We found that IFN-γ productions in $CD56^{dim}$ and $CD56^{bright}$ NK cells were higher in the high sVNT group after the first vaccination. The IFN-γ productions in $CD56^{dim}$ and $CD56^{bright}$ were lower in both older adult subjects and young subjects with lower sVNT. However, there were no differences in IFN-γ productions in

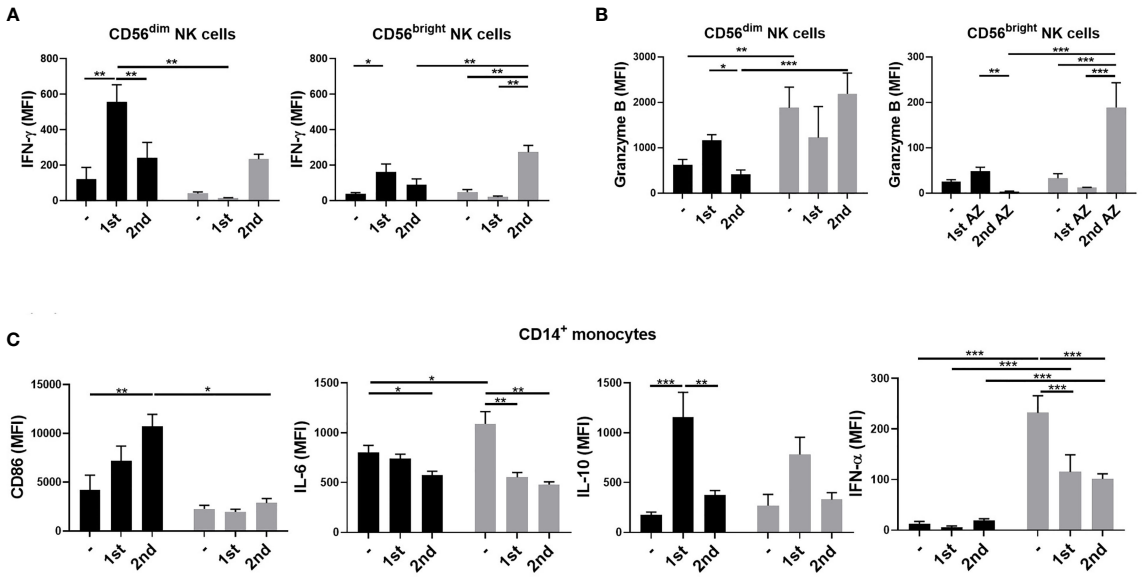

FIGURE 3 | NK cell and monocyte activation 3 days after ChAdOx1 nCoV-19 vaccination. PBMCs were isolated from young (black bars) and older adult vaccinees (gray bars) 3 days after the first and second vaccinations. IFN-γ **(A)** and granzyme B **(B)** expression in $CD3^{-}CD56^{dim}$ or $CD3^{-}CD56^{bright}$NK cells; CD86, IL-6, IL-10, and IFN-α in monocytes **(C)** of the young and older adult vaccinees were analyzed by flow cytometry. Statistical significance was determined using ANOVA with Tukey's multiple-comparisons testing between all groups. (Black: young vaccinees; Grey: older adult vaccinees). (*p value < 0.05; **p value <0.01; ***p value < 0.001).

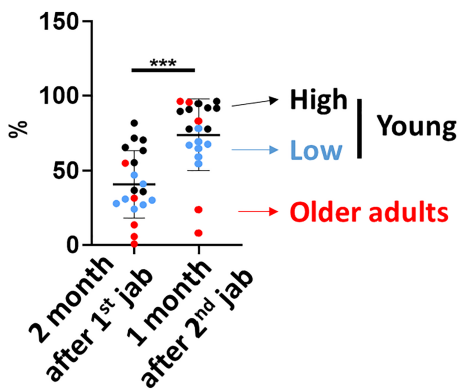

FIGURE 4 | Neutralization antibody titers 2 months after the first vaccination correlated with neutralization antibody titers 1 month after the second vaccination. The SARS-CoV-2 surrogate virus neutralization antibody titers (sVNT) were measured 2 months after the first vaccination and 1 month after the second vaccination. The high sVNT, low sVNT and older adult group all demonstrated higher sVNT 1 month after the second vaccination than 2 months after first vaccination. Statistical significance was determined using Wilcoxon signed rank test between 2 groups. (***p value < 0.001).

$CD56^{dim}$ NK cells after the second vaccination and IFN-γ productions in $CD56^{bright}$ NK cells were higher when compared with young subjects with higher sVNT (**Figures 5A, B**). We also found that monocyte CD86 expressions were higher in the high sVNT group after the first vaccination. Meanwhile, anti-inflammatory cytokine IL-10 expressions from young monocytes of the lower sVNT group were higher (**Figure 5C**). Moreover, we found that DN CD86 expression was significantly lower in older adult subjects 3 days after 2^{nd} vaccination (**Figure 5D**). Moreover, LPS- and imiquimod-induced DN B cells had higher CD86 expressions in the high sVNT group when compared with subjects with lower sVNT and older adult subjects.

DISCUSSION

In the present study, we showed that young and older vaccinees had different baseline immune cell distribution and activities. Older adult subjects had diminished TLR-induced monocyte and B cell activation compared to young subjects. The immune cells activation and intracellular cytokine expression following vaccination are different in older and young vaccinees. Importantly, we found that TLR-induced B cell activation and first-dose vaccination-induced and NK and monocyte activation correlate with the vaccine-induced neutralization antibody levels.

TLRs had been proved to be pivotal immune activators which bridges the innate and adaptive immunity. SARS-CoV-2 was known to trigger the innate immune system through TLRs 3, 7, and 8 during the early infection. The dysfunction of TLRs has been reported to be associated with severe COVID cases (21). Aging process comes with several immunological changes described as immunosenscence and inflammaging as two significant aspects of immune dysfunction in older adult people (9). Some immune functions weaken with aging (immunosenescence) while other inflammatory activity may become stronger when people become old (inflammaging). In

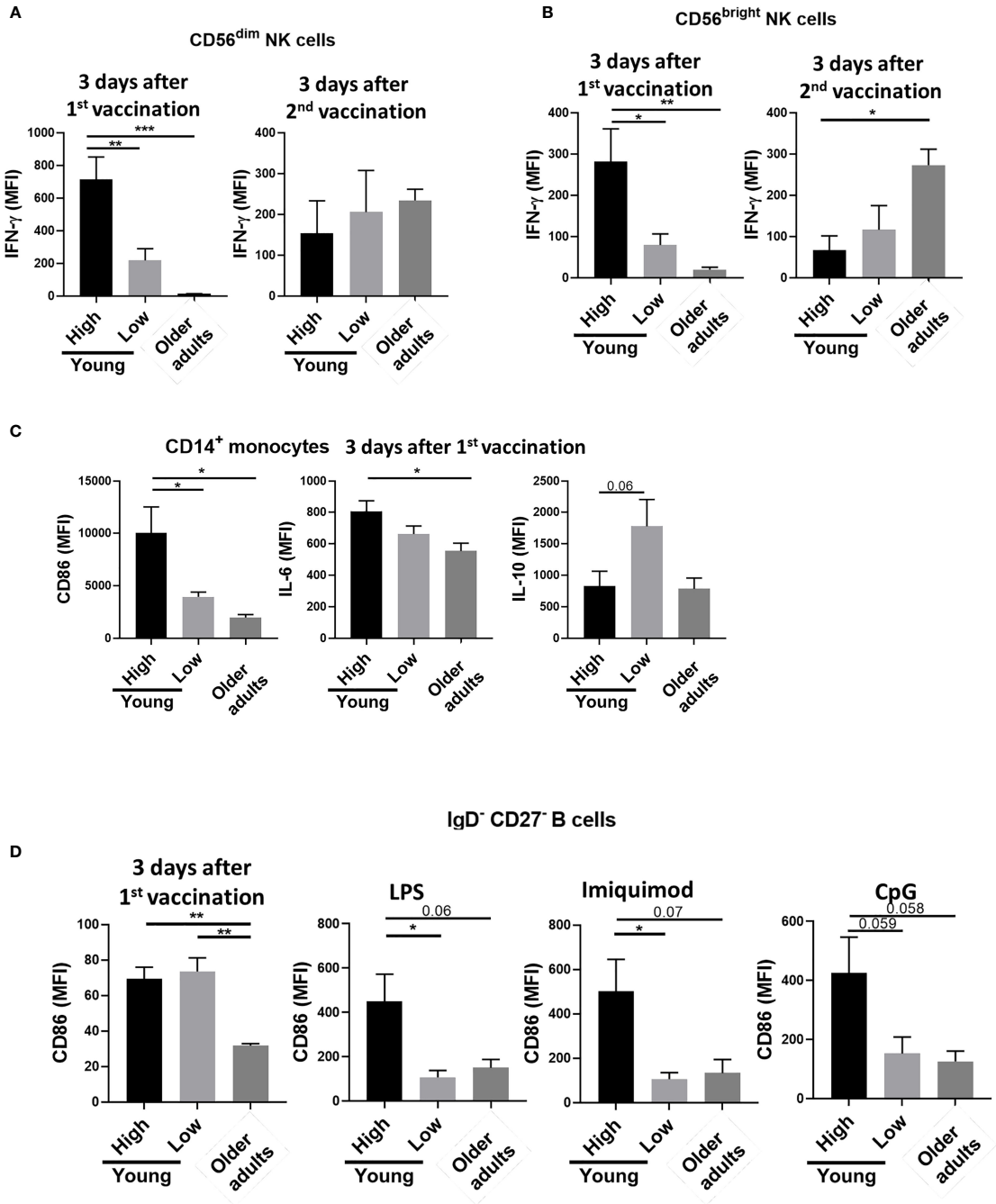

FIGURE 5 | Stronger NK and monocyte activation after the first vaccination and TLR-induced IgD-CD27-double-negative (DN) B cell activation in subjects with higher early antibody levels IFN-γ expressions in $CD3^{-}CD56^{dim}$ **(A)** or $CD3^{-}CD56^{bright}$ **(B)** NK cells; CD86, IL-6, and IL-10 expression in monocytes **(C)** 3 days after the first vaccination were compared between high and low sVNT groups of the young vaccinees and the older adult vaccinees. **(D)** CD86 expression 3 days after the first vaccination and CD86 levels after LPS, imiquimod, and CpG stimulation were compared between high and low sVNT groups. Statistical significance was determined using ANOVA with Tukey's multiple-comparisons testing between all groups. (*p value < 0.05; ** p value < 0.01; ***p value < 0.001).

our experiments, innate immune cells of young vaccinees responded more strongly and more efficiently to TLR agonist stimulation, especially more B cell activation either in CD86 expression or IFN-α production, and more monocyte with CD86 expression when compared to older vaccinees, reflecting the immunosenscence in older adult people. The older adult group had notably higher IFN-γ and granzyme B expression in $CD56^{bright}$ NK cells after the 2^{nd} jab (**Figures 3A, B**),

representing the inflammaging which may be too late to induce early protective antibody production.

NK cells are innate lymphoid cells that respond rapidly during primary infection and have adaptive characteristics enabling them to integrate innate and acquired immune responses. They are recently recognized as a key regulator of vaccine-elicited T and B cell responses and memory cells that contribute to pathogen control. This critical role of NK cell activation in vaccine-induced immunity is demonstrated in vaccination against pathogens including influenza, yellow fever, and tuberculosis (22). A previous study examining the draining lymph nodes after influenza vaccination showed that NK cells are recruited regional lymph nodes and activated by type I IFNs produced by LN macrophages. The activated NK cells subsequently produced IFN-γ, which in turn regulates the recruitment of IL-6^{+} CD11b^{+} dendritic cells (23). Actually, NK cells make both early and sustained IFN-γ responses after vaccination and represent over 70% of all IFN-γ-secreting cells (24). The activation of NK cells is critical of IL-2-secreting effector memory T cells and overall vaccine-induced response. Therefore, researchers proposed using the assays NK cell IFN-γ production, and NK cytotoxicity as the tool for evaluating correlates of vaccine-induced immunity (25). Our study demonstrated that IFN-γ expressions in NK cells after 1st jab correlated with SARS-CoV-2 vaccine-induced neutralizing antibody, which echoes previous findings. Since NK cells may play essential roles in developing efficacious vaccine-induced protection, there are discussions about NK cell-mediated modulation of the immune response and its implication on immunization strategies and the development of next-generation vaccines (26, 27).

Naïve B cells differentiate to antibody-producing plasma cells after vaccine stimulation to produce protective antibodies. The DN B cells, previously characterized as unconventional memory B cells with negative expression of both CD27 and surface IgD, were detected in healthy individuals at low levels within peripheral blood and tonsils but are expanded in peripheral blood of older adult patients with systemic lupus erythematosus (28, 29). The role of DN B cells in the humoral immune response remains unclear, but recent research has demonstrated their proinflammatory ability in autoimmune disease and protective ability following vaccination. In the present study, we demonstrated that the degree of CD86 expression of DN B cells after LPS or imiquimod stimulation positively correlated with vaccine induced neutralization antibody. This suggests that DN B cells might constitute a significant transient population during the B cell maturation process, and its activation by innate stimulation may set the stage for subsequent vaccine-induced antibody production.

CONCLUSION

Although the changes in the immune system in the older adults have been studied in recent years, the effects of aging on the innate immune activation and consequently unresponsiveness to novel COVID-19 vaccination are still unknown (9). We first found that TLR-induced monocyte and B cell activation was dampened in the older adult subjects. Different activation and intracellular protein expression profiles induced by different TLR agonists may provide further information about the critical point, which may lead to abnormal vaccine responses in older adults. We also found that TLR-induced B cell activation and the first vaccination-induced NK and monocyte activations were related to the neutralization antibody elicited by the ChAdOx1 nCoV-19 vaccination. Therefore, innate immune activation is crucial for the successful activation of protective humoral immunity during vaccination, especially with the wildly adopted viral vector vaccines (30).

DATA AVAILABILITY STATEMENT

The raw data supporting the conclusions of this article will be made available by the authors, without undue reservation.

ETHICS STATEMENT

The studies involving human participants were reviewed and approved by Institutional Review Board (IRB) of National Cheng Kung University Hospital (NCKU). The patients/participants provided their written informed consent to participate in this study.

AUTHOR CONTRIBUTIONS

C-FS and C-CS are the guarantor of the content of this manuscript, had full access to all of the data in the study and take responsibility for the integrity of the data. C-FS, C-LY, and C-CS contributed to the study conception and design, collection of data, data analysis and interpretation, and critical review of the manuscript. C-CL, P-LC and C-MC contributed to the data analysis, and critical review of the manuscript. W-CK contributed to interpretation, critical review of the manuscript. All authors contributed to the article and approved the submitted version.

FUNDING

This work was supported by the Clinical Medical Research Center, National Cheng Kung University Hospital, Taiwan (NCKUH-11002017, NCKUH-11009002, NCKUH-11102024) and Ministry of Science and Technology, Taiwan (110-2923-B-006-001-MY4).

ACKNOWLEDGMENTS

We thank Ms Shih-Wei Wang and Ms Hui-Feng Lee for the collection of clinical cases.

SUPPLEMENTARY MATERIAL

The Supplementary Material for this article can be found online at: https://www.frontiersin.org/articles/10.3389/fimmu.2022.807454/full#supplementary-material

Supplementary Figure 1 | Cytokine-producing NK and monocyte 3 days after ChAdOx1 nCoV-19 vaccination. PBMCs were isolated from young (black bars) and older adult vaccinees (gray bars) 3 days after the first and second vaccinations. The percentage of IFN-γ- **(A)** and granzyme B- **(B)** expressing cells in CD3-CD56dim or CD3-CD56brightNK cells; IL-6-, IL-10-, and IFN-α-expressing monocytes **(C)** of the young and older adult vaccinees were analyzed by flow cytometry. Statistical significance was determined using ANOVA with Tukey's multiple-comparisons testing between all groups. (Black: young vaccinees; Grey: older adult vaccinees). (*p value < 0.05; **p value < 0.01; ***p value < 0.001).

REFERENCES

1. Our World in Data. *Coronavirus Pandemic (COVID-19)* (2020). Available at: https://ourworldindata.org/coronavirus (Accessed October 13, 2021).
2. Voysey M, Clemens SAC, Madhi SA, Weckx LY, Folegatti PM, Aley PK, et al. Safety and Efficacy of the ChAdOx1 Ncov-19 Vaccine (AZD1222) Against SARS-CoV-2: An Interim Analysis of Four Randomised Controlled Trials in Brazil, South Africa, and the UK. *Lancet* (2021) 397(10269):99–111. doi: 10.1016/S0140-6736(20)32661-1
3. Soiza RL, Scicluna C, Thomson EC. Efficacy and Safety of COVID-19 Vaccines in Older People. *Age Ageing* (2021) 50(2):279–83. doi: 10.1093/ageing/afaa274
4. Ramasamy MN, Minassian AM, Ewer KJ, Flaxman AL, Folegatti PM, Owens DR, et al. Safety and Immunogenicity of ChAdOx1 Ncov-19 Vaccine Administered in a Prime-Boost Regimen in Young and Old Adults (COV002): A Single-Blind, Randomised, Controlled, Phase 2/3 Trial. *Lancet* (2021) 396(10267):1979–93. doi: 10.1016/S0140-6736(20)32466-1
5. Pardi N, Hogan MJ, Porter FW, Weissman D. mRNA Vaccines—A New Era in Vaccinology. *Nat Rev Drug Discov* (2018) 17(4):261–79. doi: 10.1038/nrd.2017.243
6. Hartman ZC, Appledorn DM, Amalfitano A. Adenovirus Vector Induced Innate Immune Responses: Impact Upon Efficacy and Toxicity in Gene Therapy and Vaccine Applications. *Virus Res* (2008) 132(1-2):1–14. doi: 10.1016/j.virusres.2007.10.005
7. Teijaro JR, Farber DL. COVID-19 Vaccines: Modes of Immune Activation and Future Challenges. *Nat Rev Immunol* (2021) 21(4):195–7. doi: 10.1038/s41577-021-00526-x
8. Connors J, Bell MR, Marcy J, Kutzler M, Haddad EK. The Impact of Immuno-Aging on SARS-CoV-2 Vaccine Development. *Geroscience* (2021) 43(1):31–51. doi: 10.1007/s11357-021-00323-3
9. Pietrobon AJ, Teixeira FME, Sato MN. I Mmunosenescence and Inflammaging: Risk Factors of Severe COVID-19 in Older People. *Front Immunol* (2020) 11:579220. doi: 10.3389/fimmu.2020.579220
10. Pereira B, Xu XN, Akbar AN. Targeting Inflammation and Immunosenescence to Improve Vaccine Responses in the Elderly. *Front Immunol* (2020) 11:583019. doi: 10.3389/fimmu.2020.583019
11. Panda A, Qian F, Mohanty S, van Duin D, Newman FK, Zhang L, et al. Age-Associated Decrease in TLR Function in Primary Human Dendritic Cells Predicts Influenza Vaccine Response. *J Immunol* (2010) 184(5):2518–27. doi: 10.4049/jimmunol.0901022
12. Lopez Bernal J, Andrews N, Gower C, Gallagher E, Simmons R, Thelwall S, et al. Effectiveness of Covid-19 Vaccines Against the B. 1.617. 2 (Delta) Variant. *N Engl J Med* (2021) 38(7):585–94. doi: 10.1056/NEJMoa2108891
13. Andrews N, Stowe J, Kirsebom F, Toffa S, Rickeard T, Gallagher E, et al. Effectiveness of COVID-19 Vaccines Against the Omicron (B. 1.1. 529) Variant of Concern. *MedRxiv* (2021) 2021.12.14.21267615. doi: 10.1101/2021.12.14.21267615
14. Lefebvre JS, Haynes L. Vaccine Strategies to Enhance Immune Responses in the Aged. *Curr Opin Immunol* (2013) 25(4):523–8. doi: 10.1016/j.coi.2013.05.014
15. DiazGranados CA, Dunning AJ, Kimmel M, Kirby D, Treanor J, Collins A, et al. Efficacy of High-Dose Versus Standard-Dose Influenza Vaccine in Older Adults. *N Engl J Med* (2014) 371(7):635–45. doi: 10.1056/NEJMoa1315727
16. O'Hagan DT, Ott GS, Nest GV, Rappuoli R, Giudice GD. The History of MF59® Adjuvant: A Phoenix That Arose From the Ashes. *Expert Rev Vaccines* (2013) 12(1):13–30. doi: 10.1586/erv.12.140
17. Cunningham AL, Garçon N, Leo O, Friedland LR, Strugnell R, Laupèze B, et al. Vaccine Development: From Concept to Early Clinical Testing. *Vaccine* (2016) 34(52):6655–64. doi: 10.1016/j.vaccine.2016.10.016
18. Ciabattini A, Nardini C, Santoro F, Garagnani P, Franceschi C, Medaglini D. Vaccination in the Elderly: The Challenge of Immune Changes With Aging. *Semin Immunol* (2018) 40:83–94. doi: 10.1016/j.smim.2018.10.010
19. Tan CW, Chia WN, Qin X, Liu P, Chen MI, Tiu C, et al. A SARS-CoV-2 Surrogate Virus Neutralization Test Based on Antibody-Mediated Blockage of ACE2-Spike Protein-Protein Interaction. *Nat Biotechnol* (2020) 38(9):1073–8. doi: 10.1038/s41587-020-0631-z
20. Jung K, Shin S, Nam M, Hong YJ, Roh EY, Park KU, et al. Performance Evaluation of Three Automated Quantitative Immunoassays and Their Correlation With a Surrogate Virus Neutralization Test in Coronavirus Disease 19 Patients and Pre-Pandemic Controls. *J Clin Lab Anal* (2021) 35 (9):e23921. doi: 10.1002/jcla.23921
21. Menezes MCS, Veiga ADM, Martins de Lima T, Kunimi Kubo Ariga S, Vieira Barbeiro H, de Lucena Moreira C, et al. Lower Peripheral Blood Toll-Like Receptor 3 Expression Is Associated With an Unfavorable Outcome in Severe COVID-19 Patients. *Sci Rep* (2021) 11(1):15223. doi: 10.1038/s41598-021-94624-4
22. Wagstaffe HR, Mooney JP, Riley EM, Goodier MR. Vaccinating for Natural Killer Cell Effector Functions. *Clin Transl Immunol* (2018) 7(1):e1010. doi: 10.1002/cti2.1010
23. Farsakoglu Y, Palomino-Segura M, Latino I, Zanaga S, Chatziandreou N, Pizzagalli DU, et al. Influenza Vaccination Induces NK-Cell-Mediated Type-II IFN Response That Regulates Humoral Immunity in an IL-6-Dependent Manner. *Cell Rep* (2019) 26(9):2307–15.e5. doi: 10.1016/j.celrep.2019.01.104
24. Long BR, Michaelsson J, Loo CP, Ballan WM, Vu BA, Hecht FM, et al. Elevated Frequency of Gamma Interferon-Producing NK Cells in Healthy Adults Vaccinated Against Influenza Virus. *Clin Vaccine Immunol* (2008) 15 (1):120–30. doi: 10.1128/CVI.00357-07
25. Horowitz A, Behrens RH, Okell L, Fooks AR, Riley EM. NK Cells as Effectors of Acquired Immune Responses: Effector CD4+ T Cell-Dependent Activation of NK Cells Following Vaccination. *J Immunol* (2010) 185(5):2808–18. doi: 10.4049/jimmunol.1000844
26. Rydyznski CE, Waggoner SN. Boosting Vaccine Efficacy the Natural (Killer) Way. *Trends Immunol* (2015) 36(9):536–46. doi: 10.1016/j.it.2015.07.004
27. Cox A, Cevik H, Feldman HA, Canaday LM, Lakes N, Waggoner SN. Targeting Natural Killer Cells to Enhance Vaccine Responses. *Trends Pharmacol Sci* (2021) 42(9):789–801. doi: 10.1016/j.tips.2021.06.004
28. Wei C, Anolik J, Cappione A, Zheng B, Pugh-Bernard A, Brooks J, et al. A New Population of Cells Lacking Expression of CD27 Represents a Notable Component of the B Cell Memory Compartment in Systemic Lupus Erythematosus. *J Immunol* (2007) 178(10):6624–33. doi: 10.4049/jimmunol.178.10.6624
29. Colonna-Romano G, Bulati M, Aquino A, Pellicano M, Vitello S, Lio D, et al. A Double-Negative (IgD-CD27-) B Cell Population Is Increased in the Peripheral Blood of Elderly People. *Mech Ageing Dev* (2009) 130(10):681–90. doi: 10.1016/j.mad.2009.08.003
30. Pulendran B, SA P, O'Hagan DT. Emerging Concepts in the Science of Vaccine Adjuvants. *Nat Rev Drug Discov* (2021) 20(6):454–75. doi: 10.1038/s41573-021-00163-y

Conflict of Interest: The authors declare that the research was conducted in the absence of any commercial or financial relationships that could be construed as a potential conflict of interest.

frontiers in Immunology

ORIGINAL RESEARCH
published: 14 February 2022
doi: 10.3389/fimmu.2022.812606

COVID-19 Recovery Patterns Across Alpha (B.1.1.7) and Delta (B.1.617.2) Variants of SARS-CoV-2

Nitya Kumar[1]*, *Suha Quadri*[1], *Abdulla Ismaeel AlAwadhi*[2] and *Manaf AlQahtani*[1,2]

[1] Department of Medicine, Royal College of Surgeons in Ireland –Bahrain, Muharraq, Bahrain, [2] Department of Pathology, Bahrain Defense Force Hospital–Royal Medical Services, Riffa, Bahrain

Background: B.1.1.7 (alpha) and B.1.617.2 (delta) variants of concern for SARS-CoV-2 have been reported to have differential infectivity and pathogenicity. Difference in recovery patterns across these variants and the interaction with vaccination status has not been reported in population-based studies.

Objective: The objective of this research was to study the length of stay and temporal trends in RT-PCR cycle times (Ct) across alpha and delta variants of SARS-CoV-2 between vaccinated and unvaccinated individuals.

Methods: Participants consisted of patients admitted to national COVID-19 treatment facilities if they had a positive RT-PCR test for SARS-CoV-2, and analysis of variants was performed (using whole genome sequencing). Information on vaccination status, age, sex, cycle times (Ct) for four consecutive RT-PCR tests conducted during hospital stay, and total length of hospital stay for each participant were ascertained from electronic medical records.

Results: Patients infected with the delta variant were younger (mean age = 35years vs 39 years for alpha, p<0.001) and had lesser vaccination coverage (54% vs 72% for alpha, p<0.001). RT-PCR Ct values were similar for both variants at the baseline test; however by the fourth test, delta variant patients had significantly lower Ct values (27 vs 29, p=0.05). Length of hospital stay was higher in delta variant patients in vaccinated (3 days vs 2.9 days for alpha variant) as well as in unvaccinated patients (5.2 days vs 4.4 days for alpha variant, p<0.001). Hazards of hospital discharge after adjusting for vaccination status, age, and sex was higher for alpha variant infections (HR=1.2, 95% CI: 1.01–1.41, p=0.029).

Conclusion: Patients infected with the delta variant of SARS-CoV-2 were found to have a slower recovery as indicated by longer length of stay and higher shedding of the virus compared to alpha variant infections, and this trend was consistent in both vaccinated and unvaccinated patients.

Keywords: SARS-CoV-2, COVID-19 vaccine, delta variant, alpha variant, hospital stay length, recovery pattern, B1.617.2, B1.1.7

OPEN ACCESS

Edited by:
Srinivasa Reddy Bonam, Institut National de la Santé et de la Recherche Médicale (INSERM), France

Reviewed by:
Nitin Saksena, Victoria University, Australia
Veronika Zarnitsyna, Emory University, United States

***Correspondence:**
Nitya Kumar
nkumar@rcsi-mub.com

Specialty section:
This article was submitted to Vaccines and Molecular Therapeutics, a section of the journal Frontiers in Immunology

Received: *10 November 2021*
Accepted: *21 January 2022*
Published: *14 February 2022*

Citation:
Kumar N, Quadri S, AlAwadhi AI and AlQahtani M (2022) COVID-19 Recovery Patterns Across Alpha (B.1.1.7) and Delta (B.1.617.2) Variants of SARS-CoV-2. Front. Immunol. 13:812606. doi: 10.3389/fimmu.2022.812606

INTRODUCTION

The respiratory infection, COVID-19, caused by the novel coronavirus 2 or SARS-CoV-2 that originated in Wuhan, China in December 2019 rapidly devolved into a worldwide pandemic in March of 2020 (1). Despite experiencing differential evolution across geographies and continuing well into 2021, this pandemic also saw unprecedented global initiatives in vaccine development, approval, and implementation efforts that have resulted in a decline in the number and severity of cases (2–5). Several studies have found vaccination to be linked with the reduced number of cases and severity of infection (6–10). However, the widespread disparity in distribution and access of the vaccines (11, 12) as well as the lack of adherence to public health measures to control the spread (13–15) saw unchecked community spread in different geographical locations. This constellation of factors gave rise to multiple mutations in the genetic make-up of the pathogen, resulting in different variants (16).

Some of the SARS-CoV-2 variants have been labeled "variants of concern" including the alpha, beta, gamma, and delta variants (17). The first identified variant was the D614G in March 2020 in China (18). Other notable variants are the beta variant found in South Africa in December 2020 and the gamma variant found in Brazil in January 2021 (19). The B.1.1.7 variant was first detected in September 2020 in Kent, United Kingdom. It was formally termed the "alpha" variant of concern in December 2020 (20).

The B.1.617.2 "delta" variant was first identified in December 2020 during the second wave of COVID-19 in India (20, 21). It garnered global attention due to a high degree of infectivity, morbidity, and mortality than previously witnessed in the pandemic and has become the dominant strain in the US and UK among over ten other countries (8). The variant infects more young patients than previous variants do, and subsequently infection rates have risen in children and adolescents since its spread (22). The viral load for this delta variant is also over a thousand times higher than the original strain (23).

The clinical presentation of the virus has also changed with the variant. Atypical symptoms such as clots, gangrene, mucormycosis, abdominal pain, nausea, diarrhea, hearing loss, myalgia, and arthralgias have been speculated to be caused by delta. Many patients also present afebrile or with mild and nonspecific symptoms (24).

The delta variant has been known to cause breakthrough infections, with some fully vaccinated individuals exhibiting symptomatic infection. Even fully vaccinated infected individuals can spread the virus to others (25). Although vaccines are effective against the variant, multiple studies have found reduced efficacy against the delta variant alone and in comparison to other variants (26). The variant has been found to be two times more communicable than previous variants. Some vaccines and antibody treatments have been less successful against this variant compared to others (27). In addition, morbidity is increased with delta, as it poses twice the risk of hospitalization and need of emergency resources (28).

Besides sporadic reports on the efficacy of various vaccines on the delta variant and preclinical and modeling studies on pathogenicity, the interaction of the effect of vaccination and the pathogenicity of variants of concern, especially the recovery pattern, remains poorly understood in clinical settings. This is partly due to the lack of comprehensive data from infections from different variants in vaccinated and unvaccinated individuals. The Kingdom of Bahrain was one of the very few states to achieve a comprehensive vaccination coverage at the population level (29)) and also saw different variants of concern. Therefore, this study was conducted with the aim of studying the length of hospital stay and pattern of RT-PCR cycle times across vaccinated and unvaccinated patients infected with the SARS-CoV-2 variants B.1.1.7 (here on referred to as the "alpha variant") and B.1.617.2 (henceforth referred to as the "delta variant").

METHODS

Study Population, Patient Selection, and Data Extraction

The study population comprised of patients admitted to COVID-19 treatment facilities under the Bahrain Ministry of Health between 1 January 2021 and 30 May 2021. Patients were included if they were above 18 years of age, had a positive RT-PCR for SARS-CoV-2, were admitted between the above specified dates, and were identified as being infected with either the alpha or delta SARS-CoV-2 variants through whole genome sequencing. Data pertaining to demographic details, COVID-19 test results, vaccination status, and length of hospital stay were extracted from the local electronic medical record (EMR) system, "I-SEHA." Data were extracted manually from EMR, and all cases were reviewed manually before inclusion into the study.

Diagnosis of COVID-19

Confirmation of an infection with SARS-CoV-2 was done using a standard reverse transcriptase polymerase chain reaction (RT-PCR) test of nasopharyngeal swab samples. The test was performed using Thermo Fisher Scientific (Waltham, MA) TaqPath 1-Step RT-qPCR Master Mix, CG on the Applied Biosystems (Foster City, CA) 7500 Fast Dx RealTime PCR instrument. This assay targeted the E gene. Once the E gene was detected, the test was confirmed by RdRP and N gene assays. E gene Ct values have been reported in this study. Ct values >40 were considered negative. Positive and negative controls have been included for quality control.

Ascertainment/Detection of Variants

Whole genome sequencing was used to identify the common variants of concerns using illumina/ARTIC and COVID-Seq protocols. The data were analyzed with the Abiomix platform. Sequencing was undertaken at the national COVID-19 molecular public health laboratory where all the samples get tested. Spike gene target status on PCR was used as a second approach for identifying each variant.

Outcome Assessment

Recovery pattern among the patients was assessed by estimating the length of hospital stay as well as the longitudinal trend in

PCR test cycle time (CT) values indicating the extent of viral shedding, across 4 consecutive PCR tests. As per Bahrain national protocol during the study period, PCR testing was required to be carried out 4 times: test 1 performed at the time of diagnosis (corresponding to day 0), test 2 (performed on day 3), test 3 (performed on day 5), and final test (either on day 10 or earlier if they are clinically stable). Subjects who stayed in the hospital for 10 or more days were tested 4 times. Those who got discharged before day 5 underwent only two tests: diagnosis test and discharge test. Those who got discharged between days 5 and 10 underwent testing three times: diagnosis, discharge, and once on day 3. All patients have minimum two tests—one performed at the time of diagnosis and one performed at the time of recovery or discharge.

Statistical Analysis

The proportion of vaccination and variants have been described using frequencies and percentages, PCR CT values have been reported as means and standard deviations, and length of hospital stay has been reported as median and interquartile range. Difference in consecutive CT values across SARS-CoV-2 variants was assessed using a mixed model analysis of variance (mixed ANOVA). Length of stay was estimated using Kaplan–Meier analysis. Hazards of hospital discharge adjusted for age and sex were computed using a Cox proportional hazards model. All analyses were performed using STATA 17 (StataCorp. 2020. Stata Statistical Software: Release 17. College Station, TX: StataCorp LLC.)

Ethics Approval and Declaration

Ethics approval for this study was obtained from the National COVID-19 Research Committee in Bahrain (approval code: CRT-COVID2021-148). All methods and analysis in this study were carried out in compliance with the local guideline and ethical guidelines of the Declaration of Helsinki 1975. All data used in this study were collected as part of regular medical procedures. Given the retrospective nature of the study and the de-identification of patients' information, the requirement for informed consent was waived by the reviewing body.

Data Availability Statement

Original data will be made available upon request to the corresponding author.

RESULTS

The demographic characteristics across the SARS-CoV-2 variants are shown in **Table 1**. Of the study subjects, 636 (44.5%) were infected with the delta variant, and 737 (55.5%) were infected with the alpha variant. Delta variant patients were significantly younger (median age = 35years) than those infected with the alpha variant (median age = 39, p<0.001). Both groups had a more or less comparable sex distribution (**Table 1**). Among the delta variant patients, 353 (54.1%) were vaccinated compared to 573 (72.4%) in the alpha variant group. The mean Ct values for the first two PCR tests were comparable across the groups; however, the mean Ct values for the subsequent two tests seemed significantly lower for the delta variant (p=0.05 for test #4). Our data were collected between January and April of 2021, when the initial vaccines to get approved in the country were Sinopharm, AstraZeneca, Pfizer-BioNTech, and subsequently Sputnik. Among our vaccinated participants, 289 had taken Sinopharm, 21 had taken AstraZeneca, 12 took Pfizer-BioNTech, and 18 were vaccinated with Sputnik (data not shown in the tables). Information on the type of vaccine was not available for the remaining 739 of the subjects who were vaccinated. All subjects who were double vaccinated have been identified as vaccinated in our study, and those who did not receive any dose have been identified as "nonvaccinated." Individuals who received a single dose or who received booster doses were not included in the study.

The difference in the Ct value trend across the four PCR tests and the difference in the trend between the variants are shown in **Figure 1**. For both variants, regardless of the vaccination status, the increase in CT values by the fourth consecutive PCR test (**Figure 1**) was significant (p<0.001) as measured by p-value for within-subject effects using a mixed ANOVA. Although patients infected with both the variants started out with similar Ct values (**Figure 1**) at the first PCR test, in subsequent tests, the alpha variant's Ct values increased faster, whereas the increase in Ct values for the delta variant was slow. In both vaccinated as well as unvaccinated patients, the difference in Ct values across variants, as measured by the between-subject effects using a mixed model ANOVA, was not significant (p=0.616).

Figure 2 conveys the gradient in median length of hospital stay across variants between vaccinated and unvaccinated patients. Unvaccinated patients infected with the delta variant

TABLE 1 | Characteristics of the study subjects.

Characteristics	Alpha variant (n=792)	Delta variant (n=636)	p-value
N (%)	792 (55.5%)	636 (44.5%)	
Age [median, (IQR)]	39 (29, 51)	35 (28, 44)	<0.001
Male [n, (%)]	467 (59.0%)	399 (62.83%)	0.145
Bahraini nationality [n, (%)]	553 (69.8%)	338 (53.1%)	<0.001
Vaccination coverage [n, (%)]	573 (72.4%)	343 (54.1%)	<0.001
PCR test 1 CT value (n=2070) [mean, (SD)]	23.1 (3.8)	22.7 (3.1)	0.13
PCR test 2 CT value (n= 1291) [mean, (SD)]	28.0 (4.0)	27.3 (3.7)	0.24
PCR test 3 CT value (n= 540) [mean, (SD)]	29.2 (4.3)	27.6 (4.2)	0.076
PCR test 4 CT value (n=2070) [mean, (SD)]	29.7 (5.1)	27.7 (3.0)	0.05

IQR, interquartile range; PCR, polymerase chain reaction; CT, cycle time.

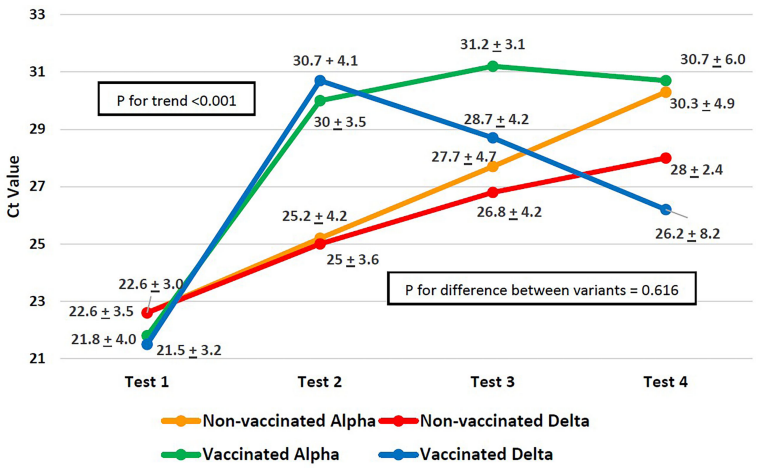

FIGURE 1 | Progression of PCR cycle time (CT) values across SARS-CoV-2 variants.

had the longest median length of stay (5.2 days), followed by unvaccinated patients infected with the alpha variant (4.4 days) and by vaccinated patients infected with the delta variant (3.0 days), and the least amount of median hospital stay was for vaccinated patients infected with the alpha variant (2.9 days). We saw 9 total deaths in our study (data not shown in the tables). Of these, two (22%) occurred in vaccinated patients, and both were infected with the alpha variant. Of the remaining 7 patients who died (78%), two were infected with the delta variant and the rest were other variants. The nonvaccinated group experienced a 1.4% mortality, which was more than thrice compared to 0.4% in the vaccinated group.

As seen in **Table 2**, after adjusting for age, sex, and vaccination status, the alpha variant's hazards to get discharged were 1.20 (compared to the delta variant, 1.01–1.41). In other words, the delta variant was 80% more likely to stay in the hospital compared to the alpha variant (p<0.001). Unvaccinated individuals were 22% more likely to stay in the hospital compared to unvaccinated counterparts, as indicated by a hazard ratio of 1.77 (1.49–2.11) for vaccinated patients. Age appeared to marginally decrease the likelihood of discharge (HR = 0.98, p<0.001). No significant difference across sex was observed.

DISCUSSION

The present study found the median length of stay to be higher in patients infected with the delta variant of SARS-CoV-2 compared

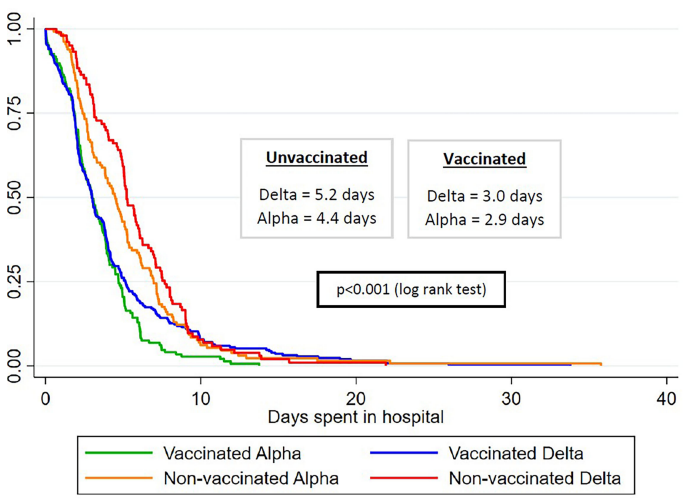

FIGURE 2 | Median length of hospital stay by variant type and vaccination status.

TABLE 2 | Hazards of discharge across variant types.

Variable	HR (95% CI)	P value
Variant		
Alpha	1.20 (1.01–1.41)	0.029
Delta	Ref	
Vaccination status		
Vaccinated	1.77 (1.49–2.11)	<0.001
Unvaccinated	Ref	
Age		
Age	0.98 (0.97–0.99)	<0.001
Sex		
Male	1.17 (0.98–1.38)	0.071
Female	Ref	

to the alpha variant. This pattern of recovery was consistent between vaccinated as well as nonvaccinated individuals.

The average age of patients infected with the delta variant compared to the alpha variant patients suggests that younger people may be more susceptible to the delta variant. The latest data from the CDC support this finding, showing higher rates of COVID-19 hospitalizations in those aged 18–49 than previously reported during the pandemic, and higher rates than older age groups (30). This may be due to increased vaccination in older ages, resulting in comparatively fewer cases in older cohorts. Data from the American Academy of Pediatrics between July 22nd and August 5th, 2021 showed a 4% rise in COVID-19 rates in children, in addition to comprising 15% of all cases (31). In accordance with our findings, a recent article from the *British Medical Journal* reported the highest outbreaks of delta in school settings and increasing COVID rates among children in the UK (22).

A higher proportion of those infected with the alpha variant in the present study were vaccinated compared to those infected with the delta variant. It is worth noting that since the data from this study were collected between January and April of 2021, the cases of the delta variant were just beginning to rise in Bahrain, and the dominant strain was still the alpha variant (32). This could be one of the reasons we saw a higher number of breakthrough infections from the alpha variant compared to the delta variant. Recent studies, however, have found vaccine efficacy against delta to be less than that of the alpha variant. In the UK, a study found that two vaccine doses sufficiently provide protection from infection by the delta variant, but to a lesser degree than against the alpha variant (33, 34). Similarly, Lopez Bernal and coworkers have reported that although there was little difference in vaccine efficacy against the alpha and delta variant infection with 2 doses of Pfizer-BioNTech and AstraZeneca vaccines, the efficacy was still greater against the alpha variant (26). Both the AstraZeneca and Pfizer-BioNTech vaccines have been reported to be less protective against hospitalization and infection caused by the delta variant in comparison to alpha (35, 36).

The Ct trend indicated no significant difference between the variants. In contrast, a US study found a higher viral load in delta demonstrated by a lower Ct value (delta 98, alpha 562), but no difference was found between vaccinated and unvaccinated groups (37). A Chinese study recorded Ct of 24 for delta compared to Ct of 34.31 of clade19a/19b. This means that the delta variant viral load is 1,260 times higher than the first strain (23). A recent study in France found lower Ct values for delta variant infection (Ct value: 17.3; 95%CI: 15–19.7) at the time of symptoms (unadjusted for time since symptoms) compared to alpha variant infection (Ct value 19.7, 95%CI: 16.2–23) (38).

The difference between our findings and the studies could be due to time elapsed since symptom or infection onset. A study on the viral load of the alpha variant commented that low Ct values alone could not predict the detection of the strain in a population being tested at different times, especially if not early in the infection when Ct values are highest, which is around the fifth day (39). Hence, those who are asymptomatic, randomly tested, or tested after established symptoms may not demonstrate high Ct values. Our finding exemplifies a real-world scenario, in which testing takes place at different points of infection, not necessarily at the onset.

The length of stay was higher in delta compared to alpha in both the vaccinated and unvaccinated. After adjusting for age and sex, the delta variant-infected patients were 80% more likely to remain at the hospital compared to their alpha variant counterparts. In accordance with our findings, a Scottish study concluded the risk of hospital admission from delta to be twice that of those with alpha. Although those vaccinated had reduced risk of admission, being infected with the delta variant rather than the alpha variant increased their risk of hospitalization (35). In the present study, we observed a small fraction of vaccinated people infected with delta with a slower recovery (length of stay >10 days) compared to unvaccinated delta infections. Upon closer analysis of demographic data from delta infections that stayed longer than 10 days, we found that vaccinated delta variant patients with >10 days of stay were significantly older and had higher proportion of males (mean age = 42.4 years, 38% males) compared to unvaccinated patients with delta variant infection (mean age =31.8 years, 18% males), suggesting that age and male gender were likely to play a role in slower recovery within delta variant infections, as also found by Hu and coworkers (40) and Butt et al. (41).

Another factor to consider in terms of breakthrough infections in vaccinated individuals is possible immune decay, especially in those who received their vaccination earliest in January. Nations such as Bahrain and United Arab Emirates, where inactivated virus (Sinopharm) was used for inoculation in the earliest stages of the vaccination roll-out, had since updated their national guidelines for such individuals to receive booster doses (42, 43), given the possibility of waning immunity (44, 45), which is also seen in vaccinated individuals (46). Since our dataset includes participants hospitalized from January till April 2021, it is possible that some of the breakthrough infections that occurred may have been in subjects who received their doses early in January and might have experienced immune decay.

A cohort study from England over March–May 2021 comparing alpha and delta variant hospitalization risk and emergency admissions with a population of similar age (31 years on average) and findings to our study established a higher risk of hospital admission and ER attendance (within 14 days of specimen collection) with delta (24). The study also found that unvaccinated delta infections had a higher admission risk compared to unvaccinated alpha counterparts. The study did not report any difference in hospital admission risk between vaccinated delta and alpha infections, similar to the results from Sheikh et al. (35).

The investigators also found delta patients to have twice the risk of hospital admission and ER use compared to alpha variant infections. Supporting our findings, the CDC Weekly Morbidity and Mortality Report from New York (47) also found vaccines to protect against hospitalization in the fully vaccinated but noted reduced efficacy against new infections even in the vaccinated when delta became the predominant strain. Prolonged hospital stay is explicable in the context of the increased admission risk and emergency facilities use caused by delta.

Despite breakthrough infections and hospital admissions, population level data on vaccinations and COVID-19 death demonstrate that the greatest protection conferred by COVID-19 vaccines worldwide is against mortality and severe disease. Nation-level COVID-19 death rates in unvaccinated individuals have been found to be anywhere between 3 and 12 times higher than that in vaccinated people in England, Northern Ireland, Singapore, and Chile (48–50). The Center for Disease Control statistics (48, 51) on COVID-19 mortality in the United States indicate that unvaccinated individuals had a death rate of 3.47 per 100,000 compared to 0.54 per 100,000 in fully vaccinated individuals (all vaccines). Similarly, data from Switzerland and Liechtenstein as reported by their Federal Office of Public Health (52), saw a death rate of 11.92 per 100,000 in unvaccinated individuals compared to 0.55 per 100,000 in vaccinated ones. Although restricted to hospitalized patients, the present study also found the mortality rate in unvaccinated subjects (1.4%) to be more than 3 times higher compared to the vaccinated group (0.4%), reiterating the global findings that COVID-19 vaccines remain highly protective against mortality and severe disease and therefore are of utmost public health significance.

Strengths and Limitations

This paper is one of the first efforts to use real-world data from vaccination roll-out in Bahrain to look at how the recovery pattern differs between alpha and delta variants of concern of SARS-CoV-2. One of the limitations of this body of work is that we did not have data on immune responses to see how immune decay in individuals vaccinated early on would have played a role in breakthrough infections.

CONCLUSION

In conclusion, the present study found patients infected with the delta variant of SARS-CoV-2 to have longer recovery periods as indicated by length of stay and pattern of PCR test CT values, within both vaccinated and unvaccinated individuals. In light of these findings, relaxation of preventative public health measures such as mask mandates needs to be evaluated in the context of proportion of SARS-CoV-2 infections that are the delta variant.

DATA AVAILABILITY STATEMENT

The raw data supporting the conclusions of this article will be made available by the authors, without undue reservation.

ETHICS STATEMENT

The studies involving human participants were reviewed and approved by the National COVID-19 Research Committee in Bahrain; Approval Code: CRT-COVID2021-148. Written informed consent for participation was not required for this study in accordance with the national legislation and the institutional requirements.

AUTHOR CONTRIBUTIONS

NK analyzed and interpreted the data, and wrote and reviewed the manuscript. SQ wrote and reviewed the manuscript. AA oversaw the data collection and reviewed the manuscript. MA was responsible for conception, design, and overall responsibility of the study, as well as wrote and reviewed the manuscript. All authors contributed to the article and approved the submitted version.

FUNDING

Financial support for open access publication was received from RCSI -Bahrain, project number: 172/22-Aug-2021.

ACKNOWLEDGMENTS

We are thankful to the Bahrain National COVID-19 Taskforce for making this study possible.

REFERENCES

1. World Health Organization. *Director-General's Opening Remarks at the Media Briefing on COVID-19 - 11 March 2020 [Press Release]*. Geneva: World Health Organization (2020).
2. Baden LR, El Sahly HM, Essink B, Kotloff K, Frey S, Novak R, et al. Efficacy and Safety of the mRNA-1273 SARS-CoV-2 Vaccine. *N Engl J Med* (2021) 384 (5):403–16. doi: 10.1056/NEJMoa2035389
3. Polack F, Thomas SJ, Kitchin N, Absalon J, Gurtman A, Lockhart S, et al. Safety and Efficacy of the BNT162b2 mRNA Covid-19 Vaccine. *N Engl J Med* (2020) 383(27):2603–15. doi: 10.1056/NEJMoa2034577
4. Voysey M, Clemens SA, Madhi SA, Weckx LY, Folegatti PM, Aley PK, et al. Safety and Efficacy of the ChAdOx1 Ncov-19 Vaccine (AZD1222) Against SARS-CoV-2: An Interim Analysis of Four Randomised Controlled Trials in Brazil, South Africa, and the UK. *Lancet* (2021) 397(10269):99–111. doi: 10.1016/S0140-6736(20)32661-1
5. Sathian B, Asim M, Banerjee I, Roy B, Pizarro AB, Mancha MA, et al. Development and Implementation of a Potential Coronavirus Disease 2019 (COVID-19) Vaccine: A Systematic Review and Meta-Analysis of Vaccine Clinical Trials. *Nepal J Epidemiol* (2021) 11(1):959–82. doi: 10.3126/nje.v11i1.36163
6. Moghadas SM, Vilches TN, Zhang K, Wells CR, Shoukat A, Singer BH, et al. The Impact of Vaccination on COVID-19 Outbreaks in the United States. *Clin Infect Dis* (2021) 73(12):ciab079. doi: 10.1093/cid/ciab079

7. Jablonska K, Aballea S, Toumi M. The Real-Life Impact of Vaccination on COVID-19 Mortality in Europe and Israel. *Public Health* (2021) 198:230–7. doi: 10.1016/j.puhe.2021.07.037
8. Liang LL, Kuo HS, Ho HJ, Wu CY. COVID-19 Vaccinations Are Associated With Reduced Fatality Rates: Evidence From Cross-County Quasi-Experiments. *J Glob Health* (2021) 11:05019. doi: 10.7189/jogh.11.05019
9. Paltiel AD, Schwartz JL, Zheng A, Walensky RP. Clinical Outcomes Of A COVID-19 Vaccine: Implementation Over Efficacy. *Health Aff (Millwood)* (2021) 40(1):42–52. doi: 10.1377/hlthaff.2020.02054
10. Rudolph JL, Hartronft S, McConeghy K, Kennedy M, Intrator O, Minor L, et al. Proportion of SARS-CoV-2 Positive Tests and Vaccination in Veterans Affairs Community Living Centers. *J Am Geriatr Soc* (2021) 69(8):2090–5. doi: 10.1111/jgs.17180
11. Peacocke EF, Heupink LF, Frønsdal K, Dahl EH, Chola L. Global Access to COVID-19 Vaccines: A Scoping Review of Factors That may Influence Equitable Access for Low and Middle-Income Countries. *BMJ Open* (2021) 11(9):e049505. doi: 10.1136/bmjopen-2021-049505
12. Boudjelal M, Almajed F, Salman AM, Alharbi NK, Colangelo M, Michelotti JM, et al. COVID-19 Vaccines: Global Challenges and Prospects Forum Recommendations. *Int J Infect Dis* (2021) 105:448–51. doi: 10.1016/j.ijid.2021.02.093reference
13. Nicolelis MA, Raimundo RL, Peixoto PS, Andreazzi CS. The Impact of Super-Spreader Cities, Highways, and Intensive Care Availability in the Early Stages of the COVID-19 Epidemic in Brazil. *Sci Rep* (2021) 11(1):1–2. doi: 10.1038/s41598-021-92263-3
14. Rambo AP, Gonçalves LF, Gonzáles AI, Rech CR, Paiva KM, Haas P. Impact of Super-Spreaders on COVID-19: Systematic Review. *Sao Paulo Med J* (2021) 139:163–9. doi: 10.1590/1516-3180.2020.0618.r1.10122020
15. Parikh PM, Hingmire S, Ghadiyalpatil N. Next Wave of COVID-19: Lessons for India From Indonesia, Israel, and Iceland. *South Asian J Cancer* (2021) 10 (01):01–2. doi: 10.1055/s-0041-1735436
16. Na W, Moon H, Song D. A Comprehensive Review of SARS-CoV-2 Genetic Mutations and Lessons From Animal Coronavirus Recombination in One Health Perspective. *J Microbiol* (2021) 59(3):332–40. doi: 10.1007/s12275-021-0660-4
17. World Health Organization. *Tracking SARS-CoV-2 Variants* (2021). Available at: https://www.who.int/en/activities/tracking-SARS-CoV-2-variants/.
18. Yurkovetskiy L, Wang X, Pascal KE, Tomkins-Tinch C, Nyalile TP, Wang Y, et al. Structural and Functional Analysis of the D614G SARS-CoV-2 Spike Protein Variant. *Cell* (2020) 183(3):739–51. doi: 10.1016/j.cell.2020.09.032
19. Alam I, Radovanovic A, Incitti R, Kamau AA, Alarawi M, Azhar EI, et al. CovMT: An Interactive SARS-CoV-2 Mutation Tracker, With a Focus on Critical Variants. *Lancet Infect Diseases* (2021) 21(5):602. doi: 10.1016/S1473-3099(21)00078-5
20. Williams H, Hutchinson D, Stone H. Watching Brief: The Evolution and Impact of COVID-19 Variants B.1.1.7, B.1.351, P.1 and B.1.617. *Global Biosecur* (2021) 3(1). doi: 10.31646/gbio.112
21. Choi JY, Smith DM. SARS-CoV-2 Variants of Concern. *Yonsei Med J* (2021) 62(11):961–8. doi: 10.3349/ymj.2021.62.11.961
22. Torjesen I. Covid-19: Delta Variant is Now UK's Most Dominant Strain and Spreading Through Schools. *BMJ* (2021) 373:n1445. doi: 10.1136/bmj.n1445
23. Li B, Deng A, Li K, Hu Y, Li Z, Xiong Q, et al. Viral Infection and Transmission in a Large Well-Traced Outbreak Caused by the Delta SARS-CoV-2 Variant. *MedRxiv* (2021). doi: 10.1101/2021.07.07.21260122
24. Twohig KA, Nyberg T, Zaidi A, Thelwall S, Sinnathamby MA, Aliabadi S, et al. Hospital Admission and Emergency Care Attendance Risk for SARS-CoV-2 Delta (B. 1.617. 2) Compared With Alpha (B. 1.1. 7) Variants of Concern: A Cohort Study. *Lancet Infect Dis* (2021) 22(1):35–42. doi: 10.1016/S1473-3099(21)00475-8
25. Brown CM, Vostok J, Johnson H, Burns M, Gharpure R, Sami S, et al. Outbreak of SARS-CoV-2 Infections, Including COVID-19 Vaccine Breakthrough Infections, Associated With Large Public Gatherings — Barnstable County, Massachusetts, July 2021. In: *MMWR Morb Mortal Wkly Rep*. Atlanta: Center for Disease Control (2021). Available at: https://www.cdc.gov/mmwr/volumes/70/wr/mm7031e2.htm.
26. Bernal JL, Andrews N, Gower C, Gallagher E, Simmons R, Thelwall S, et al. Effectiveness of Covid-19 Vaccines Against the B.1.617.2 (Delta) Variant. *N Engl J Med* (2021) 385(7):585–94. doi: 10.1056/NEJMoa2108891
27. Chia PY, Ong SWX, Chiew CJ, Ang LW, Chavatte JM, Mak TM, et al. Virological and Serological Kinetics of SARS-CoV-2 Delta Variant Vaccine-Breakthrough Infections: A Multi-Center Cohort Study. *Clin Microbiol Infect* (2021). doi: 10.1101/2021.07.28.21261295
28. Ong SWX, Chiew CJ, Ang LW, Mak TM, Cui L, Toh MPHS, et al. Clinical and Virological Features of SARS-CoV-2 Variants of Concern: A Retrospective Cohort Study Comparing B.1.1.7 (Alpha), B.1.315 (Beta) and B.1.617.2 (Delta). *SSRN J* (2021). doi: 10.2139/ssrn.3861566
29. Hannah R, Ortiz-Ospina E, Beltekian D, Mathieu E, Hasell J, Macdonald B, et al. *Coronavirus (COVID-19) Vaccinations - Statistics and Research - Our World in Data* (2021). Ourworldindata. Available at: https://ourworldindata.org/covid-vaccinations (Accessed November 2, 2021).
30. COVID-NET. *COVID-19-Associated Hospitalization Surveillance Network*. Centers for Disease Control and Prevention. Available at: https://gis.cdc.gov/grasp/COVIDNet/COVID19_5.html (Accessed on 2 November 2021).
31. American Academy of Pediatrics. *Children and COVID-19: State-Level Data Report 28 October 2021*. Available at: https://www.aap.org/en/pages/2019-novel-coronavirus-covid-19-infections/children-and-covid-19-state-level-data-report/.
32. Freunde von GISAID e.V. *Tracking of Variants*. gisaid.org. (2021). (Retrieved 11 January 2022).
33. del Rio C, Malani PN, Omer SB. Confronting the Delta Variant of SARS-CoV-2, Summer 2021. *JAMA* (2021) 326(11):1001–2. doi: 10.1001/jama.2021.14811
34. Pouwels KB, Pritchard E, Matthews P, Stoesser NB, Eyre DW, Vihta KD, et al. Impact of Delta on Viral Burden and Vaccine Effectiveness Against New SARS-CoV-2 Infections in the UK. *medRxiv* (2021). doi: 10.1101/2021.08.18.21262237
35. Sheikh A, McMenamin J, Taylor B, Robertson C. SARS-CoV-2 Delta VOC in Scotland: Demographics, Risk of Hospital Admission, and Vaccine Effectiveness. *Lancet* (2021) 397(10293):2461–2. doi: 10.1016/S0140-6736(21)01358-1
36. Puranik A, Lenehan PJ, Silvert E, Niesen MJ, Corchado-Garcia J, O'Horo JC, et al. Comparison of Two Highly-Effective mRNA Vaccines for COVID-19 During Periods of Alpha and Delta Variant Prevalence. *Preprint medRxiv* (2021):2021.08.06.21261707. doi: 10.1101/2021.08.06.21261707
37. Luo CH, Morris CP, Sachithanandham J, Amadi A, Gaston D, Li M, et al. Infection With the SARS-CoV-2 Delta Variant is Associated With Higher Infectious Virus Loads Compared to the Alpha Variant in Both Unvaccinated and Vaccinated Individuals. *medRxiv* (2021). doi: 10.1101/2021.08.15.21262077
38. Blanquart F, Abad C, Ambroise J, Bernard M, Cosentino G, Giannoli J-M, et al. Spread of the Delta Variant, Vaccine Effectiveness Against PCR-Detected Infections and Within-Host Viral Load Dynamics in the Community in France. *HAL Open Science* (2021) ffhal-03289443 https://hal.archives-ouvertes.fr/hal-03289443.
39. Hill K, Dewar R, Templeton K. A Multiregional Evaluation of Cycle Threshold Values in Severe Acute Respiratory Syndrome Coronavirus 2 VOC-20dec-01 Variant. *J Infect Dis* (2021) 224(5):927–8. doi: 10.1093/infdis/jiab303
40. Hu K, Lin L, Liang Y, Shao X, Hu Z, Luo H, et al. COVID-19: Risk Factors for Severe Cases of the Delta Variant. *Aging (Albany NY)* (2021) 13(20):23459. doi: 10.18632/aging.203655
41. Butt AA, Dargham SR, Chemaitelly H, Al Khal A, Tang P, Hasan MR, et al. Severity of Illness in Persons Infected With the SARS-CoV-2 Delta Variant vs Beta Variant in Qatar. *JAMA Internal Med* (2021). doi: 10.1001/jamainternmed.2021.7949
42. The Washington Post. *"Third Dose of Sinopharm Coronavirus Vaccine Needed for Some in UAE After Low Immune Response". By Paul Schemm, March 22, 2021*. Available at: https://www.washingtonpost.com/world/middle_east/uae-sinopharm-third-dose/2021/03/21/588fcf0a-8a26-11eb-a33e-da28941cb9ac_story.html.
43. The Washington Post. *"UAE and Bahrain Offer Sinopharm Coronavirus Booster Shots Amid Questions on Chinese Vaccine Efficacy". By Katerina Ang, May 19, 2021*. Available at: https://www.washingtonpost.com/world/2021/05/19/uae-sinopharm-third-dose-booster/.
44. Tso FY, Lidenge SJ, Poppe LK, Peña PB, Privatt SR, Bennett SJ, et al. Presence of Antibody-Dependent Cellular Cytotoxicity (ADCC) Against SARS-CoV-2 in COVID-19 Plasma. *PloS One* (2021) 16(3):e0247640. doi: 10.1371/journal.pone.0247640
45. Baraniuk C. How Long Does Covid-19 Immunity Last? *BMJ* (2021) 373: n1605. doi: 10.1136/bmj.n1605

46. Glück V, Grobecker S, Köstler J, Tydykov L, Bertok M, Weidlich T, et al. Immunity After COVID-19 and Vaccination: Follow-Up Study Over 1 Year Among Medical Personnel. *Infection* (2021) 1–8. doi: 10.1007/s15010-021-01703-9
47. Rosenberg ES, Holtgrave DR, Dorabawila V, Conroy M, Greene D, Lutterloh E, et al. New COVID-19 Cases and Hospitalizations Among Adults, by Vaccination Status—New York, May 3–July 25, 2021. *Morbidity Mortality Weekly Rep* (2021) 70(37):1306. doi: 10.15585/mmwr.mm7037a7
48. Mathieu E, Roser M. *How do Death Rates From COVID-19 Differ Between People Who Are Vaccinated and Those Who Are Not*? Our World in Data (2021). Available at: https://ourworldindata.org/covid-deaths-by-vaccination. November 23, 2021. Retrieved on 11 January 2022.
49. Office for National Statistics. Dataset. *"Deaths by Vaccination Status, England", (Version 20 Decemebr 2021)*. Available at: https://www.ons.gov.uk/peoplepopulationandcommunity/birthsdeathsandmarriages/deaths/datasets/deathsbyvaccinationstatusengland (Accessed 11 Januray 2022).
50. Singapore Ministry of Health. *Dataset "Proportion of Cases Who Died, by Age and Vaccination Status" (Version January 3, 2022)*. Available at: https://data.gov.sg/dataset/covid-19-case-numbers?resource_id=3c6c43ca-9703-48e4-a288-0d2d24a1946a (Accessed 11 January 2022).
51. Centers for Disease Control and Prevention. *COVID-19 Response. Rates of COVID-19 Cases or Deaths by Age Group and Vaccination Status Public Use Data (Version Date: December 17, 2021). Retrieved on 11 January 2022.* Available at: https://data.cdc.gov/Public-Health-Surveillance/Rates-of-COVID-19-Cases-or-Deaths-by-Age-Group-and/3rge-nu2a.
52. Federal Office of Public Health. *Dataset "COVID19Death_Vaccpersons_AKL10_w.Csv", Under "COVID-19 Switzerland"*. Available at: https://opendata.swiss/en/dataset/covid-19-schweiz.

Conflict of Interest: The authors declare that the research was conducted in the absence of any commercial or financial relationships that could be construed as a potential conflict of interest.

frontiers in Immunology

ORIGINAL RESEARCH
published: 24 March 2022
doi: 10.3389/fimmu.2022.856657

Specific Anti-SARS-CoV-2 Humoral and Cellular Immune Responses After Booster Dose of BNT162b2 Pfizer-BioNTech mRNA-Based Vaccine: Integrated Study of Adaptive Immune System Components

*Rosalia Busà[1], Maria Concetta Sorrentino[2], Giovanna Russelli[1], Giandomenico Amico[1,3], Vitale Miceli[1], Monica Miele[1,3], Mariangela Di Bella[1,3], Francesca Timoneri[1,3], Alessia Gallo[1], Giovanni Zito[1], Daniele Di Carlo[2], Pier Giulio Conaldi[1] and Matteo Bulati[1]**

[1] Research Department, Mediterranean Institute for Transplantation and Advanced Specialized Therapies (IRCCS ISMETT), Palermo, Italy, [2] Department of Laboratory Medicine and Advanced Biotechnologies, Mediterranean Institute for Transplantation and Advanced Specialized Therapies (IRCCS ISMETT), Palermo, Italy, [3] Department of Regenerative Medicine, Ri.MED Foundation, Palermo, Italy

Severe acute respiratory syndrome coronavirus 2 (SARS-CoV-2), which causes coronavirus disease 2019 (COVID-19), is modifying human activity all over the world with significant health and economic burden. The advent of the SARS-CoV-2 pandemic prompted the scientific community to learn the virus dynamics concerning transmissibility, epidemiology, and usefulness of vaccines in fighting emerging health hazards. Pieces of evidence suggest that the first and second doses of mRNA vaccines induce a significant antibody response in vaccinated subjects or patients who recovered from SARS-CoV-2 infection, demonstrating the importance of the previously formed memory. The aim of this work has been to investigate the effects of BNT162b2 Pfizer-BioNTech mRNA-based vaccine booster dose in a cohort of 11 uninfected immunocompetent (ICs), evaluating the humoral and cellular responses, with more carefulness on memory B and T cells. Our findings underscore the potential benefit of the third dose of mRNA vaccine on the lifespan of memory B and T cells, suggesting that booster doses could increase protection against SARS-CoV-2 infection.

Keywords: SARS-CoV-2, mRNA vaccine, BNT162b2, booster dose, B cells, T cells

OPEN ACCESS

Edited by:
Suryaprakash Sambhara, Centers for Disease Control and Prevention (CDC), United States

Reviewed by:
Todd Bradley, Children's Mercy Hospital, United States
Stephanie Longet, University of Oxford, United Kingdom

****Correspondence:***
Matteo Bulati
mbulati@ismett.edu

Specialty section:
This article was submitted to Vaccines and Molecular Therapeutics, a section of the journal Frontiers in Immunology

Received: *17 January 2022*
Accepted: *28 February 2022*
Published: *24 March 2022*

Citation:
Busà R, Sorrentino MC, Russelli G, Amico G, Miceli V, Miele M, Di Bella M, Timoneri F, Gallo A, Zito G, Di Carlo D, Conaldi PG and Bulati M (2022) Specific Anti-SARS-CoV-2 Humoral and Cellular Immune Responses After Booster Dose of BNT162b2 Pfizer-BioNTech mRNA-Based Vaccine: Integrated Study of Adaptive Immune System Components. Front. Immunol. 13:856657. doi: 10.3389/fimmu.2022.856657

INTRODUCTION

Severe acute respiratory syndrome coronavirus 2 (SARS-CoV-2), which causes coronavirus disease 2019 (COVID-19), is modifying human activity all over the world with significant health and economic burden. The advent of the SARS-CoV-2 pandemic prompted the scientific community to learn the virus dynamics concerning transmissibility, epidemiology, and usefulness of vaccines in fighting emerging health hazards. In the last two years, many studies on vaccinated subjects or patients who recovered from SARS-CoV-2 infection (1–3) highlighted the formation of high amounts of specific antibodies, a sign of robust protective immune responses and memory. A conspicuous number of studies reported that humoral and cellular immunity to SARS-CoV-2 reaches the peak after one month from vaccination, and then it decreases over time (4–7). Conversely, circulating specific memory B lymphocytes reach the peak after two/three months and remain constant over 8 months (1, 2). In a recent study, it has been shown that the first dose of mRNA vaccines, either Pfizer-BioNTech BNT162b2 or Moderna mRNA-1273, induces a significant antibody response in COVID-19 convalescents compared to uninfected healthy individuals, demonstrating the importance of the previously formed memory (8). The emergence of new variants of SARS-CoV-2, such as B.1.617.2 (Delta) and B.1.1.529 (Omicron), able to improve transmissibility and/or the escape from antibody binding (9, 10), and the reduced effectiveness overtime of the Pfizer-BioNTech BNT162b2 vaccine (11–13), led to a resurgence of COVID-19 cases in individuals that had been vaccinated for more than six months. For these reasons, in Italy, from September 2021, a circular from the Ministry of Health approved the use of the third dose of the BNT162b2 vaccine as an additional dose for fragile individuals and, subsequently, for those who had been vaccinated for more than 4 months, in order to achieve an adequate level of the immune response. Incorrectly, the duration of protective immunity after vaccination is sometimes related solely to the level of specific antibodies. However, the most important protection from reinfection is due to the synergistic action of memory B cells, which produce specific antibodies in response to pathogen entry, and T cells, which play a key role by helping B cells to produce high-affinity antibodies and/or by eliminating virus-infected cells. Therefore, to reach a long-lasting immunity, a vaccine should not only induce robust antibodies production but also induce strong B- and T-cell responses (14).

In this article, we investigated, in a cohort of 11 uninfected immunocompetents (ICs) from our hospital staff, humoral and cellular responses, in terms of anti-spike-specific antibody production and specific memory B- and T-cell formation. Anti-spike IgG and IgA were detected in sera collected three weeks (T1) and nine months (T2) from the second dose, and three weeks after booster dose (T3) of the BNT162b2 mRNA vaccine. Circulating anti-spike memory B cells were analyzed by using unique sets of fluorescently labeled recombinant tetramers of the SARS-CoV-2 spike protein in combination with an extensive flow cytometry panel, at T2 and T3.

At the same time points, T-cell-mediated response was detected by using the QuantiFERON SARS-CoV-2, a whole-blood assay, which is based on the same platform as the QuantiFERON-TB Plus, currently approved for the diagnosis of tuberculosis and other several viral infections (15). Interestingly, a good correlation between cellular responses detected by QuantiFERON SARS-CoV-2 with ELISpot assays has been recently demonstrated (16, 17). We decided to perform the QuantiFERON assay because it is an easy-to-use tool and the only automatable test available to detect the T cellular responses in a microenvironment as close as possible to the physiological condition (16–19). Finally, T-cell reactivity to SARS-CoV-2 specific antigens was also evaluated by flow cytometry detection of activation-induced markers (AIMs) on both CD4+ (CD40L+CD69+ and OX-40+CD137+) and CD8+ (CD69 +CD137+) T cells (20, 21) at T3. This is an alternative method that consents to detecting circulating antigen-specific T cells without using human leukocyte antigen (HLA)-multimers (22). In the cohort studied, we found a good antibody response at T1. Afterward, we observed a significant time-dependent decline of anti-SARS-CoV-2-specific IgG and IgA, which, in some cases, turned out to become a negativization, especially in the ones with the lowest response after the first vaccination cycle. Despite the decrease in specific antibodies, in all subjects studied, we showed the persistence of spike-specific memory B cells at T2. At the same time point, we did not find a significant T-cell response. As expected, at T3 the immune response is completely restored compared to that observed at T2 and even potentiates when compared to T1.

MATERIAL AND METHODS

Subjects Studied

A total of 11 uninfected immunocompetent (IC) healthy subjects (4 male and 7 female; median age 44, range 33–51), who never had positive nasopharyngeal swab (NPS) and anti-N response, were enrolled at the time of SARS-CoV-2 vaccination with the Pfizer-BioNTech BNT162b2 mRNA vaccine. Blood, PBMC, and serum samples were collected three weeks (T1) and nine months (T2) after the second dose and three weeks after the booster dose (T3) for the analysis of humoral and cellular immune response. The study was approved by the IRCCS-ISMETT Institutional Research Review Board (IRRB 00/21) and by the Ethic Committee of ISMETT, and all enrolled individuals signed the written informed consent form.

Detection of SARS-CoV-2 Antibodies

Sera samples from subjects enrolled were used to detect anti-spike immunoglobulin. The chemiluminescent immunoassay (CLIA) LIAISON® SARS-CoV-2 S1/S2 IgG (DiaSorin S.p.A.) was used for the quantitative detection of IgG antibodies to S1 and S2 fragments of the viral surface spike protein in the human serum. The test was used on the fully automated LIAISON® XL Analyser (DiaSorin S.p.A.). The SARS-CoV-2 S1/S2 IgG

antibody concentrations were expressed as arbitrary units (AU/ml) and the results were graded as follows: Negative (< 12.0 AU/ml), Equivocal (12.0–15.0 AU/ml), and Positive (> 15.0 AU/ml). The analytical performance of the assay has a good correlation to the detection of neutralizing antibodies [94.4% positive agreement to Plaque Reduction Neutralization Test (PRNT90)] and high sensitivity (95.4%) and specificity (98.6%) to ensure accurate results.

The anti-SARS-CoV-2 IgA (EUROIMMUN, Perkin Elmer Company) is an enzyme-linked immunoassay (ELISA) intended for the semiquantitative detection of IgA antibodies to S1 fragments of the viral surface spike protein, in the human serum and plasma. The test was used on the fully automated EUROIMMUN Analyzer I (EUROIMMUN, Perkin Elmer Company). The anti-SARS-CoV-2 ELISA IgA antibody concentrations were expressed as the ratio from the extinction of the sample and that of the calibrator and the results were graded as follows: Negative (< 0.8 Ratio), Equivocal (≥ 0.8 to 1.1 Ratio) and Positive (> 1.1 Ratio) With regard to performance analytical of the assay, good sensitivity (between 88.3% and 96.9%, depending on the time the sample was taken) together with high specificity (98.3%) ensures accurate results.

In order to exclude asymptomatic infection during the overall period of follow-up, anti-N response was determined on the ARCHITECT Quant test (Abbott) using the chemiluminescent assay anti-SARS-CoV-2-N-domain CMIA (IgG and IgM) (Abbott) and SARS-CoV-2 anti-N ELISpot (see ELISpot paragraph) at T3 (data not shown).

Isolation and Quantification of SARS-CoV-2-Specific B Cells

The venous blood of ICs was collected in K3EDTA tubes (Greiner Bio-One GmbH, Kremsmünster, Austria). Peripheral blood mononuclear cells (PBMCs) were isolated by density gradient centrifugation on Lympholyte Cell Separation Media (Cedarlane Laboratories Limited, Burlington, ON, Canada). Afterward, CD19+ B cells were separated from PBMCs by immune-magnetic sorting using anti-CD19 magnetic microbeads (REAlease CD19 MicroBeads Kit, Miltenyi Biotec, Auburn, CA, USA). The CD19+ B cells obtained from immune-magnetic sorting displayed a purity yield higher than 98%, which was determined by flow cytometry analysis. The isolated fraction was stained with SARS-CoV-2 spike B Cell Analysis Kit (ref. 130-128-022, Miltenyi Biotec, Auburn, CA, USA) to quantify the SARS-CoV-2-specific B cells at T2 and T3 following the manufacturer's instructions. Samples were acquired by a MACSQuant Cytometer (Miltenyi Biotec, Auburn, CA, USA) and analyzed with the Kaluza Version 2.1.1 software (Beckman Coulter, CA, USA).

QuantiFERON SARS-CoV-2 Assay

We evaluated the T-cell response at T2 and T3 by using the QuantiFERON SARS-CoV-2 kit (Qiagen, Hilden, Germany). This is an interferon gamma (IFN-γ) release assay, which contains heparinized antigen tubes that allow both to collect whole blood and to stimulate lymphocytes with a combination of three antigen peptides specific to SARS-CoV-2 (SARS-CoV-2 Ag1, Ag2, and Ag3). The SARS CoV-2 Ag1 tube contains CD4+ epitopes derived from the S1 subunit of the spike protein; the SARS CoV-2 Ag2 tube contains CD4+ and CD8+ epitopes from the S1 and S2 subunits of the spike protein; the SARS CoV-2 Ag3 tube contains CD4+ and CD8+ epitopes from S1 and S2 plus immunodominant CD8+ epitopes derived from the whole genome. After stimulation, plasma samples were analyzed for the detection of IFN-γ (IU/ml) using an ELISA-based platform. Samples were processed following the manufacturer's instructions (QuantiFERON SARS-CoV-2 Starter kit, ref. 626115; QuantiFERON SARS-CoV-2 Extended kit, ref. 626215; QuantiFERON ELISA, ref. 626410; Qiagen, Hilden, Germany). Elevated response was defined as a value at least 0.20 IU/ml greater than Nil (negative control used to subtract IFN-γ not derived from SARS-CoV-2-specific T-cell stimulation) (16).

SARS-CoV-2 ELISpot Assay

T-cell responses at T3 were also evaluated by using the ELISpot assay. Briefly, PBMCs from subjects studied were isolated by density gradient centrifugation from whole blood using a cell preparation tube with sodium citrate (BD Vacutainer ® CPT™), according to the manufacturer's protocol. PBMCs were counted by using the Sysmex XN-2000™ Hematology System. IFN-γ-secreting T cells were detected by a Human IFN-γ ELISpot plus kit (MABTECH AB, Sweden), according to the manufacturer's protocol. The assay was performed, in duplicate, stimulating $2.5x10^5 \pm 0.5x10^5$ PBMCs/ml for 20–22 h, at 37°C in a 5% CO_2 humidified atmosphere, with 1 μg/ml overlapping peptides spanning SARS-CoV-2 Spike (Mix I and II, respectively, of 158 and 157 peptides derived from a peptide scan, 15mers with 11 aa overlap) or N protein (JPT Peptide Technologies, Germany). The PBMCs were cultured in a RPMI 1640 medium (BIOWEST), supplemented with 5% GemCell U.S. Origin Human Serum AB (BIOVIT) and 1% L-Glutamine (EUROCLONE). Negative control (RPMI + 5% Human Serum AB) and positive controls, such as anti-CD3 and CEFX pepmix (a pool of 176 known peptides from various infectious agents, JPT Peptide Technologies, Germany), were also included. The number of SARS-CoV-2-specific IFN-γ-secreting cells was measured with an ELISpot Reader (Autoimmun Diagnostika (AID) GmbH, Straßberg, Germany) by using the ELISpot Software (AID). Mean spot counts for negative control wells were subtracted from the mean of test wells to generate normalized readings; these are presented as Spot Forming Unit (SFU) per million PBMCs. To determinate the lower limit to indicate a positive response (cutoff), we considered the mean value of responses of unstimulated wells plus 2 standard deviations (SD) (cutoff=121 SFC/10^6 PBMC).

Activation-Induced Marker (AIM) Memory T-cell Detection

Whole-blood aliquots (60 μl), at T3, were withdrawn from Nil (negative control) and mitogen (positive control) tubes and from the three Ag tubes (20 μl each, mixed together) of the QuantiFERON SARS-CoV-2 kit (Qiagen, Hilden, Germany)

before centrifugation, and stained with the following combination of anti-human fluorescent monoclonal antibodies: CD3BV786, CD4FITC, CD8PE, CD137APC, CD69BV711 (Becton Dickinson, San Jose, CA, USA), CD154(CD40L)APC-VIO770, and CD134(OX-40)PE-VIO770 (Miltenyi Biotec, Auburn, CA, USA). Pharm Lyse solution (Becton Dickinson, San Jose, CA, USA) was used to remove red blood cells. Then T cells were analyzed by using a 16-color FACS Celesta SORP flow cytometer (Becton Dickinson, San Jose, CA, USA) with the same instrument setting. At least 10^4 cells were analyzed using the Kaluza Version 2.1.1 software (Beckman Coulter, CA, USA). Cells were gated on the forward scatter/side scatter cell gate and then on the CD3+CD4+ gate for the quantification of CD40L +CD69+ and CD137+OX-40+ SARS-CoV-2-specific CD4 T cells, and on the CD3+CD8+ gate for the quantification of CD137+CD69+ SARS-CoV-2-specific CD8 T cells.

Statistical Analysis

Statistical analysis has been performed using GraphPad Prism 9.0 (GraphPad Software, USA). Wilcoxon matched-pairs nonparametric test, Pearson and Spearman correlation, and one-way ANOVA tests with multiple comparisons have been used according to the type of samples to compare. Statistical significance was considered at $p < 0.05$.

RESULTS

Humoral Response Elicited by Booster Dose of Pfizer-BioNTech BNT162b2 mRNA Vaccine

We measured anti-SARS-CoV-2-specific antibodies, in particular IgG and IgA, by using LIAISON® SARS-CoV-2 S1/S2 CLIA (DiaSorin S.p.A.) for the former and ELISA (EUROIMMUN) for the latter. At T1, the median value of specific IgG was 253 AU/ml (SEM=30.23), and it significantly decreased (p=0.0003) to 80.40 AU/ml (SEM=16.48) at T2, while at T3, we observed that the specific IgG significantly increased reaching the median value of 1,590 AU/ml (SEM=156.5) in 100% of the subjects (**Figure 1A**). Interestingly, we recorded a 20-fold increase between T3 and T2 (p<0.0001) and an 8-fold increase between T3 and T1 (p<0.0001). These results demonstrate the efficacy of the third dose to boost antibody response against SARS-CoV-2. As depicted in **Figure 1B**, we observed the same trend concerning specific IgA. Indeed, the median ratio was 8.35 (SEM=1.27) at T1, which significantly decreased to 1.10 (SEM=0.33) at T2 (p<0.0001). At T3, specific IgA had a significant upsurge (p<0.0001) compared to T2 reaching a median value of the ratio of 9.8 (SEM=0.52) compared to that observed at T1. These results suggest that the third dose restored the IgA response against SARS-CoV-2.

SARS-CoV-2-Specific Memory B Cells Persist After Nine Months From the 2nd Dose and Increased After the Booster Dose

To evaluate the long-term persistency of SARS-CoV-2-specific memory B cells after the second dose, and their kinetics after the booster dose, we assessed the identification and the characterization of these cells in all subjects studied. The SARS-CoV-2-specific B cells were characterized using a SARS-CoV-2-biotinylated-recombinant protein and two distinct fluorescently labeled streptavidin conjugates to make a spike tetramer solution. SARS-CoV-2-specific B cells were evaluated by flow cytometry in all 11 samples for the expression of markers for memory B cells (CD27) and cell surface immunoglobulin isotypes, such as IgG, IgA, and IgM, at T2 and T3. Despite a very significant reduction of circulating anti-spike antibodies (**Figures 1A, B**), we found that the percentage of SARS-CoV-2-specific memory B cells detected at T2 in our vaccinated subjects is comparable to current data in literature on the non-infected vaccinated (23) and, interestingly, is also comparable to

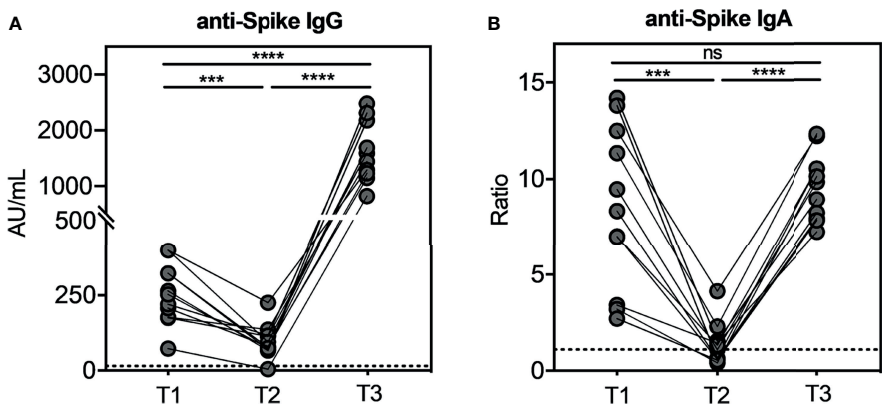

FIGURE 1 | Kinetic of total anti-SARS-CoV-2 IgG and IgA serum antibodies levels in seronegative recipients (ICs n=11) of Pfizer-BioNTech BNT162b2 mRNA-based vaccination. The evaluation of both serum antibodies was conducted at three weeks (T1) and nine months (T2) after the second dose, and three weeks after the booster dose (T3). In Figure (A) anti-SARS-CoV-2 S1/S2 IgG levels and in (B) anti-SARS-CoV-2 S1 IgA levels. The dotted lines correspond to IgG (> 15.0 AU/mL) and IgA (>1.1 Ratio) cut-off, respectively. The significance was determined using Tukey's multiple comparisons test. One-way ANOVA, ***p=0.0002; ****p<0.0001, ns, not significant.

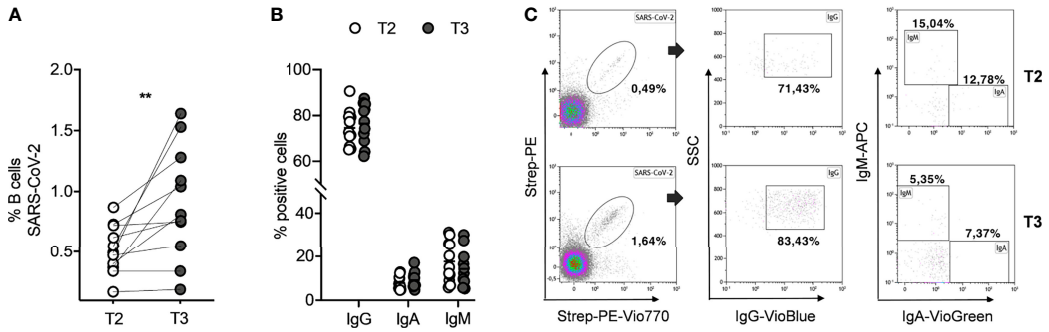

FIGURE 2 | SARS-CoV-2-specific memory B cells in seronegative recipients (ICs n=11) of Pfizer-BioNTech BNT162b2 mRNA-based vaccination before (T2) and after (T3) the booster dose. **(A)** Percentage (%) of SARS-CoV-2 specific B cells before and after the booster dose. **(B)** Comparison amid T2 and T3 of percentage (%) positive cell to surface immunoglobulin isotypes, IgG, IgA, and IgM. **(C)** Representative flow cytometry plots (one subject) showing memory B-cell subpopulations. The significance was determined using Wilcoxon matched-pairs test **(A)** and Sidak's multiple comparisons test **(B)**, one-way ANOVA, **p=0.0021

data on COVID-19 convalescent subjects (2). Indeed, as shown in **Figure 2A**, the percent of SARS-CoV-2-specific memory B cells had a median value of 0.49% (SEM=0.06%) at T2. After the booster dose (T3), this value significantly increases compared to T2 (p=0.002), reaching a median value of 0.81% (SEM=0.14%). The phenotype analysis of spike-specific memory (CD27+) B cells reveals that most of these cells express IgG (median=72.73%, SEM=2.38% at T2; median=77.46%, SEM=2.66% at T3), and the remnants expresses IgA (median=6.29%, SEM=0.91% at T2; median=7.37%, SEM=1.10% at T3) or IgM (median=15.04%, SEM=2.84% at T2; median=12.30%, SEM=2.59% at T3) at both time points, without any significant differences (**Figure 2B**). **Figure 2C** depicts a representative flow cytometry analysis used to analyze the memory B-cell subpopulations, and **Supplementary Figure 1** shows the complete gating strategy. Briefly, cells were gated on the forward scatter/side scatter cell gate and on 7AAD-negative live cells. Subsequently, CD19+ total B cells were gated on CD27+ memory subsets and then on double-positive streptavidin conjugates for the quantification of spike-specific B cells. On this gate, IgG, IgA, and IgM immunoglobulin surface expressions were quantified.

Cellular Response Elicited by Booster Dose Pfizer-BioNTech BNT162b2 mRNA Vaccine

To investigate whether the booster dose of the BNT162b2 Pfizer-BioNTech mRNA vaccine elicits a T-cell response to SARS-CoV-2, we performed a new IFN-γ release assay (QuantiFERON SARS-CoV-2 kit) on the whole blood of all subjects studied at T2 and T3. At T2, we showed a T-cell response, in terms of IFN-γ production, in 2/11 (18%) for Ag1 (**Figure 3A**), 2/11 (18%) for Ag2 (**Figure 3B**), and 2/11 (18%) for Ag3 (**Figure 3C**). A significant IFN-γ response in Ag2 (p=0.031) and Ag3 (p=0.016) tubes was observed at T3, compared to T2, whereas no significant responses were observed in the Ag1 tube. In particular, at T3, 4/11 (36%), 5/11 (45%), and 7/11 (64%) subjects overcame the IFN-γ cutoff (0.2 IU/ml) for Ag1, Ag2, and Ag3, respectively. Moreover, we compared IFN-γ production by both QuantiFERON and ELISpot assays. Spearman's statistical correlation analysis revealed a positive correlation between the SARS-CoV-2 ELISPOT and SARS-CoV-2 QuantiFERON assay results. As shown in **Figure 3D**, we found significant correlations between ELISpot and Ag1 (r=0.65, p=0.03), Ag2 (r=0.78, p=0.005), and Ag3 (r=0.91, p=0.0001). These results suggest that about half of the subjects studied did not develop a good T-cell response after the booster dose (**Figure 3E**). Lastly, to define SARS-CoV-2 memory T cells, we detected on the blood coming from Ag1, Ag2, and Ag3 Quantiferon tubes the frequency of AIM-T cells. Surprisingly, we found that, at T3, all subjects showed the presence of AIM-T cells (**Figure 4A**), namely, CD40L+CD69+ (median=0.26%, SEM=0.05%; p=0.002) and CD137+OX-40+ (median=0.07%, SEM=0.05%; p=0.002) for CD4+ T cells, and CD137+CD69+ (median=0.53%, SEM=0.14%; p=0.001) for CD8+ T cells, indicative of the presence of SARS-CoV-2-specific memory T-cell compartment (22). **Figure 4B** depicts a representative flow cytometry analysis used to analyze the memory T-cell subpopulations, including the positive control (Mitogen), and **Supplementary Figure 2** shows the complete gating strategy.

DISCUSSION

In this study, we provided an analysis of the adaptive immune response elicited by Pfizer-BioNTech mRNA BNT162b2 vaccination in a cohort of 11 uninfected ICs. The participants have completed the anti-SARS-CoV-2 vaccination cycle, with the two recommended doses, in January 2021 and received the booster dose between October and November 2021. Three weeks after the first vaccination cycle, all subjects showed an optimal serological response, being positive for both SARS-CoV-2 anti-spike-specific IgG and IgA antibodies. We observed that anti-spike IgG and IgA antibodies drop over a nine-month period in all subjects studied. Nevertheless, about 90% (10/11) and 63% (7/11) of the participants maintained, respectively, a positive IgG and IgA value. Although serum antibodies are the

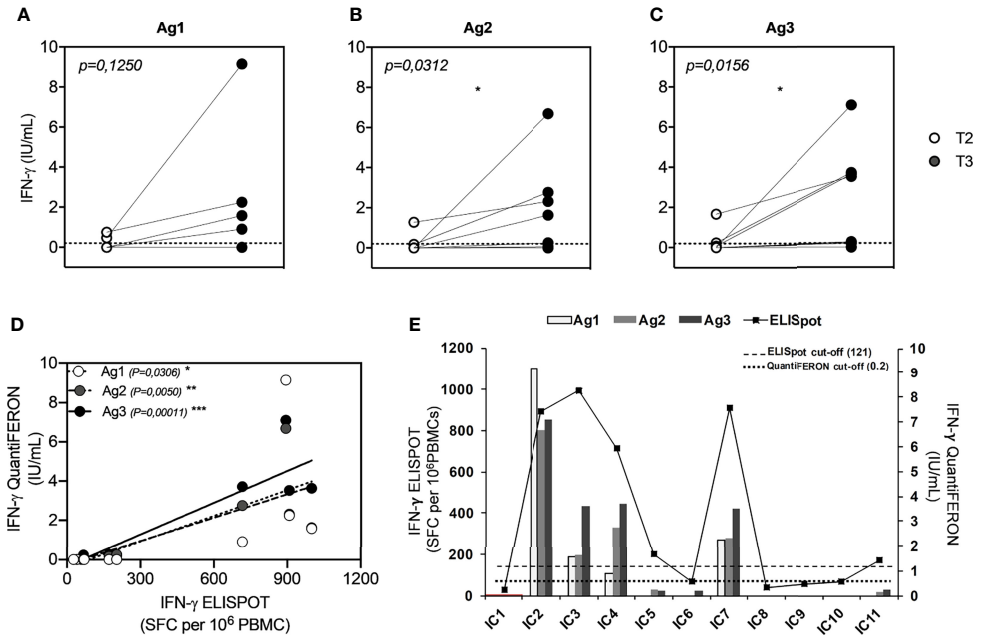

FIGURE 3 | Comparison of QuantiFERON SARS-CoV-2 antigen tube (Ag minus Nil) response, express as IFN-γ (IU/ml), in seronegative subjects (ICs n=11) before (T2) and after (T3) the booster dose of the Pfizer-BioNTech BNT162b2 mRNA-based vaccine. **(A)** QFN-SARS-CoV-2 Ag1-Nil responses; **(B)** Ag2-Nil responses; **(C)** Ag3-Nil responses. The dotted lines, in each graph, correspond to IFN-γ cutoff (0.2 IU/ml). **(D)** Correlation between IFN-γ-ELISpot and IFN-γ-QFN responses of each specific antigen (Ag1 contains CD4+ epitopes derived from the S1 subunit of the spike protein; Ag2 contains CD4+ and CD8+ epitopes from the S1 and S2 subunits of the spike protein; and Ag3 contains CD4+ and CD8+ epitopes from S1 and S2, plus immunodominant CD8+ epitopes derived from the whole genome). **(E)** Graphic comparison of IFN-γ-ELISpot and IFN-γ-QFN responses of all subjects studied. The significance was determined using Wilcoxon matched-pairs test, *p = 0.0332 **(A–C)** and Pearson correlation, *p=0.0332; **p=0.0021; ***p=0.0002.

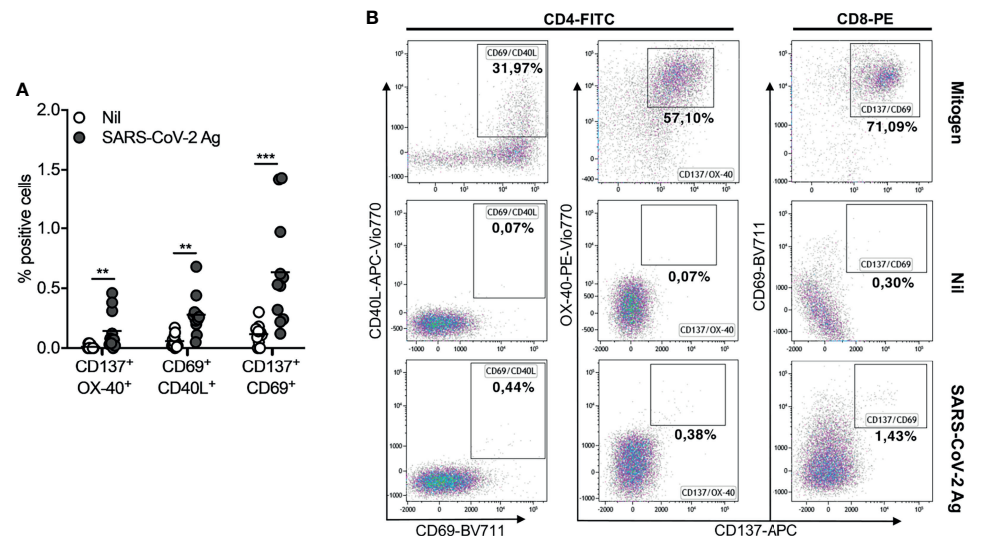

FIGURE 4 | Activation-induced memory (AIM)-T cell detection in seronegative recipients (ICs n=11) of Pfizer-BioNTech BNT162b2 mRNA-based vaccination at T3. **(A)** Comparing of percentage (%) of AIM-T cells in Nil tubes to SARS-CoV-2 antigen using specific marker CD137/OX-40, CD69/CD40L, CD137/CD69 (CD40L is uniquely expressed on activated CD4 T cells; CD69 is an activation marker of both CD4 and CD8 T cells; CD137 and OX-40, both belonging to the TNF receptor superfamily, are also markers of Ag-specific CD8 and CD4 T cells, respectively. In combinations, CD137/OX-40 and CD69/CD40L identify Ag-specific CD4 T cells, while CD137/CD69 identifies Ag-specific CD8 T cells). **(B)** Representative flow cytometry plots (one subject) showing AIM-T cell subpopulations stimulated or not (Nil) with SARS-CoV-2 antigen and the positive control (Mitogen). The significance was determined using Wilcoxon matched-pairs test, **p = 0.0021; ***p = 0.0002.

most used biomarker for the evaluation of vaccine efficacy, it emerged that they are not reliable markers able to predict the immune response outcome in response to SARS-CoV2 vaccination. It is well known that serum antibody decline normally occurs in every vaccination due to the decay of short-lived plasma cells (24). The effectiveness of a vaccine depends on its ability to generate a time-enduring immunological memory, which is mediated by long-lived antigen-specific memory B and T lymphocytes. Indeed, the quantitative and qualitative analysis of antigen-specific B and T cells toward a defined antigen allows to assess whether an individual has developed an adaptive immune response to a previous immunization. Essential properties for protective memory immunity are specificity and rapidity of action. On this purpose, memory B cells, differently from memory T cells, can improve their specificity due to repeated steps of selection and somatic hypermutation, which undergo in germinal centers. Moreover, different kinetics, duration, and evolution of memory B and T cells after SARS-CoV-2 infection have been recently demonstrated. Indeed, it has been shown that spike-specific memory B cells were more abundant at 6 months than at 1 month after symptom onset and persist for up to 8 months (1). Conversely, SARS-CoV-2-specific T cells declined with a half-life of 3 to 5 months (1). In our results, obtained at nine months from the second dose of BNT162b2, we report similar findings. In fact, even if anti-spike antibody response contracts, the presence of SARS-CoV-2 memory B cells in all subjects, predominantly IgG^+, is indicative of persisting immune memory following a second dose of vaccination. A different situation arises, instead, for the T-cell effector response, as we have shown the ability to produce IFN-γ after stimulation in a small fraction of our studied population (18%) at nine months from the primary vaccine cycle. A pronounced immune response was observed following the booster dose, including a very significant increase in anti-Spike IgG and IgA, of specific memory B cells and of T-cell response. The production of serum IgA, and the presence of IgA-expressing memory B cells, after vaccination, is of great interest because this isotype is the main antibody for protection at mucosal sites, such as the upper respiratory tracts, known to be the site of SARS-CoV-2 entry. However, in order to prevent the viral invasion of the upper airways, mucosal secretory IgA is needed (25). High levels of secretory salivary IgA have been detected in COVID-19 patients (26), but very low concentration was observed in the saliva of vaccinated individuals (27), suggesting less ability of vaccine to induce mucosal immunity. Recently, Piano Mortari et al. showed the increase in salivary IgA in vaccinated healthy individuals with a positive nasopharyngeal swab (28), demonstrating the reaction to the local infection. As a matter of fact, in most cases, vaccinated subjects with a positive nasopharyngeal swab remain asymptomatic or with mild symptoms. It could be hypothesized that part of their protection may be due to the ability of specific memory B cells to migrate to inflamed mucosal tissues, in response to attracting inflammatory molecules, and locally produce IgA. Concerning the T-cell response, after the booster dose, we observed that, despite the fact that half of the subjects did not develop a T-cell effector response, all of them present SARS-CoV-2-specific AIM-T cells, demonstrating the maintenance of long-lived memory T-cell compartment. Probably, shortening time between doses could improve the effectiveness of vaccine on the T-cell response. Although promising, these results are based on a relative short follow-up period from the booster dose and in a small cohort. Further long-term studies are necessary to investigate the duration and pliability of the immune memory induced by vaccines. The integrated study of serum antibodies, memory B cells, effector T-cell response, and memory T cells should help us to understand their time-related different kinetics and duration, with the aim to improve current or future anti-SARS-CoV-2 vaccination strategies and decisions.

DATA AVAILABILITY STATEMENT

The original contributions presented in the study are included in the article/**Supplementary Material**. Further inquiries can be directed to the corresponding author.

ETHICS STATEMENT

The studies involving human participants were reviewed and approved by the IRCCS-ISMETT Institutional Research Review Board (IRRB 00/21) and by the Ethic Committee of ISMETT. The patients/participants provided their written informed consent to participate in this study.

AUTHOR CONTRIBUTIONS

RB and MB: Conceptualization, methodology, resources, and writing original draft. RB, MB, and MCS: Methodology and data curation. RB, VM, MM, FT, and MDB: Formal analysis and software. RB, MB, VM, and AG: Visualization and investigation. GZ and GA: Investigation. GR: Clinical research coordinator. PGC and DDC revised the paper critically for important intellectual content. PGC: Funding acquisition. All authors have seen and approved the final draft of the manuscript.

FUNDING

This research was funded by Ministero della Salute Ricerca Finalizzata Progetto COVID-2020-12371760 and Ministero della Salute a valere sui fondi Ricerca Corrente Reti 2020 (RCR-2020): Rete Tematica IRCCS—Rete Cardiologica, grant number 23670065.

SUPPLEMENTARY MATERIAL

The Supplementary Material for this article can be found online at: https://www.frontiersin.org/articles/10.3389/fimmu.2022.856657/full#supplementary-material

REFERENCES

1. Dan JM, Mateus J, Kato Y, Hastie KM, Yu ED, Faliti CE, et al. Immunological Memory to SARS-CoV-2 Assessed for Up to 8 Months After Infection. *Science* (2021) 371(6529):1–13. doi: 10.1126/science.abf4063
2. Hartley GE, Edwards ESJ, Aui PM, Varese N, Stojanovic S, McMahon J, et al. Rapid Generation of Durable B Cell Memory to SARS-CoV-2 Spike and Nucleocapsid Proteins in COVID-19 and Convalescence. *Sci Immunol* (2020) 5(54):1–14. doi: 10.1126/sciimmunol.abf8891
3. Yan R, Zhang Y, Li Y, Xia L, Guo Y, Zhou Q. Structural Basis for the Recognition of SARS-CoV-2 by Full-Length Human ACE2. *Science* (2020) 367(6485):1444–8. doi: 10.1126/science.abb2762
4. Chivu-Economescu M, Bleotu C, Grancea C, Chiriac D, Botezatu A, Iancu IV, et al. Kinetics and Persistence of Cellular and Humoral Immune Responses to SARS-CoV-2 Vaccine in Healthcare Workers With or Without Prior COVID-19. *J Cell Mol Med* (2022) 26(4):1293–305. doi: 10.1111/jcmm.17186
5. Demaret J, Corroyer-Simovic B, Alidjinou EK, Goffard A, Trauet J, Miczek S, et al. Impaired Functional T-Cell Response to SARS-CoV-2 After Two Doses of BNT162b2 mRNA Vaccine in Older People. *Front Immunol* (2021) 12:778679. doi: 10.3389/fimmu.2021.778679
6. Krause PR, Fleming TR, Peto R, Longini IM, Figueroa JP, Sterne JAC, et al. Considerations in Boosting COVID-19 Vaccine Immune Responses. *Lancet* (2021) 398(10308):1377–80. doi: 10.1016/S0140-6736(21)02046-8
7. Mazzoni A, Vanni A, Spinicci M, Lamacchia G, Kiros ST, Rocca A, et al. SARS-CoV-2 Infection and Vaccination Trigger Long-Lived B and CD4+ T Lymphocytes: Implications for Booster Strategies. *J Clin Invest* (2022). doi: 10.1172/JCI157990
8. Goel RR, Apostolidis SA, Painter MM, Mathew D, Pattekar A, Kuthuru O, et al. Distinct Antibody and Memory B Cell Responses in SARS-CoV-2 Naive and Recovered Individuals Following mRNA Vaccination. *Sci Immunol* (2021) 6(58):1–13. doi: 10.1126/sciimmunol.abi6950
9. Ai J, Zhang H, Zhang Y, Lin K, Zhang Y, Wu J, et al. Omicron Variant Showed Lower Neutralizing Sensitivity Than Other SARS-CoV-2 Variants to Immune Sera Elicited by Vaccines After Boost. *Emerg Microbes Infect* (2022) 11(1):337–43. doi: 10.1080/22221751.2021.2022440
10. Perez-Gomez R. The Development of SARS-CoV-2 Variants: The Gene Makes the Disease. *J Dev Biol* (2021) 9(4):1–28. doi: 10.3390/jdb9040058
11. Barda N, Dagan N, Cohen C, Hernan MA, Lipsitch M, Kohane IS, et al. Effectiveness of a Third Dose of the BNT162b2 mRNA COVID-19 Vaccine for Preventing Severe Outcomes in Israel: An Observational Study. *Lancet* (2021) 398(10316):2093–100. doi: 10.1016/S0140-6736(21)02249-2
12. Pouwels KB, Pritchard E, Matthews PC, Stoesser N, Eyre DW, Vihta KD, et al. Effect of Delta Variant on Viral Burden and Vaccine Effectiveness Against New SARS-CoV-2 Infections in the UK. *Nat Med* (2021) 27(12):2127–35. doi: 10.1038/s41591-021-01548-7
13. Thompson RN, Hill EM, Gog JR. SARS-CoV-2 Incidence and Vaccine Escape. *Lancet Infect Dis* (2021) 21(7):913–4. doi: 10.1016/S1473-3099(21)00202-4
14. Sauer K, Harris T. An Effective COVID-19 Vaccine Needs to Engage T Cells. *Front Immunol* (2020) 11:581807. doi: 10.3389/fimmu.2020.581807
15. Shafeque A, Bigio J, Hogan CA, Pai M, Banaei N. Fourth-Generation QuantiFERON-TB Gold Plus: What Is the Evidence? *J Clin Microbiol* (2020) 58(9):1–8. doi: 10.1128/JCM.01950-19
16. Jaganathan S, Stieber F, Rao SN, Nikolayevskyy V, Manissero D, Allen N, et al. Preliminary Evaluation of QuantiFERON SARS-CoV-2 and QIAreach Anti-SARS-CoV-2 Total Test in Recently Vaccinated Individuals. *Infect Dis Ther* (2021) 10(4):2765–76. doi: 10.1007/s40121-021-00521-8
17. Martinez-Gallo M, Esperalba J, Pujol-Borrell R, Sanda V, Arrese-Munoz I, Fernandez-Naval C, et al. Commercialized Kits to Assess T-Cell Responses Against SARS-CoV-2 S Peptides. A Pilot Study in Health Care Workers. *Med Clin* (2021). doi: 10.1016/j.medcli.2021.09.013
18. Pedersen RM, Tornby DS, Bistrup C, Johansen IS, Andersen TE, Justesen US. Negative SARS-CoV-2 Antibodies, T-Cell Response and Virus Neutralization Following Full Vaccination in a Renal Transplant Recipient: A Call for Vigilance. *Clin Microbiol Infect: Off Publ Eur Soc Clin Microbiol Infect Dis* (2021) 27(9):1371–3. doi: 10.1016/j.cmi.2021.05.042
19. Van Praet JT, Vandecasteele S, De Roo A, De Vriese AS, Reynders M. Humoral and Cellular Immunogenicity of the BNT162b2 Messenger RNA Coronavirus Disease 2019 Vaccine in Nursing Home Residents. *Clin Infect Dis: Off Publ Infect Dis Soc Am* (2021) 73(11):2145–7. doi: 10.1093/cid/ciab300
20. Guerrera G, Picozza M, D'Orso S, Placido R, Pirronello M, Verdiani A, et al. BNT162b2 Vaccination Induces Durable SARS-CoV-2-Specific T Cells With a Stem Cell Memory Phenotype. *Sci Immunol* (2021) 6(66):eabl5344. doi: 10.1126/sciimmunol.abl5344
21. Tarke A, Sidney J, Methot N, Yu ED, Zhang Y, Dan JM, et al. Impact of SARS-CoV-2 Variants on the Total CD4(+) and CD8(+) T Cell Reactivity in Infected or Vaccinated Individuals. *Cell Rep Med* (2021) 2(7):100355. doi: 10.1016/j.xcrm.2021.100355
22. Takahama S, Nogimori T, Higashiguchi M, Murakami H, Akita H, Yamamoto T. Simultaneous Monitoring Assay for T-Cell Receptor Stimulation-Dependent Activation of CD4 and CD8 T Cells Using Inducible Markers on the Cell Surface. *Biochem Biophys Res Commun* (2021) 571:53–9. doi: 10.1016/j.bbrc.2021.07.037
23. Terreri S, Piano Mortari E, Vinci MR, Russo C, Alteri C, Albano C, et al. Persistent B Cell Memory After SARS-CoV-2 Vaccination is Functional During Breakthrough Infections. *Cell Host Microbe* (2022) 30(3):400–8. doi: 10.1016/j.chom.2022.01.003
24. Pollard AJ, Bijker EM. A Guide to Vaccinology: From Basic Principles to New Developments. *Nat Rev Immunol* (2021) 21(2):83–100. doi: 10.1038/s41577-020-00479-7
25. Quinti I, Mortari EP, Fernandez Salinas A, Milito C, Carsetti R. IgA Antibodies and IgA Deficiency in SARS-CoV-2 Infection. *Front Cell Infect Microbiol* (2021) 11:655896. doi: 10.3389/fcimb.2021.655896
26. Sterlin D, Mathian A, Miyara M, Mohr A, Anna F, Claer L, et al. IgA Dominates the Early Neutralizing Antibody Response to SARS-CoV-2. *Sci Trans Med* (2021) 13(577):1–10. doi: 10.1126/scitranslmed.abd2223
27. Ketas TJ, Chaturbhuj D, Portillo VMC, Francomano E, Golden E, Chandrasekhar S, et al. Antibody Responses to SARS-CoV-2 mRNA Vaccines Are Detectable in Saliva. *Pathog Immun* (2021) 6(1):116–34. doi: 10.20411/pai.v6i1.441
28. Piano Mortari E, Russo C, Vinci MR, Terreri S, Fernandez Salinas A, Piccioni L, et al. Highly Specific Memory B Cells Generation After the 2nd Dose of BNT162b2 Vaccine Compensate for the Decline of Serum Antibodies and Absence of Mucosal IgA. *Cells* (2021) 10(10):1–18. doi: 10.3390/cells10102541

Conflict of Interest: The authors declare that the research was conducted in the absence of any commercial or financial relationships that could be construed as a potential conflict of interest.

frontiers | Frontiers in Immunology

ORIGINAL RESEARCH
published: 12 April 2022
doi: 10.3389/fimmu.2022.817345

Persistence of SARS-CoV-2 Antibodies in Vaccinated Health Care Workers Analyzed by Coronavirus Antigen Microarray

Sina Hosseinian[1†], Kathleen Powers[1†], Milind Vasudev[1†], Anton M. Palma[2], Rafael de Assis[3], Aarti Jain[3], Peter Horvath[2], Paramveer S. Birring[1], Rana Andary[1], Connie Au[1], Brandon Chin[1], Ghali Khalil[1], Jenny Ventura[1], Madeleine K. Luu[4], Cesar Figueroa[5], Joshua M. Obiero[3], Emily Silzel[3], Rie Nakajima[3], William Thomas Gombrich[4], Algis Jasinskas[3], Frank Zaldivar[2,6], Sebastian Schubl[1,5], Philip L. Felgner[3], Saahir Khan[7*] and The Specimen Collection Group[1]*

[1] School of Medicine, University of California Irvine, Irvine, CA, United States, [2] Institute for Clinical and Translational Science, University of California Irvine, Irvine, CA, United States, [3] Department of Physiology and Biophysics, University of California Irvine, Irvine, CA, United States, [4] School of Biological Sciences, University of California Irvine, Irvine, CA, United States, [5] Department of Surgery, School of Medicine, University of California Irvine, Irvine, CA, United States, [6] Department of Pediatrics, University of California Irvine, Irvine, CA, United States, [7] Department of Medicine, Keck School of Medicine, University of Southern California, Los Angeles, CA, United States

OPEN ACCESS

Edited by:
Phillip Stafford, Arizona State University, United States

Reviewed by:
Maria Goossens, Sciensano, Belgium
Krupa Navalkar, Immunexpress, United States

***Correspondence:**
Saahir Khan
saahirkh@usc.edu
Philip L. Felgner
pfelgner@hs.uci.edu

†These authors have contributed equally to this work

Specialty section:
This article was submitted to Vaccines and Molecular Therapeutics, a section of the journal Frontiers in Immunology

Received: *18 November 2021*
Accepted: *14 March 2022*
Published: *12 April 2022*

Citation:
Hosseinian S, Powers K, Vasudev M, Palma AM, de Assis R, Jain A, Horvath P, Birring PS, Andary R, Au C, Chin B, Khalil G, Ventura J, Luu MK, Figueroa C, Obiero JM, Silzel E, Nakajima R, Gombrich WT, Jasinskas A, Zaldivar F, Schubl S, Felgner PL, Khan S and The Specimen Collection Group (2022) Persistence of SARS-CoV-2 Antibodies in Vaccinated Health Care Workers Analyzed by Coronavirus Antigen Microarray. Front. Immunol. 13:817345. doi: 10.3389/fimmu.2022.817345

Recent studies provide conflicting evidence on the persistence of SARS-CoV-2 immunity induced by mRNA vaccines. Here, we aim to quantify the persistence of humoral immunity following vaccination using a coronavirus antigen microarray that includes 10 SARS-CoV-2 antigens. In a prospective longitudinal cohort of 240 healthcare workers, composite SARS-CoV-2 IgG antibody levels did not wane significantly over a 6-month study period. In the subset of the study population previously exposed to SARS-CoV-2 based on seropositivity for nucleocapsid antibodies, higher composite anti-spike IgG levels were measured before the vaccine but no significant difference from unexposed individuals was observed at 6 months. Age, vaccine type, or worker role did not significantly impact composite IgG levels, although non-significant trends towards lower antibody levels in older participants and higher antibody levels with Moderna vaccine were observed at 6 months. A small subset of our cohort were classified as having waning antibody titers at 6 months, and these individuals were less likely to work in patient care roles and more likely to have prior exposure to SARS-CoV-2.

Keywords: serology, SARS-CoV-2, healthcare workers, antibodies, microarray, vaccine, mRNA

INTRODUCTION

Since the initial 2019 outbreak of the novel beta coronavirus SARS-CoV-2, rapid international spread of the COVID-19 disease has resulted in a global pandemic. In efforts to contain the spread and severity of COVID-19, the FDA approved the emergency distribution of mRNA vaccines BNT162b and mRNA1273 in December of 2020. Both vaccines provide high rates of

protective efficacy of up to 95% against the targeted virus strain following two doses administered at least 3-4 weeks apart (1, 2).

Here, we seek to analyze the persistence of SARS-CoV-2 antibody responses induced by 2-dose mRNA vaccines in a health care worker population using a coronavirus antigen microarray. This serological analysis can yield significant insight into comparative antibody responses following vaccination and natural infection. Of particular importance, binding antibodies against SARS-CoV-2 antigens have been shown to correlate strongly with neutralizing antibodies, which are a critical component of clinical immunity (3–6).

In prior studies, subjects who received two doses of mRNA vaccine developed significant levels of IgM and IgG against SARS-CoV-2 spike (S) proteins and receptor-binding domain (RBD) titers (7). Anti-spike protein IgG levels were reported to increase exponentially following initial vaccination but plateau by 21 days. After the second dose, antibody levels increased even further and remained elevated (7, 8). Recent studies provide conflicting evidence on the longitudinal efficacy of the mRNA vaccines- some studies report waning begins as early as 10 weeks (9), others show age (10), vaccine type (11), and prior exposure (11) to be significant factors in the humoral response. Others report waning over the course of 6 months (12, 13), while some report non-waning in both mRNA vaccines and non-mRNA vaccines (14, 15). Here, we evaluate the effect of these factors on humoral immunity up to 6 months following SARS-CoV-2 vaccination.

METHODS

Study Population

This study was approved by the institutional review board (IRB) of the University of California Irvine (UCI) prior to initiation of the study. Widespread mRNA vaccination of healthcare workers (HCWs) at UC Irvine Health began in December 2020, administering over 16,000 doses of mRNA1273 (Moderna Inc.) or the BNT162b (Pfizer Inc. and BioNTech Inc.) vaccines within the first 4 months. All HCWs working at the UCI Medical Center, located in Orange County CA, were invited to receive serological testing by providing serum blood samples *via* fingerstick at the time of vaccination and follow-up testing at approximately 2 months, 4 months, and 6 months post-final dose of vaccination. All blood samples were brought to the Institute for Clinical and Translational Science Core Laboratory at the UCI Medical Center. Serum samples were centrifuged using the Eppendorf 5415R and spun at 3000xg for 5 minutes. Serum was quickly transferred into a clean sterile tube and frozen at -80°C until analyzed for Igs. Reports of their serological test results were returned within 4 weeks of receiving the test. At each assessment, demographic and work-related characteristics, testing frequency, exposure risk, and symptom history were collected *via* surveys administered prior to serum sample collection. Longitudinal participation was encouraged through an aggressive email campaign as well as ensuring that participants received a report of their antibody titers, but not every subject participated at every time point. A total of 956 HCWs were recruited for longitudinal follow-up. Eligibility for this analysis was restricted to 240 HCWs who provided blood specimens and survey data at multiple time points.

Coronavirus Antigen Microarray

1,559 independent finger stick blood serum samples were collected over the 6-month period for analysis. Specimens were probed and analyzed on a coronavirus antigen microarray (CoVAM) for IgG and IgM antibodies against 37 antigens from SARS-CoV-2, other coronaviruses, and other respiratory viruses using a coronavirus antigen microarray (**eFigure 1**). The CoVAM contained 10 SARS-CoV-2 antigens including nucleocapsid protein (NP) and several varying fragments of the spike (S) protein, as well as 4 SARS, 3 MERS, 12 Common CoV, and 8 influenza antigens. A full list of antigens used in the assay can be found in **Supplementary Table 1**. Samples were tested in triplicate.

The data analysis was carried out according to the following general pipeline (see Online-Only Methods for details): For each sample, the average reactivity to the printing buffer was subtracted from each spot. The arrays were normalized according to the composite method described elsewhere (16–18). Reactivity assessment was performed using a logistic regression model consisting of a weighted combination of antigens as described elsewhere (18, 19). In summary, a generalized linear model (GLM) was built using 6 antigens (SARS.CoV.2.S1.RBD.mFc, SARS.CoV.2.Spike.RBD.His.HEK, SARS.CoV.2_S1, SARS.CoV.2.NP, SARS.CoV.2 S2, SARS.CoV.2. S1.HisTag). This model was found to be 93% sensitive and 98% specific in correctly classifying 91 PCR-positive cases and 88 pre-pandemic negative control (18, 19). The model was then used to generate a weighted composite measure of IgG reactivity on all titers, with weights corresponding to each antigen's relative importance in the model. This composite IgG reactivity measure was scaled up to represent the weighted mean fluorescence intensity (MFI) of all antigens assayed in the CoVAM. Here, we utilized a model containing all SARS-CoV-2 antigens as above with the exception of NP, as this antigen was used to classify prior exposure to SARS-CoV-2 in a subgroup analysis.

To determine the relative anti SARS-CoV-2 antibody reactive levels at the last time point, as well as to identify individuals for whom the antibody levels significantly declined, first all individuals with at least two time points were selected. Then, for each individual, the sample with the closest time point to 80 days was identified. All individuals for whom the last time point coincided with the 80 days post vaccination time point were dropped. Lastly, the individuals were classified as having waning antibodies when, the median signal intensity of all SARS-CoV-2 antigens at the final time point was lower than the median of these antigens at the closest to day 80 time point (a $p < 0.05$, Wilcoxon test, was considered significant). A boxplot of the median antibody reactivity at the last time point, for all selected individuals can be visualized on **Figure 3**. Individual demographics for either the waning or non-waning groups obtained from the consent form are listed on **Table 3**.

Statistical Analysis

In order to characterize SARS-CoV-2 antibody response over time, we fit a linear mixed effect model of the composite IgG reactivity measure using all available data from the n=240 HCWs with at least 2 time points available. Due to the variability in the timing of the tests across individuals, we report the model-estimated composite IgG reactivity means and 95% confidence intervals (CI) at pre-vaccine, 2 months, 4 months and 6 months post-first dose, and compared the changes over time. We then explored differences in long-term antibody response by individual characteristics hypothesized to influence the magnitude and durability of the vaccine-induced antibody response: sex [male or female, by self-report], age [≥55 vs. <55 years, by self-report], HCW role [patient care vs. non-patient care role], race [Asian, Latino, White, Other, by self-report], presence of obesity and/or diabetes, hypertension, vaccine type [mRNA1273 vs. BNT162b], and prior COVID-19 exposure [defined by presence of SARS-CoV-2 NP antibody reactivity at baseline]. We tested each potential moderator individually by fitting the same linear mixed effect model with the inclusion of an interaction term between that variable and time (e.g., time * age≥55 vs. <55 years). All analyses were conducted using R v4.1.1.

RESULTS

SARS-CoV-2 Antibody Levels Persist 6 Months Post-Vaccination

A total of 629 tests were collected from 240 HCWs who provided at least 2 samples (mean number of samples 2.6, range 2-6, **Table 1**). Antibody responses significantly increased in the 2 months following vaccination (mean [95% CI] composite IgG MFI: baseline: 175 [-63, 308], 2mo: 3829 [3665, 3993]; baseline to 2 months, p<0.001) and increased further at 4 months (mean [95% CI] composite IgG MFI: 4mo: 4471 [4263, 4679]; 2 to 4 months, p<0.001). Antibody levels plateaued at the 4-month timepoint; notably, we observed no evidence of significant waning from 4 to 6 months (p=0.959, **Figure 1** and **Table 2**). Comparisons by sex did not show any significant difference, although men did show a trend towards lower composite IgGs at 6 months (men vs. women at 6 months: p=0.301, **Figure 2A**). Comparisons by age showed modest waning from 4 to 6 months in the older age group who were ≥55 years; however, these differences were not statistically significant (4 to 6 months among men: p=0.949, **Figure 2B** and **Table 2**). No statistically significant differences in antibody levels were observed between participants segregated by patient care role, race, presence of obesity and/or diabetes, or affliction of hypertension (**Figures 2C–F** and **Table 2**). Similarly, no statistically significant differences in antibody levels were observed between those who received the BNT162b or mRNA1273 vaccines, although there was a non-significant trend towards higher antibody levels at 6 months with mRNA1273 (**Figure 2G**). HCWs who had evidence of prior exposure to COVID-19 as defined by NP reactivity at baseline haxd higher composite IgG levels at baseline but did not differ significantly at post-vaccine time points up to 6 months; furthermore, their antibody levels increased significantly post-vaccination (**Figure 2H**). With respect to individual antigens, vaccine-induced antibodies were directed primarily against the S1 and RBD domains of spike protein, to a lesser extent against the S2 domain, and not at all against the nucleocapsid protein as expected based on design of mRNA vaccines (**eFigures 2**–**4**).

SARS-CoV-2 Antibody Waning in Select Individuals

Although the overall reactivity did not seem to significantly wane over the observed 6-month period, as seen on **Figure 3**, a subset of study participants could be classified as having waning antibodies against SARS-CoV-2 antigens. A significant difference between individuals with waning antibodies and non-waning antibodies was identified for all SARS-CoV-2 antigens ($p < 0.05$). The observed reactivity differences are more pronounced for S1-containing antigens, although a significant difference was observed for S2 and NP antigens as well. Among 41 individuals being classified as non-waning and 58 as waning, there was no significant difference between the groups when examining age, gender, vaccine type, time since vaccination, or race (**Table 3**). However, non-waning individuals

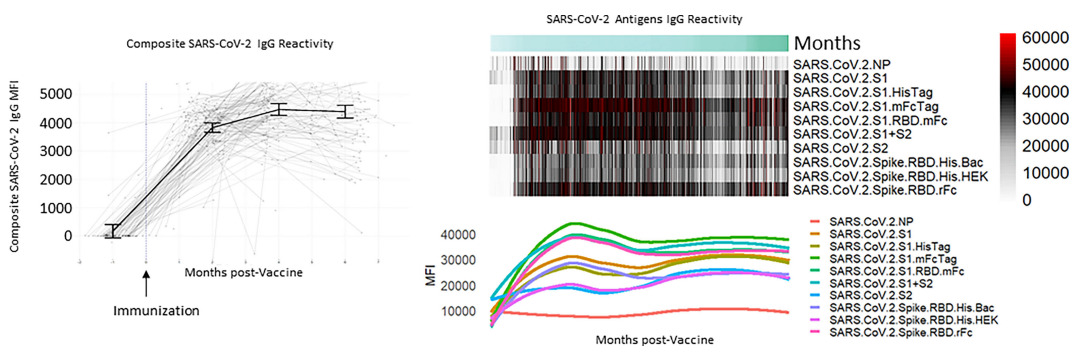

FIGURE 1 | Composite and individual SARS-CoV-2 IgG levels over time for the longitudinal cohort. Background lines (left) representing individual study participants and thick solid line representing mean antibody level at baseline, 2 months, 4 months, and 6 months with error bars representing 95% confidence intervals with heatmap and individual antibody plots.

TABLE 1 | Characteristics of study participants compared between all study participants and the longitudinal cohort who provided data at multiple time points post vaccination.

	HCWs (n=240)
No. tests	
2	152 (63%)
3	53 (22%)
4	21 (9%)
5	8 (3%)
6	6 (3%)
Gender	
Female	176 (73%)
Male	63 (26%)
Non-binary	1 (0%)
Age (years)	
20-29	52 (22%)
30-39	77 (32%)
40-49	52 (22%)
50-59	40 (17%)
60-69	20 (8%)
70+	2 (1%)
Race	
Asian	92 (38%)
White	76 (32%)
Latino	39 (16%)
Other	33 (14%)
Role	
Administrative	27 (11%)
Clinical staff	31 (13%)
Food/EVS	9 (4%)
Nurse	100 (42%)
Physician	26 (11%)
Student	22 (9%)
Other	25 (10%)
Obesity/diabetes	
BMI >30 or diabetes	47 (20%)
Neither	193 (80%)
Hypertension	
Yes	30 (13%)
No	210 (88%)
History of tobacco use	
Yes	3 (1%)
No	237 (99%)
NP reactive at baseline	
Reactive	41 (17%)
Non-reactive	199 (83%)

were less likely to work in patient care roles and were more likely to have presence of NP antibodies.

DISCUSSION

This study utilized a novel immunoassay against 10 different SARS-CoV-2 antigens to measure compositive anti-SARS-CoV-2 IgG levels amongst healthcare workers following vaccination. The test performance of SARS-CoV-2 immunoassays can vary, with more antigens correlating with a higher specificity (20, 21). The CoVAM utilizes multiple antigens to achieve test performance that compares favorably to commercially available assays (18, 22).

Using the CoVAM, we initially observed no significant decline of SARS-CoV-2 antibody levels up to 6 months after the first dose of mRNA vaccine for the general HCW population. Some prior studies show waning of SARS-CoV-2 antibody levels as soon as 10 weeks (9) or 3 months (23) following first dose of mRNA vaccine. We propose that these differences may be due to the use of more antigens in the immunoassay, which is able to detect a broader repertoire of antibodies, and the generalized linear model used to determine composite antibody level, which is able to increase the weight of antibodies specific to SARS-CoV-2. Alternatively, given the high inter-individual variability in antibody levels at all time points, it is possible that this study was underpowered to detect small differences in the antibody response across time points.

Collection of serology samples from patients who had received either the mRNA1273 or the BNT162b mRNA vaccine allowed evaluation of the relative differences in longitudinal antibody levels induced by the two vaccines. Other reports suggested that mRNA1273 may be more effective at sustaining antibody titers long-term (11). No statistically significant differences were observed in antibody responses to the two vaccines at any point time; however, at 6 months post-vaccination, subjects who received the mRNA1273 vaccine showed a non-significant trend towards higher antibody levels compared to those who received the BNT162b vaccine. A follow-up study with a larger sample size may be able to elicit whether this suggested difference is significant.

Although our overall analysis shows no significant decline in 6 months for the general HCW population, a further retrospective analysis identifies a small subset of individuals whose antibodies do in fact wane over the course of the 6 months as compared to the overall cohort. No significant difference was found between the two groups when investigating for age, gender, vaccine type, or race, but surprisingly, waning antibodies were correlated with being involved with a direct patient-care role, being defined as either a nurse, physician, student, or patient care technician. We initially hypothesized that being involved with a patient care role would result in higher, non-waning antibodies, but that is not the case in this study. It is important to note that healthcare workers not involved with patient care were still in contact with patients. In addition, the presence of the NP antibody, which is a marker for prior natural infection with SARS-CoV-2, was higher among non-waning individuals which may be driving the increased persistence of the humoral immune response in these individuals. We hypothesize that workers not involved in patient care may have had less personal protective equipment usage than patient care workers, resulting in a higher prevalence of NP antibody among non-care positions and thus having a higher, non-waning humoral response to the vaccine.

Nearly all immunocompetent individuals develop a humoral immune response following SARS-CoV-2 exposure (24–26). A fraction of our study cohort (20% of the total cohort) included subjects that had received the vaccine after previous exposure to SARS-CoV-2, assessed by presence of antibodies against nucleocapsid protein, which are only found in individuals previously exposed to the virus and not vaccinated individuals. The composite IgG antibody levels were compared between the

TABLE 2 | Composite SARS-CoV-2 IgG levels compared between time points for subgroups of study participants divided by gender, age, race, occupation role, and presence of co-morbidities.

Variable	Category	N	Composite SARS-CoV-2 IgG MFI, mean (95% CI)[a]				p-value[b]		
			Pre-vaccine	2mo	4mo	6mo	Pre vs. 2mo	2mo vs. 4mo	4mo vs. 6mo
Overall		240	175 (0, 408)	3829 (3665, 3993)	4471 (4263, 4679)	4396 (4166, 4625)	*<0.001**	*<0.001**	*0.959*
Sex[c]	Female	176	146 (0, 424)	3856 (3669, 4043)	4450 (4217, 4682)	4506 (4243, 4770)	*<0.001**	*0.001**	*0.999*
	Male	63	250 (0, 688)	3744 (3418, 4071)	4541 (4087, 4995)	3878 (3407, 4348)	*<0.001**	*0.077*	*0.430*
	Female vs. male		*0.999*	*0.999*	*0.999*	*0.301*			
Age	<55 years	196	187 (0, 453)	3814 (3635, 3992)	4515 (4282, 4748)	4524 (4265, 4784)	*<0.001**	*<0.001**	*0.999*
	≥55 years	44	122 (0, 631)	3908 (3499, 4316)	4305 (3852, 4759)	3939 (3448, 4429)	*<0.001**	*0.877*	*0.949*
	<55 years vs. ≥55 years		*0.999*	*0.999*	*0.993*	*0.434*			
Race	Asian	92	112 (0, 505)	3654 (3395, 3912)	4463 (4133, 4793)	4250 (3906, 4595)	*<0.001**	*0.009**	*0.999*
	White	76	141 (0, 518)	3846 (3544, 4149)	4136 (3768, 4503)	4365 (3969, 4762)	*<0.001**	*0.997*	*0.999*
	Latino	39	369 (0, 990)	4223 (3817, 4629)	4978 (4499, 5458)	4834 (4275, 5392)	*<0.001**	*0.501*	*0.999*
	Other	33	167 (0, 869)	3824 (3406, 4242)	4650 (4004, 5295)	4327 (3379, 5274)	*<0.001**	*0.709*	*0.999*
	By race		*0.999*	*0.999*	*<0.001**	*<0.001**			
NP reactivity	Non-reactive	199	26 (0, 191)	3712 (3595, 3828)	4413 (4196, 4630)	4362 (4118, 4606)	*<0.001**	*<0.001**	*0.999*
	Reactive	41	1093 (671, 1514)	4211 (3958, 4464)	4972 (4352, 5592)	4610 (4012, 5208)	*<0.001**	*0.388*	*0.991*
	Non-reactive vs. reactive		*0.084*	*0.435*	*0.703*	*0.995*			
Patient care	Patient care role	179	122 (-162, 407)	3755 (3573, 3938)	4436 (4186, 4685)	4320 (4041, 4599)	*<0.001**	*<0.001**	*0.998*
	Non-patient care role	61	285 (-134, 705)	4115 (3747, 4484)	4563 (4189, 4937)	4560 (4157, 4964)	*<0.001**	*0.658*	*0.999*
	By patient care role		*0.998*	*0.674*	*0.999*	*0.979*			
Hypertension	No hypertension	210	184 (-75, 444)	3839 (3666, 4012)	4543 (4315, 4771)	4415 (4161, 4669)	*<0.001**	*<0.001**	*0.995*
	Hypertension	30	102 (-465, 669)	3747 (3233, 4261)	4117 (3610, 4623)	4293 (3749, 4838)	*<0.001**	*0.964*	*0.999*
	No hypertension vs. hypertension		*0.999*	*0.999*	*0.804*	*0.999*			
Obesity/diabetes	No obesity and diabetes	193	127 (-140, 394)	3791 (3613, 3968)	4419 (4189, 4649)	4329 (4070, 4588)	*<0.001**	*<0.001**	*0.999*
	Obesity or diabetes	47	335 (-163, 833)	4029 (3603, 4455)	4710 (4227, 5194)	4646 (4148, 5145)	*<0.001**	*0.378*	*0.999*
	Any vs. none		*0.996*	*0.972*	*0.962*	*0.954*			

[a]Composite SARS-CoV-2 IgG MFI mean and 95% confidence interval bounds are post-estimated values calculated based on the fitted regression model.

[b]p-values indicate strength of evidence for change in Composite SARS-CoV-2 IgG MFI between timepoints at 2 months intervals, against a null hypothesis of no change, as estimated from Wald test on model post-estimated marginal means within each group and timepoint. Asterisks denote significant differences at p<0.05.

[c]One participant self-reported as non-binary sex and was excluded for the sex-specific analysis.

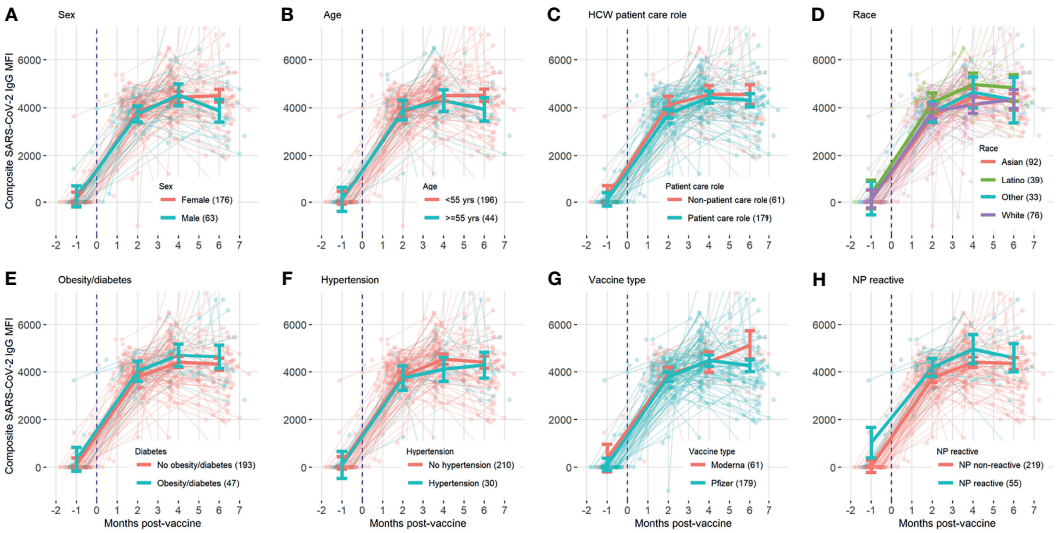

FIGURE 2 | Composite SARS-CoV-2 IgG levels over time, with background lines representing individual study participants and thick solid line representing mean antibody level at baseline, 2 months, 4 months, and 6 months with error bars representing 95% confidence intervals, compared for subgroups divided by **(A)** sex, **(B)** age, **(C)** HCW patient care role, **(D)** race, **(E)** obesity/diabetes, **(F)** hypertension, **(G)** vaccine type, and **(H)** previous exposure.

baseline NP reactive and NP non-reactive participants before and after vaccination. Participants with previous exposure to SARS-CoV-2 had higher IgG antibody levels pre-vaccine (excluding anti-NP antibodies) than participants without prior exposure. The differences in antibody levels between these groups decreased over time and were not statistically significant at any time point following vaccination. Prior studies that report differences in vaccine-induced antibody responses based on prior SARS-CoV-2 exposure focused on shorter time points at 6 to 10 weeks post vaccination (11), it is possible that with a larger sample size, this study would have detected a small difference at early post-vaccine time points, but the observed trends suggest that such a difference does not persist at later post-vaccine time points. Surprisingly, our outreach campaign revealed that many HCWs refused the vaccine due to their prior exposure, believing erroneously that prior exposure is just as effective at eliciting a humoral immune response as vaccination. Our data indicates that even in participants previously exposed to SARS-CoV-2, mRNA vaccination induces a significant increase in humoral immunity, and vaccination produces higher levels of SARS-CoV-2 antibodies compared to prior exposure, corroborating other studies that

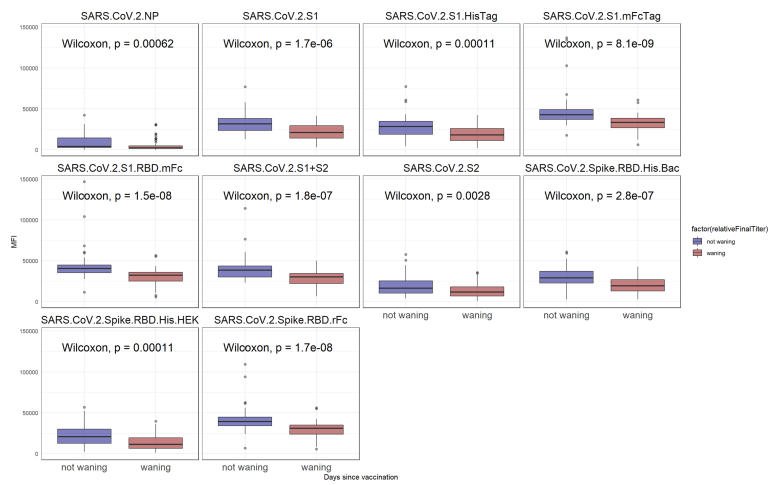

FIGURE 3 | SARS-CoV-2 reactivity after 6 months. In blue, are individuals for whom the reactivity did not significantly wane when compared to the day 80 time point. In red are samples for whom the reactivity has declined ($p < 0.05$).

TABLE 3 | Demographic variables in patients with and without waning antibody titers.

	Non-waning (n=41)	Waning (n=58)	p-value
Age	45.15	44.9	0.337
Gender			
Male	9 (21.9)	13 (22.4)	0.969
Female	31 (75.6)	44 (75.9)	
Non-binary	1 (2.4)	1 (1.7)	
Vaccine type			0.985
Moderna	5 (12.2)	7 (12.1)	
Pfizer	36 (87.8)	51 (87.9)	
Race			0.127
Asian	10 (24.4)	30 (51.7)	
White	21 (51.2)	17 (29.3)	
Latino	8 (19.5)	6 (10.3)	
Black	0 (0)	1 (1.7)	
Other	2 (4.9)	4 (6.9)	
Role			0.01*
Patient care	20 (48.8)	43 (74.1)	
Non-patient care	21 (51.2)	15 (25.9)	
NP Antigen			0.03*
Negative	29	51	
Positive	12	7	
Days since vaccine	168.41	176.91	0.262

Demographic data was obtained from survey questions on the consent form. Means are reported with percentages being reported in parenthesis. Values with an asterisk are statically significant with a p value <0.05.

have found previously infected but unvaccinated individuals to be at a higher risk for contracting severe disease compared to vaccinated individuals (27, 28).

We hypothesized that different subgroups of HCWs would have varying SARS-CoV-2 antibody levels following vaccination, with older individuals having decreasing antibody levels at later time points as observed in prior studies (10, 29, 30). While we observed a trend towards decreasing antibody levels at 6 months post vaccination in participants above the age of 55, this difference was not statistically significant. While other studies examined ages above 65, our study included very few healthcare workers older than 65, so it is possible that the lower age threshold and limited sample size resulted in insufficient power to detect age-related antibody waning. We also stratified healthcare workers by role, hypothesizing that those in patient care roles may have higher antibody levels throughout the 6-month period due to potential exposure to patients with COVID-19. Our data did not show any significant evidence to suggest that patient care role influences antibody levels in the healthcare worker population, suggesting that current approaches to infection prevention among staff in healthcare facilities are effective.

This study is particularly relevant to defining the optimal timing and target populations for additional doses of mRNA vaccine beyond the initial 2-dose series in order to sustain long-term immunity to SARS-CoV-2. Among a cohort of generally immunocompetent healthcare workers, there were some individuals whose antibody levels significantly waned over the course of 6 months. These individuals would likely benefit the most from early administration of additional doses of mRNA vaccine, but further studies are needed to define the optimal approach to identify these individuals with waning antibody levels and to characterize the magnitude of differences in antibody levels that correlate with reduction in clinical immunity.

DATA AVAILABILITY STATEMENT

The datasets presented in this study can be found in online repositories. The names of the repository/repositories and accession number(s) can be found below: GEO Data Repository, GSE199668.

ETHICS STATEMENT

The studies involving human participants were reviewed and approved by Institutional Review Board of University of California Irvine. The patients/participants provided their written informed consent to participate in this study.

SPECIMEN COLLECTION GROUP

Ariana Naaseh, Ava Runge, Shannon Skochko, Steven Tohmasi, Olivia Tsai, Justine Chinn, Jessica Colin Escobar, Christina Grabar, Amanda Leung, and Fjolla Muqolli.

AUTHOR CONTRIBUTIONS

SH, KP, MV, PB, RA, CA, BC, GK, JV, MK, SS, PF, and SK conceived and designed research. SH, KP, MV, PB, RA, CA, BC,

GK, JV, and ML collected samples. PH and FZ prepared and stored samples. PF and SK designed the microarray. RDA, AaJ, JO, ES, RN, AlJ, and WG constructed the microarray and probed samples. AP and RA analyzed data. SH, KP, MV, AP, RDA, SS, PF, and SK interpreted results of data. AP and RA prepared figures. SH, KP, MV, AP, RDA, PB, ML, and SK drafted the manuscript. SH, KP, MV, AP, RA, FZ, and SK edited and revised manuscript. SH, SS, PF, and SK obtained funding for the project. All authors approved final version of the manuscript.

FUNDING

This work was supported by two intramural research grants from the COVID-19 Basic, Translational, and Clinical Research Fund of the University of California Irvine and by the Emergency COVID-19 Research Seed Funding Opportunity from the University of California Office of the President [research grants R00RG2646, R01RG3745]. This work was supported by a grant from the Surgical Infection Society Foundation. Research reported in this publication was supported by The Institute for Clinical and Translational Science of the National Institutes of Health under award number T35DK128788. SK was supported by the National Center for Research Resources and the National Center for Advancing Translational Sciences of the National Institutes of Health [grant KL2 TR001416]. The project described was supported by the National Center for Research Resources and the National Center for Advancing Translational Sciences of the National Institutes of Health [grant UL1 TR001414]. The initial design and construction of the CoVAM was supported by the Prometheus-UMD contract sponsored by the Defense Advanced Research Projects Agency (DARPA) BTO under the auspices of Col. Matthew Hepburn [agreements N66001-17-2-4023, N66001-18-2-4015]. The findings and conclusions in this report are those of the authors and do not necessarily represent the official position or policy of the funding agencies and no official endorsements should be inferred.

REFERENCES

1. Baden LR, El Sahly HM, Essink B, Kotloff K, Frey S, Novak R, et al. Efficacy and Safety of the mRNA-1273 SARS-CoV-2 Vaccine. *N Engl J Med* (2021) 384 (5):403–16. doi: 10.1056/NEJMoa2035389
2. Polack FP, Thomas SJ, Kitchin N, Absalon J, Gurtman A, Lockhart S, et al. Safety and Efficacy of the BNT162b2 mRNA Covid-19 Vaccine. *N Engl J Med* (2020) 383(27):2603–15. doi: 10.1056/NEJMoa2034577
3. Rubio-Acero R, Castelletti N, Fingerle V, Olbrich L, Bakuli A, Wolfel R, et al. In Search of the SARS-CoV-2 Protection Correlate: Head-To-Head Comparison of Two Quantitative S1 Assays in Pre-Characterized Oligo-/Asymptomatic Patients. *Infect Dis Ther* (2021) 10:1–14. doi: 10.1007/s40121-021-00475-x
4. Khoury DS, Cromer D, Reynaldi A, Schlub TE, Wheatley AK, Juno JA, et al. Neutralizing Antibody Levels Are Highly Predictive of Immune Protection From Symptomatic SARS-CoV-2 Infection. *Nat Med* (2021) 27(7):1205–11. doi: 10.1038/s41591-021-01377-8
5. Poland GA, Ovsyannikova IG, Kennedy RB. SARS-CoV-2 Immunity: Review and Applications to Phase 3 Vaccine Candidates. *Lancet* (2020) 396 (10262):1595–606. doi: 10.1016/S0140-6736(20)32137-1
6. Letizia AG, Ge Y, Vangeti S, Goforth C, Weir DL, Kuzmina NA, et al. SARS-CoV-2 Seropositivity and Subsequent Infection Risk in Healthy Young Adults: A Prospective Cohort Study. *Lancet Respir Med* (2021) 9(7):712–20. doi: 10.1016/S2213-2600(21)00158-2
7. Wang Z, Schmidt F, Weisblum Y, Muecksch F, Barnes CO, Finkin S, et al. mRNA Vaccine-Elicited Antibodies to SARS-CoV-2 and Circulating Variants. *bioRxiv* (2021) 592:616–22. doi: 10.3410/f.739524179.793585051
8. Wisnewski AV, Campillo Luna J, Redlich CA. Human IgG and IgA Responses to COVID-19 mRNA Vaccines. *PloS One* (2021) 16(6):e0249499. doi: 10.1371/journal.pone.0249499
9. Shrotri M, Navaratnam AMD, Nguyen V, Byrne T, Geismar C, Fragaszy E, et al. Spike-Antibody Waning After Second Dose of BNT162b2 or Chadox1. *Lancet* (2021) 398(10298):385–7. doi: 10.1016/S0140-6736(21)01642-1
10. Tsatsakis A, Vakonaki E, Tzatzarakis M, Flamourakis M, Nikolouzakis TK, Poulas K, et al. Immune Response (IgG) Following Full Inoculation With BNT162b2 COVID19 mRNA Among Healthcare Professionals. *Int J Mol Med* (2021) 48(5):200. doi: 10.3892/ijmm.2021.5033
11. Steensels D, Pierlet N, Penders J, Mesotten D, Heylen L. Comparison of SARS-CoV-2 Antibody Response Following Vaccination With BNT162b2 and mRNA-1273. *JAMA* (2021) 326:1463–544. doi: 10.1001/jama.2021.15125

ACKNOWLEDGMENTS

We thank Joshua Alger and Rodrigo Romo of UCI's Institute for Clinical and Translational Science for their assistance in maintaining sample integrity. We thank Yannik Cadin for helping with the microarray mean fluorescence intensity quantification.

SUPPLEMENTARY MATERIAL

The Supplementary Material for this article can be found online at: https://www.frontiersin.org/articles/10.3389/fimmu.2022.817345/full#supplementary-material

Supplementary Table 1 | List of antigens used in SARS-CoV-2 microarray.

Supplementary Figure 1 | Content of coronavirus antigen microarray with representative microarray images for different time points.

Supplementary Figure 2 | Antigen-specific SARS-CoV-2 IgG levels over time, with background lines representing individual study participants and thick solid line representing mean antibody level at baseline, 2 months, 4 months, and 6 months with error bars representing 95% confidence intervals, for **(A)** NP, **(B)** S1+S2, and **(C)** S2 antigens.

Supplementary Figure 3 | Antigen-specific SARS-CoV-2 IgG levels over time, with background lines representing individual study participants and thick solid line representing mean antibody level at baseline, 2 months, 4 months, and 6 months with error bars representing 95% confidence intervals, for **(A)** S1, **(B)** S1 with His tag, and **(C)** S1 with mouse Fc tag antigens.

Supplementary Figure 4 | Antigen-specific SARS-CoV-2 IgG levels over time, with background lines representing individual study participants and thick solid line representing mean antibody level at baseline, 2 months, 4 months, and 6 months with error bars representing 95% confidence intervals, for **(A)** RBD with His tag produced in HEK-293 cells, **(B)** RBD with rabbit Fc tag, **(C)** RBD with mouse Fc tag, and d) RBD with His tag produced in baculovirus antigens.

Supplementary Figure 5 | SARS-CoV-2 reactivity after 6 months. Blue lines indicate individuals for whom reactivity did not significantly wane when compared to the last time point recorded, in red are samples for whom the reactivity has declined ($P < 0.05$).

12. Levin EG, Lustig Y, Cohen C, Fluss R, Indenbaum V, Amit S, et al. Waning Immune Humoral Response to BNT162b2 Covid-19 Vaccine Over 6 Months. *N Engl J Med* (2021) 385:e84. doi: 10.1056/NEJMoa2114583
13. Chemaitelly H, Tang P, Hasan MR, AlMukdad S, Yassine HM, Benslimane FM, et al. Waning of BNT162b2 Vaccine Protection Against SARS-CoV-2 Infection in Qatar. *N Engl J Med* (2021) 385:e83. doi: 10.1101/2021.08.25.21262584
14. Zhong D, Xiao S, Debes AK, Egbert ER, Caturegli P, Colantuoni E, et al. Durability of Antibody Levels After Vaccination With mRNA SARS-CoV-2 Vaccine in Individuals With or Without Prior Infection. *JAMA* (2021) 326 (24):2524–6. doi: 10.1001/jama.2021.19996
15. Flaxman A, Marchevsky NG, Jenkin D, Aboagye J, Aley PK, Angus B, et al. Reactogenicity and Immunogenicity After a Late Second Dose or a Third Dose of ChAdOx1 nCoV-19 in the UK: A Substudy of Two Randomised Controlled Trials (COV001 and COV002). *Lancet* (2021) 398(10304):981–90. doi: 10.1016/S0140-6736(21)01699-8
16. Ball C, Brazma A, Causton H, Chervitz S, Edgar R, Hingamp P, et al. Standards for Microarray Data: An Open Letter. *Environ Health Perspect* (2004) 112(12):A666–7. doi: 10.1289/ehp.112-1277123
17. Bolstad N, Warren DJ, Nustad K. Heterophilic Antibody Interference in Immunometric Assays. *Best Pract Res Clin Endocrinol Metab* (2013) 27 (5):647–61. doi: 10.1016/j.beem.2013.05.011
18. de Assis RR, Jain A, Nakajima R, Jasinskas A, Felgner J, Obiero JM, et al. Analysis of SARS-CoV-2 Antibodies in COVID-19 Convalescent Blood Using a Coronavirus Antigen Microarray. *bioRxiv* (2020) 12:6. doi: 10.1101/2020.04.15.043364
19. Khan S, Nakajima R, Jain A, de Assis RR, Jasinskas A, Obiero JM, et al. Analysis of Serologic Cross-Reactivity Between Common Human Coronaviruses and SARS-CoV-2 Using Coronavirus Antigen Microarray. *bioRxiv* (2020). doi: 10.1101/2020.03.24.006544
20. Kohmer N, Westhaus S, Ruhl C, Ciesek S, Rabenau HF. Brief Clinical Evaluation of Six High-Throughput SARS-CoV-2 IgG Antibody Assays. *J Clin Virol* (2020) 129:104480. doi: 10.1016/j.jcv.2020.104480
21. Choe PG, Kang CK, Suh HJ, Jung J, Kang E, Lee SY, et al. Antibody Responses to SARS-CoV-2 at 8 Weeks Postinfection in Asymptomatic Patients. *Emerg Infect Dis* (2020) 26(10):2484–7. doi: 10.3201/eid2610.202211
22. Assis R, Jain A, Nakajima R, Jasinskas A, Khan S, Davies H, et al. Distinct SARS-CoV-2 Antibody Reactivity Patterns in Coronavirus Convalescent Plasma Revealed by a Coronavirus Antigen Microarray. *Sci Rep* (2021) 11 (1):7554. doi: 10.1038/s41598-021-87137-7
23. Favresse J, Bayart JL, Mullier F, Elsen M, Eucher C, Van Eeckhoudt S, et al. Antibody Titres Decline 3-Month Post-Vaccination With BNT162b2. *Emerg Microbes Infect* (2021) 10(1):1495–8. doi: 10.1080/22221751.2021.1953403
24. Grifoni A, Weiskopf D, Ramirez SI, Mateus J, Dan JM, Moderbacher CR, et al. Targets of T Cell Responses to SARS-CoV-2 Coronavirus in Humans With COVID-19 Disease and Unexposed Individuals. *Cell* (2020) 181(7):1489–501.e15. doi: 10.1016/j.cell.2020.05.015
25. Suthar MS, Zimmerman MG, Kauffman RC, Mantus G, Linderman SL, Hudson WH, et al. Rapid Generation of Neutralizing Antibody Responses in COVID-19 Patients. *Cell Rep Med* (2020) 1(3):100040. doi: 10.1016/j.xcrm.2020.100040
26. Robbiani DF, Gaebler C, Muecksch F, Lorenzi JCC, Wang Z, Cho A, et al. Convergent Antibody Responses to SARS-CoV-2 in Convalescent Individuals. *Nature* (2020) 584(7821):437–42. doi: 10.1038/s41586-020-2456-9
27. Cavanaugh AM, Spicer KB, Thoroughman D, Glick C, Winter K. Reduced Risk of Reinfection With SARS-CoV-2 After COVID-19 Vaccination - Kentucky, May-June 2021. *MMWR Morb Mortal Wkly Rep* (2021) 70 (32):1081–3. doi: 10.15585/mmwr.mm7032e1
28. Gazit S, Shlezinger R, Perez G, Lotan R, Peretz A, Ben-Tov A, et al. Comparing SARS-CoV-2 Natural Immunity to Vaccine-Induced Immunity: Reinfections Versus Breakthrough Infections. *medRxiv* (2021) 2021.08.24.21262415. doi: 10.1101/2021.08.24.21262415
29. Muller L, Andree M, Moskorz W, Drexler I, Walotka L, Grothmann R, et al. Age-Dependent Immune Response to the Biontech/Pfizer BNT162b2 COVID-19 Vaccination. *Clin Infect Dis* (2021) 73:2065–72. doi: 10.1101/2021.03.03.21251066
30. Collier DA, Ferreira I, Kotagiri P, Datir RP, Lim EY, Touizer E, et al. Age-Related Immune Response Heterogeneity to SARS-CoV-2 Vaccine BNT162b2. *Nature* (2021) 596(7872):417–22. doi: 10.1038/s41586-021-03739-1

Author Disclaimer: The findings and conclusions in this report are those of the authors and do not necessarily represent the official position or policy of the University of California. The content is solely the responsibility of the authors and does not necessarily represent the official views of the NIH.

Conflict of Interest: The coronavirus antigen microarray is intellectual property of the Regents of the University of California that is licensed for commercialization to Nanommune Inc. (Irvine, CA), a private company for which PF is the largest shareholder and several co-authors (RA, AaJ, RN, and SK) also own shares. Nanommune Inc. has a business partnership with Sino Biological Inc. (Beijing, China) which expressed and purified the antigens used in this study. KP is invested in mutual funds that have either Pfizer or Moderna holdings: American Funds Fundamental, Federated Hermes Kaufman Fund, and Fidelity Biotechnology Fund.

The remaining authors declare that the research was conducted in the absence of any commercial or financial relationships that could be construed as a potential conflict of interest.

Publisher's Note: All claims expressed in this article are solely those of the authors and do not necessarily represent those of their affiliated organizations, or those of the publisher, the editors and the reviewers. Any product that may be evaluated in this article, or claim that may be made by its manufacturer, is not guaranteed or endorsed by the publisher.

frontiers | Frontiers in Immunology

ORIGINAL RESEARCH
published: 13 April 2022
doi: 10.3389/fimmu.2022.797918

BNT162b2, mRNA-1273, and Sputnik V Vaccines Induce Comparable Immune Responses on a Par With Severe Course of COVID-19

Anna Kaznadzey[1,2*†], *Maria Tutukina*[2,3,4†], *Tatiana Bessonova*[4], *Maria Kireeva*[1] *and Ilya Mazo*[1,5]

[1] VirIntel, LLC, Gaithersburg, MD, United States, [2] Institute for Information Transmission Problems, Russian Academy of Sciences (RAS), Moscow, Russia, [3] Department of Molecular and Cellular Biology, Skolkovo Institute of Science and Technology, Moscow, Russia, [4] Institute of Cell Biophysics, Russian Academy of Sciences (RAS), Federal Research Center, Puschino Scientific Center for Biological Research of the Russian Academy of Sciences (FRC PSCBR RAS), Pushchino, Russia, [5] Argentys Informatics, LLC, Gaithersburg, MD, United States

OPEN ACCESS

Edited by:
Nitin Saksena,
Australia, Australia

Reviewed by:
Julian Braun,
Charité Universitätsmedizin Berlin, Germany
Yury Goltsev,
Stanford University, United States

***Correspondence:**
Anna Kaznadzey
anna.kaznadzey@virintel.com

†These authors have contributed equally to this work and share first authorship

Specialty section:
This article was submitted to Vaccines and Molecular Therapeutics, a section of the journal Frontiers in Immunology

Received: 19 October 2021
Accepted: 23 March 2022
Published: 13 April 2022

Citation:
Kaznadzey A, Tutukina M, Bessonova T, Kireeva M and Mazo I (2022) BNT162b2, mRNA-1273, and Sputnik V Vaccines Induce Comparable Immune Responses on a Par With Severe Course of COVID-19. Front. Immunol. 13:797918. doi: 10.3389/fimmu.2022.797918

Vaccines against the severe acute respiratory syndrome coronavirus 2, which have been in urgent need and development since the beginning of 2020, are aimed to induce a prominent immune system response capable of recognizing and fighting future infection. Here we analyzed the levels of IgG antibodies against the receptor-binding domain (RBD) of the viral spike protein after the administration of three types of popular vaccines, BNT162b2, mRNA-1273, or Sputnik V, using the same ELISA assay to compare their effects. An efficient immune response was observed in the majority of cases. The obtained ranges of signal values were wide, presumably reflecting specific features of the immune system of individuals. At the same time, these ranges were comparable among the three studied vaccines. The anti-RBD IgG levels after vaccination were also similar to those in the patients with moderate/severe course of the COVID-19, and significantly higher than in the individuals with asymptomatic or light symptomatic courses of the disease. No significant correlation was observed between the levels of anti-RBD IgG and sex or age of the vaccinated individuals. The signals measured at different time points for several individuals after full Sputnik V vaccination did not have a significant tendency to lower within many weeks. The rate of neutralization of the interaction of the RBD with the ACE2 receptor after vaccination with Sputnik V was on average slightly higher than in patients with a moderate/severe course of COVID-19. The importance of the second dose administration of the two-dose Sputnik V vaccine was confirmed: while several individuals had not developed detectable levels of the anti-RBD IgG antibodies after the first dose of Sputnik V, after the second dose the antibody signal became positive for all tested individuals and raised on average 5.4 fold. Finally, we showed that people previously infected with SARS-CoV-2 developed high levels of antibodies, efficiently neutralizing interaction of RBD with ACE2 after the first dose of Sputnik V, with almost no change after the second dose.

Keywords: COVID-19, vaccine, BNT162b2, MRNA-1273, Sputnik V

INTRODUCTION

In March 2020, the World Health Organization declared the disease caused by a virus from the Coronaviridae family (1), known as the severe acute respiratory syndrome coronavirus 2 (SARS-CoV-2), a pandemic. At the time, there were 20 thousand registered cases of SARS-CoV-2 disease (COVID-19) with less than a thousand deaths. As of March 2022, over 440 million cases are reported with over 6 million deaths registered worldwide.

By March 19th, 2020, the global pharmaceutical industry announced a major commitment to address COVID-19. Vaccines, which have been in development since then, are intended to provide acquired immunity against SARS-CoV-2 among the world population and help conquer the pandemic. Knowledge about the structure and function of coronaviruses causing diseases like severe acute respiratory syndrome (SARS) and Middle East respiratory syndrome (MERS) (2, 3) aided the accelerated development of various vaccine technologies. Currently, several COVID-19 vaccines have demonstrated efficacy as high as 95% and more during Phase III trials (4–7). As of March 2022, over 10.8 billion doses of COVID-19 vaccines have been administered worldwide. The following vaccines were authorized by at least one national regulatory authority for public use: RNA vaccines (Pfizer–BioNTech BNT162b2, and Moderna mRNA-1273), conventional inactivated vaccines (Sinopharm BBIBP-CorV, Chinese Academy of Medical Sciences vaccine, CoronaVac, Covaxin, WIBP-CorV, CoviVac, COVIran Barakat, Minhai-Kangtai, and QazVac), viral vector vaccines (Oxford–AstraZeneca AZD1222, Gamaleya Sputnik V, Gamaleya Sputnik Light, Convidecia Ad5-nCoV, and Janssen-Johnson & Johnson Ad26.COV2.S), and protein subunit or peptide vaccines (EpiVacCorona, RBD-Dimer ZF2001, Abdala, and Soberana 02). Over three hundred vaccine candidates are at various stages of development (details available at https://www.who.int/publications/m/item/draft-landscape-of-covid-19-candidate-vaccines).

A vaccine typically contains an agent that resembles a disease-causing microorganism. It stimulates the immune system to define the agent as a threat to recognize and destroy it in the future (8). Although COVID-19 vaccines do not provide sterilizing immunity in every case, it has been shown that even with breakthrough infections, the viral load in vaccinated individuals is significantly decreased (9) and the risks of transmitting the infection appear to be several times as low (10–12). One of the main immune system responses to vaccines is production of antibodies. It is thus of interest to compare the antibody development characteristics in response to vaccines of various types.

Moderna mRNA-1273 and Pfizer–BioNTech BNT162b2 are RNA vaccines composed of nucleoside-modified mRNA encoding an altered version of the spike protein of SARS-CoV-2, which is encapsulated in lipid nanoparticles (13, 14). Gamaleya Sputnik V, or Gam-COVID-Vac, is a viral two-vector vaccine based on two strains of common cold human adenoviruses, Ad26 and Ad5, also containing a gene encoding the SARS-CoV-2 spike protein (15). All three vaccines require two-part administration, with a booster dose suggested in six months.

The spike (S) glycoprotein in its trimeric form is in charge of the initial interaction of the virus with the receptors of the host cell. S-protein consists of two subunits, S1 and S2, separated by the furin protease cleavage site. Cleavage of the spike protein at this site facilitates viral entry into the cell, and occurs only in SARS-CoV-2, not SARS or MERS, possibly being one of the reasons for the higher infectivity of the former (16). Receptor binding domain (RBD) is a part of the S1 subunit, represented by aminoacids from 333 to 527, that binds the angiotensin converting enzyme 2 (ACE2) receptor on the cell surface. Particular amino acids directly involved in this interaction are 438-506 (RBM) (17). Several structural studies indicated that SARS-CoV-2 has stronger affinity for the ACE2 receptor than SARS (18).

The RBD is known to stimulate production of the IgG antibodies which can bind to the virus and prevent it from attaching to the human ACE2 receptors (19–22), thus anti-RBD IgG are often called neutralizing antibodies. In recent studies, it was shown that about a third of samples from individuals with previous SARS-CoV-2 infection do not seem to contain a detectable amount of the neutralizing antibodies, and that their low or absent titers positively correlate with the possibility of critical illness (patient death) (23). This allows to suggest that obtaining a high level of neutralizing antibodies is a preferable outcome of a vaccination.

In this work, we compared development of the IgG antibodies in different individuals as an immune system response after vaccination with Pfizer–BioNTech, Moderna, or Sputnik V, using a unified ELISA-based assay previously developed in our laboratory. This assay simultaneously tests for antibodies to two types of viral antigens, nucleocapsid protein (N) and RBD (24). To assess the serum neutralization capabilities in individuals vaccinated by Sputnik V, we tested the ability of the respective serum to prevent RBD from binding to the ACE2 receptor, and compared it with that in previously infected patients. We also analyzed the levels of the anti-RBD IgG antibodies developed after vaccination and previous infection with COVID-19, studying groups of patients with light/asymptomatic or moderate/severe courses of the disease. For several patients, we have performed the test multiple times after the vaccination, to reveal the tendency for the antibody levels to drop or raise over time. Finally, we assessed the levels of the anti-RBD IgG antibodies in vaccinated patients who have had COVID-19 prior to vaccination at different time points, as well as the ability of their serum to neutralize interaction with ACE2.

MATERIALS AND METHODS

Samples

For the vaccine comparison analysis, 79 serum samples from vaccinated individuals were used; 18 samples were obtained from people vaccinated by both doses of BNT162b2 (Pfizer–BioNTech), 16 from vaccinated by both doses of mRNA-1273 (Moderna) and 58 samples from 40 people vaccinated by the

Sputnik V (Gam-COVID-Vac, Gamaleya), including 18 samples taken after the first administration of the vaccine and 40 after the second (**Supplementary Table S1**). The interval between first and second dose of the vaccine was 3 weeks in all cases. In the study comparing effects of the first and the second dose of Sputnik V, the samples were taken exactly 3 weeks after administration of each dose. In all other cases, sampling was performed 2-10 weeks after administration of the second dose of a vaccine or after recovery from the SARS-CoV-2 infection.

To compare the levels of anti-RBD levels within the same individuals over time, additional samples from 17 Sputnik V vaccinated individuals were taken 7-30 weeks after the vaccination.

For the comparison of vaccine-induced and disease-induced antibody development effects serum samples from 40 COVID-19 patients were used, with infection confirmed by RT-PCR, antigen tests, or alternative commercial SARS-CoV-2 antibody tests. Of these, 20 samples belonged to a group of patients with asymptomatic/light course of the disease (who had experienced only anosmia, fatigue, headache, fever below 37.5 C, or had no symptoms), and 20 samples belonged to a group with moderate/severe course of the disease (who had experienced fever above 37.5 C, cough, lung lesions, and, in several cases, were hospitalized) (**Supplementary Table S1**).

For the neutralization effect study 38 samples from individuals vaccinated with Sputnik V and 16 samples of previously infected individuals (8 samples from asymptomatic/light symptom group and 8 samples from moderate/severe symptom group) were used.

For the study of vaccinated individuals who previously encountered COVID-19 four additional samples were taken, with infection confirmed by RT-PCR or antigen tests.

Blood samples were taken with either venipuncture in a commercial certified laboratory, or with finger prick using 20µl Mitra Cartridge (2-Sampler, Neoteryx, USA) according to the manufacturer's protocol.

As negative controls, 8 pre-pandemic samples were used, tested HIV- and hepatitis-negative, provided by the Laboratory of cell cultures and cell engineering of the Institute of Cell Biophysics RAS.

All procedures were approved by the Commission on Biosafety and Bioethics (Institute of Cell Biophysics – Pushchino Scientific Center for Biological Research of the Russian Academy of Sciences, Permission no. 1 of June 12, 2020) in accordance with Directive 2010/63/EU of the European Parliament. The patients/participants provided their written informed consent to participate in this study.

Dual-Antigen Testing ELISA Assay

The signal of anti-RBD and anti-N IgG antibodies in the samples was analyzed using the dual-antigen VirIntel assay (24). ELISA was made as described in (20) with minor modifications. In brief, the wells of the plate were filled with 98 µL of PBS-T containing 1% casein (1× Casein in PBS ready to use solution (#37528, Thermo Fisher Scientific, USA) with 0.1% TWEEN-20 added). Then, 2 µL of each sample was added to each well, and the plate was incubated for 2 h at 23°C (RT). If a sample was collected with finger prick, then 200 µL of PBS-T containing 1% casein was added, and blood was extracted *via* the 1-hour incubation at 37°C and constant shaking. Then 70 µL of the resulting sample was added to each well. After 3 washes with 300 µL of PBS-T, 100 µL of anti-human IgG HRP-conjugated secondary antibody (A01854, GenScript, USA) diluted 1:3000 in PBS-T+1% casein was added to the wells. The plate was incubated for 1 h at 23°C (RT), washed three times with PBS-T and stained with SigmaFast OPD (P9187, Sigma, USA). The resulting absorbance was measured on a Biotek Synergy H1 plate reader (Biotek Instruments, USA) at 490 nm. Each sample was assayed in duplicate.

ELISA Result Analysis

The antibody level for each individual was determined by comparison of the obtained optical density value of the respective sample to the threshold of the assay, as specified in the VirIntel test protocol (24). The ratio of the signal to the threshold for each sample is referred to as the "signal to cut-off ratio" (S/CO) and the result is considered positive if the S/CO is above 1.

Throughout the study, the S/CO for antibodies to both RBD and N antigens were measured for each sample. All three types of studied vaccines (Moderna mRNA-1273, Pfizer–BioNTech BNT162b2 and Gamaleya Sputnik V) are based on the spike protein of the SARS-CoV-2 and were expected to yield antibody production only to the RBD antigen. If the results from the assay were also positive for the N-antigen, we presumed that the respective individual had encountered COVID-19 in the past, during or after the vaccination process. These samples were excluded from further analysis unless otherwise specified within the Results and Discussion sections.

Neutralization Assay

The ability of serum to inhibit the RBD binding to ACE2 receptor was measured using the SARS-CoV-2 Surrogate Virus Neutralization Test (sVNT) Kit (ProteoGenix, France) according to the manufacturer's protocol.

Statistical Analysis

The statistical significance calculations were done and respective P-values were obtained using the Mann-Whitney U test for comparison of S/CO value distributions between different sets of samples, and using Spearman's correlation coefficient method for estimating the S/CO difference after first and second administrations of the vaccine in individuals within the Sputnik V vaccinated group, and for assessing correlation between individual's age and S/CO. P-value of < 0.05 was used as a threshold for statistical significance evaluation.

RESULTS

Antibody Signal for the Sputnik V Vaccinated Individuals After the First and the Second Doses

To analyze the levels of immune response after the first and the second vaccine doses, 18 Sputnik V vaccinated individuals were

tested twice: shortly before second vaccination and two to three weeks after. Three tested individuals with highest levels of anti-RBD antibodies were also positive for the anti-N antibodies, which might indicate previous infection with SARS-CoV-2. One more individual had shown positive anti-N results after the second dose, presumably having been infected between the doses. After eliminating these four samples from the dataset, 14 results were left to compare and are shown on **Figure 1**. Of them, 11 demonstrated positive results for the anti-RBD antibodies after the first dose, with S/CO ratio ranging from 1.21 to 7.45 with an average of 3.31 and a median of 2.62. Three patients tested RBD-negative after the first dose of Sputnik. After two doses all 14 patients were tested positive, ranging from 4 to 16.06. The average signal was 9.59, the median 9.65.

Overall, the difference between the S/CO result distributions in samples after the first and second dose of Sputnik vaccination as measured by Mann-Whitney test was very prominent (P-value 2.67 × 10−05). The S/CO after the second dose was on average 5.4 times higher (**Figure 1**). At the same time, Spearman's coefficient analysis showed that there was no significant correlation between the signal after the first and second dose within individuals (P-value 0.39); for some individuals the signal raised much more drastically (for example, for V15 on **Figure 1**) than for others (V11 on **Figure 1**).

Antibody Signal for the Individuals After Two-Dose Vaccination by Sputnik V, Moderna, Pfizer-BioNtech, and Previously Infected Individuals

In all 40 cases of the Sputnik V-vaccinated individuals tested after the second dose, positive results for the anti-RBD antibodies were demonstrated (**Figures 1** and **2**). However, the S/CO ranged dramatically, with values between 1.06 and 21.0, with the average of 10.95 and median of 11.07.

Reasonably, highest levels of antibodies were detected in the individuals with positive S/CO for anti-N antibodies. There were 8 such cases, with respective S/CO for the anti-RBD antibodies ranging from 10.51 to 20.52, with an average of 15.1 and a median of 13.7. We excluded these cases from further analysis here. The 32 remaining Sputnik V two-dose vaccinated samples demonstrated results with an average of 9.53 and a median of 9.51. The record case was a S/CO of 21.0.

For the Pfizer-BioNTech vaccinated individuals, 18 out of 18 cases showed positive anti-RBD antibody results (**Figure 2**). 3 cases demonstrated positive results for the anti-N antibodies, and were further excluded (the respective S/CO for the anti-RBD antibodies in these cases were high, 15.73, 12.92, and 13.06). The resulting range was between 4.98 and 27.63, with the average of 11.99 and median 10.27. The record case was a S/CO of 27.63, the highest result obtained in the whole study.

All 16 Moderna-vaccinated individuals were anti-RBD antibody positive, with one further excluded positive anti-N case with the S/CO for anti-RBD antibodies of 23.72. The range was between 4.95 and 20.37, with an average of 11.32 and a median of 10.01 (**Figure 2**). The record case was a S/CO of 20.37.

All 40 studied cases of previously infected individuals (who have not been vaccinated) also demonstrated above-threshold results for the RBD antibodies (**Figure 2**). The average S/CO was 4.69, ranging from 1.01 to 17.03, with a median of 3.10. The patients in our study consisted of two groups, 20 individuals each: a group with moderate or severe symptoms, and a group with light symptoms or a completely asymptomatic course of the disease. The first group had an average S/CO of 2.22 (ranging from 1.01 to 7.07, with a median of 1.7), and the second group had an average S/CO of 7.08 (ranging from 1.52 to 17.03, with a median of 5.88). As measured by the Mann-Whitney test, we observed a significant difference between these signal distributions (P-value 1.3 × 10 −05), in consistency with our previous studies (25).

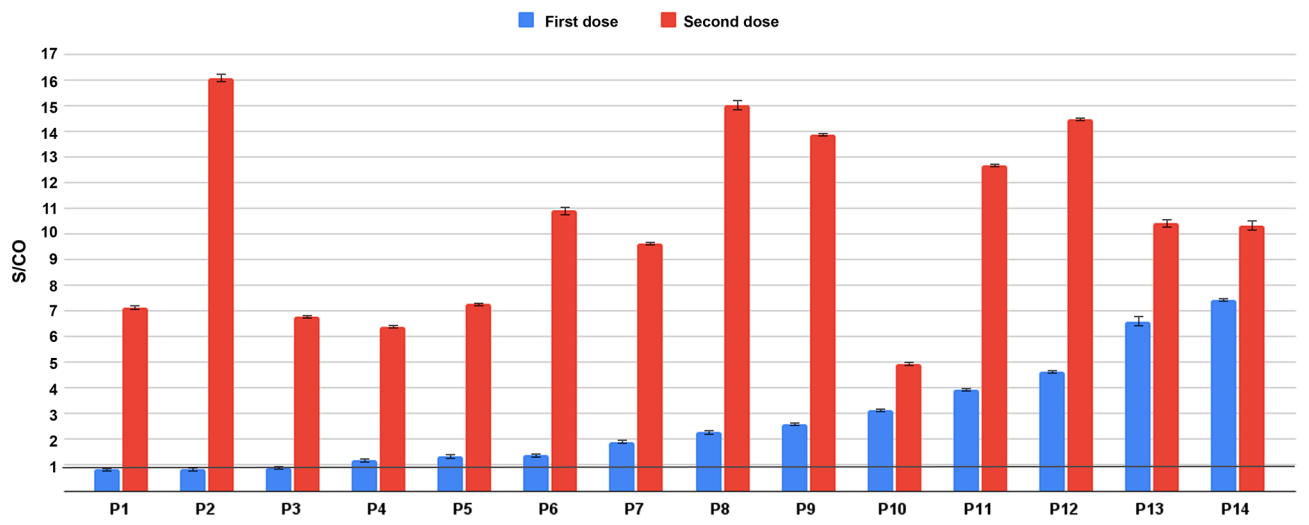

FIGURE 1 | Comparison of S/CO of IgG anti-RBD antibodies in individuals after first (blue) and second (red) administration of the Sputnik V vaccine. Threshold S/CO value is 1 and is indicated with a black horizontal line.

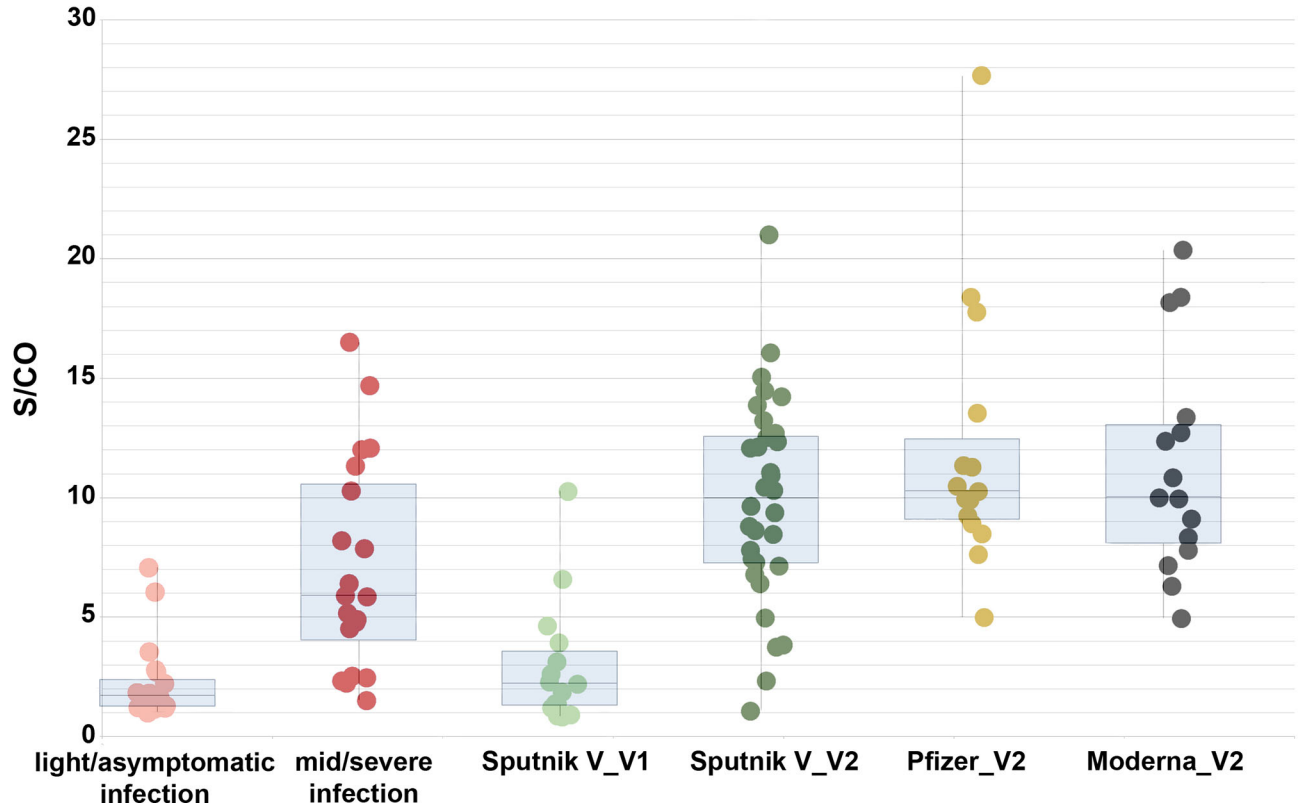

FIGURE 2 | Comparison of S/CO for the anti-RBD IgG antibodies in the individuals after light/asymptomatic course of COVID-19 (pink dots, 20 samples), moderate/severe course (red dots, 20 samples), Sputnik V single dose vaccinated (light green dots, 14 samples), Sputnik V both doses vaccinated (dark green dots, 32 samples), Pfizer vaccinated (yellow dots, 15 samples), and Moderna vaccinated individuals (black dots, 15 samples). Error bars show the maximal and the minimal meaning for each group. Boxes represent interquartile range.

Antibody Signal for the Vaccinated Groups of Individuals of Different Sex and Age

For the 35 fully vaccinated females (9 with Pfizer-BioNTech, 6 with Moderna and 20 with Sputnik V; both doses of vaccine were administered in all cases, N-positive samples were excluded) the average S/CO was 11.37, median 10.08. For the 27 males (6 vaccinated with Pfizer-BioNTech, 9 with Moderna and 12 with Sputnik V) the average S/CO was 10.98, median 9.91. The overall distributions of the respective values did not significantly differ (P-value 0.4) (**Supplementary Figure 1**).

For the 39 individuals with age less than 50 years the average S/CO was 9.99, median 9.65; for the 23 individuals 50 or older the average S/CO was 13.26, median 10.31. The two distributions of the respective values did not show a significant difference (P-value 0.1). According to Spearman's coefficient analysis there was no overall correlation between age and RBD signal levels (P-value 0.73).

Similar analysis for each of the three vaccine type groups individually did not demonstrate any significant difference between male/female or younger/older distributions of the S/CO values.

Antibody Signal Variation With Time After Full Sputnik V Vaccination

To understand how the levels of anti-RBD antibodies change with time within the scope of our study, we have taken additional samples from individuals 54 to 205 days after the full Sputnik V vaccination (**Figure 3**).

Overall, 39 measurements were taken for 17 individuals, at two to four time points for each. In 13 cases the antibody signal dropped over time, and in 9 cases the levels rose. We did not observe a significant correlation between the change in the S/CO and the time between different samplings taken after the vaccination (P-value 0.7).

There was one individual (blue line in **Figure 3**) with the signal rising by 93% in 70 days, then lowering by 64% in the next 40 days and then, in the next 34 days, rising back by 45%. Since neither symptoms, nor anti-N antibodies were detected, it seems that this person had not been infected with SARS-CoV-2. In another case (red line in **Figure 3**), where the anti-RBD antibody level rose by 114%, the anti-N antibody result also appeared to be positive. This most likely indicates an encounter with the SARS-CoV-2 infection in the period of time between the two samplings.

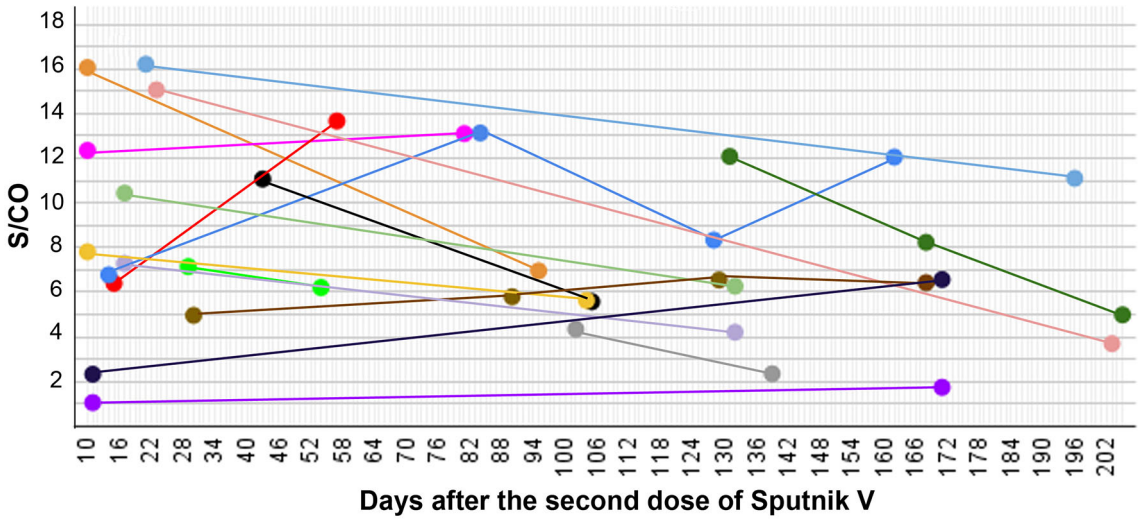

FIGURE 3 | S/CO in 17 individuals measured after full vaccination with Sputnik V at several time points presented as a time course.

Neutralization Effect in Samples From the Sputnik V Vaccinated and Infected Individuals

We have assessed the neutralization capabilities of serum after the Sputnik V vaccination using a surrogate virus neutralization system. It allows measuring the effect of antibodies coupling to the viral antigen and preventing it from binding to the human ACE2 receptor. Samples of 30 anti-N-negative individuals who received both doses of Sputnik V were tested. For all vaccinated patients, the neutralization effect was high and varied between 61.59% and 97.74% with an average of 80.69% and median of 80.51% (**Figure 4A**).

No significant correlation was observed between the neutralization effect and the antibody signal (P-value 0.2) (**Figure 4B**).

In comparison, the neutralization effect measured for patients who had been infected by the SARS-CoV-2 varied greatly, ranging between 39.03% and 89.31%, with the average for the group with no/light symptoms of 58.38% (median 62.02%) and for the group with moderate/severe symptoms of 72.74% (median 73.98) (**Figure 4A**), in consistency with our previous studies (25).

Antibody Signal and Neutralization Capabilities for Vaccinated Individuals Previously Exposed to COVID-19

As it has been mentioned previously, the observed immune response upon vaccination was higher in patients with positive S/CO for the N antigen. We tested eight such cases, of which four were confirmed with PCR or antigen test during the disease, two

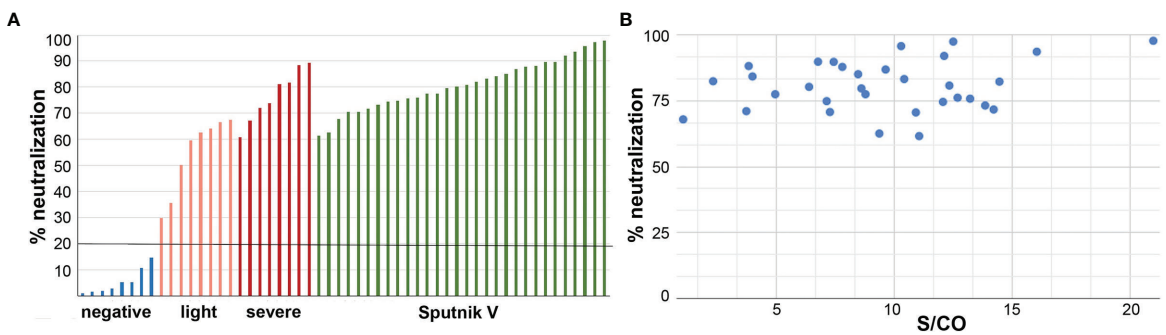

FIGURE 4 | **(A)** Serum of the Sputnik V vaccinated patients efficiently neutralize interaction of the S-protein RBD domain with ACE2 receptor. Bars for the negative controls representing samples before 2019, are in blue, asymptomatic/light symptom patients are in pink, patients with moderate/severe symptoms are in red, and for the Sputnik V vaccinated individuals are in green. Cut-off level of 20% is indicated by the black horizontal line. N-positive patients were excluded from the analysis. **(B)** Neutralization effect in samples of both-doses Sputnik V vaccinated individuals. No significant correlation was observed between the effect and the antibody signal.

claimed to have symptoms of COVID-19 at 94 to 165 days prior to vaccination, and one (PV8) was presumably infected during vaccination (**Figure 5A**).

In the last case, PV3*, patient was sampled 150, 120, and 95 days before vaccination, with stable negative results for N-antigen in all cases. No COVID-19 symptoms were reported before the vaccination. After vaccination, the patient developed extensive side effects, with high fever above 38°C for almost a week, possibly indicating infection with SARS-CoV-2 during vaccination or just before it. In line with this assumption, their respective levels of anti-N antibodies measured after the second dose (5 weeks after possible infection) slightly increased, while the anti-RBD levels increased almost 2-fold which can be a combined effect of infection and vaccination (**Figure 5B**).

We also measured the antibody levels before and after the second dose for two N-positive patients with confirmed infection (PV1 and PV2 in **Figure 5**). Neither of them demonstrated significant change in the anti-RBD S/CO after the second administration of the vaccine.

Overall, the respective results for N-positive patients were among the highest values obtained for the anti-RBD antibody signals, exceeding the threshold 12-20 times (15.13 times on average, median 13.5) (**Figures 1** and **5B**). The difference between the distributions of S/CO of the antibodies to the anti-RBD antigen within N-positive and N-negative samples as measured by Mann-Whitney test was very prominent (P-value 0.0001).

The same tendency was observed for the neutralization capability of respective serum (**Figure 5C**); 6 out of 8 samples were above the calculated median for the N-negative vaccinated individuals, and almost no changes were detected after the second vaccine administration.

DISCUSSION

It has been shown in various studies that Moderna, Pfizer-BioNTech, and Sputnik V vaccines are capable of producing a prominent immune system response, yielding vast development of the anti-spike protein antibodies (6, 15, 26). However, it was of interest to analyze the respective signals using a unified testing system which would allow us to compare them directly. In this study, we have used the VirIntel dual-antigen assay, an ELISA-based system, testing serum simultaneously for the IgG antibodies to the nucleocapsid and the receptor-binding domain of the spike protein (24). This, in particular, allowed us to separate cases of individuals possibly infected by SARS-CoV-2 before the vaccination, who had antibodies to the N-antigen. Our first goal was to compare the anti-RBD IgG antibody levels in samples obtained from the three vaccinated

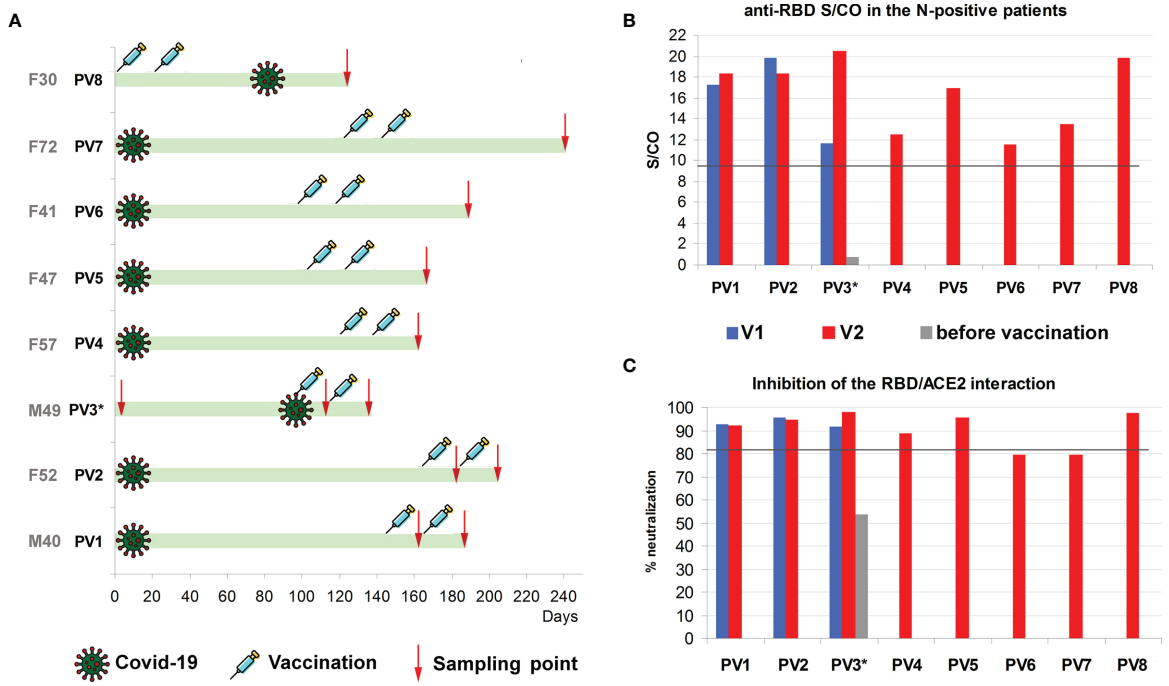

FIGURE 5 | **(A)** Time points of Covid-19 symptoms, vaccination and sampling. PV3* - no antibodies and no symptoms before vaccination, but severe "side effects" for a week after the first dose **(B)** Results for S/CO of IgG anti-RBD antibodies in the individuals with positive results for the anti-N antibodies, after first (blue) and second (red) administration of the Sputnik V vaccine. Grey bar is the anti-RBD level before vaccination. Threshold S/CO value is 1. **(C)** Inhibition of the RBD interaction with ACE2 in the individuals with positive results for the anti-N antibodies, after the first (blue) and the second (red) administration of the Sputnik V vaccine. Grey bar is the neutralization level before vaccination.

groups. Sex and age of individuals were then assessed as possible factors affecting the antibody levels. Next, we compared vaccinated individuals with two groups of patients previously infected by SARS-CoV-2, with light/asymptomatic or moderate/severe course of the disease. We also assessed the neutralization capabilities of anti-RBD antibodies in Sputnik V vaccinated individuals and how their antibody levels change within several weeks after vaccination. Finally, the antibody levels and neutralization capabilities in several individuals who had been both infected and vaccinated were studied.

Anti-RBD Antibodies Signal Levels Are Similar in Moderna, Pfizer-BioNTech, and Sputnik V Vaccinated Individuals

All three studied vaccines demonstrated a prominent immune system response, yielding the production of IgG antibodies to the viral RBD antigen. All of them require two-dose administration (later, 3rd and/or 4th booster doses were recommended). We first compared the levels of anti-RBD IgG antibodies in the individuals three weeks after the first dose and two or three weeks after the second dose of Sputnik V. After a single dose of Sputnik V only 11 out of 14 individuals demonstrated positive results. After the second dose, all the individuals demonstrated positive results. This highlights the importance of the two-stage vaccination of naive patients.

The signal levels after the second dose of Sputnik V were significantly higher than after the first, on average 5.4 fold. At the same time, we did not observe significant correlation between the signals for first and second sampling within individuals, for some of them the signal raised only slightly, for others more than 7-10 fold. This might reflect the preexisting immunity of respective individuals to either Ad26 or Ad5 (two strains of adenoviruses used for the first and second dose of Sputnik V, respectively)

For individuals vaccinated by both doses of Sputnik V, Moderna or Pfizer-BioNTech a wide range of signals was observed in each group, going up to values exceeding threshold over 20 times, with the Pfizer-BioNTech vaccine showing highest values. These ranges most likely reflect specific features of the immune system of different individuals.

At the same time, the average and median S/CO values of all three groups were similar (**Table 1**). Moreover, distributions of these values did not demonstrate significant difference (P-value above 0.05 for each possible pair of groups). This finding indicates that all three vaccines not only induce a strong immune system response, but are also comparable with each other. They yield similar levels of anti-RBD IgG antibody production, despite the difference in respective vaccine structures, Moderna and Pfizer-BioNTech being RNA-based vaccines, and Sputnik V an adenovirus vector.

TABLE 1 | Signal/Cut-off ranges, average and median values of the analyzed sets of samples from vaccinated and previously infected individuals.

Vaccine/Course of disease	Range of S/CO	Average S/CO	Median S/CO
Sputnik V	1.06 - 21.0	9.53	9.51
Pfizer-BioNTech	0.83 - 27.63	11.99	10.27
Moderna	1.07 - 17.78	11.32	10.01
Light/asymptomatic disease	1.01 - 7.07	2.22	1.7
Moderate/severe disease	1.52 - 17.03	7.08	5.88

Sex and Age Do Not Seem to Affect Anti-RBD Antibody Signals in Vaccinated Individuals

Reports indicate that the number of COVID-19 cases between men and women is similar, but men experience more severe outcomes, including hospitalization, admission to the intensive care unit, and death, the difference in risks being sometimes estimated as two-fold (27). On the other hand, females have been reported to have higher risks of acquiring side effects after vaccination against COVID-19 (28).

It was thus of interest to compare the levels of anti-RBD IgG antibody development in males and females after vaccination. This type of studies have been done for other vaccines; in most cases females have been shown to have greater immune system response (29, 30), in particular, for the influenza vaccine (31), some studies even suggest half-dose vaccination for females to be more adequate (32). The vaccines typically administered to children, such as combination measles, mumps, and rubella (MMR) vaccine also elicited higher antibody development levels in girls (33).

In our study, for the 35 studied fully vaccinated females, the antibody level was on average only 3.5% higher than for the 27 studied males. The distributions of the respective values did not demonstrate a statistically significant difference, thus we did not observe a correlation between sex and the levels of the anti-RBD IgG antibodies of vaccinated individuals.

Aging can also be a significant factor in the immune system response after different types of vaccinations, in particular, reducing the antibody development levels (31, 34–36). SARS-CoV-2 anti-spike IgG antibody levels have been recently shown to be lower for people over the age of 80 vaccinated by the Pfizer-BioNTech vaccine than for people under the age of 60 (36). However, the subject of vaccine-induced immunity correlation with age still remains unclear; other studies have reported that the vaccine efficacy is similar for younger and older cohorts of individuals. In particular, during the clinical trials of the Pfizer-BioNTech vaccine, breaking down the participants by age revealed that of 3,848 vaccine recipients older than 65 years of age only one became infected whereas 19 of 3,880 placebo recipients of that age tested positive. This translated to an estimated efficacy of 94.7%, highly similar with the 95.6% in those aged 16–55 and the 93.7% in those aged 55–65 (37).

In our study, we considered two age groups. For the fully vaccinated individuals with the age of over 50 the average signal was 14% higher than in the younger group, but the two distributions of values did not demonstrate a significant difference (P-value 0.1). Overall correlation between the signal and age values was also not observed (P-value 0.9). In particular, several samples taken from people over the age of 70 yielded results 8-16 times exceeding the threshold value, on a par with people of around 50 or 35 years old. Only one vaccinated individual of over 80 was present in our dataset (vaccinated with Moderna), and their respective anti-RBD S/CO was 6.3,

which was, in concordance with the aforementioned study, on the lower scale of the dataset values. At the same time, an over 70 years old patient vaccinated with Sputnik V demonstrated anti-RBD S/CO of 16.06 which is in the upper scale of all results. For future studies, more samples of individuals within the older age group would be required.

Anti-RBD Antibody Signals Are Similar in Vaccinated Individuals and Previously Infected Patients With Moderate or Severe Course of the Disease

It has been shown in previous studies that patients with severe COVID-19 symptoms generally develop more antibodies to the virus than in mild or asymptomatic cases (38, 39). In accordance with this, we have shown significant difference between antibody signal distributions for the two studied groups: with asymptomatic/light course of the SARS-CoV-2 infection and with moderate/severe symptoms, both in this and our previous studies (25).

Further analyzing the IgG anti-RBD results for the group of individuals with moderate/severe symptoms, we have shown that the respective distribution of obtained values also did not significantly differ from any of the studied vaccinated groups. On the other hand, each of the three vaccinated groups demonstrated significant difference with the distribution of values from the group with an asymptomatic/light course of the disease (P-value 3.4e-08, 7.3e-05 and 0.001 for Sputnik V, Moderna and Pfizer-BioNTech vaccinated groups, respectively). These results indicate that the general trend of the development of the IgG antibodies is similar for vaccinated individuals and for previously infected patients, but only with prominent symptoms of COVID-19.

Antibody Signals Do Not Necessarily Lower Within Many Weeks After full Sputnik V Vaccination

Studies about the longevity of the antibody levels to SARS-CoV-2 are not in full agreement, some reporting rapid waning of virus-specific IgG antibodies by several months after the infection (12, 40–42), and others observing stable titers detected over the same periods of time (43–45). In a study on COVID-19 patients with different courses of the disease including death cases, it was suggested that quality rather than quantity of antibodies may predict the outcome of the infection (46). Also, it is now evident that cellular immunity also provides a critical role in the outcomes of SARS-CoV-2 infection (47). On the other hand, low or undetectable titers of antibodies are sometimes a reason for considering vaccination or revaccination, even as the CDC warns against doing so.

It was recently shown that nonhuman primates infected with SARS-CoV-2 after vaccination with spike-based DNA vaccines yielded strong immune responses, including neutralizing antibodies, which possibly indicates that antibody development may in some cases be more effective in preventing than resolving the disease (48). Studies of the mRNA vaccines in humans have demonstrated that antibody levels after the administration seem to be detectable and persistent within several month periods (49, 50), although an overall decline in respective levels has been reported (42, 51). On the other hand, stable titers were reported for the adenovirus-based ChAdOx1 vaccine Oxford–AstraZeneca (52) in some studies; in other recent studies it was shown that these titers decline as well (53). It was thus of interest to assess the changes in antibody levels in the adenovirus-based Sputnik V vaccinated individuals.

Analysis of the serum of 17 Sputnik V fully vaccinated individuals in 7-30 weeks after the initial sampling demonstrated that anti-RBD levels do not have a strict tendency towards lowering with time. In 13 cases the signal dropped, and in 9 cases it rose, and there was no significant correlation between time and signal change (P-value 0.7). In the cases where more than two samplings were taken, all possible scenarios were played out, with signal raising, dropping or first dropping and then raising again and vice versa.

Such variations might reflect individual aspects of one's immune system or point to an encounter with the SARS-CoV-2 at uncertain time points between samplings, despite no reports of such encounters (no individuals experienced any COVID-19 symptoms). The rise of the anti-RBD antibody signal may indicate the respective immune response upon interacting with the virus and quickly conquering it. In one studied case after the second dose of Sputnik V the anti-nucleocapsid antibody result was positive along with the significant rise of the anti-RBD antibody level (by 113.5%). This most likely indicates that the respective individual unknowingly encountered SARS-CoV-2 infection between the two samplings and here, unlike the other cases, this interaction was long enough for their immune system to produce other kinds of antibodies as well.

Further analysis should include more samples and time points, but these results indicate that the stability of the anti-RBD IgG antibody levels over time after the Sputnik V vaccination is not easily predictable, and most likely depends on the individual characteristics of the immune system. At the same time, the S/CO stayed positive for all studied individuals, for the vast majority of samples exceeding the threshold level over four times even after more than a half year since the vaccination. This points to prominent persistence characteristics of the adenovirus-based vector vaccine Sputnik V in the studied period of time.

Sputnik V Vaccine Effect on Previously Infected Individuals

It has been recently shown that the IgG antibody titers of vaccinated individuals with preexisting immunity can be 10 to 45 times as high as those without it (54), even after administration of a single dose of the mRNA vaccines (50). It was also shown that the second dose does not significantly affect the level of the antibodies within the same individual (54). Moreover, a single immunization boosted neutralizing titers of respective antibodies by up to 1000-fold (55).

In this study we demonstrate that the adenovirus-based Sputnik V yielded similar results. We analyzed 11 samples of 8 vaccinated individuals, which showed positive results for the anti-nucleocapsid antibodies (3 samples were taken after the first dose of the vaccine, 8 after the second). The signal to cut-off ratio values for the N-positive samples taken after the first dose were all quite

high (average 15.58), while the signals for the N-negative individuals after the first dose were on average 4.5 times lower. The S/CO values for the N-positive individuals after the second dose of Sputnik V were on average 15.14, thus not showing significant difference compared to the first dose group (the average for the respective N-negative samples was 1.6 times lower).

Overall, we show that individuals who had been previously exposed to COVID-19 demonstrate very high levels of antibodies after the vaccination with Sputnik V, in concordance with the results obtained in other studies for Moderna and Pfizer- BioNTech vaccines (6, 26). This can be explained as a strong response of the immune system, which most likely treats the vaccine at least partially as a SARS-CoV-2 reinfection and yields vast antibody production. Our results indicate that a single administration of the Sputnik V (Sputnik Light) could be a sufficient boost to the immune system for those who have had the SARS-CoV-2 infection, that is in line with other studies on Sputnik Light (54, 56–59).

Neutralization Effects Are High for Sputnik V Vaccinated and Are Comparable With Previously Infected Individuals With Moderate and Severe Course of COVID-19

SARS-CoV-2 infects human cells, at least partially, *via* the interaction of the viral RBD S-domain with the ACE2 receptors on the cell surface. Respective neutralizing effects, in turn, are shown to be highly predictive in terms of protection against symptomatic course of the COVID-19 (60). Thus, one of the expected outcomes of vaccination should be the ability of serum to efficiently prevent this interaction. Such neutralization effects were demonstrated, in particular, for individuals vaccinated by mRNA-based vaccines (26, 61). In the Sputnik V clinical trials, the seroconversion level in the microneutralization assays with tissue cultures was reported to be 95.38% (4). In (62), eleven candidate vaccines were compared from the viewpoint of peak neutralizing antibody response, and according to the data available at that moment, the highest production of neutralizing antibodies were induced by BBIBP-CorV, AZD1222 and BNT162b2, followed by New Crown COVID-19 and Sputnik V.

In line with this, we observed a high capability of serum from the Sputnik V vaccinated individuals to inhibit the interaction of RBD with ACE2. We have found that the average rate of the inhibition was 81%, which was significantly higher than in the patients with light symptoms (58%), and slightly higher than in patients with a moderate/severe course of COVID-19 (72%). This is in concordance to previous observations for mRNA vaccines (62–64).

Similar to the anti-RBD IgG levels, neutralization effects were very prominent in the vaccinated individuals with previous SARS-CoV-2 infection, with a highest observed effect of 98.02%. In those cases, high neutralization rates were observed after the first dose of Sputnik V and did not significantly change after the second. This supports recent proposals for application of a single dose vaccine boost for previously infected patients (54, 65).

DATA AVAILABILITY STATEMENT

The original contributions presented in the study are included in the article/**Supplementary Material**. Further inquiries can be directed to the corresponding author.

ETHICS STATEMENT

The studies involving human participants were reviewed and approved by Commission on Biosafety and Bioethics (Institute of Cell Biophysics – Pushchino Scientific Center for Biological Research of the Russian Academy of Sciences). The patients/participants provided their written informed consent to participate in this study.

AUTHOR CONTRIBUTIONS

AK and MT have contributed equally to this work and share first authorship. MK, MT, and TB performed experiments. AK performed statistical analysis. AK and MT wrote the article. AK, MT, MK, and IM reviewed the article. IM supervised the study and obtained funding. All authors approved the submitted version.

FUNDING

This research received no external funding, it was funded by internal company funds of VirIntel LLC.

ACKNOWLEDGMENTS

We thank the Laboratory of cell cultures and cell engineering of the Institute of Cell Biophysics RAS for providing pre-pandemic samples, and Dr. Oleg S. Morenkov for useful suggestions throughout this project. We also thank Denis Kaznadzey for help with experiment logistics and for fruitful discussions.

SUPPLEMENTARY MATERIAL

The Supplementary Material for this article can be found online at: https://www.frontiersin.org/articles/10.3389/fimmu.2022.797918/full#supplementary-material

REFERENCES

1. Zhou P, Yang X-L, Wang X-G, Hu B, Zhang L, Zhang W, et al. A Pneumonia Outbreak Associated With a New Coronavirus of Probable Bat Origin. *Nature* (2020) 579:270–3. doi: 10.1038/s41586-020-2012-7
2. Tse LV, Meganck RM, Graham RL, Baric RS. The Current and Future State of Vaccines, Antivirals and Gene Therapies Against Emerging Coronaviruses. *Front Microbiol* (2020) 11:658. doi: 10.3389/fmicb.2020.00658
3. Li Y-D, Chi W-Y, Su J-H, Ferrall L, Hung C-F, Wu T-C. Coronavirus Vaccine Development: From SARS and MERS to COVID-19. *J BioMed Sci* (2020) 27:104. doi: 10.1186/s12929-020-00695-2
4. Logunov DY, Dolzhikova IV, Shcheblyakov DV, Tukhvatulin AI, Zubkova OV, Dzharullaeva AS, et al. Safety and Efficacy of an Rad26 and Rad5 Vector-Based Heterologous Prime-Boost COVID-19 Vaccine: An Interim Analysis of a Randomised Controlled Phase 3 Trial in Russia. *Lancet* (2021) 397:671–81. doi: 10.1016/S0140-6736(21)00234-8
5. Polack FP, Thomas SJ, Kitchin N, Absalon J, Gurtman A, Lockhart S, et al. Safety and Efficacy of the BNT162b2 mRNA Covid-19 Vaccine. *N Engl J Med* (2020) 383:2603–15. doi: 10.1056/NEJMoa2034577
6. Mulligan MJ, Lyke KE, Kitchin N, Absalon J, Gurtman A, Lockhart S, et al. Phase I/II Study of COVID-19 RNA Vaccine BNT162b1 in Adults. *Nature* (2020) 586:589–93. doi: 10.1038/s41586-020-2639-4
7. Baden LR, El Sahly HM, Essink B, Kotloff K, Frey S, Novak R, et al. Efficacy and Safety of the mRNA-1273 SARS-CoV-2 Vaccine. *N Engl J Med* (2021) 384:403–16. doi: 10.1056/NEJMoa2035389
8. Berkowitz FE, Jerris RC. Practical Medical Microbiology for Clinicians. *John Wiley Sons* (2016). 480 p.
9. Levine-Tiefenbrun M, Yelin I, Katz R, Herzel E, Golan Z, Schreiber L, et al. Initial Report of Decreased SARS-CoV-2 Viral Load After Inoculation With the BNT162b2 Vaccine. *Nat Med* (2021) 27:790–2. doi: 10.1038/s41591-021-01316-7
10. Mahase E. Covid-19: One Dose of Vaccine Cuts Risk of Passing on Infection by as Much as 50%, Research Shows. *BMJ* (2021) 373:n1112. doi: 10.1136/bmj.n1112
11. Scobie HM. Monitoring Incidence of COVID-19 Cases, Hospitalizations, and Deaths, by Vaccination Status — 13 U.S. Jurisdictions, April 4–July 17, 2021. *MMWR Morb Mortal Wkly Rep* (2021) 70:1284–90. doi: 10.15585/mmwr.mm7037e1
12. Goldberg Y, Mandel M, Bar-On YM, Bodenheimer O, Freedman L, Haas EJ, et al. Waning Immunity of the BNT162b2 Vaccine: A Nationwide Study From Israel. *N Engl J Med* (2021) 385:e85. doi: 10.1056/NEJMoa2114228
13. Commissioner O of the. *Moderna COVID-19 Vaccine* (2021). FDA. Available at: https://www.fda.gov/emergency-preparedness-and-response/coronavirus-disease-2019-covid-19/moderna-covid-19-vaccine (Accessed June 18, 2021).
14. Commissioner O of the. *Pfizer-BioNTech COVID-19 Vaccine* (2021). FDA. Available at: https://www.fda.gov/emergency-preparedness-and-response/coronavirus-disease-2019-covid-19/pfizer-biontech-covid-19-vaccine (Accessed June 18, 2021).
15. Jones I, Roy P. Sputnik V COVID-19 Vaccine Candidate Appears Safe and Effective. *Lancet* (2021) 397:642–3. doi: 10.1016/S0140-6736(21)00191-4
16. Örd M, Faustova I, Loog M. The Sequence at Spike S1/S2 Site Enables Cleavage by Furin and Phospho-Regulation in SARS-CoV2 But Not in SARS-CoV1 or MERS-CoV. *Sci Rep* (2020) 10:16944. doi: 10.1038/s41598-020-74101-0
17. Lan J, Ge J, Yu J, Shan S, Zhou H, Fan S, et al. Structure of the SARS-CoV-2 Spike Receptor-Binding Domain Bound to the ACE2 Receptor. *Nature* (2020) 581:215–20. doi: 10.1038/s41586-020-2180-5
18. Yuan M, Wu NC, Zhu X, Lee C-CD, So RTY, Lv H, et al. A Highly Conserved Cryptic Epitope in the Receptor Binding Domains of SARS-CoV-2 and SARS-CoV. *Science* (2020) 368:630–3. doi: 10.1126/science.abb7269
19. Rogers TF, Zhao F, Huang D, Beutler N, Burns A, He W, et al. Isolation of Potent SARS-CoV-2 Neutralizing Antibodies and Protection From Disease in a Small Animal Model. *Science* (2020) 369:956–63. doi: 10.1126/science.abc7520
20. Zost SJ, Gilchuk P, Case JB, Binshtein E, Chen RE, Nkolola JP, et al. Potently Neutralizing and Protective Human Antibodies Against SARS-CoV-2. *Nature* (2020) 584:443–9. doi: 10.1038/s41586-020-2548-6
21. Wan Y, Shang J, Graham R, Baric RS, Li F. Receptor Recognition by the Novel Coronavirus From Wuhan: An Analysis Based on Decade-Long Structural Studies of SARS Coronavirus. *J Virol* (2020) 94:e00127–20. doi: 10.1128/JVI.00127-20
22. Cao Y, Su B, Guo X, Sun W, Deng Y, Bao L, et al. Potent Neutralizing Antibodies Against SARS-CoV-2 Identified by High-Throughput Single-Cell Sequencing of Convalescent Patients' B Cells. *Cell* (2020) 182:73–84.e16. doi: 10.1016/j.cell.2020.05.025
23. Dispinseri S, Secchi M, Pirillo MF, Tolazzi M, Borghi M, Brigatti C, et al. Neutralizing Antibody Responses to SARS-CoV-2 in Symptomatic COVID-19 is Persistent and Critical for Survival. *Nat Commun* (2021) 12:2670. doi: 10.1038/s41467-021-22958-8
24. Komarov A, Kaznadzey A, Li Y, Kireeva M, Mazo I. Dual-Antigen System Allows Elimination of False Positive Results in COVID-19 Serological Testing. *Diagn (Basel)* (2021) 11:102. doi: 10.3390/diagnostics11010102
25. Tutukina M, Kaznadzey A, Kireeva M, Mazo I. IgG Antibodies Develop to Spike But Not to the Nucleocapsid Viral Protein in Many Asymptomatic and Light COVID-19 Cases. *Viruses* (2021) 13:1945. doi: 10.3390/v13101945
26. Wang Z, Schmidt F, Weisblum Y, Muecksch F, Barnes CO, Finkin S, et al. mRNA Vaccine-Elicited Antibodies to SARS-CoV-2 and Circulating Variants. *Nature* (2021) 592:616–22. doi: 10.1038/s41586-021-03324-6
27. Klein SL, Dhakal S, Ursin RL, Deshpande S, Sandberg K, Mauvais-Jarvis F. Biological Sex Impacts COVID-19 Outcomes. *PloS Pathog* (2020) 16:e1008570. doi: 10.1371/journal.ppat.1008570
28. Gee J, Marquez P, Su J, Calvert GM, Liu R, Myers T, et al. First Month of COVID-19 Vaccine Safety Monitoring — United States, December 14, 2020–January 13, 2021. *MMWR Morb Mortal Wkly Rep* (2021) 70:283–8. doi: 10.15585/mmwr.mm7008e3
29. Fink AL, Klein SL. The Evolution of Greater Humoral Immunity in Females Than Males: Implications for Vaccine Efficacy. *Curr Opin Physiol* (2018) 6:16–20. doi: 10.1016/j.cophys.2018.03.010
30. Flanagan KL, Fink AL, Plebanski M, Klein SL. Sex and Gender Differences in the Outcomes of Vaccination Over the Life Course. *Annu Rev Cell Dev Biol* (2017) 33:577–99. doi: 10.1146/annurev-cellbio-100616-060718
31. Potluri T, Fink AL, Sylvia KE, Dhakal S, Vermillion MS, Vom Steeg L, et al. Age-Associated Changes in the Impact of Sex Steroids on Influenza Vaccine Responses in Males and Females. *NPJ Vaccines* (2019) 4:29. doi: 10.1038/s41541-019-0124-6
32. Engler RJM, Nelson MR, Klote MM, VanRaden MJ, Huang C-Y, Cox NJ, et al. Half- vs Full-Dose Trivalent Inactivated Influenza Vaccine (2004-2005): Age, Dose, and Sex Effects on Immune Responses. *Arch Intern Med* (2008) 168:2405–14. doi: 10.1001/archinternmed.2008.513
33. Fischinger S, Boudreau CM, Butler AL, Streeck H, Alter G. Sex Differences in Vaccine-Induced Humoral Immunity. *Semin Immunopathol* (2019) 41:239–49. doi: 10.1007/s00281-018-0726-5
34. Frasca D, Blomberg BB. Aging Induces B Cell Defects and Decreased Antibody Responses to Influenza Infection and Vaccination. *Immun Ageing* (2020) 17:37. doi: 10.1186/s12979-020-00210-z
35. Lord JM. The Effect of Aging of the Immune System on Vaccination Responses. *Hum Vaccin Immunother* (2013) 9:1364–7. doi: 10.4161/hv.24696
36. Müller L, Andrée M, Moskorz W, Drexler I, Walotka L, Grothmann R, et al. Age-Dependent Immune Response to the Biontech/Pfizer BNT162b2 COVID-19 Vaccination. *Clin Infect Dis* (2021) 73:2065–72. doi: 10.1093/cid/ciab381
37. Pawelec G, McElhaney J. Unanticipated Efficacy of SARS-CoV-2 Vaccination in Older Adults. *Immun Ageing* (2021) 18:7. doi: 10.1186/s12979-021-00219-y
38. Rijkers G, Murk J-L, Wintermans B, van Looy B, van den Berge M, Veenemans J, et al. Differences in Antibody Kinetics and Functionality Between Severe and Mild Severe Acute Respiratory Syndrome Coronavirus 2 Infections. *J Infect Dis* (2020) 222:1265–9. doi: 10.1093/infdis/jiaa463
39. Chvatal-Medina M, Mendez-Cortina Y, Patiño PJ, Velilla PA, Rugeles MT. Antibody Responses in COVID-19: A Review. *Front Immunol* (2021) 12:633184. doi: 10.3389/fimmu.2021.633184
40. Long Q-X, Tang X-J, Shi Q-L, Li Q, Deng H-J, Yuan J, et al. Clinical and Immunological Assessment of Asymptomatic SARS-CoV-2 Infections. *Nat Med* (2020) 26:1200–4. doi: 10.1038/s41591-020-0965-6

41. Ibarrondo FJ, Fulcher JA, Goodman-Meza D, Elliott J, Hofmann C, Hausner MA, et al. Rapid Decay of Anti-SARS-CoV-2 Antibodies in Persons With Mild Covid-19. *N Engl J Med* (2020) 383:1085–7. doi: 10.1056/NEJMc2025179
42. Goel RR, Painter MM, Apostolidis SA, Mathew D, Meng W, Rosenfeld AM, et al. mRNA Vaccines Induce Durable Immune Memory to SARS-CoV-2 and Variants of Concern. *Science* (2021) 374:abm0829. doi: 10.1126/science.abm0829
43. Gudbjartsson DF, Norddahl GL, Melsted P, Gunnarsdottir K, Holm H, Eythorsson E, et al. Humoral Immune Response to SARS-CoV-2 in Iceland. *N Engl J Med* (2020) 383:1724–34. doi: 10.1056/NEJMoa2026116
44. Wang Y, Zhang L, Sang L, Ye F, Ruan S, Zhong B, et al. Kinetics of Viral Load and Antibody Response in Relation to COVID-19 Severity. *J Clin Invest* (2020) 130:5235–44. doi: 10.1172/JCI138759
45. Isho B, Abe KT, Zuo M, Jamal AJ, Rathod B, Wang JH, et al. Persistence of Serum and Saliva Antibody Responses to SARS-CoV-2 Spike Antigens in COVID-19 Patients. *Sci Immunol* (2020) 5:eabe5511. doi: 10.1126/sciimmunol.abe5511
46. Atyeo C, Fischinger S, Zohar T, Slein MD, Burke J, Loos C, et al. Distinct Early Serological Signatures Track With SARS-CoV-2 Survival. *Immunity* (2020) 53:524–532.e4. doi: 10.1016/j.immuni.2020.07.020
47. Moss P. The T Cell Immune Response Against SARS-CoV-2. *Nat Immunol* (2022) 23:186–93. doi: 10.1038/s41590-021-01122-w
48. Yu J, Tostanoski LH, Peter L, Mercado NB, McMahan K, Mahrokhian SH, et al. DNA Vaccine Protection Against SARS-CoV-2 in Rhesus Macaques. *Science* (2020) 369:806–11. doi: 10.1126/science.abc6284
49. Widge AT, Rouphael NG, Jackson LA, Anderson EJ, Roberts PC, Makhene M, et al. Durability of Responses After SARS-CoV-2 mRNA-1273 Vaccination. *N Engl J Med* (2021) 384:80–2. doi: 10.1056/NEJMc2032195
50. Ebinger JE, Fert-Bober J, Printsev I, Wu M, Sun N, Prostko JC, et al. Antibody Responses to the BNT162b2 mRNA Vaccine in Individuals Previously Infected With SARS-CoV-2. *Nat Med* (2021) 27:981–4. doi: 10.1038/s41591-021-01325-6
51. Levin EG, Lustig Y, Cohen C, Fluss R, Indenbaum V, Amit S, et al. Waning Immune Humoral Response to BNT162b2 Covid-19 Vaccine Over 6 Months. *N Engl J Med* (2021) 385:e84. doi: 10.1056/NEJMoa2114583
52. Wei J, Stoesser N, Matthews PC, Ayoubkhani D, Studley R, Bell I, et al. Antibody Responses to SARS-CoV-2 Vaccines in 45,965 Adults From the General Population of the United Kingdom. *Nat Microbiol* (2021) 6:1140–9. doi: 10.1038/s41564-021-00947-3
53. Shrotri M, Navaratnam AMD, Nguyen V, Byrne T, Geismar C, Fragaszy E, et al. Spike-Antibody Waning After Second Dose of BNT162b2 or Chadox1. *Lancet* (2021) 398:385–7. doi: 10.1016/S0140-6736(21)01642-1
54. Krammer F, Srivastava K, Alshammary H, Amoako AA, Awawda MH, Beach KF, et al. Antibody Responses in Seropositive Persons After a Single Dose of SARS-CoV-2 mRNA Vaccine. *N Engl J Med* (2021) 384:1372–4. doi: 10.1056/NEJMc2101667
55. Stamatatos L, Czartoski J, Wan Y-H, Homad LJ, Rubin V, Glantz H, et al. mRNA Vaccination Boosts Cross-Variant Neutralizing Antibodies Elicited by SARS-CoV-2 Infection. *Science* (2021) 372:1413–8. doi: 10.1126/science.abg9175
56. Rossi AH, Ojeda DS, Varese A, Sanchez L, Gonzalez Lopez Ledesma MM, Mazzitelli I, et al. Sputnik V Vaccine Elicits Seroconversion and Neutralizing Capacity to SARS-CoV-2 After a Single Dose. *Cell Rep Med* (2021) 2:100359. doi: 10.1016/j.xcrm.2021.100359
57. Tukhvatulin AI, Dolzhikova IV, Shcheblyakov DV, Zubkova OV, Dzharullaeva AS, Kovyrshina AV, et al. An Open, non-Randomised, Phase 1/2 Trial on the Safety, Tolerability, and Immunogenicity of Single-Dose Vaccine "Sputnik Light" for Prevention of Coronavirus Infection in Healthy Adults. *Lancet Regional Health – Europe* (2021) 11:100241. doi: 10.1016/j.lanepe.2021.100241
58. Claro F, Silva D, Rodriguez M, Rangel HR, De Waard JH. Immunoglobulin G Antibody Response to the Sputnik V Vaccine: Previous SARS-CoV-2 Seropositive Individuals may Need Just One Vaccine Dose. *Int J Infect Dis* (2021) 111:261–6. doi: 10.1016/j.ijid.2021.07.070
59. Komissarov AA, Dolzhikova IV, Efimov GA, Logunov DY, Mityaeva O, Molodtsov IA, et al. Boosting of the SARS-CoV-2–Specific Immune Response After Vaccination With Single-Dose Sputnik Light Vaccine. *J Immunol* (2022) 208:1139–45. doi: 10.4049/jimmunol.2101052
60. Khoury DS, Cromer D, Reynaldi A, Schlub TE, Wheatley AK, Juno JA, et al. Neutralizing Antibody Levels are Highly Predictive of Immune Protection From Symptomatic SARS-CoV-2 Infection. *Nat Med* (2021) 27:1205–11. doi: 10.1038/s41591-021-01377-8
61. Wu K, Werner AP, Koch M, Choi A, Narayanan E, Stewart-Jones GBE, et al. Serum Neutralizing Activity Elicited by mRNA-1273 Vaccine. *N Engl J Med* (2021) 384:1468–70. doi: 10.1056/NEJMc2102179
62. Rogliani P, Chetta A, Cazzola M, Calzetta L. SARS-CoV-2 Neutralizing Antibodies: A Network Meta-Analysis Across Vaccines. *Vaccines* (2021) 9:227. doi: 10.3390/vaccines9030227
63. Demonbreun AR, Sancilio A, Velez ME, Ryan DT, Saber R, Vaught LA, et al. Comparison of IgG and Neutralizing Antibody Responses After One or Two Doses of COVID-19 mRNA Vaccine in Previously Infected and Uninfected Individuals. *EClinicalMedicine* (2021) 38:101018. doi: 10.1016/j.eclinm.2021.101018
64. Walsh EE, Frenck RW, Falsey AR, Kitchin N, Absalon J, Gurtman A, et al. Safety and Immunogenicity of Two RNA-Based Covid-19 Vaccine Candidates. *N Engl J Med* (2020) 383:2439–50. doi: 10.1056/NEJMoa2027906
65. Reynolds CJ, Pade C, Gibbons JM, Butler DK, Otter AD, Menacho K, et al. Prior SARS-CoV-2 Infection Rescues B and T Cell Responses to Variants After First Vaccine Dose. *Science* (2021) 372:1418–23. doi: 10.1126/science.abh1282

Conflict of Interest: Authors IM, AK, and MK are employees and consultants of VirIntel, LLC, the company which has developed the testing system used in the article and funded this research. The funder had the following involvement with the study: design, collection, analysis, interpretation of data, the writing of this article and the decision to submit it for publication. These authors are inventors of a pending patent on this work. Author IM is also employed by Argentys Informatics, LLC.

frontiers | Frontiers in Immunology

ORIGINAL RESEARCH
published: 02 May 2022
doi: 10.3389/fimmu.2022.879036

Humoral Response to BNT162b2 Vaccine Against SARS-CoV-2 Variants Decays After Six Months

*Tulio J. Lopera[1], Mateo Chvatal-Medina[1], Lizdany Flórez-Álvarez[1], Maria I. Zapata-Cardona[1], Natalia A. Taborda[1,2], Maria T. Rugeles[1] and Juan C. Hernandez[1,3]**

[1] Grupo Inmunovirología, Facultad de Medicina, Universidad de Antioquia, Medellín, Colombia, [2] Grupo de Investigaciones Biomédicas Uniremington, Programa de Medicina, Facultad de Ciencias de la Salud, Corporación Universitaria Remington, Medellín, Colombia, [3] Infettare, Facultad de Medicina, Universidad Cooperativa de Colombia, Medellín, Colombia

OPEN ACCESS

Edited by:
Daniela F. Hozor,
Universidad Nacional de La Plata, Argentina

Reviewed by:
Jane Marie Heffernan, York University, Canada
Javier Ibarrondo, UCLA Health System, United States

***Correspondence:**
Juan C. Hernandez
juankhernandez@gmail.com

Specialty section:
This article was submitted to Vaccines and Molecular Therapeutics, a section of the journal Frontiers in Immunology

Received: 18 February 2022
Accepted: 06 April 2022
Published: 02 May 2022

Citation:
Lopera TJ, Chvatal-Medina M, Flórez-Álvarez L, Zapata-Cardona MI, Taborda NA, Rugeles MT and Hernandez JC (2022) Humoral Response to BNT162b2 Vaccine Against SARS-CoV-2 Variants Decays After Six Months. Front. Immunol. 13:879036. doi: 10.3389/fimmu.2022.879036

SARS-CoV-2 vaccines have shown very high effectiveness in real-world scenarios. However, there is compelling evidence for a fast-paced waning of immunity. The increasing number of new variants that could alter the severity, transmissibility, and potential to evade the immune response raised significant concern. Therefore, elucidating changes in the humoral immune response against viral variants induced by vaccines over time is crucial for improving immunization protocols. We carried out a 6-month longitudinal prospective study in which 60 individuals between 21 and 71 years of age who have received the complete scheme of the BNT162b2 vaccine were followed to determine titers of serum neutralizing activity. The neutralizing capacity was measured at one, three, and six-months post-vaccination by plaque reduction neutralization assay using SARS-CoV-2 B.1 (D614G) and the Gamma, Alpha, Delta, and Mu variants. Data were analyzed using GraphPad 5.0. Neutralizing activity against five different SARS-CoV-2 variants was detected in the serum samples of all vaccinated participants to a different extent after one month, with a progressive decrease according to age and gender. Overall, after one month of vaccination, the neutralizing titer was lower for all evaluated variants when compared to B.1, most remarkable against Delta and Mu, with a reduction of 83.1% and 92.3%, respectively. In addition, the Titer at 3- or 6-months follow-up decreased dramatically for all variants. Our results support the decaying of serum neutralizing activity, both over time and across SARS-CoV-2 variants, being more significant in older men. Since Delta and Mu appear to evade the neutralizing activity, these and further new variants of immune escape mutations should be considered for novel vaccine formulations.

Keywords: SARS-CoV-2, vaccine, neutralizing antibodies, immunity, immunogenicity, variant

INTRODUCTION

A few times throughout its history, humanity has faced such significant threats as the SARS-CoV-2 pandemic. The appearance of this novel coronavirus has resulted in substantial morbidity and mortality worldwide, which in turn has precipitated a vast spectrum of pharmacologic and non-pharmacologic measures to contain its impact (1). Some of the most encouraging ones include vaccines that provide immunity against symptomatic infection, reducing transmission to a variable extent (2, 3). Although overall vaccine effectiveness has proven to be very high in real-world scenarios, there is compelling evidence for a fast-paced waning of immunity. Some studies reported initial effectiveness of nearly 90% during the first month, which declined to under 50% after five months (4). A further concern has been raised with the increasing number of new variants with distinct mutations that might increase disease severity, transmissibility, and immune evasion, which might render a significant population vulnerable, either formerly immunized or not (5).

SARS-CoV-2 has undoubtedly reshaped the understanding of viral evolution. Despite its proven mechanisms for maintaining genetic fidelity, biological pressure has led to selecting highly fit specimens that are now considered variants of interest (VOIs) or variants of concern (VOCs) (6). The World Health Organization (WHO) has currently designated five VOCs -Alpha, Beta, Gamma, Delta, and Omicron- and two VOIs -Lambda and Mu-, many of which contain important mutations for immune evasion such as E484K and N501Y (5, 7). Since immunity from vaccines could exert selective pressure on viral evolution and given the possibility of potential escape from antibody neutralization by these variants, a particular emphasis must be set on how vaccine effectiveness is affected as they continue being rolled out worldwide. In fact, worrying data have already surfaced, showcasing a decrease in effectiveness against variants such as Delta, where overall vaccine effectiveness against infection varies from 51.9 to 88% (8, 9).

Extensive research has been conducted on the kinetics of immune response against this virus, both from natural infection and vaccines (10, 11). Nonetheless, there is little evidence so far regarding the behavior of such responses against multiple variants lengthwise, and this holds especially true for recently characterized variants such as Mu and Delta. Furthermore, a well-standardized study focusing on live-virus neutralization is peremptory, as these assays have allowed for some correlates of protection (12, 13). This longitudinal study aimed to evaluate the overall and variant-specific immunogenicity through live-virus neutralization of BNT162b2 against Alpha, Gamma, Delta, Mu, and B.1 SARS-CoV-2 variants in a group of individuals in Colombia.

MATERIALS AND METHODS

Study Design and Volunteers

We conducted a prospective longitudinal cohort study in Medellin, Colombia, between May and November of 2021, in BNT162b2 fully vaccinated individuals (Pfizer - BioNTech). The study was designed and conducted following the Declaration of Helsinki and Colombian legislation (Ministry of Health resolution 008430 de 1993). It was approved by the Ethics Committee of the Universidad de Antioquia (Acta 006/2021). After thoroughly explaining the project, all subjects signed a written informed consent and provided blood samples.

The study population included healthcare professionals or individuals prioritized in the early stages of vaccination in Colombia. All individuals received the BNT162b2 vaccine in a double-dose scheme, with an inter-dose interval of 3 weeks, as per the interim recommendations issued by the WHO. Eligibility criteria included an age of 18 years or older and a complete BNT162b2 vaccination schedule. In total, 60 people were included, and they were classified into four groups according to gender and age (women and men under and over 40 years).

Exclusion criteria included any history of SARS-CoV-2 infection prior to the first dose (defined as any spectrum of confirmed infection or symptoms suggestive of COVID-19), suspected SARS-CoV-2 infection at the time of inclusion in the study, incomplete schedule, or completed schedule vaccination more than 35 days ago, people in pregnancy, with autoimmune diseases, cancer, or HIV-1 infection. In the event of any symptoms associated with COVID-19 or exposure to a person infected with SARS-CoV-2, a RT-qPCR test for SARS-CoV-2 was performed. Those individuals with confirmed SARS-CoV-2 infection or who received the third vaccination dose in the follow-up period were excluded (n=4).

Follow-Up of Vaccinated Individuals

The individuals were followed for 180 days from a complete vaccination schedule. All volunteers provided a peripheral-blood sample at 30, 90, and 180 days after receiving the second vaccination dose (with a window of ± five days on days 30 and 90, and ± 28 days on day 180). At the beginning of the study, each individual completed a survey on demographic information, report of symptoms associated with vaccination, and existence of comorbidities. After the first visit, participants were followed with a virtual survey where they were asked about the onset of symptoms suggestive of COVID-19, confirmed infection by SARS-CoV-2, or the diagnosis of new comorbidities.

Plaque Reduction Neutralizing Test

Neutralizing activity of serum samples was detected by a 50% plaque reduction neutralization test (PRNT50) using Vero E6 cells. Briefly, Vero E6 cells (1.1×10^5 cells per well) were seeded into the 24-well tissue culture plates. The next day, 100 plaque-forming units (PFU) of SARS-CoV-2 were incubated with serial dilutions (1:20 until 1:5120) of heat-inactivated serum samples (56°C, 30 min) in a final volume of 500 µL for 60 min at 37°C and 5% CO2. Then, the mix was added to the Vero E6 monolayers by duplicate (200 uL per well) and incubated at 37°C for 60 min. Subsequently, the inoculum was removed, and 1 ml of the semisolid medium (1.5% carboxymethylcellulose, 2% fetal bovine serum (Gibco, Grand Island, NY, USA), 1% streptomycin (Sigma-Aldrich, St. Louis, MO, USA), and DMEM (Dulbecco's Modified Eagle Medium, Sigma-Aldrich,

St. Louis, MO, USA) was added and incubated at 37°C for 72h. Then, the semisolid medium was removed, and the monolayers were washed twice with PBS (Lonza, Rockland, ME, USA). Finally, the monolayers were fixed and stained with 1% crystal violet and 4% formaldehyde for 30 min and washed twice with PBS. A 50% reduction in plaque count was defined as the neutralization endpoint. The percentage inhibition was calculated based on the number of plaques in the infection control wells. The higher dilution with a reduction of 50% of plaques was reported as plaque reduction neutralization titer (PRNTi)

Neutralizing activity was evaluated in all participants using5 different lineages obtained from viral isolates collected in Colombia. The lineages assessed were B.1 (D614G) (hCoV-19/Colombia/ANTUdeA-200325-01/2020 ID accession: EPI_ISL_536399), variants of concern (VOC) Gamma (P.1) (hCoV-19/Colombia/ANT-UdeA-21002835v/2021 ID accession: EPI_ISL_4926393), Alpha (B.1.117) (hCoV-19/Colombia/ANT-UdeA-21001965v/2021 ID accession: and Delta (B.1.617.2) (hCoV-19/Colombia/ANT-UdeA-36211/2021 ID accession: EPI_ISL_5103929), and the variant of interest (VOI) Mu (B.1.621) (hCoV-19/Colombia/ANT-UdeA-21002149/2021 ID accession: EPI_ISL_4005445). Colombia/ANT-UdeA-21002149/2021 ID accession: EPI_ISL_4005445), and the variant of interest (VOI) Mu (B.1.621) (hCoV-19/Colombia/ANT-UdeA-36211/2021 ID accession: EPI_ISL_5103929).

Statistical Analysis

We performed an exploratory analysis to identify atypical data. The distribution of demographic, clinical, and immunological variables was assessed using the Shapiro-Wilk test. Wilcoxon test for paired samples and Spearman's rank correlation coefficient were used to determine significant differences and correlations. All data were analyzed using GraphPad Prism software, version 8.0 (California, USA), and the significance statistic was defined as p-value <0.05.

RESULTS

Sociodemographic Characteristics of Participants in the Study

Three serial serum samples have been taken from each individual up to the cut-off date, and their demographic characteristics are shown in **Table 1**. The cohort was evenly distributed among the groups of males and females, younger or older than 40. The mean body-mass index (BMI) was 24.8 $Kg/^{m2}$, and 16.6% of individuals reported comorbidities. Arterial hypertension and diabetes were the most prevalent (5% and 3.33%, respectively). Over 70% of participants in each group presented local symptoms, and over 60% presented systemic symptoms related to vaccination, except in males over 40 years, where these reactions were noticeably lower (33.3%). Concerning profession, 41.7% of the study participants were either healthcare professionals or had increased exposure to the virus and were consequently prioritized for receiving the vaccine. After six months of follow-up, 176 samples were included in the study: after 30 days (n=60), 90 days (n=60), and 180 days (n=56) (4 donors were excluded because of SARS-CoV-2 infection during the follow-up).

Immunogenicity of BNT162b2 at Day 30 Post-Vaccination

PRNTi was detected in all serum samples after 30 days of completing the vaccination schedule. Participants younger than

TABLE 1 | Demographic characteristics of participants fully vaccinated with BNT162b2.

		Female under 40 years old (n=15)	Male under 40 years old (n=15)	Female over 40 years old (n=15)	Male over 40 years old (n=15)
Age: years [range]		29 [21-39]	27 [21-40]	57 [47-68]	55 [42-71]
Body-mass index [range]		24.4 [18.0-28.9]	24.1 [19.5-31.4]	24.6 [21.1-29.3]	25.9 [23.1-30.9]
Blood type	**A (%)**	3 (20)	4 (26.7)	3 (20)	10 (66.7)
	B (%)	1 (6.7)	4 (26.7)	1 (6.7)	0 (0)
	O (%)	11 (73.3)	7 (46.7)	10 (66.7)	4 (26.7)
	AB (%)	0 (0)	0 (0)	1 (6.7)	0 (0)
Rhesus factor	**Positive (%)**	14 (93.3)	14 (93.3)	14 (93.3)	11 (73.3)
Symptoms associated with vaccination	**Local (%)**	12 (80)	13 (86.7)	13 (86.7)	7 (46.7)
	Systemic (%)	11 (73.3)	11 (73.3)	10 (66.7)	5 (33.3)
Substance consumption	**Alcohol (%)**	0 (0)	2 (13.3)	1 (6.7)	1 (6.7)
	Cigarette (%)	2 (13.3)	0 (0)	0 (0)	0 (0)
	Other (%)	0 (0)	0 (0)	0 (0)	0 (0)
Exercise	**Yes (%)**	9 (60)	13 (86.7)	8 (53.3)	7 (46.7)
	No (%)	6 (40)	2 (13.3)	8 (53.3)	10 (66.7)
	Hours per week [range]	3.5 [2-7]	4 [3-12]	4.5 [2-7]	5 [3-14]
Comorbidities	**Arterial hypertension (%)**	0 (0)	0 (0)	3 (20)	0 (0)
	Cardiovascular disease (%)	0 (0)	0 (0)	0 (0)	1 (6.7)
	Diabetes (%)	0 (0)	0 (0)	1 (6.7)	1 (6.7)
	Other* (%)	1 (6.7)	0 (0)	3 (20)	0 (0)

Other comorbidities: Dyslipidemia, Gilbert's syndrome, glaucoma, and hypothyroidism.

40 years old showed a more robust response after vaccination, with PRNTi against B.1 higher than 320 (reciprocal dilution) in most cases (**Figure 1A**). The neutralization capacity was higher in female participants than in their male counterparts, as they more often reached titers of up to 5120. The PRNTi generated after vaccination were enormously effective against the B.1 virus, but were hindered against VOCs and the VOI. In particular, VOCs Gamma and Alpha showed a reduction in PRNTi titers of 71.1% and 64.3%, respectively, when compared with those against B.1. Even more so, VOC Delta and VOI Mu showed a profound reduction in neutralizing capacity, as PNRTi decreased by up to 83.1% with and 92.3% respectively (**Figure 1B**) when compared with B.1.

Decreasing PRNTi Against All Variants in Older Individuals

To assess the difference among participants under and over 40 years old and the dramatic decrease in titers seen in all individuals against the variants, we analyzed SARS-CoV-2 PRNTis against each VOC and the VOI according to age. Older volunteers showed significantly lower PRNTi against all variants (**Figure 2**). Although a decrease in neutralization activity was observed in the entire population against the Gamma, Alpha, Delta, and Mu variants, compared with B.1, older individuals had lower PRNTi titers overall. We observed a significant decrease in neutralizing against the B.1 (r= -0.35, p= 0.0037), Gamma (r= -0.33, p= 0.0055), Alpha (r= -0.49, p< 0.0001), Delta (r= -0.37, p= 0.0017), and Mu (r= -0.39, p= 0.0011) (**Figure 2**).

Neutralizing Capacity Against All Lineages Decays Over Time

Plaque reduction neutralizing titers showed an evident decrease over time since vaccination. A noticeable reduction in neutralizing activity between 1- and 6-months post-vaccination among all variants evaluated was observed. For B.1 SARS-CoV-2, a 20% decrease at 90 days and 64.9% at 180 days post-vaccination were observed. For the variants Gamma, Alpha, Delta, and Mu, a progressive decay rate of neutralizing titer was observed during the follow-up, reducing at six months post-vaccination of 89.9%, 83.4%, 76.1%, and 68.9%, respectively. This difference was statistically significant for Gamma, Delta, and Mu variants at three- and six months post-vaccination and for B.1 and Alpha only at six months post-vaccination (**Figure 3**).

The kinetics of the PRNTi against B.1 lineage of SARS-CoV-2 were not different according to gender since both males and females had a marked drop at 180 days post-vaccination (**Figure 4**). Although women reached high neutralizing titers at day 30, after 90- and 180-days post-vaccination, they showed a marked drop, both older and younger than 40 years old (95.0% and 89.7%, respectively at 180 days) (**Figure 4**). On the other hand, in males, a significant reduction in neutralizing activity was observed after three months, only in those older than 40 years old, since the younger males only showed a significant reduction at six months (**Figure 4**).

As PRNTi against all variants was affected, we analyzed these results in independent groups according to age and gender. After six months, neutralizing titers showed a drastic reduction against

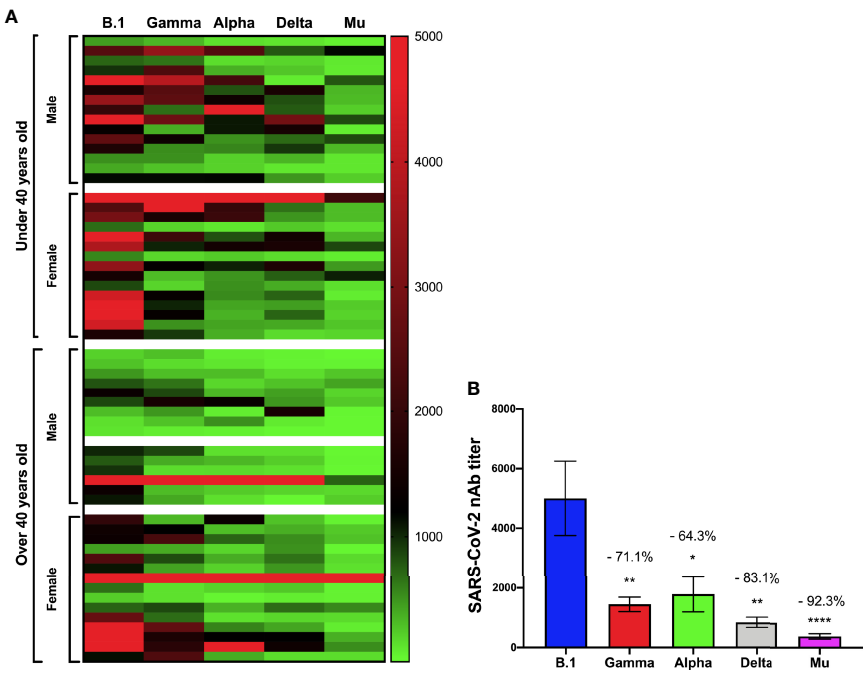

FIGURE 1 | Immunogenicity of BNT162b2 at 30 days after being fully vaccinated. The neutralizing antibody (nAb) titers against the B.1, Gamma, Alpha, Delta, and Mu variants, 30 days after being fully vaccinated according to age over or under 40 years and gender is shown in **(A)**. The percentage decrease in the neutralizing titers against the Gamma, Alpha, Delta, and Mu variants compared to B.1 lineage is shown in **(B)**. *p<0.05. **p<0.01. ****p<0.0001.

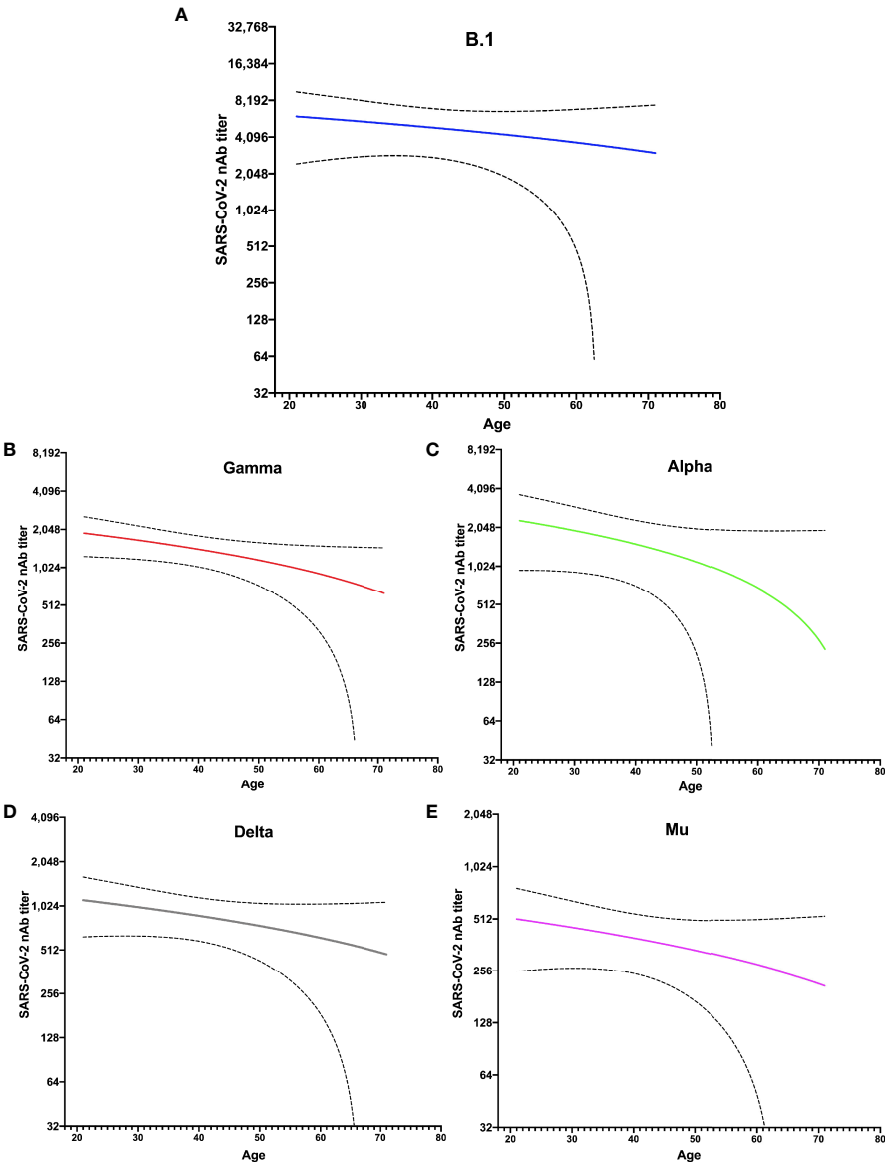

FIGURE 2 | Lower nAbs titer against five variants studied in older donors. The distribution of neutralizing antibody (nAbs) titers after 30 days of completing the vaccination scheme is shown for each variant, according to the age distribution of studied individuals: **(A)** B.1 lineage, **(B)** Gamma, **(C)** Alpha, **(D)** Delta, and **(E)** Mu. The statistical analysis was performed using Spearman's correlation.

Gamma, Alpha and Delta variants in all groups of donors. Notably, the reduction was observed for the Delta variant in all groups analyzed in both three- and six-month follow-up. For the Mu variant, the reduction in nAbs titers was differentially modulated according to age and gender (**Figure S1**).

DISCUSSION

Ever since the design of currently rolled-out vaccines against SARS-CoV-2, evidence has shown their remarkable effectiveness in preventing infection, particularly severe disease and death related to COVID-19. Yet, growing evidence has focused on the potential harm of variants against established immunity, varying from *in silico* to observational population analyses and even nationwide studies (4, 14, 15). Indeed, our results lead to a similar conclusion. When serum neutralizing activity was first evaluated at one-month post-vaccination, all individuals displayed a peak of neutralizing response against B.1 lineage SARS-CoV-2, as expected. Of note, mRNA in the BNT162b2 vaccine encodes a nearly identical Spike protein to the reference SARS-CoV-2 genome, Wuhan-Hu-1 (16), which might explain this vaccine's outstanding performance against relatively ancestral lineages such as B.1 virus, evaluated in this study.

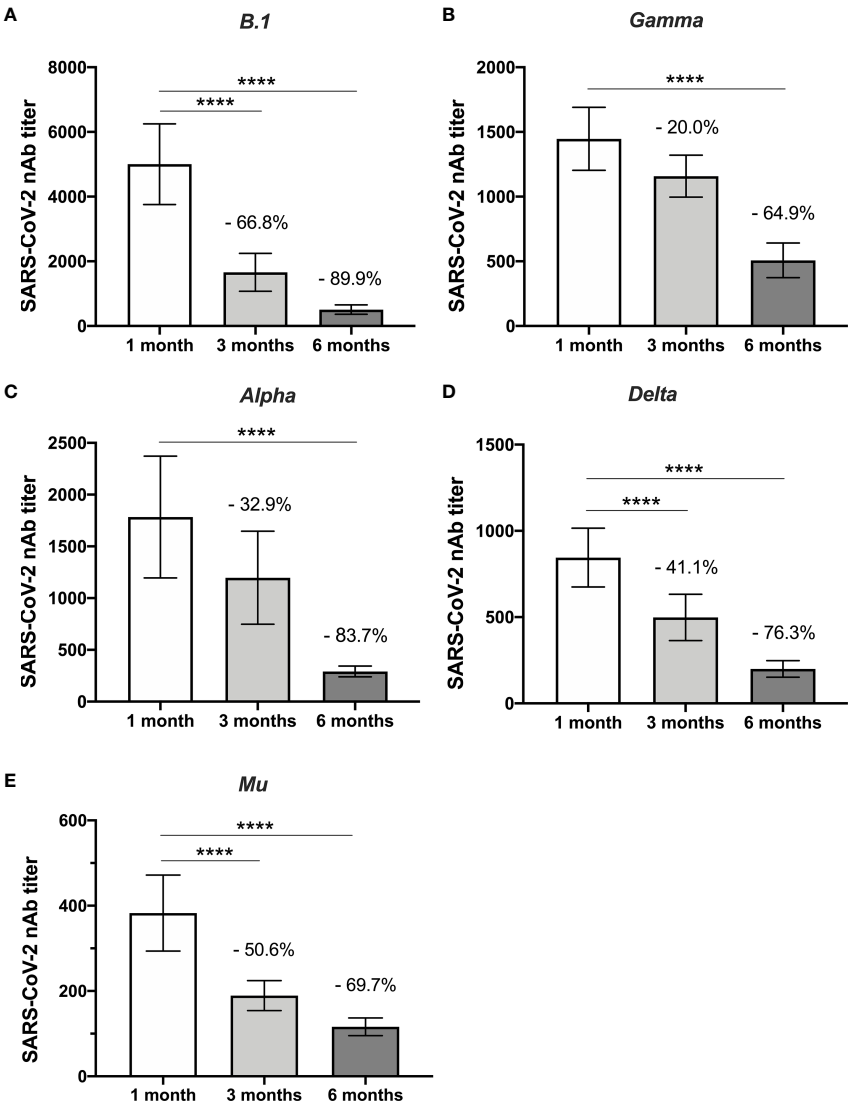

FIGURE 3 | Decrease in nAbs against five variants studied over time. The comparison between the neutralizing antibody titers of the individuals after one month and three months of being fully vaccinated are shown according to the variants: **(A)** B.1 lineage, **(B)** Gamma, **(C)** Alpha, **(D)** Delta, and **(E)** Mu. The statistical analysis was performed using Wilcoxon's test. ****p<0.0001.

From this perspective, neutralizing response reached peak levels and behaved consistently in all groups, although a lower response was seen among older individuals. Furthermore, among participants in our study, females displayed a fairly greater PNRTi than males, in concordance with previous studies with different vaccines (17).

However, once we evaluated cross-reactivity against other variants, titers fell consistently among groups. VOCs Gamma, Alpha, and Delta, many of which exhibit mutations related to immune escape such as E484K and N501Y, have been extensively documented to display an increased capacity for evading antibody responses (7). Yet, one of our most noticeable findings is that Mu, first detected in January 2021 in Colombia (18), and the WHO listed as a VOI due to its ability to increase community transmission and higher prevalence in an area, features the escape mutations E484K, N501Y, and K417N. This last mutation has been detected in Delta plus (AY.4.2) and is also related to immune evasion (19). The results obtained at 30 days post-vaccination showcase a reduced response against all variants assessed, when compared to ancestral B.1, especially for Mu which displays a significantly higher molecular divergence. Hence, our results suggest that as variants genetically drift away from the reference genome, vaccine efficacy might be compromised.

Furthermore, our evidence demonstrates that the neutralizing response against SARS-CoV-2 and its variants wanes over time in vaccinated individuals. Previous work from several authors goes in line with this as well, both in convalescent and vaccinated

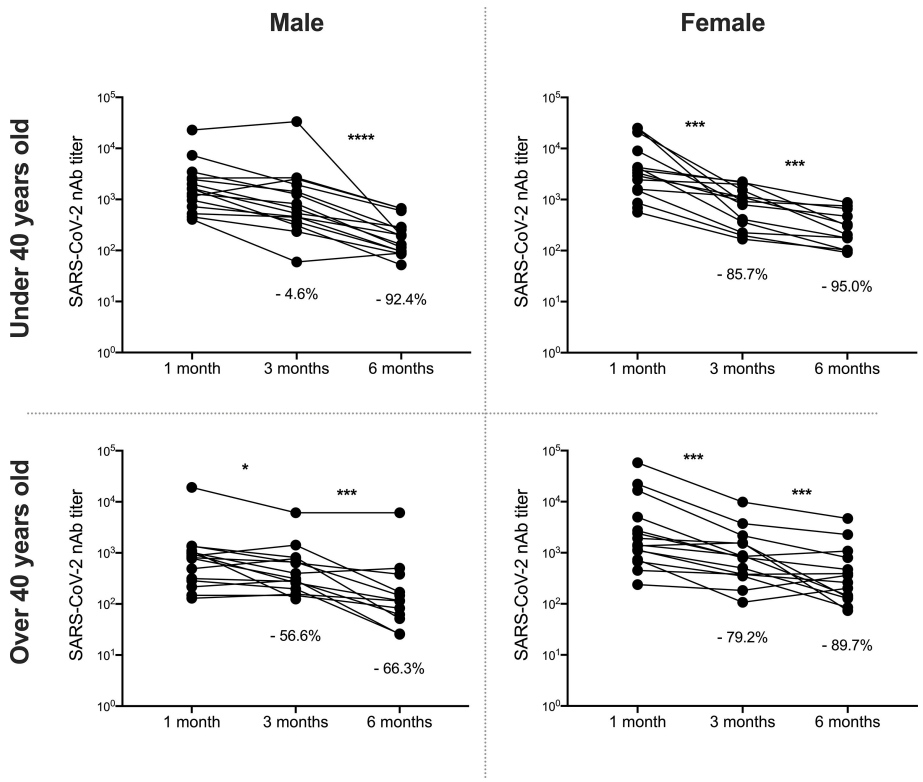

FIGURE 4 | Decrease nAbs against B.1 lineage over time, according to age and gender. Neutralizing antibody (nAbs) titers against B.1 virus are shown between individuals one month and three months after being fully vaccinated and compared according to age (over or under 40 years) and sex. The statistical analysis was performed using Wilcoxon's test. *p<0.05, ***p<0.001, ****p<0.0001.

individuals (20, 21). We observed a dramatic decrease in PNRTi titers against B.1 lineage of SARS-CoV-2 at three- and six months post-vaccination. The neutralizing response has been the predominant immunological marker for protection against SARS-CoV-2. Some studies estimate that the 50% protective neutralization levels, as a correlate of protection for severe disease, would be between 1:10 and 1:30, even though it could be as high as 1:200 (13, 22). Hence, the resulting antibody titers against B.1 at 3 and 6 months (at around 1:1660 and 1:505) would still be sufficient.

In the case of variants, the decay of humoral response is different. VOCs such as Alpha and Gamma would not likely translate into a threat for vaccinated individuals since the rates of decrease in antibody levels are not as strong (both remain over 1:1000 for the most part) as has been shown in other studies (23). For Delta, however, the decay is more remarkable, and the resulting mean nAbs titers approach 1:500 at three months, a decrease also observed by other authors (24). The most alarming data are those from Mu, as titers cross the 1:200 threshold at three months post-vaccination. Even though correlates of protection in variants may behave differently to those in B.1 lineage of SARS-CoV-2, it is safe to say that variants Delta and Mu have an outstanding ability to evade antibody responses in BNT162b2-vaccinated individuals and that immunity against them wanes faster than against other, less-circulating variants.

The results obtained from our study indicate that the humoral immune response induced by BNT162b2 holds less robustly against some of the VOCs and VOI that have circulated in Colombia, particularly against Delta and Mu, this last, the most unsuccessfully neutralized lineage assessed and the variant with the highest waning of them all (25–27). Consistent with our findings, Álvarez-Díaz et al. found that serum neutralizing activity from individuals vaccinated with BNT162b2 decreased by 75.7- and 17.7-fold against Mu, with respect to B.1.111 lineage and Gamma variant, respectively (26). In addition, Uriu et al. showed that the Mu variant was 9.1 as resistant as the ancestral lineage and 1.5 times as resistant to neutralization by serum from individuals vaccinated as the Beta variant (25). Further, Tada et al. reported that Mu and C.1.2 variants were more resistant to neutralization by BNT162b2 vaccination (6.8- and 7.3-fold decrease in titer, respectively, compared with D614G strain) (27). Based on the exposed view in Colombia and other countries (25–27), it should be considered that Mu be classified as a VOC since vaccines' effectiveness has decreased to a certain extent.

On the other hand, the decrease in antibody titers after vaccination is common for different vaccines. Some authors have reported a more significant decrease in antibodies against influenza B strains than A strains after six months of vaccination (28). Others have reported that antibody levels and avidity decrease between 8% and 23% after six months to 20 years of vaccination against measles, mumps, and rubella (29). However, in the context of vaccination for

SARS-CoV-2, our study shows that the decrease in the nAbs is more pronounced. These results suggest that time would render a substantial amount of the population susceptible to acquiring infection, especially as variants continue to emerge with increasing genetic divergence. This holds especially true for the elderly, considering that older individuals mount lower titers against all variants, and the kinetics of nAbs have shown an age dependency (30, 31). Considering that older individuals have a higher risk of suffering complications related to COVID-19, they must be protected from an ever-growing body of SARS-CoV-2 variants.

As shown herein and by other authors, the neutralizing response against mRNA vaccines decreases over time but is also commonly affected by mutations in SARS-CoV-2 variants (26, 32). This phenomenon occurs with other types of vaccines. For example, the humoral immune response triggered by adenoviral vaccines is less efficient in variants neutralization than mRNA vaccines (33, 34), and the sensitivity to neutralizing antibodies also decreases.

Our results showed a clear correlation between age, gender, and rate of decay in the post-vaccination immune response, remarkable at the peak neutralizing response and reduced near the end of the follow-up. Recently, other authors have reported that the humoral response to the BNT162b2 vaccine is affected by gender and age in studies carried out with ancestral lineages such as B.1 (31, 35, 36). The critical issue we observed in our study is that neutralization of variants also showed a differential reduction, especially in males over 40 years old. Clearly, males, especially older individuals, showed a significant decrease in nAbs titers against Alpha, Gamma, Delta, and Mu, aligning with other reports' conclusions (31). Furthermore, even though our group of older individuals did not report having several comorbidities, this population tends to accumulate more risk factors, and antibody titers tend to decline sharply (37).

An advantage of our design is the spectrum of epidemiologically, and immunologically relevant variants studied. This diverse sample allowed for a proper and direct comparison between lineages that previously depended on normalization or data extrapolation. Moreover, we assessed neutralization through PRNT at serial dilutions, which is regarded as the gold standard for measuring antibody levels for many viruses, including SARS-CoV-2. However, the study has limitations: First, the overall sample size is restricted. Second, as this is an observational study, several variables were not precisely controlled. Third, it is possible that participants could have been infected asymptomatically, which could present as a confounding variable. Despite classical vaccinology being focused on the induction of antibodies (mainly neutralizing), cellular-mediated immunity is currently being recognized as an important aim of vaccination, which needs to be assessed to understand the overall adaptive immune response. This cohort, as well as the cellular immunity, will be assessed in future studies.

In conclusion, our study provides evidence of the humoral response kinetics in a heterogeneous population followed for six months. The neutralizing capacity was evaluated against widely distributed variants in the world. Since the pandemic continues to be a public health challenge to face, it is imperative to have protection correlates after vaccination and to have extensive information on the immune response generated by these vaccines against worrisome variants, especially when it comes to malleable and quickly produced platforms. Another study evaluating the cell-mediated immunity to SARS-CoV-2 vaccination will be developed to better elucidate the immunologic effects of SARS-CoV-2 vaccines. In addition, the evaluation of immune parameters induced by SARS-CoV-2 infection in infected individuals with different clinical outcomes will be reported in future publications.

DATA AVAILABILITY STATEMENT

The original contributions presented in the study are included in the article/**Supplementary Material**. Further inquiries can be directed to the corresponding author.

ETHICS STATEMENT

The studies involving human participants were reviewed and approved by Ethics Committee of the Universidad de Antioquia (Acta 006/2021). The patients/participants provided their written informed consent to participate in this study.

AUTHOR CONTRIBUTIONS

TL and MC-M, formal analysis and writing – original draft. LF-A and MZ-C, investigation and formal analysis. NT, formal analysis, visualization, and writing - original draft. MR, conceptualization, project administration, writing - review and editing. JH, formal analysis, software, conceptualization, writing - original draft, and supervision. All authors contributed to the article and approved the submitted version.

FUNDING

This study was supported by *Universidad de Antioquia, Universidad Cooperativa de Colombia* and *Corporación Universitaria Remington*. The funders had no role in the study's design, data collection, and analysis, the decision to publish, or the preparation of the manuscript.

ACKNOWLEDGMENTS

We thank Claudia Rugeles for sampling support, and Salomon Gallego and Dayana Sepulveda for their technical assistance. We also thank Wbeimar Aguilar and Francisco J. Díaz for their contribution to VOIs isolation and identification. Finally, we thank all study participants.

SUPPLEMENTARY MATERIAL

The Supplementary Material for this article can be found online at: https://www.frontiersin.org/articles/10.3389/fimmu.2022.879036/full#supplementary-material

Supplementary Figure 1 | Decreased nAbs overtime against different variants of SARS-CoV-2, according to age and gender. Neutralizing antibody (nAb) titers against Gamma, Alpha, Delta, and Mu are shown between individuals at one, three, and six months after being fully vaccinated and compared according to age (over or under 40 years) and sex. The statistical analysis was performed using Wilcoxon's test. *p<0.05. **p<0.01. ***p<0.001.

REFERENCES

1. Johns Hopkins University & Medicine. *COVID-19 Map - Johns Hopkins Coronavirus Resource Center*. Johns Hopkins Coronavirus Resour Cent, Baltimore, Maryland (2020).
2. Polack FP, Thomas SJ, Kitchin N, Absalon J, Gurtman A, Lockhart S, et al. Safety and Efficacy of the BNT162b2 mRNA Covid-19 Vaccine. *N Engl J Med* (2020) 383:2603–15. doi: 10.1056/NEJMoa2034577
3. Baden LR, El Sahly HM, Essink B, Kotloff K, Frey S, Novak R, et al. Efficacy and Safety of the mRNA-1273 SARS-CoV-2 Vaccine. *N Engl J Med* (2020) 384:403–16. doi: 10.1056/NEJMoa2035389
4. Tartof SY, Slezak JM, Fischer H, Hong V, Ackerson BK, Ranasinghe ON, et al. Effectiveness of mRNA BNT162b2 COVID-19 Vaccine Up to 6 Months in a Large Integrated Health System in the USA: A Retrospective Cohort Study. *Lancet (London England)* (2021) 398:1407–16. doi: 10.1016/S0140-6736(21)02183-8
5. World Health Organization. *Tracking SARS-CoV-2 Variants*. WHO, Ginebra, Swizertland, (2021). Available at: https://www.who.int/en/activities/tracking-SARS-Co.
6. Romano M, Ruggiero A, Squeglia F, Maga G, Berisio R. A Structural View of SARS-CoV-2 RNA Replication Machinery: RNA Synthesis, Proofreading and Final Capping. *Cells* (2020) 9(5):1267. doi: 10.3390/cells9051267
7. Harvey WT, Carabelli AM, Jackson B, Gupta RK, Thomson EC, Harrison EM, et al. SARS-CoV-2 Variants, Spike Mutations and Immune Escape. *Nat Rev Microbiol* (2021) 19:409–24. doi: 10.1038/s41579-021-00573-0
8. Lopez Bernal J, Andrews N, Gower C, Gallagher E, Simmons R, Thelwall S, et al. Effectiveness of Covid-19 Vaccines Against the B.1.617.2 (Delta) Variant. *N Engl J Med* (2021) 385:585–94. doi: 10.1056/NEJMoa2108891
9. Folegatti PM, Ewer KJ, Aley PK, Angus B, Becker S, Belij-Rammerstorfer S, et al. Safety and Immunogenicity of the ChAdOx1 Ncov-19 Vaccine Against SARS-CoV-2: A Preliminary Report of a Phase 1/2, Single-Blind, Randomised Controlled Trial. *Lancet* (2020) 396:467–78. doi: 10.1016/S0140-6736(20)31604-4
10. Chvatal-Medina M, Mendez-Cortina Y, Patiño PJ, Velilla PA, Rugeles MT. Antibody Responses in COVID-19: A Review. *Front Immunol* (2021) 12:633184. doi: 10.3389/fimmu.2021.633184
11. Altawalah H. Antibody Responses to Natural SARS-CoV-2 Infection or After COVID-19 Vaccination. *Vaccines* (2021) 9(8):910. doi: 10.3390/vaccines9080910
12. Poonia B, Kottilil S. Immune Correlates of COVID-19 Control. *Front Immunol* (2020) 11:569611. doi: 10.3389/fimmu.2020.569611
13. Addetia A, Crawford KHD, Dingens A, Zhu H, Roychoudhury P, Huang M-L, et al. Neutralizing Antibodies Correlate With Protection From SARS-CoV-2 in Humans During a Fishery Vessel Outbreak With a High Attack Rate. *J Clin Microbiol* (2020) 58(11):2107–20. doi: 10.1128/JCM.02107-20
14. Villoutreix BO, Calvez V, Marcelin AG, Khatib AM. In Silico Investigation of the New UK (B.1.1.7) and South African (501y.V2) SARS-CoV-2 Variants With a Focus at the Ace2–Spike Rbd Interface. *Int J Mol Sci* (2021) 22:1–13. doi: 10.3390/ijms22041695
15. Charmet T, Schaeffer L, Grant R, Galmiche S, Chény O, Von Platen C, et al. Impact of Original, B.1.1.7 and B.1.351/P.1 SARS-CoV-2 Lineages on Vaccine Effectiveness of Two Doses of COVID-19 mRNA Vaccines: Results From a Nationwide Case-Control Study in France. *Lancet Reg Heal - Eur* (2021) 8:100171. doi: 10.1016/j.lanepe.2021.100171
16. Xia X. Detailed Dissection and Critical Evaluation of the Pfizer/BioNTech and Moderna mRNA Vaccines. *Vaccines* (2021) 9(7):734. doi: 10.3390/vaccines9070734
17. Fink AL, Klein SL. The Evolution of Greater Humoral Immunity in Females Than Males: Implications for Vaccine Efficacy. *Curr Opin Physiol* (2018) 6:16–20. doi: 10.1016/j.cophys.2018.03.010
18. Instituto Nacional de Salud. *Noticias coronavirus-genoma*. Inst Nac Salud, Bogotá, Colombia (2021).
19. Public Health England. SARS-CoV-2 Variants of Concern and Variants Under Investigation in England. *Sage* (2021) 01:1–50. Available at: https://www.gov.uk/government/publications/investigation-of-sars-cov-2-variants-technical-briefings.
20. Goldberg Y, Mandel M, Bar-On YM, Bodenheimer O, Freedman L, Haas EJ, et al. Waning Immunity After the BNT162b2 Vaccine in Israel. *N Engl J Med* (2021) 385:e85. doi: 10.1056/NEJMoa2114228
21. Xia W, Li M, Wang Y, Kazis LE, Berlo K, Melikechi N, et al. Longitudinal Analysis of Antibody Decay in Convalescent COVID-19 Patients. *Sci Rep* (2021) 11:16796. doi: 10.1038/s41598-021-96171-4
22. Khoury DS, Cromer D, Reynaldi A, Schlub TE, Wheatley AK, Juno JA, et al. Neutralizing Antibody Levels are Highly Predictive of Immune Protection From Symptomatic SARS-CoV-2 Infection. *Nat Med* (2021) 27:1205–11. doi: 10.1038/s41591-021-01377-8
23. Mileto D, Fenizia C, Cutrera M, Gagliardi G, Gigantiello A, De Silvestri A, et al. SARS-CoV-2 mRNA Vaccine BNT162b2 Triggers a Consistent Cross-Variant Humoral and Cellular Response. *Emerg Microbes Infect* (2021) 10:2235–43. doi: 10.1080/22221751.2021.2004866
24. Davis C, Logan N, Tyson G, Orton R, Harvey WT, Perkins JS, et al. Reduced Neutralisation of the Delta (B.1.617.2) SARS-CoV-2 Variant of Concern Following Vaccination. *PLoS Pathog* (2021) 17:e1010022. doi: 10.1371/journal.ppat.1010022
25. Uriu K, Kimura I, Shirakawa K, Takaori-Kondo A, Nakada T-A, Kaneda A, et al. Neutralization of the SARS-CoV-2 Mu Variant by Convalescent and Vaccine Serum. *N Engl J Med* (2021) 385:2397–9. doi: 10.1056/NEJMc2114706
26. Álvarez-Díaz DA, Muñoz AL, Tavera-Rodríguez P, Herrera-Sepúlveda MT, Ruiz-Moreno HA, Laiton-Donato K, et al. Low Neutralizing Antibody Titers Against the Mu Variant of SARS-CoV-2 in 31 BNT162b2 Vaccinated Individuals in Colombia. *Vaccines* (2022) 10(2):180. doi: 10.3390/vaccines10020180
27. Tada T, Zhou H, Dcosta BM, Samanovic MI, Cornelius A, Herati RS, et al. High-Titer Neutralization of Mu and C.1.2 SARS-CoV-2 Variants by Vaccine-Elicited Antibodies of Previously Infected Individuals. *Cell Rep* (2022) 38:110237. doi: 10.1016/j.celrep.2021.110237
28. Lee JH, Cho HK, Kim KH, Lee J, Kim YJ, Eun BW, et al. Evaluation of Waning Immunity at 6 Months After Both Trivalent and Quadrivalent Influenza Vaccination in Korean Children Aged 6-35 Months. *J Korean Med Sci* (2019) 34:e279. doi: 10.3346/jkms.2019.34.e279
29. Kontio M, Jokinen S, Paunio M, Peltola H, Davidkin I. Waning Antibody Levels and Avidity: Implications for MMR Vaccine-Induced Protection. *J Infect Dis* (2012) 206:1542–8. doi: 10.1093/infdis/jis568
30. Müller L, Andrée M, Moskorz W, Drexler I, Walotka L, Grothmann R, et al. Age-Dependent Immune Response to the Biontech/Pfizer BNT162b2 Coronavirus Disease 2019 Vaccination. *Clin Infect Dis* (2021) 73:2065–72. doi: 10.1093/cid/ciab381
31. Bates TA, Leier HC, Lyski ZL, Goodman JR, Curlin ME, Messer WB, et al. Age-Dependent Neutralization of SARS-CoV-2 and P.1 Variant by Vaccine Immune Serum Samples. *JAMA* (2021) 326:868–9. doi: 10.1001/jama.2021.11656
32. Noori M, Nejadghaderi SA, Arshi S, Carson-Chahhoud K, Ansarin K, Kolahi AA, et al. Potency of BNT162b2 and mRNA-1273 Vaccine-Induced Neutralizing Antibodies Against Severe Acute Respiratory Syndrome-CoV-2 Variants of Concern: A Systematic Review of *In Vitro* Studies. *Rev Med Virol* (2021) 32(2):1–23. doi: 10.1002/rmv.2277
33. Terpos E, Trougakos IP, Karalis V, Ntanasis-Stathopoulos I, Sklirou AD, Bagratuni T, et al. Comparison of Neutralizing Antibody Responses Against SARS-CoV-2 in Healthy Volunteers Who Received the BNT162b2 mRNA or the AZD1222 Vaccine: Should the Second AZD1222 Vaccine Dose be Given Earlier? *Am J Hematol* (2021) 96:E321–4. doi: 10.1002/ajh.26248
34. Tada T, Zhou H, Samanovic MI, Dcosta BM, Cornelius A, Herati RS, et al.

Neutralization of SARS-CoV-2 Variants by mRNA and Adenoviral Vector Vaccine-Elicited Antibodies. *Front. Immunol* (2022) 13:797589. doi: 10.3389/fimmu.2022.797589

35. Lustig Y, Sapir E, Regev-Yochay G, Cohen C, Fluss R, Olmer L, et al. BNT162b2 COVID-19 Vaccine and Correlates of Humoral Immune Responses and Dynamics: A Prospective, Single-Centre, Longitudinal Cohort Study in Healthcare Workers. *Lancet Respir Med* (2021) 9:999–1009. doi: 10.1016/S2213-2600(21)00220-4
36. Levin EG, Lustig Y, Cohen C, Fluss R, Indenbaum V, Amit S, et al. Waning Immune Humoral Response to BNT162b2 Covid-19 Vaccine Over 6 Months. *N Engl J Med* (2021) 385:e84. doi: 10.1056/NEJMoa2114583
37. Michos A, Tatsi E-B, Filippatos F, Dellis C, Koukou D, Efthymiou V, et al. Association of Total and Neutralizing SARS-CoV-2 Spike -Receptor Binding Domain Antibodies With Epidemiological and Clinical Characteristics After Immunization With the 1st and 2nd Doses of the BNT162b2 Vaccine. *Vaccine* (2021) 39:5963–7. doi: 10.1016/j.vaccine.2021.07.067

Conflict of Interest: The authors declare that the research was conducted in the absence of any commercial or financial relationships that could be construed as a potential conflict of interest.

Publisher's Note: All claims expressed in this article are solely those of the authors and do not necessarily represent those of their affiliated organizations, or those of the publisher, the editors and the reviewers. Any product that may be evaluated in this article, or claim that may be made by its manufacturer, is not guaranteed or endorsed by the publisher.

frontiers | Frontiers in Immunology

ORIGINAL RESEARCH
published: 26 May 2022
doi: 10.3389/fimmu.2022.879946

A SARS–CoV-2 Spike Receptor Binding Motif Peptide Induces Anti-Spike Antibodies in Mice and Is Recognized by COVID-19 Patients

Federico Pratesi[1†], Fosca Errante[2†], Lorenzo Pacini[3†], Irina Charlot Peña-Moreno[4], Sebastian Quiceno[4], Alfonso Carotenuto[5], Saidou Balam[6,7], Drissa Konaté[6], Mahamadou M. Diakité[6], Myriam Arévalo-Herrera[8], Andrey V. Kajava[9], Paolo Rovero[2], Giampietro Corradin[10], Paola Migliorini[1], Anna M. Papini[3] and Sócrates Herrera[4]*

[1] Department of Clinical and Experimental Medicine, University Hospital of Pisa, Pisa, Italy, [2] Interdepartmental Laboratory of Peptide and Protein Chemistry and Biology, Department of NeuroFarBa, University of Florence, Sesto Fiorentino, Italy, [3] Interdepartmental Laboratory of Peptide and Protein Chemistry and Biology, Department of Chemistry "Ugo Schiff", University of Florence, Sesto Fiorentino, Italy, [4] Department of Immunology, Caucaseco Scientific Research Center, Cali, Colombia, [5] Department of Pharmacy, University of Naples Federico II, Naples, Italy, [6] Immunogenetic Laboratory and Parasitology, University of Sciences, Techniques and Technologies of Bamako (USTTB), Bamako, Mali, [7] Department of Nephrology, University Hospital Regensburg, Regensburg, Germany, [8] Department of Immunology, Malaria Vaccine and Drug Development Center, Cali, Colombia, [9] CRBM, University of Montpellier, CNRS, Montpellier, France, [10] Biochemistry Department, University of Lausanne, Lausanne, Switzerland

OPEN ACCESS

Edited by:
Pedro A. Reche, Complutense University of Madrid, Spain

Reviewed by:
Nikhil Maroli, Indian Institute of Science (IISc), India
R. S. Rajmani, Indian Institute of Science (IISc), India

***Correspondence:**
Sócrates Herrera
sherrera@inmuno.org

[†]These authors have contributed equally to this work

Specialty section:
This article was submitted to Vaccines and Molecular Therapeutics, a section of the journal Frontiers in Immunology

Received: *20 February 2022*
Accepted: *26 April 2022*
Published: *26 May 2022*

Citation:
Pratesi F, Errante F, Pacini L, Peña-Moreno IC, Quiceno S, Carotenuto A, Balam S, Konaté D, Diakité MM, Arévalo-Herrera M, Kajava AV, Rovero P, Corradin G, Migliorini P, Papini AM and Herrera S (2022) A SARS–CoV-2 Spike Receptor Binding Motif Peptide Induces Anti-Spike Antibodies in Mice and Is Recognized by COVID-19 Patients. Front. Immunol. 13:879946. doi: 10.3389/fimmu.2022.879946

The currently devastating pandemic of severe acute respiratory syndrome known as coronavirus disease 2019 or COVID-19 is caused by the coronavirus SARS-CoV-2. Both the virus and the disease have been extensively studied worldwide. A trimeric spike (S) protein expressed on the virus outer bilayer leaflet has been identified as a ligand that allows the virus to penetrate human host cells and cause infection. Its receptor-binding domain (RBD) interacts with the angiotensin-converting enzyme 2 (ACE2), the host-cell viral receptor, and is, therefore, the subject of intense research for the development of virus control means, particularly vaccines. In this work, we search for smaller fragments of the S protein able to elicit virus-neutralizing antibodies, suitable for production by peptide synthesis technology. Based on the analysis of available data, we selected a 72 aa long receptor binding motif ($RBM_{436-507}$) of RBD. We used ELISA to study the antibody response to each of the three antigens (S protein, its RBD domain and the $RBM_{436-507}$ synthetic peptide) in humans exposed to the infection and in immunized mice. The seroreactivity analysis showed that anti-RBM antibodies are produced in COVID-19 patients and immunized mice and may exert neutralizing function, although with a frequency lower than anti-S and -RBD. These results provide a basis for further studies towards the development of vaccines or treatments focused on specific regions of the S virus protein, which can benefit from the absence of folding problems, conformational constraints and other advantages of the peptide synthesis production.

Keywords: SARS-CoV-2, receptor binding motif, COVID-19, immunized animals, neutralizing Abs, spike (S) protein

INTRODUCTION

The current SARS-CoV-2 (severe acute respiratory syndrome coronavirus 2) pandemic has resulted in devastating social and economic consequences worldwide, in addition to an enormous public health burden. Coronaviruses are single-stranded RNA-enveloped viruses (1). Although this type of viruses is frequently associated with a common cold with mild symptoms in humans, some of them can cause severe respiratory infection and death, mainly in elderly patients and in individuals with several comorbidities, primarily diabetes, obesity, hypertension and other cardiovascular disorders (2–4).

The ongoing coronavirus disease 2019 (COVID-19) is considered one of the world's worst pandemics, with more than 400 million cases and 5.8 million human deaths reported as of February 2022 (5). Since the beginning of the COVID-19 pandemic, the scientific community has focused intense efforts on studying the virus biology, the disease manifestations and management and its prevention (6, 7). In a short time, the SARS-CoV-2 genome, the specificity of its overall structural organization and the atomic 3D structure of the most significant proteins were revealed (8, 9).

One of the critical proteins is a trimeric spike (S) protein that allows this virus to penetrate host cells and cause infection. The S protein trimers protrude from the outer bilayer leaflet and form a characteristic crown-like halo surrounding the viral particle (hence, "corona"). The importance of the SARS-CoV2 S-protein is that it is a large self-assembled homo-trimer protein of about 1,250 aa (8, 9), expressed on the virus membrane and responsible for the virus-cell invasion. The protein is composed of two functional subunits, S1 and S2. The S1 subunit, which forms the globular head of the S protein trimer, contains the receptor-binding domain (RBD) that specifically interacts with the host receptor angiotensin-converting enzyme 2 (ACE2).

The S2 subunits form the stalk of the trimer embedded into the viral envelope. When the S protein binds to the ACE2 receptor, proteases located on the host cell membrane trigger the dissociation of S1 fragments and induce an irreversible refolding of the S2 trimer. The structural rearrangement of S2 brings together the viral and cellular membranes, leading to the fusion of the two bilayers. The atomic 3D structure of the S trimer in the prefusion conformation, the S2 trimer in the post-fusion conformation, and the RBD-ACE2 complex have been determined (10–12) and all have contributed to developing means to control virus spreading. Specifically, these features of the S protein led vaccine companies to choose it for vaccine development (13, 14).

The RBD is a monomeric domain of a smaller size (220 aa) that folds in the same stable 3D structure as part of the complete S protein and as a separate domain (15). Antiviral antibodies and cell mediated responses of multiple specificities are produced during SARS-CoV-2 infection and appear to contribute to protection (16). RBD is not only essential for virus invasion of host cells, but also targets neutralizing antibodies generated during SARS-CoV-2 infection; therefore, RBD represents another promising vaccine candidate (8, 17, 18).

While the rate of infections and deaths rapidly increased worldwide, significant efforts were invested in developing effective tools to promptly confirm diagnosis of the infection i.e., highly sensitive and specific molecular diagnostic methods (19). Likewise, given that vaccines are the primary medical option and most cost-effective means for global control of the pandemic, an unprecedented effort to develop anti-COVID-19 vaccines led to the production, clinical evaluation and approval by regulatory agencies of multiple vaccines. Along this line, given the critical functions of the S protein, the viral surface location, and the availability of detailed structural information, this protein was chosen for vaccine development (9, 20, 22).

As of February 2022, more than ten billion vaccine doses had been delivered globally, and ~60% of the world population had received at least one vaccine dose (5). Moreover, despite specific antiviral drugs having been elusive until recently, two novel antiviral medicines have already been approved by the United States Food and Drug Administration (FDA). Molnupiravir produced by Merck (23), and Nirmatrelvir/Ritonavir (Paxlovid) produced by Pfizer (24) are medicines for oral administration, with high effectiveness to reduce disease severity and prevent deaths (25).

Although the most extensively used vaccines have shown high protective efficacy, their effectivity, particularly the antibody response's longevity and the virus-neutralizing function, appears short-lasting, suggesting the need for new vaccine formulations. Based on the recent advances in understanding the structure and function of S protein, and with the aim of identifying highly effective virus proteins/fragments this work concentrate on further characterization of the S protein, focusing on shorter fragments/domains with vaccine potential. We selected the S-ACE2 receptor binding motif ($RBM_{436-507}$) which was produced as a single synthetic peptide, along with shorter sequences which were compared in their antigenicity and immunogenicity using sera from humans naturally exposed to COVID-19, and sera from immunized animals. Selected sera were also analyzed for their neutralization activity.

MATERIALS AND METHODS

Recombinant S and RBD Proteins Production

Since the S trimer is described as the primary protein responsible for inducing a protective immune response against the SARS-CoV-2 virus, first we produced a secreted and soluble form of this protein self-assembled in the trimer using Chinese Hamster Ovary (CHO) cells as previously described (26). Briefly, the transmembrane domain and the C terminal intracellular tail were removed and replaced by a T4 foldon DNA sequence and an 8xHis tag. A signal peptide sequence was added. To stabilize the prefusion structure of the S trimer in our constructs, we deactivated the original RRA furin cleavage site R by changing it to RGSA. We introduced amino-acid mutations K986P/V987P ("2P") as suggested elsewhere (12). The construct used in this work had the D614G mutation shared by most of the SARS-

CoV-2 variant of concern (B.1.1.7 - Alpha, B.1.351 - Beta, B.1.617.2 - Delta, B.1.1.529 - Omicron) widely spread during the 2020-2021 pandemic (27). This S protein construct was established to form trimers predominantly folded in the prefusion conformation (26). In addition, the RBD of the S protein (aa 319-541) was produced as a recombinant product (26) and a series of peptides covering the BIP sequence were synthesized and analyzed.

Peptide Synthesis, Purification and Characterization

Peptide sequences corresponding to the full $RBM_{436-507}$ length (72 aa) as well as shorter fragments of 20-22 amino acids (P11-P16) described in **Table 1** were synthesized and analyzed. Single cysteine residues in peptides P11, P12, and P13 (486-507, 476-495 and 466-485 of S protein, respectively) were replaced with serine to avoid unwanted spontaneous formation of disulfide dimers. Peptides were prepared by microwave-assisted solid-phase peptide synthesis (MW-SPPS), cleaved from the resin and, in the case of $RBM_{436-507}$ and P12, oxidized in solution with H_2O_2 at pH 9.0. (28) Purifications were performed by flash chromatography followed by semi-preparative HPLC to achieve purity >70% ($RBM_{436-507}$ and P16) or >87% (P11-P15). Final products were characterized by analytical UHPLC coupled with ESI single quadrupole mass spectrometry and/or MALDI-ToF analysis. Analytical data and details on the synthesis and purification procedures are available as **Supplementary Information**.

Conformational Studies by Circular Dichroism

The CD spectrum of the $RBM_{436-507}$ peptide was recorded using quartz cells of 0.1 cm path length with a JASCO J-710 CD spectropolarimeter at 25 °C. The spectrum was measured in the 260–190 nm spectral range, 1 nm bandwidth, 64 accumulations, and 100 nm/min scanning speed. The peptide was dissolved in water to a concentration of 12 μM. The secondary structure content of the peptide was predicted using the online server for protein secondary structure analyses DichroWeb (29). Input and output units and the wavelength step were θ (mdeg) and 1.0 nm, respectively.

The mean residue molar ellipticity [Θ]MR (Y-axis label) was calculated, which is defined as:

$$[\Theta]MR = \Theta/(10 \times Cr \times l)$$

where: Θ is ellipticity in mdeg, Cr is the mean residue molar concentration, l is the cell path in cm, and Cr = (n x 1000 x Cg)/Mr

where: n is the number of peptide bonds (residue), Cg is the macromolecule concentration (g/ml), Mr is the molecular weight of the peptide.The algorithm used was CDSSTR, and the reference database was set-7 (30).

The normalized root means square deviation (NRMSD) was 0.035.

Human Blood Samples

A clinical protocol was developed, submitted to and approved by the local Ethical Committees (CEAVNO, Approval # 17522) in Italy and (CECIV, approval # 04-2020) in Colombia. Whole blood (10 mL) was collected from COVID-19 patients from both Italy and Colombia. Samples were collected by arm venipuncture using dry tubes after hospitalization, and upon the patient's written informed consent, socio-demographic data and clinical manifestations were recorded. SARS-CoV-2 infection was confirmed by RT-PCR. Blood was fractionated, and sera were collected and kept frozen at -20°C until use for serology.

Mice Immunization and Sera Collection

A total of 30 male and female, 6-8 weeks old BALB/c mice of 20 ± 5 g of body weight were randomly selected and distributed in three groups (A, B and C) of 10 animals each. Each group was further divided into experimental (Exp) and control (Ctrl) subgroups of five mice each and were further immunized with SARS-CoV-19 S (group A) or RDB (group B) recombinant proteins as well as with the synthetic $RBM_{436-507}$ peptide (group C). Each group of mice was immunized subcutaneously (s.c.) at the base of the tail on days 0, 20 and 40 with 20μg of each antigen diluted in 50 μL PBS and emulsified in Montanide ISA-51 (Seppic Inc., Paris, France) according to the manufacturer's recommendations. Mice were bled from submandibular veins on days 1-2 before the first and third immunizations, 20 days after the third dose and every 60 days until day 140. Whole blood (~100 μL) was collected, and sera were separated by centrifugation and stored frozen at -20°C until use for serological analyses. Animal studies were carried out at the Caucaseco Research Center in Cali (Colombia) and approved by the Animal Ethics Committee of MVDC in Colombia. Animal care, housing, and handling were performed according to institutional guidelines and following the National Institutes of Health Guide for the Care and Use of Laboratory Animals.

TABLE 1 | Synthesized RBM peptide sequences.

Name	Sequence	Amino acids
$RBM_{436-507}$	Ac-WNSNNLDSKVGGNYNYLYRLRKSNLKPFERDISTEIYQAGSTPCNGVEGFNCYFPLQSYGFQPTNGVGYQP-NH_2	436-507
P11	Ac-FNSYFPLQSYGFQPTNGVGYQP-NH_2	486-507
P12	Ac-GSTPCNGVEGFNCYFPLQSY-NH_2	476-495
P13	Ac-RDISTEIYQAGSTPSNGVEG-NH_2	466-485
P14	Ac-FRKSNLKPFERDISTEIYQA-NH_2	456-475
P15	Ac-GGNYNYLYRLFRKSNLKPFE-NH_2	446-465
P16	Ac-WNSNNLDSKVGGNYNYLYRL-NH_2	436-455

Underlined sequences in peptides P3 and P12 represent disulfide bridges. Serine residues (S) highlighted in red in peptides P11 and P13 replace native Cysteines.

Serological Analyses

Reactivity of Mouse Antibodies to S and RBD Proteins and $RBM_{436-507}$

The reactivity of sera from mice immunized with the S, RBD and $RBM_{436-507}$ was determined by ELISA, using as antigens the specific immunogens. Briefly, 96-well plates (Nunc-Immuno Plate, Maxisorp, Roskilde, Denmark) were coated with one µg/mL $RBM_{436-507}$, RBD and Spike Trimer protein, pH 7.4 at 4°C, overnight. After plates were blocked with 5% skim milk solution [PBS 1X, 0.05% Tween 20, (PBS-T)], serum samples were added at 1:100 or three-fold serial dilutions starting at 1:100 in 2.5% skim milk in PBS-T and were incubated for 1 hour. Plates were then washed and incubated with alkaline phosphatase-conjugated anti-mouse IgG antibody (Sigma Chemical Co., St Louis, MO) at a 1:1000 dilution for 1 hour. Reactions were revealed with para-nitrophenyl phosphate substrate (*p*-NPP) (Sigma Aldrich) and read at 405 nm wavelength (Dynex Technologies, Inc., MRX Chantilly, VA).

ELISA Assays to Analyze Anti-Spike, Anti-RBD and Anti-$RBM_{436-507}$ Human Antibodies

Nunc Maxisorp polystyrene plates were coated with Spike Trimer (Excellgene, Monthey, Switzerland) or RBD (Excellgene, Monthey, Switzerland) at 1 µg/ml in PBS pH 7.4 (50 µl/well) overnight at 4°C; peptide $RBM_{436-507}$ coating was at 2 µg/ml in Carbonate buffer, pH 9.6; 20-mers P11-P16 at 10 µg/ml in PBS, pH 7.4. After blocking for 1 hr at room temperature (RT) with PBS pH 7.4, BSA 3% (A4503 - Merck KGaA, Darmstadt, Germany), sera diluted 1/100 in PBS pH 7.4, BSA 1%, Tween-20 0.05% were incubated on the plate (50 µl/well) for 2 hours at RT. After 3 washings with PBS Tween-20 0.05% (150 µl/well), goat anti-human IgG HRP (A0293 - Merck) diluted 1:5000 in PBS BSA 1% Tween-20 0.05% was added to the plates at 50 µl/well and incubated for 2 hours. For IgM and IgA determination, goat anti-human IgM HRP conjugate (A0420 – Merck) or goat anti-human IgA HRP conjugate (A0295 - Merck) diluted 1:20,000 in PBS, BSA 1%, Tween 0.05% were added to the plates. After three washings with PBS Tween-20, 0.05%, enzymatic activity was measured at 450 nm after TMB addition (T4444 - Merck) and blocked by H_2SO_4 1M.

Inhibition of ACE Binding to RBD With Anti-$RBM_{436-507}$ Specific Human Antibodies

The ability of anti-$RBM_{436-507}$ antibodies to inhibit the binding of ACE2 to RBD was evaluated using a modification of the SPIA commercial kit (Diametra Srl, Spello, Pg - Italy, ImmunoDiagnostic System Group). Anti-RBD antibodies were used as a positive control. Anti-N1 (20-mer linear peptide of SARS-CoV-2 nucleocapsid, aa 366-388) and anti-TT (tetanus toxoid) antibodies were used as virus-related and -unrelated negative controls. Specific antibodies were eluted from four sera with high anti-COVID-19 antibody titers using polystyrene plates coated with RBD, $RBM_{436-507}$, N1 and TT. Briefly, the plates were blocked with PBS BSA 3%, and COVID-19 sera diluted 1/50 in PBS BSA 1% Tween-20 0.05% and incubated for 2 hours at RT. Plates were washed three times with PBS Tween-20 0.05%, and bound antibodies were eluted with 200µl PBS pH 3.0 and immediately neutralized at pH 7.4 with basic phosphate buffer. The concentration of eluted antibodies was evaluated by A_{280} absorbance measurement with Nanodrop, and binding to the respective antigen was confirmed by indirect ELISA. For ACE inhibition assay, anti-RBD, anti- $RBM_{436-507}$, anti-N1 and anti-TT eluted antibodies were incubated onto Diametra SPIA plates coated with recombinant RBD. Calibrator and controls were loaded as per the manufacturer's instructions. Ready-to-use ACE2 conjugated with horseradish peroxidase was then added to the wells, and plates were incubated for 90 minutes at 37°C. After washings, plates were incubated with TMB for 15 minutes and acid stop solution was added before reading the absorbance at 450 nm. Results were expressed as percentage inhibition according to the manufacturer's instruction.

Statistical Analysis

Antibody titers were compared between mouse groups. A descriptive analysis was performed to evaluate differences in humoral immune responses within each group of mice. Kruskal-Wallis was performed to compare the antibody response to each protein, followed by Dunn's multiple comparison test. Results of anti-S, anti-RBD and anti- $RBM_{436-507}$ antibodies were expressed as Odd Ratio (OR) of a positive internal control set at 1.0. A *p*-value < 0.05 was considered statistically significant. Data were analyzed and plotted using GraphPad Prism software (version 5.01; GraphPad Software Inc, San Diego, California, USA).

RESULTS

Selection and Circular Dichroism Analysis of $RBM_{436-507}$ Peptide

To study the interaction between S and ACE2, we focused on the surface of the RBD involved in the ACE2 receptor binding, which should represent the target of the neutralizing antibodies. Our analysis of the 3D structure of the RBD-ACE2 complex showed that the large part of the RBD interacting surface, the Receptor Binding Motif (RBM), is composed of a 436-507 aa segment (**Figures 1A–C**). Since peptide synthesis technology has several advantages compared to recombinant proteins (31–34), we selected this RBM region for peptide synthesis and subsequent experimental studies. The central part of $RBM_{436-507}$ should mimic well the native-like conformation due to a disulfide bond. The peptide flanking parts should be unstructured and highly flexible both in peptides as well as within the 3D structure of the S-protein. In addition to the critical surface localization of the $RBM_{436-507}$ in the S protein, its amino acid sequence is specific to the SARS-CoV-2 and contains several predicted T-cell epitopes (33). The sequence of $RBM_{436-507}$ (**Table 1**) was N-terminal acetylated and C-terminal amidated to avoid including terminal charged groups not present in the native protein.

The conformation of $RBM_{436-507}$ in water at pH 7 was explored by CD spectrometry (**Figure 1D**). We then evaluated the antigenic properties of this peptide. The absence of a defined

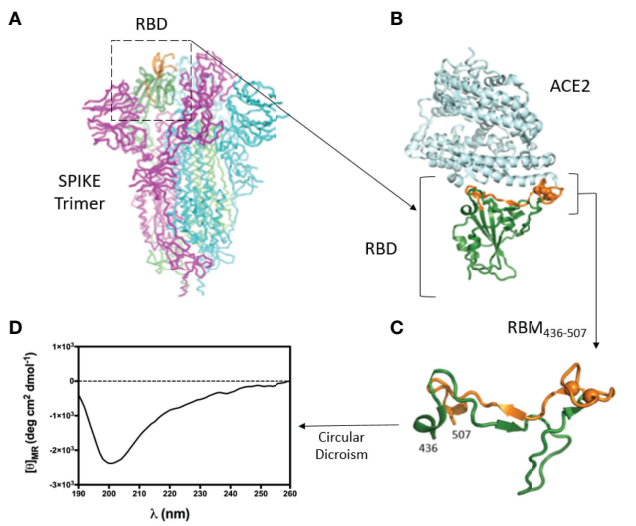

FIGURE 1 | 3D structure of the RBD-ACE2 complex and CD of $RBM_{436-507}$. **(A)** Atomic 3D structure of the S trimer in the prefusion conformation (27). RBD is shown in ribbon representation (dark green). Region 476-507 is in orange. **(B)** Complex between RBD (green-orange) and ACE2 receptor (light cyan) (12). **(C)** Conformation of the RBM peptide (436-507) within the RBD. Cysteine residues are shown as spheres. **(D)** Circular Dichroism of $RBM_{436-507}$ synthetic peptide used in this work.

minimum around 200 nm, diagnostic of random coil conformation, is compatible with a certain degree of structuration of the peptide. The secondary structure content was predicted based on the CD spectrum using the online server for protein secondary structure analyses, DichroWeb (29): 2% helix, 30% β-strand, 19% β-turn, and 49% random coil. The relatively high percentage of β-strand conformation suggests the intriguing hypothesis that $RBM_{436-507}$ peptide can partially preserve the extended conformation displayed along most of its sequence within the folded Spike protein (pdb code 6VXX) (8, 21).

Immunogenicity of S, RBD and $RBM_{436-507}$ in Mice

As shown in **Figure 2**, sera from all immunized animals tested by ELISA at 1:100 dilution, in response to the S, RBD and $RBM_{436-507}$ antigens, indicated specific IgG seroconversion after the first immunization dose. Furthermore, most of them displayed a boosting response after the second immunization dose, with the highest levels against the three proteins observed on day 40. However, while animals immunized with $RBM_{436-507}$ and RBD developed similar high level antibody profiles (3.0 to 3.5 OD), mice immunized with the S protein displayed significantly lower responses (1.0 to 2.0 OD). For $RBM_{436-507}$ and RBD, antibodies remained at high levels (>2.0 OD) after day 140, whereas antibodies against the S protein notably decreased (< 0.5 0D) during the same period. None of the control mice immunized with adjuvant alone seroconverted. The antibody titration (three-fold dilutions) using sera collected on day 140 indicated titers of 1:24,300, 1:72,900 to $RBM_{436-507}$ and RBD respectively, and 1:900 to S (**Supplementary Material**, **Figure S1**).

Reactivity of Mouse Antibodies to S, RBD and $RBM_{436-507}$

The analysis of the homologous and cross recognition of the S, RBD and $RBM_{436-507}$ antigens by antibodies elicited upon mice immunization is shown in **Figure 3**. ELISA results showed a high homologous sera reactivity but different reactivity with the other proteins/domains. Reactivity of sera diluted at 1:100 showed OD values ranging from 1.2 to 2.0 against the full-length S antigen, 3.2-3.5 to the RBD and 3.0-3-5 to the $RBM_{436-507}$ fragment. The titration of this homologous reactivity indicated that final reactivity (OD 0,2) at $1:10^4$ dilution to the S protein (**Figure 3A**), whereas at the final dilution tested ($1:10^4$) the OD values were higher for RBD (OD= 2.5-3.0) and RBM (0.5-1.7) (**Figures 3B, C**, respectively).

Regarding the analysis of the cross reactivity, anti-S antibodies displayed similar recognition of RBD and $RBM_{436-507}$ (**Figure 3**), and the anti-RBD antibodies high recognition of both the S- and -$RBM_{436-507}$ proteins, although the S-protein was better recognized. In contrast, for the anti-$RBM_{436-507}$ antibodies, only two mice presented cross reactivity with end point of $1:10^4$ whereas the remaining animals of the group presented only weak reactivity at 1:100 dilution. Notably, these antibodies did not cross react with the S-protein (**Figures 3D–I**).

The final reactivity titer of the anti-S antibodies was $1:10^4$ against the S protein, and $1.8x10^3$ against RBD and $RBM_{436-507}$. In the case of RBD, mouse immunization elicited a vigorous antibody response (**Figure 3**) with high optical densities even at $1:10^4$ dilution. Although reactivity to the S protein and the $RBM_{436-507}$ peptide were lower, recognition remained significant even at dilutions of $1:10^4$ and $5:10^3$, respectively.

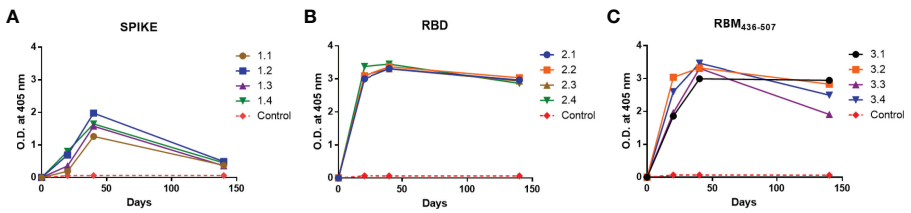

FIGURE 2 | Immunogenicity of S, RBD and $RBM_{436-507}$ in mice. Analysis of the antibody response in mice immunized at days 0, 20, 40. **(A)** Anti-S, **(B)** Anti-RBD and **(C)** Anti-$RBM_{436-507}$. SD is < 20% of the mean.

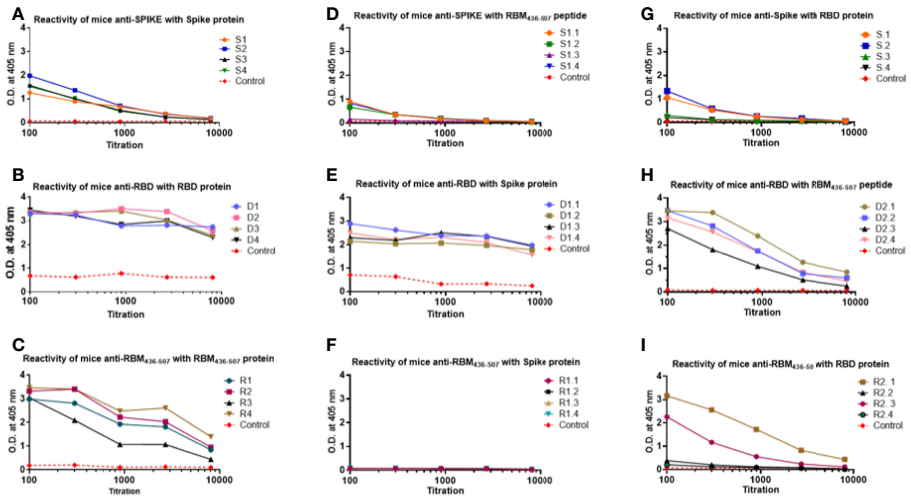

FIGURE 3 | Homologous and cross reactivity of the S, RBD and $RBM_{436-507}$ antigens with antibodies elicited upon mice immunization. **(A–C)** show reactivity of anti-S, anti-RBD and anti-$RBM_{436-507}$ produced in mice with their homologous antigens. **(D, G)** show cross reactivity of anti-S with RBM and RBD antigens. **(E, H)** of anti-RBD with S and RBM antigens. **(F, I)**, of anti RBM436-507 with S and RBD, respectively. SD is < 20% of the mean.

Sera from mice immunized with $RBM_{436-507}$ peptide also displayed high reactivity with the homologous peptide and the RBD protein; however, these sera did not react with the S protein (**Figure 3**). We further analyzed reactivity of anti-$RBM_{436-507}$ antibodies upon solid-phase capture on ELISA plates followed by glycine elution with its homologous peptide, the RBD and the S proteins. As shown in **Figure 4**, while there was significant reactivity of eluted antibodies with $RBM_{436-507}$, no recognition of the motif on the RBD and S proteins was observed.

Evaluation of Anti- $RBM_{436-507}$ Antibodies in Humans

Patient sera were first screened by ELISA using S and RBD proteins and compared to a group of pre-pandemic normal sera. IgG antibody levels higher than the 97.5th percentile of normal sera were detected in 45% (29/64) of patient sera on S and in 53% (34/64) on RBD (**Figures 5A, B**). A strong positive correlation ($p<0,0001$) was observed between antibody levels for the two recombinant proteins (**Figure 5C**).

It has been shown that low pH affects spike structure, favoring a closed conformation of the trimer (34), affecting epitope exposure (16). We thus performed the ELISA assay at acidic pH, obtaining a similar level of antibodies in patient sera (**Supplementary Figures 2A, B**). Sera from COVID-19 patients and normal subjects were tested by ELISA using RBM immobilized on polystyrene plates (see *Materials and Methods* for details). IgG anti-$RBM_{436-507}$ higher than the 97.5th percentile of the healthy population was detected in 21/60 (35%) of the COVID-19 patients. IgG antibody levels were significantly higher in patients than in controls ($p<0.05$) (**Figure 6A**) and

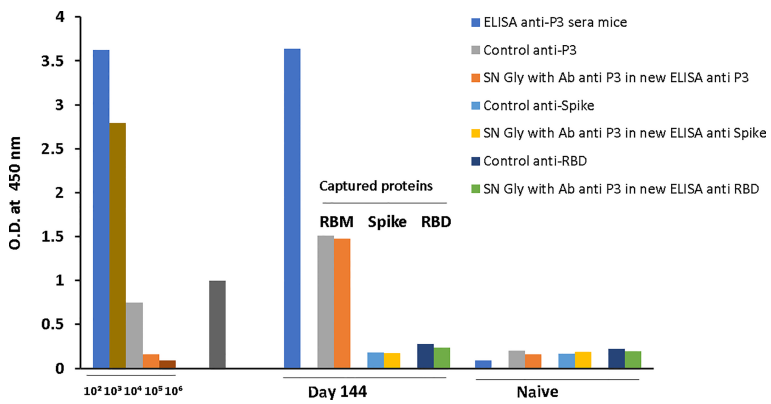

FIGURE 4 | Cross-reactivity of S and RBD with ELISA captured $RBM_{436-507}$. ELISA captured mice anti-$RBM_{436-507}$ antibodies were eluted with Gly pH 2.5 and used to determine the reactivity with RBM (homologous), and with S and RBD (heterologous) antigens ELISA reaction was developed using rabbit anti-mouse alkaline phosphatase conjugate.

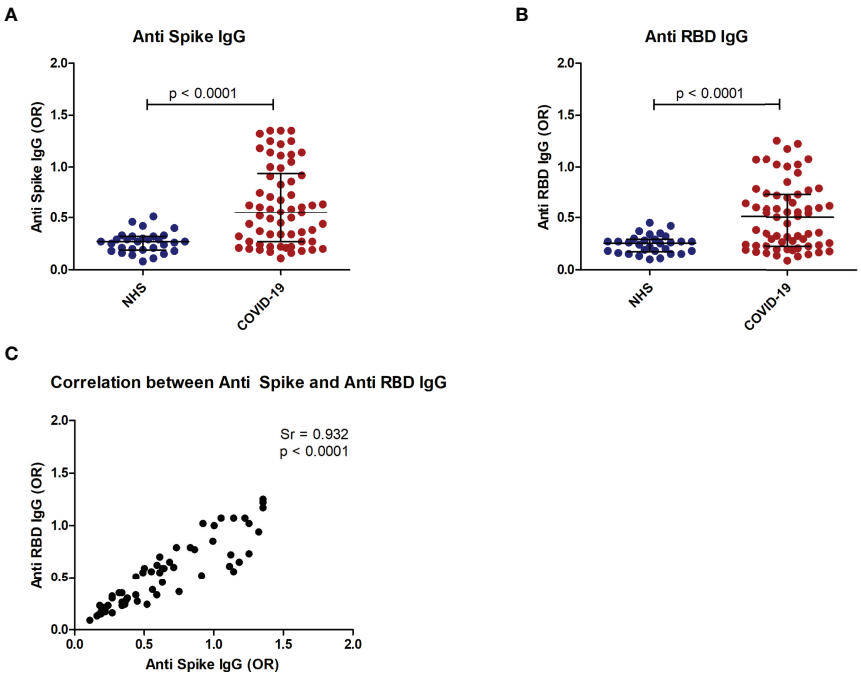

FIGURE 5 | Anti-Spike and anti-RBD antibodies in COVID-19 patients. Distribution of anti-S IgG **(A)** and anti RBD IgG **(B)** in COVID-19 patients as compared to normal controls (NHS). Correlation of anti-S IgG and anti-RBD IgG in COVID-19 patients **(C)**. $p < 0.05$ was considered significant.

were correlated with anti-S and anti-RBD antibody levels ($p < 0.01$) (**Figures 6D, E**). Anti $RBM_{436\text{-}507}$ of IgM and IgA isotype were also evaluated, with IgM anti- $RBM_{436\text{-}507}$ detected in 7/60 (11.6%) and IgA in 6/60 (10%) (**Figures 6B, C**). IgM and IgA antibody levels were not significantly different in COVID-19 patients and controls. There was coexpression of anti-$RBM_{436\text{-}507}$ Ig isotypes in COVID-19 samples (**Figure 6F**).

Epitope Mapping and Functional Activity of Murine and Human Anti-$RBM_{436\text{-}507}$ Antibodies

The analysis of the neutralizing activity of antibodies elicited by mouse immunization showed that, for mice immunized with S and RBD, the neutralization was significantly boosted after the second and third doses. Both S and RBD sera induced total neutralization after the third dose and remained high until the last test on day 115. In contrast, antibodies to $RBM_{436\text{-}507}$ reached 40% neutralization, which remained at that level until day 115 (**Figures 7A–C**).

To determine whether $RBM_{436\text{-}507}$ represents a target of neutralizing antibodies in natural conditions, we first carried out an extensive ELISA analysis of sera from both COVID-19 patients and immunized mice, and second, we compared the ACE2-RBD binding neutralization by antibodies to the whole RBD and to $RBM_{436\text{-}507}$. In the ELISA analysis of human sera (n= 100) from COVID-19 patients 35 (35%) reacted with the $RBM_{436\text{-}507}$ indicating a lower reactivity than the same sera with the S and RBD. Positive samples displayed distinct reactivity with different regions of $RBM_{436\text{-}507}$, more frequently with the N-terminal portion (P15-P16). Neutralizing activity of anti-$RBM_{436\text{-}507}$ antibodies has been evaluated by inhibition of RBD binding to ACE2, an assay considered a SARS-CoV-2 surrogate virus neutralization test (35–37). Neutralizing antibodies may bind to sequences exposed both in the closed and the open conformation of the S protein or only in the open one; most of these sequences are comprised in $RBM_{436\text{-}507}$. In contrast to human patients, mice immunized with $RBM_{436\text{-}507}$ presented good recognition of $RBM_{436\text{-}507}$ and RBD but no reactivity with S.

Since neutralizing antibodies mostly specific for RBD but also to several targeted epitopes are produced during natural infection (21, 22), in the ACE2-RBD binding neutralization assay, antibodies to the whole RBD and to $RBM_{436\text{-}507}$ were compared. In the case of humans with confirmed COVID-19 infection, sera positive to $RBM_{436\text{-}507}$ were tested using the 20-mer overlapping peptides covering the entire RBM sequence (**Table 1**). As shown in **Figure 8**, immune response mainly targets the N terminal domain (P15-P16) rather than the C-terminal part (P11-P12). To evaluate the ability of antibodies to RBD or $RBM_{436\text{-}507}$ sequences to block ACE2 binding to RBD, specific anti-RBD and anti-$RBM_{436\text{-}507}$ antibodies were eluted from COVID-19 positive sera using antigen-coated wells and incubated with labeled ACE2 on solid-phase RBD. Anti-RBD antibodies eluted from 4 COVID-19 sera inhibited the binding of labeled ACE2 to solid-phase RBD (**Figure 9**). Anti-$RBM_{436\text{-}507}$ antibodies from 2 out of 4 sera displayed some inhibition, higher than anti-N1 and anti-TT control antibodies.

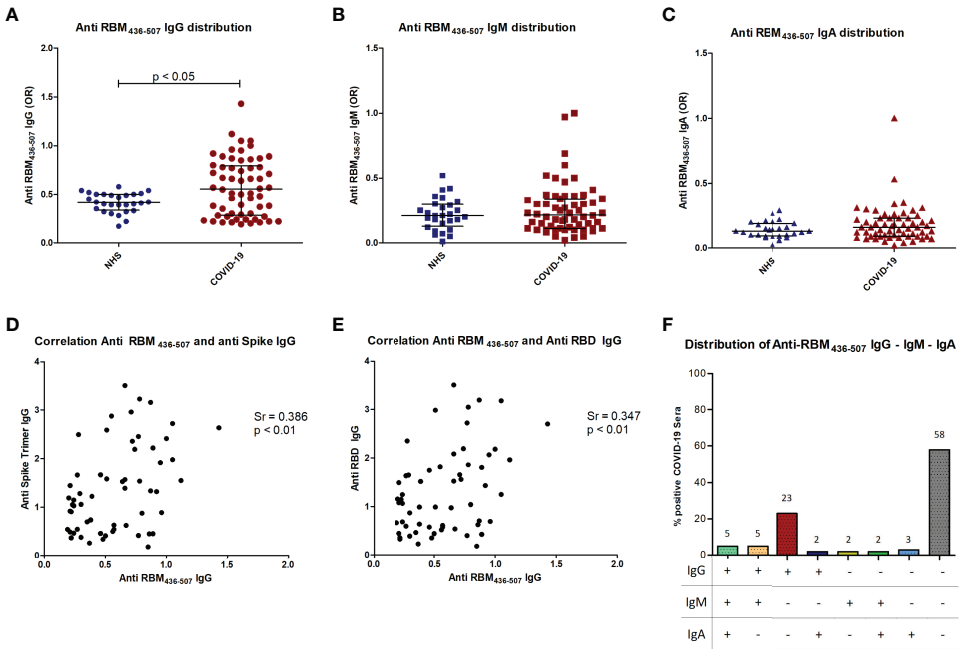

FIGURE 6 | Anti-$RBM_{436-507}$ Ig isotypes in COVID-19 patients. Distribution of anti RBM IgG **(A)**, IgM **(B)** and IgA **(C)** in COVID-19 patients is shown compared to normal controls (NHS). Correlation of anti-RBM IgG with anti-Spike **(D)** or anti-RBD **(E)** IgG in COVID-19 patients **(D)**. Distribution of anti-RBM antibody isotypes **(F)**. $p < 0.05$ was considered significant.

DISCUSSION

This study confirmed the high seroreactivity of the full-length S and RBD recombinant proteins and described the immunogenicity of the synthetic $RBM_{436-507}$ fragment. Moreover, it compared the antibody responses induced by natural human exposure to SARS-CoV-2 with that of rodents experimentally immunized with the three antigens.

Analysis of 3D structures of the S protein and RBD-ACE2 complex led to selecting a RBD 72 aa long segment ($RBM_{436-507}$) highly specific to SARS-CoV-2 and located in the RBD-ACE2 interface. Importantly, *in silico* studies confirmed the presence in this protein fragment of multiple immune epitopes (B- and T-cell epitopes) previously identified (33), and our CD data suggested that the $RBM_{436-507}$ peptide alone can partially preserve the extended beta-conformation observed in the context of the native protein structure. Indeed within the folded Spike protein, two short antiparallel beta sheets are observed (residues 453-454, 492-493 sheet1, and 473-474, 488-489, sheet2) but many other residues are in extended conformation (38/72, 53 %). The $RBM_{436-507}$ peptide shows a high percentage of random coil conformation (about 50%) as expected for an isolated peptide; however, it maintains about one half of the extended conformation of the segment 436-507 when included in the whole protein which is an interesting result especially considering that many of the epitope residues of RBM that make interactions with a human neutralizing antibody (P2B-2F6 Fab) are in extended conformation, notably K444, N448, L452, V483, E484, F490 and S494 (38)

These features, together with the high RBD immunogenicity during human natural infection, vaccination and animal

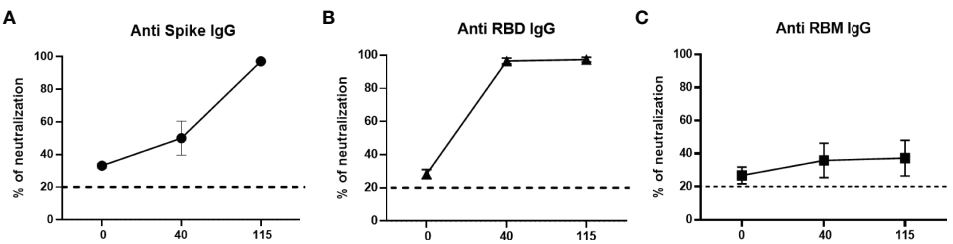

FIGURE 7 | Neutralizing ability of antibodies in mice. Neutralizing ability of anti-S **(A)**, anti-RBD **(B)** and anti-RBM **(C)** antibodies from immunized mice. Results are shown as the percentage of inhibition of specific antibodies at different days (0, 40, and 115) post-immunization.

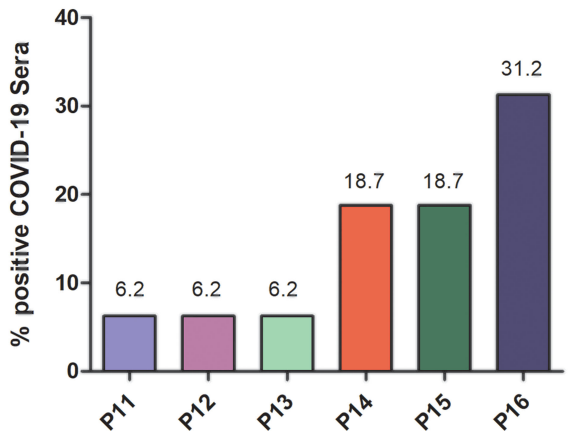

FIGURE 8 | Fine specificity of anti-RBM436-507 antibodies in COVID-19 patients. Reactivity of anti-RBM positive COVID-19 sera with 20-mers overlapping peptides (P11-P16) covering the entire $RBM_{436-507}$ sequence. Results are shown as percentage of anti-RBM positive sera reacting with the specific peptide.

immunization, as well as the efficient neutralization of the RBD-ACE2 interaction by anti-RBD antibodies, encouraged the search for a smaller fragment with vaccine potential, suitable for production by peptide synthesis technology. It was hoped that the smaller fragment could elicit virus-neutralizing antibodies with similar or superior vaccine performance than the S protein.

The multiple vaccines delivered worldwide are based on the full-length S protein using different technological platforms (39). Although most of them have displayed high protective efficacy, their effectivity, particularly the antibody response's longevity and the virus-neutralizing function, appears short-lasting. Within less than a year of a two doses immunization schedule, a third vaccine dose was required to maintain the protection level; moreover, boosting vaccine doses may be further required to offer functional immunity in the population (40). Because of the vast virus propagation capacity in the population, frequent vaccination generates a significant logistic and global economic challenge; therefore, alternative vaccine platforms are envisioned.

The strong positive correlation of the ELISA seroreactivity of the S (45% = 29/64) and RBD (53% = 34/64) proteins ($p<0,0001$) is very interesting and confirms the feasibility of using a fragment of the S protein as vaccine. In addition, this result correlates with the highly efficient neutralization induced by mouse anti-S and -RBD sera. Moreover, the IgG ELISA reactivity of these two proteins with COVID19 and pre-pandemic normal sera (>97.5th percentile) indirectly confirmed the response specificity to SARS-COV-2. In contrast, specific IgM and IgA antibodies are less frequent in COVID-19 patients. This latter finding may be explained because in the COVID-19 sera the primary IgM response and IgA had waned. These results support the idea that shorter protein fragments i.e., RBD would have the capacity to stimulate at least a similar immune response to S protein.

We show here that the antibody recognition of $RBM_{436-507}$ as an isolated fragment, i.e., as $RBM_{436-507}$ peptide, was present in a fraction of COVID-19 donors. In COVID-19 patients, a polyclonal anti-$RBM_{436-507}$ antibody response with IgM, IgG and IgA isotypes was detected in one third of the cases, in amounts correlated with the level of anti-RBD and anti-S antibodies. Our finding that COVID-19 patients recognise $RBM_{436-507}$ and smaller peptides within this sequence is in agreement with a report from 2020 (17) showing that infected subjects produced antibodies to multiple sequences, such as $S_{412-431}$ and $S_{446-465}$, that overlap ACE2 contact residues, and $S_{432-451}$ and $S_{475-494}$, that are adjacent to critical residues contacted by ACE2, all contained within $RBM_{436-507}$.

The high level of neutralization achieved by mice sera after the first immunization dose with RBD encouraged selection of a smaller protein fragment with vaccine potential. Complete neutralization is produced after the first immunization with RBD, whereas similar neutralization by anti-S antibodies is only obtained after two immunization doses. In contrast, the poor neutralization of the anti-$RBM_{436-507}$ antibodies was unexpected and deserves further studies. This result is surprising as there was significant cross reactivity of anti-RBD and anti-$RBM_{436-507}$.

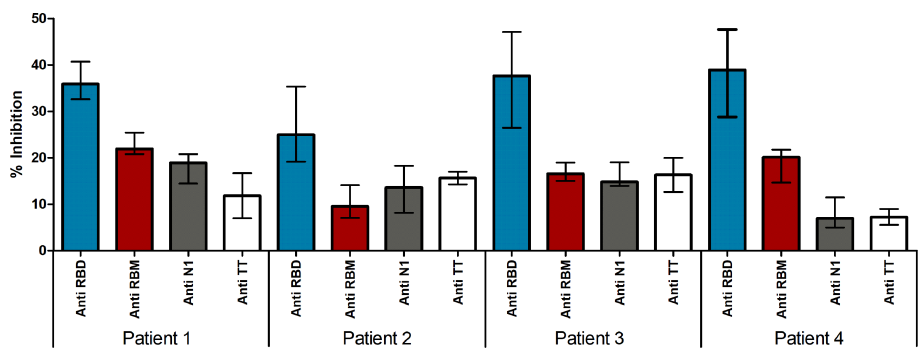

FIGURE 9 | Neutralizing ability of antibodies in Covid-19 patients. Neutralizing ability of antigen eluted anti-S, anti-RBD and anti-RBM antibodies in COVID-19 patients. Results are shown as the percentage of inhibition of ACE-HRP binding to RBD.

The neutralizing activity of anti-$RBM_{436-507}$ antibodies might be associated with the lack of recognition of the full-length S by the anti-$RBM_{436-507}$ sera. In addition, the high immunogenicity of $RBM_{436-507}$ mice confirms the presence of T-cell epitopes within this protein segment, as suggested by the analysis performed by Grifoni et al. (33).

Mouse IgG antibodies efficiently reacted with both $RBM_{436-507}$ and RBD, but not with S. The latter results can be explained by the fact that $RBM_{436-507}$ represent only 6-7% of the whole protein. Moreover, anti-$RBM_{436-507}$ specific antibodies elicited by mice immunization only partially inhibited (30-40%) the RBD-ACE2 interaction, while mouse anti S and RBD recognized RBM and induced 100% inhibition of the ligand-receptor interaction. These results suggest that the conformation of isolated $RBM_{436-507}$ only partially overlaps with the RBM structures present in S or RDB. The relatively high percentage of β-strand conformation suggests that $RBM_{436-507}$ peptide alone can partially preserve the extended conformation displayed along most of its sequence within the folded S protein (pdb code 6VXX) (21, 23).

In conclusion, our comparative analysis of immunological properties has shown that although $RBM_{436-507}$ had reduced seroreactivity compared to the S protein and RBD, it could still represent an alternative path for developing virus control means, such as vaccines. The basis for this potential lies in its small size, absence of folding problems, possibility to constraint the RBM conformation in a required state, easy incorporation in different multimeric carriers and advantages associated with peptide synthesis production.

Further studies are needed to strengthen the potential use of $RBM_{436-507}$ in vaccination strategies.

DATA AVAILABILITY STATEMENT

The raw data supporting the conclusions of this article will be made available by the authors, without undue reservation.

ETHICS STATEMENT

The studies involving human participants were reviewed and approved by Comitato etico Area Vasta Nord Ovest (Pisa - Italy) Approval N° 17522. Comitè de Etica Centro Internacional de Vacunas Approval N° 04-2020. The patients/participants provided their written informed consent to participate in this study. The animal study was reviewed and approved by Comité de Etica Centro International de Vacunas Approval N° 04-2020.

AUTHOR CONTRIBUTIONS

Conceptualization: GC, AP, AK, and SH; Formal analysis: GC, MA-H, AP, AK, and SH; Investigation: GC, PR, FP, PM, LP, FE, AC, IP-M, SB, DK, MD, SQ, MA-H, and SH; Methodology: MA-H, FP, FE, SH, and GC; Project administration: MA-H and GC; Resources: GC, SH, AK, and AP; Supervision: MA-H, SH, and GC; Validation: MA-H, GC, and AK; Visualization: MA-H, SH, and GC; Writing: PM, PR, GC, SH, FP, and AK. All authors contributed to the article and approved the submitted version.

FUNDING

This work was funded by MVDC/CIV Foundation (grant 150820) and by the Italian Ministry of Health grant COVID-2020-12371849

ACKNOWLEDGMENTS

We thank the volunteers from Pisa (Italy) and from Cali (Colombia) for their invaluable contribution to the study. We also thank Prof. Florian Wurm and Dr. Maria Wurm at Excellgene SA, Monthey (Switzerland) for providing S and RBD antigens.

SUPPLEMENTARY MATERIAL

The Supplementary Material for this article can be found online at: https://www.frontiersin.org/articles/10.3389/fimmu.2022.879946/full#supplementary-material

Supplementary Figure 1 | ELISA titration of the mouse antibody response. Humoral response induced in mice after immunization at days 0, 20, and 40: ELISA used three-fold serial dilutions of sera, starting at 1:100. Antibody titers are expressed as O.D

Supplementary Figure 2 | Effect of pH on anti-Spike and -RBD antibodies. Distribution of Anti-Spike antibodies **(A)** and anti-RBD antibodies **(B)** analyzed by ELISA under acid conditions (pH 5) and neutral conditions (pH 7.4). Results are expressed as OD 450 nm.

REFERENCES

1. Fehr AR, Perlman S. Coronaviruses: An Overview of Their Replication and Pathogenesis. *Methods Mol Biol* (2015) 1282:1–23. doi: 10.1007/978-1-4939-2438-7_1
2. Bellan M, Patti G, Hayden E, Azzolina D, Pirisi M, Acquaviva A, et al. Fatality Rate and Predictors of Mortality in an Italian Cohort of Hospitalized COVID-19 Patients. *Sci Rep* (2020) 1(1):20731. doi: 10.1038/s41598-020-77698-4
3. O'Driscoll M, Ribeiro Dos Santos G, Wang L, Cummings DAT, Azman AS, Paireau J, et al. Age-Specific Mortality and Immunity Patterns of SARS-Cov-2. *Nature* (2021) 590(7844):140–5. doi: 10.1038/s41586-020-2918-0
4. Williamson EJ, Walker AJ, Bhaskaran K, Bacon S, Bates C, Morton CE, et al. Factors Associated With COVID-19-related Death Using Opensafely. *Nature* (2020) 584(7821):430–6. doi: 10.1038/s41586-020-2521-4
5. WHO. *Weekly Epidemiological Update on COVID-19* (2022). Available at: https://www.who.int/publications/m/item/weekly-epidemiological-update-on-covid-19—15-february-2022.

6. Li CX, Noreen S, Zhang LX, Saeed M, Wu PF, Ijaz M, et al. A Critical Analysis of SARS-CoV-2 (Covid-19) Complexities, Emerging Variants, and Therapeutic Interventions and Vaccination Strategies. *BioMed Pharmacother* (2022) 146:112550. doi: 10.1016/j.biopha.2021.112550
7. Sharma O, Sultan AA, Ding H, Triggle CR. A Review of the Progress and Challenges of Developing a Vaccine for COVID-19. *Front Immunol* (2020) 11:585354. doi: 10.3389/fimmu.2020.585354
8. Walls AC, Park YJ, Tortorici MA, Wall A, McGuire AT, Veesler D, et al. Structure, Function, and Antigenicity of the SARS-CoV-2 Spike Glycoprotein. *Cell* (2020) 181(2):281–292.e6. doi: 10.1016/j.cell.2020.02.058
9. Wierbowski SD, Liang S, Liu Y, Chen Y, Gupta S, Andre NM, et al. A 3D Structural SARS-CoV-2-human Interactome to Explore Genetic and Drug Perturbations. *Nat Methods* (2021) 18(12):1477–88. doi: 10.1038/s41592-021-01318-w
10. Fan X, Cao D, Kong L, Zhang X. Cryo-EM Analysis of the Post-Fusion Structure of the SARS-CoV Spike Glycoprotein. *Nat Commun* (2020) 11 (1):3618. doi: 10.1038/s41467-020-17371-6
11. Cai Y, Zhang J, Xiao T, Peng H, Sterling SM, Walsh RM Jr, et al. Distinct Conformational States of SARS-CoV-2 Spike Protein. *Science* (2020) 369 (6511):1586–92. doi: 10.1126/science.abd4251
12. Wrapp D, Wang N, Corbett KS, Goldsmith JA, Hsieh CL, Abiona O, et al. Cryo-EM Structure of the 2019-nCoV Spike in the Prefusion Conformation. *Science* (2020) 367(6483):1260–3. doi: 10.1126/science.abb2507
13. Polack FP, Thomas SJ, Kitchin N, Absalon J, Gurtman A, Lockhart S, et al. Safety and Efficacy of the BNT162b2 Mrna Covid-19 Vaccine. *N Engl J Med* (2020) 383(27):2603–15. doi: 10.1056/NEJMoa2034577
14. Baden LR, El Sahly HM, Essink B, Kotloff K, Frey S, Novak R, et al. Efficacy and Safety of the Mrna-1273 SARS-CoV-2 Vaccine. *N Engl J Med* (2021) 384 (5):403–16. doi: 10.1056/NEJMoa2035389
15. Shang J, Ye G, Shi K, Wan Y, Luo C, Aihara H, et al. Structural Basis of Receptor Recognition by SARS-Cov-2. *Nature* (2020) 581(7807):221–4. doi: 10.1038/s41586-020-2179-y
16. Tortorici MA, Beltramello M, Lempp FA, Pinto D, Dang HV, Rosen LE, et al. Ultrapotent Human Antibodies Protect Against SARS-CoV-2 Challenge Via Multiple Mechanisms. *Science* (2020) 370(6519):950–7.doi: 10.1126/science.abe3354
17. Amanat F, Krammer F. SARS-Cov-2 Vaccines: Status Report. *Immunity* (2020) 52(4):583–9. doi: 10.1016/j.immuni.2020.03.007
18. Barnes CO, Jette CA, Abernathy ME, Dam KA, Esswein SR, Gristick HB, et al. Sars-CoV-2 Neutralizing Antibody Structures Inform Therapeutic Strategies. *Nature* (2020) 588(7839):682–7. doi: 10.1038/s41586-020-2852-1
19. Roberts A, Chouhan RS, Shahdeo D, Shrikrishna NS, Kesarwani V, Horvat M, et al. A Recent Update on Advanced Molecular Diagnostic Techniques for COVID-19 Pandemic: An Overview. *Front Immunol* (2021) 12:732756. doi: 10.3389/fimmu.2021.732756
20. Du L, He Y, Zhou Y, Liu S, Zheng BJ, Jiang S, et al. The Spike Protein of SARS-CoV–a Target for Vaccine and Therapeutic Development. *Nat Rev Microbiol* (2009) 7(3):226–36. doi: 10.1038/nrmicro2090
21. Piccoli L, Park YJ, Tortorici MA, Czudnochowski N, Walls AC, Beltramello M, et al. Mapping Neutralizing and Immunodominant Sites on the SARS-CoV-2 Spike Receptor-Binding Domain by Structure-Guided High-Resolution Serology. *Cell* (2020) 183(4):1024–2.e21. doi: 10.1016/j.cell.2020.09.037
22. Shrock E, Fujimura E, Kula T, Timms RT, Lee IH, Leng Y, et al. Viral Epitope Profiling of COVID-19 Patients Reveals Cross-Reactivity and Correlates of Severity. *Science* (2020) 370(6520). doi: 10.1126/science.abd4250
23. FDA. *Emergency Use Authorization 108* (2021). Available at: https://www.fda.gov/media/155053/download.
24. FDA. *Emergency Use Authorization 105* (2021). Available at: https://www.fda.gov/media/155049/download.
25. Parums DV. Editorial: Current Status of Oral Antiviral Drug Treatments for SARS-CoV-2 Infection in Non-Hospitalized Patients. *Med Sci Monit* (2022) 28:e935952. doi: 10.12659/MSM.935952
26. Pino P, Kint J, Kiseljak D, Agnolon V, Corradin G, Kajava AV, et al. Trimeric SARS-CoV-2 Spike Proteins Produced From CHO Cells in Bioreactors are High-Quality Antigens. *Processes* (2020) 8(12):1539. doi: 10.3390/pr8121539
27. *Sars-CoV-2 Variants of Concern as of February* (2022). Available at: https://www.who.int/en/activities/tracking-SARS-CoV-2-variants/.
28. Rizzolo F, Testa C, Lambardi D, Chorev M, Chelli M, Rovero P, et al. Conventional Microwave-Assisted SPPS Approach: A Comparative Synthesis of PTHrP (1-34) NH2. *J Pept Sci* (2011) 17(10):708–14. doi: 10.1002/psc.1395
29. Whitmore L, Wallace BA. DICHROWEB, an Online Server for Protein Secondary Structure Analyses From Circular Dichroism Spectroscopic Data. *Nucleic Acids Res* (2004) 32:W668–73. doi: 10.1093/nar/gkh371
30. Sreerama N, Woody RW. Estimation of Protein Secondary Structure From Circular Dichroism Spectra: Comparison of CONTIN, SELCON, and CDSSTR Methods With an Expanded Reference Set. *Anal Biochem* (2000) 287(2):252–60. doi: 10.1006/abio.2000.4880
31. Olugbile S, Habel C, Servis C, Spertini F, Verdini A, Corradin G, et al. Malaria Vaccines - The Long Synthetic Peptide Approach: Technical and Conceptual Advancements. *Curr Opin Mol Ther* (2010) 12(1):64–76.
32. Olugbile S, Villard V, Bertholet S, Jafarshad A, Kulangara C, Roussilhon C, et al. Malaria Vaccine Candidate: Design of a Multivalent Subunit Alpha-Helical Coiled Coil Poly-Epitope. *Vaccine* (2011) 29(40):7090–9. doi: 10.1016/j.vaccine.2011.06.122
33. Grifoni A, Sidney J, Zhang Y, Scheuermann RH, Peters B, Sette A, et al. A Sequence Homology and Bioinformatic Approach Can Predict Candidate Targets for Immune Responses to SARS-Cov-2. *Cell Host Microbe* (2020) 27 (4):671–680.e2. doi: 10.1016/j.chom.2020.03.002
34. Zhou T, Tsybovsky Y, Gorman J, Rapp M, Cerutti G, Chuang GY, et al, Cryo-EM Structures of SARS-CoV-2 Spike without and with ACE2 Reveal a pH-Dependent Switch to Mediate Endosomal Positioning of Receptor-Binding Domains. *Cell Host Microbe* (2020) 28(*6*):867–79.e5. doi: 10.1016/j.chom.2020.11.004
35. Marien J, Michiels J, Heyndrickx L, Nkuba-Ndaye A, Ceulemans A, Bartholomeeusen K, et al. Evaluation of a Surrogate Virus Neutralization Test for High-Throughput Serosurveillance of SARS-Cov-2. *J Virol Methods* (2021) 297:114228. doi: 10.1016/j.jviromet.2021.114228
36. Pratesi F, Caruso T, Testa D, Tarpanelli T, Gentili A, Gioè F, et al. BNT162b2 Mrna SARS-CoV-2 Vaccine Elicits High Avidity and Neutralizing Antibodies in Healthcare Workers. *Vaccines (Basel)* (2021) 9(6). doi: 10.3390/vaccines9060672
37. Tan CW, Chia WN, Qin X, Liu P, Chen MI, Tiu C, et al. A SARS-CoV-2 Surrogate Virus Neutralization Test Based on Antibody-Mediated Blockage of ACE2-spike Protein-Protein Interaction. *Nat Biotechnol* (2020) 38(9):1073–8. doi: 10.1038/s41587-020-0631-z
38. Ju B, Zhang Q, Ge J, Wang R, Sun J, Ge X, et al. Human Neutralizing Antibodies Elicited by SARS-CoV-2 Infection. *Nature* (2020) 584:115–9. doi: 10.1038/s41586-020-2380-z
39. Silveira MM, Moreira G, Mendonca M. DNA Vaccines Against COVID-19: Perspectives and Challenges. *Life Sci* (2021) 267:118919. doi: 10.1016/j.lfs.2020.118919
40. Krause PR, Fleming TR, Peto R, Longini IM, Figueroa JP, Sterne JAC, et al. Considerations in Boosting COVID-19 Vaccine Immune Responses. *Lancet* (2021) 398(10308):1377–80. doi: 10.1016/S0140-6736(21)02046-8

Conflict of Interest: The authors declare that the research was conducted in the absence of any commercial or financial relationships that could be construed as a potential conflict of interest.

frontiers | Frontiers in Immunology

ORIGINAL RESEARCH
published: 27 May 2022
doi: 10.3389/fimmu.2022.876533

Differences in SARS-CoV-2-Specific Antibody Responses After the First, Second, and Third Doses of BNT162b2 in Naïve and Previously Infected Individuals: A 1-Year Observational Study in Healthcare Professionals

*Manca Ogrič[1], Polona Žigon[1,2], Eva Podovšovnik[3], Katja Lakota[1,2], Snezna Sodin-Semrl[1,2], Žiga Rotar[1,4] and Saša Čučnik[1,5]**

[1] Department of Rheumatology, University Medical Centre Ljubljana, Ljubljana, Slovenia, [2] University of Primorska, Faculty of Mathematics, Natural Sciences and Information Technologies, Koper, Slovenia, [3] Valdoltra Orthopaedic Hospital, Ankaran, Slovenia, [4] Faculty of Medicine, University of Ljubljana, Ljubljana,Slovenia, [5] Faculty of Pharmacy, University of Ljubljana, Ljubljana, Slovenia

OPEN ACCESS

Edited by:
Suryaprakash Sambhara, Centers for Disease Control and Prevention (CDC), United States

Reviewed by:
Waleed Mahallawi, Taibah University, Saudi Arabia
Ricardo Ribeiro, Instituto de Investigação e Inovação em Saúde, Universidade do Porto, Portugal

***Correspondence:**
Saša Čučnik
sasa.cucnik@kclj.si

Specialty section:
This article was submitted to Vaccines and Molecular Therapeutics, a section of the journal Frontiers in Immunology

Received: 15 February 2022
Accepted: 28 April 2022
Published: 27 May 2022

Citation:
Ogrič M, Žigon P, Podovšovnik E, Lakota K, Sodin-Semrl S, Rotar Ž and Čučnik S (2022) Differences in SARS-CoV-2-Specific Antibody Responses After the First, Second, and Third Doses of BNT162b2 in Naïve and Previously Infected Individuals: A 1-Year Observational Study in Healthcare Professionals. Front. Immunol. 13:876533. doi: 10.3389/fimmu.2022.876533

Background: Safe and effective vaccines against COVID-19 are critical for preventing the spread of SARS-CoV-2, but little is known about the humoral immune response more than 9 months after vaccination. We aimed to assess the humoral immune response after the first, second, and third (booster) doses of BNT162b2 vaccine in SARS-CoV-2 naïve and previously infected healthcare professionals (HCP) and the humoral immune response after infection in vaccinated HCP.

Methods: We measured anti-spike (anti-S) and anti-nucleocapsid antibodies at different time points up to 12 months in the sera of 300 HCP who had received two or three doses of BNT162b2 vaccine. Mixed-model analyses were used to assess anti-S antibody dynamics and to determine their predictors (age, sex, BMI, and previous infection).

Results: Naïve individuals had statistically lower anti-S antibody concentrations after the first dose (median 253 BAU/ml) than previously infected individuals (median 3648 BAU/ml). After the second dose, anti-S antibody concentrations increased in naïve individuals (median 3216 BAU/ml), whereas the second dose did not significantly increase concentrations in previously infected individuals (median 4503 BAU/ml). The third dose resulted in an additional increase in concentrations (median 4844 BAU/ml in naïve and median 5845 BAU/ml in previously infected individuals). Anti-S antibody concentrations steadily decreased after the second dose and after the third dose in naïve and previously infected individuals. In addition, we found that age had an effect on the humoral immune response. Younger individuals had higher anti-S antibody concentrations after the first and second doses. After infection with the new variant Omicron, a further increase in anti-S

antibody concentrations to a median value of 4794 BAU/ml was observed in three times vaccinated HCP whose anti-S antibody concentrations were relatively high before infection (median 2141 BAU/ml). Our study also showed that individuals with systemic adverse events achieved higher anti-S antibody concentrations.

Conclusion: In this study, significant differences in humoral immune responses to BNT162b2 vaccine were observed between naïve and previously infected individuals, with age playing an important role, suggesting that a modified vaccination schedule should be practiced in previously infected individuals. In addition, we showed that the high anti-S antibodies were not protective against new variants of SARS-CoV-2.

Keywords: COVID-19, SARS-CoV-2, BNT162b2 vaccine, anti-S antibody dynamics, healthcare professionals, humoral immune response

1 INTRODUCTION

The pandemic of coronavirus disease 2019 (COVID-19) caused by severe acute respiratory syndrome coronavirus 2 (SARS-CoV-2) has greatly affected the normal life of people and the functioning of society (1). One of the key factors to prevent the spread of infection in the population is the use of safe and effective vaccines. Vaccination protects individuals and thus reduces the risk of clinically significant consequences in the event of infection. An additional issue in protecting vaccinated and previously infected individuals is the new variants of the virus, including Omicron, that are emerging in the population (2, 3).

The efficacy of different vaccines has been reported in clinical trials to be 50-95% (4–7). The efficacy of two doses of the vaccine BNT162b2 (Comirnaty, Pfizer and BioNTech), a single-stranded mRNA carrying the spike (S) protein transcript, located in lipid nanoparticles, is 95% (4), while protection against reinfection in previously infected individuals is estimated at 89% (7). The specific antibodies against SARS-CoV-2 produced during infection are antibodies against S and nucleocapsid protein (N) (anti-S and anti-N antibodies), whereas only anti-S antibodies are produced after vaccination with BNT162b2. The duration of protection that an individual develops after vaccination or after overcoming infection is still largely unclear. However, we do know that the primary humoral immune response declines over time (8–10). In addition, information about concentrations of anti-S antibodies sufficient to prevent infection is not known but would be clinically relevant, especially for the new Omicron variant.

Currently, there are limited data on the dynamics and concentrations of anti-S antibodies over a longer period after vaccination. A clinical study investigating antibody responses after initial and booster vaccination with BNT162b2 has shown strong anti-S IgG antibody responses with concentrations exceeding those in COVID-19 convalescent plasma and a decrease in antibody concentrations 85 days after the first dose (11). Longer studies, as presented by Collier et al. showed data in which decreasing vaccine immunity was observed 8 months after vaccination, not only with BNT162b2 but also with other vaccines used (12).

Responses to vaccination also vary widely due to differences between individuals. In some studies, a negative correlations between anti-S antibody concentrations and age were observed (13–16), while one study showed lower magnitude of memory B-cell responses with increasing age (17). Limited information is available on association of adverse events and anti-S antibody concentration. Specifically, Goel et al. found no significant correlation between anti-S antibody concentration and the severity of adverse events (17), while Naaber et al. reported that adverse events correlated positively with anti-S antibody concentration (13).

In our study, we primarily investigated the humoral immune response to the first, second, and third (booster) doses of BNT162b2 vaccine by measuring anti-S antibody concentrations in healthcare professionals (HCP) who were not previously infected with SARS-CoV-2 virus (so-called naïve individuals) and in previously infected individuals. We also examined the 12-month dynamics of anti-S antibody concentrations after the second dose and the 3-month dynamics after the third (booster) dose, as well as the concentrations of anti-S antibodies after infections with SARS-CoV-2 in vaccinated HCP. In addition, we performed a mixed-model analyses to determine the predictors (age, sex, BMI and previous infection) of anti-S antibody concentrations and dynamics. Finally, we compared anti-S antibody concentrations among the group of HCP with systemic, local, and no adverse events after the second dose.

2 MATERIAL AND METHODS

2.1 Sample and Data Collection

HCP, employees of the Division of Internal Medicine University Medical Centre Ljubljana, who had received at least two or three doses of the BNT162b2 mRNA vaccine were included in the study. Participants provided detailed information on their health status (presence of chronic diseases), demographics, lifestyle (age, sex, BMI), occurrence of adverse events after vaccination, and SARS-CoV-2 infection before and during vaccination *via* questionnaires.

Serum samples from HCP were collected longitudinally from December 2020 to December 2021 at different time points: before the first dose (P0), three weeks after the first dose (P1), approximately three weeks (range 2-5 weeks) after the second dose (P2), three (P3), six (P4), nine (P5) and twelve (P*) months after the first dose; and three weeks (P6) and three months (P7) after the third (booster) dose (**Figure 1**). Additional samples were collected from January to February 2022 only from HCP infected with SARS-CoV-2 after the last time point (P6 or P7).

The study was approved by the Slovenian National Medical Ethics Committee (#0120-422/2020/6). Participants signed an informed consent form before recruitment to the study. The study was conducted in accordance with the Helsinki Declaration.

2.2 Antibody Testing

Anti-S antibodies to the S1 subunit and anti-N antibodies were measured by enzyme linked immunosorbent assay (anti-SARS-CoV-2 QuantiVac ELISA (IgG) for detection of anti-S antibodies and anti-SARS-CoV-2 NCP ELISA (IgG) for detection of anti-N antibodies, both from Euroimmun, Germany). Concentrations of anti-S antibodies were used to evaluate the efficacy of vaccination, while the presence of anti-N antibodies indicated symptomatic, PCR-positive individuals and asymptomatic COVID-19 infections. ELISAs were performed according to the manufacturer`s instructions.

The manufacturer has calibrated the units of anti-S antibody concentration to the first World Health Organization (WHO)

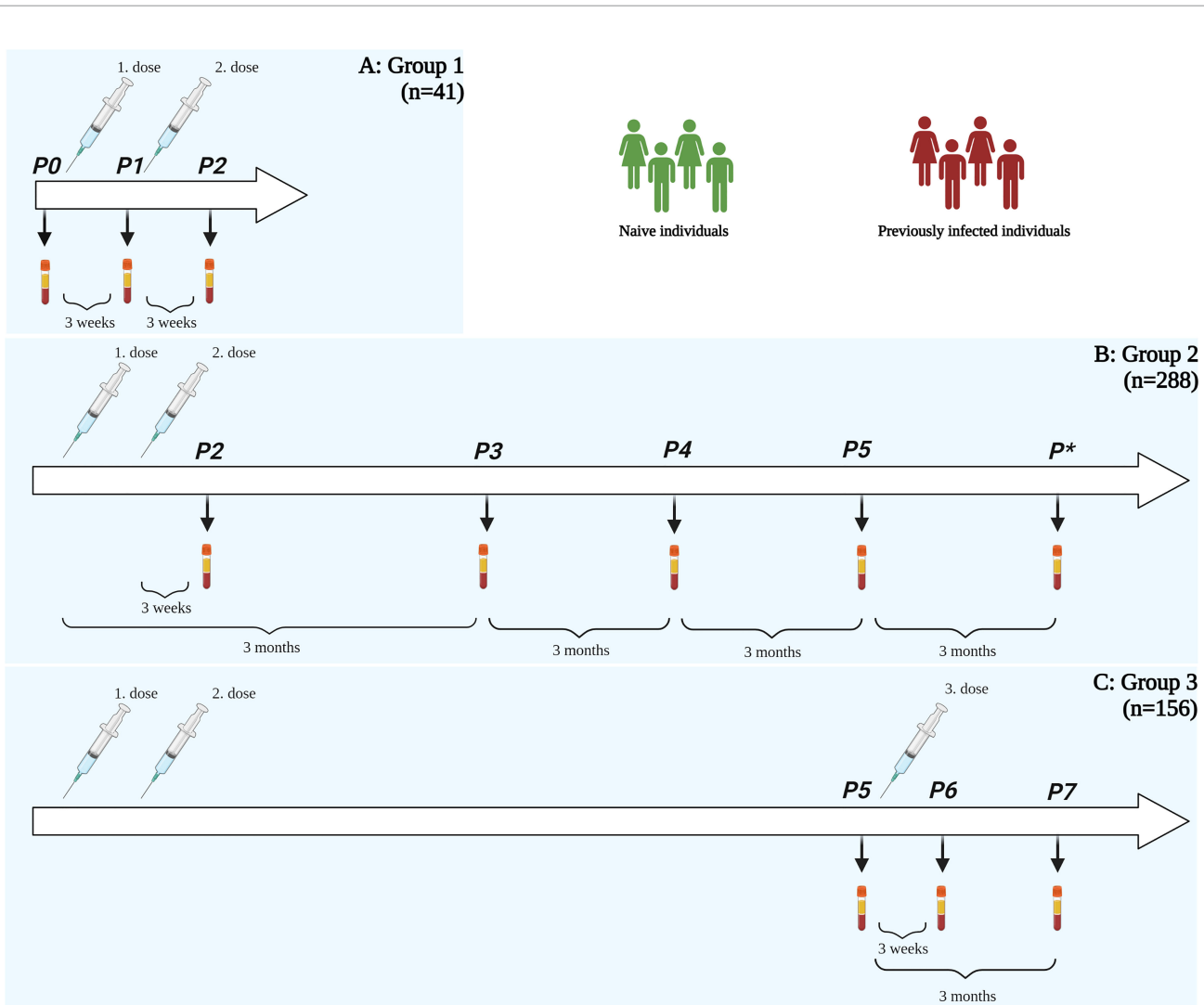

FIGURE 1 | Summary of the study. **(A)** Group 1: participants with samples in P0, P1, and P2 (n = 41) **(B)** Group 2: participants with samples in P2, P3, P4, and P5 (at least two samples, n = 288) and **(C)** Group 3: participants with samples in P5, P6 and P7 (n = 156). Legend: P0 – time point before vaccination, P1 – time point three weeks after first dose, P2 – time point three weeks after second dose, P3 – time point three months after vaccination, P4 – time point six months after vaccination, P5 – time point nine months after vaccination, P* – time point twelve months after vaccination, P6 – time point three weeks after third dose, P7 – time point three months after third dose.

standard (NIBSC code: 20/136) and recommends reporting results in binding antibody units per milliliter (BAU/ml), with values <25.6 BAU/ml reported as negative. In the case of anti-N antibodies, the ratio <0.8 is considered a negative result.

2.3 Statistics

Statistical significances were determined by nonparametric statistical tests (for independent samples - Mann-Whitney U test and Kruskal-Wallis test with Dunn's multiple comparison test, for dependent samples – Wilcoxon signed-rank test). Mixed models were used to assess the dynamics of anti-S antibodies (dependent variable) and relate these changes to age groups (<45 years and >45 years), sex, BMI groups (<25 and >25), and previous infections (fixed covariates). GraphPad Prism 8 and SPSS IBM 25 were used for statistical analysis.

3 RESULTS

The study included 300 HCP [female 239 (80%), male 61 (20%), median age 43 (IQR 35-53)]. 292 HCP provided information on chronic diseases and medications. 69/292 (24%) HCP had one or more chronic diseases (arterial hypertension, cardiovascular disease, diabetes, chronic kidney disease, chronic rheumatic disease, inflammatory bowel disease, Hashimoto`s disease, asthma…) and five of them reported receiving immunosuppressive drugs.

The participants were divided into three study groups according to the time points they had their sera collected (**Figure 1**):

- group 1: 41 participants, with serum samples collected before and following the first and second doses (time points P0, P1 and P2),
- group 2: 288 participants who sent at least two of the four samples after the second dose (time points P2, P3, P4 and P5). Within this group, 22 individuals did not receive a third dose and had their serum collected also after 12 months (P*).
- group 3: 156 participants who sent their serum samples after receiving the third (booster) dose (time point P6) and 69 participants who sent their serum samples 3 months after the third (booster) dose (time point P7).

During our study, eleven HCP were infected between the first and second dose, four between three and nine months, four between nine and twelve months after vaccination and five after the third dose. Between January and February 2022, when the Omicron variant was the predominant one, an additional 27 HCP were infected. The results of their anti-S antibody concentrations are presented separately.

3.1 Humoral Immune Response After Vaccination

3.1.1 Humoral Immune Response After the First Dose

The humoral immune response to the first dose was analyzed in the group, which included 41 HCP, 29 were naïve and 12 were previously infected individuals (8 with known infection confirmed by a positive PCR test before vaccination and 4 asymptomatic individuals with positive anti-S and/or anti-N antibodies before vaccination). Anti-N antibody levels were also tested in these samples. In the previously infected individuals, the median anti-N antibody level was 1.67 (ratio). There was no correlation between anti-N and anti-S antibody concentrations in these 12 participants. Interestingly, we found a negative correlation -0.652 (p=0.02) between anti-S antibody concentrations in P0 and the ratio of anti-S antibody concentrations between P1/P0, suggesting that those with lower anti-S antibody concentrations before vaccination had a higher increase in anti-S antibody concentration after the first dose than those with higher anti-S antibody concentrations before vaccination.

In naïve anti-S antibody concentration before the first dose was median 3.2 BAU/ml and after vaccination 253 BAU/ml, whereas in previously infected individuals it was 90 BAU/ml before and 3648 BAU/ml after the first dose. Thus, individuals with previous infection had significantly higher concentrations of anti-S antibodies before vaccination (p<0.001) and after the first dose (p<0.001) (**Table 1** and **Figure 2A**). Anti-S antibody concentrations increased after the first dose in both naïve (median 79-fold change) and in previously infected individuals (median 52-fold change).

3.1.2 Humoral Immune Response After the Second Dose

Humoral immune response after the second dose was assessed in 288 HCP, 41 HCP had been previously infected (25 with positive PCR test and 16 with positive anti-N antibodies, with a median anti-N antibody level of 2.23).

Three weeks after the second dose, median concentration of anti-S antibodies was 3216 BAU/ml in naïve individuals and 4503 BAU/ml in previously infected individuals (**Table 1** and **Figure 2B**). However, after the second dose a significant increase (median 13-fold change) was only observed in naïve individuals. In previously infected individuals, an increase after the second dose was not statistically significant. Importantly, antibody concentrations measured in previously infected individuals after the first dose were comparable to those measured in naïve individuals after the second dose (p = 0.83), pointing toward same humoral immune response in second encounter with viral proteins. In naïve individuals, median concentrations of anti-S antibodies at different time points after the second dose showed a decrease and were 1293 BAU/ml at three months, 355 BAU/ml at six months, and 232 BAU/ml at nine months after vaccination. In previously infected individuals, median concentration of anti-S antibodies were 1784 BAU/ml, 563 BAU/ml, and 507 BAU/ml at three, six, and nine months after vaccination, respectively. At all-time points, previously infected individuals had higher anti-S antibody concentrations than naïve individuals (**Table 1** and **Figure 2B**). One naïve participant did not develop anti-S antibodies after vaccination (value < 25.6 BAU/ml), and in two naïve participants anti-S antibody concentrations fell below 25.6 BAU/ml three months after vaccination. It is important to note that, two of these three

TABLE 1 | Comparison of anti-S antibody concentrations between naïve and previously infected individuals in all time-points.

		Naïve individuals	Previously infected individuals	Mann Whitney; p
P0	**anti-S (BAU/ml), median (IQR)**	3.2 (3.2-3.2)	90 (36-230)	*<0.001*
	n	29	12	
P1	**anti-S (BAU/ml), median (IQR)**	253 (133-411)	3648 (638-11278)	*<0.001*
	n	29	12	
P2	**anti-S (BAU/ml), median (IQR)**	3216 (2278-4925)	4503 (2731-7201)	*0.008*
	n	227	32	
P3	**anti-S (BAU/ml), median (IQR)**	1293 (858-2006)	1784 (1031-3146)	*0.008*
	n	240	38	
P4	**anti-S (BAU/ml), median (IQR)**	355 (228-569)	563 (318-1133)	*0.001*
	n	213	31	
P5	**anti-S (BAU/ml), median (IQR)**	232 (134-356)	507 (181-801)	*0.008*
	n	198	24	
P6	**anti-S (BAU/ml), median (IQR)**	4844 (3215-6984)	5845 (4039-7495)	*0.32*
	n	142	14	
P7	**anti-S (BAU/ml), median (IQR)**	1951 (1545-2967)	2586 (915-5053)	*0.60*
	n	62	7	
P*	**anti-S (BAU/ml), median (IQR)**	83 (51-134)	229 (101-417)	*0.09*
	n	17	5	

P0 – time point before vaccination, P1 – time point three weeks after first dose, P2 – time point three weeks after second dose, P3 – time point three months after vaccination, P4 – time point six months after vaccination, P5 – time point nine months after vaccination, P6 – time point three weeks after third dose, P7 – time point three months after third dose, P – time point twelve months after vaccination.*

participants have been treated with immunosuppressive therapy due to chronic diseases, while the third one was not receiving any immunosuppressive drugs.

In addition, 22 individuals who had not yet been vaccinated with the third dose had their sera withdrawn 12 months after they received the first dose. Five of them were previously infected individuals and tthe median concentration of anti-S antibodies was 229 BAU/ml, while the naïve individuals had a median concentration of anti-S antibodies of 83 BAU/ml 12 months after vaccination. Due to the small numbers, no statistical difference between the groups could be detected (**Table 1**).

3.1.3 Humoral Immune Response After the Third (Booster) Dose

Humoral immune response after the third (booster) dose was assessed in 156 HCP. Among them, 14 HCP had been previously infected (6 with positive PCR test and 8 with positive anti-N antibodies, with a median anti-N antibody level of 1.65).

Three weeks after the third dose, the median concentrations of anti-S were 4844 BAU/ml in naïve individuals and 5845 BAU/ml in previously infected individuals, both groups having an increase in anti-S concentration compared to levels before receiving the third dose. There was a slightly higher median fold change in naïve

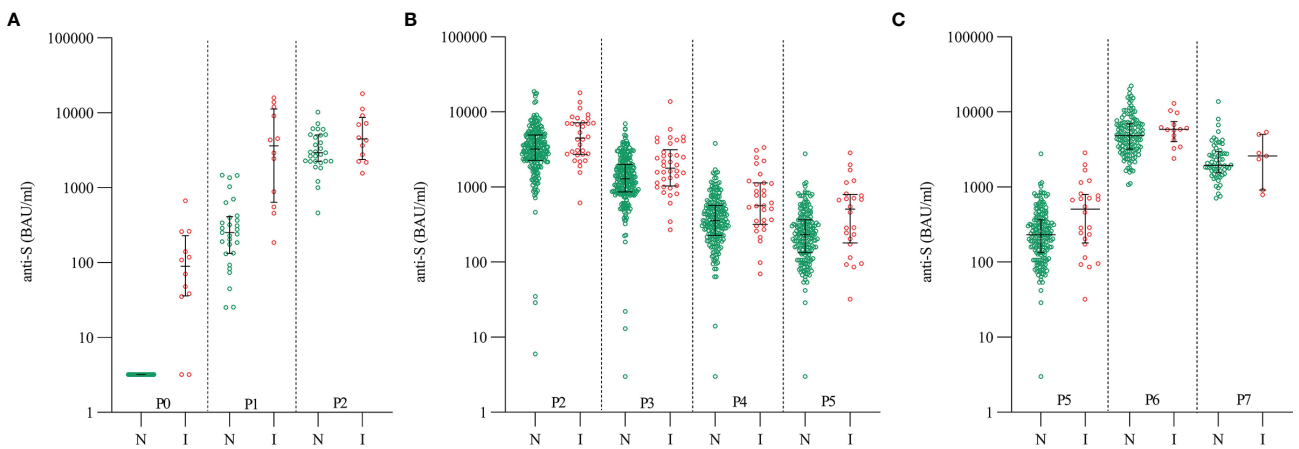

FIGURE 2 | Dynamics of anti-S antibody concentrations after vaccination with BNT162b2 in naïve (green) and previously infected (red) individuals: **(A)** Group 1: before, after the first and second doses (P0, P1 and P2), **(B)** Group 2: after the second dose (P2, P3, P4 and P5) and **(C)** Group 3: after the third dose (P5, P6 and P7). N – naïve individuals (green color), I – previously infected individuals (red color), P0 – time point before vaccination, P1 – time point three weeks after first dose, P2 – time point three weeks after second dose, P3 – time point three months after vaccination, P4 – time point six months after vaccination, P5 – time point nine months after vaccination, P6 – time point three weeks after third dose, P7 – time point three months after third dose.

individuals, that is 22-fold increase in concentrations after the third dose in comparison to concentrations before receiving the third dose, and 17-fold increase in concentrations in previously infected individuals. Three months after the third dose, 69 samples were analyzed, and median concentration of anti-S antibodies was 1951 BAU/ml in naïve individuals and 2586 BAU/ml in previously infected individuals (**Table 1** and **Figure 2C**).

3.1.4 Comparison Between Humoral Immune Responses After the Second and After the Third Dose

In addition, we found that the concentrations of anti-S antibodies were higher after the third dose than after the second dose. This difference was statistically significant in naïve ($p<0.001$) and previously infected individuals ($p=0.033$).

Additionally, we found a negative correlation between the ratio of the anti-S antibody concentrations after the third dose and after the second dose (P6/P2 ratio) and the anti-S antibody concentrations after the second dose ($r=-0.501$, $p<0.001$), showing that those individuals who had lower concentrations after the second dose had later higher concentration after the third dose. In this part both groups (naïve and previously infected individuals) were combined and analyzed together, as there was no significant difference in the P6/P2 ratio between the groups ($p=0.31$).

3.1.5 The Influence of Age, Sex, BMI, and Previous Infection on Anti-S Antibody Concentrations and Their Dynamics Using Mixed-Model Analysis

The results of the mixed-model analyses with multiple variables (age groups, sex, BMI groups, and previous infection) are presented in **Supplementary Table 1** for groups 1, 2, and 3, first for the entire group and then for the naïve individuals only.

In group 1, we found that previous infection influenced the anti-S antibody concentrations reached after the first and second doses. The results showed that previously infected individuals had higher anti-S antibody concentrations after the first and second dose than naïve individuals. In the group of naïve individuals only, an influence of age was additionally found. That is, individuals in the naïve group who were younger than 45 years had higher anti-S antibody concentrations after the first dose and after the second dose than those who were older than 45 years. Over time, anti-S antibody concentrations in this group increased after the first and second dose until time point P2.

In group 2, anti-S antibody concentrations were related to previous infection and age: individuals younger than 45 years and those with previous infection had higher anti-S antibody concentrations after the second dose. In naïve individuals, age again influenced anti-S antibody concentrations after the second dose. Anti-S antibody concentrations decreased in this group from time point P2 to P5.

Interestingly, in group 3, there was no longer an influence of previous infection, but we found that age and BMI influenced anti-S antibody concentrations after the third dose. Importantly, in this case, individuals older than 45 years and with higher BMI had higher concentrations of anti-S antibodies. In the naïve group, no influence of age was observed. Again, anti-S antibody concentrations decreased after the third dose until time point P7.

3.2 Outcomes of HCP Who Became Infected During the Observation Period

Eleven HCP who were infected with SARS-CoV-2 between the first and second dose had median anti-S antibody concentration after the second dose of 4195 BAU/ml (P2), 1975 BAU/ml (P3), 705 BAU/ml (P4) and 502 BAU/ml (P5) and after the third dose 5658 BAU/ml. Median concentrations after the second dose in these individuals were comparable to previously infected individuals (with infection before vaccination) (no significant differences in P2, P3, P4 and P5) and were higher than in naïve individuals (statistical differences in P3 ($p=0.04$) and P5 ($p=0.03$), P2 and P4 – not significant). After the third dose, no statistically significant difference in anti-S antibody concentrations between these HCP and naïve or previously infected individuals was observed.

Four HCP were infected after the second dose (three between 3 and 6 months, and one between 6 and 9 months). Two of them had positive PCR, while two of them had asymptomatic disease. In all these individuals, anti-S and anti-N antibodies increased after their infection. Their median anti-S antibody concentration after vaccination and before infection was 430 BAU/ml which increased to median concentration 2490 BAU/ml after infection.

In addition, four HCP were infected later, between 9 and 12 months after complete vaccination, all four with positive PCR. The median anti-S antibody concentration before infection was 90 BAU/ml at nine months after vaccination and increased to 4942 BAU/ml after infection. The increase after infection was significant and similar to concentrations after the third dose in naïve individuals.

Furthermore, five HCP were infected 3 weeks after the third dose, when their anti-S antibody levels were high (median 3475 BAU/ml).

3.3 Infections in HCP During the Period of High Prevalence of Omicron Variant

Four months after the third dose the Omicron variant became predominant. 27 HCP were infected during the following two-month period. Their median concentration of anti-S antibodies before infection was 2141 BAU/ml (IQR 1536-3194, samples were taken 22.5 days (median) before infection, IQR 17-41 days). After infection, anti-S antibody concentrations increased to a median concentration of 4794 BAU/ml (IQR 3414-5392) ($p<0.001$).

3.4 Adverse Events and Anti-S Antibody Concentrations After the Second Dose

249/300 (83%) participants properly answered the questionnaire on the occurrence of adverse events. Of these, 135/249 (54%) subjects had no adverse events after vaccination, while 114/249 (46%) subjects reported various adverse events such as headache, fatigue, chills, fever, muscle pain, and redness at the injection site. Subjects with adverse events were divided into two

groups according to the occurrence of local or systemic adverse events and compared with subjects reporting no adverse events. Since we had shown that anti-S antibody concentrations differed between patients and naïve subjects, we also considered the latter. We found that naïve individuals with systemic adverse events had higher concentrations of anti-S antibodies at all four time points (P2, P3, P4 and P5) after vaccination (median 3955 BAU/ml, 1651 BAU/ml and 487 BAU/ml and 285 BAU/ml, respectively) compared with those with local adverse events (median 3034 BAU/ml, 1179 BAU/ml and 335 BAU/ml and 205 BAU/ml, respectively) or no adverse events (median 2947 BAU/ml, 1205 BAU/ml, 332 BAU/ml and 218 BAU/ml, respectively). Significant differences were found in P2, P3, and P4, but only between individuals with systemic adverse events and individuals without adverse events, while there was no statistically significant significance in P5 (**Figure 3**). In contrast, in previously infected individuals, no differences in anti-S antibody concentrations were observed between individuals who reported adverse events and those who did not. The percentage of HCP reporting adverse effects after the second dose was similar in naïve and previously infected individuals (in the naïve group: 54% no adverse events, 10% with local adverse events, 36% with systemic adverse events, in the previously infected group: 58% no adverse events, 12% with local adverse events, 30% with systemic adverse events).

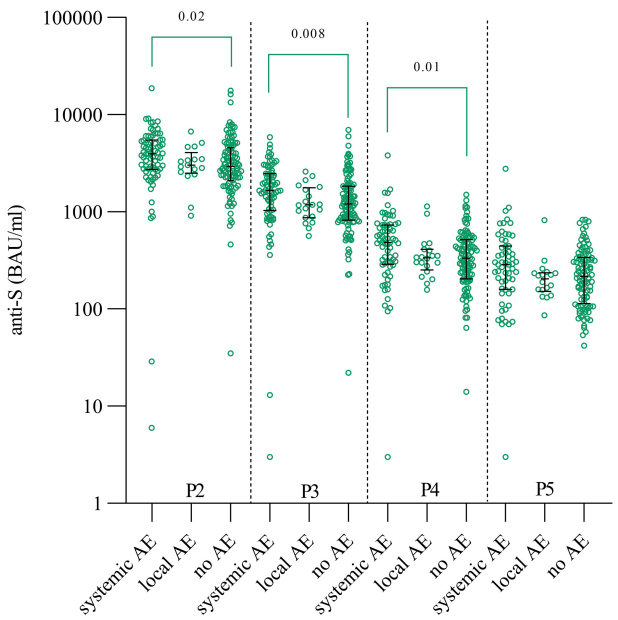

FIGURE 3 | Anti-S antibody concentrations in individuals with systemic, local and no adverse events after the second dose. Statistical differences were determined by Kruskal-Wallis test together with Dunn's multi-comparison test (significances on the graphs). AE – adverse events, P2 – time point three weeks after second dose, P3 – time point three months after vaccination, P4 – time point six months after vaccination, P5 – time point nine months after vaccination.

4 DISCUSSION

In our longitudinal study we presented data about the anti-S antibody concentrations up to twelve months after vaccination with two doses of BNT162b2 as well as following the third (booster) dose in HCP (**Figure 4**).

We found that previously infected individuals had higher concentrations of anti-S antibodies after the first dose (median 3648 BAU/ml) than naïve individuals (median 253 BAU/ml). This is consistent with the fact that almost all previously infected individuals already had anti-S antibodies before vaccination (median 90 BAU/ml), so their first vaccination actually represented their second exposure to viral proteins. Therefore, similar concentrations of anti-S antibodies (median 3216 BAU/ml) were found in naïve individuals after the second dose. Appelman et al. reported that antibody concentrations increased 4.1-fold in naïve individuals and 0.97-fold in previously infected individuals after the second dose (18). In our study, the increases were 13- and 1.1-fold, respectively. Some reports indicated that previously infected individuals had higher anti-S antibody concentration after the second dose (19), while one study reported that one week after the second dose, the naïve group and previously infected group had the same median anti-S antibody concentration (20). Overall, it has already been shown that the humoral immune response to vaccination differs significantly between individuals previously infected with SARS-CoV-2 and naïve individuals (17, 19, 21–23). An important finding of this study is that the second dose did not contribute

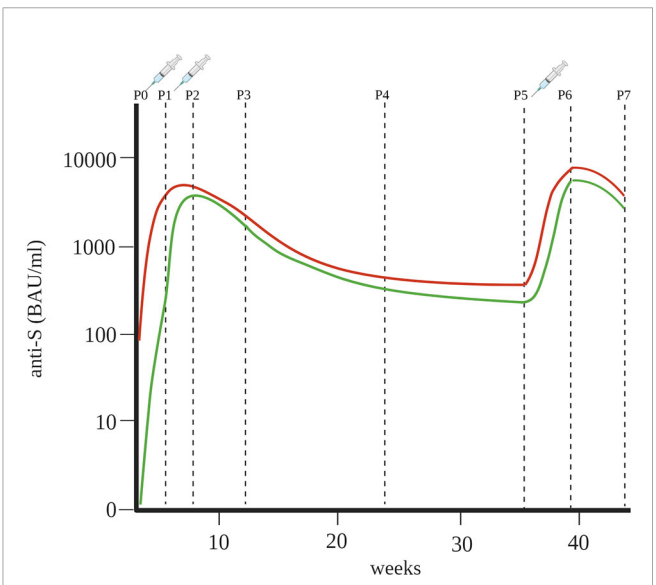

FIGURE4 | Key illustration of differences in humoral immune response between naïve individuals (green line) and previously infected individuals (red line) after the first, second and third doses of BNT162b2 (lines connect median anti-S antibody concentrations at different time points) P0 – time point before vaccination, P1 – time point three weeks after first dose, P2 – time point three weeks after second dose, P3 – time point three months after vaccination, P4 – time point six months after vaccination, P5 – time point nine months after vaccination, P6 – time point three weeks after third dose, P7 – time point three months after third dose.

to a significant increase in anti-S antibody concentrations in previously infected individuals and that the second dose may not be essential, as suggested in other studies (17, 24, 25), or may be postponed to a later time. This also justifies vaccination of naïve individuals with two doses, as third encounter in a row does not lead to an additional increase in antibody concentrations.

Consistent with these studies, our study also showed that the concentrations of anti-S antibodies in previously infected individuals after the first dose were comparable to those who had been vaccinated twice without prior SARS-CoV-2 infection. Thus, it can be concluded that infection is equivalent to one vaccination.

In our group, there were two HCP who did not develop anti-S antibodies after vaccination with BNT162b2, most likely because of taking immunosuppressive drugs due to chronic disease. In such cases, passive immunization with monoclonal antibodies, convalescent plasma (26, 27), or antiviral agents such as Remdesivir, Paxlovid is recommended at the onset of the first symptoms of COVID-19 to prevent severe complications.

Anti-S antibody concentrations decreased after 9 months from peak concentrations (median 3216 BAU/ml in naïve individuals and median 4503 BAU/ml in previously infected individuals) to the lowest point of anti-S antibody concentrations (median 232 BAU/ml in naïve individuals and median 507 BAU/ml in previously infected individuals). An additional decrease was observed 12 months after vaccination in 22 HCP, in whom anti-S antibody concentration dropped to a median value of 229 BAU/ml in previously infected, whereas the naïve individuals had a median anti-S antibody concentration of 83 BAU/ml.

The dynamics of humoral immune response in our study are consistent with the results of certain published studies. In a clinical trial of BNT162b2, similar results were obtained on anti-S antibody concentrations, with a significant increase in naïve individuals after the first vaccination (from 1 to 913 U/ml) and after the second vaccination (from 913 to 6466 U/ml – three weeks after the second dose). The decrease from 8279 U/ml, one week after second dose (29 days after the first dose), to 2543 U/ml, 85 days after first dose, was observed in naïve individuals in a clinical study (11).

Shrotri et al. (28) showed a decrease in anti-S antibody concentration from 7506 U/ml to 3320 U/ml from 21-41 days to 70 days after the second vaccination. Favresse et al. found a significant decrease in anti-S antibody concentrations after 3 months (29), and, interestingly Israel et al. showed in their 6-month study, with 2,653 individuals included that antibodies decreased by up to 40% in each subsequent month (30). There is also evidence that the early humoral immune response may be inversely associated with antibody concentrations 90 days after vaccination (31).

Little is known about humoral immune responses after the third (booster) dose. The available data refer to patients with various diseases or specific treatments that inhibit the immune system (32, 33). However, Falsey et al. presented data from a Pfizer clinical trial data with a small number of individuals (34). The recent study from Israel showed that a third dose of BNT162b2 mRNA vaccine is effective in protecting against severe COVID-19-related outcomes, compared with only two doses given at least 5 months earlier, but did not report concentrations of antibodies after the third dose (35). We found that the third dose resulted in an even higher concentrations of anti-S antibodies compared to those measured after the second dose, which is consistent with Falsey et al. (34), and that the naïve and previously infected groups reached similar anti-S antibody concentrations. We also found that those who were less responsive after the second dose had higher concentrations of anti-S antibodies after the third dose. We can explain this phenomenon in part by the kinetics of the humoral immune response after vaccination. The antibody response increases with each vaccine booster and/or infection, but eventually a plateau is reached. Accordingly, in some individuals a plateau may have been reached after the second dose and the third dose did not result in a significant increase, whereas in others the third dose contributed significantly to the antibody response. Another confirmation of this theory is the fact that 8 participants of this study who became infected after full vaccination had anti-S antibody concentrations comparable to those already reached after the third dose. This also indicates that infection could equal one vaccine dose.

As mentioned above, in our real-world study, we found a significant decrease in humoral immune response over a 12-month period. The influence of age, sex, BMI, and previous infection with anti-S antibodies were analyzed with a mixed-model analysis. We found that previously infected individuals had higher anti-S antibody concentrations in group 1 and group 2, whereas this influence was no longer found after third dose (group 3). The reason could be the plateau of the immune system, as described above. In addition, we found that in group 1 (time points P1 and P2) and group 2 (time points P2, P3, P4, and P5) anti-S antibody concentrations were higher in individuals younger than 45 years. Similar results were found in other studies in which anti-S antibody concentrations were lower in the elderly after the second dose (13, 36–38). On the contrary, after the third dose in group 3 (time points P6 and P7), the higher anti-S antibody concentrations were found in the individuals older than 45 years (however, the oldest individuals in our group 3 had 63 years with the median age in the group of 54 years), pointing to effectiveness and relevance of third dose for elder people. However, the influence of age was lost in naïve individuals of group 3. The influence of BMI on anti-S antibody concentrations was observed only in group 3, after third dose. Levin et al. has shown that neutralizing antibodies are influenced by BMI (≥30), but after the second dose, which we did not observe. The mechanism of humoral immune response to SARS-CoV-2 in obese individuals is still unclear. Some studies have also reported lower antibody concentrations in males (28, 36, 38), but this was not the case in our study. One of the reasons for this could be the small number of men who participated in our study.

Another important finding of our study is that the high concentration of anti-S antibodies measured in individuals after they received the third dose of BNT162b2 did not protect them from SARS-CoV-2 infection, the Omicron variant. This is consistent with studies reporting that the current BNT162b2

vaccine does not effectively prevent the infection with the new variants of SARS-CoV-2 (39).

Headache, fatigue, fever, and muscle pain were the most common adverse events reported by 46% of study participants. The proportion of subjects reporting adverse events in other studies varied from 66% to 93% (13, 25). Like one other study, we have shown that the individuals with adverse events had higher concentrations of anti-S antibodies (13).

Our study exhibits several strengths. To our knowledge this is the first study investigating antibody dynamics following vaccination in real-world settings for 12-months using mixed-model analysis. Also, we examined the antibody responses separately in naïve individuals and in previously infected individuals. This has revealed that separate vaccine protocols for naïve and previously infected individuals might be feasible.

This study also has certain limitations. The first limitation is the relatively small number of participants, especially pre-vaccination samples, since the study was conducted at a single center and because of rapid vaccination implementation in our Medical Centre. However, due to urgency of providing information on antibody responses after vaccination, the results of this study are very important as they comprise new and potentially very useful data for future vaccination protocols and thus should be published timely. The second important note is that the study was conducted in an apparently healthy population of HCP and that the disease course of included previously infected individuals was rather mild. Thus we do not provide information on humoral immune response of different patient population. The third limitation of the study is that the neutralizing properties of the antibodies were not evaluated.

Our study contains several important conclusions. First, under real world conditions, we confirmed that the different vaccination schedules are appropriate for previously infected individuals, as their concentrations after the first dose were as high as in naïve individuals after the second dose. Second, we found that anti-S antibody concentrations were consistently higher in previously infected individuals than in naïve individuals at all-time points after the second dose. Third, the humoral immune response decline after the second dose and also after the third dose. Fourth, participants with lower concentrations after the second dose achieved higher concentrations after the third dose. Fifth, age had a significant effect on the humoral immune response after vaccination. Younger individuals had higher anti-S antibody concentrations after the first and second doses. Sixth, 24 HCP became infected during the 1-year observation period, five of whom became infected after the booster dose. Seventh, high anti-S antibody concentrations did not effectively prevent the infection with Omicron variant, and eight, individuals with systemic adverse events achieved higher concentrations after the second dose than those with local or no adverse events.

Our study provides new data on the response to vaccination after three doses of BNT162b2 and reports the decline in anti-S antibodies in naïve and previously infected individuals, comprising real data from a 12-month observation period using mixed-model analysis. Because of the many factors that influence humoral response and the intervariability between individuals, such studies are important to confirm previously reported data and to substantiate the new findings. Furthermore, we show that the high concentrations of anti-S antibodies were not protective against new variants of SARS-CoV-2, indicating the need to optimize vaccines for the different variants.

DATA AVAILABILITY STATEMENT

Raw data supporting the conclusions of this article will be made available by the authors, without undue reservation.

ETHICS STATEMENT

The studies involving human participants were reviewed and approved by Slovenian National Medical Ethics Committee (#0120-422/2020/6). The participants provided their written informed consent to participate in this study.

AUTHOR CONTRIBUTIONS

MO, ŽR and SČ participated in research design. MO participated in data curation and sample acquisition. MO, PŽ, EP and KL participated in data analysis. MO, PŽ, KL and SČ participated in the writing of the paper. EP, SS-S and ŽR participated in the review and editing of the paper. SS-S, ŽR and SČ participated in funding acquisition and project administration. All authors contributed to the article and approved the submitted version.

FUNDING

The study was supported by the University Medical Centre Ljubljana with a tertiary project and by the Slovenian Research Agency ARRS with the National Research Program #P3-0314.

ACKNOWLEDGEMENT

We would like to thank all the employees of the Division of Internal Medicine of the University Medical Centre Ljubljana who voluntarily participated in the study.

SUPPLEMENTARY MATERIAL

The Supplementary Material for this article can be found online at: https://www.frontiersin.org/articles/10.3389/fimmu.2022.876533/full#supplementary-material

Supplementary Table 1 | Mixed-model analysis of variables (age, sex, body mass index (BMI), previous infection and time) and anti-S antibody concentrations in group 1, group 2 and group 3, presented first for the entire group and then for the naïve individuals only.

REFERENCES

1. Cheng MP, Yansouni CP, Basta NE, Desjardins M, Kanjilal S, Paquette K, et al. Serodiagnostics for Severe Acute Respiratory Syndrome-Related Coronavirus 2: A Narrative Review. *Ann Intern Med* (2020) 173(6):450–60. doi: 10.7326/M20-2854
2. Wang P, Nair MS, Liu L, Iketani S, Luo Y, Guo Y, et al. Antibody Resistance of SARS-CoV-2 Variants B.1.351 and B.1.1.7. *Nature* (2021) 593(7857):130–5. doi: 10.1038/s41586-021-03398-2
3. Wilhelm A, Widera M, Grikscheit K, Toptan T, Schenk B, Pallas C, et al. Reduced Neutralization of SARS-CoV-2 Omicron Variant by Vaccine Sera and Monoclonal Antibodies. *medRxiv* (2021) 12:07.21267432.
4. Polack FP, Thomas SJ, Kitchin N, Absalon J, Gurtman A, Lockhart S, et al. Safety and Efficacy of the BNT162b2 mRNA Covid-19 Vaccine. *N Engl J Med* (2020) 383(27):2603–15. doi: 10.1056/NEJMoa2034577
5. Chodick G, Tene L, Rotem RS, Patalon T, Gazit S, Ben-Tov A, et al. The Effectiveness of the TWO-DOSE BNT162b2 Vaccine: Analysis of Real-World Data. *Clin Infect Dis* (2022) 74(3):472–78. doi: 10.1093/cid/ciab438
6. Dagan N, Barda N, Kepten E, Miron O, Perchik S, Katz MA, et al. BNT162b2 mRNA Covid-19 Vaccine in a Nationwide Mass Vaccination Setting. *N Engl J Med* (2021) 384(15):1412–23. doi: 10.1056/NEJMoa2101765
7. Kim JH, Marks F, Clemens JD. Looking Beyond COVID-19 Vaccine Phase 3 Trials. *Nat Med* (2021) 27(2):205–11. doi: 10.1038/s41591-021-01230-y
8. Wheatley AK, Juno JA, Wang JJ, Selva KJ, Reynaldi A, Tan HX, et al. Evolution of Immune Responses to SARS-CoV-2 in Mild-Moderate COVID-19. *Nat Commun* (2021) 12(1):1162. doi: 10.1038/s41467-021-21444-5
9. Gaebler C, Wang Z, Lorenzi JCC, Muecksch F, Finkin S, Tokuyama M, et al. Evolution of Antibody Immunity to SARS-CoV-2. *Nature* (2021) 591 (7851):639–44. doi: 10.1038/s41586-021-03207-w
10. Dan JM, Mateus J, Kato Y, Hastie KM, Yu ED, Faliti CE, et al. Immunological Memory to SARS-CoV-2 Assessed for Up to 8 Months After Infection. *Science* (2021) 371(6529). doi: 10.1126/science.abf4063
11. Sahin U, Muik A, Vogler I, Derhovanessian E, Kranz LM, Vormehr M, et al. BNT162b2 Vaccine Induces Neutralizing Antibodies and Poly-Specific T Cells in Humans. *Nature* (2021) 595(7868):572–7. doi: 10.1038/s41586-021-03653-6
12. Collier AY, Yu J, McMahan K, Liu J, Chandrashekar A, Maron JS, et al. Differential Kinetics of Immune Responses Elicited by Covid-19 Vaccines. *N Engl J Med* (2021) 385(21):2010–2. doi: 10.1056/NEJMc2115596
13. Naaber P, Tserel L, Kangro K, Sepp E, Jürjenson V, Adamson A, et al. Dynamics of Antibody Response to BNT162b2 Vaccine After Six Months: A Longitudinal Prospective Study. *Lancet Reg Health Eur* (2021) 10:100208. doi: 10.1016/j.lanepe.2021.100208
14. Shrotri M, Fragaszy E, Geismar C, Nguyen V, Beale S, Braithwaite I, et al. Spike-Antibody Responses to ChAdOx1 and BNT162b2 Vaccines by Demographic and Clinical Factors (Virus Watch Study). *medRxiv* (2021) 05:12.21257102.
15. Müller L, Andrée M, Moskorz W, Drexler I, Walotka L, Grothmann R, et al. Age-Dependent Immune Response to the Biontech/Pfizer BNT162b2 COVID-19 Vaccination. *Clin Infect Dis* (2021) 73(11):2065–72. doi: 10.1093/cid/ciab381
16. Abu Jabal K, Ben-Amram H, Beiruti K, Batheesh Y, Sussan C, Zarka S, et al. Impact of Age, Ethnicity, Sex and Prior Infection Status on Immunogenicity Following a Single Dose of the BNT162b2 mRNA COVID-19 Vaccine: Real-World Evidence From Healthcare Workers, Israel, December 2020 to January 2021. *Euro Surveill* (2021) 26(6). doi: 10.2807/1560-7917.ES.2021.26.6.2100096
17. Goel RR, Apostolidis SA, Painter MM, Mathew D, Pattekar A, Kuthuru O, et al. Distinct Antibody and Memory B Cell Responses in SARS-CoV-2 Naïve and Recovered Individuals Following mRNA Vaccination. *Sci Immunol* (2021) 6(58). doi: 10.1126/sciimmunol.abi6950
18. Appelman B, van der Straten K, Lavell AHA, Schinkel M, Slim MA, Poniman M, et al. Time Since SARS-CoV-2 Infection and Humoral Immune Response Following BNT162b2 mRNA Vaccination. *EBioMedicine* (2021) 72:103589. doi: 10.1016/j.ebiom.2021.103589
19. Ebinger JE, Fert-Bober J, Printsev I, Wu M, Sun N, Prostko JC, et al. Antibody Responses to the BNT162b2 mRNA Vaccine in Individuals Previously Infected With SARS-CoV-2. *Nat Med* (2021) 27(6):981–4. doi: 10.1038/s41591-021-01325-6
20. Samanovic MI, Cornelius AR, Wilson JP, Karmacharya T, Gray-Gaillard SL, Allen JR, et al. Poor Antigen-Specific Responses to the Second BNT162b2 mRNA Vaccine Dose in SARS-CoV-2-Experienced Individuals. *medRxiv* (2021) 02:07.21251311.
21. Anichini G, Terrosi C, Gandolfo C, Gori Savellini G, Fabrizi S, Miceli GB, et al. SARS-CoV-2 Antibody Response in Persons With Past Natural Infection. *N Engl J Med* (2021) 385(1):90–2. doi: 10.1056/NEJMc2103825
22. Manisty C, Otter AD, Treibel TA, McKnight Á, Altmann DM, Brooks T, et al. Antibody Response to First BNT162b2 Dose in Previously SARS-CoV-2-Infected Individuals. *Lancet* (2021) 397(10279):1057–8. doi: 10.1016/S0140-6736(21)00501-8
23. Saadat S, Rikhtegaran Tehrani Z, Logue J, Newman M, Frieman MB, Harris AD, et al. Binding and Neutralization Antibody Titers After a Single Vaccine Dose in Health Care Workers Previously Infected With SARS-CoV-2. *Jama* (2021) 325(14):1467–9. doi: 10.1001/jama.2021.3341
24. Ibarrondo FJ, Hofmann C, Fulcher JA, Goodman-Meza D, Mu W, Hausner MA, et al. Primary, Recall, and Decay Kinetics of SARS-CoV-2 Vaccine Antibody Responses. *ACS Nano* (2021) 15(7):11180–91. doi: 10.1021/acsnano.1c03972
25. Krammer F, Srivastava K, tP t, Simon V. Robust Spike Antibody Responses and Increased Reactogenicity in Seropositive Individuals After a Single Dose of SARS-CoV-2 mRNA Vaccine. *medRxiv* (2021), 29.21250653.
26. Pavia CS, Wormser GP. Passive Immunization and its Rebirth in the Era of the COVID-19 Pandemic. *Int J Antimicrob Agents* (2021) 57(3):106275. doi: 10.1016/j.ijantimicag.2020.106275
27. El-Masry EA. Immunization Against Severe Acute Respiratory Syndrome Coronavirus 2: An Overview. *Afr Health Sci* (2021) 21(4):1574–83. doi: 10.4314/ahs.v21i4.11
28. Shrotri M, Navaratnam AMD, Nguyen V, Byrne T, Geismar C, Fragaszy E, et al. Spike-Antibody Waning After Second Dose of BNT162b2 or Chadox1. *Lancet* (2021) 398(10298):385–7. doi: 10.1016/S0140-6736(21)01642-1
29. Favresse J, Bayart JL, Mullier F, Elsen M, Eucher C, Van Eeckhoudt S, et al. Antibody Titres Decline 3-Month Post-Vaccination With BNT162b2. *Emerg Microbes Infect* (2021) 10(1):1495–8. doi: 10.1080/22221751.2021.1953403
30. Israel A, Shenhar Y, Green I, Merzon E, Golan-Cohen A, Schäffer AA, et al. Large-Scale Study of Antibody Titer Decay Following BNT162b2 mRNA Vaccine or SARS-CoV-2 Infection. *medRxiv* (2021). doi: 10.1101/2021.08.19.21262111
31. Cocomazzi G, Piazzolla V, Squillante MM, Antinucci S, Giambra V, Giuliani F, et al. Early Serological Response to BNT162b2 mRNA Vaccine in Healthcare Workers. *Vaccines (Basel)* (2021) 9(8):913. doi: 10.3390/vaccines9080913
32. Bensouna I, Caudwell V, Kubab S, Acquaviva S, Pardon A, Vittoz N, et al. SARS-CoV-2 Antibody Response After a Third Dose of the BNT162b2 Vaccine in Patients Receiving Maintenance Hemodialysis or Peritoneal Dialysis. *Am J Kidney Dis* (2022) 79(2):185–192.e1. doi: 10.1053/j.ajkd.2021.08.005
33. Dekervel M, Henry N, Torreggiani M, Pouteau LM, Imiela JP, Mellaza C, et al. Humoral Response to a Third Injection of BNT162b2 Vaccine in Patients on Maintenance Haemodialysis. *Clin Kidney J* (2021) 14(11):2349–55. doi: 10.1093/ckj/sfab152
34. Falsey AR, Frenck RW, Walsh EE, Kitchin N, Absalon J, Gurtman A, et al. SARS-CoV-2 Neutralization With BNT162b2 Vaccine Dose 3. *New Engl J Med* (2021) 385(17):1627–9. doi: 10.1056/NEJMc2113468
35. Barda N, Dagan N, Cohen C, Hernán MA, Lipsitch M, Kohane IS, et al. Effectiveness of a Third Dose of the BNT162b2 mRNA COVID-19 Vaccine for Preventing Severe Outcomes in Israel: An Observational Study. *Lancet* (2021) 398(10316):2093–2100. doi: 10.1016/S0140-6736(21)02249-2
36. Nomura Y, Sawahata M, Nakamura Y, Kurihara M, Koike R, Katsube O, et al. Age and Smoking Predict Antibody Titres at 3 Months After the Second Dose of the BNT162b2 COVID-19 Vaccine. *Vaccines (Basel)* (2021) 9(9):1042. doi: 10.3390/vaccines9091042
37. Richards NE, Keshavarz B, Workman LJ, Nelson MR, Platts-Mills TAE, Wilson JM. Comparison of SARS-CoV-2 Antibody Response by Age Among Recipients of the BNT162b2 vs the mRNA-1273 Vaccine. *JAMA*

Network Open (2021) 4(9):e2124331–e. doi: 10.1001/jamanetworkopen.2021.24331
38. Levin EG, Lustig Y, Cohen C, Fluss R, Indenbaum V, Amit S, et al. Waning Immune Humoral Response to BNT162b2 Covid-19 Vaccine Over 6 Months. *New Engl J Med* (2021) 385(24):e84. doi: 10.1056/NEJMoa2114583
39. Abu-Raddad LJ, Chemaitelly H, Ayoub HH, AlMukdad S, Yassine HM, Al-Khatib HA, et al. Effect of mRNA Vaccine Boosters Against SARS-CoV-2 Omicron Infection in Qatar. *N Engl J Med* (2022) 386(19):1804–1816. doi: 10.1056/NEJMoa2200797

Conflict of Interest: The authors declare that the research was conducted in the absence of any commercial or financial relationships that could be construed as a potential conflict of interest.

Publisher's Note: All claims expressed in this article are solely those of the authors and do not necessarily represent those of their affiliated organizations, or those of the publisher, the editors and the reviewers. Any product that may be evaluated in this article, or claim that may be made by its manufacturer, is not guaranteed or endorsed by the publisher.

frontiers | Frontiers in Immunology

ORIGINAL RESEARCH
published: 02 June 2022
doi: 10.3389/fimmu.2022.882515

mRNA or ChAd0x1 COVID-19 Vaccination of Adolescents Induces Robust Antibody and Cellular Responses With Continued Recognition of Omicron Following mRNA-1273

Alexander C. Dowell[1†], Annabel A. Powell[2†], Chris Davis[3], Sam Scott[3], Nicola Logan[3], Brian J. Willett[3], Rachel Bruton[1], Morenike Ayodele[1], Elizabeth Jinks[1], Juliet Gunn[1], Eliska Spalkova[1], Panagiota Sylla[1], Samantha M. Nicol[1], Jianmin Zuo[1], Georgina Ireland[2], Ifeanyichukwu Okike[2,4], Frances Baawuah[2], Joanne Beckmann[5], Shazaad Ahmad[6], Joanna Garstang[7], Andrew J. Brent[8,9], Bernadette Brent[8], Marie White[10], Aedin Collins[11], Francesca Davis[10], Ming Lim[12,13], Jonathan Cohen[14], Julia Kenny[13,14], Ezra Linley[15], John Poh[2], Gayatri Amirthalingam[2], Kevin Brown[2], Mary E. Ramsay[2], Rafaq Azad[16], John Wright[16], Dagmar Waiblinger[16], Paul Moss[1†] and Shamez N. Ladhani[2,17†]*

[1] Institute of Immunology & Immunotherapy, College of Medical and Dental Sciences, University of Birmingham, Birmingham, United Kingdom, [2] Immunisation and Vaccine Preventable Diseases Division, United Kingdom (UK) Health Security Agency, London, United Kingdom, [3] Medical Research Council (MRC)-University of Glasgow Centre for Virus Research, Glasgow, United Kingdom, [4] University Hospitals of Derby and Burton National Health Service (NHS) Foundation Trust, Derby, United Kingdom, [5] East London National Health Service (NHS) Foundation Trust, London, United Kingdom, [6] Manchester University National Health Service (NHS) Foundation Trust, Manchester, United Kingdom, [7] Birmingham Community Healthcare National Health Service (NHS) Trust, Aston, United Kingdom, [8] Nuffield Department of Medicine, Oxford University Hospitals National Health Service (NHS) Foundation Trust, Oxford, United Kingdom, [9] University of Oxford, Oxford, United Kingdom, [10] Department of General Paediatrics, Evelina London Children's Hospital, London, United Kingdom, [11] The National Children's Hospital, Tallaght University Hospital, Dublin, Ireland, [12] Children's Neurosciences, Evelina London Children's Hospital at Guy's and St Thomas' National Health Service (NHS) Foundation Trust, King's Health Partners Academic Health Science Centre, London, United Kingdom, [13] Department Women and Children's Health, School of Life Course Sciences (SoLCS), King's College London, London, United Kingdom, [14] Department of Paediatric Infectious Diseases and Immunology Evelina London Children's Hospital, London, United Kingdom, [15] United Kingdom (UK) Health Security Agency, Manchester Royal Infirmary, Manchester, United Kingdom, [16] Bradford Institute for Health Research, Bradford Teaching Hospitals National Health Service (NHS) Foundation Trust, Bradford, United Kingdom, [17] Paediatric Infectious Diseases Research Group, St. George's University of London, London, United Kingdom

Children and adolescents generally experience mild COVID-19. However, those with underlying physical health conditions are at a significantly increased risk of severe disease. Here, we present a comprehensive analysis of antibody and cellular responses in adolescents with severe neuro-disabilities who received COVID-19 vaccination with either ChAdOx1 (n=6) or an mRNA vaccine (mRNA-1273, n=8, BNT162b2, n=1). Strong immune responses were observed after vaccination and antibody levels and neutralisation titres were both higher after two doses. Both measures were also higher after mRNA vaccination and were further enhanced by prior natural infection where one

OPEN ACCESS

Edited by:
Srinivasa Reddy Bonam, University of Texas Medical Branch at Galveston, United States

Reviewed by:
Stephanie Longet, University of Oxford, United Kingdom
Alexander William Tarr, University of Nottingham, United Kingdom

***Correspondence:**
Shamez N. Ladhani
Shamez.Ladhani@phe.gov.uk

[†]These authors have contributed equally to this work

Specialty section:
This article was submitted to Vaccines and Molecular Therapeutics, a section of the journal Frontiers in Immunology

Received: *23 February 2022*
Accepted: *09 May 2022*
Published: *02 June 2022*

Citation:
Dowell AC, Powell AA, Davis C, Scott S, Logan N, Willett BJ, Bruton R, Ayodele M, Jinks E, Gunn J, Spalkova E, Sylla P, Nicol SM, Zuo J, Ireland G, Okike I, Baawuah F, Beckmann J, Ahmad S, Garstang J, Brent AJ, Brent B, White M, Collins A, Davis F, Lim M, Cohen J, Kenny J, Linley E, Poh J, Amirthalingam G, Brown K, Ramsay ME, Azad R, Wright J, Waiblinger D, Moss P and Ladhani SN (2022) mRNA or ChAd0x1 COVID-19 Vaccination of Adolescents Induces Robust Antibody and Cellular Responses With Continued Recognition of Omicron Following mRNA-1273. Front. Immunol. 13:882515. doi: 10.3389/fimmu.2022.882515

vaccine dose was sufficient to generate peak antibody response. Robust T-cell responses were generated after dual vaccination and were also higher following mRNA vaccination. Early T-cells were characterised by a dominant effector-memory CD4+ T-cell population with a type-1 cytokine signature with additional production of IL-10. Antibody levels were well-maintained for at least 3 months after vaccination and 3 of 4 donors showed measurable neutralisation titres against the Omicron variant. T-cell responses also remained robust, with generation of a central/stem cell memory pool and showed strong reactivity against Omicron spike. These data demonstrate that COVID-19 vaccines display strong immunogenicity in adolescents and that dual vaccination, or single vaccination following prior infection, generate higher immune responses than seen after natural infection and develop activity against Omicron. Initial evidence suggests that mRNA vaccination elicits stronger immune responses than adenoviral delivery, although the latter is also higher than seen in adult populations. COVID-19 vaccines are therefore highly immunogenic in high-risk adolescents and dual vaccination might be able to provide relative protection against the Omicron variant that is currently globally dominant.

Keywords: COVID-19, vaccine, paediatric, T-cell, antibody, neuro-disabilities, high-risk patients

INTRODUCTION

SARS-CoV-2 infection in children and adolescents is generally mild, transient and self-limiting, however those with underlying co-morbidities have a higher risk of developing severe and fatal COVID-19 (1–3). As such, vaccination of high-risk children and adolescents against COVID-19 is of considerable importance. Recent studies have indicated mRNA vaccination of adolescents is highly protective against severe and critical COVID-19 (4–6), including in high risk groups (7). The immunogenicity of COVID-19 vaccines in high-risk paediatric groups, however, has not been assessed.

COVID-19 vaccines were first licensed for adults in December 2020 and have proven to be highly effective. In the United Kingdom, the Joint Committee on Vaccination and Immunisation (JCVI) recommended COVID-19 vaccination for older children aged ≥12 years with severe neuro-disabilities at the same time as adults, even though the vaccines were not authorised for this age-group at the time, because they were at higher risk of severe and fatal COVID-19 (1). In March 2021, Public Health England (PHE) (now known as the UK Health Security Agency) initiated the SAFE-KIDS study to assess immune responses in children receiving a COVID-19 vaccine as part of the JCVI recommendation. At the time Moderna (mRNA-1273), and Pfizer-BioNTech (BNT162b2) mRNA vaccines and the AstraZeneca adenoviral-vector (ChAdOx1) vaccine were recommended for adults and high-risk adolescents. Contrary to the marketing authorisation of 3-4 weeks, the JCVI recommended a 12-week interval between COVID-19 vaccine doses. As such, this provided a unique opportunity to compare after one and two doses the relative immunogenicity of adenoviral vector vaccines to mRNA vaccines in adolescence. Currently no comparative data exist.

Here, we provide detailed characterisation of the antibody and cellular immune response to COVID-19 vaccination in fifteen adolescent individuals with severe neuro-disabilities aged 12-16 years. Uniquely, donors received either ChAdOx1 (n=6) or mRNA vaccine (n=8 mRNA-1273, n=1 BNT162b2). Three donors receiving mRNA-1273 had serological evidence of SARS-CoV-2 infection prior to vaccination. Participant characteristics are summarised in **Supplementary Table 1**, with details of vaccination and sample timing in **Figure 1**.

RESULTS

Characterization of Antibody Titres Following First and Second Dose of COVID-19 Vaccination

We firstly determined the antibody response using the Meso-Scale Diagnostics (MSD) assay platform, allowing comparison with other studies using the same platform (8, 9). Samples were assessed longitudinally from baseline. All vaccines induced robust spike-specific (**Figure 2A**) and receptor-binding domain- (RBD-) specific (**Figure 2B**) antibodies. mRNA vaccine, however, induced 4.4-fold and 6.6-fold higher spike-specific antibody responses than the adenovirus-based vaccine after the first and second dose, respectively. Individuals who were previously naturally infected prior to vaccination demonstrated a marked increase in antibody levels after the first mRNA vaccine. Spike-specific antibody levels were significantly higher than one or two doses of ChAdOx1, and significantly higher than one dose of mRNA vaccine (p=0.001, 0.004 and 0.003 respectively, one-way ANOVA with Dunnett's multiple comparisons test). Two doses of mRNA vaccine in previously uninfected individuals achieved similar antibody levels to donors who had received one dose of vaccine after prior natural infection. Antibody levels for all cohorts are shown relative to the WHO reference standard in **Supplementary Table 2**. Additionally, antibody titres specific for the seasonal human coronaviruses, Influenza-A, -B, and

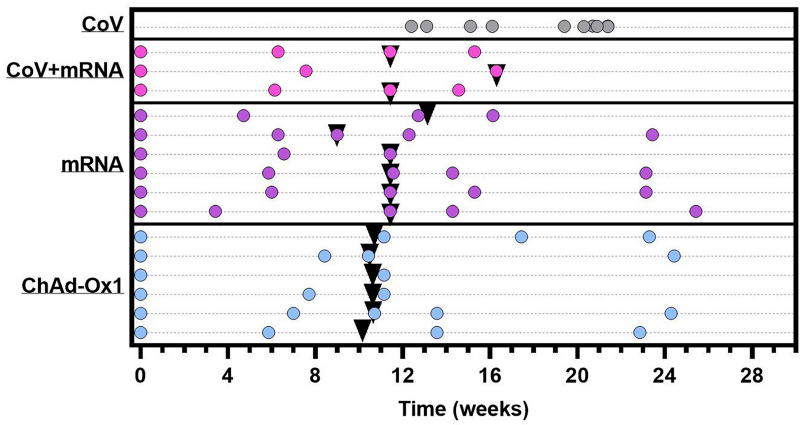

FIGURE 1 | Graphical representation of sample collection and vaccine administration. CoV+mRNA (pink dots) = seropositive adolescents receiving mRNA vaccination (n = 3) mRNA (purple dots) = seronegative adolescents receiving mRNA vaccination (n = 6). ChAdOx1 (blue dots) = seronegative adolescents receiving ChAdOx1 vaccination (n = 6). CoV (grey dots) = naturally infected adolescents with definitive PCR results, for comparison (n = 10). Each dot represents a sample collection. Black triangles indicate time of second dose. Time for all vaccinated donors is relative to administration of first dose. Time of blood sampling for naturally infected donors (CoV) is relative to the date of PCR.

Respiratory Syncytial Virus (common respiratory viruses), were determined and found to be comparable to healthy donors (**Supplementary Table 3**).

We next assessed functional neutralisation using live wild-type (B), Alpha (B1.1.7), Beta (B1.351) or Delta (B1.617.2) viral variants. For comparison, we also included samples from 10 healthy adolescent donors who had PCR-confirmed SARS-CoV-2 infection 2-4 months before sampling. After the first dose of vaccine, in naïve donors, neutralisation titres (NT50) were similar or below that of natural infection against WT virus. Neutralisation of variants was in general below detection. In contrast, previously infected donors induced high neutralising titres to wild type and all viral variants after one dose (**Figure 2C**). Following second dose in naïve donors, neutralizing titres were improved, including to variants (**Figure 2D**). Comparable results were also seen against these and other variants in a ACE2-Spike binding inhibition assay (**Supplementary Figure 1**). There was considerable variability between donors receiving ChAdOx1 or mRNA vaccine, with the latter inducing higher neutralising titres than the former in this limited cohort.

Characterization of the Cellular Response Following COVID-19 Vaccination

We next investigated the cellular immune response after two vaccine doses (median 23-days, range 20-48), in three ChAdOx1 and seven mRNA vaccinated adolescents, including two with prior infection. The timing of sampling is shown in **Figure 1**. Spike-specific cellular responses were assessed using an activation-induced marker (AIM) assay to identify T-cells responding to stimulation with a pool of overlapping-peptides from spike protein, an example is provided in **Supplementary Figure 2**. As previously reported in adults (10), responses were dominated by CD4 T-cells, with ~10-fold lower CD8 T-cell responses. The CD4 T-cell response was higher in mRNA-1273 vaccinated adolescents compared to those vaccinated with ChAdOx1 (**Figures 3A, B**). Cellular samples were also available after one vaccine dose for adolescents receiving mRNA vaccine, allowing the trajectory of T-cell responses to be assessed. The T-cell response appeared to peak after one dose in the two previously-infected donors. In contrast, the CD4 T-cell response increased significantly ($p=0.047$, two-tailed paired t-test) following second dose in infection-naïve donors (**Figure 3A**). Characterisation of the CD4 T-cell response in more detail showed, in all vaccine types, the predominant phenotype was early (CD27+CD28+) effector memory, with elements of central memory, indicating induction of a memory response (**Figure 3C**). CXCR3 and CCR4 expression characterise Th1 and Th2 CD4+ populations, respectively, and both were represented within the spike-specific response at similar frequencies. CXCR5+ T follicular helper cells were also present within the antigen-specific pool (**Figure 3D**).

The cytokine profile of spike-specific T-cells was determined by analysis of supernatant from AIM assay cultures. Type-I cytokines were found at high levels, with IFNγ and IL-2 predominating; release of TNF was also notable, consistent with a Type-I cytokine profile. The level of IFNγ was significantly higher in mRNA vaccinated donors compared to ChAdOx1 ($p=0.016$, RM two-way ANOVA with Geisser-Greenhouse correction and Tukey's multiple comparison test), consistent with the higher frequency of responding cells. Cells also demonstrated cytotoxic potential, with release of perforin, granzyme A and B. In contrast, high IL-10 concentrations were also found within the supernatant. There was, however, little evidence of IL-4 production, with levels generally below 10pg/ml, although it is interesting to note increased detection of IL-4 in mRNA-vaccinated individuals which may be associated with the increased proportion of responding cells. This level of IL-4 is not consistent with the high proportion of activated CCR4-

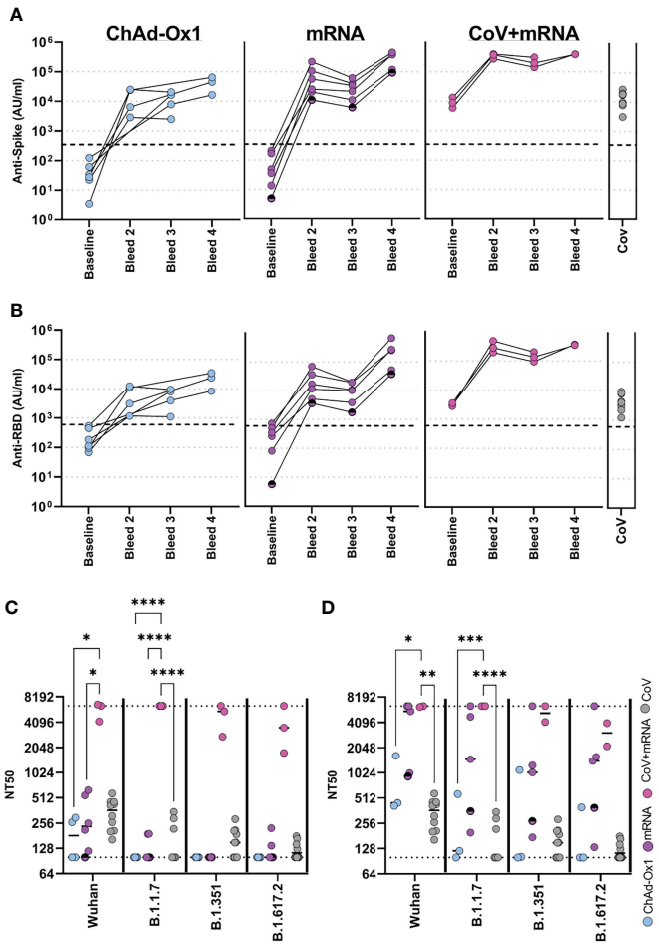

FIGURE 2 | Antibody responses in adolescents following COVID-19 vaccination. Antibody levels to Spike **(A)** and RBD **(B)** measured by MSD assay in adolescents receiving COVID-19 vaccination (ChAdOx1 – seronegative adolescents receiving ChAdOx1 vaccination, (n = 6), mRNA – seronegative adolescents receiving mRNA vaccination (n = 6), CoV+mRNA – seropositive adolescents receiving mRNA vaccination (n = 3), half shaded mRNA symbol indicates the individual who received BNT162b2 vaccine). Antibody levels 2-4 months after natural SARS-CoV-2 infection [CoV, (n = 10)] are shown for comparison. **(C**, **D)** Neutralisation of live virus, either B (Wild Type; PHE-2), B.1.1.7 (Alpha), B.1.351 (Beta) or B.1.617.2 (Delta) variants, following first dose **(C)** or second dose **(D)**. Dotted lines represent upper and lower limits of detection. RM Two-way ANOVA with Geisser-Greenhouse correction and Tukey's multiple comparison test. *p<0.05, **p<0.01, ***p<0.001, ****p<0.0001.

expressing cells being Th2-polarised. IL-17A was also detected but below 10pg/ml (**Figure 3E**). The profile of cytokine release did not change between first and second dose in mRNA vaccinated children (**Supplementary Figure 3**) and was consistent between naïve and previously-infected individuals.

Durability of Antibody Responses and Neutralisation of Omicron Variant 3 Months Post-Vaccination

Rapid waning of the spike-specific antibody level following vaccination is evident in adults, with the greatest decline seen in the initial period following mRNA vaccination (11, 12). In vaccinated adolescents, there was also reduction of the spike-specific antibody level between first and second dose of mRNA vaccination of naïve adolescent donors (**Figure 1A**). Irrespective of vaccine type, modest reduction of the spike-specific antibody level was evident 3 months after the second dose, with a 1.5- and 1.8-fold decrease in mRNA and ChAdOx1 vaccinated adolescents respectively (**Figure 4A**). A greater reduction was evident in RBD-specific antibody levels with a 2.2 - and 1.9-fold reduction following mRNA and ChAdOx1 vaccination respectively (**Figure 4B**).

A direct comparison could now be made between vaccinated donors and the cohort of naturally infected adolescents, as these donors were at a similar timepoint after infection. Antibody levels were significantly higher in the mRNA-1273 vaccinated individuals, compared to naturally infected individuals (p=0.0058, Kruskal-Wallis test with Dunn's multiple comparisons test). Spike-specific antibody levels were 2.1 and 18-fold higher than the naturally infected donors in the ChAdOX1 and mRNA-1273 vaccinated groups, respectively (**Figure 4A**; **Supplementary Table 2**).

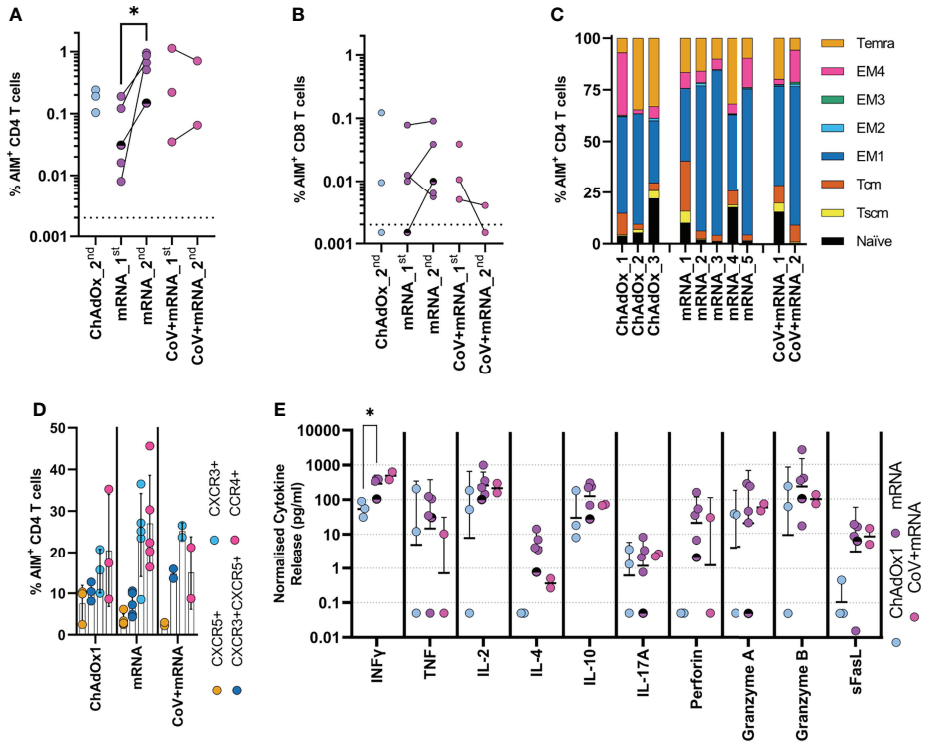

FIGURE 3 | Initial cellular responses in adolescents following COVID-19 vaccination. Analysis of the T-cell response following the second dose of vaccine. A flow cytometry-based AIM assay was used to identify responding **(A)** CD4 (CD69+CD40L+) and **(B)** CD8 (CD69+CD137+) T-cell frequency following overnight stimulation with an overlapping spike peptide pool. Where possible frequency was assessed 6 weeks after first dose _1st or 3 weeks after second dose _2nd. Dots indicate individual donors. n = 3 ChAdOx1 (ChAdOx), n = 5 mRNA and n = 2 CoV+mRNA, half shaded mRNA symbol indicates the individual who received BNT192b2 vaccine. **(C)** Responding AIM+ CD4 T-cells from donors after second dose, were phenotyped, to assess memory state. Bars represent individual donors receiving the indicated vaccine type, numbers indicate individual donors and show the proportion of the AIM+ CD4 T-cell population with each memory phenotype in each donor. T effector memory (CD45RA-CCR7-, EM) are subdivided as EM1 – CD27+CD28+, EM2 – CD27+CD28-, EM3 – CD27-CD28-, EM4 - CD27-CD28+). **(D)** the expression of homing and polarisation markers CXCR5, CXCR3, and CCR4 by AIM+ CD4 T-cell population was also assessed and expressed as a proportion of the total AIM+ CD4 T-cell population. Dots indicate individual donors, bars indicate mean ± SD. **(E)** Supernatant from overnight stimulated cultures were analysed to identify cytokine production. Data was normalised to $1x10^6$ PBMC per well and minus background cytokine production from unstimulated (DMSO) wells. Dots indicate individual donors; bars indicate geometric mean ± geo.SD. Repeated measure two-way ANOVA with Geisser-Greenhouse correction and Tukey multiple comparisons test. *p<0.05.

We tested whether neutralising antibody titres were retained to a similar degree as total spike- and RBD-specific antibodies at three months after the second dose, using a pseudotyped virus neutralisation assay. Reduction of neutralising titres was evident in both ChAdOx1 and mRNA-1273 vaccinated individuals, compared to titres after the second vaccine dose (**Figure 4C**). Neutralising titres were reduced by 2.1- and 1.9-fold in mRNA and ChAdOx1 vaccinated adolescents respectively, comparable to the reduction in RBD-specific antibody levels. Neutralisation titres from mRNA-1273 vaccinated individuals, however, remained significantly higher than titres in healthy adolescents 2-4mths after natural infection (n=10), (p=0.019, Kruskal-Wallis test with Dunn's multiple comparisons test), although considerable variability in titre was evident. Titres from ChAdOx1 vaccinated donors were also similar to natural infection.

The emergence of the Omicron (B.1.1.529) variant has reduced the effectiveness of vaccine protection against infection after two doses of vaccine in adults, requiring further booster vaccinations to elicit higher antibody titres (13, 14). As such, understanding of the longer-term neutralisation of Omicron in vaccinated adolescents is vital. Given this, we tested the neutralisation of Omicron variant in mRNA-1273 vaccinated individuals three months after vaccination. Titres were reduced against Omicron in comparison to the Wuhan sequence, with considerable variation between donors although, importantly, 3 of 4 individuals had measurable neutralisation titres against Omicron (**Figure 4D**). Indeed, titres from individuals with measurable neutralisation titres against Omicron, were similar to or above titres against Wuhan spike from naturally infected healthy adolescents.

Durability of the T-Cell Response and Response to the Omicron Variant 3 Months After Second Dose

Finally, we examined the T-cell response in three ChAdOx1 and four mRNA-1273 adolescents who had cellular samples available

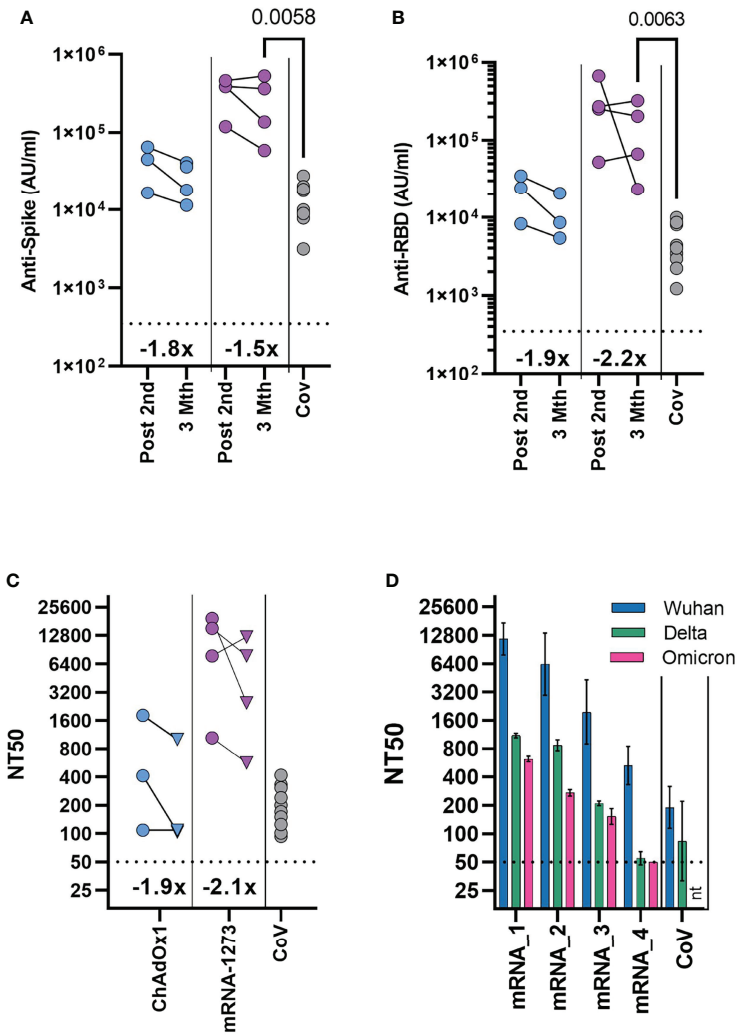

FIGURE 4 | Durability of antibody response and neutralisation of the Omicron variant 3 months after second dose. Antibody levels to Spike **(A)** and RBD **(B)** measured by MSD assay in previously seronegative adolescents receiving two COVID-19 vaccinations (ChAdOx1 – (n = 3), mRNA-1273 – (n = 4), either following second dose (Post 2nd), or three months after second dose (3 Mth). Antibody levels 2-4 months following natural SARS-CoV-2 infection [CoV, (n = 10)] are shown for comparison. **(C)** Neutralising antibody titres quantified using HIV (SARS-CoV-2) pseudotypes bearing the Wuhan spike glycoprotein. Each point represents the mean of three replicates, circles indicate following second dose, triangle three months after second dose. **(A–C)** Inset show the fold change in geometric mean titre. **(D)** Neutralising antibody titres quantified three months after second dose in four mRNA-1273 vaccinated individuals using HIV (SARS-CoV-2) pseudotypes bearing either Wuhan, B.1.617.2 (Delta) or B.1.1.529 (Omicron) spike glycoprotein. mRNA1-4 indicate individual donors. Bars indicate mean (± geometric SD). Neutralisation titres 2-4 months following natural SARS-CoV-2 infection [CoV, (n=10)] are shown for comparison. Kruskal-Wallis test with Dunn's multiple comparison correction.

for assessment three months after second vaccination. We assessed responses to pools of overlapping peptides from either Wuhan or Omicron (B.1.1.529) sequence spike protein using IFNγ ELISpot. Consistent with the initial response measured by AIM assay, T-cell responses were higher in mRNA-1273 vaccinated donors, although variation was evident between donors. Importantly all donors irrespective of vaccine type retained robust T-cell responses to Wuhan peptide pools 3 months after vaccination, similar to that previously observed in children following natural infection (**Figure 5A**) (15). In comparison to the Wuhan sequence, the T-cell response was reduced to Omicron spike peptide pool, with the response on average 84% (range 92.2-76%) of the response to the Wuhan spike peptide pool (**Figure 5A**). The majority of mutations in the Omicron spike sequence occur in the S1 domain of the spike protein (14). Comparing the response to peptides derived from the S1 and S2 domains of Wuhan and Omicron (B.1.1.529) spike sequence, we found that, while the reduction in total spike response was relatively consistent across donors, the relative reduction in response to S1 and S2 domains showed a degree of donor variation (**Figure 5B**).

We again used the AIM assay to assess the phenotype of T-cell response at three months. Sufficient cellular samples were available from three mRNA-1273 vaccinated donors. These donors were

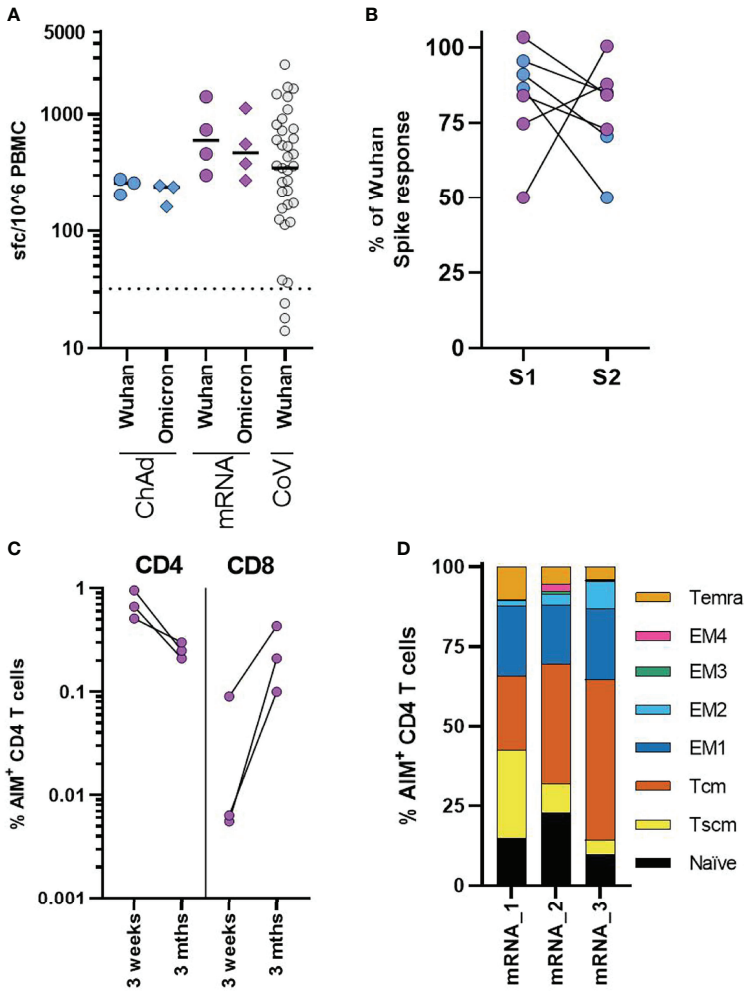

FIGURE 5 | Cellular responses in adolescents three months after COVID-19 vaccination. **(A)** Analysis of the T-cell response in ChAdOx1 (n = 3) and mRNA-1273 (n = 4) adolescents three months after second dose. Results from IFNγ ELISpot assay are normalised to the DMSO control and expressed as spot forming cells (sfc) per million input PBMC. Response to overlapping peptide pools from Wuhan (circles) or B1.1.529 (diamonds) sequence spike protein. Results from previously published data from n = 37 seropositive children aged 4-11 are shown for comparison, dotted line indicates response threshold. **(B)** Shows the relative change in the response to peptide pools containing peptides from the S1 and S2 spike protein domains of Omicron, expressed relative to the size of the response to Wuhan sequence peptide pools. **(C, D)** A flow cytometry-based AIM assay was used to identify responding CD4 (CD69+CD40L+) and CD8 (CD69+CD137+) T-cell frequency following overnight stimulation with overlapping Wuhan spike peptides in three adolescents who received mRNA-1273 vaccination. **(C)** Dots indicate individual donors and frequency of AIM+ CD4 and CD8 T-cells following second dose of vaccine (3 weeks) or three months after second dose (3 Mths). **(D)** AIM+ CD4 T-cells, were phenotyped to assess memory state, bars represent indicate individual donors (numbered 1-3) and show the proportion of the AIM+ CD4 T-cell population. T effector memory (CD45RA-CCR7-, EM) are subdivided as EM1 – CD27+CD28+, EM2 – CD27+CD28-, EM3 – CD27-CD28-, EM4 - CD27-CD28+).

also assessed ~3 weeks after the second vaccine dose by AIM assay (**Figure 3A–C**). The CD4 T-cell response was found to be lower in all donors, compared with the earlier peak response. In contrast, an increase in the frequency of AIM+ CD8 T-cells was observed (**Figure 5C**). Initially following vaccination, AIM+ CD4 T-cells were predominantly effector memory (CD45RA-CCR7-) phenotype (**Figure 3C**) but, three months after vaccination AIM+ CD4 T-cells were predominantly central (CD45RA-CCR7+) and stem cell memory (CD45RA+CCR7+CD95+) phenotype in all donors (**Figure 5D**). There was a corresponding reduction in T effector/effector memory phenotype cells. These data, therefore, indicate the successful formation of long-term memory T-cell responses following vaccination.

DISCUSSION

The UK JCVI decision to recommend COVID-19 vaccination for adolescents with neuro-disabilities, soon after COVID-19 vaccines were authorised for adults, provided a unique opportunity to rapidly assess immune responses to two different types of vaccines in this high-risk group in a real-

world setting. While there is growing evidence of clinical efficacy of vaccination, there are limited data characterising the immune responses to COVID-19 vaccination in children and adolescents, especially in high-risk groups, and none comparing responses in adolescents who received ChAdOx1 against an mRNA vaccine (4–7). Uniquely, instead of the 3-4 week interval used by most other countries, the JCVI recommendations included a 12-week interval between COVID-19 vaccine doses, to maximise population first dose coverage. In adults, it is now evident that an extended interval schedule provides higher peak antibody responses after the second dose and, potentially, longer duration of protection (16). Importantly, the extended interval also provided a unique opportunity to assess the immunogenicity of the initial vaccine dose, prior to the second dose.

The higher immunogenicity with mRNA vaccine we observed compared to ChAdOx1 vaccine is consistent with data in adults (8, 9, 11, 17), including studies reporting the extended 12-week interval schedule (8, 16). The antibody level after mRNA vaccination was comparable to those previously reported in adults (8), but higher in adolescents than in adults after ChAdOx1 vaccination (9). It is noted the single donor who received BNT162b2 had similar antibody levels as ChAdOx1 vaccinated donors. In adults, the highest antibody levels are reported following mRNA-1273 followed closely by BNT162b2 (13). Further study will be required to define the relative antibody response induced by mRNA-1273, BNT162b2, and ChAdOx1 in larger adolescent cohorts. Our preliminary data, however, indicate that ChAdOx1 may be more immunogenic in adolescents than adults, and confirm that both vaccine types provide robust antibody responses using an extended-interval schedule in these higher-risk adolescents.

Rapid waning of spike-specific antibody level following vaccination is evident in adults, with the greatest decline seen following mRNA vaccination, and the most rapid waning occurring soon after vaccination (11, 12). It was, therefore, encouraging to observe comparatively stable antibody responses between 21 days (range 20-27 days) after the second dose and three months later. Antibody titres reduced by 1.5-fold, compared to an approximate 3.7-fold decline reported in adults receiving an extended-interval BNT162b2 vaccine schedule, measured at similar timepoints using the MSD platform (8). These data showing retained antibody titres are consistent with the better clinical protection in adolescents 3 months after vaccination compared to adults (6).

A key aim of vaccination is the induction of neutralising antibodies. The use of a 12-week vaccination schedule uniquely allowed us to explore the relative immunogenicity of one and two vaccine doses in adolescents. Our data show that a second dose significantly increases immune responses in infection-naïve adolescents, with improved neutralising titres after the second vaccine dose, including to the viral variants tested. While mRNA vaccines induced higher neutralising titres, there was considerable variability between donors, again with the BNT162b2 vaccinated donor being similar to ChAdOx1. We also assessed neutralisation at three months after vaccination, an important point at which to evaluate the durability of response, given the waning in protection observed in adults (11, 18). We chose to use a pseudotype neutralisation assay as isolates of Omicron were not yet available. Both live virus and pseudotype assays give comparable results and are regarded to be well correlated (19), as such these results should be representative of live virus neutralisation assays. Despite the relatively stable total spike-specific antibody responses, there was evidence of waning of neutralisation titres, which mirrored the reduction in RBD-specific-antibody level highlighting the need for further long-term assessment in larger groups of adolescents and children. We have previously shown that antibody responses in children are durable up to 12 months after natural infection (15).

Given the ability of Omicron to evade vaccine immunity (13, 14), it was vital to assess the immune response against this variant. Three months after vaccination provided an informative point to address this. As in adults, Omicron-neutralisation titres were significantly reduced compared to Wuhan (13, 14). However, titres were similar to those seen in adults after booster mRNA vaccination (13), indicating comparable neutralising response in dual vaccinated adolescents. Surprisingly, mRNA-1273 vaccinated adolescents who retained a measurable Omicron neutralising titre, had similar or enhanced titres compared to neutralising titres against Wuhan spike in naturally infected healthy adolescents, highlighting that mRNA-1273 vaccination of adolescents, and likely children, may offer improved and broader immunity to Omicron than natural infection. However, further evaluation of neutralisation titres in larger cohorts and real-world epidemiological studies are required.

Cellular immune responses are ultimately likely to be more durable than antibody responses and provide longer-term protection against severe disease (20, 21). Additionally, T-cells are likely to be less susceptible to changes in viral variants (22). Importantly, we found that, while T-cell responses were reduced towards the Omicron spike sequence when compared to the neutralising antibody response, the T-cell response was retained at a robust level towards the Omicron variant spike peptide pool. The relative reduction in responses to S1 and S2 domains showed donor variation, potentially indicating differences in the epitope and immunodominance of epitopes between donors. The T-cell response was observed to peak after one dose in the two previously-infected children, consistent with results from adults (23), although a larger cohort is required to fully assess this. The CD4 T-cell response in infection-naïve adolescents was, however, significantly enhanced by a second dose of vaccine, again indicating the requirement for two vaccine doses in infection-naïve adolescents.

The T-cell response retained at three months after vaccination was similar to the range of responses observed after SARS-CoV-2 infection in younger children aged 4-11 years, which was also significantly higher than in adults (15). As such, this showed that vaccination elicits robust T-cell responses in adolescents similar to that produced following natural infection. Given the range of responses following natural infection, larger cohorts will be required to assess whether the lower response after ChAdOx1 is a result of differences between vaccine type or donor variation.

However, the finding that the mRNA-1273 vaccine generates strong spike-specific cellular responses in adolescents contrasts with previous reports in older adults where cellular responses after ChAdOx1 are somewhat higher than after mRNA vaccination (8, 9, 24). Cellular responses displayed an effector memory phenotype early after the second vaccine, representing recent antigenic stimulation (25), and it was therefore reassuring to observe the formation of a potential long-term memory pool three months later.

Spike-specific T-cells displayed a predominant Type-I cytokine profile, but high IL-10 concentrations were also observed and is noteworthy as this combination has been reported previously as a feature of mild or asymptomatic infection (10, 15, 26). The presence of spike-specific T-cells expressing CCR4 in the absence of IL-4 may also be important as this is a specific phenotypic profile of lung/skin homing (27) rather than Th2 polarisation.

A limitation of this study is the small number of participants, mainly due to very low vaccine uptake in eligible groups during the first 6 months of 2021 (28). While considered as high-risk because of severe neuro-disabilities, our participants are clinically immune competent and their antibody levels against other respiratory viruses were comparable to healthy donors, indicating normal immune function. As such the robust immune responses to SARS-CoV-2 vaccine in these donors should be representative of the general adolescent population. One participant did have Down syndrome, which is associated with unspecified immune dysfunction (29), although our participant mounted a robust immune response after vaccination.

Our study provides a detailed and unique insight into the relative immunogenicity of mRNA and adenoviral-vector vaccines in infection-naïve and previously infected adolescents, following one and two doses of vaccine. Overall, these findings show that COVID-19 vaccination in adolescents can elicit coordinated and durable cellular and antibody responses with activity against Omicron variant. Further investigation in larger cohorts is required to confirm these findings.

METHODS

Sample Collection

Eligible children (**Supplementary Table 1**) aged 12-16 years were recruited into SAFE-KIDS by paediatricians. The current study was reviewed and approved by the PHE Research Ethics and Governance Group (REGG) reference NR0264. Written informed consent was obtained for all participants from parents or guardians.

Blood samples taken at baseline (before or within 48 hours of first vaccination), ~6 weeks follow prime (bleed 2), at boost (bleed 3), ~2-4 weeks following boost (bleed 4) and ~3 months following boost (bleed 5) (**Figure 1**). The vaccine administered was not pre-determined, children received vaccine as part of the national vaccine campaign, as such vaccine type was dependent on availability at each site. The full SAFE-KIDS protocol is available online at https://www.gov.uk/guidance/covid-19-paediatric-surveillance.

Sero-status was determined as described below using the baseline sample. Nucleocapsid-specific antibody responses were assessed at each timepoint to exclude the possibility of SARS-CoV-2 infection during the study. Routine surveillance PCR testing was not performed during this study.

Convalescent plasma samples were also available from the Born in Bradford study (30). 10 children aged 10-13 years with PCR-confirmed SARS-CoV-2 infection between October and December 2020, had samples taken a median of 18 weeks after PCR (**Supplementary Table 1**).

PBMC and Plasma Preparation

Lithium Heparin blood tubes were processed within 24hrs of collection. Briefly tubes were spun at 300g for 10mins prior to removal of plasma which was then spun at 800g for 10mins and stored as aliquots at -80°C. Remaining blood was diluted with RPMI and PBMC isolated on ficol density gradient, washed with RPMI and frozen in 90%FBS+10%DMSO, samples were stored in the vapour phase of liquid nitrogen.

Serological Analysis of SARS-CoV-2-Specific Immune Response

Quantitative IgG antibody titres were measured using Mesoscale Diagnostics multiplex assays as previously described (15), following the manufacturer instructions. Briefly, samples were diluted at 1:5000 and added wells of the 96 well plate alongside reference standards and controls. After incubation, plates were washed and anti-IgG-Sulfo tagged detection antibody added. Plates were washed and were immediately read using a MESO TM QuickPlex SQ 120 system. Data was generated by Methodological Mind software and analysed with MSD Discovery Workbench (v4.0) software. Data are presented as arbitrary units (AU)/ml relative to the standard. Anti-Spike and anti-RBD AU/ml were converted to WHO reference standard Binding Antibody units (BAU)/ml using the provided correction values, using the following formula: anti-spike - AU/ml*0.00901=BAU/ml, anti-RBD - AU/ml*0.0272=BAU/ml. Positive and negative cut-off values were used as previously defined (15), using plasma samples taken prior to the pandemic.

Live Virus Neutralisation Assay

Clinical isolates used in the study were provided by Public Health England and Imperial College London. A549-ACE2-TMPRSS2 (31) cells were seeded at a cell density of $1x10^4$/well in 96-well plates 24hrs before inoculation. Serum was titrated starting at a 1:100 dilution-1:6400 dilution. The specified virus was then incubated at an MOI 0.01 with the Serum for 1hr prior to infection. All wells were performed in triplicate. 72hrs later infection plates were fixed with 8% formaldehyde and stained with Coomassie blue for 30 mins. Plates were washed and dried overnight before quantification using a Celigo Imaging Cytometer (Nexcelom) to measure the staining intensity. Percentage cell survival was assessed by comparing the intensity of the staining to uninfected wells. Antibody titre was then estimated by interpolating the point at which infectivity had been reduced to 50% of the value for the no serum control samples.

Pseudotype-Based Neutralisation Assays

Constructs and 293-ACE2 cells were previously described (13, 15). The assay was performed as previously described (13, 15), briefly neutralising activity in each sample was measured by a serial dilution approach. Each sample was serially diluted in triplicate from 1:50 to 1:36450 in complete DMEM prior to incubation with approximately $1x10^6$ CPS (counts per second) per well of HIV (SARS-CoV-2) pseudotypes, incubated for 1 hour, and plated onto 239-ACE2 target cells. After 48-72 hours, luciferase activity was quantified by the addition of Steadylite Plus chemiluminescence substrate and analysis on a Perkin Elmer EnSight multimode plate reader (Perkin Elmer, Beaconsfield, UK). Antibody titre was then estimated by interpolating the point at which infectivity had been reduced to 50% of the value for the no serum control samples.

Spike-ACE2 Receptor Blocking Assay

Inhibition of ACE-2 binding to trimeric SARS-CoV-2 Spike protein from variants of concern were measured using the MSD V-PLEX COVID-19 ACE2 Neutralization Kit (SARS-CoV-2 Plate 13) following manufacturer's instructions. Briefly, samples were diluted 1:10 in diluent, known neutralizing antibody dilutions were included as a reference standard, and pre-incubated on the plate, which was coated with trimeric spike from SARS-CoV-2 variants. After incubation, Sulfo-tagged Human ACE-2 Protein was added to the plate and incubated for 1 hour. Plates were washed and read immediately using a MESO ^{TM} QuickPlex SQ 120 system. Data was generated by Methodological Mind software and analysed with MSD Discovery Workbench (v4.0) software. Presented data were adjusted for sample dilution and expressed as neutralising antibody ug/ml as determined using the reference standard.

Activation Induced Marker Assay

Cryopreserved PBMC were thawed and rested for at least 6 hours in filtered R10 - RPMI+10%FBS (Sigma). Cells were counted and divided between two wells of a round bottom 96-well plate (1-$3x10^6$/well) in a final volume of 200ul, purified anti-CD40 antibody (Biolegend) was included at a final concentration 1µg/ml. Cells were then stimulated with a pool of overlapping peptides from Wuhan sequence SARS-CoV-2 Spike (JPT technologies) at final concentration of 1µg/ml per peptide, or DMSO as an unstimulated control. Cells were incubated at 37°C overnight for 18 hours. Following stimulation, plates were spun for 2 min at 250g, and 150ul of supernatant removed and immediately frozen at -80°C. Cells were transferred to FACS tubes and washed with cold wash buffer (PBS+0.5% BSA+0.1% EDTA), Fc-block was added for 5 minutes (Biolegend), An antibody mastermix was made using 50µl of brilliant staining buffer (BD biosciences) per sample, to which appropriate volumes of antibody were added as shown in **Supplementary Table 4**. Antibody was added to the cell suspension and cells stained at 4°C for 30 minutes. Cells were then washed and fixed with 1.6% paraformaldehyde for 30 minutes at RT in the dark, washed and run on a BD Symphony A3 flow cytometer (BD Biosciences). Data was collected using BD FACS Diva 8 and analysis was carried out using FlowJo v10.7.1.

Cytokine Release Profiling

Supernatants from AIM assay cultures were assessed using a LEGENDplex CD8/NK cytokine-profile 13-plex kit (Biolegend) following manufacturer's instructions. Samples were analysed in duplicate. Cytokine levels were normalised to be equivalent to $1x10^6$ cells per well, cytokine levels in DMSO controls were then removed. Data was analysed using LEGENDplex v8.0 Software (Biolegend).

IFN-γ ELISpot

T-cell responses were measured using an IFN-γ ELISpot Pro kit (Mabtech) as previously described (15). Briefly, fresh PBMC were rested overnight prior to assay and $0.25\text{-}0.3x10^6$ PBMC were added in duplicate per well containing either pep-mix, anti-CD3 (positive) or DMSO (negative) control. Samples were incubated for 16-18hrs. Plates were developed following the manufacturer's instructions and read using an AID plate reader (AID).

Pepmixes pool containing 15-mer peptides overlapping by 10aa from either SARS-CoV-2 spike S1 or S2 domains from the Wuhan or Omicron (B1.1.529) variant were purchased from JPT technologies.

Data Visualisation and Statistics

Data was visualised and statistical tests, including normality tests, performed as indicated using GraphPad Prism v9 software. Only results found to be significant ($p<0.05$) are displayed.

DATA AVAILABILITY STATEMENT

The raw data supporting the conclusions of this article will be made available by the authors, without undue reservation.

ETHICS STATEMENT

The studies involving human participants were reviewed and approved by PHE Research Ethics and Governance Group (REGG) reference NR0264. Written informed consent to participate in this study was provided by the participants' legal guardian/next of kin.

AUTHOR CONTRIBUTIONS

Conceptualization: AD, GI, PM, and SL. Methodology: AD, CD, and BW. Formal analysis: AD, CD, and BW. Investigation: AD, CD, SS, and NL. Resources: AP, MA, EJ, JGu, PS, ES, SN, GI, IO, BW, JB, SA, JGa, AB, BB, MW, AC, ML, JK, JC, MR, EL, JP, GA, KB, RA, DW, and JW. Data curation: AD and AP. Writing – original draft: AD, AP, PM, and SL. Writing - review and editing: all authors. Visualization: AD, PM, and SL. Supervision: AD, RB, DW, CD, BW, JZ, PM, and SL. Project administration: RB, AP, GI, PM, and SL.

Funding acquisition: CD, BW, PM, and SL. All authors contributed to the article and approved the submitted version.

FUNDING

This work was partly funded by UKRI/NIHR through the UK Coronavirus Immunology Consortium (UK-CIC) (PM). The study was also funded in part by the MRC (MC UU 1201412) (CD and BW).

ACKNOWLEDGMENTS

We would like to express our gratitude to the parents and especially children who took part in this study.

SUPPLEMENTARY MATERIAL

The Supplementary Material for this article can be found online at: https://www.frontiersin.org/articles/10.3389/fimmu.2022.882515/full#supplementary-material

REFERENCES

1. Wong BLH, Ramsay ME, Ladhani SN. Should Children Be Vaccinated Against COVID-19 Now? *Arch Dis In Childhood* (2021) 106:1147–8. doi: 10.1136/archdischild-2020-321225
2. Ward JL, Harwood R, Smith C, Kenny S, Clark M, Davis PJ, et al. Risk Factors for PICU Admission and Death Among Children and Young People Hospitalized With COVID-19 and PIMS-TS in England During the First Pandemic Year. *Nat Med* (2022) 28(1):193–200. doi: 10.1038/s41591-021-01627-9
3. Smith C, Odd D, Hardwood R, Ward J, Linney M, Clark M, et al. Deaths in Children and Young People in England After SARS-Cov-2 Infection During the First Pandemic Year. *Nat Med* (2022) 28(1):185–92. doi: 10.1038/s41591-021-01578-1
4. Ali K, Berman G, Zhou H, Deng W, Faughnan V, Coronado-Voges M, et al. Evaluation of Mrna-1273 SARS-Cov-2 Vaccine in Adolescents. *N Engl J Med* (2021) 385:2241–51. doi: 10.1056/NEJMoa2109522
5. Frenck RW, NP K, Kitchin N, Gurtman A, Absalon J, Lockhart S, et al. Safety, Immunogenicity, and Efficacy of the BNT162b2 Covid-19 Vaccine in Adolescents. *N Engl J Med* (2021) 385(33):239–50. doi: 10.1056/NEJMoa2107456
6. Tartof SY, Slezak JM, Fischer H, Hong V, Ackerson BK, Ranasinghe ON, et al. Effectiveness of Mrna BNT162b2 COVID-19 Vaccine Up to 6 Months in a Large Integrated Health System in the USA: A Retrospective Cohort Study. *Lancet* (2021) 398(10309):1407–16. doi: 10.1016/S0140-6736(21)02183-8
7. Olson SM, Newhams MM, Halasa NB, Price AM, Boom JA, Sanhi LC, et al. Effectiveness of BNT162b2 Vaccine Against Critical Covid-19 in Adolescents. *N Engl J Med* (2022) 386: 713–23. doi: 10.1056/NEJMoa2117995
8. Payne RPayne RP, Longet S, JA A, DT S, Dejnirattisai W, Adele S, et al. Immunogenicity of Standard and Extended Dosing Intervals of BNT162b2 mRNA Vaccine. *Cell* (2021) 184(23):5699–714. doi: 10.1016/j.cell.2021.10.011
9. Folegatti PM, Ewer KJ, Aley PK, Angus B, Becker S, Belij-Rammerstorfer S, et al. Safety and Immunogenicity of the Chadox1 Ncov-19 Vaccine Against SARS-Cov-2: A Preliminary Report of a Phase 1/2, Single-Blind, Randomised Controlled Trial. *Lancet* (2020) 396(10249):467–78. doi: 10.1016/S0140-6736(20)31604-4
10. Zuo J, Dowell A, Pearce H, Verma K, Long H, Begum J, et al. Robust SARS-Cov-2-Specific T-Cell Immunity Is Maintained at 6 Months Following Primary Infection. *Nat Immunol* (2020) 22:620–6. doi: 10.1038/s41590-021-00902-8
11. Shrotri M, Navaratnam AMD, Nguyen V, Byrne T, Geismar C, Fragaszy E, et al. Spike-Antibody Waning After Second Dose of BNT162b2 or Chadox1. *Lancet* (2021) 398(10298):385–7. doi: 10.1016/S0140-6736(21)01642-1
12. Pegu A, O'Connell SE, Schmidt SD, O'Dell S, Talana CA, Lai L, et al. Durability of Mrna-1273 Vaccine Induced Antibodies Against SARS-Cov-2 Variants. *Science (New York NY)* (2021) 373(6561):1372–7. doi: 10.1126/science.abj4176
13. Willett BJ, Grove J, MacLean OA, Wilkie C, Logan N, Lorenzo GD, et al. The Hyper-Transmissible SARS-Cov-2 Omicron Variant Exhibits Significant Antigenic Change, Vaccine Escape and a Switch in Cell Entry Mechanism. *medRxiv* (2022) 03:21268111. doi: 10.1101/2022.01.03.21268111
14. Garcia-Beltran WF, St. Denis KJ, Hoelzemer A, Lam EC, Nitido AD, Sheehan ML, et al. Mrna-Based COVID-19 Vaccine Boosters Induce Neutralizing Immunity Against SARS-Cov-2 Omicron Variant. *Cell* (2021) 185(3):457–66. doi: 10.2139/ssrn.3985605
15. Dowell AC, Butler MS, Jinks E, Tut G, Lancaster T, Sylla P, et al. Children Develop Robust and Sustained Cross-Reactive Spike-Specific Immune Responses Following SARS-Cov-2 Infection. *Nat Immunol* (2022) 23:40–9. doi: 10.1038/s41590-021-01089-8
16. Parry H, Bruton R, Stephens C, Brown K, Amirthalingam G, Hallis B, et al. Extended Interval BNT162b2 Vaccination Enhances Peak Antibody Generation in Older People. *Medrxiv* (2021) 15:21257017. doi: 10.1101/2021.05.15.21257017
17. Sadarangani M, Marchant A, Kollmann TR. Immunological Mechanisms of Vaccine-Induced Protection Against COVID-19 in Humans. *Nat Rev Immunol* (2021) 21(8):475–84. doi: 10.1038/s41577-021-00578-z
18. Levin EG, Lustig Y, Cohen C, Fluss R, Indenbaum V, Amit S, et al. Waning Immune Humoral Response to BNT162b2 Covid-19 Vaccine Over 6 Months. *N Engl J Med* (2021) 385(24):e84. doi: 10.1056/NEJMoa2114583
19. Fenwick C, Turelli P, Pellaton C, Farina A, Campos J, Raclot C, et al. A High-Throughput Cell- and Virus-Free Assay Shows Reduced Neutralization of SARS-Cov-2 Variants by COVID-19 Convalescent Plasma. *Sci Transl Med* (2021) 13(605). doi: 10.1126/scitranslmed.abi8452
20. Ng KW, Faulkner N, Cornish GH, Rosa A, Harvey R, Hussain S, et al. Preexisting and De Novo Humoral Immunity to SARS-Cov-2 in Humans. *Science (New York NY)* (2020) 370(6522):1339–43. doi: 10.1126/science.abe1107
21. Tang F, Quan Y, Xin ZT, Wrammert J, Ma MJ, Lv H, et al. Lack of Peripheral Memory B Cell Responses in Recovered Patients With Severe Acute Respiratory Syndrome: A Six-Year Follow-Up Study. *J Immunol (Baltimore Md: 1950)* (2011) 186(12):7264–8. doi: 10.4049/jimmunol.0903490
22. Skelly DT, Harding AC, Gilbert-Jaramillo J, Knight ML, Longet S, Brown A, et al. Two Doses of SARS-CoV-2 Vaccination Induce Robust Immune Responses to Emerging SARS-CoV-2 Variants of Concern. *Nat Commun* (2021) 12(1):5061. doi: 10.1038/s41467-021-25167-5
23. Mazzoni A, Di Lauria N, Maggi L, Salvati L, Vanni A, Capone M, et al. First-Dose mRNA Vaccination Is Sufficient to Reactivate Immunological Memory to SARS-CoV-2 in Subjects Who Have Recovered From COVID-19. *J Clin Invest* (2021) 131(12):e149150. doi: 10.1172/JCI149150
24. Parry H, Bruton R, Stephens C, Brown K, Amirthalingam G, Otter A, et al. Differential Immunogenicity of BNT162b2 or ChAdOx1 Vaccines After Extended-Interval Homologous Dual Vaccination in Older People. *Immun Ageing* (2021) 18(1):34. doi: 10.1186/s12979-021-00246-9
25. Turner JS, O'Halloran JA, Kalaidina E, Kim W, Schmitz AJ, Zhou JQ, et al. SARS-CoV-2 mRNA Vaccines Induce Persistent Human Germinal Centre Responses. *Nature* (2021) 596(7870):109–13. doi: 10.1038/s41586-021-03738-2
26. Le Bert N, Clapham HE, Tan AT, Chia WN, Tham CYL, Lim JM, et al. Highly Functional Virus-Specific Cellular Immune Response in Asymptomatic SARS-CoV-2 infectionSARS-CoV-2–Specific T Cells in Asymptomatic. *J Exp Med* (2021) 218(5):e20202617. doi: 10.1084/jem.20202617
27. Mikhak Z, Strassner JP, Luster AD. Lung Dendritic Cells Imprint T Cell Lung Homing and Promote Lung Immunity Through the Chemokine Receptor Ccr4. *J Exp Med* (2013) 210(9):1855–69. doi: 10.1084/jem.20130091
28. Aiano F, Campbell C, Saliba V, ME R, Ladhani SN. COVID-19 Vaccine Given to Children With Comorbidities in England, December 2020–June

2021. *Arch Dis Child* (2021) 107(3):e16. doi: 10.1136/archdischild-2021-323162
29. Dieudonné Y, Uring-Lambert B, Jeljeli MM, Gies V, Alembik Y, Korganow A-S, et al. Immune Defect in Adults With Down Syndrome: Insights Into a Complex Issue. *Front Immunol* (2020) 11: doi: 10.3389/fimmu.2020.00840
30. Bird PK, McEachan RRC, Mon-Williams M, Small N, West J, Whincup P, et al. Growing Up in Bradford: Protocol for the Age 7–11 Follow Up of the Born in Bradford Birth Cohort. *BMC Public Health* (2019) 19(1):939. doi: 10.1186/s12889-019-7222-2
31. Rihn SJ, Merits A, Bakshi S, Turnbull ML, Wickenhagen A, Alexander AJT, et al. A Plasmid DNA-Launched SARS-CoV-2 Reverse Genetics System and Coronavirus Toolkit for COVID-19 Research. *PLoS Biol* (2021) 19(2): e3001091. doi: 10.1371/journal.pbio.3001091

Conflict of Interest : MR received funding for the COV-BOOST trial under contract *via* University Hospital Southampton NHS Foundation Trust, Funded by the UK NIHR/Vaccine Task Force (NIHR203292). Post-marketing surveillance reports on pneumococcal and meningococcal infection have been provided to vaccine manufacturers for which a cost recovery charge was made to GSK and Pfizer.

The remaining authors declare that the research was conducted in the absence of any commercial or financial relationships that could be construed as a potential conflict of interest.

Publisher's Note: All claims expressed in this article are solely those of the authors and do not necessarily represent those of their affiliated organizations, or those of the publisher, the editors and the reviewers. Any product that may be evaluated in this article, or claim that may be made by its manufacturer, is not guaranteed or endorsed by the publisher.

frontiers | Frontiers in Immunology

BRIEF RESEARCH REPORT
published: 23 June 2022
doi: 10.3389/fimmu.2022.907343

Individuals With Weaker Antibody Responses After Booster Immunization Are Prone to Omicron Breakthrough Infections

Birte Möhlendick[1], Ieva Čiučiulkaitė[1], Carina Elsner[2], Olympia E. Anastasiou[2], Mirko Trilling[2], Bernd Wagner[3], Denise Zwanziger[4], Karl-Heinz Jöckel[5], Ulf Dittmer[2] and Winfried Siffert[1]*

[1] Institute of Pharmacogenetics, University Hospital Essen, University of Duisburg-Essen, Essen, Germany, [2] Institute for Virology, University Hospital Essen, University of Duisburg-Essen, Essen, Germany, [3] Department of Clinical Chemistry and Laboratory Medicine, University-Hospital Essen, University of Duisburg-Essen, Essen, Germany, [4] Department of Endocrinology, Diabetes and Metabolism and Division of Laboratory Research, University-Hospital Essen, University of Duisburg-Essen, Essen, Germany, [5] Institute of Medical Informatics, Biometry and Epidemiology, University of Duisburg-Essen, Essen, Germany

OPEN ACCESS

Edited by:
Pedro A. Reche, Complutense University of Madrid, Spain

Reviewed by:
Massimo Pieri, University of Rome Tor Vergata, Italy
Javier Carbone, Gregorio Marañón Hospital, Spain

***Correspondence:**
Birte Möhlendick
birte.moehlendick@uk-essen.de

Specialty section:
This article was submitted to Vaccines and Molecular Therapeutics, a section of the journal Frontiers in Immunology

Received: *29 March 2022*
Accepted: *27 May 2022*
Published: *23 June 2022*

Citation:
Möhlendick B, Čiučiulkaitė I, Elsner C, Anastasiou OE, Trilling M, Wagner B, Zwanziger D, Jöckel K-H, Dittmer U and Siffert W (2022) Individuals With Weaker Antibody Responses After Booster Immunization Are Prone to Omicron Breakthrough Infections. Front. Immunol. 13:907343. doi: 10.3389/fimmu.2022.907343

Background: Despite the high level of protection against severe COVID-19 provided by the currently available vaccines some breakthrough infections occur. Until now, there is no information whether a potential risk of a breakthrough infection can be inferred from the level of antibodies after booster vaccination.

Methods: Levels of binding antibodies and neutralization capacity after the first, one and six month after the second, and one month after the third (booster) vaccination against COVID-19 were measured in serum samples from 1391 healthcare workers at the University Hospital Essen. Demographics, vaccination scheme, pre-infection antibody titers and neutralization capacity were compared between individuals with and without breakthrough infections.

Results: The risk of developing an Omicron breakthrough infection was independent of vaccination scheme, sex, body mass index, smoking status or pre-existing conditions. In participants with low pre-infection anti-spike antibodies (≤ 2641.0 BAU/ml) and weaker neutralization capacity (≤ 65.9%) against Omicron one month after the booster vaccination the risk for developing an Omicron infection was 10-fold increased (P = 0.001; 95% confidence interval, 2.36 - 47.55).

Conclusion: Routine testing of anti-SARS-CoV-2 IgG antibodies and surrogate virus neutralization can quantify vaccine-induced humoral immune response and may help to identify subjects who are at risk for a breakthrough infection. The establishment of

thresholds for SARS-CoV-2 IgG antibody levels identifying "non"-, "low" and "high"-responders may be used as an indication for re-vaccination.

Keywords: SARS-CoV-2, booster vaccination, breakthrough infection, COVID-19, humoral immune response, neutralization, anti-spike antibodies

1 INTRODUCTION

Despite the undeniable success of anti-Coronavirus disease 2019 (COVID-19) vaccines, some breakthrough infections occur. So far, the predisposing factors remain largely elusive. The lack of knowledge is based on three factors: (I) Retrospective surveillance studies lack clinical specimens predating the infection event. (II) Post-infection immune profiling is necessarily confounded by anamnestic immune responses. (III) Breakthrough infections are rare events. Thus, only well-powered prospective studies enroll sufficient participants to allow for a stratification according to the occurrence of breakthrough infections and a look-back assessment of pre-infection immunity. Here we report, to our knowledge for the first time, on such humoral immune responses being present in boostered vaccinees prior to severe acute respiratory syndrome coronavirus 2 (SARS-CoV-2) breakthrough infection with the Omicron variant.

Only two days after its description, the variant B.1.1.529 was declared as a variant of concern and designated with the Greek letter Omicron on November 26, 2021 (1). Omicron is highly transmissible, able to evade the immune system and currently approved vaccines are less effective against this variant (2–6).

The increased number of breakthrough infections observed during the Omicron wave allowed us to analyze pre-infection immune responses in a comprehensive longitudinal monocentric observational study cohort. Also, we were able to determine a threshold for anti-spike antibody levels and neutralization capacity at which the risk for a breakthrough infection significantly increases.

2 METHODS

2.1 Study Cohort

Since April 2021, we have recruited 2526 healthcare workers at the University Hospital Essen (Essen, Germany) as participants for a comprehensive study on immune responses to vaccines against COVID-19.

Up to now 1391 participants have received their third SARS-CoV-2 vaccination (booster) with an mRNA vaccine after a first and a second vaccination with either mRNA (BNT162b2, BioNTech SE or mRNA-1273, Moderna Inc.), an adenoviral vector vaccine (AZD1222, AstraZeneca), or a combination of both. All individuals were vaccinated in accordance with recommendations of the national vaccine commission (STIKO). Study participants had to self-administer rapid SARS-CoV-2 nucleocapsid protein antigen tests at least twice a week since December 1, 2021. All subjects completed questionnaires at regular intervals delivering information on demographics, general health, and any known SARS-CoV-2 infection including symptoms and course of disease.

Between November 29, 2021, and March 5, 2022, 102 (7.3%) participants self-reported a SARS-CoV-2 infection. All infections were confirmed by real-time reverse transcription-PCR (RT-PCR). In 16 individuals (15.7%), an infection with the Omicron variant (B.1.1.529; BA.1 or BA.1.1) was confirmed by sequencing. Except for one case which occurred before the last week of December 2021, all other cases were observed when the Omicron variant was already predominantly or exclusively detected in healthcare workers and patients at the University Hospital Essen (**Supplementary Figure 1**). Our observations are consistent with the data reported by the Robert Koch Institute for Germany during this period (7). Thus, it is very unlikely, that variants other than Omicron contributed significantly to herein analyzed breakthrough infections. Association of age, body mass index (BMI, kg/m^2) to breakthrough infection were estimated by Mann-Whitney test. *P*-value, odds ratio (OR) and 95% confidence interval (CI) were calculated for association of sex, pre-existing conditions, smoking status, or vaccination scheme to SARS-CoV-2 vaccination breakthrough infection.

2.2 Laboratory and Statistical Methods

2.2.1 SARS-CoV-2 Spike Protein Immunoassay

The determination of anti-spike SARS-CoV-2 antibody concentrations was performed at specific time points (**Supplementary Figure 2**) using SARS-CoV-2 S1 RBD IgG/sCOVG test on Siemens Atellica® IM System (Siemens Healthcare GmbH, Erlangen, Germany) according to the manufacturers' instructions. Results of anti-spike antibody levels were given in binding antibody units per milliliter serum (BAU/ml). The detection limit for positivity was 21.8 BAU/ml.

Distribution of data was assessed by Shapiro-Wilk test prior association analysis. Data were not normally distributed ($P < 0.0001$). Association of anti-spike antibody levels with vaccination breakthrough was estimated by Mann-Whitney test. To determine a threshold above which the risk for a breakthrough infection significantly increases, the frequency distribution of anti-spike antibody levels at the 25% percentile (2816.0 BAU/ml) of all study participants one month after booster vaccination was analyzed and *P*-value by Fisher's exact test as well as OR and 95% CI were calculated. Sensitivity and specificity of the selected cut-off were estimated by ROC analysis (sensitivity = 0.8; specificity = 0.6).

2.2.2 SARS-CoV-2 Nucleocapsid Protein Immunoassay

All samples were also analyzed at the same time points (**Supplementary Figure 2**) for SARS-CoV-2 IgG antibodies

against the nucleocapsid protein on the Architect i2000SR system (CoV-2 IgG, Abbott Diagnostics, IL, USA) to detect participants with previous SARS-CoV-2 infection. An index of ≥ 1.4 specimen calibrator (s/c) was considered as positive for a previous infection.

2.2.3 SARS-CoV-2 Surrogate Neutralization Test (sVNT)

To detect circulating neutralizing antibody against SARS-CoV-2 which block the interaction between wild type (WT)- or Omicron-receptor binding domain (RBD; Accession #P0DTC2) we used a SARS-COV-2 surrogate virus neutralization test (sVNT; GenScript Biotech, Leiden, Netherlands). sVNTs have a high sensitivity and specificity and show a good correlation to conventional plaque reduction neutralization tests (8, 9) and, thus, can be used as a substitute test for cell-based neutralization assays.

All available samples of infected individuals (N = 62) one month after booster vaccination were analyzed and compared with a non-infected cohort (N = 53) matched in age, sex and vaccination scheme. Association of anti-spike antibody titers to breakthrough infection as seen in the complete cohort could be confirmed in this selected cohort (**Supplementary Figure 4**, 3477.0 BAU/ml vs 6935.0 BAU/ml, $P < 0.0001$).

Samples were diluted 1:576 for WT-RBD and 1:9 for Omicron-RBD and then incubated with the horseradish-peroxidase (HRP)-conjugated WT- or Omicron-RBD. The mixture was added to a capture plate coated with human ACE2 receptor protein (hACE2). Circulating neutralization antibodies which bound to the HRP-RBD complexes remained in the supernatant, whereas unbound WT- or Omicron-HRP-RBD were captured on the plate. After washing, 3,3',5,5'-Tetramethylbenzidine (TMB) solution was added to the plate as a substrate for HRP. After the reaction was quenched by adding a stop solution, absorbance at 450 nm was measured on a microplate reader (FLUOstar Omega, BMG Labtech, Ortenberg, Germany). The absorbance of the sample is inversely correlated to the neutralization capacity of the sample. The inhibition rates (%) as an expression of the neutralization capacity for WT- and Omicron-RBD of the sample was calculated against negative control, respectively.

Distribution of data was assessed by Shapiro-Wilk test prior association analysis. Data were not normally distributed ($P < 0.0001$). Association of inhibition rate against Omicron-RBD and breakthrough infection risk was calculated by Mann-Whitney test. To determine a threshold above which the risk for a breakthrough infection significantly increases we analyzed the frequency distribution of inhibition rates at the 25% percentile (65.9%) in the breakthrough infection cohort compared to the matched controls one month after booster vaccination and calculated *P*-value by Fisher's exact test, OR and 95% CI. Combined risk estimation was performed with cases and matched controls of the breakthrough infection cohort. Frequency distributions at the 25% percentiles of antibody titers (2641.0 BAU/ml, sensitivity = 1.0; specificity = 0.7 as estimated by ROC analysis) plus inhibition rates against Omicron-RBD (65.9%, sensitivity = 0.9; specificity = 0.7 as estimated by ROC analysis) were analyzed to determine a threshold above which breakthrough infection risk increases significantly.

3 RESULTS

Between November 29, 2021, and March 5, 2022, 102 (7.3%) participants reported an RT-PCR-confirmed SARS-CoV-2 infection, whereas 1289 (92.7%) participants remained uninfected. On average, breakthrough infections occurred after 52 days (10 - 127) after the booster vaccination. With the exception of a slightly but significantly younger age (37 vs. 41 years, $P = 0.004$) SARS-CoV-2-infected subjects did not differ regarding vaccination scheme, sex, BMI, smoking status, or any other pre-existing conditions from the non-infected subjects (**Supplementary Table 1**).

The source of infection remained elusive for 28 subjects (27.4%). The majority of individuals reported that they had been infected in the familial or domestic environment (53.0%). In 27.0% of these cases, the infection could be traced back to other SARS-CoV-2-positive household members, such as the partner or roommates, and in 26.0% of the cases to a contact with their SARS-CoV-2-positive child. Eleven percent of the participants reported being infected while traveling or sporting activity. Only 8.0% of the subjects self-reported being infected at work.

All infections were described as a mild to moderate ″cold-like″ illness without a need for hospitalization. On average, symptoms lasted for six days (0 - 22 days), with rhinitis (53.9%), sore throat (52.9%), headache or cough (both 45.1%), and fatigue (34.3%) being the most prevalent symptoms. Other symptoms typically associated with COVID-19 such as fever (21.6%), dyspnea (15.7%), dysosmia (9.8%), and dysgeusia (6.9%) were rarely observed. Ten individuals (9.8%) remained asymptomatic.

We stratified our cohort according to the occurrence of an Omicron breakthrough infection, and then applied a look-back assessment to compare pre-infection antibody titers at various time points after vaccination but prior to infection (**Supplementary Figure 2**). Anti-spike antibody titers were indistinguishable between individuals with and without a later Omicron breakthrough infection after the first as well as one and six month after the second vaccination (**Supplementary Figure 3**).

In clear contrast we observed a significant difference in anti-spike antibody levels one month after the booster vaccination between subjects with and without breakthrough infection before they became actually infected (3477.0 BAU/ml vs 4733.0 BAU/ml, $P = 0.02$; **Figure 1A**).

Study participants with an anti-spike antibody level of 2816.0 BAU/ml or less had a 2-fold increased risk for a breakthrough infection compared to individuals with antibody levels exceeding this cut-off (OR: 2.12, 95% CI: 1.24 - 3.58, $P = 0.01$).

Remarkably, inhibition rates against Omicron in the sVNT were also significantly lower in infected individuals prior to infection (77.1% vs 88.5%, $P = 0.002$; **Figure 1B**). Subjects with inhibition rates of 65.9% or less had a 3.6-fold increased risk for a breakthrough infection compared to SARS-CoV-2-negative study participants (OR: 3.61, 95% CI: 1.42 - 9.01, $P = 0.01$).

Subsequently, we combined the inhibition rates obtained in the sVNT together with anti-spike antibody levels of both infected and non-infected individuals (**Figure 1C**) and estimated the risk for breakthrough infections at low anti-spike binding titers and sVNT inhibition rates. Individuals with anti-spike antibody titers of 2641.0 BAU/ml or less plus a sVNT inhibition against Omicron

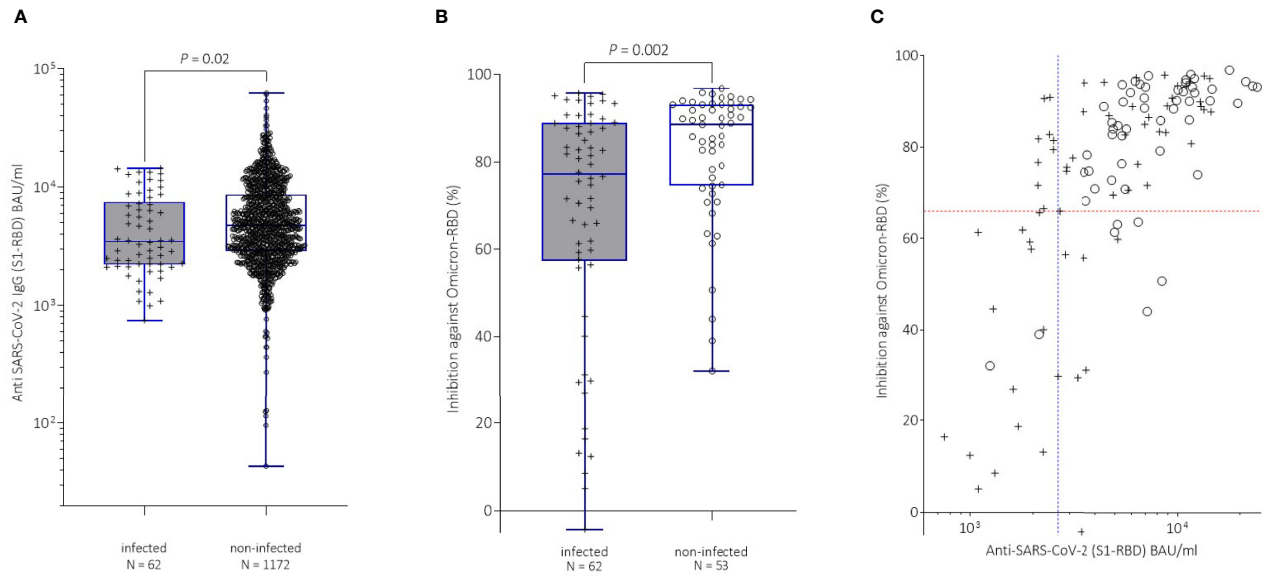

FIGURE 1 | **(A)** Comparison of anti-spike antibody titers in study participants, with (+, grey boxplots) or without (o, white boxplots) breakthrough infection after the third vaccination. Antibody levels were determined one month after the third vaccination (booster). Median values between infected (3477.0 BAU/ml) and non-infected (4733.0 BAU/ml) individuals differed significantly (Mann-Whitney test; $P = 0.02$). **(B)** Comparison of neutralization capacity as measured by inhibition (%) against Omicron in the study participants with breakthrough infection (+, grey boxplots) with matched non-infected controls (o, white boxplots) after booster vaccination. Median inhibition rates between infected (77.1 %) and non-infected (88.5%) individuals differed significantly (Mann-Whitney test; $P = 0.002$). **(C)** Comparison of anti-spike antibody levels (BAU/ml) with inhibition rates (%) against Omicron-RBD in breakthrough infection cohort (+) and matched non-infected controls (o) by. The red dashed line indicates the 25% percentile (65.9 %) of inhibition rate. The blue dashed line denotes the 25%percentile (2641.0 BAU/ml) of anti-spike antibody level.

of 65.9% or less showed a 10-fold increased risk for breakthrough infection compared with individuals with titers above these thresholds (OR: 10.4, 95% CI: 2.36 - 47.55).

4 DISCUSSION

To the best of our knowledge, this is the first comprehensive study reporting lower antibody levels and a diminished neutralization capacity in individuals prior to a SARS-CoV-2 breakthrough infection with the Omicron variant compared to non-infected individuals based on a cohort of uniformly boostered vaccinees. Our data suggest that routine anti-SARS-CoV-2 IgG antibody determinations in combination with sVNT can identify subjects who are at a higher risk for a breakthrough infection.

Although a weaker immune response upon COVID-19 vaccination has been described for particular groups, like elderly or immune-compromised individuals (10–13), we observed differences in immune response independent from these factors. Genetic variations might explain some of the differences in the strength of innate immune response (14).

Higher humoral immune responses as determined by antispike-antibody determinations and sVNT tests have been reported for boostered vaccinees by several studies (15–20). Additionally, a higher immune response in boostered vaccinees compared to individuals, who only have been vaccinated twice, against the Omicron variant, which nevertheless is weaker than against the wild type virus, has been reported as well (21, 22). However, no thresholds for a higher probability of SARS-CoV-2 breakthrough infection have been established based on other comprehensive longitudinal studies so far.

Up to now, testing of anti-SARS-CoV-2 antibodies or neutralization capacity is not routinely performed after vaccination and, thus, “non”- or “low”-responders who might require a re-vaccination remain unidentified. Otherwise, the interval to re-vaccination in individuals with “high” response might be extended. Therefore, further studies are urgently needed to set a threshold for “non”, “low” and high” vaccination response to better plan vaccination strategies.

DATA AVAILABILITY STATEMENT

The original contributions presented in the study are included in the article/**Supplementary Material**. Further inquiries can be directed to the corresponding author.

ETHICS STATEMENT

The studies involving human participants were reviewed and approved by Ethics Committee of the Medical Faculty of the

University of Duisburg-Essen (21-10005-BO). The patients/participants provided their written informed consent to participate in this study.

AUTHOR CONTRIBUTIONS

BM, WS, and K-HJ conceptualized and designed the study. BM obtained ethics approval. BM and IC obtained informed consent, demographic data, and samples from the participants, organized logistics and performed laboratory analyses. Additionally, CE, OA, MT, BW, and DZ performed laboratory investigations. BM performed statistical analyses. BM, UD, and WS drafted and wrote the manuscript which was reviewed by all authors. All authors had full access to the data and approved submission of this article. BM and WS had the final responsibility to submit for publication.

FUNDING

This work was supported by the Ministry of Culture and Science of North Rhine-Westphalia; VIRus Alliance NRW). The funder of the study had no role in study design, data collection, data analysis, data interpretation, writing of the report, or in decision of submitting the paper for publication. We acknowledge support by the Open Access Publication Fund of the University of Duisburg-Essen.

ACKNOWLEDGMENTS

We gratefully acknowledge the participants of the study. We kindly thank Iris Manthey, Grit Müller and Stephanie Büscher for technical support (Institute of Pharmacogenetics). We thank Dr. Lothar Volbracht and Dr. Marc Wichert for their support with the samples analyzed at the central laboratory (University Hospital Essen) and Dr. Frank Mosel (Department of Clinical Microbiology) for his support with coordination of the study.

SUPPLEMENTARY MATERIAL

The Supplementary Material for this article can be found online at: https://www.frontiersin.org/articles/10.3389/fimmu.2022.907343/full#supplementary-material

REFERENCES

1. World Health Organization. *Classification of Omicron (B.1.1.529): SARS-CoV-2 Variant of Concern* (2021). Available at: https://www.who.int/news/item/26-11-2021-classification-of-omicron-(b.1.1.529)-sars-cov-2-variant-of-concern.
2. Planas D, Saunders N, Maes P, Guivel-Benhassine F, Planchais C, Buchrieser J, et al. Considerable Escape of SARS-CoV-2 Omicron to Antibody Neutralization. *Nature* (2021) 602(7898). doi: 10.1038/s41586-021-04389-z
3. Pajon R, Doria-Rose NA, Shen X, Schmidt SD, O'Dell S, McDanal C, et al. SARS-CoV-2 Omicron Variant Neutralization After mRNA-1273 Booster Vaccination. *N Engl J Med* (2022) 386(11):1088–1091. doi: 10.1056/NEJMc2119912
4. Andrews N, Stowe J, Kirsebom F, Toffa S, Rickeard T, Gallagher E, et al. Covid-19 Vaccine Effectiveness Against the Omicron (B.1.1.529) Variant. *N Engl J Med* (2022) 386(16):1532–1546. doi: 10.1056/NEJMoa2119451
5. Abu-Raddad LJ, Chemaitelly H, Ayoub HH, AlMukdad S, Yassine HM, Al-Khatib HA, et al. Effect of mRNA Vaccine Boosters Against SARS-CoV-2 Omicron Infection in Qatar. *N Engl J Med* (2022) 386(19):1804–1816. doi: 10.1056/NEJMoa2200797
6. Dimeglio C, Migueres M, Mansuy J-M, Saivin S, Miedougé M, Chapuy-Regaud S, et al. Antibody Titers and Breakthrough Infections With Omicron SARS-CoV-2. *J Infect* (2022) 84(4):e13–e15. doi: 10.1016/j.jinf.2022.01.044
7. Robert Koch Institute. *Weekly Reports on COVID-19* . Available at: https://www.rki.de/EN/Content/infections/epidemiology/outbreaks/COVID-19/COVID19.html.
8. Tan CW, Chia WN, Qin X, Liu P, Chen MI-C, Tiu C, et al. A SARS-CoV-2 Surrogate Virus Neutralization Test Based on Antibody-Mediated Blockage of ACE2-Spike Protein-Protein Interaction. *Nat Biotechnol* (2020) 38:1073–8. doi: 10.1038/s41587-020-0631-z
9. Ramos A, Cardoso MJ, Ribeiro L, Guimarães JT. Assessing SARS-CoV-2 Neutralizing Antibodies After BNT162b2 Vaccination and Their Correlation With SARS-CoV-2 IgG Anti-S1, Anti-RBD and Anti-S2 Serological Titers. *Diagnostics (Basel)* (2022) 12(1):205. doi: 10.3390/diagnostics12010205
10. Collier DA, Ferreira IA, Kotagiri P, Datir RP, Lim EY, Touizer E, et al. Age-Related Immune Response Heterogeneity to SARS-CoV-2 Vaccine BNT162b2. *Nature* (2021) 596:417–22. doi: 10.1038/s41586-021-03739-1
11. Müller L, Andrée M, Moskorz W, Drexler I, Walotka L, Grothmann R, et al. Age-Dependent Immune Response to the Biontech/Pfizer BNT162b2 Coronavirus Disease 2019 Vaccination. *Clin Infect Dis* (2021) 73:2065–72. doi: 10.1093/cid/ciab381
12. Korth J, Jahn M, Dorsch O, Anastasiou OE, Sorge-Hädicke B, Eisenberger U, et al. Impaired Humoral Response in Renal Transplant Recipients to SARS-CoV-2 Vaccination With BNT162b2 (Pfizer-BioNTech). *Viruses* (2021) 13 (5):756. doi: 10.3390/v13050756
13. Willuweit K, Frey A, Passenberg M, Korth J, Saka N, Anastasiou OE, et al. Patients With Liver Cirrhosis Show High Immunogenicity Upon COVID-19 Vaccination But Develop Premature Deterioration of Antibody Titers. *Vaccines (Basel)* (2022) 10(3):377. doi: 10.3390/vaccines10030377
14. Kimman TG, Vandebriel RJ, Hoebee B. Genetic Variation in the Response to Vaccination. *Community Genet* (2007) 10:201–17. doi: 10.1159/000106559
15. Wanlapakorn N, Suntronwong N, Phowatthanasathian H, Yorsaeng R, Thongmee T, Vichaiwattana P, et al. Immunogenicity of Heterologous Inactivated and Adenoviral-Vectored COVID-19 Vaccine: Real-World Data. *Vaccine* (2022) 40:3203–9. doi: 10.1016/j.vaccine.2022.04.043
16. Yorsaeng R, Suntronwong N, Phowatthanasathian H, Assawakosri S, Kanokudom S, Thongmee T, et al. Immunogenicity of a Third Dose Viral-Vectored COVID-19 Vaccine After Receiving Two-Dose Inactivated Vaccines in Healthy Adults. *Vaccine* (2022) 40:524–30. doi: 10.1016/j.vaccine.2021.11.083
17. Benning L, Morath C, Bartenschlager M, Kim H, Reineke M, Beimler J, et al. Neutralizing Antibody Response Against the B.1.617.2 (Delta) and the B.1.1.529 (Omicron) Variants After a Third mRNA SARS-CoV-2 Vaccine Dose in Kidney Transplant Recipients. *Am J Transplant* (2022). doi: 10.1111/ajt.17054
18. Belik M, Jalkanen P, Lundberg R, Reinholm A, Laine L, Väisänen E, et al. Comparative Analysis of COVID-19 Vaccine Responses and Third Booster Dose-Induced Neutralizing Antibodies Against Delta and Omicron Variants. *Nat Commun* (2022) 13:2476. doi: 10.1038/s41467-022-30162-5
19. Poh XY, Tan CW, Lee IR, Chavatte J-M, Fong S-W, Prince T, et al. Antibody Response of Heterologous vs Homologous mRNA Vaccine Boosters Against the SARS-CoV-2 Omicron Variant: Interim Results From the PRIBIVAC Study, A Randomized Clinical Trial. *Clin Infect Dis* (2022). doi: 10.1093/cid/ciac345

20. Zuo F, Abolhassani H, Du L, Piralla A, Bertoglio F, de Campos-Mata L, et al. Heterologous Immunization With Inactivated Vaccine Followed by mRNA-Booster Elicits Strong Immunity Against SARS-CoV-2 Omicron Variant. *Nat Commun* (2022) 13:2670. doi: 10.1038/s41467-022-30340-5
21. Furukawa K, Tjan LH, Kurahashi Y, Sutandhio S, Nishimura M, Arii J, et al. Assessment of Neutralizing Antibody Response Against SARS-CoV-2 Variants After 2 to 3 Doses of the BNT162b2 mRNA COVID-19 Vaccine. *JAMA Netw Open* (2022) 5:e2210780. doi: 10.1001/jamanetworkopen.2022.10780
22. Du Y, Chen L, Shi Y. Booster COVID-19 Vaccination Against the SARS-CoV-2 Omicron Variant: A Systematic Review. *Hum Vaccin Immunother* (2022), 1–19. doi: 10.1080/21645515.2022.2062983

Conflict of Interest: The authors declare that the research was conducted in the absence of any commercial or financial relationships that could be construed as a potential conflict of interest.

frontiers | Frontiers in Immunology

CASE REPORT
published: 23 June 2022
doi: 10.3389/fimmu.2022.875637

Misdiagnosis of Reactive Lymphadenopathy Remotely After COVID-19 Vaccination: A Case Report and Literature Review

Qian Yu[1†], *Wei Jiang*[2†], *Ni Chen*[1], *Jia Li*[3], *Xiaohui Wang*[4], *Maoping Li*[1], *Dong Wang*[1] *and Lan Jiang*[1*]

[1] Department of Ultrasound, First Affiliated Hospital of Chongqing Medical University, Chongqing, China, [2] Department of Orthopaedics, First Affiliated Hospital of Chongqing Medical University, Chongqing, China, [3] Department of Radiology, The First Affiliated Hospital, Chongqing Medical University, Chongqing, China, [4] Department of Respiratory and Critical Care Medicine, First Affiliated Hospital of Chongqing Medical University, Chongqing, China

OPEN ACCESS

Edited by:
Nitin Saksena,
Victoria University, Australia

Reviewed by:
Vivek Gupta,
Government Institute of Medical Sci, India
Alexander Roesch,
Essen University Hospital, Germany

***Correspondence:**
Lan Jiang
helene_jiang@sohu.com

[†]These authors have contributed equally to this work

Specialty section:
This article was submitted to Vaccines and Molecular Therapeutics, a section of the journal Frontiers in Immunology

Received: 14 February 2022
Accepted: 20 May 2022
Published: 23 June 2022

Citation:
Yu Q, Jiang W, Chen N, Li J, Wang X, Li M, Wang D and Jiang L (2022) Misdiagnosis of Reactive Lymphadenopathy Remotely After COVID-19 Vaccination: A Case Report and Literature Review. Front. Immunol. 13:875637. doi: 10.3389/fimmu.2022.875637

Keywords: COVID-19, vaccine, lymphadenopathy, axillary lymph nodes, ultrasonography, contrast-enhanced ultrasonography, side effect

INTRODUCTION

Globally, large-scale COVID-19 vaccination programs are in progress to control the severe acute respiratory syndrome coronavirus 2 (SARS-CoV-2) pandemic (1). As of February 10, 2022, 10.3 billion doses of the vaccines have been administered globally (2). Reactive hyperplasia of the ipsilateral axillary lymph nodes is a side effect of vaccination (3), which has been reported in 0.3% of the participants in the clinical trial of Pfizer (4, 5). Additionally, it has been reported to be rare in the trials of Moderna, Novavax, Sinovac, Johnson & Johnson, and AstraZeneca vaccines (6–10). In reality, the rate is likely to be higher. The Centers for Disease Control and Prevention of the United States (CDC) have reported 11.6 and 16.0% of axillary swelling or tenderness after receiving the first and second doses of Moderna, respectively (11). The frequency of imaging-detected lymphadenopathy ranged between 14.5 and 53% (12). This side effect is a frequent finding after COVID-19 vaccination.

Herein we present a misdiagnosed case of remote lymphadenopathy after receiving the CoronaVac vaccine from Sinovac. We highlight its prolonged course, discuss the clinical findings and imaging features, and analyze our misdiagnosis in combination with a relevant literature review.

CASE DESCRIPTION

A 34-year-old woman presented with left axillary pain for a week and transient fever (38.6°C) for a day. She denied a medical history of allergic disease, tuberculosis, past malignant tumors, recent infection, trauma, specific medication history, and travel or social history. She received the first and second doses of CoronaVac 5 and 4 months ago, respectively, with both doses delivered to the left deltoid muscle. The possibility of side effects was neglected, as the detection exceeded the expected time interval for an adverse reaction to the vaccine. Physical examination revealed left axillary

swelling and tenderness with no localized skin or soft tissue lesions, particularly on the head, neck, chest, or left arm.

Ultrasonography (US) revealed multiple abnormal left axillary lymph nodes with "alarming" signs (**Figures 1A**, **2A–C**). The relevant diagnostic workup revealed the following: complete blood count (CBC) demonstrated a slight decrease in eosinophils (0.01×10^9/L), the computed tomography (CT) of the head, neck, and chest was normal, and the US of the thyroid, breast, and lymph nodes in other parts of the body and abdomen was also normal (**Figure 2E**). Contrast-enhanced ultrasonography (CEUS) using SonoVue (sulfur hexafluoride microbubbles, Bracco, Netherlands) revealed an internal hypoperfusion area (**Figure 1α**). The sign was misinterpreted as an alarming "necrotic" change and "evidence" of tuberculosis. A US-guided fine-needle aspiration (**Figure 2D**) of one abnormal lymph node (different to the largest one) was performed to confirm the diagnosis; however, the Xpert MTB/RIF assay was negative for the tuberculous gene, the cell smear demonstrated neutrophils and lymphocytes, and the T-cell spot (T-SPOT TB) test and purified protein derivative test were also negative. Thus, tuberculosis and malignancy were excluded, lymphadenopathy was inferred to be bacterial, and treatment with cefaclor (750 mg per os, twice daily for 7 days) was given. The puncture site was fully recovered, but the abnormal lymph nodes never demonstrate a remission.

At 1 week later, the patient presented with transient febrile (40.5°C) again. The US features of the abnormal lymph nodes remained nearly the same, whereas CEUS revealed a noticeable reduction in the hypoperfusion area (**Figures 1B, β**). The laboratory investigations revealed the following parameters: CBC demonstrated decreases in white cell count (3.13×10^9/L), lymphocyte count (0.59×10^9/L), hemoglobin (113 g/L), and hematocrit value (33.8%); the peripheral smear showed normal erythrocyte and leucocyte morphology; the coagulation function showed an increase in D-dimer concentration (1.55 mg/L), fibrinogen (3.92 g/L), and prothrombin time (14.6 s); the liver function test showed an increase in lactic dehydrogenase (762 U/L); the inflammatory biomarkers of procalcitonin (PCT, 0.13 ng/ml), serum ferritin (SF, 354.5 ng/ml), and erythrocyte sedimentation rate (ESR, 69 mm/h) were increased, whereas C-reactive protein and the rheumatoid factors were normal. Immunological tests exhibited negative values for specific infections, including serum IgM antibody titers against influenza virus A/B, parainfluenza virus, respiratory syncytial virus, Epstein–Barr virus, adenovirus, legionella pneumophila, *Mycoplasma pneumoniae*, *Chlamydia pneumoniae*, *Rickettsia*, IgG against hepatitis virus C, syphilis, and HIV antibodies. The quantifications of serum hepatitis B surface antigen (0.00 IU/ml), blood cytomegalovirus DNA ($<1.0 \times 10^3$), blood Epstein–Barr virus DNA ($<1.0 \times 10^3$), and serum fungus (1, 3)-β-D glucan (<10 pg/ml) were negative. The aerobic and anaerobic blood cultures were negative for pathogens. The nasopharyngeal swab for the SARS-CoV-2 nucleic acid PCR test was negative for the *ORFlab*

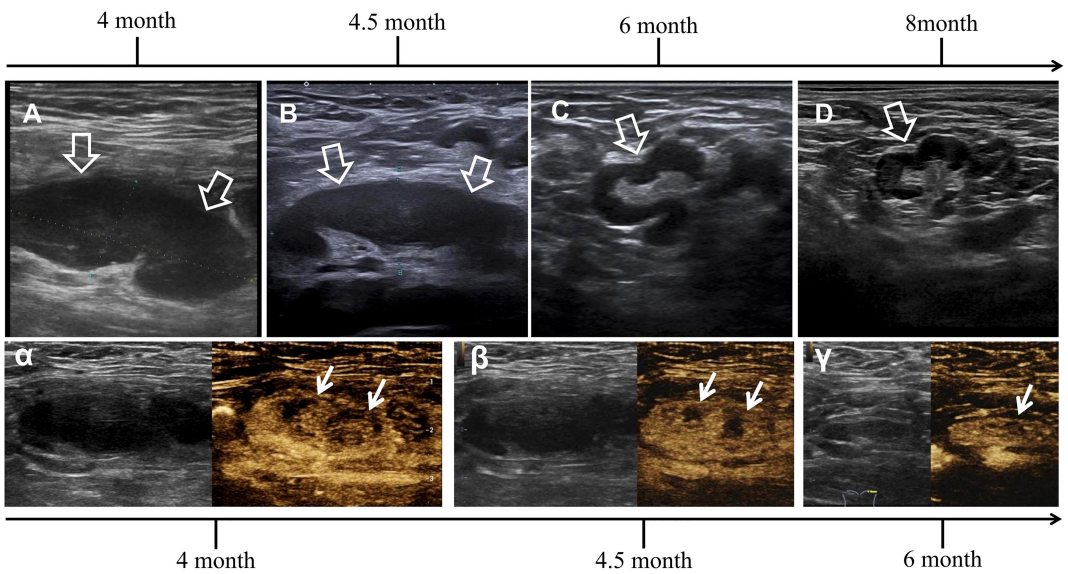

FIGURE 1 | Successive ultrasonography (US) and contrast-enhanced ultrasonography (CEUS) images of the same largest lymph node, with dynamic changes during progression and regression. **(A)** The initial US showed the lymph node was in deep position, flat oval in shape, 40 mm on the long axis and 15 mm on the short axis, with a long/short ratio of >2. The lymphatic cortex was notably thickened to 12 mm and presented as a homogeneous hypoechoic area with a visible lymphatic hilum. **(B)** The second US showed indistinctive decrease in cortical thickness and the same lymph node size from the previous examination. **(C)** The third US in the follow-up showed a distinctive decrease in lymph node size and cortical thickness having irregular shape. **(D)** The last US showed normalized lymph node (indicated by hollow arrows). **(α)** The initial diagnosis of CEUS was based on centripetal perfusion enhancement in the asynchronous type, with a notable area in the deviated center showing hypoperfusion, covering half of the area of the lymph node. **(β)** The second CEUS showed distinctive decrease in hypoperfusion area. **(γ)** The third CEUS in the follow-up showed normalized enhancement and near invisibility of the hypoperfusion area (indicated by arrows).

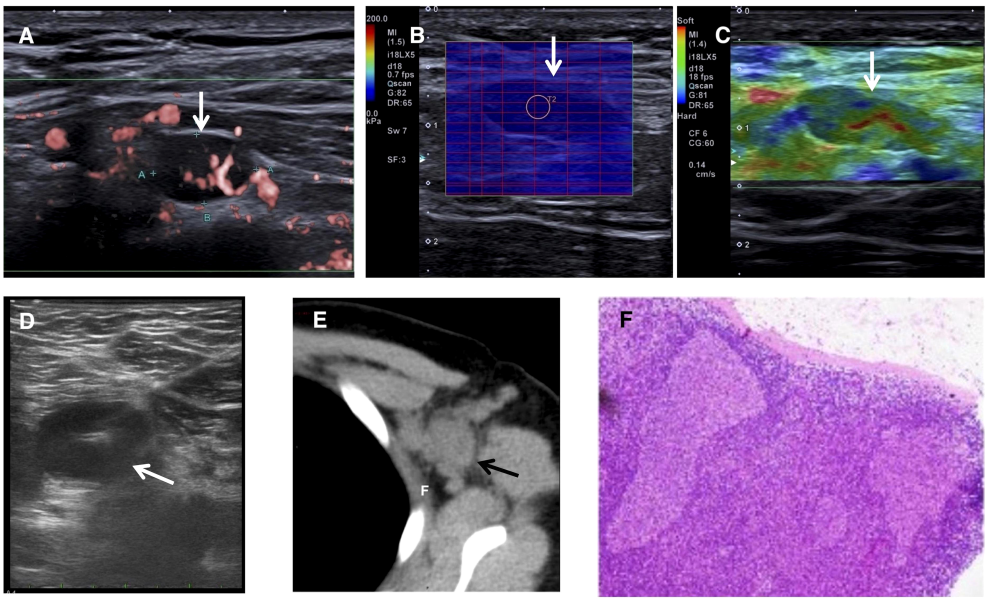

FIGURE 2 | **(A–E)** Images of multiple abnormal lymph nodes (indicated by arrows) at 4 months after vaccination. **(A)** One small abnormal lymph node in the nearly spherical shape, with a long/short ratio of <2, the notably thickened lymphatic cortex with an invisible lymphatic hilum, yet superb microvascular imaging confirmed the blood distribution of hilar type. **(B, C)** Elastography of one of the same abnormal lymph nodes. **(B)** Shear wave elastography demonstrated a modulus of 9.7 kPa. **(C)** Real-time tissue elastography demonstrated the hardness ranging from 'median' to 'soft'. **(D)** US-guided fine-needle aspiration of one superficial lymph node. **(E)** Computed tomography demonstrated the left axillary lymphadenopathy. **(F)** Hematoxylin and eosin staining under 100x magnification showed reactive hyperplasia.

and *N* genes. The suspicion of infected lymphadenitis was essentially excluded, and the only remaining concern was histiocytic necrotizing lymphadenitis.

The patient was anxious due to the prolonged diagnostic course and requested a histopathological examination. Macroscopically, the resected abnormal lymph node was soft and yellow-grayish; the microscopy revealed nonspecific reactive hyperplasia (**Figure 2F**), and the immunohistochemistry was negative for tumors. All possible concerns were ruled out except for the idea that vaccination history was reconsidered as the cause. All medical interventions were suspended. In the follow-up at 6 months after vaccination, US demonstrated a notable decrease in the size and cortical thickness of the largest lymph node; the previous hypoperfusion area shown on CEUS was hardly visible (**Figures 1C, γ**). Her laboratory tests of CBC and inflammatory markers were normal. The US indicated complete resolution on the second follow-up at 8 months after vaccination (**Figure 1D**). The lymphadenopathy was finally attributed to COVID-19 vaccine side effects based on clinical, laboratory, imaging, and histopathological findings, and this was confirmed in the prognosis. The timeline of diagnosis, interventions, and prognosis for this case is shown in **Figure 3**.

DISCUSSION

Duration

A prolonged course most characterized the presented case of remote reactive lymphadenopathy after COVID-19 vaccination. The symptoms and signs were noticed 4 months after receiving the second dose of CoronaVac, after which the patient improved in 6 months and recovered in 8 months. To our knowledge, no cases of such a remote nature have been previously reported.

In CDC reports, lymphadenopathy occurred within 2 to 4 days after vaccination with Moderna and lasted for 1 to 2 days (11), and the duration in radiologic observational reports was longer (between 4 days and 10 weeks) (12–18). However, most of these cases were retrospective studies in the patients who recently received the COVID-19 vaccine and underwent positron emission tomography (PET). Therefore, there could be selection bias, short observational periods, and lack of reports involving other imaging modalities. This case may be an exception due to individual differences. Nonetheless, the existence of such a prolonged course challenged the current perception about the duration of this side effect.

Guidelines

Based on the abovementioned observations, current guidelines emphasize the timing for imaging after COVID-19 vaccination. A multidisciplinary expert panel recommended the postponement of imaging for at least 6 weeks after completion of the vaccination (19). The Breast Imaging Society also recommended a scheduling exam conducted at 4–6 weeks following the second dose for screening and a short-term follow-up examination at 4–12 weeks for ipsilateral axillary adenopathy patients who received the COVID-19 vaccine within 4 weeks (20). The recommended timing is practical; however, it cannot encompass exceptional situations, and a

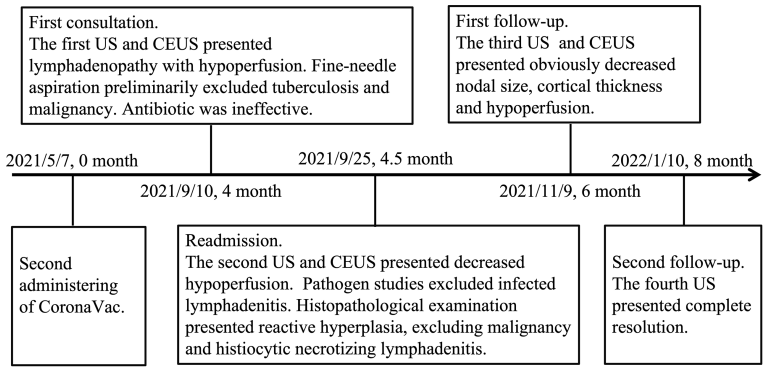

FIGURE 3 | Timeline of diagnosis, interventions, and prognosis. US, ultrasonography; CEUS, contrast-enhanced ultrasonography.

cautious approach is needed when facing lymphadenopathy potentially related to vaccines, even in unexpected situations.

Analysis of Misdiagnosis

This lymphadenopathy case was particularly unusual because the detection occurred outside of the expected time interval with the presence of other clinical findings, of which we were not aware. In hindsight, most of the diagnostic interventions were unnecessary, which resulted in physical and psychological burdens on the patient. Additionally, the misinterpretation of hypoperfusion on CEUS as "perfusion defect" supported the misdiagnosis, as it often suggests "necrosis" of tuberculous or malignant lymphadenopathy (21). Therefore, we must emphasize the importance of rational and subtle image interpretations to avoid both over- and underdiagnosis.

A limitation of this case was the lack of evidence of nucleic acid elements or SARS-CoV-2 antigen on PCR, western blot, or immunohistochemistry tests, which was mainly due to the misdiagnosis that resulted in all of the chosen tests being conducted to verify inflammation or tumors. We propose that biopsy of needle aspiration for PCR or western blot testing would be practical for future diagnostic quandaries that need genetic verification. Additionally, activated lymphocytes should also be examined as an important indicator.

Imaging Modalities

An accurate diagnosis of lymphadenopathy after vaccination is important. In this case report, we discussed the diagnostic perplexity in an individual without combined medical conditions, whereas reports have also focused on cancer patients (12, 13, 15, 22). A modeling study suggested a large proportion of missed cancer diagnoses due to the pandemic (23). Therefore, subtle imaging interpretation is crucial in patient management.

Concerning imaging-detected reactive lymphadenopathy after COVID-19 vaccination, the majority of cases were identified on PET scans, mainly during cancer surveillance. This condition normally involved transient 18-fluorine-fluorodeoxyglucose (^{18}F-FDG) uptake in ipsilateral lymph nodes, ranging from intense to gradually regressed after administration (13, 19, 22, 24–26). However, the maximal standardized uptake value (SUVmax) should not be solely used to differentiate between benign and malignant lymph nodes (14). There were attempts to improve the diagnostic rate by comparing the SUVmax of the ipsilateral lymph nodes to the contralateral lymph nodes (27) as well as the increased uptake in the deltoid muscle (28, 29) or using different tracers (30). PET is the most sensitive imaging modality for differentiating lymphadenopathy, whereas the radioactive nature and high cost are limitations.

Few of the cases were detected *via* magnetic resonance imaging (MRI) (31, 32), CT (15), and mammography (33). These techniques are common diagnostic workups that provide relevant information, especially in the case of breast or lung cancers which often involve axillary lymph node metastasis. They provide good overall observations but relatively few morphological details of abnormal lymph nodes compared to the US (34). Additionally, they cannot provide metabolic features compared to PET (35).

Role of US

The US has a high diagnostic value in the screening, evaluation, and follow-up of lymphadenopathy (36); it presents high-resolution images of superficial lymph nodes with subtle morphological details that CT or MRI may not have been able to assess (37). We reviewed the full-text accessible literature on US-detected reactive lymphadenopathy after COVID-19 vaccination with a complete vaccination history and explicit image description. The US findings are shown in **Table 1** (34, 38–46). In general, the size, shape, cortex-hilum structure, vascularity patterns, and stiffness of lymph node were essential signs to consider. Rational judgments should be made based on the combined information. It should be noted that there were "alarming" signs mentioned, such as spherical shape, thickened lymphatic cortex, hilum absence, and peripheral vascularity, which have often been observed in malignant or specifically infected lymph nodes (37).

In this case, the patient underwent 4 successive US examinations that demonstrated dynamic changes during progression and regression. Initially, the US showed increases

TABLE 1 | Ultrasonographic features of 10 published articles on COVID-19 vaccine-related lymphadenopathy (only full-text accessible articles between January 1 and December, 2021 with complete vaccination history and US image description were included).

First author	Interval between US and vaccine	Sum of cases (*N*)	Subclinical ratio	Sum of abnormal lymph nodes in cases (*N*)		Maximum length of LAD (mm)	Maximum thickness of cortex (mm)	Nearly sphere or L/S ratio <2 (*N*)	Hilum		Vascularity patterns			Outcome
				n > 3	*n* < 3				Present (*N*)	Absent (*N*)	Hilar (*N*)	Peripheral (N)	Mixed (*N*)	
Washington (38)	12 days	1	–	1	–	31	NA	NA	1	–	NA	NA	NA	Resolved
Granta (39)	1 to 2 days	18	50%	7	11	16	NA	*n* = 12	*n* = 51	*n* = 4	NA	NA	NA	NA
D'Auria (34)	2–8 days	6	1%	6	–	26	6	3	3	3	5	1	–	Reduced
Faermann (40)	1–38 days	125	98%	NA	NA	48	15	NA	NA	NA	NA	NA	NA	Reduced
Mehta (41)	5–13 days	4	100%	2	1	27	7	NA	4	–	3	–	1	NA
Cocco (42)	1–16 days	24	46%	4	20	28	NA	6	16	8	10	1	13	Resolved
Placke (43)	<6 weeks	8	100%	8	–	16	NA	1	2	–	–	–	8	PA
Cristina (44)	1–7 days	91	NA	91	–	Mean: 24	Mean: 4.6	NA	91	–	NA	NA	NA	Resolved
Igual-Rouilleault (45)	20–38 days	10	NA	NA	NA	Thickness: 23	NA	NA	10	–	NA	NA	NA	Resolved: 5 PA: 5
Tsumura (46)	3 weeks	1	100%	NA	NA	35	NA	NA	1	–	–	1	–	NA

N, number of cases; n, number of abnormal lymph nodes; mm, millimeter; L/S, long/short ratio; NA, not available; PA, pathologically verified; -, none.

in the number and size of abnormal lymph nodes, with notably thickened lymphatic cortex (**Figures 1A**, **2A–C**). Regarding the progression of the largest lymph node, the second US showed an indistinctive decrease in cortical thickness, whereas the nodal size remained almost the same. Both size and cortical thickness markedly decreased and eventually resolved at the follow-up examination (**Figures 1A–D**). Based on these trends, we supposed that the thickened cortex might be related to nodal hyperplasia, and it began to subside in the early stage of nodal regression. The decrease in cortical thickness in the US may be an early imaging sign of improvement that should be considered.

CEUS Findings

To our knowledge, this case was the first to report the CEUS findings of reactive lymphadenopathy after COVID-19 vaccination. The patient underwent 3 successive CEUS scans that also demonstrated dynamic changes. Initially, CEUS demonstrated hypoperfusion in the deviated center of the largest lymph node. It was markedly narrowed in the second CEUS and became nearly invisible in the third exam (**Figures 1α–γ**). In hindsight, we noted that the initial hypoperfusion area overlapped with the most thickened cortex; moreover, it regressed even earlier than the cortex attenuation. A decrease of hypoperfusion may be an even earlier sign of improvement. We speculated that the COVID-19 vaccine might stimulate immune cells in the nodal cortex, which leads to excessive pressure on tissue microcirculation. The insufficiency of perfusion was represented as filling insufficiency on CEUS. However, this was merely a conjecture regarding pathogenesis without the support of systematic research, and further work is required to elucidate this mechanism.

Concomitant Manifestations

In this case, accompanying manifestations interfered with the diagnosis, including transient fever, decreased white cell and lymphocyte counts, increased inflammatory markers (ESR, PCT, and SF), and abnormal coagulation function. A previous study reported a decrease in lymphocytes after COVID-19 vaccination (26), and elevated PCT and CRP were independent risk factors for death in patients with COVID-19 (47). As all tests for specific infections were negative, and the patient fully recovered without medical intervention, we retrospectively supposed that these manifestations were also vaccine reactions. However, local and systemic inflammatory reactions after COVID-19 vaccination should be transient, and further studies are needed to describe remote reactions after COVID-19 vaccination. Additionally, the patient presented with mild anemia in the second CBC, possibly due to malnutrition because of anxiety.

Vaccine Type

Concerning the type of COVID-19 vaccine that causes reactive lymphadenopathy, there have been more than 2,000 reported cases after mRNA vaccines and 14 reported cases after adenoviral vectored vaccines (12, 22), yet there have been no specific case reports related to protein subunit vaccines. In theory, regardless of the type, all COVID-19 vaccines might cause reactive lymphadenopathy, and this case can serve as a supplement to observational side effect studies.

CONCLUSION

Radiologists and clinicians should recognize that reactive lymphadenopathy has become frequently observed in association with the general administration of COVID-19 vaccines. It should be considered a frequent and important differential diagnosis. Rational judgment should be made in the context of vaccination information and subtle imaging interpretations. Herein we propose the existence of a prolonged course of this side effect, the value of US as a diagnostic workup and evaluation, and the first introduction of CEUS through the presented case.

DATA AVAILABILITY STATEMENT

The original contributions presented in the study are included in the article/supplementary material. Further inquiries can be directed to the corresponding author.

ETHICS STATEMENT

Written informed consent was obtained from the individual for the publication of any potentially identifiable images or data included in this article.

AUTHOR CONTRIBUTIONS

QY and JL were major contributors in preparation of the manuscript. LJ interpreted the patient data and drafted the paper. QY did the literature review. WJ drafted the paper. NC and ML performed the US and CEUS. JL, XW, and DW interpreted the patient data. All authors contributed to the article and approved the submitted version.

ACKNOWLEDGMENTS

We appreciate all supports from the patient.

REFERENCES

1. Duman N, ALzaidi Z, Aynekin B, Taskin D, Demirors B, Yildirim A, et al. COVID-19 Vaccine Candidates and Vaccine Development Platforms Available Worldwide. *J Pharm Anal* (2021) 11(6):675–82. doi: 10.1016/j.jpha.2021.09.004
2. *Our World in Data*. Available at: https://ourworldindata.org/covid-vaccinations (Accessed Feb 10, 2021).

3. Fishbein DB, Baer GM. Animal Rabies: Implications for Diagnosis and Human Treatment. *Ann Intern Med* (1988) 109(12):935–7. doi: 10.7326/0003-4819-109-12-935
4. Wang X. Safety and Efficacy of the BNT162b2 mRNA Covid-19 Vaccine. *N Engl J Med* (2021) 384(16):1577–8. doi: 10.1056/NEJMc2036242
5. Polack FP, Thomas SJ, Kitchin N, Absalon J, Gurtman A, Lockhart S, et al. Safety and Efficacy of the BNT162b2 mRNA Covid-19 Vaccine. *N Engl J Med* (2020) 383(27):2603–15. doi: 10.1056/NEJMoa2034577
6. El Sahly HM, Baden LR, Essink B, Doblecki-Lewis S, Martin JM, Anderson EJ, et al. Efficacy of the mRNA-1273 SARS-CoV-2 Vaccine at Completion of Blinded Phase. *N Engl J Med* (2021) 385(19):1774–85. doi: 10.1056/NEJMoa2113017
7. Zeng G, Wu Q, Pan H, Li M, Yang J, Wang L, et al. Immunogenicity and Safety of a Third Dose of CoronaVac, and Immune Persistence of a Two-Dose Schedule, in Healthy Adults: Interim Results From Two Single-Centre, Double-Blind, Randomised, Placebo-Controlled Phase 2 Clinical Trials. *Lancet Infect Dis* (2022) 22(4):483–95. doi: 10.1016/S1473-3099(21)00681-2
8. Sadoff J, Le Gars M, Shukarev G, Heerwegh D, Truyers C, de Groot AM, et al. Interim Results of a Phase 1-2a Trial of Ad26.COV2.S Covid-19 Vaccine. *N Engl J Med* (2021) 384(19):1824–35. doi: 10.1056/NEJMoa2034201
9. Falsey AR, Sobieszczyk ME, Hirsch I, Sproule S, Robb ML, Corey L, et al. Phase 3 Safety and Efficacy of AZD1222 (ChAdOx1 Ncov-19) Covid-19 Vaccine. *N Engl J Med* (2021) 385(25):2348–60. doi: 10.1056/NEJMoa2105290
10. Heath PT, Galiza EP, Baxter DN, Boffito M, Browne D, Burns F, et al. Safety and Efficacy of NVX-CoV2373 Covid-19 Vaccine. *N Engl J Med* (2021) 385 (13):1172–83.
11. *Centers for Disease Control and Prevention* . Available at: https://www.cdc.gov/vaccines/covid-19/info-by-product/moderna/reactogenicity.html (Accessed Feb 10, 2021).
12. Garreffa E, Hamad A, O'Sullivan CC, Hazim AZ, York J, Puri S, et al. Regional Lymphadenopathy Following COVID-19 Vaccination: Literature Review and Considerations for Patient Management in Breast Cancer Care. *Eur J Cancer* (2021) 159:38–51. doi: 10.1016/j.ejca.2021.09.033
13. Özütemiz C, Krystosek LA, Church AL, Chauhan A, Ellermann JM, Domingo-Musibay E, et al. Lymphadenopathy in COVID-19 Vaccine Recipients: Diagnostic Dilemma in Oncologic Patients. *Radiology* (2021) 300(1):E296–300. doi: 10.1148/radiol.2021210275
14. Cohen D, Krauthammer SH, Wolf I, Even-Sapir E. Hypermetabolic Lymphadenopathy Following Administration of BNT162b2 mRNA Covid-19 Vaccine: Incidence Assessed by [18F]FDG PET-CT and Relevance to Study Interpretation. *Eur J Nucl Med Mol Imaging* (2021) 48(6):1854–63. doi: 10.1007/s00259-021-05314-2
15. Nishino M, Hatabu H, Ricciuti B, Vaz V, Michael K, Awad MM. Axillary Lymphadenopathy After Coronavirus Disease 2019 Vaccinations in Patients With Thoracic Malignancy: Incidence, Predisposing Factors, and Imaging Characteristics. *J Thorac Oncol* (2022) 17(1):154–9. doi: 10.1016/j.jtho.2021.08.761
16. Ferrari C, Nappi AG, Santo G, Mammucci P, Rubini D, Tucci M, et al. The Day After Mass COVID-19 Vaccination: Higher Hypermetabolic Lymphadenopathy Detection on PET/CT and Impact on Oncologic Patients Management. *Cancers (Basel)* (2021) 13(17):4340. doi: 10.3390/cancers13174340
17. Eshet Y, Tau N, Alhoubani Y, Kanana N, Domachevsky L, Eifer M. Prevalence of Increased FDG PET/CT Axillary Lymph Node Uptake Beyond 6 Weeks After mRNA COVID-19 Vaccination. *Radiology* (2021) 300(3):E345–7. doi: 10.1148/radiol.2021210886
18. El-Sayed MS, Wechie GN, Low CS, Adesanya O, Rao N, Leung VJ. The Incidence and Duration of COVID-19 Vaccine-Related Reactive Lymphadenopathy on 18F-FDG PET-Ct. *Clin Med (Lond)* (2021) 21(6): e633–8. doi: 10.7861/clinmed.2021-0420
19. Becker AS, Perez-Johnston R, Chikarmane SA, Chen MM, El Homsi M, Feigin KN, et al. Multidisciplinary Recommendations Regarding Post-Vaccine Adenopathy and Radiologic Imaging: Radiology Scientific Expert Panel. *Radiology* (2021) 300(2):E323–7. doi: 10.1148/radiol.2021210436
20. Grimm L, Destounis S, Dogan B, Nicholson B, Dontchos B, Sonnenblick E, et al. *SBI Recommendations for the Management of Axillary Adenopathy in Patients With Recent COVID-19 Vaccination: Society of Breast Imaging Patient Care and Delivery Committee* (2021). Available at: https://www.sbi-online.org/Portals/0/Position%20Statements/2021/SBI-recommendations-for managing-axillary-adenopathy-post-COVID-vaccination.pdf.
21. Zhang X, Wang L, Feng N, Ni T, Tang W. Reassessing the Value of Contrast-Enhanced Ultrasonography in Differential Diagnosis of Cervical Tuberculous Lymphadenitis and Lymph Node Metastasis of Papillary Thyroid Carcinoma. *Front Oncol* (2021) 11:694449. doi: 10.3389/fonc.2021.694449
22. Lim J, Lee SA, Khil EK, Byeon SJ, Kang HJ, Choi JA. COVID-19 Vaccine-Related Axillary Lymphadenopathy in Breast Cancer Patients: Case Series With a Review of Literature. *Semin Oncol* (2021) 48(4-6):283–91. doi: 10.1053/j.seminoncol.2021.10.002
23. Maringe C, Spicer J, Morris M, Purushotham A, Nolte E, Sullivan R, et al. The Impact of the COVID-19 Pandemic on Cancer Deaths Due to Delays in Diagnosis in England, UK: A National, Population-Based, Modelling Study. *Lancet Oncol* (2020) 21(8):1023–34. doi: 10.1016/S1470-2045(20)30388-0
24. Treglia G, Cuzzocrea M, Giovanella L, Elzi L, Muoio B. Prevalence and Significance of Hypermetabolic Lymph Nodes Detected by 2-[18F]FDG PET/CT After COVID-19 Vaccination: A Systematic Review and a Meta-Analysis. *Pharm (Basel)* (2021) 14(8):762. doi: 10.3390/ph14080762
25. McIntosh LJ, Bankier AA, Vijayaraghavan GR, Licho R, Rosen MP. COVID-19 Vaccination-Related Uptake on FDG PET/CT: An Emerging Dilemma and Suggestions for Management. *AJR Am J Roentgenol* (2021) 217(4):975–83. doi: 10.2214/AJR.21.25728
26. Seban RD, Richard C, Nascimento-Leite C, Ghidaglia J, Provost C, Gonin J, et al. Absolute Lymphocyte Count After COVID-19 Vaccination is Associated With Vaccine-Induced Hypermetabolic Lymph Nodes on 18F-FDG PET/CT: A Focus in Breast Cancer Care. *J Nucl Med* (2021). doi: 10.2967/jnumed.121.263082
27. Advani P, Chumsri S, Pai T, Li Z, Sharma A, Parent E. Temporal Metabolic Response to mRNA COVID-19 Vaccinations in Oncology Patients. *Ann Nucl Med* (2021) 35(11):1264–9. doi: 10.1007/s12149-021-01675-8
28. Eifer M, Tau N, Alhoubani Y, Kanana N, Domachevsky L, Shams J, et al. COVID-19 mRNA Vaccination: Age and Immune Status and Its Association With Axillary Lymph Node PET/CT Uptake. *J Nucl Med* (2022) 63(1):134–9. doi: 10.2967/jnumed.121.262194
29. Orevi M, Chicheportiche A, Ben-Haim S. Lessons Learned From Post-COVID-19 Vaccination PET/CT Studies. *J Nucl Med* (2021) 63(3):453–60. doi: 10.2967/jnumed.121.262348
30. Schroeder DG, Jang S, Johnson DR, Takahashi H, Navin PJ, Broski SM, et al. Frequency and Characteristics of Nodal and Deltoid FDG and 11C-Choline Uptake on PET Performed After COVID-19 Vaccination. *AJR Am J Roentgenol* (2021) 217(5):1206–16. doi: 10.2214/AJR.21.25928
31. Edmonds CE, Zuckerman SP, Conant EF. Management of Unilateral Axillary Lymphadenopathy Detected on Breast MRI in the Era of COVID-19 Vaccination. *AJR Am J Roentgenol* (2021) 217(4):831–4. doi: 10.2214/AJR.21.25604
32. Plaza MJ, Wright J, Fernandez S. COVID-19 Vaccine-Related Unilateral Axillary Lymphadenopathy: Pattern on Screening Breast MRI Allowing for a Benign Assessment. *Clin Imaging* (2021) 80:139–41. doi: 10.1016/j.clinimag.2021.07.011
33. Lehman CD, Lamb LR, D'Alessandro HA. Mitigating the Impact of Coronavirus Disease (COVID-19) Vaccinations on Patients Undergoing Breast Imaging Examinations: A Pragmatic Approach. *AJR Am J Roentgenol* (2021) 217(3):584–6. doi: 10.2214/AJR.21.25688
34. D'Auria D, Fulgione L, Romeo V, Stanzione A, Maurea S, Brunetti A. Ultrasound and Shear-Wave Elastography Patterns of COVID-19 mRNA Vaccine-Related Axillary, Supra and Subclavicular Lymphadenopathy. *Clin Transl Imaging* (2021) 9(5):539–45. doi: 10.1007/s40336-021-00441-0
35. Adin ME, Isufi E, Kulon M, Pucar D. Association of COVID-19 mRNA Vaccine With Ipsilateral Axillary Lymph Node Reactivity on Imaging. *JAMA Oncol* (2021) 7(8):1241–2. doi: 10.1001/jamaoncol.2021.1794
36. Net JM, Mirpuri TM, Plaza MJ, Escobar CA, Whittington EE, Collado-Mesa F, et al. Resident and Fellow Education Feature: US Evaluation of Axillary Lymph Nodes. *Radiographics* (2014) 34(7):1817–8. doi: 10.1148/rg.347140081
37. Furukawa MK, Furukawa M. Diagnosis of Lymph Node Metastases of Head and Neck Cancer and Evaluation of Effects of Chemoradiotherapy Using Ultrasonography. *Int J Clin Oncol* (2010) 15(1):23–32. doi: 10.1007/s10147-009-0017-1

38. Washington T, Bryan R, Clemow C. Adenopathy Following COVID-19 Vaccination. *Radiology* (2021) 299(3):E280–1. doi: 10.1148/radiol.2021210236
39. Granata V, Fusco R, Setola SV, Galdiero R, Picone C, Izzo F, et al. Lymphadenopathy After BNT162b2 Covid-19 Vaccine: Preliminary Ultrasound Findings. *Biol (Basel)* (2021) 10(3):214. doi: 10.3390/biology10030214
40. Faermann R, Nissan N, Halshtok-Neiman O, Shalmon A, Gotlieb M, Yagil Y, et al. COVID-19 Vaccination Induced Lymphadenopathy in a Specialized Breast Imaging Clinic in Israel: Analysis of 163 Cases. *Acad Radiol* (2021) 28 (9):1191–7. doi: 10.1016/j.acra.2021.06.003
41. Mehta N, Sales RM, Babagbemi K, Levy AD, McGrath AL, Drotman M, et al. Unilateral Axillary Adenopathy in the Setting of COVID-19 Vaccine: Follow-Up. *Clin Imaging* (2021) 80:83–7. doi: 10.1016/j.clinimag.2021.06.037
42. Cocco G, Delli Pizzi A, Fabiani S, Cocco N, Boccatonda A, Frisone A, et al. Lymphadenopathy After the Anti-COVID-19 Vaccine: Multiparametric Ultrasound Findings. *Biol (Basel)* (2021) 10(7):652. doi: 10.3390/biology10070652
43. Placke JM, Reis H, Hadaschik E, Roesch A, Schadendorf D, Stoffels I, et al. Coronavirus Disease 2019 Vaccine Mimics Lymph Node Metastases in Patients Undergoing Skin Cancer Follow-Up: A Monocentre Study. *Eur J Cancer* (2021) 154:167–74. doi: 10.1016/j.ejca.2021.06.023
44. Igual-Rouilleault AC, Soriano I, Quan PL, Fernández-Montero A, Elizalde A, Pina L. Unilateral Axillary Adenopathy Induced by COVID-19 Vaccine: US Follow-Up Evaluation. *Eur Radiol* (2021) 32(5):3199–206. doi: 10.1007/s00330-021-08309-7
45. Giorgis S, Garlaschi A, Brunetti N, Tosto S, Rescinito G, Monetti F, et al. Axillary Adenopathy After COVID-19 Vaccine in Patients Undergoing Breast Ultrasound. *J Ultrason* (2021) 21(87):e361–4. doi: 10.15557/JoU.2021.0060
46. Tsumura Y, Asakura K, Takahashi I, Akaihata M, Takahashi Y, Ishida Y. New Mimic of Relapse or Regional Lymph Node Metastasis in a Cancer Survivor: A Case of mRNA COVID-19 Vaccine-Induced Lymphadenitis With High FDG Uptake. *Immunol Med* (2022) 45(1):45–7. doi: 10.1080/25785826.2021.1999786
47. Xu JB, Xu C, Zhang RB, Wu M, Pan CK, Li XJ, et al. Associations of Procalcitonin, C-Reaction Protein and Neutrophil-to-Lymphocyte Ratio With Mortality in Hospitalized COVID-19 Patients in China. *Sci Rep* (2020) 10 (1):15058. doi: 10.1038/s41598-020-72164-7

Conflict of Interest: The authors declare that the research was conducted in the absence of any commercial or financial relationships that could be construed as a potential conflict of interest.

Publisher's Note: All claims expressed in this article are solely those of the authors and do not necessarily represent those of their affiliated organizations, or those of the publisher, the editors and the reviewers. Any product that may be evaluated in this article, or claim that may be made by its manufacturer, is not guaranteed or endorsed by the publisher.

frontiers | Frontiers in Immunology

ORIGINAL RESEARCH
published: 30 June 2022
doi: 10.3389/fimmu.2022.911738

Seroconversion Rate After SARS-CoV-2 Infection and Two Doses of Either ChAdOx1-nCOV COVISHIELD™ or BBV-152 COVAXIN™ Vaccination in Renal Allograft Recipients: An Experience of Two Public and Private Tertiary Care Center

Narayan Prasad[1], Shyam Bihari Bansal[2], Brijesh Yadav[1], Neha Manhas[2], Deependra Yadav[1], Sonam Gautam[1], Ravishankar Kushwaha[1], Ankita Singh[1], Dharmendra Bhadauria[1], Monika Yachha[1], Manas Ranjan Behera[1] and Anupama Kaul[1]*

[1] Department of Nephrology and Renal Transplantation, Sanjay Gandhi Postgraduate Institute of Medical Sciences, Lucknow, India, [2] Medanta The Medicity Hospital, Gurgaon, India

Introduction: Vaccination is an effective strategy for preventing SARS-CoV-2 infection and associated mortality. Renal Transplant Recipients (RTRs) are vulnerable to acquiring infection and high mortality due to their immunocompromised state. Varying responses to the different vaccines, depending on types of vaccines and population, have been reported. Vaccines supply is also limited. The current study evaluated the seroconversion rate after SARS-CoV-2 infection and 2 doses of either COVAXIN™ or COVISHIELD™ vaccination in RTR.

Methods: The serum anti-SARS-CoV-2 spike protein neutralizing antibody titer was measured in 370 RTRs who acquired SARS-CoV-2 infection (n=172), yet not vaccinated; and those vaccinated with COVAXIN™ (n=78), and COVISHIELD™ (n=120) by chemiluminescence microparticle immunoassay methods from serum.

Result: Overall, the seroconversion rate either after vaccination or infection was 85.13% (315/370). The vaccine-associated seroconversion was 80.30% (159/198). SARS-CoV-2 infection-associated seroconversion was 90.69% (156/172), COVISHIELD™ associated seroconversion was 79.2% (95/120), and COVAXIN™ associated seroconversion was 82.05% (64/78). The median IgG titer in the SARS-CoV-2 infection group was 646.50 AU/ml (IQR: 232.52-1717.42), in the COVAXIN™ group was 1449.75 AU/ml (IQR: 400.0-3068.55), and the COVISHIELD™ vaccination group was 1500.51 AU/ml (IQR: 379.47-4938.50). The seroconversion rate and antibody titers were similar irrespective of the place of sampling. Patient's age-associated seroconversion in <45 years was 88.01% (213/242), 45.1-60 years was 83.18% (94/113), and > 60 years was 58.3% (7/12).

OPEN ACCESS

Edited by:
Nitin Saksena, Victoria University, Australia

Reviewed by:
Pragya Dhruv Yadav, ICMR-National Institute of Virology, India
Swayam Prakash, University of California, Irvine, United States

***Correspondence:**
Narayan Prasad
narayan.nephro@gmail.com

Specialty section:
This article was submitted to Vaccines and Molecular Therapeutics, a section of the journal Frontiers in Immunology

Received: *03 April 2022*
Accepted: *02 June 2022*
Published: *30 June 2022*

Citation:
Prasad N, Bansal SB, Yadav B, Manhas N, Yadav D, Gautam S, Kushwaha R, Singh A, Bhadauria D, Yachha M, Behera MR and Kaul A (2022) Seroconversion Rate After SARS-CoV-2 Infection and Two Doses of Either ChAdOx1-nCOV COVISHIELD™ or BBV-152 COVAXIN™ Vaccination in Renal Allograft Recipients: An Experience of Two Public and Private Tertiary Care Center. Front. Immunol. 13:911738. doi: 10.3389/fimmu.2022.911738

Conclusions: Both infection and vaccination induce robust antibody formation in RTRs. The seroconversion rate after SARS-CoV-2 infection was higher but with a lower antibody titer than vaccines. The vaccines, COVAXIN™ and COVISHIELD™, induce more elevated antibody titers than natural infection. The seroconversion rate and antibody titer in Indian RTRs appears to be better than in the western population, irrespective of their vaccination status.

Keywords: vaccination, anti- SARS-CoV-2 antibody, humoral immunity, COVISHIELD™, COVAXIN™

INTRODUCTION

Vaccination is one of the most effective strategies in preventing SARS-CoV-2 infection and transmission during a pandemic (1–3). There has been the emergence of multiple SARS-CoV-2 variants and repeated infection episodes in several people. However, the vaccines prevented morbidity, hospitalization, and mortality of patients suffering from coronavirus diseases 19 (COVID19). Several vaccines have been developed against the SARS-CoV-2 virus in multiple countries, including India. The high demand for vaccines from across the world has limited the availability of vaccines in low resources countries (4). Well-validated mRNA-based vaccines BNT162b2 (Pfizer-BioNTech, USA) are mainly limited to developed countries. The vaccines have shown high seroconversion rate in the general population up to the tune of 95%, however, had a poor seroconversion rate in renal transplant recipient (RTR) (5–7). Data of mRNA-based vaccination showed a 48% of seroconversion rate in RTRs after the 28th day of the 2nd dose of vaccination (1, 6, 8).

Adenovirus vector-based vaccines ChAdOx1-nCOV (COVISHIELD™, AstraZeneca–Oxford University and Serum Institute, India) and inactivated whole virus-based BBV-152 (COVAXIN™, The Bharat Biotech, India) vaccine are available in India. These vaccines have also shown a good seroconversion rate in a healthy population (2). However, the seroconversion data is limited to a small single-center study in RTRs (9). A single-center study showed seroconversion of about 70% in RTRs, which is higher than that reported from mRNA-based vaccines (1, 10). A lesser amount of antibody formation and poor seroconversion rate after vaccination and SARS-CoV-2 infection is expected in RTRs because of immunosuppressive medicines (1, 6, 7). A reduction of immunosuppression may boost the antibody formation in these patients, although this may pose patients at risk of allograft rejection.

Few studies have reported the incidence of allograft rejection after the vaccination (1, 11, 12). Notably, a 100% seroconversion rate was observed after a single vaccination dose in RTRs, infected previously with SARS-CoV-2 (13, 14). Elicitation of antibodies after vaccination depends on the (i) nature of the antigens and adjuvants, (ii) dose of antigen, and (iii) mode of vaccine delivery (15). The antigenic material used in mRNA-based, vector-based, and inactivated whole virus-based vaccines are known to be different. Therefore, it may be interesting to hypothesize and study whether a whole inactivated virus-based vaccine-like BBV-152 (COVAXIN™) may be more effective in immunocompromised RTRs, who are at a higher risk of acquiring SARS-CoV-2 infection and develop severe COVID-19 and related mortality. The cause for such heterogeneous response to vaccination in RTRs may vary on the duration and degree of immunosuppression (8). Developing and testing the efficacy of other vaccines in antibody formation remained a high priority research area. In the present two center studies, we aimed to study the overall seroconversion rate after (i) two doses of anti-SARS-CoV-2 vaccination and (ii) SARS-CoV-2 infection among non-vaccinated RTRs. Further, we have carefully evaluated the potential association of clinical variables influencing antibody formation in RTRs.

MATERIALS AND METHODS

Patient Population

A total of 370 RTRs were included in the study from two centers, Medanta Medicity hospital Gurugram, New Delhi, India, a private sector tertiary care center, and Sanjay Gandhi Postgraduate Institute of Medical Sciences, Lucknow, India, a public sector tertiary care teaching institute between 1st June 2021 to 30th November 2021. This study was approved by the Institutional Ethics Committee and adhered to the ethical standards of the declaration of Istanbul and Helsinki. The ethics approval code was 2021-36-IP-EXP-36. All patients were reverse transcriptase-polymerase chain reaction (RT-PCR) negative at the time of sample collection. The demographic and clinical details were noted at the time of sample collection from the patient's medical record. The prior history of SARS-CoV-2 infection was 78 (range, 56-90) days. Vaccination history and associated side effects fever, myalgias, headache, back pain, body ache, and giddiness were obtained from each participating individual. The type and dose of vaccines were confirmed from the vaccination certificate issued by the Ministry of Health and Family Welfare, Government of India. RTRs who had SARS-CoV-2 infection and yet not received vaccines and those who received two doses of vaccines were asked for the blood sampling for anti-SARS-CoV-2 spike protein IgG measurement. The mean gap between two doses of either brand of vaccination and samples collection was 21.10 ± 4.27 days. The median interval between 1st and 2nd dose for COVISHIELD™ vaccine was 69 (range, 42-112) days, and for COVAXIN™, it was 36 (range, 28-42) days.

For the analysis purpose, patients were categorized into three groups. Group-1, those who had a history of SARS-CoV-2 infection yet did not receive any dose of vaccines (n=172).

Group-2, those who had received 2 doses of COVAXIN™ (n=78), and Group-3, those who had received 2 doses of COVISHIELD™ vaccine (n=120).

Anti-SARS-CoV-2 Spike Protein IgG Titer Measurement by Chemiluminescence Immunoassay Methods

A five ml blood sample was collected in a plain vial with blood clot activating factors and centrifugation at 1500RPM for 5 minutes. The serum was separated and stored at -80^{0}C. Anti-SARS-CoV-2 spike protein IgG titer was determined using the chemiluminescent magnetic microparticle Immunoassay (CMIA) analyzer per the manufacturer's instruction (Abbott diagnostic, Ireland).

In brief, in this process, the first serum anti-SARS-CoV-2 IgG antibody was captured on an antigen-coated paramagnetic microparticle bead and buffer. The non-specific binding was removed by the washing. The antigen-antibody complex mixture was further incubated with acridinium labeled anti-human IgG conjugate. The complex mixture was again washed with buffer to remove non-specific binding. Further, a pre-trigger and trigger solution of hydrogen peroxide and sodium hydroxide was added, resulting in a chemiluminescent mixture on the Architect platform (Abbott diagnostic, Ireland). The intensity of the chemiluminescent mixture was measured in a relative light unit (RLU) that was directly proportional to the concentration of anti-SARS-CoV-2 antibody present in the serum. The sample's RLU values were normalized with the calibrator RLU as per the World Health Organization standard (16, 17).

Statistical Analysis

Statistical analysis was performed using the SPSS software version 20 (IBM corporation, Armonk, NY, USA). Kruskal Wallis test was used to compare the median of nonparametrically distributed variables between the groups. Median and interquartile range was calculated for the antibody titer. For the comparison of continuous variables among the group, a one-way analysis of variance (ANOVA) was applied. The mean and standard deviation was calculated. The Chi-square test or the Fischer exact test was used per the application required to compare the categorical variables. Multivariate analysis was also performed for variables predicting seroconversion. Graphs were plotted with Prism version 8 for Windows, GraphPad Software, La Jolla, CA, USA.

RESULTS

Demographic and Clinical Characteristics of the Patients

Demographic and clinical profiles of the patients are given in **Table 1**. Eighty-five (317/370) percent of patients were male, and 46.48% (172/370) had previous SARS-CoV-2 infection without a history of any dose of vaccination. Of these, 21.08% (78/370) of patients were vaccinated with COVAXIN™, and 32.43% (120/370) patients were vaccinated with COVISHIELD™. The mean age of the patients was 40.84 years and the median post-transplant period to sample collection for testing anti-SARS-CoV-2 spike protein IgG was 78.99 months. All patients were live-related renal allograft recipients, and the majority, 93.78% (347/370) were ABO compatible RTRs.

Anti-SARS-CoV-2 Spike Protein-Specific IgG Seroconversion Rate Among RTRs

The overall cumulative seroconversion rate, either due to vaccination or infection, was 85.13% (315/370). The vaccine-associated seroconversion was 80.30% (159/198). The SARS-CoV-2 infection-associated seroconversion was 90.69% (156/172); COVISHIELD™ vaccination-associated seroconversion was 79.2% (95/120), and the COVAXIN™ associated seroconversion was 82.05% (64/78). However, the antibody titer was higher after vaccination than the titer developed only with natural SARS-CoV-2 infection. The median IgG titer in the SARS-CoV-2 infection group was 646.50 AU/ml (IQR: 232.52-1717.42). In the COVAXIN™ group, was 1449.75 AU/ml (IQR: 400.00-3068.55) and in the COVISHIELD™ vaccination group was 1500.51 AU/ml (IQR: 379.47-4938.50). (**Table 2**, **Figure 1**). Further, we compared the percentage of seroconversion and antibodies titer at two different centers. Vaccination associated seroconversion rate was similar between both the center. COVAXIN™ associated seroconversion was 83.9% (47/56) at SGPGIMS compared to 82.05% (64/78) at Medanta Medicity. COVISHIELD™ associated seroconversion in SGPGIMS was 73.8% (31/42) compared to 77% (17/22) in the Medanta Medicity. **Table 3**.

Clinical Variables Associated With Seroconversion

The clinical variables associated with seroconversion rate are shown in **Table 4**. Patients with age <45 years had a seroconversion rate of 88.01% (213/242). In the age group 45.1-60 years, seroconversion was 83.18% (94/113), and in patients with age >60 years, seroconversion was only 58.3% (7/12). Older patients had a poor seroconversion rate. There was no impact of BMI, post-transplant interval, gender, blood groups, immunosuppressive regimen, and serum creatinine values on seroconversion (**Table 4**).

Predictor Clinical Variables for Seroconversion on Multivariate Analysis

On multivariate analysis, we observed that the age of the recipients was the significant predictor for seroconversion (B=0.041, Exp (B)=1.04; P=0.004). Other variables like BUN, serum creatinine, total leukocyte count, hemoglobin, BMI, post-transplant gap, eGFR, and trough tacrolimus level were not the predictors of seroconversion (**Table 5**).

Side Effects of Vaccination

The major side effects reported by the RTRs for both of the vaccines (COVISHIELD™ and COVAXIN™) were similar. RTRs vaccinated with COVISHIELD™, the mild degree fever was in 13.3%, myalgias in 24.16%, headache in 15.8%, back pain in 4.1%, body- ache in 10%, and giddiness in 12.5%. Whereas

TABLE 1 | Demographic and clinical characteristic of patients in SARS-CoV-2 infection and Vaccination.

Characteristics		Total	SARS-CoV-2 infection (n=172)	COVAXIN™Vaccination (n=78)	COVISHIELD™Vaccination (n=120)	P Value
Age (Years)		40.84 ± 10.84	39.65 ± 10.02	41.87 ± 10.79	41.89 ± 11.86	0.14*
Male/Female		317/53	150/22	65/13	102	0.69**
ABOc/ABOi		347/23	164/8	76/2	107/13	0.032**
Post-transplant interval in Month (mean ± SD)		78.99 ± 52.3	82.19 ± 56.18	85.61 ± 54.35	70.09 ± 43.61	0.068*
BMI(Kg/M^2)		23.72 ± 4.82	23.73 ± 5.16	23.41 ± 3.14	23.90 ± 5.22	0.78*
Hemoglobin(g/dl)		12.54 ± 2.05	13.02 ± 1.85	11.39 ± 2.38	12.61 ± 1.80	<0.001*
BUN (mg/dl)		23.76 ± 11.81	19.83 ± 7.82	27.09 ± 13.38	27.22 ± 13.67	0.001*
Baseline serum creatinine(mg/dl)		0.87 ± 0.41	1.03 ± 0.40	0.71 ± 0.39	0.76 ± 0.35	<0.001*
Serum creatinine(mg/dl)		1.34 ± 0.60	1.47 ± 0.79	1.23 ± 0.29	1.23 ± 0.34	0.001*
TLC (X10$^{3/}$µl)		7.63 ± 2.46	8.26 ± 2.58	6.75 ± 2.06	7.30 ± 2.30	<0.001*
eGFR (ml/min)		73.41 ± 34.62	70.42 ± 45.17	75.92 ± 21.21	76.05 ± 21.68	0.30*
Tacrolimus level(µg/l)		5.44 ± 1.94	5.56 ± 2.18	5.19 ± 1.09	5.45 ± 2.00	0.37*
Systolic BP (mmHg)		133.17 ± 14.37	130.13 ± 15.10	131.27 ± 12.56	135.67 ± 13.85	<0.004*
Diastolic BP (mmHg)		82.24 ± 10.31	80.48 ± 10.02	82.51 ± 9.79	84.57 ± 10.64	0.004*
Patient blood group	A^{+ve}	99	51	19	29	0.35**
	B^{+ve}	135	54	30	51	
	O^{+ve}	91	48	16	27	
	AB^{+ve}	45	19	13	13	
Induction regimen	None/Basiliximab/ ATG	155/148/67	74/81/17	35/22/21	46/45/29	0.001**
MMF+ Steroid+	Tacrolimus/ Cyclosporin	355/15	166/6	72/6	117/3	0.17**

** ANOVA test, ** Chie square test; ABOc, ABO compatible; ABOi, ABO incompatible; BMI, Body mass index; TLC, Total leucocyte count; BUN, Blood urea nitrogen; eGFR, estimated glomerular filtration rate; BP, Blood group; ATG, Anti-thymocyte globulin; MMF, Mycophenolate mofetil.*

RTRs vaccinated with COVAXIN™, the mild degree fever was observed in 10.2%, myalgias in 23.07%, headache in 10.2%, back pain in 3.8%, body ache, and giddiness in 14.10%. In our cohort, no RTRs experienced any major side effects, such as blood clots or thrombotic microangiopathy, similar to the healthy population reported in other studies (18, 19) (**Table 6**).

DISCUSSION

The current two-center study found that both COVISHIELD™ and COVAXIN™ yielded robust seroconversion up to 80.3% in RTRs at both centers. We also observed that the elderly of more than 60 years had a poor seroconversion rate. The seroconversion rate is inferior to the general population but higher than that reported from mRNA-based vaccines in RTRs from western population studies.

The poor seroconversion is expected in RTRs because of an immunocompromised state because of immunosuppressions like calcineurin inhibitors, mycophenolate mofetil, and corticosteroids. Studies have shown that the use of mycophenolate mofetil significantly hampers the seroconversion after vaccination in RTRs (5, 20). All our patients were on mycophenolate mofetil at the time of sampling. Therefore, antibody formation is less than that expected in the general population (1). However, the SARS-CoV-2 infection alone induced seroconversion in 90% of patients, similar to seroconversion in liver transplant recipients (21). The data from mRNA-based vaccines BNT162b2 (Pfizer–BioNTech, USA) showed a 48% seroconversion rate in RTRs after vaccination, which increased to 49-64% after 3rd dose of vaccination (22, 23). The seroconversion in Indian RTRs appeared much higher than in the European and the USA renal transplant cohorts in both scenarios after infection and vaccination (24–26). The reason for blunted seroconversion in the western population is not known. One of the factors could be the older age of allograft recipients and mainly deceased donor transplantation. Our results found that the seroconversion rate decreased significantly with the increase in the recipient's age (**Table 2**). Further, multivariate analysis showed age as the best predictor of overall seroconversion. Similar findings were also observed in other studies (24, 25). In our cohort, the

TABLE 2 | $Anti-SARS-CoV-2 antibody titer and seroconversion among renal transplant recipients.

S.No.	SARS-CoV-2 infection (n=172)		COVAXIN™ (n=78)		COVISHIELD™(n=120)		P value
Median titer (Interquartile range)	646.50 (232.52-1717.42)		1449.75 (400.0-3068.55)		1500.51 (379.47-4938.50)		a vs b, p=0.009*; a vs c, p=0.004*; b vs c, p=0.45*
Overall anti-SARS-CoV-2 spike protein antibody seroconversion	Yes 156(90.69%)	No 16(9.3%)	Yes 64(82.05%)	No 14 (17.94%)	Yes 95(79.2%)	No 25(20.83%)	0.017**

*$- Indicates seroconversion in patient who had anti SARS-CoV-2 Spike protein antibody titer >50AU/ml. *Kruskal Wallis Test; **Chi Square test.*

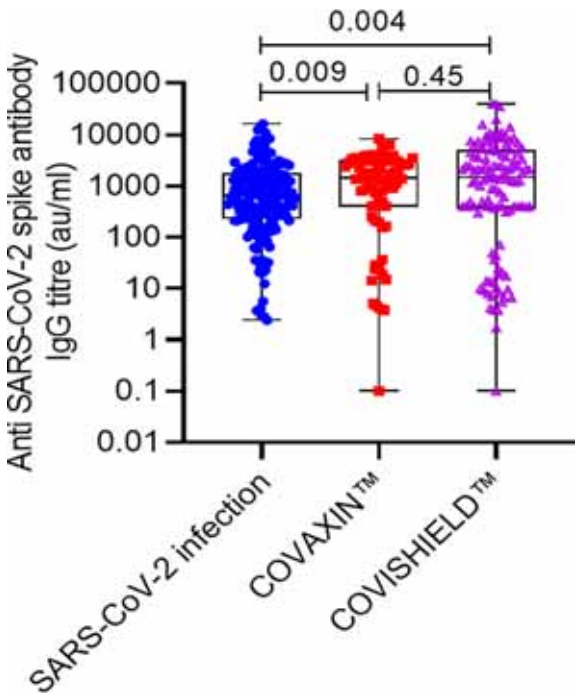

FIGURE 1 | Anti-SARS-CoV-2 spike protein antibody titer in RTRs infected with SARS-CoV-2 or vaccinated with 2 doses of either COVISHIELD™ or COVAXIN™ vaccine.

median age of the patient was 40.50 years, which was younger than German and UK transplant cohorts (median age 54 and 57 years) (24, 25). The relatively depressed immune system of older people with top-up immunosuppression may have resulted in poor immune response (27). Another important factor associated with seroconversion is the body mass index (BMI) of patients. A poor seroconversion has been reported in obese persons (28). Although, we did not find any difference in seroconversion between lean and obese RTRs. Although, obese patients tended to increase seroconversion rates, similar to the finding by Maria et al. (7). The deceased donor-associated transplant may be another important factor that may influence seroconversion. All patients underwent live-related renal transplantation in our study, and overall, 85.13% (315/370) of patients developed antibodies. In the UK and the German-based cohorts, most patients were undergone deceased donor-organ transplantation (24, 25). Deceased donor-associated allograft recipients usually receive a higher degree of immunosuppression to avoid the risk of rejection. It may be another reason for the lower seroconversion rate in western organ transplant recipients. In our study, the graft dysfunction measured in terms of BUN, Creatinine, and e GFR was not associated with seroconversion. A few studies have shown an association of seroconversion with graft dysfunction. Patients with lower eGFR had poor seroconversion (29, 30). The finding may be because of the fact that the RTRs included in our study had relatively better graft function with a mean serum creatinine value of 1.34 ± 0.60 mg/dl. The longer duration of transplantation indicates a larger duration of immunosuppression, which reduces the chance of antibody formation (29).

One of the exciting findings in our study was the higher seroconversion rate (79.2%) after COVISHIELD™ vaccination at both centers, while the seroconversion rate was only 44% the UK study (31). Besides the age factors, BMI of patients, living versus deceased donor RTS, the seroconversion was also determined by several other factors like genetic makeup of an individual, exposure to antigens, gut microbiota, etc. The vigorous immune response against vaccination in Indian patients may be due to a higher immune response to the pathogens. One of the possible reasons could be Bacille Calmette-Guerin (BCG) vaccination in all RTRs. BCG to prevent tuberculosis disease (TB) is universally given to every child soon after birth in India and other Asian countries with a high prevalence of tuberculosis (32). BCG provokes a non-specific immunity. The cross-protective effects of the BCG vaccine on non-tuberculosis-related diseases are well established (33). The cross-protective effect may be in response to trained innate immune memory (33). It is characterized by non-permanent epigenetic reprogramming of macrophages that leads to increased inflammatory cytokine production and consequently potent immune responses. BCG vaccination was associated with a lower incidence of sepsis and respiratory tract infections that reduced child mortality (34). It has also been observed that BCG vaccination protects against various viral

TABLE 3 | [$]Seroconversion and antibody titer after vaccination at both center.

Seroconversion and antibody titer in SGPGI Lucknow							
S.No.	**SARS-CoV-2 infection (n=172)**		**COVAXIN™b(n=78)**		**COVISHIELD™c(n=120)**		**P value**
Median titer (Interquartile range)	646.50 (232.52-1717.42)		1586.0 (501.95-3000.0)		1572.95 (22.82-7522.75)		a vs b; p=0.033* a vs c; p=0.014* b vs c; p=0.33*
Over all anti-SARS-CoV-2 spike protein antibody seroconversion	Yes 156(90.69%)	No 16(9.3%)	Yes 47(83.9%)	No 9 (16.07%)	Yes 31(73.8%)	No 11(26.19%)	0.012**
Seroconversion and antibody titer in Medanta, Gurugram, India							
Median titer (Interquartile range)			1310.0 (309.05-4000.0)		1400.0 (398.0-4414.52)		0.85*
Over all anti-SARS-CoV-2 spike protein antibody seroconversion			64(82.05%)	14(18%)	17 (77%)	5 (22.7%)	0.76**

*$- Indicates seroconversion in patient who had anti SARS-CoV-2 Spike protein antibody titer >50AU/ml. *Kruskal Wallis Test, **Chi Square test.*

TABLE 4 | Clinical variables associated with seroconversion among the group.

Characteristics	Variable stratification	Seroconversion		P value
		Yes	No	
Age (years)	<45	213 (88.01%)	29 (11.98%)	0.012
	45.1-60	94 (83.18%)	19 (16.81%)	
	>60	7 (58.3%)	5 (41.66%)	
	<45	213 (88.01%)	29 (11.98%)	
Gender	M	271 (85.5%)	46 (14.51%)	0.67
	F	44 (83.01%)	9 (16.98%)	
Post-transplant interval (month)	2-60	133 (86.36%)	21 (13.63%)	0.29
	60.1-120	120 (85.10%)	21 (14.89%)	
	120.1-180	38 (79.16%)	10 (20.83%)	
	>180	23 (95.8%)	1 (4.16%)	
BMI (kg/m^2)	<18.4	43 (84.3%)	8 (15.68%)	0.38
	18.5-24.99	152 (82.60%)	32 (17.4%)	
	25.0-24.99	92 (90.2%)	10 (9.8%)	
	>30	28 (84.8%)	5 (15.15%)	
Blood group	A^{+ve}	86 (86.8%)	13 (13.13%)	0.43
	B^{+ve}	110 (81.5%)	25 (18.51%)	
	AB^{+ve}	38 (84.4%)	7 (15.5%)	
	O^{+ve}	81 (89.0%)	10 (10.98%)	
Blood group compatibility	ABOc	298 (85.8%)	49 (14.12%)	0.13
	ABOi	17 (73.91%)	6 (26.08%)	
Serum creatinine (mg/dl)	<1.4	210 (84.33%)	39 (15.6%)	0.64
	>1.4	105 (86.77%)	16 (13.22%)	
Immunosuppression	Tacrolimus	302 (85.07%)	53 (14.92%)	1.00
	Cyclosporin	13 (86.6%)	2 (13.3%)	

BMI, Body mass index; ABOc, ABO compatible; ABOi, ABO-incompatible.

infections such as influenza virus, yellow fever virus, herpes simplex viruses, respiratory syncytial virus, and human papilloma virus (35). The findings confirm a non-targeted beneficial effect of BCG vaccination (33).

The immune system imposes a vigorous response against the SARS-CoV-2 for its clearance, and as a result, there is profuse neutralizing anti-spike IgG antibody formation (36). The higher titer of neutralizing antibody titer in patients with either brand of vaccines in India compared to titers after natural SARS-CoV-2 infection suggests antigenicity of the adjuvants and viral components in sensitization of the immune system for seroconversion is important. This finding gives the clue about designing population-specific vaccines with natural viral components and potent antigenic adjuvants. The seroconversion rate was higher with natural infection but the antibody titer was lower than that occurred after vaccination. The lower antibody titer may be due to the waning of the antibody over time (3, 37). It is speculated that whole virus-based vaccines may induce the robust seroconversion and elicitation of antibody titer as reflected in our finding (**Table 2**) (10).

As SARS-CoV-2 virus induce innate immune components leading to proinflammatory cytokines secretion such as IL-1β, and IL-18 (Cytokine storm) (38). A higher inflammatory state

TABLE 5 | Multivariate analysis predicting seroconversion in RTRs.

Variables	B	Exp (B)	95% CI for EXP (B) (Lower-Upper)	P value
Age (Years)	0.041	1.04	1.03-1.07	0.004
Post-transplant interval (months)	-0.001	0.99	0.99-1.005	0.73
BMI (kg/m^2)	-0.030	0.97	0.90-1.03	0.36
BUN (mg/dl)	0.005	1.005	0.98-1.03	0.70
Hemoglobin(g/dl)	-0.101	0.90	0.77-1.05	0.197
Serum creatinine(mg/dl)	-0.193	0.82	0.39-1.70	0.60
TLC (X10$^{3/}$µl)	0.008	1.008	0.88-1.14	0.90
eGFR(ml/min)	0.005	1.005	0.980-1.03	0.70
Tacrolimus level(µg/l)	0.13	1.13	0.98-1.31	0.073

TLC, Total leucocyte count; BUN, blood urea nitrogen; eGFR, estimated glomerular filtration rate; BMI, body mass index.

TABLE 6 | Side effects associated with vaccination.

Characteristics	COVISHIELD™(n=120)	COVAXIN™ (n=78)	P value
Myalgia (%)	29 (24.16)	18 (23.07)	0.86
Headache (%)	19 (15.83)	8 (10.2)	0.26
Backpain (%)	5 (4.1)	3 (3.8)	0.91
Body ache (%)	12 (10)	11 (14.10)	0.38
Giddiness (%)	15 (12.5)	11 (14.10)	0.74
Fever (%)	16 (13.3)	8 (10.2)	0.51
Myalgia+ Body ache+ Fever (%)	24 (20)	19 (24.3)	0.47

leads higher seroconversion rate after vaccination in solid organ transplant recipients (39). A study showed a 100% seroconversion rate in RTRs after the first dose of mRNA-based vaccination in previous SARS-CoV-2 infected patients (13). Again, suggesting the importance of the co-stimulating effect of viral components in seroconversion. Alternatively, reducing the immunosuppressive dose may help in raising the antibody titer. Although, it may increase the chances of rejection. Alternatively, using more antigenic material in vaccine preparation may improve the vaccine efficacy for these patients. The present two-center study confirms the finding of our single-center study of higher seroconversion rate with COVISHIELD™ and COVAXIN™ in living donor renal transplant patients in India (10). The side-effects profile suggests the safety of these vaccines in RTRs. It is also prudent to understand whether a single dose of vaccination is sufficient in a previously infected person or whether complete vaccination with two doses is required. It is particularly important for low-middle income and resource-limited countries where vaccination of the entire population is still a dream. Owing to the fourth wave of SARS-CoV-2 infection, vaccination with either of these two vaccines will be helpful in elicitating the effective SARS-CoV-2 neutralizing antibody in population.

CONCLUSIONS

Both infection and vaccination induce robust antibody formation in RTRs. SARS-CoV-2 infection induces a higher seroconversion but poor antibody titer. The vaccines induce more elevated antibodies titer than natural infection. The response rate in Indian RTRs appears better than the western population.

DATA AVAILABILITY STATEMENT

The raw data supporting the conclusions of this article will be made available by the authors, without undue reservation.

ETHICS STATEMENT

The studies involving human participants were reviewed and approved by Institute Ethics Committe, SGPGI. The patients/participants provided their written informed consent to participate in this study.

AUTHOR CONTRIBUTIONS

NP, BY and SB Conceived the project, counselled patients for sample donation, supervised the progress of project, edited the final draft of manuscript. BY collected the sample, analyzed the IgG titer, analyzed the data, wrote the initial draft of manuscript NM collected the samples and helped in IgG titer analysis. DY, SG, and AK helped in sample collection and analysis of the IgG titer. RK, DB, MY, MB, and AK coordinated with the patients for sample donation and reviewed the final draft of manuscript. All authors contributed to the article and approved the submitted version.

ACKNOWLEDGMENTS

Brijesh Yadav received the Young Scientist Research Grant (Grant No YSS/2020/000202/PRCYSS) support from the Department of Health Research, New Delhi, India.

REFERENCES

1. Benotmane I, Gautier-Vargas G, Cognard N, Olagne J, Heibel F, Braun-Parvez L, et al. Low Immunization Rates Among Kidney Transplant Recipients Who Received 2 Doses of the mRNA-1273 SARS-CoV-2 Vaccine. *Kidney Int* (2021) 99:1498–500. doi: 10.1016/j.kint.2021.04.005
2. Singh AK, Phatak SR, Singh R, Bhattacharjee K, Singh NK, Gupta A, et al. Antibody Response After First and Second-Dose of ChAdOx1-nCOV (CovishieldTM®) and BBV-152 (CovaxinTM®) Among Health Care Workers in India: The Final Results of Cross-Sectional Coronavirus Vaccine-Induced Antibody Titre (COVAT) Study. *Vaccine* (2021) 39:6492–509. doi: 10.1016/j.vaccine.2021.09.055
3. Favresse J, Bayart JL, Mullier F, Elsen M, Eucher C, Van Eeckhoudt S, et al. "Antibody Titres Decline 3-Month Post-Vaccination With BNT162b2. *Emerg Microbes Infect* (2021) 10:1495–8. doi: 10.1080/22221751.2021.1953403
4. Lindstrand A, Cherian T, Chang-Blanc D, Feikin D, O'Brien KL. The World of Immunization: Achievements, Challenges, and Strategic Vision for the Next Decade. *J Infect Dis* (2021) 224(12 Suppl 2):S452–67. doi: 10.1093/infdis/jiab284
5. Vaiciuniene R, Sitkauskiene B, Bumblyte IA, Dalinkeviciene E, Ziginskiene E, Bagdonas D, et al. Immune Response After SARS-CoV-2 Vaccination in Kidney Transplant Patients. *Medicina (Kaunas)* (2021) 57:1327. doi: 10.3390/medicina57121327
6. Rincon-Arevalo H, Choi M, Stefanski AL, Halleck F, Weber U, Szelinski F, et al. Impaired Humoral Immunity to SARS-CoV-2 BNT162b2 Vaccine in

Kidney Transplant Recipients and Dialysis Patients. *Sci Immunol* (2021) 6: eabj1031. doi: 10.1126/sciimmunol.abj1031
7. Magicova M, Fialova M, Zahradka I, Rajnochova-Bloudickova S, Hackajlo D, Raska P, et al. Humoral Response to SARS-CoV-2 is Well Preserved and Symptom Dependent in Kidney Transplant Recipients. *Am J Transplant* (2021) 21:3926–35. doi: 10.1111/ajt.16746
8. Benotmane I, Gautier-Vargas G, Cognard N, Olagne J, Heibel F, Braun-Parvez L, et al. Weak Anti-SARS-CoV-2 Antibody Response After the First Injection of an mRNA COVID-19 Vaccine in Kidney Transplant Recipients. *Kidney Int* (2021) 99:1487–9. doi: 10.1016/j.kint.2021.03.014
9. Meshram HS, Kute VB, Shah N, Chauhan S, Navadiya VV, Patel AH, et al. COVID-19 in Kidney Transplant Recipients Vaccinated With Oxford-AstraZeneca COVID-19 Vaccine (Covishield): A Single-Center Experience From India. *Transplantation* (2021) 105:e100–3. doi: 10.1097/TP.0000000000003835
10. Prasad N, Yadav B, Singh M, Gautam S, Bhadauria D, Patel M, et al. Humoral Immune Response of SARS-CoV-2 Infection and Anti-SARS-CoV-2 Vaccination in Renal Transplant Recipients. *Vaccines (Basel)* (2022) 10:385. doi: 10.3390/vaccines10030385
11. Del Bello A, Marion O, Delas A, Congy-Jolivet N, Colombat M, Kamar N. Acute Rejection After Anti-SARS-CoV-2 mRNA Vaccination in a Patient Who Underwent a Kidney Transplant. *Kidney Int* (2021) 100(1):238–9. doi: 10.1016/j.kint.2021.04.025
12. Phylactou M, Li J-PO, Larkin DFP. Characteristics of Endothelial Corneal Transplant Rejection Following Immunisation With SARS-CoV-2 Messenger RNA Vaccine. *Br J Ophthalmol* (2021) 105(7):893–6. doi: 10.1136/bjophthalmol-2021-319338
13. Benotmane I, Gautier-Vargas G, Gallais F, Gantner P, Cognard N, Olagne J, et al. Strong Antibody Response After a First Dose of a SARS-CoV-2 mRNA-Based Vaccine in Kidney Transplant Recipients With a Previous History of COVID-19. *Am J Transplant* (2021) 21(11):3808–10. doi: 10.1111/ajt.16764
14. Caillard S, Thaunat O. COVID-19 Vaccination in Kidney Transplant Recipients. *Nat Rev Nephrol* (2021) 17(12):785–7. doi: 10.1038/s41581-021-00491-7
15. Zimmermann P, Curtis N. Factors That Influence the Immune Response to Vaccination. *Clin Microbiol Rev* (2019) 32:e00084–18. doi: 10.1128/CMR.00084-18
16. Abbott Laboratories. *SARS-CoV-2 IgG [Package Insert]* (2020).
17. Knezevic I, Mattiuzzo G, Page M, Minor P, Griffiths E, Nuebling M, et al. WHO International Standard for Evaluation of the Antibody Response to COVID-19 Vaccines: Call for Urgent Action by the Scientific Community. *Lancet Microbe* (2022) 3:e235–40. doi: 10.1016/S2666-5247(21)00266-4
18. Kaur RJ, Dutta S, Bhardwaj P, Charan J, Dhingra S, Mitra P, et al. Safety and Immunogenicity of an Inactivated SARS-CoV-2 Vaccine, BBV152: A Double-Blind, Randomised, Phase 1 Trial. *Lancet Infect Dis* (2021) 21:637–46. doi: 10.1016/S1473-3099(20)30942-7
19. Kamal D, Thakur V, Nath N, Malhotra T, Gupta A, Batlish R. Adverse Events Following ChAdOx1 Ncov-19 Vaccine (COVISHIELD) Amongst Health Care Workers: A Prospective Observational Study. *Med J Armed Forces India* (2021) 77:S283–8. doi: 10.1016/j.mjafi.2021.06.014
20. Kantauskaite M, Müller L, Kolb T, Fischer S, Hillebrandt J, Ivens K, et al. Intensity of Mycophenolate Mofetil Treatment is Associated With an Impaired Immune Response to SARS-CoV-2 Vaccination in Kidney Transplant Recipients. *Am J Transplant* (2022) 22:634–9. doi: 10.1111/ajt.16851
21. Becchetti C, Broekhoven AGC, Dahlqvist G, Fraga M, Zambelli MF, Ciccarelli O, et al. Humoral Response to SARS-CoV-2 Infection Among Liver Transplant Recipients. *Gut* (2022) 71(4):746–56. doi: 10.1136/gutjnl-2021-326609
22. Benotmane I, Gautier G, Perrin P, Olagne J, Cognard N, Fafi-Kremer S, et al. Antibody Response After a Third Dose of the mRNA-1273 SARS-CoV-2 Vaccine in Kidney Transplant Recipients With Minimal Serologic Response to 2 Doses. *JAMA* (2021) 326(11):1063–5. doi: 10.1001/jama.2021.12339
23. Kamar N, Abravanel F, Marion O, Couat C, Izopet J, Del Bello A. Three Doses of an mRNA Covid-19 Vaccine in Solid-Organ Transplant Recipients. *N Engl J Med* (2021) 385:661–2. doi: 10.1056/NEJMc2108861
24. Choi M, Bachmann F, Naik MG, Duettmann W, Duerr M, Zukunft B, et al. Low Seroprevalence of SARS-CoV-2 Antibodies During Systematic Antibody Screening and Serum Responses in Patients After COVID-19 in a German Transplant Center. *J Clin Med* (2020) 9:E3401. doi: 10.3390/jcm9113401
25. Willicombe M, Gleeson S, Clarke C, Dor F, Prendecki M, Lightstone L, et al. Identification of Patient Characteristics Associated With SARS-CoV-2 Infection and Outcome in Kidney Transplant Patients Using Serological Screening. *Transplantation* (2021) 105:151–7. doi: 10.1097/TP.0000000000003526
26. Zervou FN, Ali NM, Neumann HJ, Madan RP, Mehta SA. SARS-CoV-2 Antibody Responses in Solid Organ Transplant Recipients. *Transpl Infect Dis* (2021) 23:e13728. doi: 10.1111/tid.13728
27. Collier DA, Ferreira IATM, Kotagiri P, Datir RP, Lim EY, Touizer E, et al. Age-Related Immune Response Heterogeneity to SARS-CoV-2 Vaccine BNT162b2. *Nature* (2021) 596:417–22. doi: 10.1038/s41586-021-03739-1
28. Frasca D, Reidy L, Cray C, Diaz A, Romero M, Kahl K, et al. Influence of Obesity on Serum Levels of SARS-CoV-2-Specific Antibodies in COVID-19 Patients. *PloS One* (2021) 16:e0245424. doi: 10.1371/journal.pone.0245424
29. Chukwu CA, Mahmood K, Elmakki S, Gorton J, Kalra PA, Poulikakos D, et al. Evaluating the Antibody Response to SARS-COV-2 Vaccination Amongst Kidney Transplant Recipients at a Single Nephrology Centre. *PloS One* (2022) 17:e0265130. doi: 10.1371/journal.pone.0265130
30. Mulley WR, Visvanathan K, Hurt AC, Brown FG, Polkinghorne KR, Mastorakos T, et al. Mycophenolate and Lower Graft Function Reduce the Seroresponse of Kidney Transplant Recipients to Pandemic H1N1 Vaccination. *Kidney Int* (2012) 82:212–9. doi: 10.1038/ki.2012.106
31. Prendecki M, Thomson T, Clarke CL, Martin P, Gleeson S, De Aguiar RC, et al. Immunological Responses to SARS-CoV-2 Vaccines in Kidney Transplant Recipients. *Lancet* (2021) 398:1482–4. doi: 10.1016/S0140-6736(21)02096-1
32. Lobo N, Brooks NA, Zlotta AR, Cirillo JD, Boorjian S, Black PC, et al. 100 Years of Bacillus Calmette-Guérin Immunotherapy: From Cattle to COVID-19. *Nat Rev Urol* (2021) 18:611–22. doi: 10.1038/s41585-021-00481-1
33. Moorlag S. J. C. F. M., Arts RJW, van Crevel R, Netea MG. Non-Specific Effects of BCG Vaccine on Viral Infections. *Clin Microbiol Infect* (2019) 25:1473–8. doi: 10.1016/j.cmi.2019.04.020
34. Garly ML, Martins CL, Balé C, Baldé MA, Hedegaard KL, Gustafson P, et al. BCG Scar and Positive Tuberculin Reaction Associated With Reduced Child Mortality in West Africa. A non-Specific Beneficial Effect of BCG? *Vaccine* (2003) 21:2782–90. doi: 10.1016/s0264-410x(03)00181-6
35. Stensballe LG, Nante E, Jensen IP, Kofoed PE, Poulsen A, Jensen H, et al. Acute Lower Respiratory Tract Infections and Respiratory Syncytial Virus in Infants in Guinea-Bissau: A Beneficial Effect of BCG Vaccination for Girls Community Based Case-Control Study. *Vaccine* (2005) 23:1251–7. doi: 10.1016/j.vaccine.2004.09.006
36. Charmetant X, Espi M, Benotmane I, Heibel F, Buron F, Gautier-Vargas G, et al. Comparison of Infected and Vaccinated Transplant Recipients Highlights the Role of Tfh and Neutralizing IgG in COVID-19 Protection. *MedRxiv* (2021) 24:1–44. doi: 10.1101/2021.07.22.21260852
37. Zhuang C, Liu X, Chen Q, Sun Y, Su Y, Huang S, et al. Protection Duration of COVID-19 Vaccines: Waning Effectiveness and Future Perspective. *Front Microbiol* (2022) 13:828806. doi: 10.3389/fmicb.2022.828806
38. Diamond MS, Kanneganti T-D. Innate Immunity: The First Line of Defense Against SARS-CoV-2. *Nat Immunol* (2022) 23:165–76. doi: 10.1038/s41590-021-01091-0
39. Karaba AH, Zhu X, Benner SE, Akinde O, Eby Y, Wang KH, et al. Higher Proinflammatory Cytokines Are Associated With Increased Antibody Titer After a Third Dose of SARS-CoV-2 Vaccine in Solid Organ Transplant Recipients. *Transplantation* (2022) 106(4):835–41. doi: 10.1097/TP.0000000000004057

Conflict of Interest: The authors declare that the research was conducted in the absence of any commercial or financial relationships that could be construed as a potential conflict of interest.

frontiers | Frontiers in Immunology

TYPE Original Research
PUBLISHED 25 July 2022
DOI 10.3389/fimmu.2022.882918

OPEN ACCESS

EDITED BY
Morten Agertoug Nielsen,
University of Copenhagen, Denmark

REVIEWED BY
Judith H Aberle,
Medical University of Vienna, Austria
Stephanie Longet,
University of Oxford, United Kingdom

*CORRESPONDENCE
Janis A. Müller
janismueller@uni-marburg.de

†These authors have contributed equally to this work and share first authorship

SPECIALTY SECTION
This article was submitted to Vaccines and Molecular Therapeutics, a section of the journal Frontiers in Immunology

RECEIVED 24 February 2022
ACCEPTED 28 June 2022
PUBLISHED 25 July 2022

CITATION
Seidel A, Zanoni M, Groß R, Krnavek D, Erdemci-Evin S, von Maltitz P, Albers DPJ, Conzelmann C, Liu S, Weil T, Mayer B, Hoffmann M, Pöhlmann S, Beil A, Kroschel J, Kirchhoff F, Münch J and Müller JA (2022) BNT162b2 booster after heterologous prime-boost vaccination induces potent neutralizing antibodies and T cell reactivity against SARS-CoV-2 Omicron BA.1 in young adults. *Front. Immunol.* 13:882918. doi: 10.3389/fimmu.2022.882918

BNT162b2 booster after heterologous prime-boost vaccination induces potent neutralizing antibodies and T cell reactivity against SARS-CoV-2 Omicron BA.1 in young adults

Alina Seidel[1†], Michelle Zanoni[1†], Rüdiger Groß[1†], Daniela Krnavek[1], Sümeyye Erdemci-Evin[1], Pascal von Maltitz[1], Dan P. J. Albers[1], Carina Conzelmann[1], Sichen Liu[1], Tatjana Weil[1], Benjamin Mayer[2], Markus Hoffmann[3,4], Stefan Pöhlmann[3,4], Alexandra Beil[5], Joris Kroschel[5], Frank Kirchhoff[1], Jan Münch[1,6] and Janis A. Müller[7,1*]

[1]Institute of Molecular Virology, Ulm University Medical Center, Ulm, Germany, [2]Institute for Epidemiology and Medical Biometry, Ulm University, Ulm, Germany, [3]Infection Biology Unit, German Primate Center – Leibniz Institute for Primate Research, Göttingen, Germany, [4]Faculty of Biology and Psychology, Georg-August-University Göttingen, Göttingen, Germany, [5]Central Department for Clinical Chemistry, University Hospital Ulm, Ulm, Germany, [6]Core Facility Functional Peptidomics, Ulm University Medical Center, Ulm, Germany, [7]Institute of Virology, Philipps University of Marburg, Marburg, Germany

In light of the decreasing immune protection against symptomatic SARS-CoV-2 infection after initial vaccinations and the now dominant immune-evasive Omicron variants, 'booster' vaccinations are regularly performed to restore immune responses. Many individuals have received a primary heterologous prime-boost vaccination with long intervals between vaccinations, but the resulting long-term immunity and the effects of a subsequent 'booster', particularly against Omicron BA.1, have not been defined. We followed a cohort of 23 young adults, who received a primary heterologous ChAdOx1 nCoV-19 BNT162b2 prime-boost vaccination, over a 7-month period and analysed how they responded to a BNT162b2 'booster'. We show that already after the primary heterologous vaccination, neutralization titers against Omicron BA.1 are recognizable but that humoral and cellular immunity wanes over the course of half a year. Residual responsive memory T cells recognized spike epitopes of the early SARS-CoV-2 B.1 strain as well as the Delta and BA.1 variants of concern (VOCs). However, the remaining antibody titers hardly neutralized these VOCs. The 'booster' vaccination was well tolerated and elicited both high antibody titers and increased memory T

cell responses against SARS-CoV-2 including BA.1. Strikingly, in this young heterologously vaccinated cohort the neutralizing activity after the 'booster' was almost as potent against BA.1 as against the early B.1 strain. Our results suggest that a 'booster' after heterologous vaccination results in effective immune maturation and potent protection against the Omicron BA.1 variant in young adults.

KEYWORDS

COVID-19, delta, B.1.1.529.1, BA.1, humoral immunity, memory T cells, ChadOx1 nCoV-19, vaccination interval

Introduction

Vaccination against the severe acute respiratory syndrome coronavirus 2 (SARS-CoV-2) is the key strategy to control the coronavirus disease 2019 (COVID-19) pandemic (1) and has already reduced incidences, hospitalizations, and deaths in several countries (2). Unfortunately, waning humoral immunity over time (3) and the emergence of immune evasive SARS-CoV-2 variants of concern (VOC) (4) impair vaccine effectiveness (5) and allow rebounds in infection rates (6, 7). The winter of 2021/2022 and the following summer came with the challenge of decreasing population immunity as initial vaccinations date back to early 2021 and the sudden appearance and rapid spread of the highly mutated immune evasive Omicron VOC (PANGO lineages B.1.1.529; BA.1, BA.2 and BA.3, BA.4, BA.5) (8–16). Therefore, 'booster' vaccinations are of enormous relevance to reestablish efficient protection (17, 18) and have been shown to induce humoral and cellular immune responses also against the Omicron VOC (9–14, 16, 19–21). 'Boosters' are performed as additional single vaccinations with a vaccine not necessarily matching the previous regimen. Generally, boosting triggers humoral and cellular responses. However, the degree might vary dependent on the specific combination of the initial vaccination regimen and the 'booster' vaccine (22). In at least 11 states of the European Union, individuals have received an initially unscheduled heterologous primary vaccination regimen consisting of a ChAdOx1 nCoV-19 (Vaxzevria, AstraZeneca) prime followed by a BNT162b2 (Comirnaty, BioNTech/Pfizer) boost after 8–12 weeks (23). This schedule had not been evaluated in clinical trials before application, but proven effective (24). The immunological responses were even superior to homologous vaccinations (25–28). However, the effect of a 'booster' following this regimen has not yet been described.

Here, we closely monitored the antibody titers and memory T cell immunity in a heterologously vaccinated cohort of young adults (25) over 7 months of follow-up and assessed the effect of a BNT162b2 'booster'. Our data show that immunity gradually declines over the course of 5.5 months but antibody and memory T cell responses are restored and increased after the 'booster'. Responsive T cells recognized all SARS-CoV-2 variants, while the Omicron BA.1 VOC efficiently evaded neutralization by antibodies induced by initial vaccination. Strikingly, in this young cohort of heterologously vaccinated individuals where the primary vaccination had a longer interval than typically in homologous vaccinations, the 'booster' induced humoral immune responses that neutralized the Omicron BA.1 VOC almost as effectively as the early B.1 strain.

Materials and methods

Study design

Our cohort of 26 hospital employees who received a primary vaccination consisting of a ChAdOx1 nCoV-19 prime followed by a BNT162b2 boost after an 8-week interval has been previously described (25) (Table 1). Of these individuals, 23 agreed to participate in a follow-up study determining the course of immunity over time. Participants were eligible for recruitment if they had received a primary ChAdOx1 nCoV-19 BNT162b2 prime-boost vaccination. SARS-CoV-2 infections were determined by medical history and by measuring anti-SARS-CoV-2-nucleocapsid antibody levels before beginning and at the last time point of the study. One convalescent individual was detected and excluded from all statistical analyses. At 6.5 months after the primary vaccination, 18 participants decided to get a BNT162b2 'booster' vaccination. Serum samples were taken every 1.5–2.5 months. In addition, of those participants who received a 'booster', 12 agreed to donate peripheral blood mononuclear cells (PBMCs).

TABLE 1 Study participants:.

	Serum			T cells		
	Total	m	f	Total	m	f
			Longitudinal follow-up			
Participants	23	8	15	12	6	6
Age median	29.5 (26-60)	32 (26-49)	30 (26-60)	36 (26-49)	36 (26-49)	35.5 (26-40)
Prior SARS-CoV-2 infection	1	0	1	0	0	0
			'Booster'			
Participants	18	8	10	12	6	6
Age median	29.5 (26-49)	32 (26-49)	29.5 (26-40)	36 (26-49)	36 (26-49)	35.5 (26-40)
Prior SARS-CoV-2 infection	0	0	0	0	0	0

Vaccine reactogenicity

Solicited adverse reactions (SAR) were self-reported by the participants *via* questionnaire following the 'booster' vaccination. Participants were asked to list symptoms, their duration (<1 h, few hours, 1 day or more than 1 day), and severity (mild (grade 1), moderate (grade 2), severe (grade 3)). Grading criteria were adapted from the US Department of Health and Human Services CTCEA (Common Terminology Criteria for Adverse Events, v4.03) (29), with grades 1–2 being considered for some symptoms, grade 1–3 for most, as previously described (25).

Collection of serum and PBMC samples

At 5.5 months after the heterologous primary vaccination, and 2 weeks (antibody titers peaked around 14–19 days post initial heterologous vaccination (25)) after the BNT162b2 'booster' (7 months post primary vaccination), blood was drawn into S-Monovette® Serum Gel (Sarstedt) or S-Monovette® K3 EDTA tubes. Serum gel collection tubes were centrifuged at 1,500 × g at 20°C for 15 min, aliquoted, and stored at -20°C until further use. PBMCs were obtained from EDTA tubes using density gradient centrifugation by Pancoll human (Pan Biotech, Germany), and erythrocytes were removed by ACK lysis buffer (Lonza, Walkersville, MD, USA). Mononuclear cells were counted for viability using a Countess II Automated Cell Counter (Thermo Fisher) with trypan blue stain and were cryopreserved in aliquots of up to 1×10^7 cells in 10% DMSO in heat-inactivated FCS.

Determination of antibody titers

IgG and IgM titers were measured as units per ml (U/ml) which correlates 1:1 with the WHO standard unit for the SARS-CoV-2 binding antibody units per ml (BAU/ml). To this end, serum was analysed using the commercial electrochemiluminescence Elecsys Anti-SARS-CoV-2 S immunoassay (Roche, Mannheim, Germany) by a cobas® e801 immunoassay analyser according to the manufacturer's instructions (Roche).

Cell culture

Vero E6 (African green monkey, female, kidney; CRL-1586, ATCC, RRID : CVCL_0574) cells were grown in Dulbecco's modified Eagle's medium (DMEM, Gibco) which was supplemented with 10% heat-inactivated foetal calf serum (FCS), 100 units/ml penicillin, 100 µg/ml streptomycin, 2 mM L-glutamine, 1 mM sodium pyruvate, and 1× non-essential amino acids. HEK293T (human, female, kidney; ACC-635, DSMZ, RRID: CVCL_0063) cells were grown in DMEM with supplementation of 10% FCS, 100 units/ml penicillin, 100 µg/ml streptomycin, and 2 mM L-glutamine. All cells were grown at 37°C in a 5% CO_2 humidified incubator. Cell lines were recently purchased from the indicated companies and used without further authentication. All cell lines were regularly tested for mycoplasma contamination and remained negative.

Preparation of pseudotyped viral particles

Expression plasmids for vesicular stomatitis virus (VSV, serotype Indiana) glycoprotein (VSV-G) and SARS-CoV-2 spike variants Wuhan-Hu-1 D614G (B.1) (30), Delta (B.1.617.2) (31), and Omicron (B.1.1.529.1; BA.1) (9) (codon-optimized; with a C-terminal truncation for increased pseudovirus packaging) have been described elsewhere (32). Transfection of cells was carried out by Transit LT-1 (Mirus). Rhabdoviral pseudotype particles were prepared as previously described (33). A replication-deficient VSV vector in which the

genetic information for VSV-G was replaced by genes encoding two reporter proteins enhanced green fluorescent protein and firefly luciferase (FLuc) and VSV∗ΔG-FLuc (34) (kindly provided by Gert Zimmer, Institute of Virology and Immunology, Mittelhäusern, Switzerland (34)) was used for pseudotyping. One day after transfection of HEK293T cells to express the viral glycoprotein, they were inoculated with VSV∗ΔG-FLuc and incubated for 1–2 h at 37°C. Then the inoculum was removed, cells were washed with PBS, and fresh medium was added. After 16–18 h, the supernatant was collected and centrifuged (2,000 × g, 10 min, room temperature) to clear cellular debris. Cell culture medium containing anti-VSV-G antibody (I1-hybridoma cells; ATCC no. CRL-2700) was then added to block residual VSV-G-containing particles. Samples were then aliquoted and stored at -80°C.

Pseudovirus neutralization assay

For pseudovirus neutralization experiments, Vero E6 cells were seeded in 96-well plates 1 day prior (6,000 cells/well) in medium containing 2.5% FCS. Heat-inactivated (56°C, 30 min) sera were serially titrated (fourfold titration series with seven steps + buffer only control) in PBS, pseudovirus stocks added (1:1, v/v), and the mixtures incubated for 30 min at 37°C before being added to cells in duplicates (final on-cell dilution of sera: 20; 80; 320; 1,280; 5,120; 20,480; 81,920-fold). After an incubation period of 16–18 h, transduction efficiency was analysed. For this, the supernatant was removed, and cells were lysed by incubation with Cell Culture Lysis Reagent (Promega) at room temperature. Lysates were then transferred into white 96-well plates, and luciferase activity was measured using a commercially available substrate (Luciferase Assay System, Promega) and a plate luminometer (Orion II Microplate Luminometer, Berthold). For analysis of raw values (RLU/s), the background signal of an uninfected plate was subtracted and values normalized to pseudovirus treated with PBS only. Results are given as serum dilution resulting in 50% pseudovirus neutralization (PVNT50) on cells, calculated by non-linear regression ([Inhibitor] vs. normalized response – Variable slope) in GraphPad Prism Version 9.1.1.

Determination of SARS-CoV-2 spike-specific $CD4^+$ and $CD8^+$ T cell responses by intracellular cytokine staining (ICS)

Cryopreserved PBMCs of study participants were thawed and rested overnight at 37°C with 1 µl/ml of DNase (DNase I recombinant, RNase-free (10,000 U) Roche), in RPMI medium supplemented to contain a final concentration of 10% FCS, 10 mM HEPES, 1× MEM non-essential amino acids (Corning Life Sciences/Media Tech Inc., Manassas, VA), 1 mM sodium pyruvate (Lonza, Walkersville, MD, USA), 1 mM penicillin/streptomycin, and 1× 2-mercaptoethanol (Gibco, Invitrogen, Carlsbad, CA, USA). Stimulation of PBMCs for detection of cytokine production by T cells was adapted from Kasturi et al. (2020) (35). Briefly, 1×10^6 PBMCs were cultured in 200 µl final volume in a 96-well U bottom plate in the presence of 1 µg/ml anti-CD28 and anti-CD49d (BioLegend) under the following conditions: a) negative DMSO control, b) 2 µg/ml SARS-CoV-2 spike peptide pools (1-315 peptides from Wuhan-Hu-1, Delta (B.1.617.2), and Omicron (B.1.1.529.1; BA.1) SARS-CoV-2 spike, JPT Germany), c) 2 µg/ml of CEFX Ultra Super Stim peptide pool (176 peptide epitopes for a broad range of HLA subtypes of 18 different infectious agents including clostridium tetani, coxsackievirus B4, influenza A virus, haemophilus influenza, helicobacter pylori, human adenovirus 5, human herpesvirus 1/2, human herpesvirus 3, human herpesvirus 4, human herpesvirus 5, human herpesvirus 6, human papillomavirus, JC polyomavirus, measles virus, rubella virus, toxoplasma gondii, and vaccinia virus, JPT Germany) as SARS-CoV-2 vaccination-independent control of d) positive control phorbol 12-myristate 13-acetate (PMA) (50 ng/ml) and ionomycin (500 ng/ml). Cells were cultured for 2 h before adding 10 µg/ml brefeldin A (Sigma-Aldrich, St. Louis, MO) for an additional 5 h. Cells were then washed with PBS and prestained for dead cells (Live/Dead Fixable; Aqua from Thermo Fisher) and for the chemokine receptor 7 by APC/Cy7-anti-human CCR7 (clone G043H7) for 30 min at 37°C, 5% CO_2. Cells were incubated with surface antibody cocktail (prepared in 1:1 of FACS buffer and brilliant staining buffer) for 30 min at room temperature with BV510-anti-human CD14 (clone M5E2), BV510-anti-human CD19 (clone HIB19), AF700 anti-human CD3 (clone OKT3), BV605 CD4 (clone OKT4), PerCP-Cy5.5 CD8 (clone RPA-T8), and PE/Fire 700-anti-human CD45RA (clone HI100) from BioLegend. Next, cells were fixed using Cytofix/Cytoperm buffer (BD Biosciences, CA) for 20 min at room temperature and then kept in FACS buffer at 4°C overnight. Perm/Wash (1×, BD Biosciences, CA) was used for cell permeabilization for 10 min at room temperature followed by intracellular staining for 30 min at room temperature with AF647 anti-human IFNγ (clone 4S.B3) and AF488 anti-human IL-2 (clone MQ1-17H12) from BioLegend, and PE/Cy7 anti-human TNFα (clone Mab11) from Thermo Fisher Scientific. Up to 100,000 live $CD3^+$ T cells were acquired on an LSRFortessa flow cytometer (BD Biosciences), equipped with FACSDiva software. Analysis of the acquired data was performed using FlowJo software (version 10.7.1). The background was corrected by subtracting the signal of the DMSO control from the spike-treated cells.

Statistical analysis

The SARS-CoV-2 convalescent individual was excluded in all statistical analyses. Non-parametric Spearman rank correlation was used to check for possible associations at single blood sample measurements. To include neutralizing antibody titers lower than the detection limit of 20, values were set to 10. Longitudinal antibody measurements were analysed by means of a mixed linear regression model including a random intercept to account for the repeated-measure structure of the underlying data. The mixed linear model approach enabled to simultaneously account for possible confounding due to participants' age and for the presence of missing data (36). Therefore, no formal imputation of missing interim values was required. Comparison between variants and of T cell responsiveness was done by the Mann–Whitney-U test because of skewed distributions and with Wilcoxon signed-rank test for matched pairs. A two-sided alpha error of 5% was applied to analyses. All analyses were done by GraphPad Prism version 9.1.1 for Windows, GraphPad Software, San Diego, CA, USA, www.graphpad.com, R (version 4.0.1) and SAS (version 9.4).

Results

A previously described cohort of 26 individuals, of whom one had a history of SARS-CoV-2 infection, received a primary vaccination of a heterologous ChAdOx1 nCoV-19 prime and BNT162b2 boost within an 8-week interval in early 2021 (25). We performed a follow-up study of this young cohort (23 participants, median age 29.5 years, Table 1) for a duration of 7 months after primary vaccination and analysed humoral and cellular immunity over time, as well as reactogenicity and immune responses after a BNT162b2 'booster' vaccination 6.5 months later (18 participants).

The 'booster' vaccination was well tolerated and associated with a lower overall reactogenicity compared to the initial two heterologous doses (25). The major solicited adverse reactions were pain at the injection site (94%, 17/18 participants), fatigue (44.4%, 8/18), and headache (33.3%, 6/18). No serious adverse events were observed (Figure 1).

As described previously (25), 2 weeks after primary vaccination, the cohort showed median cumulative anti-SARS-CoV-2-spike IgM and IgG (IgM/G) titers of 8,815 (1,206–19,046) BAU/ml, which decreased to 2,039 (235–5,926) BAU/ml over the course of 3 months. In the (slightly smaller) follow-up cohort, they further declined to 1,120 (125–3,287) BAU/ml after 5.5 months, corresponding to an eightfold decrease (Figure 2A). After 6.5 months, 18 of the participants (median 1,243 BAU/ml) received a BNT162b2 'booster'. Two weeks later, the median IgM/G titers had increased by 21-fold to 25,775 BAU/ml (2,092–49,627; $p < 0.001$, mixed model) in boosted individuals, while further decreasing to 753 (474–3,076, $p = 0.0186$, mixed model) BAU/ml in non-boosted participants (Figure 2A). This corresponds to a 34-fold higher median titre in the boosted versus non-boosted group at the 7-month time point ($p = 0.0033$, mixed model) and exceeds the initial titers

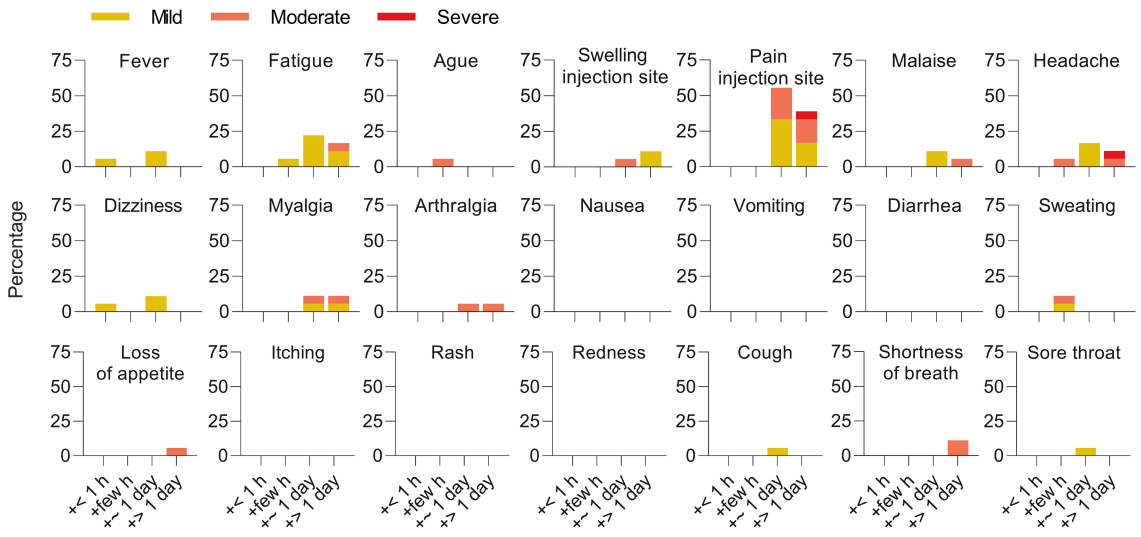

FIGURE 1
Reactogenicity of a 'booster' after heterologous primary vaccination. Solicited adverse reactions following BNT162b2 'booster' vaccination. Percentages of n = 18 participants with individual symptoms following vaccination are shown. Severity is graded on a scale of 1–2 (for some symptoms) or 1–3 (for most), as adapted from the Common Terminology Criteria for Adverse Events (US Department of Health and Human Services, Version 4.03).

determined after the primary vaccination by ~2-fold [median 11,339 BAU/ml (25)].

Using vesicular stomatitis virus (VSV)-based pseudoviruses (PVs) carrying the SARS-CoV-2 spike protein, we analysed the neutralizing activity of the sera. Two weeks after the primary vaccination, median 50% pseudovirus neutralization (PVNT50) titers against PV carrying the SARS-CoV-2 Wuhan-Hu-1 D614G (B.1) spike protein were 2,418 (350–6,383). PVNT50 titers remained stable for 1.5 months but decreased 12-fold to 204 (24–601) over the course of 5.5 months (Figure 2B, $p < 0.0001$, mixed model). In comparison, titers against the Delta VOC after 5.5 months were eightfold lower with median titers of 24 (<20–481) (Figures 2B, S1, $p < 0.0001$, mixed model). In contrast to studies on homologous vaccinations, but in line with other studies on sera from heterologously vaccinated individuals (9, 15, 37), median neutralization titers of 345 (<20–4541) were already detected against the Omicron BA.1 VOC 2 weeks after primary vaccination in 15/16 (94%) participants. These titers decayed to <20 (<20–299) after 5.5 months, with 12/22 (55%) participants showing no detectable neutralizing activity at all. This corresponds to a 7–20-fold immune evasion compared to B.1 (Figures 2B, S1, $p < 0.0001$, mixed model). After the 'booster', titers against the B.1 variant increased ninefold to 1,929 (474–4,942), 45-fold to 1,094 (51–2,895) for Delta, and >88-fold to 1,768 (<20–3,760) against BA.1 (Figures 2B, C, S1, $p < 0.0001$, mixed model). Strikingly, the neutralizing titers 2 weeks after the 'booster' against Delta and BA.1 were similar and only slightly lower than for B.1 (Figures 2B, C, S1, $p = 0.9608$, $p = 0.0198$, $p = 0.0211$, mixed model). At 5.5 months after primary vaccination, the neutralizing activity correlated weakly with IgM/G titers; however, after the 'booster' (7 months after primary vaccination), the correlation was highly significant for all variants, indicating that induction of high titers is associated with potent neutralization (Figure 2D, $r \geq 0.73$,

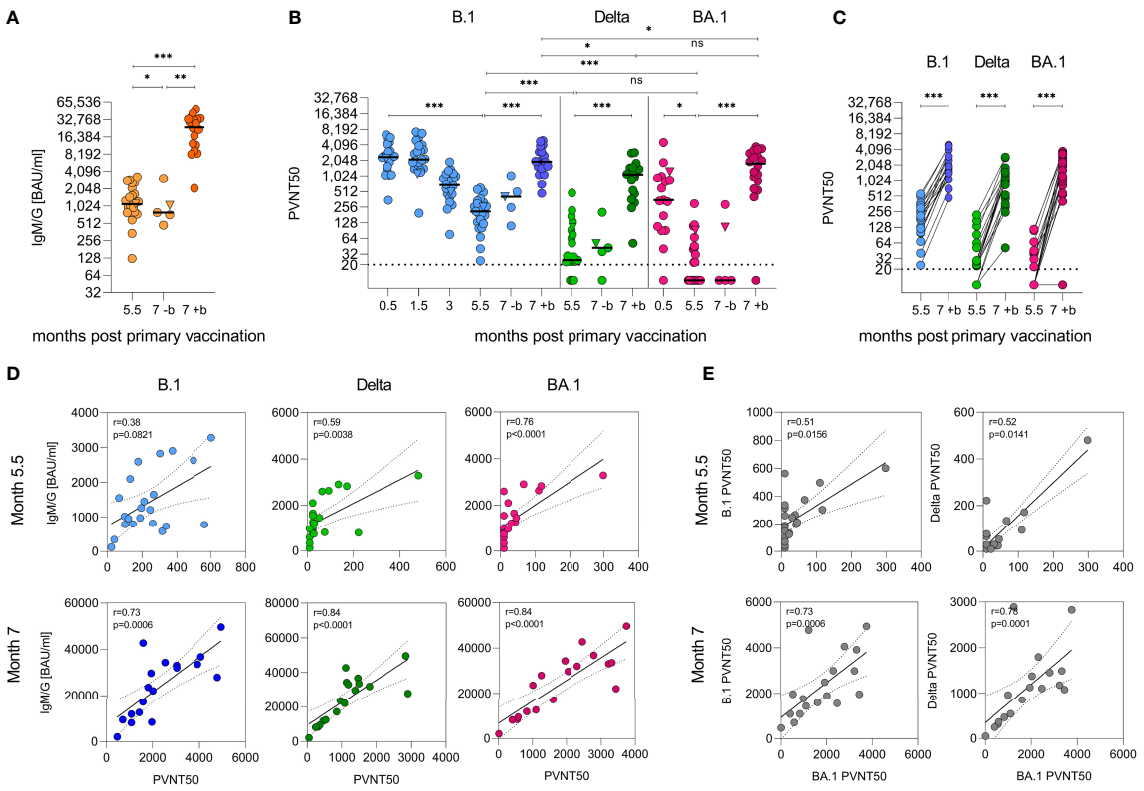

FIGURE 2
Humoral immunity against SARS-CoV-2 after heterologous vaccination followed by a 'booster' vaccination. **(A)** Quantification of cumulative anti-SARS-CoV-2 spike IgG and IgM responses as binding antibody units per ml (BAU/ml) by immunoassay with (+b) or without (-b) 'booster' after 6.5 months. **(B)** VSV-based B.1, Delta, and Omicron (BA.1) SARS-CoV-2 spike pseudovirus neutralization assay. Titers expressed as serum dilution resulting in 50% pseudovirus neutralization (PVNT50) were obtained from three experiments in duplicate infections. Triangle indicates SARS-CoV-2 convalescent individual, who was excluded from all statistical analyses. Dashed horizontal lines indicate lower limit of detection. Samples were obtained from n = 23 participants. Booster samples were taken 2 weeks after vaccination. Longitudinal antibody measurements were analysed by means of a mixed linear regression model. **(C)** Data from **(B)** illustrated as paired values pre and post 'booster'. **(D)** Spearman correlation of IgG/IgM and neutralizing titers and **(E)** between neutralizing titers, two-tailed p values, dashed lines indicate 95% confidence interval. ***p < 0.001, **p < 0.01, *p < 0.05, ns, not significant..

Spearman). Notably, the neutralizing titers obtained for the three variants correlated only weakly before but became strongly significant after the 'booster' immunization (**Figure 2E**, r ≥ 0.73, Spearman). These results indicate that the 'booster' induces broadly neutralizing antibodies that are even effective against the highly divergent Omicron BA.1 variant. Results were not confounded by participant age or sex.

To evaluate cellular immunity, we isolated peripheral blood mononuclear cells (PBMCs) from blood samples provided by 12 participants 5.5 months after the primary vaccination, as well as samples 2 weeks after the 'booster'. Cells were exposed to pools of 315 peptides spanning the spike sequences of SARS-CoV-2 Wuhan-Hu-1 (Wu), Delta (B.1.617.2), or Omicron (B.1.1.529.1; BA.1) and analysed for intracellular cytokines IFNγ, IL-2, and TNFα. Increased cytokine production upon peptide stimulation was evaluated to determine responsive and spike-specific $CD4^+$ and $CD8^+$ memory T cells (Figures S2, S3). At 5.5 months after primary vaccination, only five of the 12 donors showed remaining $CD4^+$ memory T cells responding to either spike peptide stimulation by IL-2 or TNFα production, respectively (Figure 3). In contrast, most participants (10 of 12) showed remaining memory $CD4^+$ T cells responding by IFNγ production (median 0.005%–0.011% reactive cells). Notably, the magnitude of responses to SARS-CoV-2 BA.1 spike did not differ from Wu or Delta (Figure 3, $p > 0.05$, Mann–Whitney-U), indicating efficient cross-reactivity. After the 'booster', spike-specific IFNγ $CD4^+$ memory T cell responses and the fraction of reactive cells further increased to 11 of 12 participants and the median ranged from 0.02% to 0.04% responsive cells for the spike peptide variants ($p = 0.0273$, $p = 0.0137$, $p = 0.0098$; Wilcoxon signed-rank). However, $CD4^+$ T cells responding by IL-2 or TNFα secretion were not affected by the 'booster'. $CD8^+$ memory T cells showed a longer durability and typically remained reactive over the course of 5.5 months, with 8 of 12 participants responding to Wu, Delta, or BA.1 spike peptide challenge by IL-2 (0.004%–0.009%), all by TNFα (0.027%–0.052%) and IFNγ production (0.055%–0.081%) (Figure 3). Again, the 'booster' significantly enhanced IFNγ responses for all variants (0.105%–0.208%) (Figure 3, $p = 0.0005$, $p = 0.0049$, $p = 0.0137$; Wilcoxon signed-rank). IL-2 and TNFα responses also showed an increase, but not significant. Stimulation with a pool of 176 peptide epitopes from 18 infectious agents (CEFX) confirmed that the 'booster' did not unspecifically affect T cell responses. Of note, 11 of 12 participants developed $CD4^+$ and all participants $CD8^+$ T cell memory against BA.1. Altogether, 5.5 months after heterologous vaccination participants showed stable $CD8^+$ memory T cell levels but a decreased humoral and $CD4^+$ memory T cell immunity. A BNT162b2 'booster', however, reactivated and enhanced T cell immunity and induced potent antibody responses also against the Omicron BA.1 VOC.

Discussion

Heterologous primary ChAdOx1 nCoV-19 prime, BNT162b2 boost vaccination induces potent immune responses against SARS-CoV-2 (25–28) resulting in effective protection from COVID-19 (24). Data about long-term immunity and protection conferred by this vaccination regimen, as well as reaction toward a 'booster' vaccination and its efficacy toward the Omicron VOC, are, however, scarce, in particular for younger individuals (24). T cells generally show broad cross-reactivity against SARS-CoV-2 variants (25, 38) including Omicron (39–41), which is expected, because the majority of mutations in the Omicron spike are not located in known T cell epitopes (42, 43) and because the large HLA allele diversity on population level makes T cell evasion unlikely (44). In contrast, BA.1 showed neutralization-evading properties (9–14, 20, 21) which consequently results in loss of protection from symptomatic infection (45–47). Thus, 'booster' vaccinations are performed aiming for enhanced immune protection especially from Omicron (9–14, 16, 19–21). 'Booster' vaccinations after homologous BNT162b2 or ChAdOx1 nCoV-19 vaccination regimen have been described as safe (22) and shown to restore protection from the Delta VOC (17, 18) and to reduce Omicron breakthrough infections and the secondary attack rate (48).

We here show for a young cohort with a median age of 29.5 years that heterologous primary vaccination already resulted in antibody titers with moderate Omicron BA.1-neutralizing activity, which declined over the course of 5.5 months to levels hardly neutralizing this VOC. In line, spike-specific $CD4^+$ memory T cells showed remaining but limited reactivity 5.5 months after heterologous vaccination. However, $CD8^+$ memory T cells remained responsive and also reacted to BA.1 spike epitopes. This is in line with the observation that individuals that received homologous primary vaccination remain partly protected from hospitalization upon Omicron infection (49–51) but also with the fact that Omicron shows increased breakthrough infections (52). The 'booster' resulted in lower reactogenicity than determined in the first two vaccinations (25) and elicited both high antibody titers and enhanced memory T cell responses against the tested SARS-CoV-2 variants including BA.1. Strikingly, the induced neutralizing antibodies were as potent against BA.1 as against Delta and almost as potent as against B.1. This is in contrast to earlier studies focusing on homologous short-interval primary vaccinations that also found 'boosters' to induce BA.1-neutralizing titers but where this variant still shows some degree of evasion (9–14, 20, 21). This highlights the major benefits of a third dose regimen (50, 51, 53) especially after heterologous primary vaccination in young adults to protective humoral and cellular immunity against SARS-CoV-2 variants.

In this cohort, the BNT162b2 'booster' induced titers that were neutralizing BA.1 almost as potently as B.1. In light of the immune evasive properties of Omicron and the results from studies on homologous vaccinations, this finding is somewhat surprising. As potential confounding factors, unnoticed SARS-CoV-2 infection of

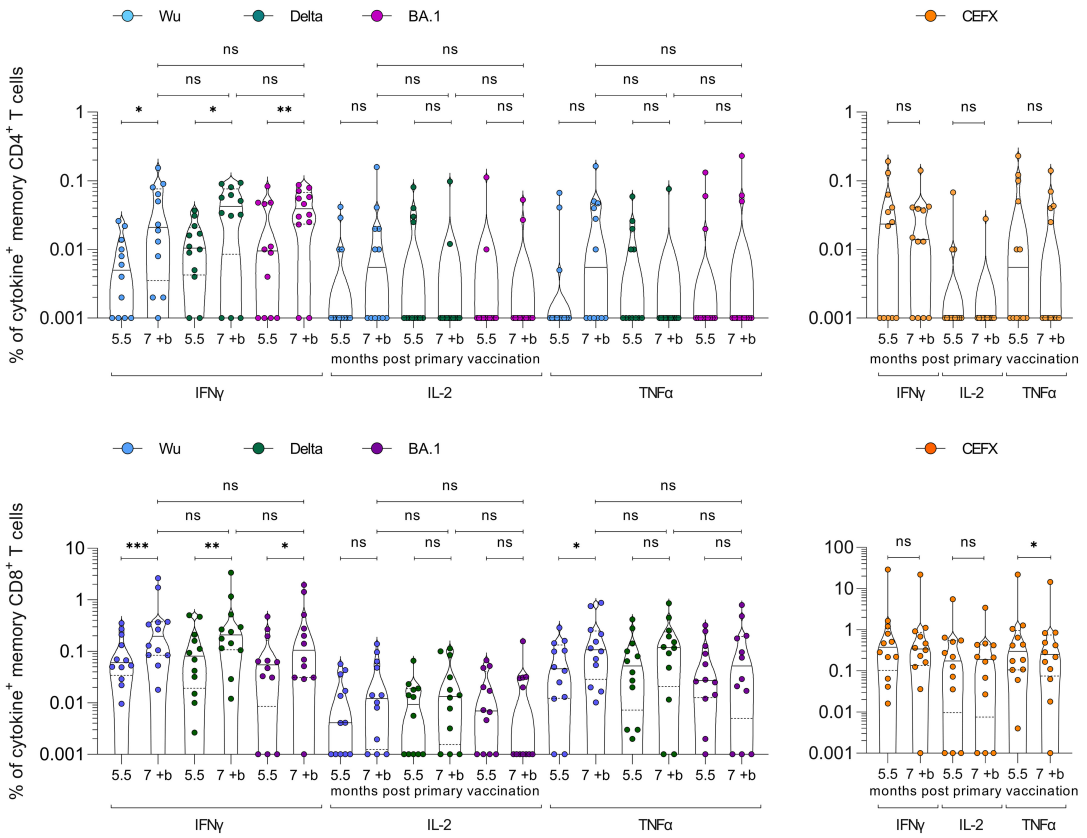

FIGURE 3
SARS-CoV-2 spike-specific $CD4^+$ and $CD8^+$ memory T cell responses after heterologous vaccination followed by a 'booster' vaccination. PBMCs isolated from samples of n = 12 study participants were obtained 5.5 months after the heterologous primary vaccination, and 2 weeks after the BNT162b2 'booster' (7 months post primary vaccination). PBMCs were stimulated with SARS-CoV-2 Wuhan-Hu-1 (Wu), Delta, or Omicron (BA.1) spike peptide-pool (left panels) or control pools of different infectious agents (CEFX, right panels) and cytokine production determined by flow cytometry. $CD4^+$ (upper panel) and $CD8^+$ (lower panel) memory T cells were gated and analysed for IFNγ, IL-2, and TNFα cytokine production. Cytokine$^+$ T cells were background-corrected for unstimulated cells (Figures S2, S3), and zero values set to 0.001%. Wilcoxon matched-pair signed-rank test compares cytokine-positive cells before and after the 'booster'. Mann–Whitney-U test compares cytokine-positive cells post 'booster' between variants. ***p < 0.001, **p < 0.01, *p < 0.05, ns, not significant.

the participants was excluded by nucleocapsid antibody detection and adequate sensitivity of the used neutralization assay has been validated previously (54). Therefore, this exceptionally efficient neutralization of BA.1 is most likely due to the extremely high antibody levels after the 'booster' as well as the long-term germinal center reaction, ongoing affinity maturation after vaccination (55), and reactivation of memory B cells (56). The Delta VOC was also potently neutralized after the 'booster', resulting in titers that were lower than against B.1 but similar to BA.1, indicating immune evasion by these VOCs but at the same time a broad cross-reactivity of 'booster'-induced antibodies. These remarkable potent and broadly active antibodies might be a result of the heterologous vaccination where DNA and mRNA vaccines encoding non- and pre-fusion-stabilized spike protein variants are mixed (57). Another explanation for the strikingly effective neutralization of the Omicron BA.1 VOC might be the relatively young age and associated potent immunity (58–61) of the here analysed cohort with median age of 29.5 years. Also timing might play a role, as the intervals in the primary vaccination and between the 'booster' influence humoral as well as cellular responses (62, 63). Studies on homologous primary BNT162b2 vaccinations with a 3-week interval detected neutralizing titers of 306–604 against B.1 but only undetectable-13 against BA.1 (9–11, 20, 21). In our study, we already detected a titre of 345 after primary vaccination, and similar results have been obtained in other studies looking at BA.1 neutralization of sera from heterologously ChAdOx1-BNT162b2-vaccinated individuals with an interval of 8–12 weeks (9, 15, 37). This is in line with the finding that longer intervals in heterologous or homologous primary vaccinations result in higher neutralization capacities of SARS-CoV-2 VOCs (21, 28, 62, 64–66). This might be attributed to ongoing antibody maturation before primary boost (55, 56, 67) as has also been observed for vaccination against influenza virus (68). Thus, the typically longer interval within heterologous primary vaccination might result in affinity

maturation already before the second vaccine dose and explain the strikingly potent cross-neutralization of BA.1 after the 'booster'.

After the 'booster', memory $CD4^+$ T cells became strongly reactive toward SARS-CoV-2 spike peptides of all variants. Also the reactivity of the residual $CD8^+$ T cells was further enhanced by the 'booster' dose, which agrees with data after homologous primary vaccinations showing that a third dose enhances preexisting cellular responses (69, 70). The finding that SARS-CoV-2-specific T cells are generally reactive to spike peptides derived from the Omicron VOC is supported by recent data (19, 40, 70) and suggests that the 'booster' might also enhance protection of Omicron-infected individuals from severe disease (71).

The Omicron VOC seems to form a new antigenic cluster (72–74), of which the BA.2 variant has rapidly expanded, now followed by BA.5. First results indicate that neutralization capacity is similar between BA.1 and BA.2 (75, 76) and lower against BA.5 (77, 78); however, the general cross-reactivity of T cells suggests that the 'booster' is likely also effective against these variants. Therefore, it will now be of importance to elucidate the longevity of humoral and cellular immunity after the 'booster' against circulating variants and most importantly its durable effectiveness in preventing infection and disease (79). In addition, fourth vaccine doses (80) or an adaptation of the vaccines to BA.1 (81) need yet to be proven useful to provide effective protection from these old and new variants. Yet unvaccinated individuals might benefit from an updated vaccine that establishes a high degree of protection against Omicron already after two doses. Altogether, our results suggest that a 'booster' 6 months after initial heterologous vaccination of young adults induces good humoral and cellular protection against SARS-CoV-2 Omicron, even though the antigen of immunization is the ancestral Wuhan-Hu-1 spike. Thus, a 'booster' following the heterologous vaccination is highly warranted especially in the light of the immune evading Omicron variants.

Data availability statement

The raw data supporting the conclusions of this article will be made available by the authors, without undue reservation.

Ethics statement

The studies involving human participants were reviewed and approved by the ethics committee of Ulm University. The patients/participants provided their written informed consent to participate in this study.

Author contributions

Conceptualization, JMü, JM, AS, MZ, RG. Funding acquisition, JMü, JM, FK, SP. Investigation, AS, MZ, RG, DK, SE-E, DA, CC, SL, PM, TW, AB, JK, JMü. Essential resources, BM, MH, SP, FK, JM, JMü. Writing, JMü, AS, MZ, RG. Review and editing, all authors. AS, MZ, RG contributed equally. AS, MZ, RG and JMü verified the underlying data. All authors read and approved the final version of the manuscript.

Funding

This project has received funding from the European Union's Horizon 2020 research and innovation programme under grant agreement no. 101003555 (Fight-nCoV) to JM, the German Research Foundation (CRC 1279) to FK and JM, MU 4485/1-1 to JMü, the BMBF to FK (Restrict SARS-CoV-2), and the Robert Koch Institute (RKI). Additional funding was provided to SP from BMBF (01KI1723D, 01KI20328A, 01KI20396, 01KX2021) and the county of Lower Saxony (14-76103-184, MWK HZI COVID-19) and to JM by the DFG (KL 2544/8-1, FR 2974/3-1).

Acknowledgments

We thank all participants for regular blood donations. We thank Nicola Schrott, Regina Burger, Jana Romana Fischer, and Birgit Ott for skilful laboratory assistance. We thank Sarah Warth and Simona Ursu of the flow cytometry core facility for support with flow cytometric analysis. R.G., A.S., C.C, and T.W. are part of the International Graduate School in Molecular Medicine Ulm.

Conflict of interest

The authors declare that the research was conducted in the absence of any commercial or financial relationships that could be construed as a potential conflict of interest.

Publisher's note

Supplementary material

The Supplementary Material for this article can be found online at: https://www.frontiersin.org/articles/10.3389/fimmu.2022.882918/full#supplementary-material..

References

1. Mathieu E, Ritchie H, Ortiz-Ospina E, Roser M, Hasell J, Appel C, et al. A global database of COVID-19 vaccinations. *Nat Hum Behav* (2021) 5:947–53. doi: 10.1038/s41562-021-01122-8

2. Meslé MM, Brown J, Mook P, Hagan J, Pastore R, Bundle N, et al. Estimated number of deaths directly averted in people 60 years and older as a result of COVID-19 vaccination in the WHO European region, December 2020 to November 2021. *Eurosurveillance* (2021) 26:1–8. doi: 10.2807/1560-7917.ES.2021.26.47.2101021

3. Levin EG, Lustig Y, Cohen C, Fluss R, Indenbaum V, Amit S, et al. Waning immune humoral response to BNT162b2 covid-19 vaccine over 6 months. *N Engl J Med* (2021) e84:1–11. doi: 10.1056/NEJMoa2114583

4. Lazarevic I, Pravica V, Miljanovic D, Cupic M. Immune evasion of SARS-CoV-2 emerging variants: What have we learnt so far? *Viruses* (2021) 13:1192. doi: 10.3390/v13071192

5. Tartof SY, Slezak JM, Fischer H, Hong V, Ackerson BK, Ranasinghe ON, et al. Effectiveness of mRNA BNT162b2 COVID-19 vaccine up to 6 months in a large integrated health system in the USA: a retrospective cohort study. *Lancet (London England)* (2021) 2:1–10. doi: 10.1016/S0140-6736(21)02183-8

6. Goldberg Y, Mandel M, Bar-On YM, Bodenheimer O, Freedman L, Haas EJ, et al. Waning immunity after the BNT162b2 vaccine in Israel. *N Engl J Med* (2021) 385:e85. doi: 10.1056/NEJMoa2114228

7. Gupta RK, Topol EJ. COVID-19 vaccine breakthrough infections. *Sci (80-)* (2021) 374:1561–2. doi: 10.1126/science.abl8487

8. Viana R, Moyo S, Amoako DG, Tegally H, Scheepers C, Althaus CL, et al. Rapid epidemic expansion of the SARS-CoV-2 omicron variant in southern Africa. *Nature* (2022) 603:679–86. doi: 10.1038/d41586-021-03832-5. 2021.12.19.21268028.

9. Hoffmann M, Krüger N, Schulz S, Cossmann A, Rocha C, Kempf A, et al. The omicron variant is highly resistant against antibody-mediated neutralization: Implications for control of the COVID-19 pandemic. *Cell* (2022) 185:447–456.e11. doi: 10.1016/j.cell.2021.12.032

10. Gruell H, Vanshylla K, Tober-Lau P, Hillus D, Schommers P, Lehmann C, et al. mRNA booster immunization elicits potent neutralizing serum activity against the SARS-CoV-2 omicron variant. *Nat Med* (2022) 28:477–80. doi: 10.1038/s41591-021-01676-0

11. Garcia-Beltran WF, St. Denis KJ, Hoelzemer A, Lam EC, Nitido AD, Sheehan ML, et al. mRNA-based COVID-19 vaccine boosters induce neutralizing immunity against SARS-CoV-2 omicron variant. *Cell* (2022) 185:457–466.e4. doi: 10.1016/j.cell.2021.12.033

12. Schmidt F, Muecksch F, Weisblum Y, Da Silva J, Bednarski E, Cho A, et al. Plasma neutralization of the SARS-CoV-2 omicron variant. *N Engl J Med* (2022) 386:599–601. doi: 10.1056/NEJMc2119641

13. Wilhelm A, Widera M, Grikscheit K, Toptan T, Schenk B, Pallas C, et al. Reduced neutralization of SARS-CoV-2 omicron variant by vaccine sera and monoclonal antibodies. *medRxiv* (2021). doi: 10.1101/2021.12.07.21267432. 2021.12.07.21267432.

14. Zeng C, Evans JP, Qu P, Faraone J, Zheng Y-M, Carlin C, et al. Neutralization and stability of SARS-CoV-2 omicron variant. *bioRxiv* (2021). doi: 10.1101/2021.12.16.472934. 2021.12.16.472934.

15. Rössler A, Riepler L, Bante D, von Laer D, Kimpel J. SARS-CoV-2 omicron variant neutralization in serum from vaccinated and convalescent persons. *N Engl J Med* (2022) 386:698–700. doi: 10.1056/NEJMc2119236

16. Doria-Rose NA, Shen X, Schmidt SD, McDanal C, Feng W, Tong J, et al. Booster of mRNA-1273 strengthens SARS-CoV-2 omicron neutralization. *medRxiv* (2021). doi: 10.1101/2021.12.15.21267805. 2021.12.15.21267805.

17. Arbel R, Hammerman A, Sergienko R, Friger M, Peretz A, Netzer D, et al. BNT162b2 vaccine booster and mortality due to covid-19. *N Engl J Med* (2021) 385:2413–20. doi: 10.1056/NEJMoa2115624

18. Barda N, Dagan N, Cohen C, Hernán MA, Lipsitch M, Kohane IS, et al. Effectiveness of a third dose of the BNT162b2 mRNA COVID-19 vaccine for preventing severe outcomes in Israel: An observational study. *Lancet* (2021) 398:2093–100. doi: 10.1016/S0140-6736(21)02249-2

19. Jergović M, Coplen CP, Uhrlaub JL, Beitel SC, Burgess JL, Lutrick K, et al. Cutting edge: T cell responses to B.1.1.529 (Omicron) SARS-CoV-2 variant induced by COVID-19 infection and/or mRNA vaccination are largely preserved. *J Immunol* (2022) 208:2461–5. doi: 10.4049/jimmunol.2200175

20. Planas D, Saunders N, Maes P, Guivel-Benhassine F, Planchais C, Buchrieser J, et al. Considerable escape of SARS-CoV-2 omicron to antibody neutralization. *Nature* (2022) 602:671–5. doi: 10.1038/s41586-021-04389-z

21. Belik M, Jalkanen P, Lundberg R, Reinholm A, Laine L, Väisänen E, et al. Comparative analysis of COVID-19 vaccine responses and third booster dose-induced neutralizing antibodies against delta and omicron variants. *Nat Commun* (2022) 13:2476. doi: 10.1038/s41467-022-30162-5

22. Munro APS, Janani L, Cornelius V, Aley PK, Babbage G, Baxter D, et al. Safety and immunogenicity of seven COVID-19 vaccines as a third dose (booster) following two doses of ChAdOx1 nCov-19 or BNT162b2 in the UK (COV-BOOST): a blinded, multicentre, randomised, controlled, phase 2 trial. *Lancet* (2021) 398:2258–76. doi: 10.1016/S0140-6736(21)02717-3

23. European Medicines Agency. Heterologous primary and booster COVID-19 vaccination. In: *Biol heal threat vaccine strateg off (COVID-ETF), EMA pandemic task force COVID-19* Amsterdam, Netherlands: European Medicines Agency (2021). EMA/349565/2021.

24. Nordström P, Ballin M, Nordström A. Effectiveness of heterologous ChAdOx1 nCoV-19 and mRNA prime-boost vaccination against symptomatic covid-19 infection in Sweden: A nationwide cohort study. *Lancet Reg Heal - Eur* (2021) 11:100249. doi: 10.1016/j.lanepe.2021.100249

25. Groß R, Zanoni M, Seidel A, Conzelmann C, Gilg A, Krnavek D, et al. Heterologous ChAdOx1 nCoV-19 and BNT162b2 prime-boost vaccination elicits potent neutralizing antibody responses and T cell reactivity against prevalent SARS-CoV-2 variants. *EBioMedicine* (2022) 75:103761. doi: 10.1016/j.ebiom.2021.103761

26. Borobia AM, Carcas AJ, Pérez-Olmeda M, Castaño L, Bertran MJ, García-Pérez J, et al. Immunogenicity and reactogenicity of BNT162b2 booster in ChAdOx1-s-primed participants (CombiVacS): A multicentre, open-label, randomised, controlled, phase 2 trial. *Lancet* (2021) 398:121–30. doi: 10.1016/S0140-6736(21)01420-3

27. Hillus D, Schwarz T, Tober-Lau P, Vanshylla K, Hastor H, Thibeault C, et al. Safety, reactogenicity, and immunogenicity of homologous and heterologous prime-boost immunisation with ChAdOx1 nCoV-19 and BNT162b2: a prospective cohort study. *Lancet Respir Med* (2021) 2600:1255–65. doi: 10.1016/S2213-2600(21)00357-X. 2021.05.19.21257334.

28. Pozzetto B, Legros V, Djebali S, Barateau V, Guibert N, Villard M, et al. Immunogenicity and efficacy of heterologous ChAdOx1–BNT162b2 vaccination. *Nature* (2021) 600:701–6. doi: 10.1038/s41586-021-04120-y

29. National Cancer Institute (U.S.). *Common terminology criteria for adverse events : (CTCAE)* (2010). Available at: https://evs.nci.nih.gov/ftp1/CTCAE/CTCAE_4.03/Archive/CTCAE_4.0_2009-05-29_QuickReference_8.5x11.pdf.

30. Korber B, Fischer WM, Gnanakaran S, Yoon H, Theiler J, Abfalterer W, et al. Tracking changes in SARS-CoV-2 spike: Evidence that D614G increases infectivity of the COVID-19 virus. *Cell* (2020) 182:812–827.e19. doi: 10.1016/j.cell.2020.06.043

31. Wang L, Zhou T, Zhang Y, Yang ES, Schramm CA, Shi W, et al. Ultrapotent antibodies against diverse and highly transmissible SARS-CoV-2 variants. *Sci (80-)* (2021) 373:eabh1766. doi: 10.1126/science.abh1766

32. Hoffmann M, Arora P, Groß R, Seidel A, Hörnich BF, Hahn AS, et al. SARS-CoV-2 variants B.1.351 and P.1 escape from neutralizing antibodies. *Cell* (2021) 184:2384–2393.e12. doi: 10.1016/j.cell.2021.03.036

33. Kleine-Weber H, Elzayat MT, Hoffmann M, Pöhlmann S. Functional analysis of potential cleavage sites in the MERS-coronavirus spike protein. *Sci Rep* (2018) 8:16597. doi: 10.1038/s41598-018-34859-w

34. Berger Rentsch M, Zimmer G. A vesicular stomatitis virus replicon-based bioassay for the rapid and sensitive determination of multi-species type I interferon. *PloS One* (2011) 6:e25858. doi: 10.1371/journal.pone.0025858

35. Kasturi SP, Rasheed MAU, Havenar-Daughton C, Pham M, Legere T, Sher ZJ, et al. 3M-052, a synthetic TLR-7/8 agonist, induces durable HIV-1 envelope–specific plasma cells and humoral immunity in nonhuman primates. *Sci Immunol* (2020) 5:eabb1025. doi: 10.1126/sciimmunol.abb1025

36. European Medicines Agency. *Missing data in confirmatory clinical trials* (2010). Available at: https://www.ema.europa.eu/en/missing-data-confirmatory-clinical-trials.

37. Kaku CI, Champney ER, Normark J, Garcia M, Johnson CE, Ahlm C, et al. Broad anti–SARS-CoV-2 antibody immunity induced by heterologous ChAdOx1/mRNA-1273 vaccination. *Sci (80-)* (2022) 375:1041–7. doi: 10.1126/science.abn2688

38. Collier AY, Yu J, McMahan K, Liu J, Chandrashekar A, Maron JS, et al. Differential kinetics of immune responses elicited by covid-19 vaccines. *N Engl J Med* (2021) 385:2010–2. doi: 10.1056/NEJMc2115596

39. Gao Y, Cai C, Grifoni A, Müller TR, Niessl J, Olofsson A, et al. Ancestral SARS-CoV-2-specific T cells cross-recognize omicron. *Nat Med* (2022) 28:1–20. doi: 10.1038/d41591-022-00017-z

40. Keeton R, Tincho MB, Ngomti A, Baguma R, Benede N, Suzuki A, et al. T cell responses to SARS-CoV-2 spike cross-recognize omicron. *Nature* (2022) 603:488–92. doi: 10.1038/s41586-022-04460-3

41. Tarke A, Coelho CH, Zhang Z, Dan JM, Yu ED, Methot N, et al. SARS-CoV-2 vaccination induces immunological T cell memory able to cross-recognize variants from alpha to omicron. *Cell* (2022) 185:847–859.e11. doi: 10.1016/j.cell.2022.01.015

42. Redd AD, Nardin A, Kared H, Bloch EM, Abel B, Pekosz A, et al. Minimal crossover between mutations associated with omicron variant of SARS-CoV-2 and CD8 + T cell epitopes identified in COVID-19 convalescent individuals. *MBio* (2022) 13:e03617–21. doi: 10.1128/mbio.03617-21. 2021.12.06.471446.

43. Ahmed SF, Quadeer AA, McKay MR. SARS-CoV-2 T cell responses elicited by COVID-19 vaccines or infection are expected to remain robust against omicron. *Viruses* (2022) 14:79. doi: 10.3390/v14010079

44. Grifoni A, Sidney J, Vita R, Peters B, Crotty S, Weiskopf D, et al. SARS-CoV-2 human T cell epitopes: Adaptive immune response against COVID-19. *Cell Host Microbe* (2021) 29:1076–92. doi: 10.1016/j.chom.2021.05.010

45. Khoury DS, Cromer D, Reynaldi A, Schlub TE, Wheatley AK, Juno JA, et al. Neutralizing antibody levels are highly predictive of immune protection from symptomatic SARS-CoV-2 infection. *Nat Med* (2021) 27:1205–11. doi: 10.1038/s41591-021-01377-8

46. Gilbert PB, Montefiori DC, McDermott AB, Fong Y, Benkeser D, Deng W, et al. Immune correlates analysis of the mRNA-1273 COVID-19 vaccine efficacy clinical trial. *Sci (80-)* (2022) 375:43–50. doi: 10.1126/science.abm3425

47. Cromer D, Steain M, Reynaldi A, Schlub TE, Wheatley AK, Juno JA, et al. Neutralising antibody titers as predictors of protection against SARS-CoV-2 variants and the impact of boosting: a meta-analysis. *Lancet Microbe* (2022) 3: e52–61. doi: 10.1016/S2666-5247(21)00267-6

48. Lyngse FP, Mortensen LH, Denwood MJ, Christiansen LE, Møller CH, Skov RL, et al. SARS-CoV-2 omicron VOC transmission in Danish households. *medRxiv* (2021). doi: 10.1101/2021.12.27.21268278. 2021.12.27.21268278.

49. Ferguson N, Ghani A, Hinsley W, Volz E, College I. Report 50: Hospitalisation risk for omicron cases in England. *Imp Coll London* (2021). doi: 10.25561/93035

50. Public Health England. SARS-CoV-2 variants of concern and variants under investigation in England. *Sage* (2021), 1–50.

51. Thompson MG, Natarajan K, Irving SA, Rowley EA, Griggs EP, Gaglani M, et al. Effectiveness of a third dose of mRNA vaccines against COVID-19–associated emergency department and urgent care encounters and hospitalizations among adults during periods of delta and omicron variant predominance — VISION network, 10 states, august 2021–. *MMWR Morb Mortal Wkly Rep* (2022) 71:139–45. doi: 10.15585/mmwr.mm7104e3

52. Christensen PA, Olsen RJ, Long SW, Snehal R, Davis JJ, Ojeda Saavedra M, et al. Signals of significantly increased vaccine breakthrough, decreased hospitalization rates, and less severe disease in patients with coronavirus disease 2019 caused by the omicron variant of severe acute respiratory syndrome coronavirus 2 in Houston, Texas. *Am J Pathol* (2022) 192:642–52. doi: 10.1016/j.ajpath.2022.01.007

53. Abu-Raddad LJ, Chemaitelly H, Ayoub HH, AlMukdad S, Yassine HM, Al-Khatib HA, et al. Effect of mRNA vaccine boosters against SARS-CoV-2 omicron infection in Qatar. *N Engl J Med* (2022) 386:1804–16. doi: 10.1056/NEJMoa2200797. 2022.01.18.22269452.

54. Jahrsdörfer B, Groß R, Seidel A, Wettstein L, Ludwig C, Schwarz T, et al. Characterization of the SARS-CoV-2 neutralization potential of COVID-19–convalescent donors. *J Immunol* (2021) 206:2614–22. doi: 10.4049/jimmunol.2100036

55. Kim W, Zhou JQ, Horvath SC, Schmitz AJ, Sturtz AJ, Lei T, et al. Germinal centre-driven maturation of b cell response to mRNA vaccination. *Nature* (2022) 604:141–5. doi: 10.1038/s41586-022-04527-1

56. Goel RR, Painter MM, Lundgreen KA, Apostolidis SA, Baxter AE, Giles JR, et al. Efficient recall of omicron-reactive b cell memory after a third dose of SARS-CoV-2 mRNA vaccine. *Cell* (2022) 185:1875–87. doi: 10.1016/j.cell.2022.04.009. 2022.02.20.481163.

57. Dai L, Gao GF. Viral targets for vaccines against COVID-19. *Nat Rev Immunol* (2021) 21:73–82. doi: 10.1038/s41577-020-00480-0

58. Collier DA, Ferreira IATM, Kotagiri P, Datir RP, Lim EY, Touizer E, et al. Age-related immune response heterogeneity to SARS-CoV-2 vaccine BNT162b2. *Nature* (2021) 596:417–22. doi: 10.1038/s41586-021-03739-1

59. Muecksch F, Weisblum Y, Barnes CO, Schmidt F, Schaefer-Babajew D, Wang Z, et al. Affinity maturation of SARS-CoV-2 neutralizing antibodies confers potency, breadth, and resilience to viral escape mutations. *Immunity* (2021) 54:1853–1868.e7. doi: 10.1016/j.immuni.2021.07.008

60. Ghraichy M, Galson JD, Kovaltsuk A, von Niederhäusern V, Pachlopnik Schmid J, Recher M, et al. Maturation of the human immunoglobulin heavy chain repertoire with age. *Front Immunol* (2020) 11:1734. doi: 10.3389/fimmu.2020.01734

61. Müller L, Andrée M, Moskorz W, Drexler I, Walotka L, Grothmann R, et al. Age-dependent immune response to the Biontech/Pfizer BNT162b2 coronavirus disease 2019 vaccination. *Clin Infect Dis* (2021) 73:2065–72. doi: 10.1093/cid/ciab381

62. Payne RP, Longet S, Austin JA, Skelly DT, Dejnirattisai W, Adele S, et al. Immunogenicity of standard and extended dosing intervals of BNT162b2 mRNA vaccine. *Cell* (2021) 184:5699–5714.e11. doi: 10.1016/j.cell.2021.10.011

63. Sallusto F, Lanzavecchia A, Araki K, Ahmed R. From vaccines to memory and back. *Immunity* (2010) 33:451–63. doi: 10.1016/j.immuni.2010.10.008

64. Hall VG, Ferreira VH, Wood H, Ierullo M, Majchrzak-Kita B, Manguiat K, et al. Delayed-interval BNT162b2 mRNA COVID-19 vaccination enhances humoral immunity and induces robust T cell responses. *Nat Immunol* (2022) 23:380–5. doi: 10.1038/s41590-021-01126-6

65. Chatterjee D, Tauzin A, Marchitto L, Gong SY, Boutin M, Bourassa C, et al. SARS-CoV-2 omicron spike recognition by plasma from individuals receiving BNT162b2 mRNA vaccination with a 16-week interval between doses. *Cell Rep* (2022) 38:110429. doi: 10.1016/j.celrep.2022.110429

66. Grunau B, Goldfarb DM, Asamoah-Boaheng M, Golding L, Kirkham TL, Demers PA, et al. Immunogenicity of extended mRNA SARS-CoV-2 vaccine dosing intervals. *JAMA* (2022) 327:279. doi: 10.1001/jama.2021.21921

67. Garg AK, Mittal S, Padmanabhan P, Desikan R, Dixit NM. Increased b cell selection stringency in germinal centers can explain improved COVID-19 vaccine efficacies with low dose prime or delayed boost. *Front Immunol* (2021) 12:776933. doi: 10.3389/fimmu.2021.776933

68. Belshe RB, Frey SE, Graham I, Mulligan MJ, Edupuganti S, Jackson LA, et al. Safety and immunogenicity of influenza a H5 subunit vaccines: Effect of vaccine schedule and antigenic variant. *J Infect Dis* (2011) 203:666–73. doi: 10.1093/infdis/jiq093

69. Atmar RL, Lyke KE, Deming ME, Jackson LA, Branche AR, El Sahly HM, et al. Homologous and heterologous covid-19 booster vaccinations. *N Engl J Med* (2022) 386:1046–57. doi: 10.1056/NEJMoa2116414

70. Tan CS, Collier AY, Liu J, Yu J, Wan H, McMahan K, et al. Ad26.COV2.S or BNT162b2 boosting of BNT162b2 vaccinated individuals. *medRxiv* (2021). doi: 10.1101/2021.12.02.21267198. 2021.12.02.21267198.

71. Peng Y, Mentzer AJ, Liu G, Yao X, Yin Z, Dong D, et al. Broad and strong memory CD4+ and CD8+ T cells induced by SARS-CoV-2 in UK convalescent individuals following COVID-19. *Nat Immunol* (2020) 21:1336–45. doi: 10.1038/s41590-020-0782-6

72. Burki TK. Omicron variant and booster COVID-19 vaccines. *Lancet Respir Med* (2022) 10:e17. doi: 10.1016/S2213-2600(21)00559-2

73. van der Straten K, Guerra D, van Gils MJ, Bontjer I, Caniels TG, van Willigen HDG, et al. Mapping the antigenic diversification of SARS-CoV-2. *medRxiv* (2022). doi: 10.1101/2022.01.03.21268582. 2022.01.03.21268582.

74. Wilks SH, Muhlemann B, Shen X, Tureli S, LeGresley EB, Netzl A, et al. Mapping SARS-CoV-2 antigenic relationships and serological responses. *bioRxiv* (2022). doi: 10.1101/2022.01.28.477987. 2022.01.28.477987.

75. Yu J, Collier AY, Rowe M, Mardas F, Ventura JD, Wan H, et al. Neutralization of the SARS-CoV-2 omicron BA.1 and BA.2 variants. *N Engl J Med* (2022) 386:1579–80. doi: 10.1056/NEJMc2201849

76. Yamasoba D, Kimura I, Nasser H, Morioka Y, Nao N, Ito J, et al. Virological characteristics of the SARS-CoV-2 omicron BA.2 spike. *Cell* (2022) 185:2103–115. doi: 10.1016/j.cell.2022.04.035. 2022.02.14.480335.

77. Qu P, Faraone J, Evans JP, Zou X, Zheng Y-M, Carlin C, et al. Neutralization of the SARS-CoV-2 omicron BA.4/5 and BA.2.12.1 subvariants. *N Engl J Med* (2022) 386:2526–8. doi: 10.1056/NEJMc2206725

78. Quandt J, Muik A, Salisch N, Lui BG, Lutz S, Krüger K, et al. Omicron BA.1 breakthrough infection drives cross-variant neutralization and memory b cell formation against conserved epitopes. *Sci Immunol* (2022). doi: 10.1126/sciimmunol.abq2427

79. Juno JA, Wheatley AK. Boosting immunity to COVID-19 vaccines. *Nat Med* (2021) 27:1874–5. doi: 10.1038/s41591-021-01560-x

80. Regev-Yochay G, Gonen T, Gilboa M, Mandelboim M, Indenbaum V, Amit S, et al. Efficacy of a fourth dose of covid-19 mRNA vaccine against omicron. *N Engl J Med* (2022) 386:1377–80. doi: 10.1056/NEJMc2202542

81. Waltz E. Omicron-targeted vaccines do no better than original jabs in early tests. *Nature* (2022). doi: 10.1038/d41586-022-00003-y

frontiers | Frontiers in Immunology

TYPE Original Research
PUBLISHED 28 July 2022
DOI 10.3389/fimmu.2022.960733

OPEN ACCESS

EDITED BY
Srinivasa Reddy Bonam,
University of Texas Medical Branch at Galveston, United States

REVIEWED BY
Sridhar Goud Nerella,
National Institutes of Health (NIH), United States
Ritwika Basu,
University of Texas Medical Branch at Galveston, United States

*CORRESPONDENCE
Praveen M. Varghese
praveenmathewsvarghese@gmail.com
Uday Kishore
ukishore@hotmail.com

†These authors have contributed equally to this work

SPECIALTY SECTION
This article was submitted to Vaccines and Molecular Therapeutics, a section of the journal Frontiers in Immunology

RECEIVED 03 June 2022
ACCEPTED 28 June 2022
PUBLISHED 28 July 2022

CITATION
Beirag N, Kumar C, Madan T, Shamji MH, Bulla R, Mitchell D, Murugaiah V, Neto MM, Temperton N, Idicula-Thomas S, Varghese PM and Kishore U (2022) Human surfactant protein D facilitates SARS-CoV-2 pseudotype binding and entry in DC-SIGN expressing cells, and downregulates spike protein induced inflammation.
Front. Immunol. 13:960733.
doi: 10.3389/fimmu.2022.960733

Human surfactant protein D facilitates SARS-CoV-2 pseudotype binding and entry in DC-SIGN expressing cells, and downregulates spike protein induced inflammation

Nazar Beirag[1†], Chandan Kumar[2†], Taruna Madan[3], Mohamed H. Shamji[4], Roberta Bulla[5], Daniel Mitchell[6], Valarmathy Murugaiah[1], Martin Mayora Neto[7], Nigel Temperton[7], Susan Idicula-Thomas[2], Praveen M. Varghese[1,8*] and Uday Kishore[1,9*]

[1]Biosciences, College of Health, Medicine and Life Sciences, Brunel University London, Uxbridge, United Kingdom, [2]Biomedical Informatics Centre, National Institute for Research in Reproductive and Child Health, ICMR, Mumbai, Maharashtra, India, [3]Department of Innate Immunity, National Institute for Research in Reproductive and Child Health, ICMR, Mumbai, India, [4]Immunomodulation and Tolerance Group, Allergy and Clinical Immunology, Department of National Heart and Lung Institute and NIHR Biomedical Research Centre, Asthma UK Centre in Allergic Mechanisms of Asthma, Imperial College London, London, United Kingdom, [5]Department of Life Sciences, University of Trieste, Trieste, Italy, [6]WMS - Biomedical Sciences, Warwick Medical School, University of Warwick, Coventry, United Kingdom, [7]Viral Pseudotype Unit, Medway School of Pharmacy, University of Kent and Greenwich, United Kingdom, [8]School of Biosciences and Technology, Vellore Institute of Technology, Vellore, India, [9]Department of Veterinary Medicine, U.A.E. University, Al Ain, United Arab Emirates

Lung surfactant protein D (SP-D) and Dendritic cell-specific intercellular adhesion molecules-3 grabbing non-integrin (DC-SIGN) are pathogen recognising C-type lectin receptors. SP-D has a crucial immune function in detecting and clearing pulmonary pathogens; DC-SIGN is involved in facilitating dendritic cell interaction with naïve T cells to mount an anti-viral immune response. SP-D and DC-SIGN have been shown to interact with various viruses, including SARS-CoV-2, an enveloped RNA virus that causes COVID-19. A recombinant fragment of human SP-D (rfhSP-D) comprising of α-helical neck region, carbohydrate recognition domain, and eight N-terminal Gly-X-Y repeats has been shown to bind SARS-CoV-2 Spike protein and inhibit SARS-CoV-2 replication by preventing viral entry in Vero cells and HEK293T cells expressing ACE2. DC-SIGN has also been shown to act as a cell surface receptor for SARS-CoV-2 independent of ACE2. Since rfhSP-D is known to interact with SARS-CoV-2 Spike protein and DC-SIGN, this study was aimed at investigating the potential of rfhSP-D in modulating SARS-CoV-2 infection. Coincubation of rfhSP-D with Spike protein improved the Spike Protein: DC-SIGN interaction. Molecular dynamic studies revealed that rfhSP-D stabilised the interaction between DC-SIGN and Spike protein. Cell binding analysis with

DC-SIGN expressing HEK 293T and THP- 1 cells and rfhSP-D treated SARS-CoV-2 Spike pseudotypes confirmed the increased binding. Furthermore, infection assays using the pseudotypes revealed their increased uptake by DC-SIGN expressing cells. The immunomodulatory effect of rfhSP-D on the DC-SIGN: Spike protein interaction on DC-SIGN expressing epithelial and macrophage-like cell lines was also assessed by measuring the mRNA expression of cytokines and chemokines. RT-qPCR analysis showed that rfhSP-D treatment downregulated the mRNA expression levels of pro-inflammatory cytokines and chemokines such as TNF-α, IFN-α, IL-1β, IL- 6, IL-8, and RANTES (as well as NF-κB) in DC-SIGN expressing cells challenged by Spike protein. Furthermore, rfhSP-D treatment was found to downregulate the mRNA levels of MHC class II in DC expressing THP-1 when compared to the untreated controls. We conclude that rfhSP-D helps stabilise the interaction between SARS- CoV-2 Spike protein and DC-SIGN and increases viral uptake by macrophages *via* DC-SIGN, suggesting an additional role for rfhSP-D in SARS-CoV-2 infection.

KEYWORDS

innate immune system, collectins, rfhSP-D, SARS-CoV-2, COVID-19, cytokine response

Introduction

Pathogen recognition receptors (PRRs) are germline-encoded host sensors that detect pathogen-associated-molecular patterns (PAMPs) (1). PRRs play a vital part in the regular functioning of the innate immune system (2). They are expressed by innate immune cells, including dendritic cells (DCs), macrophages, neutrophils and monocytes (3). Toll-like receptors (TLRs) and C-type lectin receptors (CLRs) are key PRRs involved in host immunity against pathogens (4). Although CLRs are primarily expressed on myeloid cells such as DCs and macrophages, they vary between cell types, allowing specific immune response modifications upon target recognition (5). Receptors such as Dectin-2, Mincle, MGL (Macrophage galactose lectin), Langerin and DC-SIGN (Dendritic Cell-Specific Intercellular adhesion molecules-3-Grabbing Non-integrin) are CLRs that play a major role in the recognition of pathogenic fungi, bacteria, parasites, and viruses (6). The interaction of these CLRs with their ligands allows DCs to moderate the immune response towards either activation or tolerance, which is done through antigen presentation in lymphoid organs and the release of cytokines (7). DCs are responsible mainly for initiating antigen-specific immune responses. Therefore, they are localised at and patrol the sites of first contact with a pathogen, such as mucosal surfaces, including the pulmonary and nasopharyngeal mucosa. Likewise, alveolar macrophages are present in the lung alveoli (8).

DC-SIGN is a surface molecule on DCs that binds to the cell adhesion molecule ICAM-3 on T cells, enhancing DC-T cell contact (9). DC-SIGN is a 44 KDa type II integral membrane protein with a single C-terminal CRD (carbohydrate recognition domain) supported by an α-helical neck region with 7 and a half tandem repeats of a 23 amino-acid residue sequence (10, 11). A single transmembrane region anchors the protein, a cytoplasmic domain with recycling, internalisation, and intracellular signalling characteristics (11, 12). DC-SIGN forms oligomers on the cell surface, which improves the avidity of ligand binding and the specificity towards multiple repeated units that are likely to be related to the microbial surface features (13). Recently, DC-SIGN has been associated with promoting cis/trans infection of several viruses such as HIV, Cytomegalovirus, Dengue, Ebola and Zika (14–18). The ability of DCs to transmit HIV-1 to $CD4^+$ lymphocytes *via* DC-SIGN coupled with normal DC trafficking suggests that binding of the virus to DC-SIGN could be important in mucosal transmission of HIV-1 because DC-$SIGN^+$ DCs are present in the lamina propria at the mucosal surfaces (19). Recently, DC-SIGN has been reported to bind and enhance Severe acute respiratory syndrome coronavirus (SARS-CoV) and SARS-CoV-2 infection independent of ACE2 expression (20).

Another CLR molecule is human surfactant protein D (SP-D). SP-D belongs to the collectin family with a crucial role in pulmonary surfactant homeostasis and mucosal immunity. SP-D is primarily synthesised and secreted into the air space of the lungs by alveolar type II and Clara cells. Its primary structure is organised into four regions: a cysteine-rich N-terminus, a triple-helical collagen region, a neck region, and a C-terminal C-type

lectin or CRD. SP-D binds to glycosylated ligands on pathogens and initiates opsonisation, aggregation, and direct killing of microbes, facilitating their clearance by phagocytic cells such as macrophages. SP-D was also recently found to bind to the Spike protein of SARS-CoV-2, and inhibit viral replication in Caco-2 cells by promoting viral aggregation *in vitro* (21). A recombinant fragment of human SP-D (rfhSP-D), composed of homotrimer neck, CRD, and eight N-terminal Gly-X-Y regions, has been shown to have comparable immunological activities to native SP-D (22). It was shown to bind the HA protein of IAV and act as an entry inhibitor of IAV infection on A549 lung epithelial cells (23). Furthermore, rfhSP-D binds to gp120 and inhibits HIV-1 infectivity and replication in U937 monocytic cells, Jurkat T cells and PBMCs, inhibiting HIV-1 triggered cytokines storm (24). Importantly, rfhSP-D can directly bind to DC-SIGN. This interaction modulates HIV-1 capture and transfer to $CD4^+$ T cells (25). Recently, it has been shown rfhSP-D acts as an entry inhibitor of SARS-CoV-2 infection in Vero cells and HEK293T cells expressing ACE2 and TMPRSS2 (26, 27).

SARS-CoV-2, the causative pathogen of Coronavirus Disease 2019 (COVID-19), has resulted in around three million mortality worldwide (28, 29). The most common symptoms are fever, fatigue, and dry cough. The virus has been classified into Alpha, Beta, Gamma, Delta and Omicron variants based on mutations (30, 31). Some individuals can develop severe respiratory distress (32). SARS-CoV-2 is an enveloped RNA virus that uses a homotrimeric glycosylated spike (S) protein to interact with host cell receptors and promote fusion upon proteolytic activation (33). The transmembrane protease TMPRSS2 is known to mediate proteolytic cleavage at the S1/S2 and S2 domains. The receptor binding domain (RBD) is released by S1/S2 cleavage for high-affinity interaction with ACE2, whereas the S2 domain is released by S2 cleavage for effective virus fusion with the plasma membrane (23, 24). As a result, the virus is internalised by the host cells, resulting in viral replication. New copies of SARS-CoV 2 are internalised to infect more cells, increasing the viral load in the lungs, exacerbating the pro-inflammatory response, and extending the cellular and epithelial lung damage (34).

The sequence of events around the Spike protein/ACE2 interaction is well established; however, much remains to be unravelled about additional factors facilitating the infection, such as SARS-CoV-2 delivery to the ACE2 receptor (35). Indeed, Spike protein from both SARS-CoV and SARS-CoV-2 have similar affinity for ACE2 but show very different transmission rates (36, 37). The enhanced transmission rate of SARS-CoV-2 relative to SARS-CoV might result from an efficient viral adhesion through host-cell attachment factor, which may promote efficient infection of $ACE2^+$ cells (38, 39). In this framework, DC-SIGN bearing DCs and alveolar macrophages can play a role both in viral attachment and immune activation in the lungs (40–42).

Several studies have established the immune surveillance role of SP-D in terms of its ability to recognise viruses and modulate unwanted inflammatory responses (21, 25–27, 43–46). The interaction between SP-D and DC-SIGN during HIV-1 infection further provides an insight into the ability of SP-D to block DC-SIGN-mediated viral pathogenesis (25). In case of SARS-CoV-2, SP-D and rfhSP-D have been shown to bind to the S protein of the virus and inhibit viral infection and replication (21, 26, 27). Furthermore, DC-SIGN has also been reported to act as a facilitator and an entry receptor for SARS-CoV-2 infection, independent of ACE-2 expression (20, 47, 48). Thus, this study aimed to investigate the effects of rfhSP-D on DC-SIGN-mediated SARS-CoV-2 infection. Additionally, since DC-SIGN is highly expressed by DCs and macrophages, the study also explored the role of rfhSP-D on SARS-CoV-2 viral uptake by macrophage-like cells.

Materials and methods

Cell culture

HEK 293T cells were maintained in growth media, Dulbecco's Modified Eagle's Medium (DMEM) with Glutamax (Gibco) supplemented with 10% v/v foetal bovine serum (FBS), 100U/ml penicillin (Gibco), and 100µg/ml streptomycin (Gibco). The cells were cultured at 37°C in the presence of 5% v/v CO_2 until they were 70% confluent. HEK 293T cells were transiently transfected with a plasmid expressing human DC-SIGN (HG10200-UT; Sino Biological), using Promega FuGENE™ HD Transfection Reagent (Fisher Scientific). Next day, the cells were washed and cultured in the presence of hygromycin to select DC-SIGN expressing HEK-293T cells (DC HEK) (Thermo Fisher Scientific). Similarly, THP-1 cells were cultured in growth media. THP-1 cells were induced PMA to express DC-SIGN surface molecules (10 ng/mL) in combination with IL-4 (1000 units/mL) and incubated for 72 h (49).

Expression and purification of a recombinant fragment of human SP-D (rfhSP-D) containing neck and CRD regions

A recombinant fragment of human SP-D (rfhSP-D) was expressed under bacteriophage T7 promoter in *Escherichia coli* BL21 (λDE3) pLysS (Invitrogen), transformed with plasmid containing cDNA sequences for neck, CRD regions and 8 Gly-X-Y repeats of human SP-D (26). Briefly, a primary inoculum of 25 ml bacterial culture was inoculated into 500 mL of Luria-Bertani (LB) broth containing 100 µg/ml ampicillin and 34 µg/ml chloramphenicol (Sigma-Aldrich), and grown to OD_{600} of 0.6. The bacterial culture was then induced with 0.5 mM

isopropyl β-D-1-thiogalactopyranoside (IPTG) (Sigma -Aldrich) for 3 hours. The bacterial cell pellet was harvested and resuspended in lysis buffer [50 mM Tris-HCl pH 7.5, 200 mM NaCl, 5 mM EDTA pH 8, 0.1% Triton X–100, 0.1 mM phenyl-methyl-sulfonyl fluoride (PMSF), 50μg/ml lysozyme] and sonicated (ten cycles, 30 seconds each). The sonicate was centrifuged at 12000 x g for 30 minutes, followed by solubilisation of the pellet containing inclusion bodies in refolding buffer (50 mM Tris-HCl pH 7.5, 100 mM NaCl, 10 mM 2-Mecraptoethanol) containing 8M urea. The solubilised fraction was dialysed stepwise against refolding buffer containing 4M, 2M, 1M and 0M urea. The clear dialysate was loaded onto a maltose-agarose column (5ml; Sigma-Aldrich). The bound rfhSP-D was eluted using 50 mM Tris-HCl pH 7.5, 100 mM NaCl and 10 mM EDTA. The eluted fractions were then passed through a polymyxin B column in sodium deoxycholate buffer (Pierce™ High-Capacity Endotoxin Removal Spin Columns, Thermo Fisher) to remove endotoxin. The endotoxin levels were measured using ToxinSensor™ Chromogenic LAL Endotoxin Assay Kit (Genescript). The amount of endotoxin present in the rfhSP-D batches was ~4 pg/μg of rfhSP-D.

Expression and purification of soluble tetrameric DC-SIGN

The pT5T construct expressing tetrameric form of human DC-SIGN was transformed into *Escherichia coli* BL21 ((λDE3). Protein expression was performed using bacterial culture in LB medium containing 50 μg/ml ampicillin at 37°C until OD_{600} reached 0.7. The bacteria culture was induced with 10 mM IPTG (Sigma -Aldrich) and incubated for 3 h at 37°C. Bacterial cells (1 L) were centrifuged at 4,500 x g for 15 min at 4°C. Next, the cell pellet was treated with 22 ml of lysis buffer containing 100 mM Tris-HCl pH 7.5, 0.5 mM NaCl, 2.5 mM EDTA pH 8, 0.5 mM PMSF, and 50μg/ml lysozyme, and left to stir for 1 h at 4°C. Cells were then sonicated for 10 cycles for 30 s with 2 min intervals. The sonicated suspension was spun at 10,000 g for 15 minutes at 4°C. The inclusion bodies present in the pellet were solubilised in 20 ml buffer containing 10 mM Tris-HCl, pH 7.0, 0.01% β-mercaptoethanol and 6 M urea by rotating on a shaker for 1 h at 4°C. The mixture was then centrifuged at 13,000 x g for 30 min at 4°C. The supernatant was drop-wise diluted fivefold with loading buffer containing 25 mM Tris-HCl pH 7.8, 1 M NaCl and 2.5mM $CaCl_2$ with gentle stirring. This was then dialysed against 2 L of loading buffer with three buffer changes every 3 h. Following further centrifugation at 13,000 x g for 15 min at 4°C, the supernatant was loaded onto a mannan-agarose column (5 ml; Sigma) pre-equilibrated with loading buffer. The column was washed with five-bed volumes of the loading buffer, and the bound protein was eluted in 1 ml fractions using the elution buffer containing 25 mM Tris-HCl pH 7.8, 1 M NaCl, and 2.5 mM EDTA. The absorbance was read at 280 nm, and the peak fractions were frozen at -20°C. The purity of the protein was analysed by 15% w/v SDS-PAGE.

ELISA

Decreasing concentrations of recombinant DC-SIGN or rfhSP-D (2, 1, 0.5 or 0 μg 100μl/well) were coated on polystyrene microtiter plates (Sigma-Aldrich) at 4°C overnight using carbonate/bicarbonate (CBC) buffer, pH 9.6 (Sigma-Aldrich). The microtiter wells were washed three times next day with PBST Buffer (PBS + 0.05% Tween 20) (Fisher Scientific). The wells were then blocked using 2% w/v BSA in PBS (Fisher Scientific) for 2 h at 37°C and washed three times using PBST. Constant concentration (2 μg 100μl/well) of recombinant SARS-CoV-2 spike protein (RP-87680, Invitrogen) was added to the wells. After a 2-h incubation at 37°C, the wells were washed with PBST to eliminate any unbound protein. Polyclonal rabbit anti-SARS-CoV-2 spike (NR-52947, Bei-Resources) was used to probe the wells (1:5,000) in PBS and incubated for an additional 1 h at 37°C. Goat anti-rabbit IgG conjugated to horseradish peroxidase (HRP) (1:5,000) (Promega) was used to detect the bound protein. The colour was developed using 3,3',5,5'-tetramethylbenzidine (TMB) (Biolegend), and the reaction was stopped using 1M H_2SO_4 (50 μl/well; Sigma-Aldrich) and read at 450 nm spectrophotometrically.

For competitive ELISA, microtiter wells were coated overnight at 4°C with DC-SIGN protein (2 μg; 100 μl/well) and blocked. A fixed concentration of SARS-CoV-2 Spike protein (2μg; 100μl/well) and decreasing concentration (4.0, 2.0, 1.0, 0.5, 0 μg; 100μl/well) of rfhSP-D in calcium buffer, was added to the well as competing proteins. The plate was incubated at 37°C for 1.5 h and then at 4°C for another 1.5 h. To remove any unbound protein, the wells were rinsed three times with PBST. Next, the wells were probed with polyclonal rabbit anti-SARS CoV-2 spike (1:5,000) in PBS and incubated for an additional 1 h at 37°C. The bound protein was detected using goat anti-rabbit IgG conjugated to HRP (1:5000), and the colour was developed using TMB (100 μl/well). The reaction was stopped using 1M H_2SO_4 (50 μl/well; Sigma-Aldrich). The plate was read at 450 nm using a microplate reader (BioRad).

Cell binding assay

SARS-CoV-2 spike pseudotypes were produced as previously described (44). Briefly, HEK 293Tcells were cultured in growth media to 70-80% confluence at 37°C under 5% v/v CO_2. Cells were co-transfected using FuGENE® HD Transfection Reagent (Promega) with Opti-MEM® diluted plasmids (450 ng of pCAGGS-SARS-CoV-2 spike, 500ng of

p8.91-lentiviral vector and 750 ng of pCSFLW). The transfected cells were incubated for 48h at 37°C under 5% v/v CO_2. Post incubation, the medium containing the pseudotypes was harvested without disturbing the cell monolayer. The medium was then passed through a syringe driven 0.45 µm filter to remove any cell debris and the pseudotypes were harvested and stored at -80°C until further use.

DC-HEK and DC-THP-1 cells were seeded in microtiter wells separately in growth medium (1 x 10^5 cells/well) and incubated overnight at 37°C. The wells were washed three times with PBS, then rfhSP-D (20 µg/ml), pre-incubated with SARS-CoV-2 spike pseudotypes, were added to the corresponding wells and incubated at room temperature (RT) for 2 h. The microtiter wells were rinsed three times with PBS and fixed with 1% v/v paraformaldehyde (PFA) for 1 min at RT. The wells were washed again with PBS and incubated with polyclonal rabbit anti-SARS-CoV-2 spike (1:200 diluted in PBS) and incubated for 1 h at 37°C. After washing three times with PBST, the corresponding wells were probed with Alexa Fluor 488 conjugated goat anti-rabbit antibody (Abcam) diluted in PBS (1:200) for 1 h at RT. Readings were measured using a Clariostar Plus Microplate Reader (BMG Labtech).

Fluorescence microscopy

DC-HEK cells were cultured on 13 mm glass coverslips to form a monolayer, followed by incubation with SARS-CoV-2 spike pseudotypes (50µl) at 37°C. For 30 min, cells were rinsed with PBS and fixed using 1% w/v PFA for 1 min. The cells were washed three times with PBS, then blocked with 5% w/v BSA in PBS (Fisher Scientific) for 30 minutes. The cells were incubated for 30-min with mouse anti-human DC-SIGN antibodies to detect DC-SIGN and rabbit anti-SARS-CoV-2 Spike antibodies. Next, cells were washed and incubated with a staining buffer containing Alexa Fluor 647 conjugated goat anti-mouse antibody (Abcam), Alexa fluor 488 conjugated goat anti-rabbit antibody (Abcam), and Hoechst (Invitrogen, Life Technologies). This incubation was done in the dark for 45 min. After rinsing with PBS, the mounted coverslips were visualised under a Leica DM4000 microscope.

Luciferase reporter activity assay

SARS-CoV-2 spike pseudotypes, pre-incubated with rfhSP-D (20µg/ml), were added to DC-HEK and DC-THP-1 cells separately in a 96-well plate and incubated at 37°C for 24 h. The medium was removed, and cells were washed twice with PBS to remove any unbound SARS-CoV-2 spike pseudotypes and rfhSP-D. Fresh growth medium was added and incubated at 37°C for 48h. The cells were washed, and luciferase activity (RLU) was measured using ONE-Glo™ Luciferase Assay System (Promega) and read on Clariostar Plus Microplate Reader (BMG Labtech).

Quantitative qRT-PCR Analysis

DC-HEK and DC-THP-1 cells (0.5 X 10^6) were seeded overnight in growth medium. Next day, SARS-CoV-2 Spike protein (500 ng/ml) was pre-incubated with rfhSP-D (20 µg/ml) for 2h at RT and added to DC-THP-1 cells in serum-free medium. Post incubation at 6h, 12h, 24h and 48h, the cells were washed with PBS gently and pelleted. GenElute Mammalian Total RNA Purification Kit (Sigma-Aldrich) was used to extract the total RNA. After RNA extraction, DNase I (Sigma-Aldrich) treatment was performed to remove any DNA contaminants, then the amount of RNA was quantified at A260 nm using a NanoDrop 2000/2000c (ThermoFisher). The purity of RNA was assessed using the ratio A260/A280. Two micrograms of total RNA were used to synthesize cDNA, using High-Capacity RNA to cDNA Kit (Applied Biosystems). The primer BLAST software (Basic Local Alignment Search Tool) was used to design primer sequences as listed in Table 1. qRT-PCR assay was performed using the Step One Plus system (Applied Biosciences). Each qPCR reaction was conducted in triplicates, containing 75 nM of forward and reverse primers, 5 µl Power SYBR Green Master Mix (Applied Biosystems), and 500 ng of cDNA. qPCR samples were run for 50°C, and 95°C for 2 and 10 min, followed by running the amplification template for 40 cycles, each cycle involving 15 s at 95°C and 1 min at 60°C. 18S rRNA was used as an endogenous control to normalise the gene expression.

Molecular docking

Tripartite complex models of DC-SIGN tetramer, Spike trimer and rfhSP-D trimer were predicted through blind molecular docking using ZDOCK module of Discovery Studio 2021. The structural coordinates for DC-SIGN (CRD), spike and rfhSP-D were retrieved from PDB with IDs as 1K9I, 6XM3, and 1PW9, respectively. Docking was performed in two stages. In the first stage, DC-SIGN (CRD) tetramer was blind docked individually with rfhSP-D trimer (complex A) and spike trimer (complex B). The top ranked poses were analysed for intermolecular interactions and corroborated based on previous studies (25).

In the second stage, the selected docked pose of complex A was further blind docked with spike trimer to build a tripartite complex of DC-SIGN (CRD), Spike and rfhSP-D (complex C). The tripartite complex was selected based on the docking score and intermolecular interactions that were in agreement with reports (26).

TABLE 1 Forward and reverse primers used for RT-qPCR.

Target Primer	Forward Primer	Reverse Primer
18S	5′-ATGGCCGTTC TTAGTTGGTG-3′	5′-CGCTGAGCCA GTCAGTGTAG-3′
TNF-α	5′-AGCCCATGTT GTAGCAAACC-3′	5′-TGAGGTACAG GCCCTCTGAT-3′
IL-6	5′-GAAAGCAGCA AAGAGGCACT-3	5′-TTTCACCAGG CAAGTCTCCT-3′
IL-8	5′-GGTGCAGTTTTT GCCAAGGAG-3′	5′-CACCCAGTTTT CCTTGGGGT-3′
NF-κB	5′-GTATTTCAACCA CAGATGGCACT-3′	5′-AACCTTTGCTG GTCCCACAT-3′
RANTES	5′-GCGGGTACCAT GAAGATCTCTG-3′	5′-GGGTCAGAATC AAGAAACCCTC-3′
IFN-α	5′-TTTCTCCTG CCTGAAGGACAG-3′	5′-GCTCATGATTTC TGCTCTGAC A-3′
IFN-β	5′-GGCTTTTCAGCT CTGCATCG-3′	5′-TCTGTCAC TCTCCTC TTTCCA-3
MHC II	5′-TAAGGCACATGGA GGTGATG-3′	5′-GTACGGAGC AATCGAAGAGG-3′

Molecular dynamics (MD) simulation

MD simulations for the complexes B, C1 and C2 were performed using GROMACS v2020.6 (50). The force field AMBER99SB was applied with improved protein side-chain torsion potentials (51). All the three complexes were solvated in triclinic periodic box condition using TIP3P water molecules with a distance of 1.5 nm from the center of the complex. Complexes were neutralized by adding Na^+ counter ions and subsequently minimized for 5000 energy steps using steepest descent algorithm with a tolerance of 1000 kJ/mol/nm. Equilibration was performed using NVT and NPT ensembles for 50,000 steps. Finally, MD was run at constant temperature (300 K) and pressure (1 atm) for 20ns. The analyses of obtained MD trajectories were carried out using GROMACS utility tools.

Statistical analysis

Graphs were generated using GraphPad Prism 8.0 software. The statistical significance was considered as indicated in the figure legends between treated and untreated conditions. Error bars show SD or SEM as stated in the figure legends.

Results

Both DC-SIGN and rfhSP-D bind to SARS-CoV 2 spike protein

An indirect ELISA was performed by coating microtiter plates with decreasing concentration of either rfhSP-D or DC-SIGN and probing with anti-SARS-CoV-2 spike antibody to confirm the protein-protein interaction between the two proteins. Both DC-SIGN (Figure 1A) and rfhSP-D (Figure 1B) independently exhibited a dose-dependent increase in binding at all tested concentrations. Since both rfhSP-D and DC-SIGN bound SARS-CoV-2 Spike protein independently, a completive ELISA was performed to evaluate if rfhSP-D would interfere with the binding between Spike protein and DC-SIGN. As a matter of fact, addition of rfhSP-D enhanced the binding of DC-SIGN to the Spike protein in a dose-dependent manner (Figure 1C).

rfhSP-D treatment enhances DC-SIGN mediated binding and uptake of SARS-CoV-2 pseudotyped viral particles

Since rfhSP-D was found to interact with DC-SIGN and Spike protein, we evaluated the ability of rfhSP-D to mediate the binding of SARS-CoV-2 to DC-SIGN expressing cells. HEK 293T cells were transfected with a construct containing a DNA sequence of full-length human DC-SIGN to induce DC-SIGN cell surface expression. As previous studies have established the ability of SARS-CoV-2 spike protein to bind DC-SIGN, the binding of the SARS-CoV-2 spike protein-expressing pseudotypes to DC-HEK cells was also confirmed microscopically (Figure 2). To assess the effect of rfhSP-D on pseudotypes binding to DC HEK cells, the cells were challenged with rfhSP-D (20μg/ml) treated SARS-CoV-2 Spike protein-expressing pseudotype. Increased binding (~50%) in the treated samples (DC-HEK + SARS-CoV-2 spike Pseudotypes + rfhSP-D) compared to their untreated counterparts (DC-HEK + SARS-CoV-2 spike Pseudotypes) was observed (Figure 3A). The quantitative evaluation of the binding of the pseudotypes was also performed using THP-1 cells treated with PMA and IL-4 to induce the expression of native DC-SIGN. A similar result was

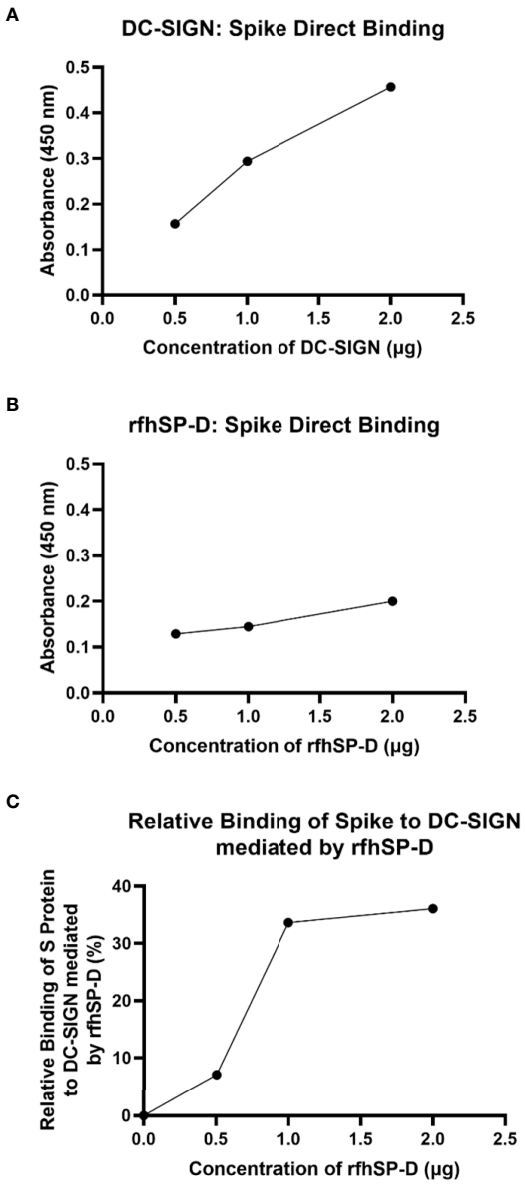

FIGURE 1
rfhSP-D promotes interaction between SARS-CoV-2 Spike protein and DC-SIGN. The binding of immobilised DC-SIGN **(A)** or immobilised rfhSP-D **(B)** to SARS-CoV-2 spike protein was analysed by ELISA. Microtiter wells were coated with a decreasing concentration of DC-SIGN or rfhSP-D (2, 1, 0.5 or 0 µg per well) proteins and incubated with a constant amount of SARS-CoV-2 Spike protein (2 µg per well). Both proteins were found to bind Spike protein in a dose-dependent manner. Competitive ELISA **(C)** was performed to analyse the effect of rfhSP-D on DC-SIGN: Spike protein interaction. rfhSP-D brought about increased binding between Spike protein and DC-SIGN. Since increasing the concentration of rfhSP-D was found to increase the detectable amount of Spike protein, it seems to suggest the existence of distinct binding sites for the Spike protein on both C type lectins. The data were expressed as a mean of three independent experiments done in triplicates ± SEM.

obtained using DC-SIGN expressing THP-1 macrophage-like cells. rfhSP-D treatment was found to increase the binding efficiency of the pseudotypes to the THP-1 cells expressing DC-SIGN by ~25%, compared to the untreated controls (Figure 3B).

To evaluate the impact of rfhSP-D on the transduction of pseudotypes to DC-HEK cells, the cells were treated with rfhSP-D (20µg/ml) and challenged with SARS-CoV-2 Spike protein-expressing pseudotypes for 24h. Higher luciferase activity (~190%) in the treated samples (DC-HEK + SARS-CoV-2 spike pseudotypes + rfhSP-D) as compared with their untreated counterparts (DC-HEK + SARS-CoV-2 spike pseudotypes) was noticed (Figure 4A). A similar observation was made using DC-SIGN expressing DC-THP-1 cells

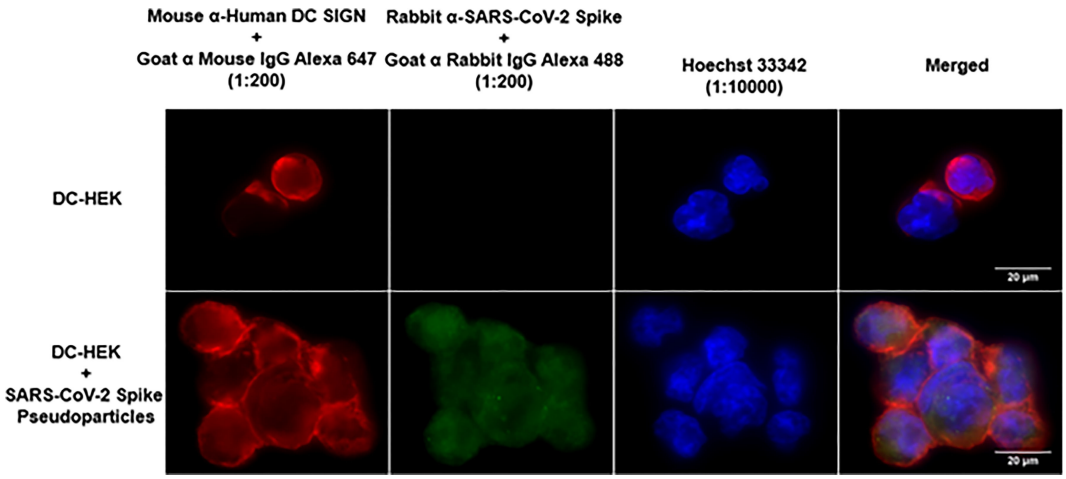

FIGURE 2
Binding of SARS-CoV-2 Spike-Pseudotypes to DC-SIGN expressing cells. DC-HEK cells were incubated with SARS-CoV-2 Spike Pseudotypes for 30 min at 37°C. Spike Pseudotypes challenged DC-HEK cells were fixed with 4% paraformaldehyde, washed, and blocked with 5% FCS. The cells were probed with rabbit anti-SARS-CoV-2 Spike antibody and mouse anti-DC-SIGN to detect the presence of Spike-Pseudotypes and DC-SIGN expressed on the cells, respectively. Alexa Fluor 647 conjugated goat anti-mouse antibody (Abcam), Alexa fluor 488 conjugated goat anti-rabbit antibody (Abcam), and Hoechst (Invitrogen, Life Technologies) were used to detect the primary antibodies and nucleus.

compared to untreated controls. rfhSP-D treatment increased the transduction effectiveness of the pseudotypes in DC-THP-1 cells by ~ 90% (Figure 4B).

rfhSP-D modulates pro-inflammatory cytokines and chemokines response in SARS-CoV-2 spike protein challenged DC-HEK cells

Pro-inflammatory cytokines and chemokines such as TNF-α, IFN-α, RANTES, and NF-κB transcription factors characterise SARS-CoV-2 infection in the lower respiratory epithelium that express DC-SIGN. DC-HEK cells were challenged with SARS-CoV-2 Spike protein pre-incubated with rfhSP-D to assess the effect of rfhSP-D on the pro-inflammatory cytokines/chemokines released during SARS-CoV-2 infection. The total RNA extracted from the cells was then used in qRT-PCR, with cells challenged with SARS-CoV-2 Spike protein that had not been treated with rfhSP-D serving as the control. rfhSP-D treatment decreased mRNA levels of TNF-α, IFN-α, RANTES, and NF-κB in DC-HEK cells that were challenged with Spike protein. TNF-α mRNA levels were reduced by (~ -3.3 $\log_{10}$) (Figure 5C), while IFN-α mRNA levels were downregulated (~ -2.1 $\log_{10}$) (Figure 5B). As RANTES is induced by detection of viral components within infected cells, rfhSP-D treatment reduced the mRNA levels of RANTES in DC-HEK cells challenged with Spike (~ -1.3 $\log_{10}$) (Figure 5D). Antiviral cytokines/chemokines are regulated by the transcription factor NF-κB; NF-κB mRNA levels were also reduced (~ -1.2 $\log_{10}$) (Figure 5A).

Modulation of immune response in SARS-CoV-2 spike protein-challenged DC-THP-1 cells by rfhSP-D

Lung macrophages secrete pro-inflammatory mediators such as IL-1, IL-6, IL-8, and TNF-α in response to SARS-CoV-2 infection. To further understand the role of rfhSP-D in modulating the production of pro-inflammatory cytokines/chemokines from lung macrophage expressing DC-SIGN during SARS-CoV-2 infection, rfhSP-D treated/untreated SARS-CoV-2 Spike protein was used to challenge DC-THP-1 cells. qRT-PCR was used to assess the mRNA levels of pro-inflammatory cytokines and chemokines in cells after treatment at 6h and 12h time points (Figure 6). In DC THP-1 cells challenged with Spike protein, rfhSP-D treatment reduced mRNA levels of IL-1, IL-6, IL- 8, TNF-α, and NF-κB (Figure 6). mRNA levels of NF- κB at 6h were slightly reduced (~ -1 $\log_{10}$). At 12 h, it was significantly downregulated (~ -4 $\log_{10}$) in rfhSP-D treated DC-THP-1 cells challenged with Spike protein (Figure 6A). Cells challenged with Spike protein and treated with rfhSP-D at 6h and 12h exhibited a reduction in the gene expression levels of TNF-α (~ -3.1 $\log_{10}$ and ~ -6.8 $\log_{10}$, respectively) (Figure 6B). In rfhSP-D treated DC-THP-1 cells

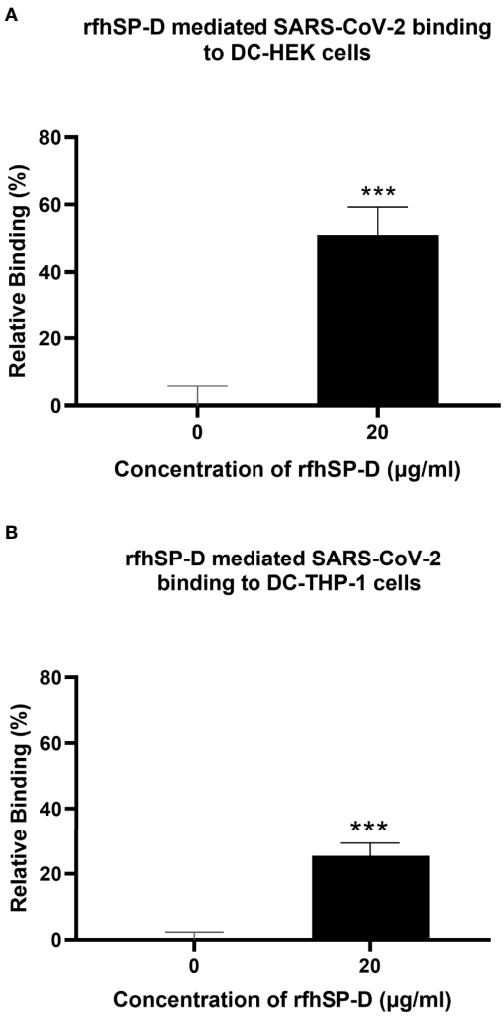

FIGURE 3
rfhSP-D promotes interaction between SARS-CoV-2 Spike Pseudotypes and DC-SIGN expressing cells. DC-HEK cells **(A)** and DC-THP-1 cells **(B)** were treated with rfhSP-D and SARS-CoV-2 Spike-Pseudotypes. The cell binding was analysed using Alexa Fluor 488 (FTIC) and Alexa Fluor 647 (APC); the fluorescence intensity was measured using a GloMax 96 Microplate Luminometer (Promega). An increased fluorescence intensity was observed in DC-HEK and DC-THP-1 cells treated with 20 µg/ml of rfhSP-D compared to cells challenged with Spike pseudotypes alone. Experiments were conducted in triplicates, and error bars represent ± SEM. Unpaired t-test was used to calculate the significance (*$p < 0.05$, **$p < 0.01$, and ***$p < 0.001$) (n = 3). (0, untreated sample; 20, treated sample).

challenged with Spike protein, IL-1β mRNA levels were reduced (~ -2.5 $\log_{10}$) after 6 h and (~ -4 $\log_{10}$) 12 h after treatment (Figure 6C). Furthermore, IL-6 levels were significantly downregulated at 12h (- 5 $\log_{10}$) in rfhSP-D treated DC-THP-1 cells challenged with Spike protein (Figure 6D). Reduced levels of IL-8 at 6h (~ -2.3 $\log_{10}$) and 12h (~ -4.8 $\log_{10}$) were detected in DC-THP-1 cells challenged with Spike protein and treated with rfhSP-D (Figure 6E). MHC class II molecules play a key role in bridging innate and adaptive immunity during anti-viral immune response. rfhSP-D reduced MHC class II expression levels at 6 (- 2 $\log_{10}$) and 12h (- 2.7 $\log_{10}$) in DC-THP-1 cells challenged with Spike protein (Figure 6F).

SP-D interacts with RBD and DC-SIGN interacts with NTD of SARS-CoV-2 spike protein

DC-SIGN and SP-D are known to interact through their CRDs (25). This interaction was observed in complex A (docked pose 2) of the current study (Figure 7A; Table 2). The binding site of DC-SIGN (CRD) and Spike protein is not known; therefore, a blind docking approach was attempted to generate complex B. Analysis of the top ranked docked pose of complex B revealed that NTD (N-terminal domain) of spike protein interacted with the CRD domain of DC-SIGN (Figure 7B;

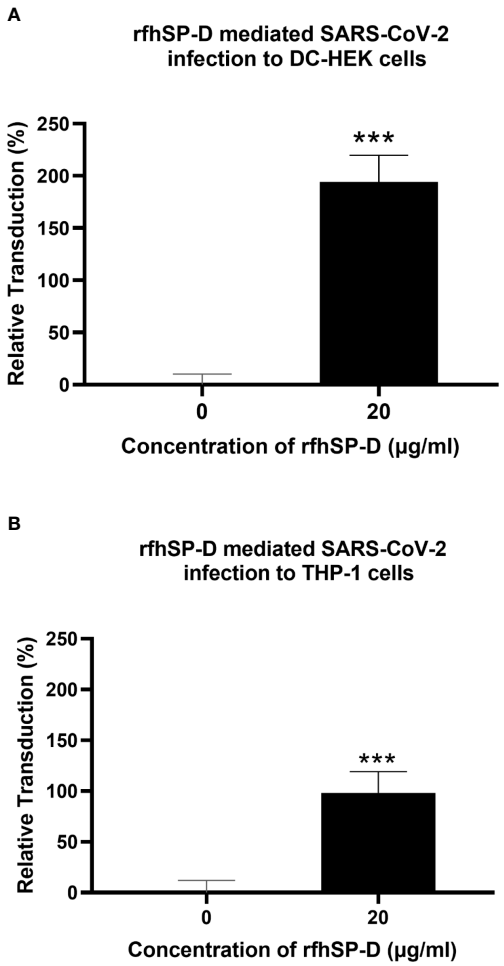

FIGURE 4
rfhSP-D enhances SARS-CoV-2 Spike pseudotype transduction by DC-HEK and DC-THP-1 cells. Purified Spike pseudotypes were used to transduce DC-HEK **(A)** and DC-THP-1 cells **(B)**, and the luciferase reporter activity was measured. Higher levels of luciferase reporter activities were observed in DC-HEK and DC-THP-1 cells when treated with 20 µg/ml of rfhSP-D compared to cells challenged with Spike pseudotypes only. Experiments were conducted in triplicates, and error bars represent ± SEM. Unpaired t-test was used calculate the significance (*$p < 0.05$, **$p < 0.01$, and ***$p < 0.001$) (n = 3).

Table 2). Since it was known that Spike protein interacted with SP-D through its receptor binding domain (RBD) (26), we postulated that Spike protein could interact with both SP-D and DC-SIGN (CRD) through two distinct RBD and NTD domains, respectively. This inference is further supported by the *in vitro* observation that binding of DC-SIGN to Spike protein was enhanced by rfhSP-D (Figure 1C). Tripartite complex was generated by docking complex A (DC-SIGN and SP-D) with Spike protein. The top two docked poses (complexes C1 and C2) were analysed for intermolecular interactions (Figure 8; Table 2). In both C1 (Figure 8A) and C2 (Figure 8B) complexes, DC-SIGN (CRD) interacted with NTD domain of Spike protein. In C1, there were no molecular interactions between Spike protein and rfhSP-D (Figure 8A; Table 2). In C2, Spike protein interacted with rfhSP-D through RBD (Figure 8B; Table 2).

SP-D stabilises DC-SIGN and SARS-CoV-2 spike protein interaction

MD simulations were performed to assess the effect of SP-D on DC-SIGN (CRD) and Spike protein interaction. The root mean square deviation (RMSD) of complexes C1 and C2 was less than complex B through the course of simulation, indicating that the binding of SP-D enhances the stability of DC-SIGN and spike interaction (Figure 9A). This observation was supported by potential energy (PE), distance, and H-bond profile. Trajectory

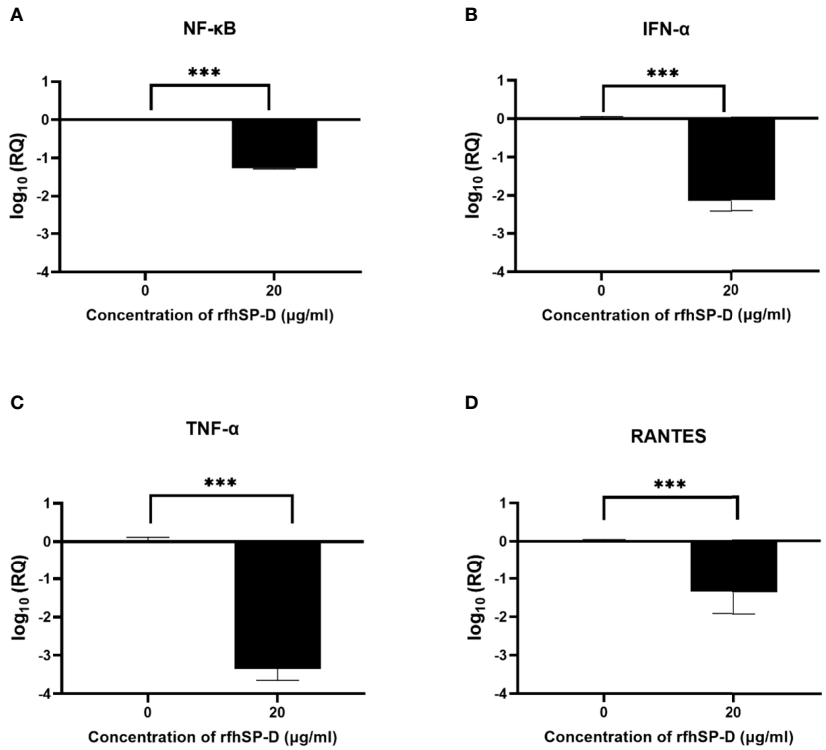

FIGURE 5
rfhSP-D downregulates pro-inflammatory cytokines and chemokines in DC-HEK cells. SARS-CoV-2 Spike protein incubated with 20µg/ml of rfhSP-D was used to challenge DC-HEK cells. Cells were harvested at 6 h to analyse the expression of cytokines. RNA was purified and converted into cDNA. The gene expression levels of NF-κB **(A)**, IFN-α **(B)**, TNF-α **(C)**, and RANTES **(D)** were assessed using RT-qPCR. 18S rRNA was used as an endogenous control. The relative expression (RQ) was calculated using cells challenged with Spike protein untreated with rfhSP-D as the calibrator. The RQ value was calculated using RQ = $2^{-\Delta\Delta Ct}$. Assays were conducted in triplicates, and error bars represent ± SEM. Significance was determined using the two-way ANOVA test (**p < 0.01, and ****p < 0.0001) (n = 3).

analysis of PE, intermolecular distance and H-bonds between DC-SIGN and spike indicated higher stability of C1 and C2 complexes as compared to B (Figures 9B, 10A–C, 10D–F). Between the tripartite complexes, C1 exhibited slightly better stability than C2 (Figures 9, 10). These analyses suggest that the interaction of DC-SIGN and spike gets stabilized in the presence of SP-D.

Discussion

Specific molecular structures on the surfaces of pathogens (PAMP) are directly recognised by pattern recognition receptors (PRRs) (4). PRRs serve as a link between nonspecific and specific immunity. PRRs can exert nonspecific anti-infection, anti-tumour, and other immune-protective actions by recognising and binding non-self ligands (52). CLRs are PRRs, which use calcium to recognise carbohydrate residues on harmful bacteria and viruses (53). DC-SIGN and SP-D are CLRs that play an important role in anti-viral immunity, including SARS-CoV-2, the causative agent of coronavirus induced illness 2019 (COVID-19) (54, 55). The availability of virus receptors and entry cofactors on the surface of host cells determines tissue tropism for many viruses (56, 57). We found rfhSP-D potentiated SARS-CoV-2 binding and entry to DC-SIGN expressing cells. Furthermore, rfhSP-D treatment was also found to impair downstream signalling induced by the binding of Spike protein to DC-SIGN resulting in the downregulation of pro-inflammatory mediators' gene expression. However, further experiments using DC-SIGN expressing cells challenged with rfhSP-D treated SARS-CoV-2 clinical isolates need to be undertaken to confirm the rfhSP-D mediated cytokine modulation observed. Our findings elucidate a novel interaction between rfhSP-D, DC-SIGN and SARS-CoV-2, which may uncover therapeutic potential for controlling SARS-CoV- 2 infection and subsequent cytokine storm.

DC-SIGN, widely expressed on DCs and alveolar macrophages in the lungs, interacts with SARS-CoV-2 through Spike protein (47). DC-SIGN has previously been shown to interact with SARS-CoV, HIV-1 and Ebola virus (41, 58, 59).

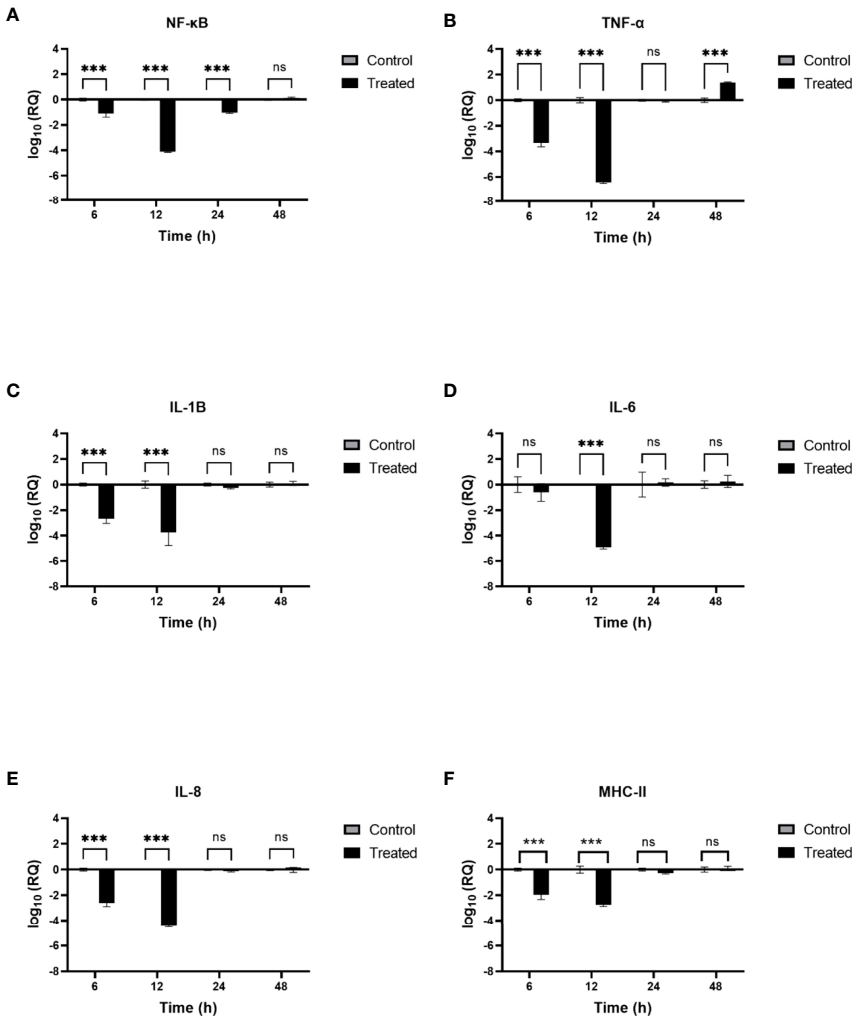

FIGURE 6
rfhSP-D modulates immune response in DC-THP-1 cells. SARS-CoV-2 Spike protein incubated with 20μg/ml of rfhSP-D was used to challenge DC-THP-1 cells. Cells were harvested at 6h, 12h, 24h, and 48h to analyse the expression of cytokines and MHC class II. Cells were lysed, and purified RNA was converted into cDNA. The expression levels of NF-κB **(A)**, TNF-α **(B)**, IL-1β **(C)**, IL-6 **(D)**, IL-8 **(E)** and MHC class II **(F)** were measured using RT-qPCR, and the data were normalised against 18S rRNA expression as a control. Experiments were conducted in triplicates, and error bars represent ± SEM. The relative expression (RQ) was calculated using cells challenged with Spike protein untreated with rfhSP-D as the calibrator. RQ = $2^{-\Delta\Delta Ct}$ was used to calculate the RQ value. Significance was determined using the two-way ANOVA test (**p < 0.01, and ****p < 0.0001) (n = 3).

SARS-CoV uses DC-SIGN for entry into DCs (47). In addition to its role as a virus attachment receptor, DC-SIGN has been implicated in triggering DC maturation, myeloid cell cytokine response, and T cell priming. Another CLR, SP-D, has been shown to have antiviral properties against SARS-CoV-2, HIV-1 and IAV infection (43, 45). We previously demonstrated that rfhSP-D reduced SARS-CoV-2 S1 protein binding to HEK293T cells overexpressing ACE2 receptors and infection in A549 cells by restricting viral entry (27). However, the role of SP-D in SARS-CoV-2 and DC-SIGN interaction is not well understood.

The binding of the SARS-CoV-2 Spike protein to the host cell *via* the ACE2 receptor is one of the critical steps in the SARS-CoV-2 infection (60). The receptor binding motif (RBM) (455-508) within the RBD of S1 protein interacts with the virus-binding residues consisting of Lys31, Glu35, and Lys353 of dimeric ACE2 (61). Although the sequence of events around the Spike protein/ACE2 association is becoming more evident, additional factors that aid infection remains unknown, for example, SARS-CoV-2 transport to the ACE2 receptor (36). Both SARS-CoV and SARS-CoV-2 Spike proteins have the same affinity for ACE2, but the transmission rate are drastically different (37). It has been suggested that the higher transmission rate of SARS-CoV-2 compared to SARS-CoV is due to more efficient viral adherence *via* host-cell attachment

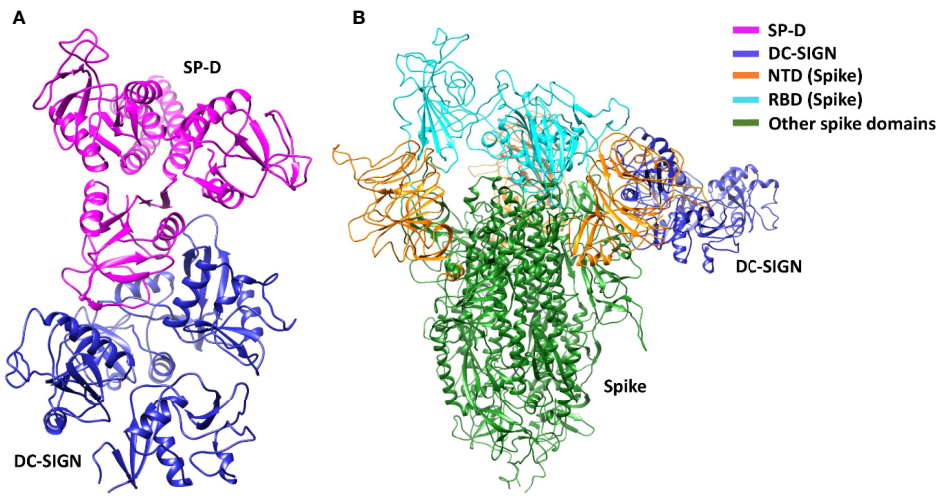

FIGURE 7
DC-SIGN interacts with both SP-D and SARS-CoV-2 spike. Docked poses of **(A)** complex A, and **(B)** complex B selected for docking and MD simulations respectively. In complex B, spike interacts with DC-SIGN (CRD) through the NTD domain (orange).

factors, leading to improved infection of ACE2 expressing cells (38, 39). DC-SIGN has also been identified as a SARS-CoV Spike protein receptor capable of enhancing cell entry in $ACE2^{+}$ pneumocytes *via* DC transfer (40). Recently, it has been shown that DC-SIGN binds to SARS-CoV-2 Spike protein and promotes trans-infection (20). In this study, we investigated the potential of rfhSP-D in inhibiting SARS-CoV-2 binding and entry into DC-SIGN expressing cells. Targeting viral entry into a host cell is a new approach for developing antiviral drugs that could interfere with viral propagation early in the SARS-CoV-2 viral cycle (62). We have independently confirmed the previously reported interaction between SARS-CoV-2 and rfhSP-D or DC-SIGN (20, 26, 27).

Here, we show that rfhSP-D enhances the binding of the SARS-CoV-2 Spike to DC-SIGN. This is further confirmed by *in-silico* molecular dynamics studies which indicate that SP-D stabilises the binding interactions between DC-SIGN CRD and N-terminal domain of SARS-CoV-2 Spike protein. The consequence of this tripartite complex involving DC-SIGN, SARS-CoV-2 Spike protein and rfhSP-D on viral infection was assessed using SARS-CoV-2 Spike protein-expressing replication-incompetent lentiviral pseudotyped viral particles since they are a safe alternative to the live virus. Using these pseudotypes, we demonstrate that rfhSP-D enhances spike protein binding and uptake in DC-SIGN expressing cells. A significant increase in spike protein binding and transduction was observed compared to untreated samples (Cells + SARS-CoV-2) to rfhSP-D (20 μg/ml) treatment. It has been shown previously that SP-D enhances the clearance of IAV from the lung *in vivo* (44). Similarly, the interaction of rfhSP-D with DC-

TABLE 2 Interaction analysis of the docked complexes of DC-SIGN, spike and SP-D.

Complex	DockedPose	Receptor	Ligand	H-bonding residues	
				Receptor	Ligand
A	2	DC-SIGN	SP-D	PHE262, GLN264, GLN274, ARG275, ASN362, SER383 CYS384	GLN263, GLN281, GLN282, ASN288, ASN316, TRP317, GLY320, ASP325
B	1	DC-SIGN	Spike	CYS253, HIS254, LYS285, GLY288, LEU321, ASN322, GLN323, GLU324, GLU353, ASN370, LYS379, SER380, ALA382, SER383	TYR28, ASN30, PHE58, PHE59, ASN61, VAL83, ASN87, ARG237, GLN239, PRO527, LYS529, SER530, THR531, ASN532, LEU533
C1 (A + Spike)	1	DC-SIGN	Spike	LEU321, GLY325, THR326, ARG345, ASN349, ASN350	ALA27, TYR28, HIS69, SER98, ASN211, ARG214
C2 (A + Spike)	2	DC-SIGN	Spike	ASN276, ASN322, GLN328, VAL330, GLY352, ASP355, ASN370	ASP111, GLU132, ASP138, PHE140, TYR160, ALA163, TYR248, THR250, SER254
		Spike	SP-D	ARG408, GLN409, VAL445, GLY502	ASN288, LYS299, SER328, GLY346

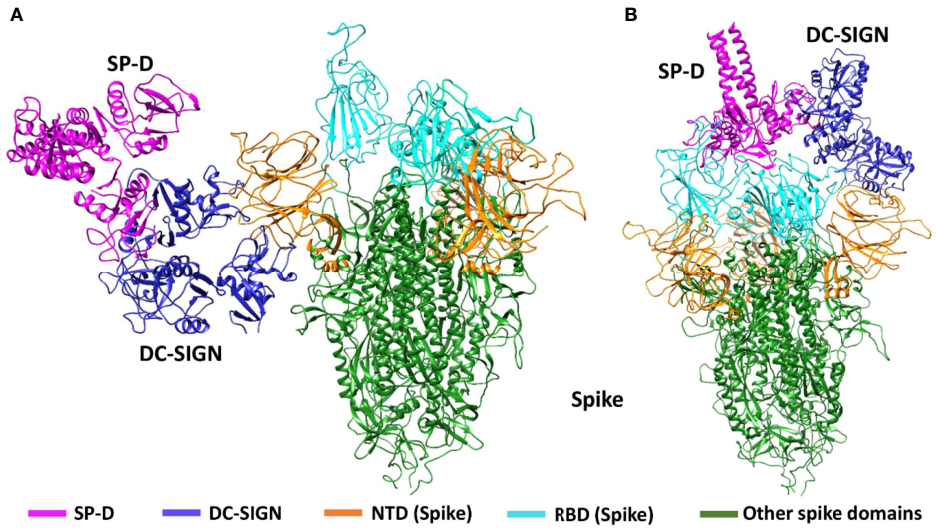

FIGURE 8
Tripartite complex of SP-D, DC-SIGN and SARS-CoV-2 Spike. Docked poses of tripartite complexes selected for MD simulation analysis. In complex C1, DC-SIGN (CRD) interacts with NTD of spike **(A)**; and in complex C2, DC-SIGN (CRD) interacts with NTD of spike and SP-D interacts with RBD of spike **(B)**.

SIGN may augment SARS-CoV-2 binding and uptake by macrophages, indicating that rfhSP-D may promote the clearance of SARS-CoV-2 *via* DC-SIGN.

The effect of rfhSP-D on gene expression levels of pro-inflammatory mediators in SARS-CoV-2 Spike protein challenged DC-HEK and DC-THP-1 cells were investigated in the current study. To our knowledge, this is the first study looking at the impact of rfhSP-D on DC-SIGN cells challenged with SARS-CoV-2. rfhSP-D showed anti-inflammatory effects on DC-SIGN expressing cells, as evident from the reduction in the levels of cytokines/chemokines such as TNF-α and IL-8.

DC-SIGN present on DC surface has been implicated in activating the STAT3 pathway during viral infection (63, 64). STAT3 plays a crucial role in activating transcription factor NF-κB in SARS-CoV-2 infection in myeloid cells, which may trigger subsequent cytokine production and stimulate pathological inflammation (65, 66). The activation of NF-κB in viral infection induces gene expression of a wide range of cytokines (e.g., IL-1, IL-2, IL-6, IL-12, TNF-α, LT-α, LT-β, and GM-CSF), and chemokines (e.g., IL-8, MIP-1, MCP1, RANTES, and eotaxin) (67). These inflammatory mediators are involved in antiviral immunity and essential for infection resistance (67). Nevertheless, in moderate and severe SARS-CoV 2 infection, the activation of NF-κB in various cells, including macrophages in the lungs, liver, kidney, central nervous system, gastrointestinal system, and cardiovascular system, results in the production of

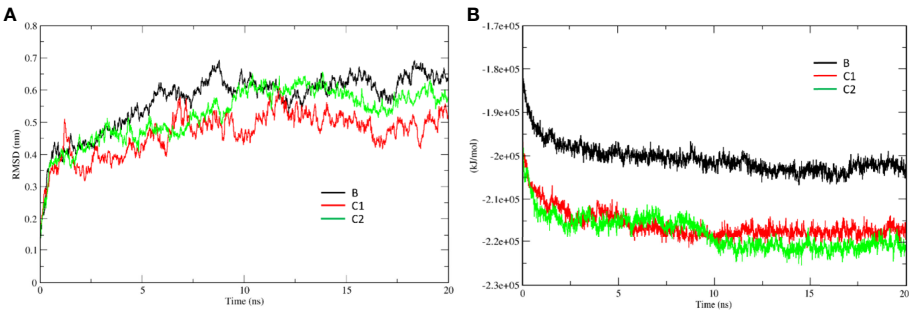

FIGURE 9
SP-D stabilises SARS-CoV-2 Spike interaction with DC-SIGN. Comparative MD simulation profile for complexes B, C1 and C2 of **(A)** root mean square deviation (RMSD) and **(B)** potential energy (PE). RMSD and PE of C1 and C2 are lesser than B indicating stability of tripartite complexes.

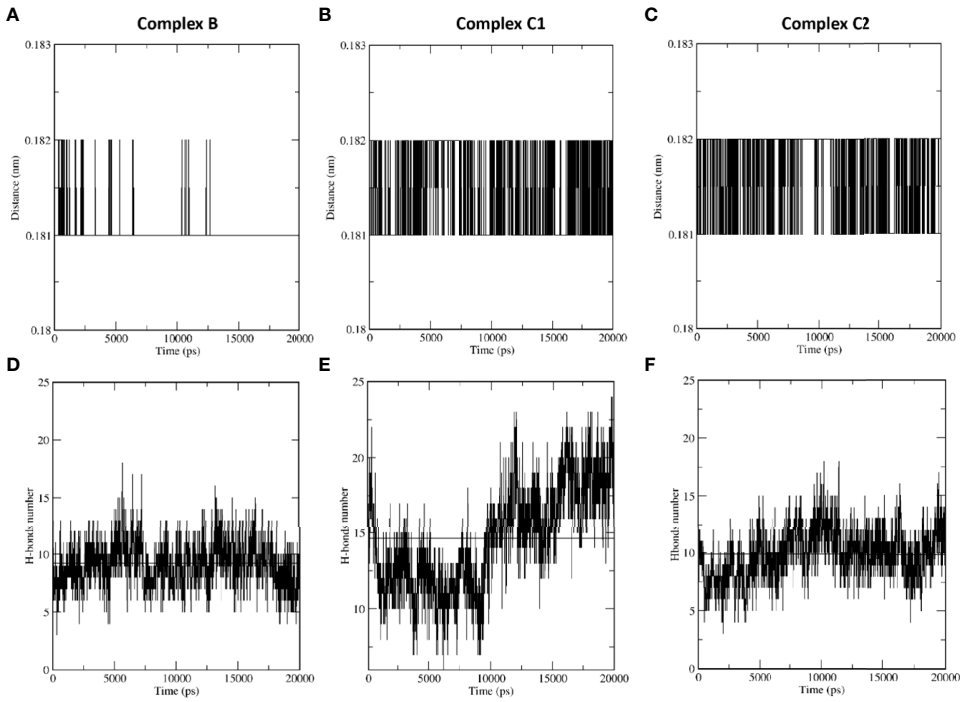

FIGURE 10
SP-D stabilises SARS-CoV-2 Spike interaction with DC-SIGN. Comparative MD simulation profile of complexes B, C1 and C2 for average distance **(A–C)** and H-bonds **(D–F)** between DC-SIGN and spike. The intermolecular distance is conserved across the simulation period for tripartite complexes C1 and C2 as compared to complex **(B)** The number of intermolecular H-bonds between DC-SIGN and spike are also higher for complexes C1 and C2 as compared to **(B)** These observations indicate the stabilising effect of SP-D on spike and DC-SIGN (CRD) interaction.

IL-1β, IL-6, IL-8, and TNF- α (68). This may result in cytokine storm and organ failure, and consequently, morbidity and mortality (68, 69). Immunomodulation at the level of NF-κB activation and inhibitors of NF-κB degradation may reduce the cytokine storm and lessen the severity of SARS-CoV-2 infection (68, 70). Pro-inflammatory mediators have been shown to be induced by SARS-CoV-2 Spike protein in THP-1 cells as *in vitro* model for lung macrophages (71). In this study, the inflammatory response was evaluated *via* measuring the gene expression levels of NF-κB in DC-HEK and DC-THP-1 challenged with SARS-CoV 2 spike protein. Our findings show that rfhSP-D downregulates the gene expression levels of NF-κB in DC-HEK and DC-THP-1 challenged with SARS-CoV-2 Spike protein. Thus, rfhSP-D suppresses pro-inflammatory immune response in DC-SIGN expressing immune cells.

Another critical element in the pathophysiology of SARS-CoV-2 infection is TNF-α, which is produced in the airway by macrophages, mast cells, T cells, epithelial cells, and smooth muscle cells (4, 72). TNF-α synthesis is predominantly stimulated by PAMPs through NF-κB activation (73). Various studies have reported that patients with severe SARS-CoV-2 infection display elevated plasma levels of TNF-α (74–76). This causes airway inflammation due to recruitment of mostly neutrophils (77). In addition, TNF-α stimulates the production of cytokines like IL-1β and IL-6 (78). DC-HEK and DC-THP-1, challenged with SARS-CoV-2 Spike protein, pre-treated with rfhSP-D, caused downregulation in the gene expression levels of TNF-α as compared to rfhSP-D-untreated cells. The results suggest an important immunomodulatory role of rfhSP-D in SARS-CoV-2-mediated inflammation.

IL-1β is released following activation of the inflammasome in response to a variety of infections, including SARS-CoV-2 (79). When compared to non-infected subjects, high levels of IL-1β were found in the plasma of severe as well as moderate CoVID-19 cases (75). Cell pyroptosis is a highly inflammatory form of programmed cell death typically seen with cytopathic viruses. An increase in IL-1β production is a downstream sign of pyroptosis (80). As a result, pyroptosis plays an essential role in the pathogenesis of SARS-CoV-2 and is a likely trigger for the uncontrolled inflammatory response (81). In this study, DC-THP-1 cells challenged by Spike protein, pre-treated with rfhSP-D, exhibited low mRNA levels of IL-1β as compared to the control. Thus, rfhSP-D may reduce the unnecessary inflammatory response to SARS-CoV-2 infection *via* reduction in IL-1β production.

IL-6 is a glycoprotein that regulates the immune system, haematopoiesis, inflammation and is a major player in SARS-

CoV-2 infection (82). Many cell types, including T and B lymphocytes, monocytes/macrophages, DCs fibroblasts and endothelial, express IL-6 (82, 83). A higher level of IL-6 in the plasma has been linked with the severity of SARS-CoV-2 infection (84, 85). rfhSP-D-treated DC-THP-1 cells challenged by Spike protein showed downregulation of IL-6 transcripts as compared with untreated cells. This suggests a role for SP-D in preventing IL-6 immunopathogenesis due to SARS-CoV2.

IFN-α is a cytokine mainly secreted by virus-infected cells associated with stimulation of immune response and limiting viral infection (86). Nonetheless, elevated expression levels of IFN-stimulated genes (ISGs) are triggered by SARS-CoV 2, which exhibits immunopathogenic potential (58). IFN-α expression levels are downregulated in rfhSP-D treated DC-HEK cells challenged with SARS-CoV-2 spike protein compared to the control. The results suggest rfhSP-D may elevate immunopathological potential of SARS-CoV-2.

Another element that may aid viral infectivity of DCs is MHC class II molecule. SARS-CoV-2 has been shown to upregulate MHC class II gene expression (87). High expression level of MHC class II molecules on the surface of antigen-presenting cells is crucial for regulating and inducing an adaptive immune response to respiratory viruses (88). However, limited-expression levels of MHC class II molecules on type II alveolar cells and macrophages improve respiratory viral disease outcomes (89). The binding of SARS-CoV-2 Spike protein to THP-1 cells polarises towards M1-like phenotype together with an increase in MHC class II molecules (71). DC-THP-1 cells challenged with SARS-CoV-2 Spike protein and treated with rfhSP-D showed downregulation of MHC class II mRNA expression levels. Thus, SP-D may have a role in modulating antigen presentation in order to avoid an unwanted and exaggerated adaptive immune response.

Chemokines, such as IL-8 and RANTES, are vital for recruiting inflammatory cells from the intravascular space across the endothelium and epithelium to the inflammation site (90). IL-8, commonly known as CXCL8, is a crucial mediator of inflammation with a direct chemotactic and priming action on neutrophils (91). In addition, IL-8 induces NETosis (Neutrophil extracellular traps/NETs). SARS-CoV-2 infected patients exhibit elevated levels of citrullinated histone H3 (Cit-H3) and myeloperoxidase (MPO)-DNA, which are specific markers of NETs that may cause organ damage (92). DC-THP-1 challenged with Spike protein and treated with rfhSP-D had low mRNA levels of IL-8 as compared to the control. There appears a role for SP-D in preventing IL-8-associated pathogenies due to SARS-CoV-2.

RANTES is a chemokine that has been linked with enhanced pathogenicity and mortality in SARS-CoV-2 infection (93). Compared to healthy control, SARS-CoV-2 infected patients contain higher serum RANTES and IL-6 levels which correlated with severity of CoVID-19 (94). In this study, the mRNA expression levels of RANTES were found to be considerably downregulated in DC-HEK cells challenged with Spike protein and treated with rfhSP-D. Thus, SP-D may modulate leukocyte recruitment to infection areas.

Thus, the results of this study help support the hypothesis that rfhSP-D facilitates the binding and uptake of SARS-CoV-2 pseudotypes and downregulates the virus-induced inflammatory response in DC-SIGN expressing cells. However, further study is required to assess the expression of DC-SIGN in individuals with mild/severe SARS-CoV-2 infection. SARS-CoV-2 is also known to affect organs other than the lungs. Thus, it is imperative to study the possibility of viral transfer to secondary sites *via* DC-SIGN and the effect of SP-D on this process. Furthermore, the interaction of rfhSP-D and/or DC-SIGN with the Spike protein of various SARS-CoV-2 variants and lineages need to be investigated to explore the viability of rfhSP-D as a universal treatment against SARS-CoV-2 infection. Additionally, the effects of rfhSP-D mediated DC-SIGN: SARS-CoV-2 interaction needs to be studied in the lung microenvironment using established animal models for COVID-19 such as Hamsters, Mouse, Ferret, Mink, Tree Shrew, and Non-human Primates.

In conclusion, our study reveals that rfhSP-D can effectively increase the binding and uptake of SARS-CoV-2 by DC-SIGN expressing cells. We also show that rfhSP-D causes substantial downregulation of pro-inflammatory cytokines such as IL-1β, TNF-α and IL-6, and chemokines like IL-8 and RANTES, in DC-SIGN expressing cells. These findings provide further credence to the evidence that rfhSP-D has a significant protective role against lung viral infection and immunopathogenesis. Our data suggests that rfhSP-D stabilises the interaction between SARS-CoV-2 Spike protein and DC-SIGN and helps in enhancing viral uptake by macrophages, suggesting an additional role for rfhSP-D in SARS-CoV-2 infection.

Data availability statement

The datasets presented in this study can be found in online repositories. The names of the repository/repositories and accession number(s) can be found below: https://biorxiv.org/cgi/content/short/2022.05.16.491949v1.

Author contributions

NB, PV, CK, MM, VM, and NT carried out crucial experiments; PV, TM, SI-T, and UK supervised most experiments; MS, RB, DM, MM, and NT generated crucial reagents; PV and UK produced the draft. All authors contributed to the article and approved the submitted version.

Funding

CK and SI-T are grateful to the grants received from the Department of Biotechnology, India [No. BT/PR40165/BTIS/

137/12/2021]. NT and MM are funded by the Wellcome Trust (GB-CHC-210183).

Conflict of interest

The authors declare that the research was conducted in the absence of any commercial or financial relationships that could be construed as a potential conflict of interest.

Publisher's note

References

1. Takeuchi O, Akira S. Pattern recognition receptors and inflammation. *Cell* (2010) 140(6):805–20. doi: 10.1016/j.cell.2010.01.022

2. Akira S, Uematsu S, Takeuchi O. Pathogen recognition and innate immunity. *Cell* (2006) 124(4):783–801. doi: 10.1016/j.cell.2006.02.015

3. Kumar H, Kawai T, Akira S. Pathogen recognition in the innate immune response. *Biochem J* (2009) 420(1):1–16. doi: 10.1042/BJ20090272

4. Akira S. Pathogen recognition by innate immunity and its signaling. *Proc Japan Academy Ser B* (2009) 85(4):143–56. doi: 10.2183/pjab.85.143

5. Stambach NS, Taylor ME. Characterization of carbohydrate recognition by langerin, a c-type lectin of langerhans cells. *Glycobiology* (2003) 13(5):401–10. doi: 10.1093/glycob/cwg045

6. Drickamer K, Taylor ME. Recent insights into structures and functions of c-type lectins in the immune system. *Curr Opin Struct Biol* (2015) 34:26–34. doi: 10.1016/j.sbi.2015.06.003

7. Qian C, Cao X. Dendritic cells in the regulation of immunity and inflammation. *Semin Immunol* (2018) 35:3–11. doi: 10.1016/j.smim.2017.12.002

8. Worbs T, Hammerschmidt SI, Förster R. Dendritic cell migration in health and disease. *Nat Rev Immunol* (2017) 17(1):30–48. doi: 10.1038/nri.2016.116

9. Geijtenbeek TB, Torensma R, van Vliet SJ, van Duijnhoven GC, Adema GJ, van Kooyk Y, et al. Identification of DC-SIGN, a novel dendritic cell–specific ICAM-3 receptor that supports primary immune responses. *Cell* (2000) 100 (5):575–85. doi: 10.1016/S0092-8674(00)80693-5

10. Pednekar L, Pandit H, Paudyal B, Kaur A, Al-Mozaini MA, Kouser L, et al. Complement protein C1q interacts with DC-SIGN via its globular domain and thus may interfere with HIV-1 transmission. *Front Immunol* (2016) 7:600. doi: 10.3389/fimmu.2016.00600

11. Mitchell DA, Fadden AJ, Drickamer K. A novel mechanism of carbohydrate recognition by the c-type lectins DC-SIGN and DC-SIGNR: Subunit organization and binding to multivalent ligands. *J Biol Chem* (2001) 276(31):28939–45. doi: 10.1074/jbc.M104565200

12. Hodges A, Sharrocks K, Edelmann M, Baban D, Moris A, Schwartz O, et al. Activation of the lectin DC-SIGN induces an immature dendritic cell phenotype triggering rho-GTPase activity required for HIV-1 replication. *Nat Immunol* (2007) 8(6):569–77. doi: 10.1038/ni1470

13. Frison N, Taylor ME, Soilleux E, Bousser M-T, Mayer R, Monsigny M, et al. Oligolysine-based oligosaccharide clusters: Selective recognition and endocytosis by the mannose receptor and dendritic cell-specific intercellular adhesion molecule 3 (ICAM-3)-Grabbing nonintegrin. *J Biol Chem* (2003) 278(26):23922–9. doi: 10.1074/jbc.M302483200

14. Halary F, Amara A, Lortat-Jacob H, Messerle M, Delaunay T, Houlès C, et al. Human cytomegalovirus binding to DC-SIGN is required for dendritic cell infection and target cell trans-infection. *Immunity* (2002) 17(5):653–64. doi: 10.1016/S1074-7613(02)00447-8

15. Alvarez CP, Lasala F, Carrillo J, Muñiz O, Corbí AL, Delgado R. C-type lectins DC-SIGN and l-SIGN mediate cellular entry by Ebola virus in cis and in trans. *J Virol* (2002) 76(13):6841–4. doi: 10.1128/JVI.76.13.6841-6844.2002

16. Carbaugh DL, Baric RS, Lazear HM. Envelope protein glycosylation mediates zika virus pathogenesis. *J Virol* (2019) 93(12):e00113–19. doi: 10.1128/JVI.00113-19

17. Geijtenbeek TB, Kwon DS, Torensma R, Van Vliet SJ, Van Duijnhoven GC, Middel J, et al. DC-SIGN, a dendritic cell–specific HIV-1-Binding protein that enhances trans-infection of T cells. *Cell* (2000) 100(5):587–97. doi: 10.1016/S0092-8674(00)80694-7

18. Navarro-Sanchez E, Altmeyer R, Amara A, Schwartz O, Fieschi F, Virelizier JL, et al. Dendritic-Cell-Specific ICAM3-grabbing non-integrin is essential for the productive infection of human dendritic cells by mosquito-Cell-Derived dengue viruses. *EMBO Rep* (2003) 4(7):723–8. doi: 10.1038/sj.embor.embor866

19. Manches O, Frleta D, Bhardwaj N. Dendritic cells in progression and pathology of HIV infection. *Trends Immunol* (2014) 35(3):114–22. doi: 10.1016/j.it.2013.10.003

20. Thépaut M, Luczkowiak J, Vivès C, Labiod N, Bally I, Lasala F, et al. Dc/L-SIGN recognition of spike glycoprotein promotes SARS-CoV-2 trans-infection and can be inhibited by a glycomimetic antagonist. *PLoS Pathog* (2021) 17(5):e1009576. doi: 10.1371/journal.ppat.1009576

21. Arroyo R, Grant SN, Colombo M, Salvioni L, Corsi F, Truffi M, et al. Full-length recombinant hSP-d binds and inhibits SARS-CoV-2. *Biomolecules* (2021) 11 (8):1114. doi: 10.3390/biom11081114

22. Singh M, Madan T, Waters P, Parida SK, Sarma PU, Kishore U. Protective effects of a recombinant fragment of human surfactant protein d in a murine model of pulmonary hypersensitivity induced by dust mite allergens. *Immunol Lett* (2003) 86(3):299–307. doi: 10.1016/S0165-2478(03)00033-6

23. Liu M-Y, Zheng B, Zhang Y, Li J-P. Role and mechanism of angiotensin-converting enzyme 2 in acute lung injury in coronavirus disease 2019. *Chronic Dis Trans Med* (2020) 6(2):98–105. doi: 10.1016/j.cdtm.2020.05.003

24. Luan B, Huynh T, Cheng X, Lan G, Wang H-R. Targeting proteases for treating COVID-19. *J Proteome Res* (2020) 19(11):4316–26. doi: 10.1021/acs.jproteome.0c00430

25. Dodagatta-Marri E, Mitchell DA, Pandit H, Sonawani A, Murugaiah V, Idicula-Thomas S, et al. Protein–protein interaction between surfactant protein d and DC-SIGN via c-type lectin domain can suppress HIV-1 transfer. *Front Immunol* (2017) 8:834. doi: 10.3389/fimmu.2017.00834

26. Madan T, Biswas B, Varghese PM, Subedi R, Pandit H, Idicula-Thomas S, et al. A recombinant fragment of human surfactant protein d binds spike protein and inhibits infectivity and replication of SARS-CoV-2 in clinical samples. *Am J Respir Cell Mol Biol* (2021) 65(1):41–53. doi: 10.1165/rcmb.2021-0005OC

27. Hsieh M-H, Beirag N, Murugaiah V, Chou Y-C, Kuo W-S, Kao H-F, et al. Human surfactant protein d binds spike protein and acts as an entry inhibitor of SARS-CoV-2 pseudotyped viral particles. *Front Immunol* (2021) 12:1613. doi: 10.3389/fimmu.2021.641360

28. Dessie ZG, Zewotir T. Mortality-related risk factors of COVID-19: A systematic review and meta-analysis of 42 studies and 423,117 patients. *BMC Infect Dis* (2021) 21(1):1–28. doi: 10.1186/s12879-021-06536-3

29. Abate SM, Checkol YA, Mantefardo B. Global prevalence and determinants of mortality among patients with COVID-19: A systematic review and meta-analysis. *Ann Med Surg* (2021) 64:102204. doi: 10.1016/j.amsu.2021.102204

30. Chen N, Zhou M, Dong X, Qu J, Gong F, Han Y, et al. Epidemiological and clinical characteristics of 99 cases of 2019 novel coronavirus pneumonia in wuhan, China: A descriptive study. *Lancet* (2020) 395(10223):507–13. doi: 10.1016/S0140-6736(20)30211-7

31. Hirabara SM, Serdan TD, Gorjao R, Masi LN, Pithon-Curi TC, Covas DT, et al. SARS-COV-2 variants: Differences and potential of immune evasion. *Front Cell Infection Microbiol* (2022) p:1401. doi: 10.3389/fcimb.2021.781429

32. Wu Z, McGoogan JM. Characteristics of and important lessons from the coronavirus disease 2019 (COVID-19) outbreak in China: Summary of a report of 72 314 cases from the Chinese center for disease control and prevention. *JAMA* (2020) 323(13):1239–42. doi: 10.1001/jama.2020.2648

33. Ludwig S, Zarbock A. Coronaviruses and SARS-CoV-2: A brief overview. *Anesth analgesia* (2020) 131(1):93–6. doi: 10.1213/ANE.0000000000004845

34. Shirbhate E, Pandey J, Patel VK, Kamal M, Jawaid T, Gorain B, et al. Understanding the role of ACE-2 receptor in pathogenesis of COVID-19 disease: A potential approach for therapeutic intervention. *Pharmacol Rep* (2021) 73(6):1539–50. doi: 10.1007/s43440-021-00303-6

35. Ni W, Yang X, Yang D, Bao J, Li R, Xiao Y, et al. Role of angiotensin-converting enzyme 2 (ACE2) in COVID-19. *Crit Care* (2020) 24(1):1–10. doi: 10.1186/s13054-020-03120-0

36. Walls AC, Park Y-J, Tortorici MA, Wall A, McGuire AT, Veesler D. Structure, function, and antigenicity of the SARS-CoV-2 spike glycoprotein. *Cell* (2020) 181(2):281–92.e6. doi: 10.1016/j.cell.2020.02.058

37. Petersen E, Koopmans M, Go U, Hamer DH, Petrosillo N, Castelli F, et al. Comparing SARS-CoV-2 with SARS-CoV and influenza pandemics. *Lancet Infect Dis* (2020) 20(9):e238–44. doi: 10.1016/S1473-3099(20)30484-9

38. Sungnak W, Huang N, Bécavin C, Berg M, Queen R, Litvinukova M, et al. SARS-CoV-2 entry factors are highly expressed in nasal epithelial cells together with innate immune genes. *Nat Med* (2020) 26(5):681–7. doi: 10.1038/s41591-020-0868-6

39. Backovic M, Rey FA. Virus entry: Old viruses, new receptors. *Curr Opin Virol* (2012) 2(1):4–13. doi: 10.1016/j.coviro.2011.12.005

40. Yang Z-Y, Huang Y, Ganesh L, Leung K, Kong W-P, Schwartz O, et al. pH-dependent entry of severe acute respiratory syndrome coronavirus is mediated by the spike glycoprotein and enhanced by dendritic cell transfer through DC-SIGN. *J Virol* (2004) 78(11):5642–50. doi: 10.1128/JVI.78.11.5642-5650.2004

41. Marzi A, Gramberg T, Simmons G, Moüller P, Rennekamp AJ, Krumbiegel M, et al. DC-SIGN and DC-SIGNR interact with the glycoprotein of marburg virus and the s protein of severe acute respiratory syndrome coronavirus. *J Virol* (2004) 78(21):12090–5. doi: 10.1128/JVI.78.21.12090-12095.2004

42. Mangalmurti N, Hunter CA. Cytokine storms: Understanding COVID-19. *Immunity* (2020) 53(1):19–25. doi: 10.1016/j.immuni.2020.06.017

43. Al-Ahdal MN, Murugaiah V, Varghese PM, Abozaid SM, Saba I, Al-Qahtani AA, et al. Entry inhibition and modulation of pro-inflammatory immune response against influenza a virus by a recombinant truncated surfactant protein d. *Front Immunol* (2018) 9:1586. doi: 10.3389/fimmu.2018.01586

44. LeVine AM, Whitsett JA, Hartshorn KL, Crouch EC, Korfhagen TR. Surfactant protein d enhances clearance of influenza a virus from the lung in vivo. *J Immunol* (2001) 167(10):5868–73. doi: 10.4049/jimmunol.167.10.5868

45. Pandit H, Gopal S, Sonawani A, Yadav AK, Qaseem AS, Warke H, et al. Surfactant protein d inhibits HIV-1 infection of target cells via interference with Gp120-CD4 interaction and modulates pro-inflammatory cytokine production. *PLoS One* (2014) 9(7):e102395. doi: 10.1371/journal.pone.0102395

46. Pandit H, Kale K, Yamamoto H, Thakur G, Rokade S, Chakraborty P, et al. Surfactant protein d reverses the gene signature of transepithelial HIV-1 passage and restricts the viral transfer across the vaginal barrier. *Front Immunol* (2019) 10:264. doi: 10.3389/fimmu.2019.00264

47. Amraei R, Yin W, Napoleon MA, Suder EL, Berrigan J, Zhao Q, et al. CD209L/L-SIGN and CD209/DC-SIGN act as receptors for SARS-CoV-2. *ACS Cent Sci* (2021) 7(7):1156–65. doi: 10.1021/acscentsci.0c01537

48. Lempp FA, Soriaga LB, Montiel-Ruiz M, Benigni F, Noack J, Park Y-J, et al. Lectins enhance SARS-CoV-2 infection and influence neutralizing antibodies. *Nature* (2021) 598(7880):342–7. doi: 10.1038/s41586-021-03925-1

49. Jin C, Wu L, Li J, Fang M, Cheng L, Wu N. Multiple signaling pathways are involved in the interleukine-4 regulated expression of DC-SIGN in THP-1 cell line. *J Biomedicine Biotechnol* (2012) 2012:357060. doi: 10.1155/2012/357060

50. Abraham MJ, Murtola T, Schulz R, Páll S, Smith JC, Hess B, et al. GROMACS: High performance molecular simulations through multi-level parallelism from laptops to supercomputers. *SoftwareX* (2015) 1-2:19–25. doi: 10.1016/j.softx.2015.06.001

51. Lindorff-Larsen K, Piana S, Palmo K, Maragakis P, Klepeis JL, Dror RO, et al. Improved side-chain torsion potentials for the amber Ff99sb protein force field. *Proteins* (2010) 78(8):1950–8. doi: 10.1002/prot.22711

52. Mogensen TH. Pathogen recognition and inflammatory signaling in innate immune defenses. *Clin Microbiol Rev* (2009) 22(2):240–73. doi: 10.1128/CMR.00046-08

53. Li D, Wu M. Pattern recognition receptors in health and diseases. *Signal Transduct Targeted Ther* (2021) 6(1):1–24. doi: 10.1038/s41392-021-00687-0

54. Lai C-C, Shih T-P, Ko W-C, Tang H-J, Hsueh P-R. Severe acute respiratory syndrome coronavirus 2 (SARS-CoV-2) and coronavirus disease-2019 (COVID-19): The epidemic and the challenges. *Int J Antimicrob Agents* (2020) 55(3):105924. doi: 10.1016/j.ijantimicag.2020.105924

55. Hu B, Guo H, Zhou P, Shi Z-L. Characteristics of SARS-CoV-2 and COVID-19. *Nat Rev Microbiol* (2021) 19(3):141–54. doi: 10.1038/s41579-020-00459-7

56. Xu J, Xu X, Jiang L, Dua K, Hansbro PM, Liu G. SARS-CoV-2 induces transcriptional signatures in human lung epithelial cells that promote lung fibrosis. *Respir Res* (2020) 21(1):1–12. doi: 10.1186/s12931-020-01445-6

57. Perrotta F, Matera MG, Cazzola M, Bianco A. Severe respiratory SARS-CoV2 infection: Does ACE2 receptor matter? *Respir Med* (2020) 168:105996. doi: 10.1016/j.rmed.2020.105996

58. Marzi A, Möller P, Hanna SL, Harrer T, Eisemann J, Steinkasserer A, et al. Analysis of the interaction of Ebola virus glycoprotein with DC-SIGN (Dendritic cell–specific intercellular adhesion molecule 3–grabbing nonintegrin) and its homologue DC-SIGNR. *J Infect Dis* (2007) 196(Supplement_2):S237–46. doi: 10.1086/520607

59. Poühlmann S, Leslie GJ, Edwards TG, Macfarlan T, Reeves JD, Hiebenthal-Millow K, et al. DC-SIGN interactions with human immunodeficiency virus: Virus binding and transfer are dissociable functions. *J Virol* (2001) 75(21):10523–6. doi: 10.1128/JVI.75.21.10523-10526.2001

60. Benton DJ, Wrobel AG, Xu P, Roustan C, Martin SR, Rosenthal PB, et al. Receptor binding and priming of the spike protein of SARS-CoV-2 for membrane fusion. *Nature* (2020) 588(7837):327–30. doi: 10.1038/s41586-020-2772-0

61. Shang J, Ye G, Shi K, Wan Y, Luo C, Aihara H, et al. Structural basis of receptor recognition by SARS-CoV-2. *Nature* (2020) 581(7807):221–4. doi: 10.1038/s41586-020-2179-y

62. Murgolo N, Therien AG, Howell B, Klein D, Koeplinger K, Lieberman LA, et al. SARS-CoV-2 tropism, entry, replication, and propagation: Considerations for drug discovery and development. *PLoS Pathog* (2021) 17(2):e1009225. doi: 10.1371/journal.ppat.1009225

63. Liu J, Zhang X, Cheng Y, Cao X. Dendritic cell migration in inflammation and immunity. *Cell Mol Immunol* (2021) 18(11):2461–71. doi: 10.1038/s41423-021-00726-4

64. Marongiu L, Valache M, Facchini FA, Granucci F. How dendritic cells sense and respond to viral infections. *Clin Sci* (2021) 135(19):2217–42. doi: 10.1042/CS20210577

65. Farahani M, Niknam Z, Amirabad LM, Amiri-Dashatan N, Koushki M, Nemati M, et al. Molecular pathways involved in COVID-19 and potential pathway-based therapeutic targets. *Biomed Pharmacother* (2022) 145:112420. doi: 10.1016/j.biopha.2021.112420

66. Yang L, Xie X, Tu Z, Fu J, Xu D, Zhou Y. The signal pathways and treatment of cytokine storm in COVID-19. *Signal Transduct Targeted Ther* (2021) 6(1):1–20. doi: 10.1038/s41392-021-00679-0

67. Mogensen TH, Paludan SR. Molecular pathways in virus-induced cytokine production. *Microbiol Mol Biol Rev* (2001) 65(1):131–50. doi: 10.1128/MMBR.65.1.131-150.2001

68. Kircheis R, Haasbach E, Lueftenegger D, Heyken WT, Ocker M, Planz O. NF-κb pathway as a potential target for treatment of critical stage COVID-19 patients. *Front Immunol* (2020) 11:3446. doi: 10.3389/fimmu.2020.598444

69. Hirano T, Murakami M. COVID-19: A new virus, but a familiar receptor and cytokine release syndrome. *Immunity* (2020) 52(5):731–3. doi: 10.1016/j.immuni.2020.04.003

70. Kircheis R, Haasbach E, Lueftenegger D, Heyken WT, Ocker M, Planz O. Perspective: NF-κb pathway as a potential target for treatment of critical stage COVID-19 patients. (2020) 11:598444. doi: 10.3389/fimmu.2020.598444

71. Barhoumi T, Alghanem B, Shaibah H, Mansour FA, Alamri HS, Akiel MA, et al. SARS-CoV-2 coronavirus spike protein-induced apoptosis, inflammatory, and oxidative stress responses in THP-1-Like-Macrophages: Potential role of angiotensin-converting enzyme inhibitor (Perindopril). *Front Immunol* (2021) 12. doi: 10.3389/fimmu.2021.728896

72. Mukhopadhyay S, Hoidal JR, Mukherjee TK. Role of tnfα in pulmonary pathophysiology. *Respir Res* (2006) 7(1):1–9. doi: 10.1186/1465-9921-7-125

73. Muñoz-Carrillo JL, Contreras-Cordero JF, Gutiérrez-Coronado O, Villalobos-Gutiérrez PT, Ramos-Gracia LG, Hernández-Reyes VE. Cytokine profiling plays a crucial role in activating immune system to clear infectious pathogens. In: *Immune response activation and immunomodulationed*. IntechOpen (2018) 2019. doi: 10.5772/intechopen.80843

74. Chen G, Wu D, Guo W, Cao Y, Huang D, Wang H, et al. Clinical and immunological features of severe and moderate coronavirus disease 2019. *J Clin Invest* (2020) 130(5):2620–9. doi: 10.1172/JCI137244

75. Huang C, Wang Y, Li X, Ren L, Zhao J, Hu Y, et al. Clinical features of patients infected with 2019 novel coronavirus in wuhan, China. *Lancet* (2020) 395 (10223):497–506. doi: 10.1016/S0140-6736(20)30183-5

76. Qin C, Zhou L, Hu Z, Zhang S, Yang S, Tao Y, et al. Dysregulation of immune response in patients with COVID-19 in wuhan, china; clinical infectious diseases; Oxford academic. *Clin Infect Dis* (2020) 28;71(15):762–8. doi: 10.1093/cid/ciaa248

77. Makwana R, Gozzard N, Spina D, Page C. TNF-α-Induces airway hyperresponsiveness to cholinergic stimulation in Guinea pig airways. *Br J Pharmacol* (2012) 165(6):1978–91. doi: 10.1111/j.1476-5381.2011.01675.x

78. Peiris J, Lai S, Poon L, Guan Y, Yam L, Lim W, et al. Coronavirus as a possible cause of severe acute respiratory syndrome. *Lancet* (2003) 361 (9366):1319–25. doi: 10.1016/S0140-6736(03)13077-2

79. Chen I-Y, Moriyama M, Chang M-F, Ichinohe T. Severe acute respiratory syndrome coronavirus viroporin 3a activates the NLRP3 inflammasome. *Front Microbiol* (2019) 10:50. doi: 10.3389/fmicb.2019.00050

80. Warke T, Fitch P, Brown V, Taylor R, Lyons J, Ennis M, et al. Exhaled nitric oxide correlates with airway eosinophils in childhood asthma. *Thorax* (2002) 57 (5):383–7. doi: 10.1136/thorax.57.5.383

81. Wang X, Jiang W, Yan Y, Gong T, Han J, Tian Z, et al. RNA Viruses promote activation of the NLRP3 inflammasome through a RIP1-RIP3-DRP1 signaling pathway. *Nat Immunol* (2014) 15(12):1126–33. doi: 10.1038/ni.3015

82. Jones SA, Jenkins BJ. Recent insights into targeting the IL-6 cytokine family in inflammatory diseases and cancer. *Nat Rev Immunol* (2018) 18(12):773–89. doi: 10.1038/s41577-018-0066-7

83. Tanaka T, Narazaki M, Kishimoto T. IL-6 in inflammation, immunity, and disease. *Cold Spring Harbor Perspect Biol* (2014) 6(10):a016295. doi: 10.1101/cshperspect.a016295

84. Chen X, Zhao B, Qu Y, Chen Y, Xiong J, Feng Y, et al. Detectable serum SARS-CoV-2 viral load (RNAaemia) is closely correlated with drastically elevated interleukin 6 (IL-6) level in critically ill COVID-19 patients. *Clin Infect Dis* (2020) 71(8):1937–42. doi: 10.1093/cid/ciaa449

85. Herold T, Jurinovic V, Arnreich C, Lipworth BJ, Hellmuth JC, von Bergwelt-Baildon M, et al. Elevated levels of IL-6 and CRP predict the need for mechanical ventilation in COVID-19. *J Allergy Clin Immunol* (2020) 146(1):128–136. e4. doi: 10.1016/j.jaci.2020.05.008

86. Lee AJ, Ashkar AA. The dual nature of type I and type II interferons. *Front Immunol* (2018), 11, 9:2061. doi: 10.3389/fimmu.2018.02061

87. Hargadon KM, Zhou H, Albrecht RA, Dodd HA, Garcia-Sastre A, Braciale TJ. Major histocompatibility complex class II expression and hemagglutinin subtype influence the infectivity of type a influenza virus for respiratory dendritic cells. *J Virol* (2011) 85(22):11955–63. doi: 10.1128/JVI.05830-11

88. Braciale TJ, Sun J, Kim TS. Regulating the adaptive immune response to respiratory virus infection. *Nat Rev Immunol* (2012) 12(4):295–305. doi: 10.1038/nri3166

89. Toulmin SA, Bhadiadra C, Paris AJ, Lin JH, Katzen J, Basil MC, et al. Type II alveolar cell MHCII improves respiratory viral disease outcomes while exhibiting limited antigen presentation. *Nat Commun* (2021) 12(1):1–15. doi: 10.1038/s41467-021-23619-6

90. Sokol CL, Luster AD. The chemokine system in innate immunity. *Cold Spring Harbor Perspect Biol* (2015) 7(5):a016303. doi: 10.1101/cshperspect.a016303

91. Kobayashi Y. The role of chemokines in neutrophil biology. *Front Biosci* (2008) 13(1):2400–7. doi: 10.2741/2853

92. Zuo Y, Yalavarthi S, Shi H, Gockman K, Zuo M, Madison JA, et al. Neutrophil extracellular traps in COVID-19. *JCI Insight* (2020) 5(11):e138999. doi: 10.1172/jci.insight.138999

93. Posch W, Vosper J, Noureen A, Zaderer V, Witting C, Bertacchi G, et al. C5aR inhibition of nonimmune cells suppresses inflammation and maintains epithelial integrity in SARS-CoV-2–infected primary human airway epithelia. *J Allergy Clin Immunol* (2021) 147(6):2083–97.e6. doi: 10.1016/j.jaci.2021.03.038

94. Patterson BK, Seethamraju H, Dhody K, Corley MJ, Kazempour K, Lalezari J, et al. Disruption of the CCL5/RANTES-CCR5 pathway restores immune homeostasis and reduces plasma viral load in critical COVID-19. *MedRxiv* (2020) 5:2020.05.02.20084673. doi: 10.1101/2020.05.02.20084673

frontiers | Frontiers in Immunology

TYPE Original Research
PUBLISHED 11 August 2022
DOI 10.3389/fimmu.2022.968991

OPEN ACCESS

EDITED BY
Nitin Saksena,
Victoria University, Australia

REVIEWED BY
Vitale Miceli,
Mediterranean Institute for Transplantation and Highly Specialized Therapies (ISMETT), Italy
Samuel Brennan,
Genieus Genomics, Australia

*CORRESPONDENCE
Luisa Barzon
luisa.barzon@unipd.it

†These authors have contributed equally to this work and share first authorship

‡These authors share last authorship

SPECIALTY SECTION
This article was submitted to Vaccines and Molecular Therapeutics, a section of the journal Frontiers in Immunology

RECEIVED 14 June 2022
ACCEPTED 20 July 2022
PUBLISHED 11 August 2022

CITATION
Giannella A, Riccetti S, Sinigaglia A, Piubelli C, Razzaboni E, Di Battista P, Agostini M, Dal Molin E, Manganelli R, Gobbi F, Ceolotto G and Barzon L (2022) Circulating microRNA signatures associated with disease severity and outcome in COVID-19 patients.
Front. Immunol. 13:968991.
doi: 10.3389/fimmu.2022.968991

Circulating microRNA signatures associated with disease severity and outcome in COVID-19 patients

Alessandra Giannella[1†], Silvia Riccetti[2†], Alessandro Sinigaglia[2], Chiara Piubelli[3], Elisa Razzaboni[3], Piero Di Battista[4], Matteo Agostini[2], Emanuela Dal Molin[2], Riccardo Manganelli[2,5], Federico Gobbi[3‡], Giulio Ceolotto[1‡] and Luisa Barzon[2,5*‡]

[1]Department of Medicine, University of Padova, Padova, Italy, [2]Department of Molecular Medicine, University of Padova, Padova, Italy, [3]Department of Infectious-Tropical Diseases and Microbiology, Istituto di Ricovero e Cura a Carattere Scientifico (IRCCS), Sacro Cuore Don Calabria Hospital, Verona, Italy, [4]Maternal and Child Health Department, University of Padova, Padova, Italy, [5]Microbiology and Virology Unit, Padova University Hospital, Padova, Italy

Background: SARS-CoV-2 induces a spectrum of clinical conditions ranging from asymptomatic infection to life threatening severe disease. Host microRNAs have been involved in the cytokine storm driven by SARS-CoV-2 infection and proposed as candidate biomarkers for COVID-19.

Methods: To discover signatures of circulating miRNAs associated with COVID-19, disease severity and mortality, small RNA-sequencing was performed on serum samples collected from 89 COVID-19 patients (34 severe, 29 moderate, 26 mild) at hospital admission and from 45 healthy controls (HC). To search for possible sources of miRNAs, investigation of differentially expressed (DE) miRNAs in relevant human cell types *in vitro*.

Results: COVID-19 patients showed upregulation of miRNAs associated with lung disease, vascular damage and inflammation and downregulation of miRNAs that inhibit pro-inflammatory cytokines and chemokines, angiogenesis, and stress response. Compared with mild/moderate disease, patients with severe COVID-19 had a miRNA signature indicating a profound impairment of innate and adaptive immune responses, inflammation, lung fibrosis and heart failure. A subset of the DE miRNAs predicted mortality. In particular, a combination of high serum miR-22-3p and miR-21-5p, which target antiviral response genes, and low miR-224-5p and miR-155-5p, targeting pro-inflammatory factors, discriminated severe from mild/moderate COVID-19 (AUROC 0.88, 95% CI 0.80-0.95, p<0.0001), while high leukocyte count and low levels of miR-1-3p, miR-23b-3p, miR-141-3p, miR-155-5p and miR-4433b-5p predicted mortality with high sensitivity and specificity (AUROC 0.95, 95% CI 0.89-1.00, p<0.0001). *In vitro* experiments showed that some of the DE miRNAs were modulated directly by SARS-CoV-2 infection in permissive lung epithelial cells.

Conclusions: We discovered circulating miRNAs associated with COVID-19 severity and mortality. The identified DE miRNAs provided clues on COVID-19 pathogenesis, highlighting signatures of impaired interferon and antiviral responses, inflammation, organ damage and cardiovascular failure as associated with severe disease and death.

KEYWORDS

COVID-19, microRNA, biomarkers, innate immunity, inflammation, interferon, SARS-CoV-2, RNA-sequencing

Introduction

Severe acute respiratory syndrome coronavirus 2 (SARS-CoV-2), the cause of coronavirus disease 2019 (COVID-19), induces a spectrum of clinical conditions ranging from asymptomatic infection to life threatening severe disease, characterized by respiratory failure, shock and multi-organ dysfunction requiring admission in the intensive care unit (ICU). Old age, male sex, presence of co-morbidities like hypertension, diabetes, immunosuppression, defective interferon (IFN) response and genetic predisposition, have been identified as risk factors for severe COVID-19 and associated with increased mortality (1–3).

Several studies searched for diagnostic biomarkers of severe COVID-19 and for prognostic biomarkers of ICU admission and risk of death. For example, abnormal levels of several clinical and laboratory parameters, such as renal dysfunction, elevated C reactive protein (CRP) and D-dimer levels, high serum levels of interleukin-6 (IL-6) and tumor necrosis factor-α (TNF-α) were identified as predictors of worsening outcome in COVID-19 (4, 5). Systems biological analysis identified increased plasma levels of inflammatory mediators and defects of type I IFN response as associated with severe COVID-19 (6), while single cell transcriptomics of immune cells in critically ill COVID-19 patients identified increased expression of genes involved in cell cycle regulation, cell-specific activation markers, and antibody processing within B-, T-, and NK-cell subsets in patients who survived (7).

Circulating microRNAs (miRNAs) have been proposed as candidate biomarkers for clinical conditions, such as malignancy, cardiovascular diseases, and infectious diseases (8–11), including COVID-19 (12). MiRNA are small non-coding RNA molecules of about 22 nucleotide in length, generated from the endogenous cellular mRNAs, long noncoding RNAs, and tRNAs (13). These small RNA molecules play a key role in the fine tuning of cell functions by suppression of protein synthesis from target mRNAs (14). Host miRNAs exert an important role in innate and adaptive immune cell development, especially during infections, (11) and have been involved in the cytokine storm driven by SARS-CoV-2 infection and proposed a candidate diagnostic and prognostic biomarkers in COVID-19 patients (15–24).

In this study, we analyzed by small RNA-sequencing a large cohort of COVID-19 patients at the time of hospital admission and healthy controls (HC) to identify signatures of circulating serum miRNAs associated with SARS-CoV-2 infection, disease severity and mortality. To search for possible sources of the differentially expressed (DE) serum miRNAs, we analyzed their expression in relevant human cell types *in vitro* upon SARS-CoV-2 infection and IFN type I treatment.

Materials and methods

Ethics statement

All subjects or their legal representatives provided written informed consent. Serum samples were collected at admission and stored in Tropica Biobank (BBMRI-eric ID: IT_1605519998080235) upon use. The study, which was conducted in accordance with the ethical principles of the Declaration of Helsinki, was approved by the local Ethics Committee (Comitato Etico per la Sperimentazione Clinica delle Province di Verona e Rovigo) on November 24, 2020 (study protocol n 63471).

Study subjects

The study population included 89 COVID-19 patients, who were admitted at the IRCCS Sacro Cuore Don Calabria hospital, Negrar, Verona, Italy, in the period between May 2020 and December 2020. Inclusion criteria for the study were age ≥18 years and diagnosis of SARS-CoV-2 infection confirmed by molecular testing on nasopharyngeal swabs. As exclusion criteria, pregnant women were not enrolled. Disease severity

was scored into mild, moderate, and severe at the time of hospital admission according to World Health Organization COVID-19 disease severity classification criteria (25). In particular, individuals who tested positive for SARS-CoV-2 using a virologic test (i.e., a nucleic acid amplification test or an antigen test) but had no symptoms consistent with COVID-19 were classified as asymptomatic or with presymptomatic infection; individuals who had any of the various signs and symptoms of COVID-19 (e.g., fever, cough, sore throat, malaise, headache, muscle pain, nausea, vomiting, diarrhea, loss of taste and smell) but who did not have shortness of breath, dyspnea, or abnormal chest imaging were classified as mild COVID-19; individuals who showed evidence of lower respiratory disease during clinical assessment or imaging and who had an oxygen saturation (SpO2) ≥94% on room air at sea level were classified as moderate COVID-19; individuals who had SpO2 <94% on room air at sea level, a ratio of arterial partial pressure of oxygen to fraction of inspired oxygen (PaO2/FiO2) <300 mm Hg, a respiratory rate >30 breaths/min, or lung infiltrates >50% were classified ad severe COVID-19; individuals who had respiratory failure, septic shock, and/or multiple organ dysfunction were classified as cases of critical COVID-19. No cases of asymptomatic infection or critical COVID-19 at the time of hospital admission were enrolled in the study. Peripheral blood samples were collected at the time of hospital admission, and before starting medications. Sera were separated from whole blood by centrifugation for 15 min at 3,000 rpm at 4°C and stored at -80°C until processing. Serum samples from 45 healthy volunteers collected before September 2019 and stored at -80°C were used as negative control group (25 females, 20 males; median age 45, range 24-76).

Small RNA library preparation and quantification for next generation sequencing

Small RNA libraries from serum samples were obtained using QIAseq® miRNA Library kit (Qiagen, Hilden, Germany), according to the manufacturer protocol. NGS Library Quality Control (QC) analysis and quantification were performed before sequencing: a) High sensitivity DNA electrophoresis by LabChip GX Touch Nucleic Acid Analyzer (PerkinElmer, Massachusetts, USA) using HT DNA 5K/RNA LABCHIP kit (D-MARK Biosciences, Toronto, Canada) according to the manufacturer's instructions. We obtained typical electropherograms from small RNA libraries that show a peak between 170-180 bp corresponding to miRNA-sized library; b) quantitative polymerase chain reaction (qPCR) according to the manufacturer's protocol, using three different primers provided by QIAseq® miRNA Library kit (Qiagen): the first, called NGS 3C Primer, for assessing the performance of 3' adapter ligation; the second, NGS 5C Primer, for assessing the performance of 5' adapter ligation and the third, NGS RTC Primer, for the performance of reverse transcription reaction. We obtained a value of threshold cycle (CT) less than 28 indicating all these steps were performed correctly. NGS library concentration was determined by Qubit dsDNA HS assay (Thermo Fisher Scientific) by Qubit® 4.0 Fluorimeter, according to the manufacturer's protocol.

Small RNA library sequencing

Equimolar amounts (1 nM) of pooled libraries normalized to 10 nM were generated to sequence in multiplexing. PhiX DNA 1.5 pM was added to pooled libraries prior to sequencing at a final concentration of 10% in order to increase the sequence diversity of the libraries. Pooled small RNA libraries (1.7 pM) were sequenced using NextSeq™ 550 System (Illumina, San Diego, California, USA) following manufacturer's instructions. NextSeq 500/550 High Output Kit v2.5 (75 Cycles) was used for sequencing in single reads of 75 pb fragments for small RNA library. This flow cell allows generating around 400 million reads per run, therefore 45 libraries per run were loaded to guarantee around 9 million reads per sample. Calculation of qualitative scores of the NGS runs (cluster density, Passing Filter clusters, % PF, and Q-score) was done with the Real-Time Analysis software (Illumina) and checked by using the Illumina Sequencing Analysis Viewer (Illumina). In our experiments, we obtained 10,313.55 ± 142.6 Kreads/sample, with an optimal cluster density (242.67± 5.03 K/mm2), high % PF (80.38 ± 1.12) and Q30 (Q-Score) with an average value of 91.93% ± 0.58. Finally, the data were collected as FastQ files.

Bioinformatics analysis of mature miRNAs

Reads in fastq files were processed using CLC Genomics Workbench 21.0.3 (Qiagen), a bioinformatics software that provides specific pipelines for small RNAs analysis. Adapter sequences were trimmed and sequences <15 nucleotides or without adapter nor unique molecular index were discarded. A sequential alignment strategy was used to map sequences on the reference GRCh38 human genome, using miRBase v.22.1 as annotation model (26). All the sequences recognized in miRBase were retrieved as mature miRNAs. Before normalization and DE analysis, data were filtered to include small RNAs with a minimum number of reads count (mean read count) >2. DE analysis was performed using Generalized Linear Model (GLM) and Trimmed mean of M-values (TMM) normalized counts (CPM) as input data, considering significant Benjamini-Hochberg adjusted p-values ≤ 0.05.

Bioinformatics analysis of isomiRNAs

At first, reads in fastq files were processed by Cutadapt v2.5 (27) to trim the adapter and filter good quality reads (mean base Qphred > 30 and length range between 10 and 35 nucleotides). After quality control with FastQC (28), reads were mapped using IsoMiRmap v5 (29) both on the GRCh38 human genome assembly and the known hairpins sequences in miRBase v22. According to the IsoMiRmap method, isomiRs were identified, assigning universally unique identifiers, and quantified. Finally, the expression matrix with raw counts of exclusive-isomiRs was normalized for sequencing depth and RNA composition and DE isomiRs were assessed with DESeq2 v1.30.1 (30), considering significant Benjamini-Hochberg adjusted p-values ≤ 0.05.

Identification of miRNA putative gene targets and network analysis

Gene targets for candidate miRNAs were identified using bioinformatics tools with online target prediction algorithm, MIENTURNET and miRWalk 3.0 (31, 32). Significant target genes for these miRNAs were selected using gene set enrichment analysis (GSEA) and implemented with Search Tool for the Retrieval Interacting Genes (STRING) v11.5, through gene ontology (GO) functional analysis and annotation databases, i.e., KEGG pathways (33), WikiPathways (34), and Disease Ontology (35), FDR<0.05. Visualization summary networks were created by Cytoscape v3.9.0 (36).

Cells and culture conditions

Vero E6 cells (CRL-1586, American Type Culture Collection, ATCC, Manassas, VA) and Calu-3 cells (HTB-55, ATCC) were maintained in Dulbecco's modified Eagle's medium (DMEM, Thermo Fisher Scientific) supplemented with 20% v/v of filtered fetal bovine serum (FBS, Thermo Fisher Scientific), 1% v/v penicillin/streptomycin (Pen/Strep, Thermo Fisher Scientific) and 1% v/v of GlutaMAX supplement (Thermo Fisher Scientific). Human epithelial colorectal adenocarcinoma cell line Caco-2 (HTB-37, ATCC) was cultured in Minimum Essential Medium (Thermo Fisher Scientific) supplemented with 20% FBS, 1% Pen/Strep, and 1% GlutaMAX supplement. Primary human umbilical vein endothelial cells (HUVEC), pooled from multiple donors, were supplied by Invitrogen (Thermo Fisher Scientific) cryopreserved at the end of the primary culture stage. These cells were cultured in adhesion in Medium 200 (M200, Thermo Fisher Scientific), supplemented with 1% v/v Large Vessel Endothelial Supplement (LVES 50x, Thermo Fisher Scientific) and 1% v/v Pen/Strep. Peripheral blood mononuclear cells were purified by Ficoll-Paque PREMIUM (Merck) gradient from healthy blood donors and grown in RPMI 1640 Medium (Thermo Fisher Scientific) supplemented with 10% FBS, 1% Pen/Strep, 1% GlutaMAX and 1% Hepes. For the experiments, cells were seeded in 6-well or 12-well plates and maintained at 37°C in a humidified 5% CO2 incubator.

SARS-CoV-2 infection and IFN-α treatment experiments.

The SARS-COV-2 isolate (lineage B1) used in infection experiments was obtained from a nasopharyngeal swab collected for diagnostic purpose. The virus was propagated in Vero E6 cells, titrated by end-point dilution assay. A lysate from uninfected Vero-E6 cells was used as a mock infection control. Infection was done at the indicated MOI for 1.5 h at 37°C to allow the adsorption of the virus. Then, the viral inoculum was removed, the cells were washed two times with PBS, and fresh medium with FBS added. Viral load was measured in cell supernatant by 50% tissue culture infective dose (TCID50) assay, as previously described (37). Viral RNA load was quantified in cells and cell supernatant by qRT-PCR. Immunofluorescence staining of SARS-CoV-2 Nucleocapsid protein was done with a rabbit monoclonal primary antibody (40143-R019; Sino Biological Inc., Beijing, China) at the dilution of 1:1000 and anti-rabbit IgG Alexa Fluor-546 secondary antibody (goat, 1:2000, Thermo Fisher Scientific). Images were achieved by Nikon Eclipse Ti confocal microscope and acquired using Nis-Element software (Nikon, Tokyo, Japan). For type I IFN stimulation experiments, cells were treated for 24 h with human recombinant IFN-α2 (Merck & Co., White House Station, NJ, USA) using a final concentration of 1,000 U/mL.

Real-time RT-PCR analyses

Total RNA was isolated from the cells using miRNeasy Tissue/Cells advanced Mini Kit (Qiagen) and reverse transcribed to cDNA by using Murine Leukemia Virus (MuLV) reverse transcriptase (Thermo Fisher Scientific). Expression of *IFIT1*, *IFIT2*, *IL6*, *IL1B*, *TLR7*, *TLR8*, *RIG-I*, and *MDA5* mRNA was determined by real-time RT-PCR, as previously described (37). For miRNA analysis, cDNA for miRNAs was generated using TaqMan Advanced miRNA cDNA Synthesis kit (Thermo Fisher Scientific) according to manufacturer's instructions. Then, miRNA levels were determined by real-time RT-PCR using TaqMan Fast Advanced Master mix and TaqMan Advanced miRNA Assays (Thermo Fisher Scientific) as indicated by the manufacturer. RNU6B was used as internal control for normalization of miRNA expression. Expression changes relative to mock were determined by the 2-ΔΔCT method.

Statistical analysis

Power analysis for NGS data was computed as previously reported (38, 39). Sample size was estimated to be at least 20 subjects per group to reach the desired power of 90%, with a standard deviation (SD) estimated at 0.5, an average power with FDR of 0.05 and fold change of 2. Since our experimental design for NGS analysis provides 89 COVID-19 patients, divided into groups of more than 25 individuals, and 45 healthy controls, the sample size was considered large enough to reach the required power.

Comparisons among groups were done by Pearson's χ^2 test, one-way ANOVA, Student's t test, non-parametric Wilcoxon-Mann-Whitney test, Kruskal–Wallis test, receiver operating characteristic (ROC) curve analysis, multiple logistic regression analysis, and Kaplan-Meyer survival curve analysis, as appropriate. Comparisons among multiple groups were corrected with Turkey or Bonferroni-Dunn methods. For analysis across multiple miRNAs, raw p-values were corrected for multiple testing by the Benjamini-Hochberg FDR method. Relationships between variables were assessed by Pearson correlation and Spearman's correlation, as appropriate. Results were considered statistically significant with a P value ≤ 0.05.

Data visualization

All the graphs and statistical analysis were done using Prism GraphPad 9.2 (Graph-Pad Software, Inc. La Jolla, CA, USA). Data in graphs and tables are reported as median and IQR, number (n) and percentage (%), mean ± standard deviation (SD), geometric mean ± SD of geometric mean. Networks of miRNA gene targets were visualized by Cytoscape v3.9.0 (36).

Results

Patient demographics, clinical and laboratory findings, and disease course

Overall, 89 patients with laboratory-confirmed diagnosis of acute SARS-CoV-2 infection were enrolled in the study, including 26 with mild COVID-19, 29 with moderate disease, and 34 with severe disease. Demographic and clinical features of COVID-19 patients are summarized in Table 1. The severity of COVID-19 was significantly associated with male sex, longer hospitalization, intensive care unit (ICU) admission, and death or long-term sequelae (Table 1 and Supplementary Figure 1). The results of routine laboratory tests, which were performed at the time of hospital admission, when serum samples were also collected, are shown in Table 1 and Supplementary Figure 2. The absolute number of leukocytes, the levels of CRP and the levels of creatine phosphokinase (CPK) were significantly higher in patients with severe COVID-19 than in moderate and mild COVID-19 groups.

Association of serum miRNAs with COVID-19 and disease severity

Analysis of small RNA sequencing data obtained from serum of COVID-19 patients and HC identified 161 miRNAs that were consistently expressed across groups. Principal component analysis (PCA) showed that their expression profile well discriminated between COVID-19 patients and HC (Figure 1A). DE analysis identified 23 upregulated miRNAs and 27 downregulated miRNAs in COVID-19 patients *vs.* HC (Figures 1B, C and Supplementary Table 1). ROC curve analysis of the DE miRNAs identified several miRNAs that could discriminate between COVID-19 patients, regardless of disease severity, and HC with high sensitivity and specificity. Among these miRNAs, high levels of miR-320 family members and miR-483-5p and low levels of miR-30d-5p, miR-25-3p, miR-93-5p, miR-16-5p showed >90% sensitivity and >90% specificity in discriminating between COVID-19 patients and HC (Table 2).

Furthermore, comparative analysis of serum miRNA levels among COVID-19 patients in accordance with disease severity (mild, moderate, and severe disease) identified as upregulated in patients with severe COVID-19 miR-21-5p, miR-22-3p, miR-29c-3p, miR-92a-3p, miR-101-3p, miR-194-5p, miR-378a-3p, miR-451a, miR-486-5p, miR-501-3p, and as downregulated let-7e-5p, miR-20a-5p, miR-23b-3p, miR-146a-5p, miR-155-5p, miR-224-5p, miR-339-5p and miR-4433b-5p (Figure 1C). Among these DE miRNAs, ROC curve analysis identified a group of miRNAs that could discriminate between severe COVID-19 and moderate/mild COVID-19 (Table 3). In particular, high levels of miR-22-3p and miR-21-5p showed about 90% sensitivity and >50% specificity, while low levels of miR-224-5p and miR-155-5p showed low sensitivity but >85% specificity in discriminating between severe COVID-19 and moderate/mild COVID-19. Multiple logistic regression analysis showed that a signature combining these four miRNAs improved the classification performance (area under the ROC curve, AUROC = 0.88, 95% CI 0.80-0.95, p<0.0001; negative predictive power 82.1% and positive predictive power 82.0%). Classification performance was further improved by a signature comprising the 17 DE miRNAs reported in Table 3 (AUROC = 0.96, 95% CI 0.93-0.99, p<0.0001; negative predictive power 85.3% and positive predictive power 90.9%) (Figure 1D).

Circulating isomiR signatures in COVID-19 patients according to disease severity

-.2IsomiRs are miRNA isoforms produced during miRNA maturation that differ from their canonical counterpart in length at their 3' or 5' end and/or in their internal sequence. IsomiRs have variable expression in different organs and tissue types and

TABLE 1 Demographics data, clinical characteristics and laboratory findings in patients with SARS-CoV-2 infection at the time of hospital admission (n = 89).

Feature	Mild COVID-19 (n = 26)	Moderate COVID-19 (n = 29)	Severe COVID-19 (n = 34)	*p* value
Age, years	69 (62-78)	73 (66-80)	67 (57-73)	0.1808
Sex				**0.0225**
Men	14 (53.9%)	18 (62.1%)	29 (85.3%)	
Women	12 (46.1%)	11 (37.9%)	5 (14.7%)	
Any comorbidity	24 (92.3%)	24 (82.8%)	29 (85.3%)	0.6871
Hypertension	13 (50.0%)	13 (44.8%)	19 (55.9%)	0.1254
Dyslipidemia	3 (11.5%)	8 (27.6%)	7 (20.6%)	0.3341
Diabetes	4 (15.4%)	8 (27.6%)	10 (29.4%)	0.3003
Malignancy	2 (7.7%)	6 (20.7%)	4 (11.8%)	0.3457
Cardiovascular Diseases	7 (26.9%)	11 (37.9%)	10 (29.4%)	0.6448
Lung disease	5 (19.2%)	8 (27.6%)	9 (26.5%)	0.739
Chronic liver disease	1 (3.9%)	1 (3.5%)	5 (14.7%)	0.169
Days of hospitalization	10 (8-15)	16 (10-21)	24 (13-50)	**<0.0001**
ICU admission	0 (0%)	2 (6.9%)	25 (73.5%)	**<0.0001**
Outcome				**<0.0001**
Recovery	23 (88.5%)	25 (86.2%)	13 (38.2%)	
Sequelae	3 (11.5%)	2 (6.9%)	11 (32.3%)	
Death	0 (0%)	2 (6.9%)	10 (29.4%)	
Laboratory test (normal range)				
Leukocytes count (4.3-10.8 10^9/L)	6.4 (4.8-8.5)	6.7 (5.6-9.1)	8.9 (4.9-11.0)	**0.0361**
CRP (<5 mg/L)	64.9 (21.2-103.3)	101.3 (36.5-171.5)	115.0 (75.0-177.2)	**0.0177**
Procalcitonin (<0.5 μg/L)	0.1 (0.06-0.22)	0.2 (0.09-0.46)	0.46 (0.18-1.13)	0.5418
Fibrinogen (1.8–3.5 g/L)	5.5 (5.0-6.1)	5.4 (4.4-6.2)	4.6 (3.9-6.4)	0.6501
D-dimer (<500 μg/L FEU)	820 (517.5-1095)	949 (580-1827)	857 (679-1709)	0.7089
CPK (46-171 U/L)	67.5 (43.8-139)	95 (73-186)	140 (69.8-343.3)	**0.0465**
Troponin (<20 ng/L)	7.4 (5.2-12.3)	11.1 (6.6-21.1)	10.1 (6.3-30)	0.5392
LDH (<247 U/L)	248 (219-311)	298.5 (255-347)	311 (273-408)	0.2913
Ferritin (23.9 – 336.2 μg/L)	424 (238-790)	408 (293-862)	697 (393-1448)	0.2042
IL-6 (<7 pg/mL)	17.1 (3.8-37.7)	42.5 (20.3-130.7)	65.3 (14.3-120.6)	0.0643

Data are median (IQR) or number (%). P values comparing mild, moderate and severe COVID-19 are from χ^2 test and one-way ANOVA, as appropriate. CRP, C-reactive protein; CPK, creatine phosphokinase; LDH, Lactate dehydrogenase; IL-6, interleukin-6. P values of statistically significant test results defined as <0.05 are in bold.

may differ in their targeted mRNA spectrum (42). Since small RNA sequencing can identify isomiRs, we searched for DE isomiRs in our dataset. DE analysis and PCA showed that also serum isomiR levels clearly discriminated COVID-19 patients from HC, while differences among severe, moderate and mild COVID-19 conditions were less clear (Figures 2A, B). DE analysis between all COVID-19 patients and HC identified 122 DE serum isomiRs (58 upregulated and 64 downregulated). Among these DE isomiRs, 32 were highly expressed (above average values) and showed absolute log2 fold change >1 (Figure 2C and Supplementary Table 2). Among DE isomiRs, the top upregulated serum isomiRs in COVID-19 patients included isoforms of miR-320 family members and miR-483-5p, while the maximum downregulated serum isomiRs in COVID-19 patients included isoforms of miR-486-5p and miR-16-5p (Supplementary Table 2). Comparison between severe and mild COVID-19 identified 57 DE serum isomiRs, including 29 highly expressed isomiRs (above average values) with absolute log2 fold change >0.5, among which isoforms of miR-21-5p, miR-451a, and miR-22-3p as the most upregulated and isoforms of let-7 family members and miR-146a-5p among the most downregulated (Figure 2D and Supplementary Table 3).

Signaling networks of COVID-19-associated serum miRNAs

Network analysis of the genes targeted by DE miRNAs in COVID-19 *vs.* HC is represented in Figures 3A, B and in Supplementary Tables 4, 5. These networks included genes involved in cell response to oxidative stress, autophagy, mitophagy, apoptosis, cell senescence, and angiogenesis. In particular, the upregulated miR-320 family targets several genes involved in antiviral defense, such as genes encoding

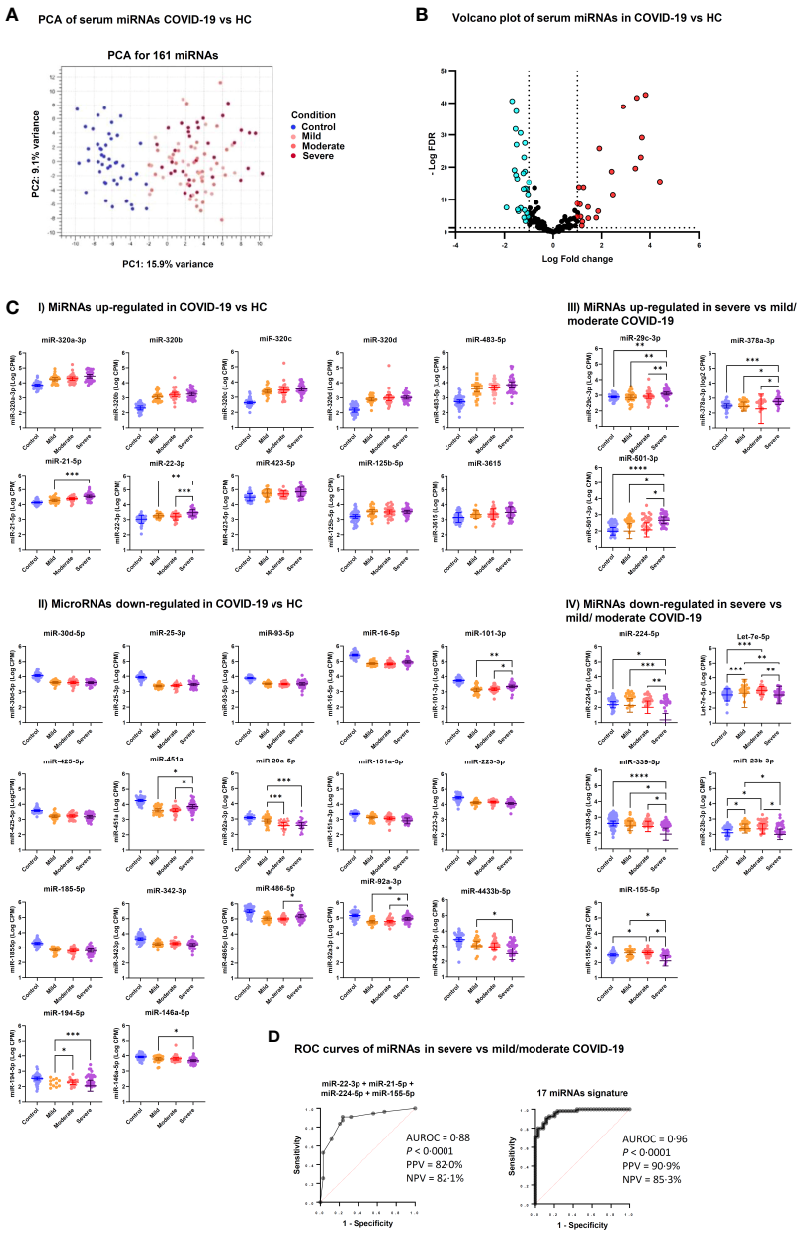

FIGURE 1
Differentially expressed serum miRNAs in COVID-19 patients. **(A)** Unsupervised principal component analysis of miRNA expression profiles in COVID-19 and HC samples (phenotype); condition is red for HC and blue, green, violet for COVID-19 severity. **(B)** Volcano plot of 161 miRNAs analyzed for differential expression (DE); vertical lines delineate > ± 2-fold change; horizontal line delineate adjusted p < 0.05. Adjusted p-values using Generalized Linear Model and trimmed mean of M-values normalized counts were used as input data and adjusted for multiple testing using the Benjamini–Hochberg false discovery rate (FDR) method; light blue dots indicate downregulated miRNA and red dots upregulated miRNAs. **(C)** Scatter dot plots of candidate DE serum miRNAs in COVID-19 patients. MicroRNA expression is reported as Log_{10} counts per million reads (Log CPM). Panels I and II show miRNAs that were up- and downregulated in severe, moderate and mild COVID-19 *vs.* HC, while Panels III and IV show DE miRNAs in severe COVID-19 *vs.* moderate and mild disease. Geometric mean values with 95% confidence interval (95% CI) are indicated by lines and error bars. Pairwise comparison between groups was done by Kruskal Wallis test for multiple comparisons, considering Benjamini-Hochberg adjusted p-values ≤ 0.05. Groups include healthy controls (Control, n = 45), mild COVID-19 (Mild, n = 26), moderate COVID-19 (Moderate, n = 29), and severe COVID-19 (Severe, n = 34). ****p<0.0001, ***p<0.001, **p<0.01, *p<0.05. Since Panels I and II include miRNAs that were DE in all COVID-19 groups (mild, moderate and severe) *vs.* HC, statistical significance is indicated only for comparisons among COVID-19 groups. **(D)** Candidate miRNA biomarkers to classify severe COVID-19 *vs.* mild/moderate COVID-19. *P* values and receiver operating characteristic (ROC) curves were calculated by multiple logistic regression analysis. AUROC, area under the ROC curve; PPV, positive predictive power; NPV, negative predictive power.

10.3389/fimmu.2022.968991

TABLE 2 ROC curve analysis of differentially expressed serum microRNAs in COVID-19 patients *vs.* healthy controls.

miRNA	AUC (95% CI)	*P* value	Cutpoint	Sensitivity % (95% CI)	Specificity % (95% CI)	Likelihood ratio
Upregulated in COVID-19 vs. healthy control						
miR-320b	0.97 (0.95-1.00)	<0.0001	> 509.3	94.4 (87.5-97.6)	95.6 (85.2-99,2)	21.24
miR-320c	0.97 (0.95-1.00)	<0.0001	> 1154	89.9 (81.9-94.6)	95.6 (85.7-99.2)	20.22
miR-320d	0.97 (0.94-0.99)	<0.0001	> 398.5	91.1 (79.3-96.5)	92.1 (84.6-96.1)	11.58
miR-483-5p	0.94 (0.91-0.98)	<0.0001	> 1371	91.0 (83.3-95.4)	91.1 (79.3-96.5)	10.24
miR-320a-3p	0.92 (0.87-0.97)	<0.0001	> 11648	80.9 (71.5-87.7)	88.9 (76.5-95.2)	7.28
miR-21-5p	0.83 (0.76-0.90)	<0.0001	> 19821	69.7 (59.5-78.2)	88.9 (76.5-95.2)	5.23
miR-22-3p	0.81 (0.74-0.89)	<0.0001	> 1478	82.0 (72.8-88.6)	66.7 (52.7-78.6)	2.46
miR-423-5p	0.79 (0.71-0.88)	<0.0001	> 38886	80.9 (71.5-87.7)	73.3 (59.0-84.0)	3.03
miR-125b-5p	0.73 (0.64-0.82)	<0.0001	> 2664	62.9 (52.6-72.3)	73.3 (59.0-84.0)	2.36
miR-3615	0.72 (0.62-0.81)	<0.0001	> 1168	88.8 (80.5-93.8)	51.1 (37.0-65.0)	1.82
Downregulated in COVID-19 vs. healthy control						
miR-30d-5p	0.98 (0.96-1.00)	<0.0001	< 6822	94.4 (87.5-97.6)	91,1 (79.3-96.5)	10.62
miR-25-3p	0.98 (0.95-1.00)	<0.0001	< 5160	96.6 (90.6-99.1)	91.1 (79.3-96.5)	10.87
miR-93-5p	0.97 (0.95-1.00)	<0.0001	< 5523	94.4 (87.5-97.6)	93.3 (82.1-97.7)	14.16
miR-16-5p	0.97 (0.94-1.00)	<0.0001	< 140526	92.1 (84.6-96.1)	95.6 (85.2-99.2)	20.73
miR-101-3p	0.96 (0.93-0.99)	<0.0001	< 3572	88.8 (80.5-93.8)	86.7 (73.8-93.7)	6.66
miR-185-5p	0.94 (0.90-0.98)	<0.0001	< 1094	86.8 (77.8-92.4)	88.9 (76.5-95.2)	7.81
miR-425-5p	0.92 (0.87-0.96)	<0.0001	< 2609	83.2 (74.0-89.5)	95.6 (85.2-99.2)	18.7
miR-451a	0.91 (0.87-0.96)	<0.0001	< 10205	85.4 (76.6-91.3)	82.2 (68.7-90.7)	4.80
miR-20a-5p	0.91 (0.86-0.96)	<0.0001	< 719	78.7 (69.1-85.9)	93.3 (82.1-97.7)	11.8
miR-151a-3p	0.91 (0.86-0.96)	<0.0001	< 1675	80.9 (71.5-87.7)	91.1 (79.3-96.5)	9.10
miR-223-3p	0.88 (0.80-0.95)	<0.0001	< 21788	95.5 (89.0-98.2)	71.1 (56.6-82.3)	3.31
miR-342-3p	0.85 (0.78-0.92)	<0.0001	< 3617	88.8 (80.5-93.8)	66.7 (52.1-78.6)	2.66
miR-486-5p	0.85 (0.78-0.92)	<0.0001	< 229399	85.4 (76.6-91.3)	73.3 (59.0-84.0)	3.20
miR-92a-3p	0.82 (0.75-0.90)	<0.0001	< 104438	79.8 (70.3-86.8)	68.9 (54.3-80.5)	2.56
miR-4433b-5p	0.80 (0.72-0.88)	<0.0001	< 2006	75.3 (65.4-83.1)	73.3 (59.0-84.0)	2.82
miR-194-5p	0.80 (0.72-0.87)	<0.0001	< 244	75.0 (65.0-82.9)	77.8 (63.7-87.5)	3.38
miR-146a-5p	0.75 (0.67-0.84)	<0.0001	< 7681	78.7 (69.1-85.9)	62.2 (47.6-74.9)	2.08

TABLE 3 ROC curve analysis of DE serum miRNAs in severe COVID-19 *vs.* mild and moderate COVID-19.

miRNA	AUC (95% CI)	*P* value	Cutpoint	Sensitivity % (95% CI)	Specificity % (95% CI)	Likelihood ratio
Upregulated in severe vs. mild/moderate COVID-19						
miR-22-3p	0.80 (0.69-0.89)	<0.0001	> 2656	89.1 (78.2-94.9)	58.8 (42.2-73.6)	2.16
miR-21-5p	0.75 (0.64-0.86)	<0.0001	> 35108	90.9 (80.4-96.1)	52.9 (36.7-68.6)	1.93
miR-101-3p	0.74 (0.64-0.85)	0.0001	> 2067	80.0 (67.6-88.5)	61.8 (45.0-76.1)	2.09
miR-194-5p	0.74 (0.64-0.85)	0.0001	> 92.01	61.1 (47.8-73.0)	82.4 (66.5-91.7)	3.46
miR-29c-3p	0.72 (0.61-0.83)	0.0005	> 1097	74.1 (61.1-83.9)	67.7 (50.8-80.9)	2.29
miR-451a	0.72 (0.60-0.83)	0.0006	> 8364	90.9 (80.4-96.1)	44.1 (28.9-60.6)	1.63
miR-92a-3p	0.71 (0.60-0.82)	0.0009	> 67074	69.1 (56.0-80.0)	70.6 (53.8-83.2)	2.35
miR-378a-3p	0.71 (0.60-0.82)	0.0012	> 609.1	75.9 (63.1-85.4)	61.8 (45.0-76.1)	1.99
miR-486-5p	0.68 (0.56-0.80)	0.0040	> 124558	72.7 (60.0-82.7)	64.7 (47.9-78.5)	2.06
miR-501-3p	0.68 (0.57-0.79)	0.0042	> 547.0	72.7 (60.0-82.7)	55.9 (39.5-71.1)	1.65
Downregulated in severe vs. mild/moderate COVID-19						
miR-224-5p	0.74 (0.63-0.84)	0.0002	< 255.7	60.0 (46.8-71.9)	85.3 (69.9-93.6)	4.08
let-7e-5p	0.71 (0.60-0.82)	0.0009	< 1074	72.7 (59.8-82.7)	67.7 (50.8-80.9)	2.25
miR-339-5p	0.70 (0.59-0.81)	0.0014	< 383.6	60.0 (46.8-71.9)	73.5 (56.9-85.4)	2.27
miR-23b-3p	0.67 (0.55-0.79)	0.0074	< 192.4	81.8 (69.7-90.0)	52.9 (36.7-68.6)	1.74
miR-155-5p	0.67 (0.56-0.78)	0.0075	< 509.7	43.6 (31.4-56.7)	88.2 (73.4-95.3)	3.71
miR-146a-5p	0.66 (0.55-0.78)	0.0103	< 5002	67.3 (54.1-78.2)	64.7 (47.9-78.5)	1.91

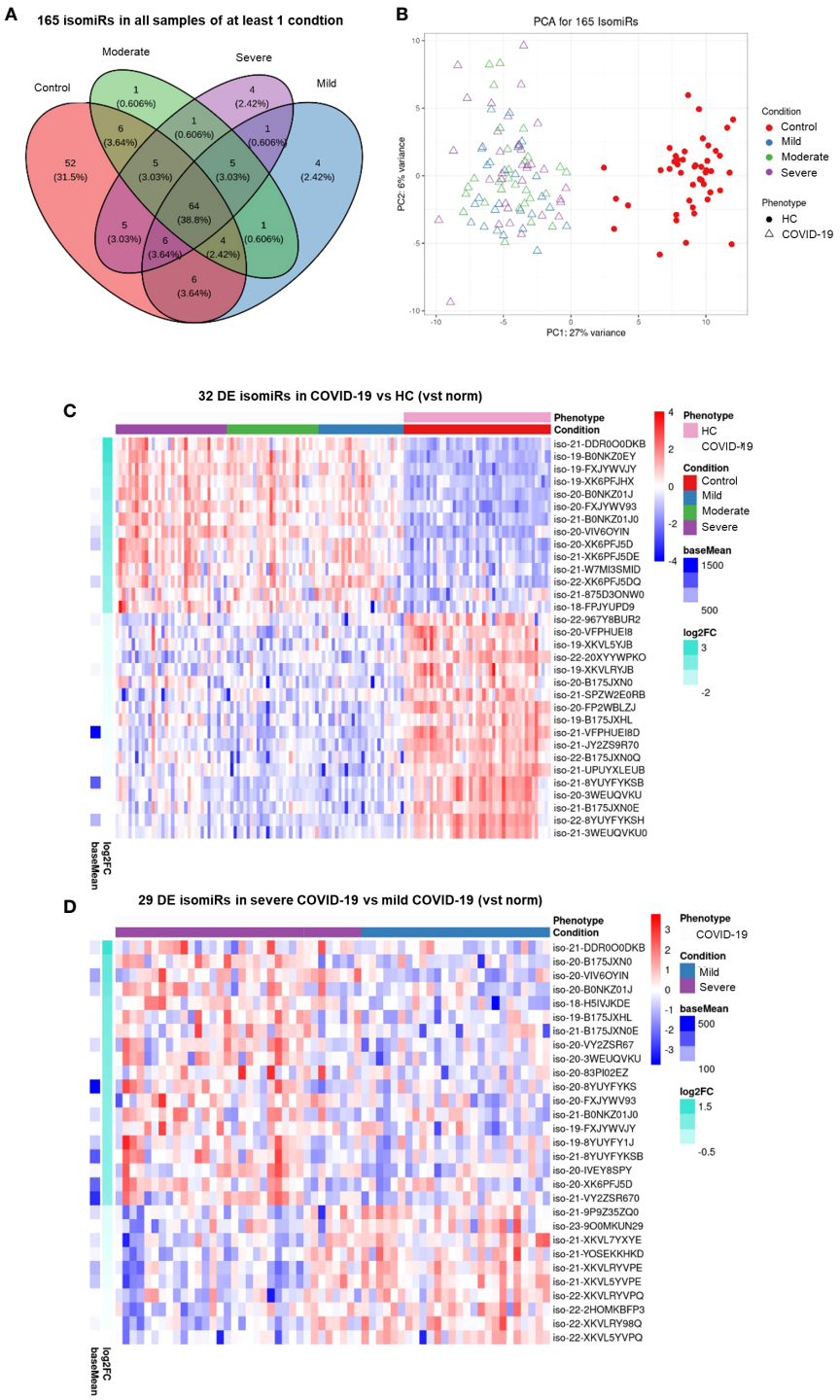

FIGURE 2
Serum isomiR analysis in COVID-19 patients. **(A)** Venn diagram showing the 165 isomiRs detected by small RNA-seq in serum samples of all individuals belonging to at least one condition. Conditions included healthy control (HC, n = 45), mild COVID-19 (n = 26), moderate COVID-19 (n = 29), and severe COVID-19 (n = 34). **(B)** Unsupervised principal component analysis of the isomiR expression profiles in COVID-19 and HC samples (phenotype); condition is red for HC and blue, green, violet for COVID-19 severity. Heatmaps **(C)** of the 32 differentially expressed (DE) serum isomiRs between COVID-19 and HC (p-value ≤ 0.01, absolute log2 Fold Change (Log2FC) ≥ 1) and **(D)** of the 29 DE serum isomiRs between severe and mild COVID-19 (p-value ≤ 0.05, absolute Log2FC ≥ 0.5); standardized expression; the baseMean column on the left indicate the mean expression for each isomiR in all samples.

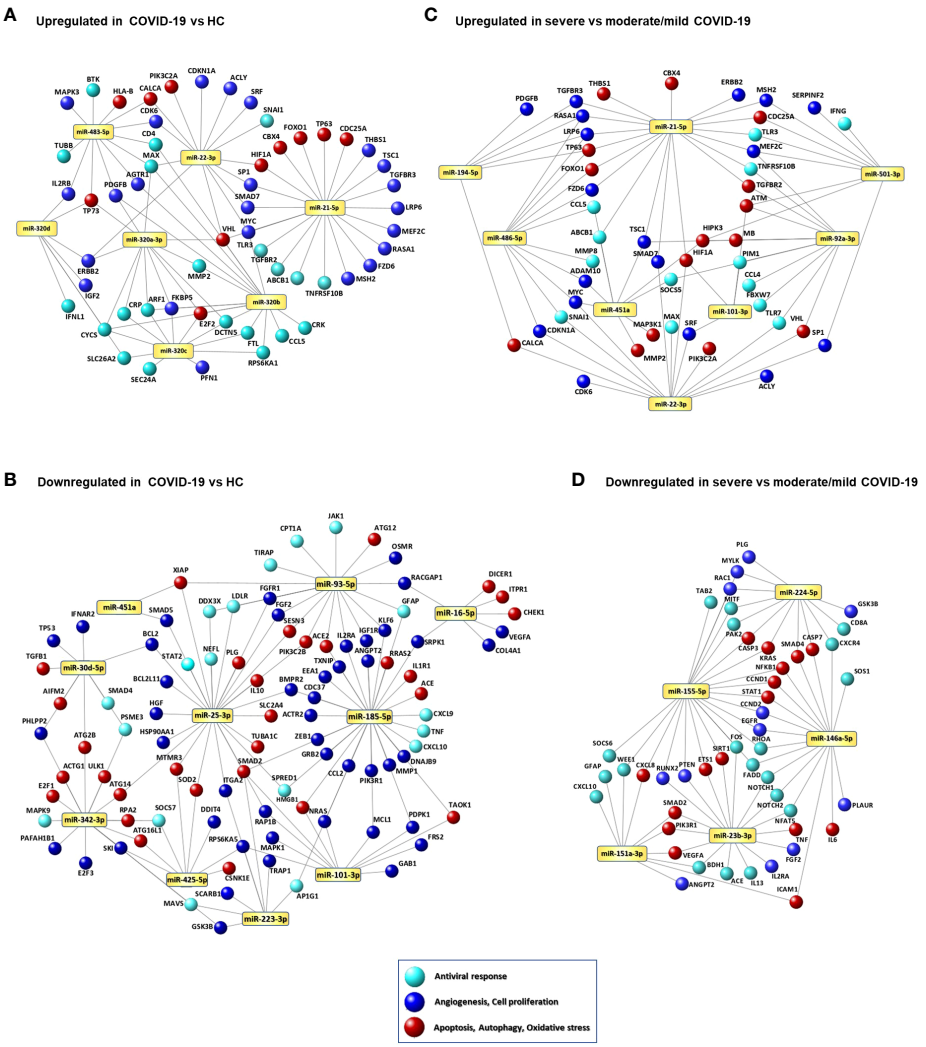

FIGURE 3
Signaling networks of COVID-19-associated serum miRNAs. Networks of putative target genes for circulating miRNAs that were significantly upregulated **(A)** and downregulated **(B)** in COVID-19 patients *vs.* healthy controls (HCs) and significantly upregulated **(C)** and downregulated **(D)** in patients with severe COVID-19 *vs.* patients with mild/moderate COVID-19. Methods for target gene identification and selection and network visualization are described in the Methods section.

cytokines, chemokines and cytokine receptors (*IFNL1, CCL5, IL2RB*), C-reactive protein (*CRP*), ferritin light chain (*FTL*), cytochrome c (*CYCS*), matrix metalloproteinase 2 (*MMP2*), and proteins involved in intracellular trafficking (*ARF1, DTCN5, SEC24A, SLC26A2*). Additional targets of this miRNA family include the angiotensin II receptor *AGTR1*, genes involved stress response and angiogenesis (*FKBP5, PDGFB, VHL*), and in cell proliferation (*CRK, E2F2, ERBB2, IGF2, MAX, RPS6KA11*). Targets of the upregulated miR-483-5p involved in antiviral response and angiogenesis are shared with miR-320 family gene targets. MiR-21-5p and miR-22-3p, both upregulated in COVID-19 patients, target several genes involved in cell signaling, cell proliferation and angiogenesis (e.g., *HIF1A, MYC, SP1, SMAD7, VHL*). MiRNAs that were downregulated in serum of COVID-19 patients mainly target genes promoting angiogenesis (e.g., *VEGFA, ANGPT2, COL4A1, FGF2, ZEB1*), apoptosis, autophagy, stress response (e.g., *ATG12, ATG14, ATG2B, SOD2, TXNIP*), and inflammation (e.g., *CXCL9, CXCL10, IL1R1, TNF*). The SARS-CoV-2 receptor gene ACE2 was targeted by miR-93-5p and miR-185-5p, both downregulated in COVID-19 patients.

Network analysis of the DE miRNAs in severe COVID-19 compared with mild and moderate COVID-19 are shown in Figures 3C, D and Supplementary Tables 6, 7. Upregulated miRNAs in severe COVID-19 target key antiviral response genes (*CCL4, CCL5, IFNG, STAT1, TLR3, TLR7*), genes

involved in myocardial disease (*MMP2, MMP9*), lung disease (*PTEN, HMGB1, SIRT1, HIF1A, BSG, AKT1, ERBB2*), cell response to stress, autophagy, cell senescence, and angiogenesis (e.g., *IGF1R, FOXO1, PTEN, PIK3R1, CDKN1A, SIRT1, AKT1*) (Figure 3C), while downregulated miRNAs target genes encoding pro-inflammatory factors (*IL6, TNF, CXCL8, CXCL10*) and involved in respiratory failure, acute respiratory distress syndrome, pulmonary fibrosis, myocardial infarction, and peripheral vascular disease (*CXCR4, CXCL8, NFKB1, STAT1, ICAM1, SMAD2, IL6, RHOA, CCND1, PLAUR*) (Figure 3D).

Association of laboratory parameters and serum miRNAs with COVID-19 clinical course

To identify biomarkers that could predict the risk of a worsened disease progression, such as ICU admission, death or development of long-term sequelae, we analyzed the results of routine laboratory tests and the levels of circulating miRNAs according to these outcome parameters. This analysis showed that COVID-19 patients admitted at ICU had significantly higher levels of serum miR-22-3p, miR-101-3p, and miR-451a, and lower levels of miR-155-5p at the time of hospitalization than patients who did not require ICU care (Figure 4A). At variance, no routine laboratory parameters were significantly associated with the risk of ICU admission.

Regarding COVID-19 outcome, a significant association was found with the absolute leukocyte count, since patients with long-term sequelae and those who died had increased leukocyte count (Figure 4B). Among miRNAs, low levels of miR-1-3p, miR-23b-3p, miR-141-3p, miR-155-5p, and miR-4433b-5p were significantly associated with COVID-19-related sequelae and/or death (Figure 4B).

Survival curve analysis confirmed that high leukocyte count (>9 × 10^9/L) and low serum levels of miR-1-3p, miR-23b-3p, miR-141-3p, miR-155-5p, and miR-4433b-5p at the time of hospital admission were associated with increased mortality evaluated at 28 days after hospitalization (Figure 4C). Multiple logistic regression analysis showed that a signature combining high leukocyte count with low levels of these five miRNAs was a good predictor of mortality (AUROC 0.95, 95% CI 0.89-1.00, $p<0.0001$; negative predictive power 78% and positive predictive power 94%) (Figure 4D).

Correlation between circulating miRNAs and laboratory parameters in COVID-19 patients

To determine if the DE circulating miRNAs in COVID-19 patients were associated with inflammation, coagulation disorders, and myocardial damage, we performed correlation analysis between miRNAs and the laboratory parameters reported in Table 1. This analysis identified statistically significant positive correlations between the absolute leukocyte count and miR-3615 levels; between CRP, ferritin, LDH (inflammatory biomarkers) and the miR-320 family and miR-3615; between miR-21-5p and IL-6 and CPK (biomarkers of inflammation and myocardial damage, respectively). At variance, statistically significant negative correlations were found between miR-101-3p and fibrinogen and between miR-151a-3p and miR-4433b-3p and inflammation and myocardial damage biomarkers (procalcitonin, IL-6, and troponin) (Figure 4E).

Correlation analysis among the DE miRNAs in patients with severe COVID-19 displayed a strong positive association among members of the miR-320 family, miR-423-5p, and miR-3615 and between miR-16-5p and miR-451a, suggesting that these miRNAs might be co-regulated (Supplementary Figure 3).

MicroRNAs associated with sex and age of COVID-19 patients

Analysis of serum miRNAs according to sex of COVID-19 patients showed that the levels of several miRNAs resulting upregulated in COVID-19 *vs.* HC or in severe *vs.* mild/moderate COVID-19 (miR-21-5p, miR-22-3p, miR-92a-3p, miR-101-3p, miR-320a-3p, miR-423-5p, miR-451a, miR-486-5p, miR-501-3p, miR-3615) were significantly higher in males than in females. Moreover, serum levels of miR-223-3p, which was downregulated in COVID-19 patients *vs.* HC, were significantly lower in males than in females (Figure 5A). Analysis of serum miRNAs according to age found a statistically significant negative correlation between miR-92a-3p and COVID-19 patients' age (Figure 5B).

Evaluation of the DE miRNAs in *in vitro* cell models

In COVID-19 patients, circulating miRNAs could derive from cells, tissues, and organs that are directly damaged by SARS-CoV-2 infection or indirectly affected by innate immune and inflammatory responses to viral infection. To investigate the possible origin of the DE serum miRNAs, we analyzed expression of these miRNAs in human lung epithelial cancer cell line (Calu-3), human epithelial colon carcinoma cell line (Caco-2), human umbilical vein endothelial cells (HUVEC), and human PBMCs after infection with SARS-CoV-2 or treatment with type I IFN. These cells were characterized by different permissiveness to SARS-CoV-2 infection and replication (SARS-CoV-2 could efficiently infect and replicate in Calu-3 cells and, less efficiently, in Caco-2 cells, Figures 6A, B), responsiveness to

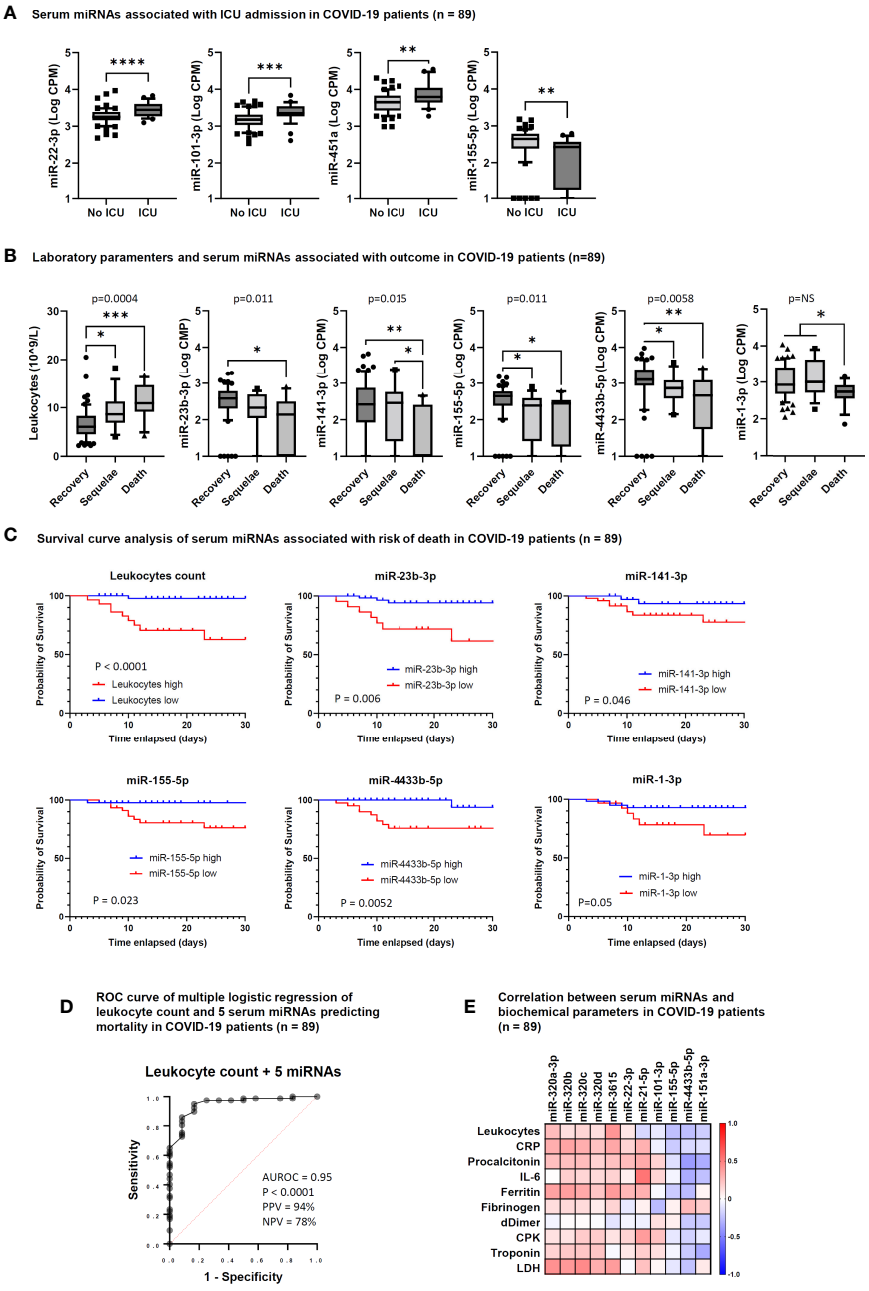

FIGURE 4
Serum microRNAs associated with intensive care unit (ICU) admission and outcome in COVID-19 patients. **(A)** Box and whiskers plot of differentially expressed (DE) miRNAs between COVID-19 patients hospitalized at ICU (ICU, n = 28) and not hospitalized at ICU (No ICU, n = 61). Wishers represent 10-90 percentile; *p* values indicated by * were determined by unpaired Mann Whitney test. **(B)** Box and whiskers plot of leukocyte counts and DE miRNAs among COVID-19 patients who recovered (Recovery, n = 61), showed COVID-19-related sequelae (Sequelae, n = 16) or had died (Death, n = 12) by day 90 after hospitalization. Wishers represent 10-90 percentile; *p* values indicated by * were determined by Kruskal Wallis test for multiple comparisons, considering two stage linear step-up procedure of Benjamini, Krieger and Yekutieli adjusted p-values ≤0.05. One-way ANOVA p value results of comparisons among the three groups are shown in the graphs. **(C)** Survival curve analysis of serum miRNAs significantly associated with the risk of death at 28 days after hospitalization. Comparisons between groups were made by Log-rank test or Gehan-Breslow-Wilcoxon test. *P* values are shown in the graphs and statistical significance was defined by p <0.05. Cut-off values for low and high miRNA levels in serum were determined by ROC curve analysis. **(D)** Candidate miRNA biomarkers to predict the risk of death in COVID-19 patients. *P* value and receiver operating characteristic (ROC) curve were calculated by multiple logistic regression analysis. AUROC, area under the ROC curve; PPV, positive predictive power; NPV, negative predictive power. The five serum miRNAs include miR-1-3p, miR-23b-3p, miR-141-3p, miR-155-5p, and miR-4433b-5p. **(E)** Correlation matrix between serum miRNAs and laboratory parameters in COVID-19 patients (n = 89). The heatmap represents Spearman *r* values of miRNAs showing one or more statistically significant correlation with any laboratory parameter. *p<0.05; **p<0.01; ***p<0.001; ****p<0.0001.

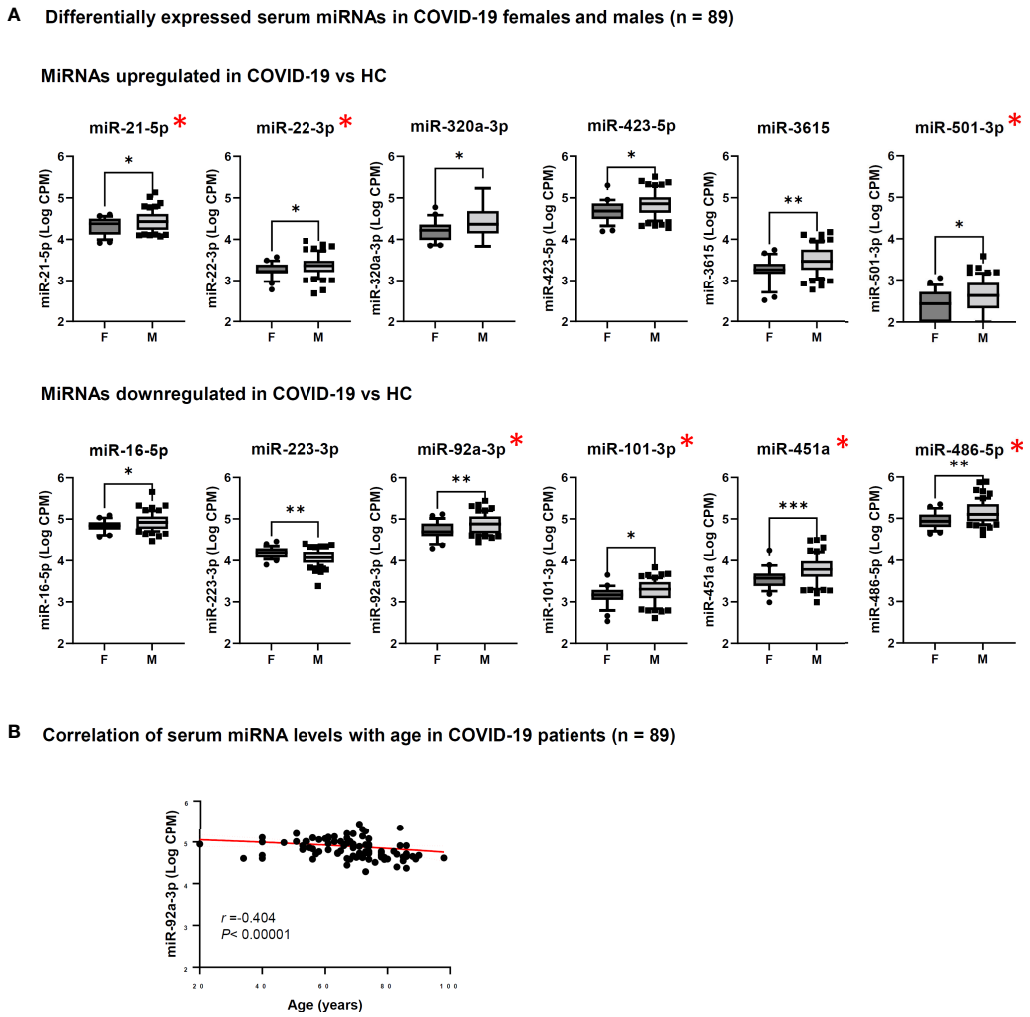

FIGURE 5
Analysis of serum miRNAs according to sex and age of COVID-19 patients. Serum miRNAs resulting significantly upregulated or downregulated in COVID-19 patients *vs.* healthy controls (HC) were included in the analyses. The red asterisk indicates miRNAs resulting significantly upregulated in patients with severe COVID-19 *vs.* mild/moderate COVID-19. **(A)** Comparison of serum miRNA levels between male (M, n = 62) and female (F, n = 27) COVID-19 patients was done by Mann-Whitney test. *p<0.05; **p<0.01; ***p<0.001. **(B)** Correlation between serum miRNA levels and age (years) of COVID-19 patients (n = 89) was done by Spearman rank correlation analysis. F, female; M, male. *r*: Spearman's correlation coefficient. A statistically significantly correlation was found for miR-92a-3p.

IFN type I (Calu-3 cells did not respond to treatment with IFN-α2b, Figure 6C), and induction of IFN and inflammatory responses upon SARS-CoV-2 infection (induction of the viral sensors RIG-I and MDA5, the IFN response markers IFIT1 and IFIT2, and the inflammatory markers IL-6 and IL-1β in Calu-3 and in PBMCs, but not in Caco-2 and HUVEC, Figure 6C) and IFN type I stimulation (Calu-3 cells did not respond to IFN-α2b, Figure 6C). Analysis by qPCR of a subset of the DE serum miRNAs identified in COVID-19 patients showed variable expression in baseline conditions among cell types, suggesting tissue-specific expression (e.g., high levels of miR-21-5p in Caco-2 and Calu-3, miR-25-3p and miR-30d-5p in Caco-2, miR-92a-3p and miR-125b-5p in HUVEC, and miR-146a-5p in PBMCs, Figure 7A). Changes of miRNAs induced by SARS-CoV-2 infection were more prominent in the highly permissive Calu-3 cells than in other cell lines, with up-regulation of miR-320a-3p, miR-320b, miR-423-5p, miR-483-5p, miR-185-5p, miR-146a-5p, and miR-155-5p, while other miRNAs (miR-22-3p, miR-125b-5p, and miR-101-3p) were downregulated at 24 hpi, when cells showed cytopathic effects (Figure 7B). Treatment with IFN-α2b for 24 h led to upregulation of miR-21-5p in Caco-2, miR-483-5p in HUVEC, and miR-29c-3p, miR-378a-3p, and miR-146a-5p in PBMCs. At variance, treatment led to downregulation of miR-423-5p and miR-29c-3p in Caco-2 and downregulation of miR-30d-5p, miR-93-5p, miR-101-3p, miR-185-5p in HUVEC and PBMCs (Figure 7C).

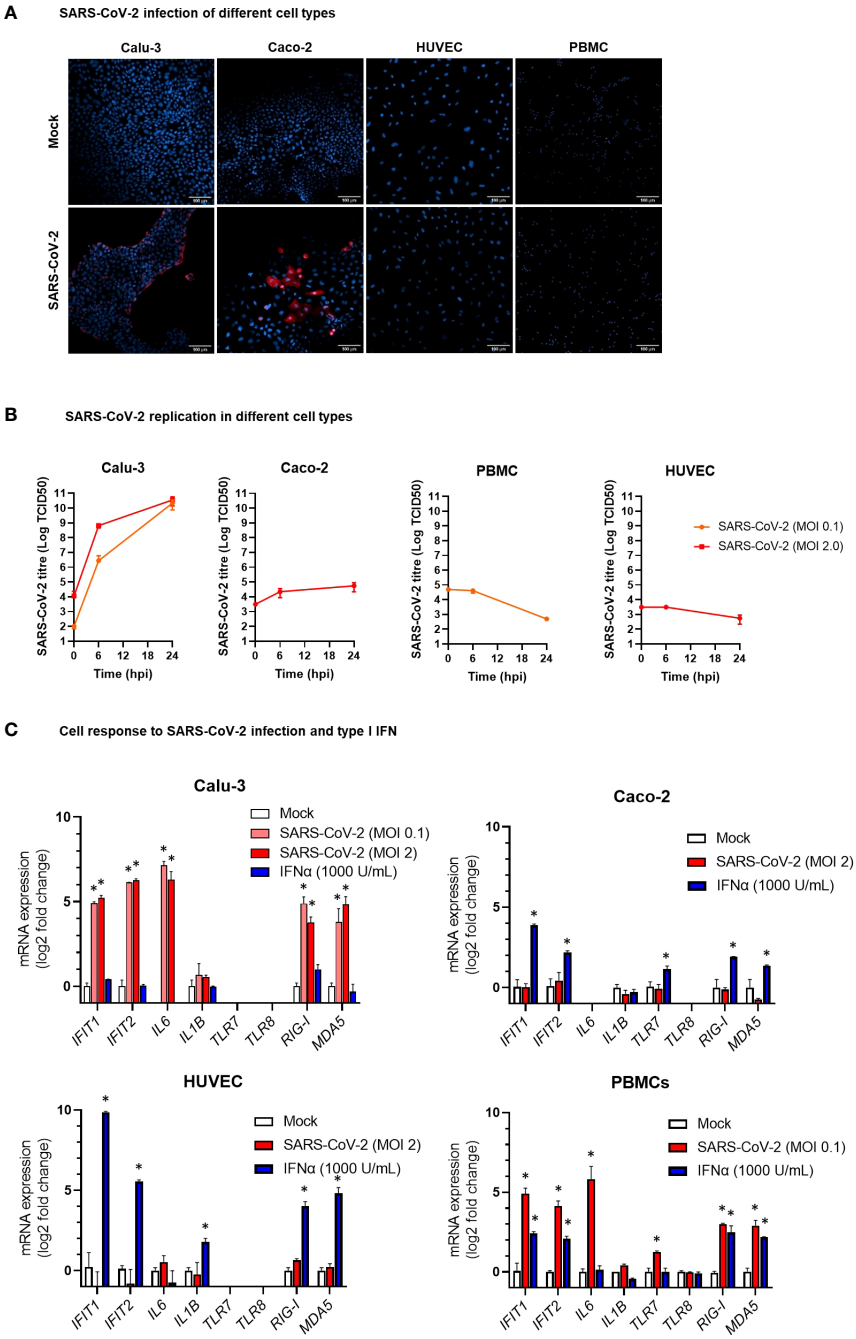

FIGURE 6
Modelling SARS-CoV-2 infection and IFNα stimulation in different human cell types. **(A)** Representative confocal microscopy images of lung carcinoma epithelial cells Calu-3, colon carcinoma epithelial cells Caco-2, human umbilical vein endothelial cells HUVEC, and peripheral blood mononuclear cells (PBMC) infected with SARS-CoV-2 or mock infected. Cells were stained with anti-SARS-CoV-2 nucleoprotein antibody (red) at 24 hours post infection. Nuclei were stained with draq5 (blue). 20× magnification. **(B)** Kinetics of SARS-CoV-2 replication in Calu-3, Caco-2, HUVEC, and PBMC. Viral load was measured by TCID50 assay in cell culture supernatant collected at different hours post infection (hpi) with SARS-CoV-2 at MOI 0.1 or 2. Viral titer is represented as mean ± SD of Log TCID50 values obtained from two experiments conducted in triplicate. **(C)** Expression of the IFN stimulated genes *IFIT1* and *IFIT2*, the pro-inflammatory cytokine genes *IL6* and *IL1B*, and the ssRNA sensor genes *TLR7* and TLR8 in HUVEC, PBMC, Caco-2 and Calu-3 cells at 24 hpi with SARS-CoV-2 at MOI 01 or 2 or treatment with IFN-α2b 1000 U/mL. mRNA expression was measured by real-time RT-PCR and represented as mean ± SD of log2 fold change *vs.* mock (calculated with the $2^{-\Delta\Delta CT}$ method) obtained from two experiments conducted in triplicate. Comparison between groups (infected or treated cells *vs.* mock) was down by Mann-Whitney U test. *p<0.05.

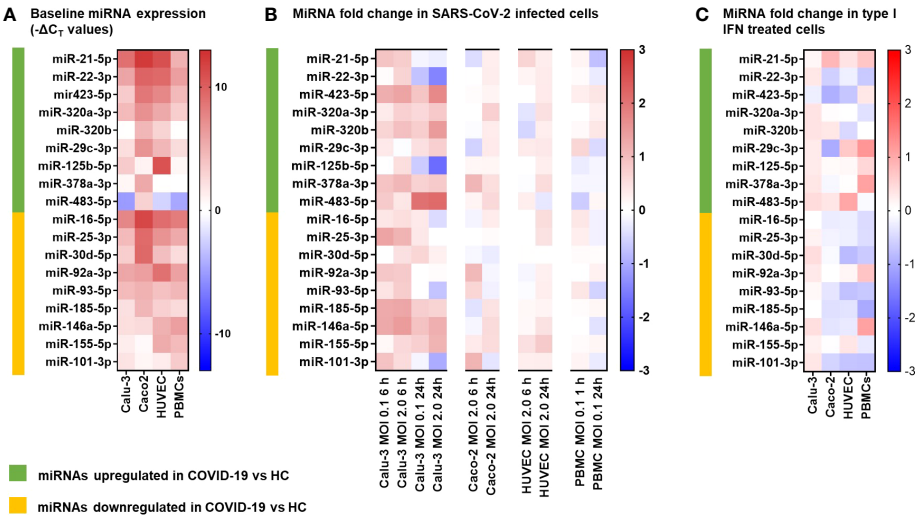

FIGURE 7
MicroRNA expression following SARS-CoV-2 infection and IFNα stimulation in different human cell types. The miRNAs investigated *in vitro* were selected among the differentially expressed (9 upregulated and 9 downregulated) serum miRNAs identified by the study in COVID-19 patients *vs.* healthy controls (HC). **(A)** Heatmap representing baseline miRNAs expression in lung carcinoma epithelial cells Calu-3, colon carcinoma epithelial cells Caco-2, human umbilical vein endothelial cells HUVEC, and peripheral blood mononuclear cells (PBMC). Data represent -ΔC_T values of miRNA normalized to the endogenous control *RNU6B* in triplicate samples. The color scale bar represents -ΔC_T values. **(B)** Heatmap representing miRNA fold change in cells infected with SARS-CoV-2 at MOI 0.1 or 2 *vs.* mock infected cells at 6 h and 24 h post infection. mRNA expression was measured by real-time RT-PCR and represented as mean log2 fold change *vs.* mock (calculated with the $2^{-\Delta\Delta CT}$ method) obtained from two experiments conducted in triplicate. The color scale bar represents mean log2 fold change *vs.* mock. **(C)** Heatmap representing miRNA fold change in cells treated for 24 h with IFNα 1000 U/mL *vs.* mock treated cells. mRNA expression was measured by real-time RT-PCR and represented as mean log2 fold change *vs.* mock (calculated with the $2^{-\Delta\Delta CT}$ method) obtained from two experiments conducted in triplicate. The color scale bar represents mean log2 fold change *vs.* mock.

Discussion

In this study, we investigated a cohort of COVID-19 patients at the time of hospital admission to discover signatures of DE circulating miRNAs associated with COVID-19 severity and disease outcome. The results of this study identified serum miRNA profiles, which could discriminate between COVID-19 and HC, between severe COVID-19 and moderate/mild disease, or predict the risk of ICU admission, COVID-19 related sequelae and death (Figure 8A). Expression analysis of DE miRNAs in relevant cell types *in vitro* upon SARS-CoV-2 exposure or type I IFN treatment provided hints to their possible sources (Figure 8B).

Through small RNA sequencing of serum miRNAs, we showed that miR-320 family members and miR-483-5p were the maximally upregulated serum miRNAs in COVID-19 patients in comparison with HC. In the literature, miR-320 family members were found as upregulated in plasma of patients with COVID-19 and especially in those with severe COVID-19 compared to those with moderate disease (17). High levels of miR-320b and miR-483-5p were also associated with increased risk of in-hospital mortality in COVID-19 patients (41) and upregulated in extracellular vesicles-enriched sera of atherosclerotic patients, indicating a possible role in vascular and endothelial injury (42). In our study, the levels of serum miR-320 family showed a positive correlation with inflammatory and tissue injury biomarkers, suggesting a role for these miRNAs in inflammatory response. Particularly strong was the positive correlation between miR-320 family and LDH, which is pathognomonic for pyroptosis and other forms of necrotic cell death and associated with severe COVID-19 (43). Interestingly, *in vitro* experiments showed that both miR-320 and miR-483-5p were significantly upregulated in lung Calu-3 cells upon SARS-CoV-2 infection.

The maximally downregulated miRNAs in serum of COVID-19 patients *vs.* HC included miR-30d-5p, miR-25-3p, miR-93-5p, miR-16-5p, miR-101-3p, miR-185-5p, miR-425-5p, miR-451a, miR-20a-5p, and miR-151-3p, which could discriminate between COVID-19 patients and HC with AUROC >0.90. These miRNAs target several pro-inflammatory cytokine and chemokine genes (e.g., *TNF, CCL2, CXCL9, CXCL10, IL10, VEGFA*) as well as cytokine and chemokine receptors and transduction factors (*IL1R1, IL2RA, IFNAR2*), reported as upregulated and associated with mortality in COVID-19 patients (44, 45). Genes involved in angiogenesis, immune cell proliferation and regulation, apoptosis, autophagy, and oxidative stress (e.g., *ACE2, ANGPT2, BCL2, FGF2, HGF, TP53*, and *ZEB1*) represented additional targets of the

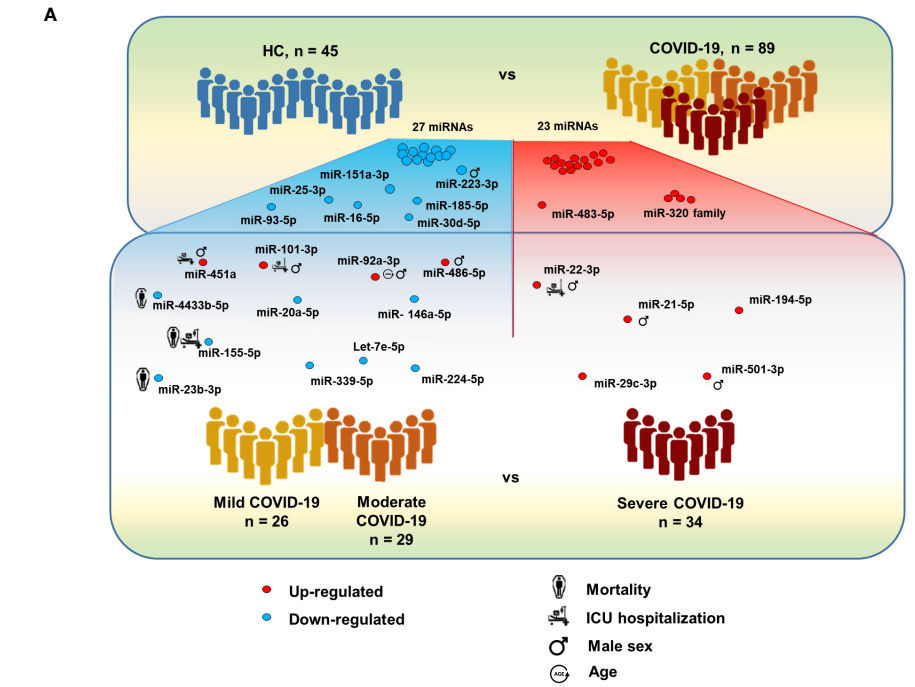

FIGURE 8
MicroRNAs modulated in COVID-19 patients. **(A)** Illustration of the study design and results, highlighting relevant serum miRNAs that were differentially expressed between COVID-19 patients *vs.* HC and between severe COVID-19 *vs.* mild and moderate COVID-19. The figure also shows serum miRNAs significantly associated with the risk of intensive care unit (ICU) hospitalization and death in COVID-19 patients, as well as male sex and age. **(B)** Illustration of the results of *in vitro* experiments, summarizing the effects of SARS-CoV-2 infection and IFN-α2b treatment on human lung (Calu-3), colon (Caco-2), endothelial (HUVEC), and peripheral blood mononuclear cells (PBMCs). Upregulated and downregulated miRNAs are represented in red and blue, respectively.

downregulated miRNAs in COVID-19. Since down-regulation of miRNAs leads to the up-regulation of their target genes, repression of these miRNAs in COVID-19 may contribute to the impaired innate and adaptive immune responses, the excessive systemic inflammation, the cytokine storm and cardiovascular injury that characterizes COVID-19 (46, 47).

While a miRNA signature could clearly discriminate between COVID-19 and HC, the differences in serum miRNA profile between severe COVID-19 cases and mild/moderate cases were subtle. Patients with severe COVID-19 had higher serum levels of a set of miRNAs, including miR-21-5p and miR-22-3p, which were also upregulated in COVID-19 patients *vs* HCs, in agreement with literature data (18). MiR-21-5p has been implicated in different regulatory pathways and high circulating levels were associated with lung disease and cardiac fibrosis (48, 49). Accordingly, in our COVID-19 cohort, miR-21-5p levels showed positive correlations with serum IL-6 and CPK, which are biomarkers of inflammation and myocardial damage, respectively. MiR-22-3p negatively regulates type I IFN and inflammatory cytokine production (50–52) and high circulating levels of miR-22-3p were found to predict COVID-19 mortality (17) and heart failure (53). In our study, network

analysis showed that miR-21-5p and miR-22-3p share targets involved in cell signaling, cell proliferation and angiogenesis.

Additional upregulated miRNAs in severe COVID-19 compared to mild/moderate disease included miR-101-3p, miR-194-5p, miR-451a, miR-486-5p, miR-29c-3p, and miR-501-3p, while levels of circulating let-7e-5p, miR-20a-5p, miR-23b-3p, miR146a-5p, miR-155-5p, miR-224-5p, miR-339-5p, and miR-4433b-5p were significantly downregulated. Relevant targets of the up-regulated miRNAs include several genes involved in antiviral innate immune response (e.g., *IFNG, TLR3, TLR7, CCL4, CCL5*), while down-regulated miRNAs target pro-inflammatory cytokine and chemokine genes (e.g., *IL6, TNF, NFKB1, CXCL8, CXCL10, VEGFA*), which are upregulated in severe COVID-19 patients and associated with mortality (5, 45, 46). Thus, since miRNAs inhibit their target gene expression, the modulated miRNAs in severe COVID-19 would lead to the inhibition of antiviral response and to the induction of inflammation. Let-7 family is induced by IL-15 signaling in natural killer T cells, leading to IFN-γ production (54). Specifically, let-7e-5p targets *RIPK1*, *CASP8*, and *TNF*, which control signaling pathways leading to inflammation and apoptotic or necroptotic cell death. In our study, let-7e-5p levels were increased in serum of patients with mild and moderate COVID-19, but not in patients with severe disease. Likewise, other key miRNAs regulating innate antiviral response, i.e., miR-23b-3p, miR-92a-3p, miR-101-3p, miR-155-5p, miR-224-5p, miR-451a, and miR-486-5p, were modulated in patients with mild/moderate COVID-19 but not in those with severe disease. This finding is in agreement with the activation of effective antiviral responses in patients with mild and moderate COVID-19, but not in patients with severe disease, who typically have impaired innate immunity (55).

In this study, some of the circulating miRNAs that were associated with severe disease were also predictive of the clinical course and disease outcome. In particular, the levels of miR-22-3p, miR-101-3p and miR-451a were significantly higher and miR-155-5p significantly lower in patients hospitalized in ICU than in those not requiring ICU. In addition, a signature characterized by low levels of miR-1-3p, miR-23b-3p, miR-141-3p, miR-155-5p and miR-4433b-5p and high leukocyte count predicted an increased risk of COVID-19-related sequelae and/or death. Dysregulation of these miRNAs was observed is physiological and pathological processes such as immunity, inflammation, and cardiovascular diseases. In our study, circulating miR-101-3p levels showed a negative correlation with fibrinogen levels, which were low in severe COVID-19 patients and associated with poor prognosis (56). Increased serum levels of miR-101-3p were observed also in neonatal sepsis (57). MiR-451a, mostly expressed in blood cells and released in extracellular vesicles, attenuates type I IFN and IL-6 responses (58, 59) and was reported to progressively decrease with COVID-19 severity (19–21). MiR-155-5p plays a key role in the homeostasis and function of the immune system (60). It is highly expressed in activated B-cells and T-cells and in monocytes/macrophages and targets a variety of genes (61), resulting in enhancement of type I IFN signaling and subsequent innate and adaptive immune responses (62). In agreement with our data, significantly lower levels of serum miR-155-5p were found in patients with severe COVID-19 and in those who died (63). Regarding the other miRNAs associated with the risk of death and/or sequelae, miR-1-3p is muscle-specific and its expression is diminished in heart disease (64); miR-23b-3p promotes cell differentiation and inhibits cell proliferation and angiogenesis (65); miR-141-3p targets the chemokine gene *CXCL12* (66), which plays a key role in immune cell recruitment and is upregulated in severe COVID-19 (67); miR-4433b-5p is significantly down-regulated in COVID-19 patients requiring supplementary oxygen therapy (68), but its functions remain unknown. Our study showed a statistically significant negative correlation between miR-4433b-3p and inflammation and myocardial damage biomarkers suggesting it might have a role in cardiac function. This miRNA, as well as the other miRNAs predictive of mortality, warrant further research as potential therapeutic targets, once their functions in health and disease are elucidated.

Analysis of the DE serum miRNAs according to sex of COVID-19 patients, regardless of disease severity, highlighted an association between male sex and the dysregulated miRNA signature observed especially in severe COVID-19. Male patients had higher levels of serum miRNAs implicated in pro-inflammatory responses (such as miR-miR-21-5p, miR-320a-3p, miR-101-3p) and lower levels of serum miR-223-3p, which was downregulated in COVID-19 patients and identified as a negative regulator of pro-inflammatory cytokine secretion and NLRP3 inflammasome activation in the lung of SARS-CoV-2 infected mice (15). In our study, serum levels of miR-92a-3p negatively correlated with patients' age and were down-regulated in patients with mild/moderated COVID-19 but not in those with severe disease. Interestingly, this miRNA was found to be highly expressed in mesenchymal stem-cell-derived extracellular vesicles and to target both a conserved 3'-untranslated region of SARS-CoV-2 genome and inflammatory response genes (69).

Taken together, our results from the clinical study showed that COVID-19 patients had a circulating miRNA signature characterized by upregulation of miRNAs associated with lung disease, vascular damage and inflammation and downregulation of miRNAs that inhibit expression and activity of pro-inflammatory cytokines and chemokines, angiogenesis, and stress response. Compared to patients with mild/moderate COVID-19, patients with severe COVID-19 and hospitalized in ICU had a circulating miRNA signature indicating a profound impairment of innate and adaptive immune responses, inflammation, cytokine storm, lung fibrosis and heart failure. A subset of the DE miRNAs predicted mortality in COVID-19 patients.

Circulating miRNAs are released by various cell types, mostly macrophages, lymphocytes, endothelial cells, and

platelets, but also by passive leakage from damaged cells as a consequence of tissue injury, inflammation, necrosis, or apoptosis (70).

To search for the possible source of the DE circulating miRNAs in COVID-19 patients, we analyzed the expression of these miRNAs *in vitro* in relevant cell types, i.e., lung carcinoma epithelial cells Calu-3, colon carcinoma epithelial cells Caco-2, endothelial cells HUVEC, and PBMCs, characterized by different tissue origin, permissiveness to SARS-CoV-2 infection and replication, capacity to sense RNA viruses and trigger antiviral response, and integrity of type I IFN response pathway. These cells are representative of the main tissues involved in COVID-19 pathogenesis, i.e., the pulmonary epithelium, which is the primary target of SARS-CoV-2 infection and injury, and the gut epithelium, which is also productively infected by SARS-CoV-2 *in vivo* (71). Endothelial cells express low levels of ACE2 and TMPRSS2 (72) and are poorly susceptible to SARS-CoV-2 infection (71). However, endothelial cells are involved in COVID-19 pathogenesis with endothelitis and thrombo-embolic manifestations and, in animal models, SARS-CoV-2 spike protein or its S1 subunit can cause endothelial damage (73, 74). Blood cells are not productively infected by SARS-CoV-2 but can sense the virus activating innate antiviral responses (55). Accordingly, our experiments showed that Calu-3 cells were permissive to SARS-CoV-2 replication, which induced CPE and triggered IFN and inflammatory responses. The virus replicated less efficiently in Caco-2 cells without CPE nor induction of IFN or inflammatory response. PBMC stimulation with SARS-CoV-2 induced the expression of IFN stimulated genes (ISGs), while HUVEC were not infected by SARS-CoV-2 nor responded to the virus.

The results of miRNA analysis in these *in vitro* models highlighted cell-specific differences of miRNA levels in baseline conditions. Upon SARS-CoV-2 infection, most changes in intracellular miRNA levels occurred in the highly permissive epithelial lung carcinoma cell line Calu-3. In these cells, SARS-CoV-2 infection upregulated miR-185-5p, miR-320, miR-423-5p, and miR-483-5p, which promote inflammation and inhibit antiviral responses, as well as miR-146a-5p and miR-155-5p, which act antagonistically to produce a robust inflammatory response (11). Upregulation of miR-155-5p following SARS-CoV-2 infection was previously described in Calu-3 cells and associated with induction of antiviral and pro-inflammatory responses triggered by sensors of RNA viruses (75). Conversely, SARS-CoV-2 infection of Calu-3 cells led to down-regulation of miR-22-3p and miR-125b-5p. These miRNAs play a key role in the regulation of cell self-renewal, differentiation, autophagy and their overexpression lead to uncontrolled cell proliferation and defective differentiation *via* TGFβ and Wnt signaling pathways and DNA methylation (11). This miRNA signature was in agreement with the robust activation of the ISGs *IFIT1* and *IFIT2* and the pro-inflammatory cytokine genes *IL6* and *IL1B* and upon SARS-CoV-2 infection, which was conceivably sensed by RIG-I and MDA5. The colon carcinoma cell line Caco-2, which is permissive to SARS-CoV-2 but unable to activate innate antiviral and IFN responses, and the non-permissive HUVEC and PBMCs did not show relevant changes of miRNA expression upon SARS-CoV-2 infection. However, theses miRNA responses may not be totally representative of miRNA expression profiles in healthy primary lung cell or gut cells experiencing SARS-CoV-2, since the colorectal and lung cells used in this study were derived from cancer cell lines. Likewise, the umbilical endothelial cells might not be representative of the endothelial cells in the lung vasculature and PBMCs may not fully represent local immune-inflammatory cells in the alveoli.

Treatment with IFN-α modulated expression of some of the selected DE miRNAs in the IFN-responsive Caco-2, HUVEC and PBMCs, but not in Calu-3 cells, characterized by a poor response to type I IFN stimulation. In Caco-2, HUVEC, and PBMC, several miRNAs downregulated in COVID-19, such as miR-93-5p, miR-185-5p, and miR-101-3p, were consistently downregulated by IFNα stimulation. In PBMC, IFNα treatment upregulated miR-29c-3p (upregulated in serum of COVID-19 patients), which is known to target the IFN receptor *IFNAR1* as negative feedback to limit type I IFN response (76), as well as miR-146a-5p and miR-378a-3p, which, respectively, inhibit TLR-mediated innate immune responses (11) and promote NET formation by granulocytes in sepsis (77). Another overexpressed miRNA in the serum of COVID-19 patients with severe disease, miR-483-5p, was markedly induced by IFN-α treatment of HUVEC endothelial cells and by SARS-CoV-2 infection in Calu-3 cells. Overexpression of this miRNA, which leads to suppression of cell proliferation and production of inflammatory cytokines (78) was observed in the lung tissues of mice with sepsis-induced acute lung injury (79).

In conclusion, this study discovered signatures of circulating miRNAs associated with COVID-19 severity and mortality, which warrant further investigation and validation as candidate prognostic biomarkers. The identified DE circulating miRNAs provided clues on COVID-19 pathogenesis, highlighting signatures of impaired IFN and antiviral responses, inflammation, organ damage and cardiovascular failure as associated with severe disease and death. *In vitro* experiments showed that some of these miRNAs were modulated directly by SARS-CoV-2 infection or indirectly by IFN.

Data availability statement

The datasets presented in this study can be found in online repositories. The names of the repository/repositories and accession number(s) can be found below: Gene Expression Omnibus under accession number GSE201790.

Ethics statement

The studies involving human participants were reviewed and approved by Comitato Etico per la Sperimentazione Clinica delle Province di Verona e Rovigo. The patients/participants provided their written informed consent to participate in this study.

Author contributions

AG, SR, AS, CP, RM, FG, GC, and LB contributed to the study design. CP, ER, and FG contributed to patient recruitment, data collection, and clinical analysis. AG, SR, AS, MA, and EM contributed to wet-lab data generation and *in vitro* analysis. AG, PB, GC, and LB contributed to small RNA sequencing analysis and statistical analysis. AG, GC, and LB wrote and revised the manuscript. All authors discussed and commented on the manuscript. RM, FG, GC, and LB provided funding to support this study. All authors contributed to the article and approved the submitted version.

Funding

This work was funded by the European Union's Horizon 2020 Research and Innovation Program, under grant agreement no. 874735 (VEO), and by PRID grant from the University of Padova. The work at IRCCS Sacro Cuore Don Calabria Hospital was supported by the Italian Ministry of Health "Fondi Ricerca Corrente – L1P6" and by the Italian Ministry of Health - COVID-2020-12371675. Small RNA-sequencing was performed by a NextSeq 550 Instrument purchased by the DIMAR Excellence project funding (DImed and MAlattie Rare) of the Department of Medicine, University of Padua.

Acknowledgments

We wish to thank Andrea Benetti (Department of Medicine, University of Padova) for technical assistance.

Conflict of interest

The authors declare that the research was conducted in the absence of any commercial or financial relationships that could be construed as a potential conflict of interest.

Publisher's note

Supplementary material

The Supplementary Material for this article can be found online at: https://www.frontiersin.org/articles/10.3389/fimmu.2022.968991/full#supplementary-material

References

1. Gupta RK, Harrison EM, Ho A, Docherty AB, Knight SR, van Smeden M, et al. Development and validation of the ISARIC 4C deterioration model for adults hospitalised with COVID-19: A prospective cohort study. *Lancet Respir Med* (2021) 9:349–59. doi: 10.1016/S2213-2600(20)30559-2

2. Pathak GA, Singh K, Miller-Fleming TW, Wendt FR, Ehsan N, Hou K, et al. Integrative genomic analyses identify susceptibility genes underlying COVID-19 hospitalization. *Nat Commun* (2021) 12:4569. doi: 10.1038/s41467-021-24824-z

3. Wong LR, Perlman S. Immune dysregulation and immunopathology induced by SARS-CoV-2 and related coronaviruses - are we our own worst enemy? *Nat Rev Immunol* (2022) 22:47–56. doi: 10.1038/s41577-021-00656-2

4. Gorog DA, Storey RF, Gurbel PA, Tantry US, Berger JS, Chan MY, et al. Current and novel biomarkers of thrombotic risk in COVID-19: A consensus statement from the international COVID-19 thrombosis biomarkers colloquium. *Nat Rev Cardiol* (2022) 19:475–95. doi: 10.1038/s41569-021-00665-7

5. Del Valle DM, Kim-Schulze S, Huang HH, Beckmann ND, Nirenberg S, Wang B, et al. An inflammatory cytokine signature predicts COVID-19 severity and survival. *Nat Med* (2020) 26:1636–43. doi: 10.1038/s41591-020-1051-9

6. Arunachalam PS, Wimmers F, Mok CKP, Perera RAPM, Scott M, Hagan T, et al. Systems biological assessment of immunity to mild versus severe COVID-19 infection in humans.. *Science* (2020) 369:1210–20. doi: 10.1126/science.abc6261

7. Amrute JM, Perry AM, Anand G, Cruchaga C, Hock KG, Farnsworth CW, et al. Cell specific peripheral immune responses predict survival in critical COVID-19 patients. *Nat Commun* (2022) 13:882. doi: 10.1038/s41467-022-28505-3

8. Pritchard CC, Cheng HH, Tewari M. MicroRNA profiling: Approaches and considerations. *Nat Rev Genet* (2012) 13:358–69. doi: 10.1038/nrg3198

9. Lu D, Thum T. RNA-Based diagnostic and therapeutic strategies for cardiovascular disease. *Nat Rev Cardiol* (2019) 16:661–74. doi: 10.1038/s41569-019-0218-x

10. Ceolotto G, Giannella A, Albiero M, Kuppusamy M, Radu C, Simioni P, et al. miR-30c-5p regulates macrophage-mediated inflammation and pro-atherosclerosis pathways. *Cardiovasc Res* (2017) 113:1627–38. doi: 10.1093/cvr/cvx157

11. Mehta A, Baltimore D. MicroRNAs as regulatory elements in immune system logic. *Nat Rev Immunol* (2016) 16:279–94. doi: 10.1038/nri.2016.40

12. Bautista-Becerril B, Pérez-Dimas G, Sommerhalder-Nava PC, Hanono A, Martínez-Cisneros JA, Zarate-Maldonado B, et al. MiRNAs, from evolutionary junk to possible prognostic markers and therapeutic targets in covid-19. *Viruses* (2021) 14:41. doi: 10.3390/v14010041

13. Treiber T, Treiber N, Meister G. Regulation of microRNA biogenesis and its crosstalk with other cellular pathways. *Nat Rev Mol Cell Biol* (2019) 20:5–20. doi: 10.1038/s41580-018-0059-1

14. Gebert LFR, MacRae IJ. Regulation of microRNA function in animals. *Nat Rev Mol Cell Biol* (2019) 20:21–37. doi: 10.1038/s41580-018-0045-7

15. Morales L, Oliveros JC, Enjuanes L, Sola I. Contribution of host miRNA-223-3p to SARS-CoV-induced lung inflammatory pathology. *mBio* (2022) 13: e0313521. doi: 10.1128/mbio.03135-21

16. Maranini B, Ciancio G, Ferracin M, Cultrera R, Negrini M, Sabbioni S, et al. microRNAs and inflammatory immune response in SARS-CoV-2 infection: A narrative review. *Life (Basel)* (2022) 12:288. doi: 10.3390/life12020288

17. Fernández-Pato A, Virseda-Berdices A, Resino S, Ryan P, Martínez-González O, Pérez-García F, et al. Plasma miRNA profile at COVID-19 onset predicts severity status and mortality. *Emerg Microbes Infect* (2022) 11:676–88. doi: 10.1080/22221751.2022.2038021

18. Gutmann C, Khamina K, Theofilatos K, Diendorfer AB, Burnap SA, Nabeebaccus A, et al. Association of cardiometabolic microRNAs with COVID-19 severity and mortality. *Cardiovasc Res* (2022) 118:461–74. doi: 10.1093/cvr/cvab338

19. de Gonzalo-Calvo D, Benítez ID, Pinilla L, Carratalá A, Moncusí-Moix A, Gort-Paniello C, et al. Circulating microRNA profiles predict the severity of COVID-19 in hospitalized patients. *Clin Trial* (2021) 236:147–59. doi: 10.1016/j.trsl.2021.05.004

20. Wilson JC, Kealy D, James SR, Plowman T, Newling K, Jagger C, et al. Integrated miRNA/cytokine/chemokine profiling reveals severity-associated step changes and principal correlates of fatality in COVID-19. *iScience* (2021) 25:103672. doi: 10.1016/j.isci.2021.103672

21. Yang P, Zhao Y, Li J, Liu C, Zhu L, Zhang J, et al. Downregulated miR-451a as a feature of the plasma cfRNA landscape reveals regulatory networks of IL-6/IL-6R-associated cytokine storms in COVID-19 patients. *Cell Mol Immunol* (2021) 18:1064–6. doi: 10.1038/s41423-021-00652-5

22. Gustafson D, Ngai M, Wu R, Hou H, Schoffel AC, Erice C, et al. Cardiovascular signatures of COVID-19 predict mortality and identify barrier stabilizing therapies. *EBioMedicine* (2022) 78:103982. doi: 10.1016/j.ebiom.2022.103982

23. Zeng Q, Qi X, Ma J, Hu F, Wang X, Qin H, et al. Distinct miRNAs associated with various clinical presentations of SARS-CoV-2 infection. *iScience* (2022) 25:104309. doi: 10.1016/j.isci.2022.104309

24. Garcia-Giralt N, Du J, Marin-Corral J, Bódalo-Torruella M, Blasco-Hernando F, Muñoz-Bermúdez R, et al. Circulating microRNA profiling is altered in the acute respiratory distress syndrome related to SARS–CoV–2 infection. *Sci Rep* (2022) 12:6929. doi: 10.1038/s41598-022-10738-3

25. World Health Organization. *Clinical management of COVID-19: interim guidance* (2020). Available at: https://apps.who.int/iris/handle/10665/332196.

26. Kozomara A, Birgaoanu M, Griffiths-Jones S. miRBase: from microRNA sequences to function. *Nucleic Acids Res* (2019) 47:D155–62. doi: 10.1093/nar/gky1141

27. Martin M. Cutadapt removes adapter sequences from high-throughput sequencing reads. *EMBnet J* (2011) 17:10–2. doi: 10.14806/ej.17.1.200

28. Wingett SW, Andrews S. FastQ screen: A tool for multi-genome mapping and quality control. *F1000Res* (2018) 7:1338. doi: 10.12688/f1000research.15931.2

29. Loher P, Karathanasis N, Londin E, Bray P, Pliatsika V, Telonis AG, et al. IsoMiRmap-fast, deterministic, and exhaustive mining of isomiRs from short RNA-seq datasets. *Bioinformatics* (2021) 37:1828–38. doi: 10.1093/bioinformatics/btab016

30. Love MI, Huber W, Anders S. Moderated estimation of fold change and dispersion for RNA-seq data with DESeq2. *Genome Biol* (2014) 15:550. doi: 10.1186/s13059-014-0550-8

31. Licursi V, Conte F, Fiscon G, Paci P. MIENTURNET: an interactive web tool for microRNA-target enrichment and network-based analysis. *BMC Bioinf* (2019) 20:545. doi: 10.1186/s12859-019-3105-x

32. Sticht C, de la Torre C, Parveen A, Gretz N. miRWalk: An online resource for prediction of microRNA binding sites. *PloS One* (2018) 13:e0206239. doi: 10.1371/journal.pone.0206239

33. Kanehisa M, Sato Y, Kawashima M, Furumichi M, Tanabe M. KEGG as a reference resource for gene and protein annotation. *Nucleic Acids Res* (2016) 44: D457–62. doi: 10.1093/nar/gkv1070

34. Slenter DN, Kutmon M, Hanspers K, Riutta A, Windsor J, Nunes N, et al. WikiPathways: A multifaceted pathway database bridging metabolomics to other omics research. *Nucleic Acids Res* (2018) 46:661–7. doi: 10.1093/nar/gkx1064

35. Kibbe WA, Arze C, Felix V, Mitraka E, Bolton E, Fu G, et al. Disease ontology 2015 update: An expanded and updated database of human diseases for linking biomedical knowledge through disease data. *Nucleic Acids Res* (2015) 43:1071–8. doi: 10.1093/nar/gku1011

36. Shannon P, Markiel A, Ozier O, Baliga NS, Wang JT, Ramage D, et al. Cytoscape: a software environment for integrated models of biomolecular interaction networks. *Genome Res* (2003) 13:2498–504. doi: 10.1101/gr.1239303

37. Riccetti S, Sinigaglia A, Desole G, Nowotny N, Trevisan M, Barzon L. Modelling West Nile virus and Usutu virus pathogenicity in human neural stem cells. *Viruses* (2020) 12:882. doi: 10.3390/v12080882

38. Kok MGM, de Ronde MWJ, Moerland PD, Ruijter JM, Creemers EE, Pinto-Sietsma SJ. Small sample sizes in high-throughput miRNA screens: A common pitfall for the identification of miRNA biomarkers. *Biomol Detect Quantif* (2017) 15:1–5. doi: 10.1016/j.bdq.2017.11.002

39. Hart SN, Therneau TM, Zhang Y, Poland GA, Kocher JP. Calculating sample size estimates for RNA sequencing data. *J Comput Biol* (2013) 20:970–8. doi: 10.1089/cmb.2012.0283

40. Cloonan N, Wani S, Xu Q, Gu J, Lea K, Heater S, et al. MicroRNAs and their isomiRs function cooperatively to target common biological pathways. *Genome Biol* (2011) 12:R126. doi: 10.1186/gb-2011-12-12-r126

41. Giuliani A, Matacchione G, Ramini D, Di Rosa M, Bonfigli AR, Sabbatinelli J, et al. Circulating miR-320b and miR-483-5p levels are associated with COVID-19 in-hospital mortality. *Mech Ageing Dev* (2022) 202:111636. doi: 10.1016/j.mad.2022.111636

42. Hildebrandt A, Kirchner B, Meidert AS, Brandes F, Lindemann A, Doose G, et al. Detection of atherosclerosis by small RNA-sequencing analysis of extracellular vesicle enriched serum samples. *Front Cell Dev Biol* (2021) 9:729061. doi: 10.3389/fcell.2021.729061

43. Junqueira C, Crespo Â, Ranjbar S, de Lacerda LB, Lewandrowski M, Ingber J, et al. FcγR-mediated SARS-CoV-2 infection of monocytes activates inflammation. *Nature* (2022) 606:576–84. doi: 10.1038/s41586-022-04702-4

44. Abers MS, Delmonte OM, Ricotta EE, Fintzi J, Fink DL, de Jesus AAA, et al. An immune-based biomarker signature is associated with mortality in COVID-19 patients. *JCI Insight* (2021) 6:e144455. doi: 10.1172/jci.insight.144455

45. Youngs J, Provine NM, Lim N, Sharpe HR, Amini A, Chen YL, et al. Identification of immune correlates of fatal outcomes in critically ill COVID-19 patients. *PloS Pathog* (2021) 17:e1009804. doi: 10.1371/journal.ppat.1009804

46. Nishiga M, Wang DW, Han Y, Lewis DB, Wu JC. COVID-19 and cardiovascular disease: from basic mechanisms to clinical perspectives. *Nat Rev Cardiol* (2020) 17:543–58. doi: 10.1038/s41569-020-0413-9

47. Fajgenbaum DC, June CH. Cytokine storm. *N Engl J Med* (2020) 383:2255–73. doi: 10.1056/NEJMra2026131

48. Kim RY, Sunkara KP, Bracke KR, Jarnicki AG, Donovan C, Hsu AC, et al. A microRNA-21-mediated SATB1/S100A9/NF-κB axis promotes chronic obstructive pulmonary disease pathogenesis. *Sci Transl Med* (2021) 13:eaav7223. doi: 10.1126/scitranslmed.aav7223

49. Ramanujam D, Schön AP, Beck C, Vaccarello P, Felician G, Dueck A, et al. MicroRNA-21-dependent macrophage-to-fibroblast signaling determines the cardiac response to pressure overload. *Circulation* (2021) 143:1513–25. doi: 10.1161/CIRCULATIONAHA.120.050682

50. Polioudakis D, Bhinge AA, Killion PJ, Lee BK, Abell NS, Iyer VR. A myc-microRNA network promotes exit from quiescence by suppressing the interferon response and cell-cycle arrest genes. *Nucleic Acids Res* (2013) 41:2239–54. doi: 10.1093/nar/gks1452

51. Wan S, Ashraf U, Ye J, Duan X, Zohaib A, Wang W, et al. MicroRNA-22 negatively regulates poly(I:C)-triggered type I interferon and inflammatory cytokine production *via* targeting mitochondrial antiviral signaling protein (MAVS). *Oncotarget* (2016) 7:76667–83. doi: 10.18632/oncotarget.12395

52. Sun J, Mao S, Ji W. LncRNA H19 activates cell pyroptosis *via* the miR-22-3p/NLRP3 axis in pneumonia. *Am J Transl Res* (2021) 13:11384–98.

53. Galluzzo A, Gallo S, Pardini B, Birolo G, Fariselli P, Boretto P, et al. Identification of novel circulating microRNAs in advanced heart failure by next-generation sequencing. *ESC Heart Fail* (2021) 8:2907–19. doi: 10.1002/ehf2.13371

54. Pobezinsky LA, Etzensperger R, Jeurling S, Alag A, Kadakia T, McCaughtry TM, et al. Let-7 microRNAs target the lineage-specific transcription factor PLZF to regulate terminal NKT cell differentiation and effector function. *Blood* (2015) 16:517–25. doi: 10.1038/ni.3146

55. Severa M, Diotti RA, Etna MP, Rizzo F, Fiore S, Ricci D, et al. Differential plasmacytoid dendritic cell phenotype and type I interferon response in asymptomatic and severe COVID-19 infection. *PloS Pathog* (2021) 17:e1009878. doi: 10.1371/journal.ppat.1009878

56. Tang N, Li D, Wang X, Sun Z. Abnormal coagulation parameters are associated with poor prognosis in patients with novel coronavirus pneumonia. *J Thromb Haemost* (2020) 18:844–7. doi: 10.1111/jth.14768

57. Zhang J, Xu X, Wang M. Clinical significance of serum miR-101-3p expression in patients with neonatal sepsis. *Per Med* (2021) 18:541–50. doi: 10.2217/pme-2020-0182

58. Francuzik W, Pažur K, Dalke M, Dölle-Bierke S, Babina M, Worm M. Serological profiling reveals hsa-miR-451a as a possible biomarker of anaphylaxis. *JCI Insight* (2022) 7:e156669. doi: 10.1172/jci.insight.156669

59. Okamoto M, Fukushima Y, Kouwaki T, Daito T, Kohara M, Kida H, et al. MicroRNA-451a in extracellular, blood-resident vesicles attenuates macrophage and dendritic cell responses to influenza whole-virus vaccine. *J Biol Chem* (2018) 293:18585–600. doi: 10.1074/jbc.RA118.003862

60. Rodriguez A, Vigorito E, Clare S, Warren MV, Couttet P, Soond DR, et al. Requirement of bic/microRNA-155 for normal immune function. *Science* (2007) 316:608–11. doi: 10.1126/science.1139253

61. Elton TS, Selemon H, Elton SM, Parinandi NL. Regulation of the MIR155 host gene in physiological and pathological processes. *Gene* (2013) 532:1–12. doi: 10.1016/j.gene.2012.12.009

62. Wang P, Hou J, Lin L, Wang C, Liu X, Li D, et al. Inducible microRNA-155 feedback promotes type I IFN signaling in antiviral innate immunity by targeting suppressor of cytokine signaling 1. *J Immunol* (2010) 185:6226–33. doi: 10.4049/jimmunol.1000491

63. Kassif-Lerner R, Zloto K, Rubin N, Asraf K, Doolman R, Paret G, et al. MiR-155: A potential biomarker for predicting mortality in COVID-19 patients. *J Pers Med* (2022) 12:324. doi: 10.3390/jpm12020324

64. Ikeda S, Kong SW, Lu J, Bisping E, Zhang H, Allen PD, et al. Altered microRNA expression in human heart disease. *Physiol Genomics* (2007) 31:367–3731. doi: 10.1152/physiolgenomics.00144.2007

65. Grossi I, Salvi A, Baiocchi G, Portolani N, De Petro G. Functional role of microRNA-23b-3p in cancer biology. *MicroRNA* (2018) 7:156–66. doi: 10.2174/2211536607666180629155025

66. Chen DL, Sheng H, Zhang DS, Jin Y, Zhao BT, Chen N, et al. The circular RNA circDLG1 promotes gastric cancer progression and anti-PD-1 resistance through the regulation of CXCL12 by sponging miR-141-3p. *Mol Cancer* (2021) 20:166. doi: 10.1186/s12943-021-01475-8

67. Martínez-Fleta P, Vera-Tomé P, Jiménez-Fernández M, Requena S, Roy-Vallejo E, Sanz-García A, et al. A differential signature of circulating miRNAs and cytokines between COVID-19 and community-acquired pneumonia uncovers novel physiopathological mechanisms of COVID-19. *Front Immunol* (2022) 12:815651. doi: 10.3389/fimmu.2021.815651

68. Farr RJ, Rootes CL, Rowntree LC, Nguyen THO, Hensen L, Kedzierski L, et al. Altered microRNA expression in COVID-19 patients enables identification of SARS-CoV-2 infection. *PloS Pathog* (2021) 17:e1009759. doi: 10.1371/journal.ppat.1009759

69. Park JH, Choi Y, Lim CW, Park JM, Yu SH, Kim Y, et al. Potential therapeutic effect of microRNAs in extracellular vesicles from mesenchymal stem cells against SARS-CoV-2. *Cells* (2021) 10:2393. doi: 10.3390/cells10092393

70. Zhao C, Sun X, Li L. Biogenesis and function of extracellular miRNAs. *ExRNA* (2019) 1:1–9. doi: 10.1186/S41544-019-0039-4

71. Trevisan M, Riccetti S, Sinigaglia A, Barzon L. SARS-CoV-2 infection and disease modelling using stem cell technology and organoids. *Int J Mol Sci* (2021) 22 (5):2356. doi: 10.3390/ijms22052356

72. Benedetti F, Silvestri G, Mavian C, Weichseldorfer M, Munawwar A, Cash MN, et al. Comparison of SARS-CoV-2 receptors expression in primary endothelial cells and retinoic acid-differentiated human neuronal cells. *Viruses* (2021) 13:2193. doi: 10.3390/v13112193

73. Lei Y, Zhang J, Schiavon CR, He M, Chen L, Shen H, et al. SARS-CoV-2 spike protein impairs endothelial function *via* downregulation of ACE 2. *Circ Res* (2021) 128:1323–6. doi: 10.1161/CIRCRESAHA.121.318902

74. Nuovo GJ, Magro C, Shaffer T, Awad H, Suster D, Mikhail S, et al. Endothelial cell damage is the central part of COVID-19 and a mouse model induced by injection of the S1 subunit of the spike protein. *Ann Diagn Pathol* (2021) 51:151682. doi: 10.1016/j.anndiagpath.2020.151682

75. Wyler E, Mösbauer K, Franke V, Diag A, Gottula LT, Arsiè R, et al. Transcriptomic profiling of SARS-CoV-2 infected human cell lines identifies HSP90 as target for COVID-19 therapy. *iScience* (2021) 24:102151. doi: 10.1016/j.isci.2021.102151

76. Forster SC, Tate MD, Hertzog PJ. MicroRNA as type I interferon-regulated transcripts and modulators of the innate immune response. *Front Immunol* (2015) 6:334. doi: 10.3389/fimmu.2015.00334

77. Jiao Y, Li W, Wang W, Tong X, Xia R, Fan J, et al. Platelet-derived exosomes promote neutrophil extracellular trap formation during septic shock. *Crit Care* (2020) 24:380. doi: 10.1186/s13054-020-03082-3

78. Zhou J, Lin J, Zhao Y, Sun X. Deregulated expression of miR-483-3p serves as diagnostic biomarker in severe pneumonia children with respiratory failure and its predictive value for the clinical outcome of patients. *Mol Biotechnol* (2022) 64:311–9. doi: 10.1007/s12033-021-00415-7

79. Leng C, Sun J, Xin K, Ge J, Liu P, Feng X. High expression of miR-483-5p aggravates sepsis-induced acute lung injury. *J Toxicol Sci* (2020) 45:77–86. doi: 10.2131/jts.45.77

frontiers | Frontiers in Immunology

TYPE Original Research
PUBLISHED 24 August 2022
DOI 10.3389/fimmu.2022.956369

OPEN ACCESS

EDITED BY
Nitin Saksena,
Victoria University, Australia

REVIEWED BY
Gonzalo Valenzuela Galaz,
Pontifical Catholic University of Chile, Chile
Juan C. Hernandez,
Cooperative University of Colombia, Colombia

*CORRESPONDENCE
Pu Liao
liaopu@sina.com
Liang Qiao
liang_qiao@fudan.edu.cn

†These authors have contributed equally to this work

SPECIALTY SECTION
This article was submitted to Vaccines and Molecular Therapeutics, a section of the journal Frontiers in Immunology

RECEIVED 30 May 2022
ACCEPTED 01 August 2022
PUBLISHED 24 August 2022

CITATION
Zhang W, Li D, Xu B, Xu L, Lyu Q, Liu X, Li Z, Zhang J, Sun W, Ma Q, Qiao L and Liao P (2022) Serum peptidome profiles immune response of COVID-19 Vaccine administration. *Front. Immunol.* 13:956369. doi: 10.3389/fimmu.2022.956369

Serum peptidome profiles immune response of COVID-19 Vaccine administration

Wenjia Zhang[1†], Dandan Li[2†], Bin Xu[3†], Lanlan Xu[1], Qian Lyu[3], Xiangyi Liu[4], Zhijie Li[1], Jian Zhang[5], Wei Sun[5], Qingwei Ma[3], Liang Qiao[2*] and Pu Liao[1*]

[1]Department of Clinical Laboratory, Chongqing General Hospital, Chongqing, China, [2]Department of Chemistry, Fudan University, Shanghai, China, [3]Bioyong Technologies, Inc., Beijing, China, [4]Department of Laboratory Medicine, Beijing Tongren Hospital, Capital Medical University, Beijing, China, [5]State Key Laboratory of Proteomics, Beijing Proteome Research Center, National Center for Protein Sciences (Beijing), Beijing Institute of Lifeomics, Beijing, China

Background: Coronavirus disease 2019 (COVID-19) caused by severe acute respiratory syndrome coronavirus 2 (SARS-CoV-2) has caused significant loss of life and property. In response to the serious pandemic, recently developed vaccines against SARS-CoV-2 have been administrated to the public. Nevertheless, the research on human immunization response against COVID-19 vaccines is insufficient. Although much information associated with vaccine efficacy, safety and immunogenicity has been reported by pharmaceutical companies based on laboratory studies and clinical trials, vaccine evaluation needs to be extended further to better understand the effect of COVID-19 vaccines on human beings.

Methods: We performed a comparative peptidome analysis on serum samples from 95 participants collected at four time points before and after receiving CoronaVac. The collected serum samples were analyzed by matrix-assisted laser desorption/ionization time-of-flight mass spectrometry (MALDI-TOF MS) to profile the serum peptides, and also subjected to humoral and cellular immune response analyses to obtain typical immunogenicity information.

Results: Significant difference in serum peptidome profiles by MALDI-TOF MS was observed after vaccination. By supervised statistical analysis, a total of 13 serum MALDI-TOF MS feature peaks were obtained on day 28 and day 42 of vaccination. The feature peaks were identified as component C1q receptor, CD59 glycoprotein, mannose-binding protein C, platelet basic protein, CD99 antigen, Leucine-rich alpha-2-glycoprotein, integral membrane protein 2B, platelet factor 4 and hemoglobin subunits. Combining with immunogenicity analysis, the study provided evidence for the humoral and cellular immune responses activated by CoronaVac. Furthermore, we found that it is possible to distinguish neutralizing antibody (NAbs)-positive from NAbs-negative individuals after complete vaccination using the serum peptidome profiles by MALDI-TOF MS together with machine learning methods, including random forest (RF), partial least squares-discriminant analysis (PLS-DA), linear support vector machine (SVM) and logistic regression (LR).

Conclusions: The study shows the promise of MALDI-TOF MS-based serum peptidome analysis for the assessment of immune responses activated by COVID-19 vaccination, and discovered a panel of serum peptides biomarkers for COVID-19 vaccination and for NAbs generation. The method developed in this study can help not only in the development of new vaccines, but also in the post-marketing evaluation of developed vaccines.

KEYWORDS

COVID-19, vaccine, MALDI-TOF, peptidome, serum, immune response

Introduction

Coronavirus disease 2019 (COVID-19) has caused considerable loss of life and property since its outbreak. To curb the pandemic, physical strategies, such as personal protective equipment distribution, social distancing rules and quarantine policies, have been widely implemented. Compared with physical strategies, herd immunity is a critical approach to control the pandemic. To date, different types of COVID-19 vaccines have been developed, approved, and widely distributed across the world, such as mRNA vaccines (Pfizer–BioNTech and Moderna), adenovirus vector vaccines (Oxford–AstraZeneca), inactivated virus vaccines (Sinovac and Sinopharm), etc. (1). Based on these licensed vaccine products, herd immunization has been boosted. As of July 2022, University of Oxford confirmed that more than 12 billion doses of COVID-19 vaccine have been administered worldwide (2) and the number is increasing continuously. Nevertheless, in response to the urgent and huge demand for COVID-19 vaccines, the development cycle of vaccines was greatly compressed (3). Besides, the natural immune response induced by severe acute respiratory syndrome coronavirus 2 (SARS-CoV-2) is still not fully understood. Given the paucity of development experience and the greatly shortened vaccine development time, there is a lack of thorough knowledge on the immune response induced by COVID-19 vaccination.

Vaccine efficacy and safety are the most important factors to be considered (4, 5). The immunogenicity of vaccine is frequently evaluated, involving both humoral and cellular immune response analyses (6). Immunogenicity is a sophisticated and informative indicator that is associated with the vaccine-induced immune responses and their change over time (6). For the assessment of immunogenicity, production of antibody is measured (7). Antibody monitoring, particularly on total antibody (TAbs) and neutralizing antibody (NAbs), is the primary laboratory strategy to test the protective ability of vaccines against SARS-CoV-2 (8, 9). There are several methods to measure NAbs. The common ones are plaque reduction neutralization test (PRNT), fluorescent neutralization assay (FNA), microneutralization assay (MNA), pseudovirus neutralization assay (PSVNA), and surrogate virus neutralization test (SVNT) (10). PRNT is the gold standard to evaluate immune protection using live virus (11), but need to be accomplished in bio-safety level 3 (BSL-3) laboratory, which limits its application scenario (8). FNA can provide equivalent results to PRNT, but sometimes it also needs to be performed in BSL-3 laboratory (8). MNA involves live SARS-CoV-2 virus as well, and is limited not only by safety risks but also by the disadvantages of time-consuming and high cost. Compared to PRNT, MNA and FNA, PSVNA is a safe method to test NAbs in Biosafety Level 2 (BSL2) laboratory by using pseudo virus without replicating ability. PSVNA is of high sensitivity, accuracy, and repeatability (12), but requires complicated procedure. SVNT has the characteristics of high-throughput and easy-to-operate without the requirement of live virus, and it also detects designated NAbs (8). To date, the currently used methods of NAbs analysis are mainly limited by the requirement of bio-safety laboratory, throughput, time costs and economic costs (8, 11, 13). Development of new strategies is of interest for the ongoing vaccine evaluation work with mass vaccination efforts underway.

Apart from antibody monitoring, cellular immune responses are also widely monitored for vaccine development (14, 15). Prendecki et al. showed that mRNA (BNT162b2, mRNA-1273) and viral-vector vaccines can elicit strong T cell response against SARS-CoV-2 (16). A recent article evaluated the T cell response induced by BBIBP-CorV (Sinopharm, inactivated virus) with a focus on IFN-γ (17). Recently, Zhao et al. reported the humoral and cellular immune responses of 136 participants activated by two-dose of CoronaVac after 1, 3, 6, and 12 moths (18). Jiang et al. reported the immune features of CoronaVac based on 13 healthy people and 12 people that recovered from COVID-19 infection (19). Although pharmaceutical companies have reported the efficacy, safety and immunogenicity of COVID-19 vaccines based on laboratory studies and clinical trials, additional vaccine evaluation is needed to better understand

the effect of COVID-19 vaccines on human beings, and new strategies for the evaluation of immune response against vaccines are needed.

Matrix-assisted laser desorption/ionization time-of-flight mass spectrometry (MALDI-TOF MS) is widely used in clinical scenarios, particularly microbial identification and biomarker discovery, due to its advantages, such as rapid analysis, high-throughput, easy operation, low-cost in consumables, etc. The peptide mass fingerprint generated by MALDI-TOF MS can describe a complex mixture of proteolytically derived peptides in human body fluids associated with biological events happening throughout the whole body. Many studies have reported that MALDI-TOF MS can be used to diagnose diseases, such as multiple myeloma (20), liver cancer (21), prostate cancer (22), active mycobacterium tuberculosis (Mtb) infection (23), etc., by screening a panel of protein and peptide biomarkers in human body fluids. Responding to the COVID-19 pandemic, MALDI-TOF-based serum peptides fingerprint, i.e., MALDI-TOF-based serum peptidome profiling, has been developed for the rapid screening of COVID-19 infectious people and COVID-19 illness severity (24, 25). MALDI-TOF MS combining liquid chromatography-tandem mass spectrometry (LC-MS/MS) has also been performed on serum and nasopharyngeal swabs from COVID-19 patients (24–27) to identify potential biomarkers of SARS-CoV-2 infection. Herein, we performed a comparative peptidome analysis on human serum before and after receiving CoronaVac.

Materials and methods

Sample collection and storage

Ninety-five participants were recruited. The subjects had no previous infection with COVID-19 and no COVID-19 vaccination before the study. The whole sampling was accomplished between February and April 2021. During this period, all participants were injected with a two-dose COVID-19 inactivated vaccine (CoronaVac, Sinovac Biotech Co., Ltd, Beijing, China) in Chongqing General Hospital, and four batches of blood samples were collected before and after vaccination. The sampling time was determined as day 0 (on the day but before the first injection), day 21 (3 weeks after the first injection, and on the day but before the second injection), day 28 (1 week after the second injection) and day 42 (3 weeks after the second injection). After centrifugation at 2264 g for 10 min and sterilization at 56°C for 30 min, the serum samples were aliquoted and frozen at −80°C until use. Erythrocyte-lysed whole blood was prepared from the samples collected on day 0 and day 28, and immediately subjected to lymphocytes subpopulation analysis.

Immunogenicity profiling

TAbs and NAbs were analyzed for all the collected serum at the four time points. TAbs were quantified using TAbs chemiluminescence reagent kits (Xiamen Wantaicare Company, batch 20210101, Xiamen, China) on an automated chemiluminescence immunoassay analyzer (Xiamen Youmic Company, Caris 200, Xiamen, China). Negative and positive TAbs were determined according to the instructions provided with the kit. NAbs were quantified using chemiluminescence reagent kits targeting at SARS-CoV-2 receptor binding domain (RBD) (Shenzhen Yahuilong company reagent, batch 20210101, Shenzhen, China) on an automated chemiluminescence analyzer (Shenzhen Yahuilong Biotechnology Co., Ltd., iFlash 3000-A, Shenzhen, China). Negative and positive NAbs were determined according to the instructions provided with the kit.

Cytokines were analyzed for serum sample collected on day 0 and day 28 by cytokines assay kits (Weimi Bio-Tech Co., Guangzhou, China) using a BD FACS CantoII flow cytometer (Becton, Dickinson and Company, Franklin Lakes, New Jersey, U.S.) following the manufacturer's' instructions. The kits included 14 types of microbeads with distinct fluorescence intensities and coated with, respectively, specific antibodies against IL-17F, IL-21, IL-2, IL-4, IL-5, IL-6, IL-8, IL-1β, IL-17A, IL-10, TNF-α, TNF-β, IL-12p70 and IFN-γ. After incubation with serum sample, the immunocomplex was further combined with PE fluorescently labeled detection antibody to form a double-antibody sandwich complex, and the fluorescence intensity of the complex was analyzed by flow cytometer to quantify the cytokines. The data were analyzed using the FCAP Array Software v3.0.

Lymphocytes subpopulation were analyzed by a MultiTEST TM IMK kit (Becton, Dickinson and Company, Franklin Lakes, New Jersey, U.S.) using a BD FACS CantoII flow cytometer (Becton, Dickinson and Company, Franklin Lakes, New Jersey, U.S.) following the manufacturer's' instructions. Absolute counts of T lymphocytes (CD3+), B lymphocytes (CD19+), helper T lymphocytes (CD3+CD4+), cytotoxic T lymphocytes (CD3+CD8+), and natural killer (NK) cells (CD16+CD56+) were quantified in erythrocyte-lysed whole blood samples collected on day 0 and day 28.

MALDI-TOF MS analysis

For all the samples, 5 μl serum was diluted 10 times using dilution buffer (PMFpre kit 1010305, Bioyong Technologies Inc., Beijing, China), and 10 μl of the diluted serum was mixed with 10 μl sinapinic acid matrix. One μl of the mixture was dropped on a sample spot of a stainless-steel target plate. The sample was dried at room temperature followed by MALDI-TOF MS (Clin-TOF-II; Bioyong Technologies Inc., Beijing, China) analysis

under the linear positive mode. The mass spectrometer was calibrated with a standard calibration mixture of peptides and proteins. The calibration tolerance was 500 ppm. The mass range was m/z 3,000 to m/z 30,000. Each spectrum was accumulated from 50 positions of a sample spot with 10 laser shots per position.

MALDI-TOF MS data processing and analysis

Raw data of MALDI-TOF MS were processed by an R package, MALDIquant (28), with operations including sqrt transformation, savitzkyGolay smoothing with a halfWindowsize of 5, and SNIP baseline correction. Then, peak detection was performed using the MAD method with a halfWindowsize of 20 and a signal-to-noise (S/N) threshold of 6. Minifrequency was set as 0.25. Peaks were then binned by binPeaks with a tolerance of 0.005 for all samples. Mass range was from 3,000 m/z to 30,000 m/z. The data obtained as a matrix table was then further processed by log 2 transformation, quantile normalization, and missing values imputing using Metaboanalyst (29) (McGill University, Montreal, Canada, https://www.metaboanalyst.ca/).

Statistical analysis

Unsupervised and supervised statistical analysis was performed using Metaboanalyst, including principal component analysis (PCA), partial least squares-discriminant analysis (PLS-DA) and volcano plot. Significant MALDI-TOF feature peaks were determined by PLS-DA (VIP > 2.0) and volcano plot (FC > 1.5, p-value < 0.05). P-value was calculated by the Wilcoxon test to confirm the significant difference of feature peaks between the same set of people at different time points, or by the Mann-Whitney test to confirm the significant difference of feature peaks between two independent sets of samples, i.e., between the NAbs positive and negative groups.

Proteomic analysis

The serum samples from three participants (Sample 23, 41, 78) were selected for proteomic analysis, since the samples showed intensive significant MALDI-TOF MS feature peaks (identified using the statistical analysis method described in 2.5). The samples were mixed, and four mixed samples at four collection time points were obtained (day 0, day 21, day 28 and day 42). For each sample, abundant proteins were removed using High Select Top14 Abundant Protein Depletion Mini Spin Columns (A36370, Thermo Fisher Scientific, Waltham, MA, USA). The remaining samples were then dissolved in a protein lysis solution containing 8M urea (U6504, Sigma-Aldrich Co., St. Louis, MO, USA) and 0.1% SDS (L6026, Sigma-Aldrich Co., St. Louis, MO, USA). BCA quantification kit (P0010, Beyotime Biotechnology, Beijing, China) was used to quantify the final protein concentration of all samples. After tris (2-carboxyethyl) phosphine (TCEP, Thermo Fisher Scientific, Waltham, MA, USA) reduction at 37°C for 1 h and iodoacetamide (IAA, Sigma-Aldrich Co., St. Louis, MO, USA) alkylation at 25°C for 1 h, 6 volume of pre-cooled acetone was added to precipitate proteins at −20°C for 4 h. The precipitate was collected by centrifugation and washed twice with 90% pre-cooled acetone. Then the protein samples were re-dissolved in 100 µl ammonium bicarbonate solution (25 mM). Proteome sequencing grade trypsin (Hualishi scientific, Beijing, China) was added at 1:50 (w:w) enzyme-to-sample ratio for protein digestion at 37°C overnight. After digestion, a C18 column (Thermo Fisher Scientific, Waltham, MA, USA) was used for desalting followed by peptide quantification using Pierce™ quantitative colorimetric peptide assay (Thermo Fisher Scientific, Waltham, MA, USA). Afterwards, the samples were lyophilized by an LNG-T98 freeze concentration centrifugation dryer (Taicang Huamei, Taicang, Jiangsu, China) for further LC-MS/MS analysis.

The processed samples were then redissolved in 0.1% formic acid (FA) aqueous solution (solvent A) to a concentration of 0.5 µg/µl. Four µL of the sample was injected into an Orbitrap Fusion Lumos spectrometer (Thermo Fisher Scientific, Waltham, MA, USA) coupled with a nanoLC system (Thermo-ESAY-nLC, Thermo Fisher Scientific, Waltham, MA, USA) using a 25 cm analytical column (75 µm inner diameter, 1.9 µm resin, Dr Maisch, Ammerbuch-Entringen, Germany), and separated using a 120-minute gradient. The flow rate of the nanoLC was maintained at 600 nL/min and the column temperature was 50°C. Water and ACN (both containing 0.1% FA) were used as solvents A and B, respectively, with the following gradient elution program: 0-4-79-108-110-120 min, 4%-7%-20%-30%-90%-90% of solvent B, with an electrospray voltage of 2.2 kV. The mass spectrometer was operated in data independent acquisition mode with MS and MS/MS automatically switched. The parameters were (1) MS: scan range (m/z) = 350-1500; resolution = 120,000; AGC target = 40,0000; maximum injection time = 50 ms; (2) HCD-MS/MS: resolution = 30,000; AGC target = 20,000; collision energy = 32%; maximum injection time = 72 ms (3) DIA: Variable isolation windows; 1 m/z overlap per window; number of windows = 60.

Raw MS data were used to search against the Homo sapiens database downloaded from UniProtKB (20,600 entries) using Spectronaut (version 15.2, Biognosys, Schlieren, Switzerland). Default parameters were retained except the quantitative method was set as the first level.

Annotation of MALDI-TOF MS feature peaks and bioinformatic analysis

Matching between the MALDI-TOF mass spectra feature peaks and the proteomic analysis results was performed under the criteria: the molecular weight of an identified protein/protein fragment was consistent with the m/z of the MALDI-TOF MS peak within a tolerance of 2000 ppm; only the charge state of 1+ was considered for MALDI-TOF MS peaks; the quantity changes of the protein/protein fragment by LC-MS/MS showed the same trend as the intensity change of the matched MALDI-TOF MS peak. If more than one protein/protein fragment matched to the feature peak under the given criteria, priority was given to the protein fragments containing N or C terminal, and then the one with the smallest mass difference. The gene ontology (GO) enrichment analysis was performed by Metascape (30) involving all the identified features.

Results

Cohort establishment and immunogenicity analysis

An overview of the study design is shown in Figure 1. Ninety-five participants (21-59 years) accepted two doses of CoronaVac vaccines. Among the 95 participants, the percentage of male (42%) and female (58%) was balanced, with 29% people aged 20-30, 17% people aged 30-40, 19% people aged 40-50 and 35% aged over 50 years (Table S1). Regarding past medical history, one of the subjects had coronary artery disease and four had hypertension or diabetes. After vaccination, records showed few symptoms of adverse reactions among the 95 participants. There were two cases of muscle aches, three cases of injection site pain or itching, one case of dizziness and palpitations, without any fever cases. More demographic information of the participants can be found in Table S1. Blood samples were collected from the participants during the 6-week recovery phase. Pre-vaccinated blood samples were also collected as the control group. Finally, four batches of blood samples were collected on day 0 (on the day but before the 1st injection), day 21 (on the day but before the 2nd injection), day 28 and day 42 (Figure 1A). Sera were separated from the blood samples (Figure 1B) and analyzed by MALDI-TOF MS (Figure 1C). Statistical analysis was performed on the MALDI-TOF mass spectra for the identification of significant features related to CoronaVac vaccination and NAbs generation (Figures 1D, E).

The immunogenicity profiling of antibodies, cytokines and lymphocyte was performed to quantify TAbs, NAbs, IL-17F, IL-21, IL-2, IL-4, IL-5, IL-6, IL-8, IL-1β, IL-17A, IL-10, TNF-α, TNF-β, IL-12p70, IFN-γ, CD3+, CD19+, CD3+CD4+, CD3+CD8+, and CD16+CD56+ (Figure 1C). From Figure S1A, it can be observed that the positive rates of TAbs (TAbs positive: s/co ≥ 1.00) and

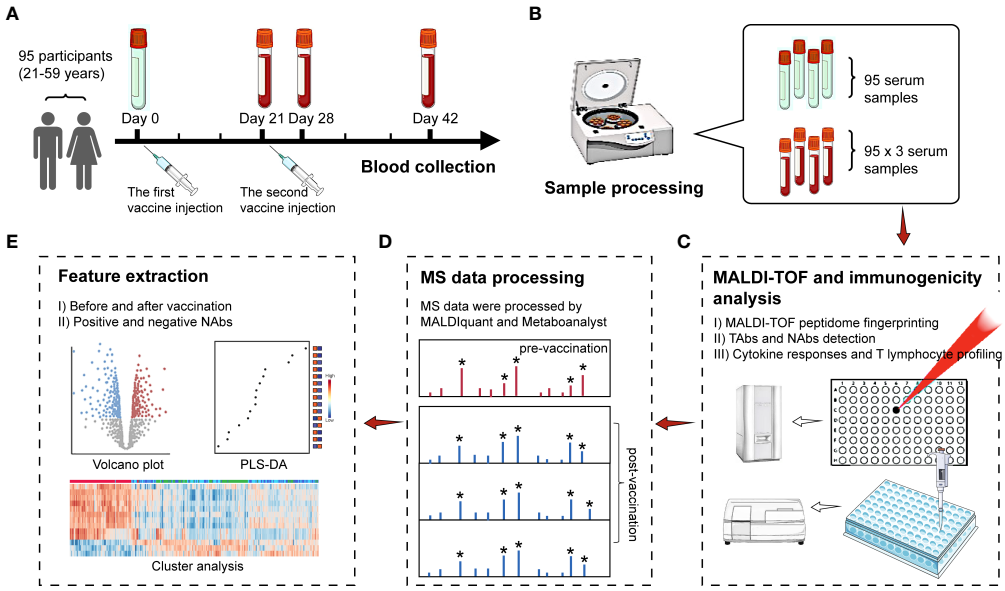

FIGURE 1
Study design. **(A)** Ninety-five participants were recruited and received two doses of CoronaVac vaccines. Blood samples were collected at four time points before and after vaccine injection. **(B)** Serum separation. **(C)** MALDI-TOF MS and immunogenicity analysis on all the collected serum samples. **(D)** MALDI-TOF MS data processing using MALDIquant and Metaboanalyst. **(E)** Feature selection based on volcano plot and variable importance in projection (VIP) scores by PLS-DA. Hierarchical cluster analyses (HCA) showed the intensity distribution of the selected features among samples. Peaks with an asterisk are peaks of higher intensity filtered by the signal-to-noise ratio and are included in the analysis. Peaks without an asterisk are by default noise peaks and are not included in the analysis.

NAbs (NAbs positive: ≥10.00 AU/mL) were zero on day 0 and were both below 40% on day 21. TAbs positive rate climbed up to over 80% on day 28 and over 90% on day 42. The high positive rate of TAbs on day 42 indicated that the immune response was activated by COVID-19 vaccination for most participants. For NAbs, the positive rate was consistently below 50% until day 28, and ascended to 73% on day 42, with 26 people still NAbs negative. Within the 26 negative NAbs people, the distribution of female (54%) and male (46%) was almost even (Figure S1B). However, more than half (54%) of the people were over 50 years old (Figure S1C), while the people > 50 years old only accounted 35% of the whole cohort. People aged 50-59 had lower rates of NAbs production than those aged under 50 (Table S1).

Serum cytokine profiling revealed that IL-21 and IL-8 increased significantly comparing day 28 to day 0, while IL-17F, IL-17A, IL-10, IL-12p70, TNF-α, TNF-β and IFN-γ decreased significantly, when considering all the participants (Figure S2). When considering separately the group with age > 50 and those with age < 50, the overall regulation trend kept consistent but IL-21, IL-17A, IL-10 and IFN-γ were only significant in the group with age < 50 (Figures S3 and S4). Lymphocyte subpopulation analysis demonstrated the significant up-regulation of CD3+CD4+ and significant down-regulation of CD3+CD8+, CD19+ and CD16+CD56+ comparing day 28 to day 0 considering all the participants (Figure S2). The significant regulation of CD19+ and CD16+CD56+ were only observed for the group with age < 50; while the significant regulation of CD3+CD4+ was only observed for the group with age > 50 (Figre S3 and S4).

Vaccination-induced serum peptidome change

A total of 380 mass spectra were collected from the 95 participants. The extracted peaks of the mass spectra are shown in supplementary Data S1. After vaccination, the number of peaks increased (Figure S5), indicating the increase of serum peptides expression. 327 peaks were obtained after peak alignment within the mass range of m/z 3,000 to m/z 30,000 (m/z, mass-to-charge ratio). Raw mass spectra of Sample 58 at four time points are shown in Figure 2. A global view of the four MALDI-TOF mass spectra revealed a high similarity of serum peptidome pattern before and after vaccination (Figure 2A). Nevertheless, a few peaks, such as m/z 13,761, m/z 13,882, m/z 13,939, m/z 14,044, m/z 14,091, m/z 14,150 and m/z 28,195 were downregulated after vaccination (Figure 2B).

Principal component analysis (PCA) was performed on the collected serum peptidome profiles. As shown in Figure 3, day 0 can be clearly discriminated from day 21, day 28 and day 42. The degree of discrimination diminished with the increase of time interval. Day 0 and day 21 presented the largest difference. In contrast, the MALDI-TOF mass spectra from day 21, day 28 and day 42 cannot be well distinguished by PCA (Figure 3). These results demonstrated that the serum peptidome was significantly changed before and after vaccination, the changes were more significant in short term, and the differences were not from batch bias effect. To further demonstrate the classification, a heat map of cluster analysis was performed on the collected serum peptidome profiles, which showed that the pre-vaccine samples clustered mostly together (Figure S6).

With the significant difference in serum peptidome before and after vaccination, significant MALDI-TOF MS features associated with the vaccination were mined. The feature selection procedure is illustrated in Figure 4A. Day 28 and day 42 with full doses of vaccination were chosen to identify distinctive features compared to day 0. The top 15 contributory features with the highest VIP scores in PLS-DA analysis between day 0 and day 28 are shown in Figure S7A. The up and down regulations of mass spectrometry features by volcano-plot analysis between day 0 and day 28 are shown in Figure S7B. By taking the intersection of the candidate features selected by

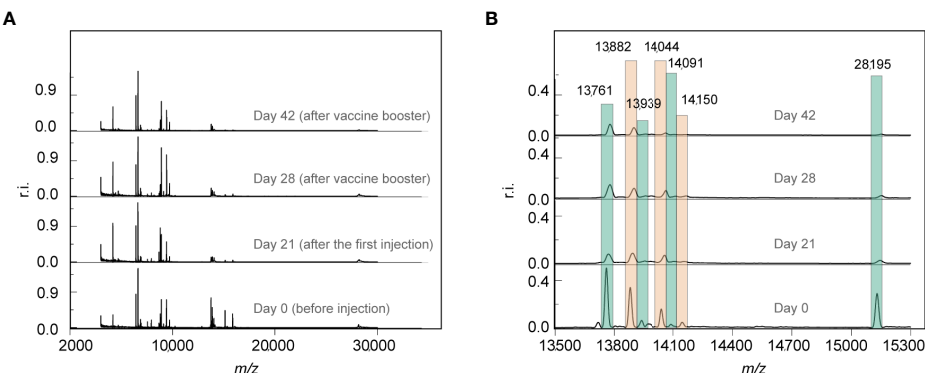

FIGURE 2
(A) The representative MALDI-TOF mass spectra of one participant at four time points pre-vaccination and post-vaccination. **(B)** Partial enlarged view of **(A)**. The mass spectra were normalized against the strongest peak. r.i.: relative intensity.

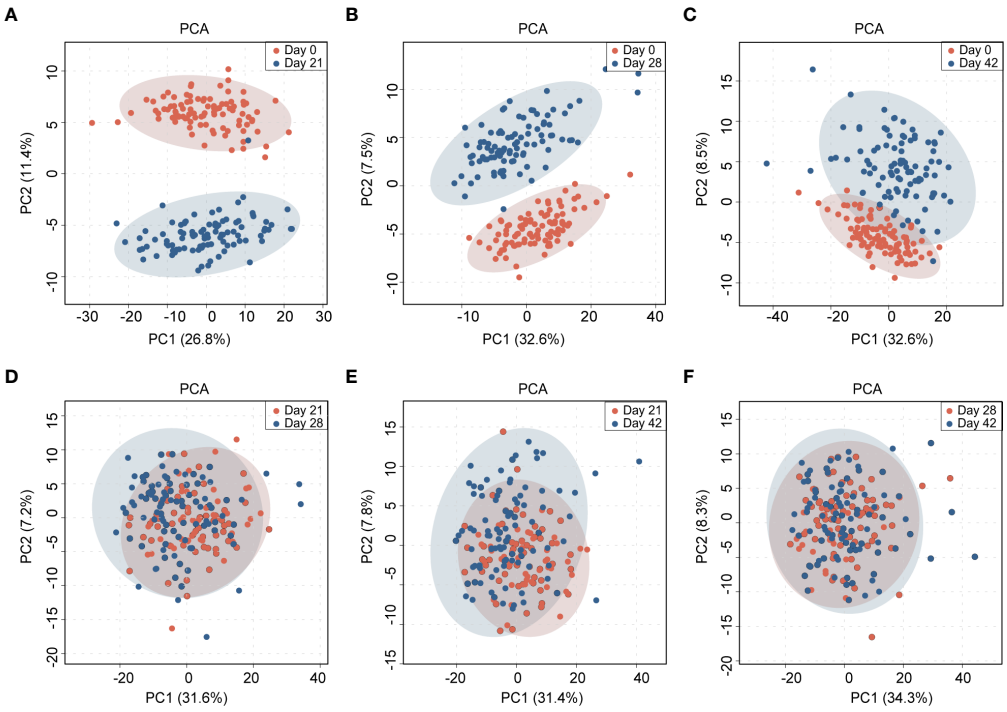

FIGURE 3
Principal component analysis (PCA) of the MALDI-TOF MS-based serum peptidome profiles collected at 4 time points before and after vaccination: **(A)** between day 0 and day 21; **(B)** between day 0 and day 28; **(C)** between day 0 and day 42; **(D)** between day 21 and day 28; **(E)** between day 21 and day 42; **(F)** between day 28 and day 42. The shadow ovals represent 95% confidence interval.

both PLS-DA and volcano-plot, a group of 12 candidate significant features between day 0 and day 28 was obtained (Table S2). Similarly, the same inclusion criteria were used for feature selection between day 0 and day 42 (Figure S7C for PLS-DA and Figure S7D for volcano-plot analysis). A group of 11 candidate features was obtained (Table S3). Combining the features between day 0 and day 28, as well as between day 0 and day 42, a panel of 13 vaccine features were determined. Cluster analysis of the 13 feature peaks among all the samples is visualized as a heat map (Figure 4B). It was observed that most of the 13 feature peaks were downregulated after vaccine injection. The downregulated peaks include m/z 3025, m/z 13,761, m/z 13,882, m/z 13,939, m/z 14,044, m/z 14,092, m/z 14,150, m/z 15,124, m/z 15,868 and m/z 28,195. Only three peaks were upregulated, including m/z 3198, m/z 3213 and m/z 6609. The relative intensities of the 13 feature peaks before vaccination and during the 6-week recovery phase after vaccination are shown in Figure S8. Proteomic analysis was performed to identify the 13 MALDI-TOF MS feature peaks of vaccination. The features were identified as component C1q receptor (m/z 6609), CD59 glycoprotein (m/z 14,150), mannose-binding protein C (MBL) (m/z 14,092), platelet basic protein (m/z 13,882), CD99 antigen (m/z 3025), Leucine-rich alpha-2-glycoprotein (LRG1) (m/z 28,195), and hemoglobin (Hb) subunits (m/z 14,044, m/z 15,124 and m/z 15,868) (Table S4). The identified proteins showed significant down-regulation after vaccination, except component C1q receptor. Gene ontology (GO) enrichment analysis revealed that these identified proteins have a close relationship with the pathways of oxygen transport, neutrophil degranulation, complement system, and hemostasis (Figure 4C).

Correlation between serum peptidome profile and NAbs generation by vaccination

Serum samples from day 42 with the NAbs positive rate of 73% were selected to study the correlation between MALDI-TOF serum peptidome profile and NAbs generation. All the samples were divided into two cohorts, NAbs positive and NAbs negative on day 42. As shown in Figure 5A, PLS-DA analysis of the MALDI-TOF mass spectra cannot well differentiate the two cohorts. Then, gender-specific PLS-DA analyses were conducted. When the 55 female samples were analyzed, the classification performance was significantly enhanced, as shown in Figure 5B. The overlap of the 95% confidence interval of the NAbs positive and NAbs negative included only 6 positive and 2 negative samples. When the 40 male samples were analyzed, the overlap of the 95% confidence interval of the NAbs positive and

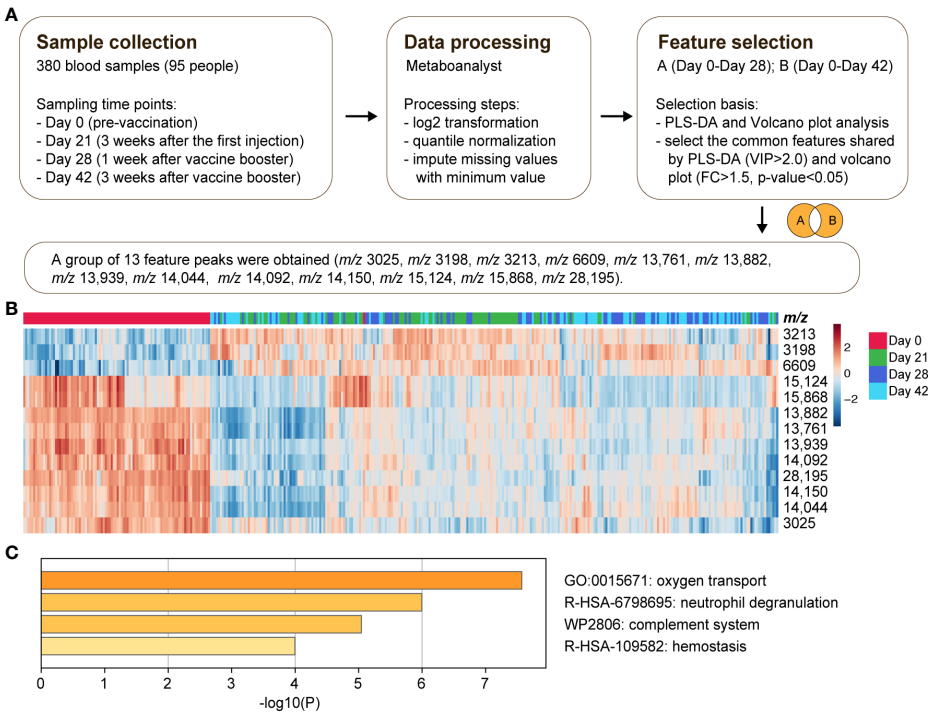

FIGURE 4
Selection of feature peaks of vaccination. **(A)** A general scheme of sample collection, data processing and feature selection. **(B)** Cluster analysis of the 13 feature peaks of vaccination among all the samples. **(C)** The Gene Ontology (GO) enrichment analysis by Metascape involving all the identified features.

NAbs negative included 7 positives and 6 negatives samples, as shown in Figure 5C. Better classification performance could be achieved with the gender-specific analyses, and the classification performance was better for female than male, indicating that gender can be a significant factor influencing the serum peptidome related to NAbs generation.

The samples collected on day 42 from female participants were then selected to explore the feasibility of building a classification model to identify NAbs generation based on MALDI-TOF serum peptidome. Figure 5D summarized the steps of feature selection and model establishment. All the 55 samples from female participants were divided into a training set (41 samples, 10 negative and 31 positive) and a test set (14 samples, 4 negative and 10 positive). Six significant feature peaks were obtained from the training set, including m/z 3496, m/z 6609, m/z 6980, m/z 9928, m/z 13,939 and m/z 14,083 (Figure S9; Table S5). As the heatmap represented, 4 features (m/z 6609, m/z 6980, m/z 13939 and m/z 14,083) were more abundant in the females with NAbs negative, and 2 features (m/z 3496 and m/z 9928) were more abundant in the females with NAbs positive (Figure 5E). With the 6 features, we tried to build a classification model to distinguish females with and without NAbs production. Verification was carried out on the 14 unlabeled test samples (Table S6). Four machine learning methods consisting of random forest (RF), PLS-DA, linear support vector machine (SVM) and logistic regression (LR) were employed to build the models, and compared in the aspects of accuracy, sensitivity, specificity and precision. The results showed that all algorithms had a high precision of over 70% but a relatively low specificity of 50% (Figure 5F). The accuracy, precision and sensitivity of the RF-based model all outnumbered 70%, better than LR, linear SVM and PLS-DA-based models (Figure 5F). By proteomic analysis, four feature peaks were identified as proteins or protein fragments, including integral membrane protein 2B (m/z 6980), complement component C1q receptor (m/z 6609), platelet factor 4 (PF4) (m/z 9928) and MBL (m/z 14,083) (Table S7).

Discussion

In this study, we profiled the serum peptidome changes induced by CoronaVac vaccination by MALDI-TOF MS, and correlated the significant changes in serum peptidome with the immune protection effect. The significant figures related to vaccination were identified as proteins or protein fragments closely associated with the pathways of oxygen transport, neutrophil degranulation, complement system, and hemostasis.

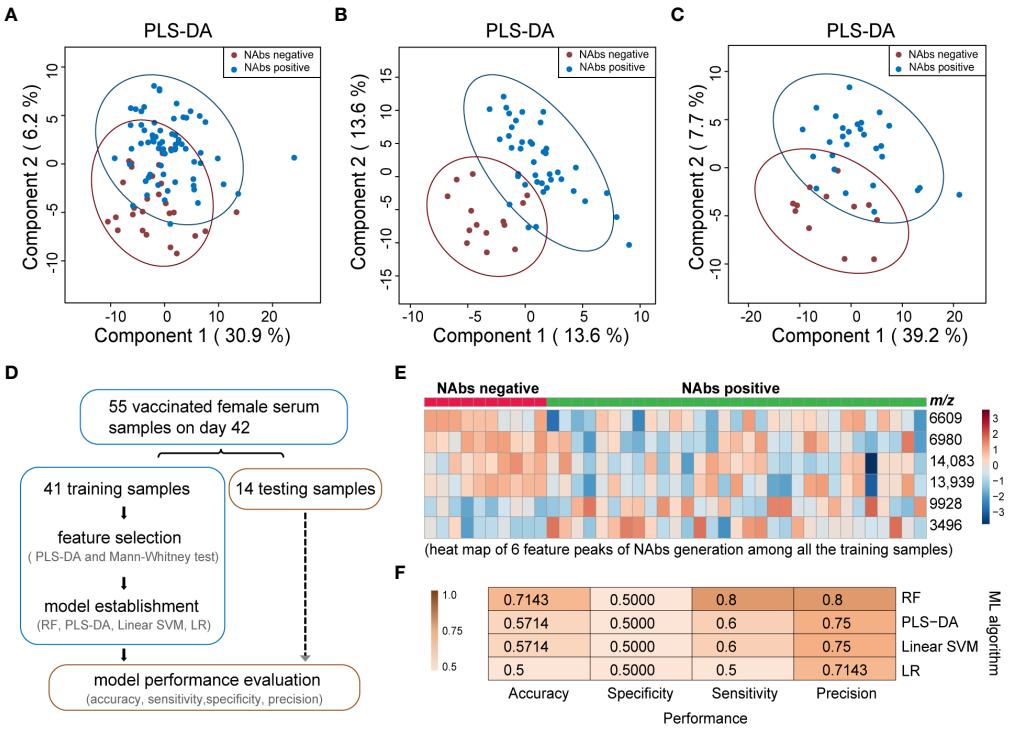

FIGURE 5
Classification of NAbs positive and negative based on MALDI-TOF MS serum peptidome. **(A)** PLS-DA analysis of all the 95 samples collected on day 42 to classify NAbs positive and negative; **(B)** PLS-DA analysis of 55 samples collected on day 42 from female individuals to classify NAbs positive and negative; **(C)** PLS-DA analysis of 40 samples collected on day 42 from male individuals to classify NAbs positive and negative; **(D)** a general scheme for feature selection and model establishment to classify NAbs positive and negative; **(E)** heat map of six feature peaks of NAbs generation among all the training samples; **(F)** performance of four classification models on the 14 test samples for NAbs generation prediction. N: negative, P: positive, RF: random forest, PLS-DA: partial least squares discriminant analysis, SVM: linear support vector machine, LR: logistic regression. The colored ovals represent 95% confidence interval.

We have also profiled the TAbs and NAbs generation, as well as serum cytokines and lymphocytes subpopulations. The regulation of serum cytokines and lymphocytes subpopulations also suggested neutrophil degranulation.

Modulation of CD3+CD8+ T cells detected in our study provides evidence of stimulated neutrophil under the influence of CoronaVac. Different evidence provided by proteomic, hematological and inflammatory analyses supported a significant increase of neutrophils in severe COVID-19 patients (31), and high level of neutrophils were found in the bronchoalveolar lavage of COVID-19 patients (32–34). A clinical study on COVID-19 hospitalized patients emphasized that the development and activation of neutrophil is a prominent signature of critically ill patients (35). IL-8 is a key chemokine recruiting neutrophils (36). It was reported that IL-8 can act as a marker of COVID-19 severity from non-hospitalized, non-ICU to ICU patients (35). A study confirmed the high IL-8 levels and increased number of neutrophils comparing COVID-19 patients with healthy controls (37). Yadav et el. reported that IL-8 and RBD IgG elevated in rhesus macaques with the administration of inactivated SARS-CoV-2 vaccine BBV152 (36). We also observed the significant upregulation of IL-8 in human serum after CoronaVac vaccination. Similar to COVID-19 infection, neutrophil degranulation was probably activated by the administration of CoronaVac.

Platelet basic protein, CD59 glycoprotein, LRG1 and complement component C1q receptor are proteins associated with neutrophil degranulation, and are significantly correlated with CoronaVac injection. Platelet basic protein is a platelet-derived growth factor belonging to the CXC chemokine family. It has been reported that the protein can down-regulate the function of neutrophil, and can desensitize platelet-derived neutrophil-activating peptide 2–induced neutrophil degranulation (38). In our study, we observed the significant downregulation of platelet basic protein, which can benefit the activation of neutrophil. CD 59 glycoprotein can protect host cells from lysis by complement system attack and is involved in lymphocyte signal transduction. A study of transcriptional profiling indicated that the complement gene of CD59 glycoprotein down-regulated in COVID-19 patients, compared

with negative controls (39). Here, we observed downregulation of CD59 glycoprotein after injection of the inactivated SARS-CoV-2 vaccine. LRG1 is a member of the leucine-rich repeat (LRR) family proteins. A proteomic study pointed out that LRG1 upregulated in severe COVID-19 patients as a function of IL-6 levels (40). This is opposite to the regulation direction in CoronaVac vaccinated people found in our study. Also, the changes of IL-6 in serum after vaccination were not significant in our study. Complement component C1q receptor, which is a critical protein belonging to the complement system, upregulated in human blood after receiving the inactivated virus vaccine. The protein can enhance antibody neutralization activity by binding to antibodies (41–43). It is released from its synthetic place in liver to bloodstream, and the process can be accelerated by virus infection (44). A clinical study focusing on the immunology of 71 confirmed COVID-19 cases found that complement component C1q dropped in severe COVID-19 patients significantly compared with mild-ill patients (31). The CoronaVac-induced regulation of complement C1q subcomponent was also detected by Jiang et al (19).

A recent study profiled the changes of the complement system signaling and associated inflammatory mediators between COVID-19 patients and healthy controls (37). The complement system is part of the immune system that enhances the clearance of antibodies and phagocytes, promotes inflammation, and attacks the cell membranes of pathogens. Complement system is a component of native plasma that plays key roles in human immunity, especially in innate immune response (42, 45), and can neutralize enveloped or non-enveloped viruses in case of virus infection (42). Following infection, macrophages are induced by the complement system anaphylatoxins to generate pro-inflammatory cytokines and chemokines. Our study showed that the complement system can be activated by CoronaVac vaccination. There are three complement system activation pathways, including the classical, the alternative and the MBL pathways (42, 46). The upregulation of complement component C1q receptor demonstrated the activation of the classical pathway of the complement system. We found that the level of MBL protein descended after CoronaVac vaccination. MBL is a pattern recognition molecule of the innate immune system. Jiang et al. detected the changes of mannan-binding lectin serine proteases induced by CoronaVac (19). The reduction of MBL serum level or MBL protein concentration has been observed in SARS patients compared to healthy people (45, 47). There were studies reporting that MBL can activate the complement system by binding to SARS-CoV and SARS-CoV-2 spike protein (45, 48, 49). Yu et al. pointed out that recombinant SARS-CoV-2 proteins can activate MBL and hence the MBL pathways for the complement system activation (50). Based on the previous reports, we speculate that inactivated coronavirus in the vaccine may retain the activity of binding MBL, and the complement system can also be activated by vaccination via the MBL pathway.

It is worth noting that the subunits of Hb alpha and Hb beta were significantly downregulated in the CoronaVac vaccinated people. Hb is mainly made up of alpha and beta subunits and iron-containing heme groups. The plummet of hemoglobin subunits prompted that Hb in blood descended after vaccination with the inactivated virus. Previous studies have shown that Hb decreased in COVID-19 infected patients, especially in severely ill patients (51). Wenping Zhang et al. proposed Hb as one of the diagnosis indicators to predict the severity of COVID-19 patients (52). The decline of hemoglobin concentration may correspond to an aggravated clinical condition of patients (51, 53, 54). In the early stage of COVID-19 outbreak, a hypothesis that COVID-19 virus may bind to hemoglobin, release iron ions from porphyrin and damage the oxygen binding ability of hemoglobin was proposed (55). The hypothesis attracted many researchers to focus on studying the interaction between Hb and coronavirus (38, 53, 56). However, no study can reveal the binding mechanism between Hb and coronavirus to date. The change of Hb after vaccination deserves more attention, and long-term surveillance of COVID-19 vaccine safety is necessary, especially on people with hemoglobin-related diseases.

Our study also revealed the downregulation of CD99 antigen. CD99 is involved in T-cell adhesion processes. In 2021, Siwy et al. demonstrated highly significant reduction of CD99 in severe/critical COVID-19, indicating the reduction of endothelial integrity and interference with transendothelial migration of monocytes, neutrophils, and T-cell recruitment (57). The reduction of CD99 in inactivated virus vaccinated people should be further studied.

This study profiled serum cytokines and lymphocyte subpopulation between day 0 and day 28, i.e., before vaccination and one week after complete vaccination. Significant variation of a number of cytokines and lymphocyte subpopulations was observed, suggesting a potential role of helper/inducer T lymphocytes and suppressor/cytotoxic T lymphocytes during the CoronaVac-induced immunization. The regulation was more significant in the relatively young participants (< 50 years) than the middle-aged participants (50-59 years). Since the cytokines were measured from serum without the knowledge of production cells and were only measured on two days, further information on the role of the cytokines in CoronaVac vaccination cannot be obtained in this study. Zhao et al. (18) and Jiang et al. (19) have studied the regulation of cytokines and lymphocytes induced by CoronaVac in a comprehensive way in their respective studies. Jiang et al. characterized the lymphocyte subpopulations before and after vaccination, and found that after the second vaccination, CD8+ cytotoxic T cell levels decreased and the serum NAbs titers increased (19), in consistent with our results, which can suggest a

balance between cellular and humoral immune responses dominating at early and late stages of vaccination, respectively.

The analysis of antibody among different age groups revealed that the middle-aged people, especially for people older than 50, displayed the lowest positive rate of NAbs after completion of the CoronaVac vaccination. Indeed, the World Health Organization's Emergency Use Listing (EUL) authorized the use of CoronaVac in June 2021 with the finding that there is a gap in evidence of the CoronaVac effectiveness for adults over 60 years. An early to mid-stage trial conducted by Sinovac suggested that the immune response of elderly subjects was slightly lower than that of young people. A case-control study observed that the vaccine efficiency descended with increasing age among the elderly people (≥70 years) in Brazil(2021). Recently, a significant reduction in T-cell and antibody responses to inactivated coronavirus vaccination has been reported in people aged 55 years or older (58). With much attention that has been paid to the immune response of elderly people (≥60 years) after vaccination, the protection effectiveness of CoronaVac against SARS-CoV-2 in middle-aged people (50-59 years) deserves more attention.

We tried to distinguish NAbs generation based on serum peptides mass fingerprinting. However, the differentiation performance was not efficient for all samples. Interestingly, gender specific models performed better for the differentiation of NAbs positive and negative individuals, especially on samples from female, demonstrating that gender is a significant factor influencing the serum peptidome correlation to NAbs generation. Comorbidities, such as obesity, have been reported to lower immune response (57). There were only 2 participants with body mass index (BMI) > 30 kg/m2 out of the 95 subjects in our study (Table S1). Therefore, obesity factors were not analyzed in association with vaccine immune response.

According to the results of feature annotation by proteomic analysis, NAbs generation is associated with integral membrane protein 2B, complement component C1q receptor, platelet factor 4 (PF4) and MBL. The correlation between complement component C1q and MBL with the immunogenicity via the activation of the complement system has been discussed above. For integral membrane protein 2B, a recent serological study demonstrated that the antibodies produced by COVID-19 patients showed an unexpected immune response against integral membrane proteins, which can be used to detect SARS-CoV-2 variants or test vaccine effectiveness (59). We found that integral membrane protein 2B was less abundant in the NAbs positive individuals. There have been studies confirming the relationship between NAbs generation induced by COVID-19 vaccination and PF4, and we observed more abundant PF4 in the NAbs positive individuals. Platelets are primarily associated with thrombosis (60). Thrombo-inflammation can be induced by platelet activation, and PF4 levels upregulate significantly in COVID-19 patients and especially critically ill patients (52, 60–63). Positive PF4 can also be induced by adenoviral vector COVID-19 vaccine or RNA COVID-19 vaccine with low clinical relevance. Vaccine-induced immune thrombotic thrombocytopenia (VITT) seldomly occurs after vaccination (64). However, a recent study reported the formation of antigenic complexes between vaccine components and PF4 on the platelet surface driven by electric charge after receiving ChAdOx1 nCoV-19 (AstraZeneca) vaccine, which eventually lead to VITT (65). Whether there is the generation of these similar complexes after receiving CoronaVac vaccine remains to be studied.

There are also limitations of the current study. We performed an observational study to characterize the changes of human serum peptidome after receiving deactivated virus COVID-19 vaccine. The recruited participants were mainly young and middle-aged adults. Only limited information on cytokines and lymphocytes was obtained. We detected the generation of NAbs by immunoassay to assess the immune protection ability induced by CoronaVac. Live virus assays, such as PRNT, is the gold standard to evaluate immune protection, but are restricted by biosafety. False positive antibody test results could be obtained by the immunoassay-based methods due to the insufficient specificity of assay kits. On the other hand, false negative results may also be obtained due to improper specimen handling which can lead to low concentration of antibodies extracted. Nevertheless, in most cases, the measurement of NAbs is still considered as an effective mean of immune protection assessment. The performance of the established model for NAbs generation prediction based on serum peptidome is still unsatisfactory, and the analysis of patient demographic characteristics is not sufficiently in-depth. In the future, it is important to carry out validation work on the NAbs generation assessment methods with large sample sizes and multicenter clinical trials. Long-term serum sampling after COVID-19 vaccination should also be performed to enable an in-depth mapping of the serum peptidome dynamic response to COVID-19 vaccination.

In summary, the method developed in this work can monitor the serum peptidome changes induced by CoronaVac injection and can identify features associated with vaccination and NAbs generation. Similar study can also be applied to other COVID-19 vaccines or vaccines for other infectious diseases. With the method, immune responses induced by vaccination can be conveniently monitored. It is also possible to assess vaccine safety by the method. Pre-marketing studies cannot fully guarantee the safety of a vaccine, and follow-up studies should be conducted to re-evaluate the efficacy and safety of vaccines after the product being licensed. The new method developed in our study has the advantage of high throughput,

low cost and easy-operation, thereby is especially suitable for large-scale post-marketing monitoring of the efficacy and safety of developed vaccines

Data availability statement

The mass spectrometry proteomics data have been deposited to the ProteomeXchange Consortium (http://proteomecentral.proteomexchange.org) via the iProX partner repository (66) with the dataset identifier PXD036159.

Ethics statement

The studies involving human participants were reviewed and approved by Ethical Committee of Chongqing General Hospital. Written informed consent for participation was not required for this study in accordance with the national legislation and the institutional requirements.

Author contributions

WZ performed the vaccination and collected the sample. DL analyzed the data and wrote the draft of the manuscript. BX collected the mass spectrometry data. LX assisted in the sample collection. QL assisted in the mass spectrometry analysis. XL assisted in the data analysis. ZL assisted in the sample collection. JZ assisted in the data analysis. WS was involved in the study design. QM designed the study and supervised the mass spectrometry analysis. LQ designed the study, supervised the data analysis, and finalized the manuscript. PL designed the study and supervised the clinical model establishment. All authors contributed to the article and approved the submitted version.

Funding

This work was supported by the Ministry of Science and Technology of China (MOST, 2020YFF0426500), the Chongqing Department of Science and Technology: 2021 Chongqing Talent Program (2021-07-12-230) and the National Natural Science Foundation of China (NSFC, 22022401, 22074022, 21934001).

Conflict of interest

Authors BX, QL and QM were employed by Bioyong Technologics, Inc.

The remaining authors declare that the research was conducted in the absence of any commercial or financial relationships that could be construed as a potential conflict of interest.

Publisher's note

Supplementary material

The Supplementary Material for this article can be found online at: https://www.frontiersin.org/articles/10.3389/fimmu.2022.956369/full#supplementary-material

References

1. Jara A, Undurraga EA, González C, Paredes F, Fontecilla T, Jara G, et al. Effectiveness of an inactivated SARS-CoV-2 vaccine in Chile. *N Engl J Med* (2021) 385(10):875–84. doi: 10.1056/NEJMoa2107715

2. Ritchie H, Mathieu E, Rodés-Guirao L, Appel C, Giattino C, Ortiz-Ospina E, et al. "*Coronavirus Pandemic (COVID-19)*". (2020) Published online at OurWorldInData.org. Retrieved from: https://ourworldindata.org/coronavirus [Online Resource]

3. Lurie N, Saville M, Hatchett R, Halton J. Developing covid-19 vaccines at pandemic speed. *N Engl J Med* (2020) 382(21):1969–73. doi: 10.1056/NEJMp2005630

4. Ella R, Vadrevu KM, Jogdand H, Prasad S, Reddy S, Sarangi V, et al. Safety and immunogenicity of an inactivated SARS-CoV-2 vaccine, BBV152: a double-blind, randomised, phase 1 trial. *Lancet Infect Dis* (2021) 21(5):637–46. doi: 10.1016/S1473-3099(20)30942-7

5. Sadoff J, Gray G, Vandebosch A, Cárdenas V, Shukarev G, Grinsztejn B, et al. Safety and efficacy of single-dose Ad26.COV2.S vaccine against covid-19. *N Engl J Med* (2021) 384(23):2187–201. doi: 10.1056/NEJMoa2101544

6. Hodgson SH, Mansatta K, Mallett G, Harris V, Emary KRW, Pollard AJ. What defines an efficacious COVID-19 vaccine? a review of the challenges assessing the clinical efficacy of vaccines against SARS-CoV-2. *Lancet Infect Dis* (2021) 21(2):e26–35. doi: 10.1016/S1473-3099(20)30773-8

7. Hussain A, Rafeeq H, Asif HM, Shabbir S, Bilal M, Mulla SI, et al. Current scenario of COVID-19 vaccinations and immune response along with antibody titer in vaccinated inhabitants of different countries. *Int Immunopharmacol.* (2021) 99:108050. doi: 10.1016/j.intimp.2021.108050

8. Lu YY, Wang J, Li QL, Hu H, Lu JH, Chen ZL. Advances in neutralization assays for SARS-CoV-2. *Scand J Immunol* (2021) 94(3):e13088. doi: 10.1111/sji.13088

9. Sadarangani M, Marchant A, Kollmann TR. Immunological mechanisms of vaccine-induced protection against COVID-19 in humans. *Nat Rev Immunol* (2021) 21(8):475–84. doi: 10.1038/s41577-021-00578-z

10. Yu S, Chen K, Fang L, Mao H, Lou X, Li C, et al. Comparison and analysis of neutralizing antibody levels in serum after inoculating with SARS-CoV-2, MERS-CoV, or SARS-CoV vaccines in humans. *Vaccines* (2021) 9(6):588. doi: 10.3390/vaccines9060588

11. Perera RA, Mok CK, Tsang OT, Lv H, Ko RL, Wu NC, et al. Serological assays for severe acute respiratory syndrome coronavirus 2 (SARS-CoV-2), march 2020. *Euro Surveill.* (2020) 25(16): pii=2000421. doi: 10.2807/1560-7917.ES.2020.25.16.2000421

12. Nie JH, Li QQ, Wu JJ, Zhao CY, Hao H, Liu H, et al. Establishment and validation of a pseudovirus neutralization assay for SARS-CoV-2. *Emerg Microbes Infect* (2020) 9(1):680–6. doi: 10.1080/22221751.2020.1743767

13. Muruato AE, Fontes-Garfias CR, Ren P, Garcia-Blanco MA, Menachery VD, Xie X, et al. A high-throughput neutralizing antibody assay for COVID-19 diagnosis and vaccine evaluation. *Nat Commun* (2020) 11(1):4059. doi: 10.1038/s41467-020-17892-0

14. Folegatti PM, Bittaye M, Flaxman A, Lopez FR, Bellamy D, Kupke A, et al. Safety and immunogenicity of a candidate middle East respiratory syndrome coronavirus viral-vectored vaccine: a dose-escalation, open-label, non-randomised, uncontrolled, phase 1 trial. *Lancet Infect Dis* (2020) 20(7):816–26. doi: 10.1016/S1473-3099(20)30160-2

15. Sahin U, Muik A, Derhovanessian E, Vogler I, Kranz LM, Vormehr M, et al. COVID-19 vaccine BNT162b1 elicits human antibody and T1 T cell responses. *Nature* (2020) 586(7830):594–9. doi: 10.1038/s41586-020-2814-7

16. Prendecki M, Clarke C, Brown J, Cox A, Gleeson S, Guckian M, et al. Effect of previous SARS-CoV-2 infection on humoral and T-cell responses to single-dose BNT162b2 vaccine. *Lancet* (2021) 397(10280):1178–81. doi: 10.1016/S0140-6736(21)00502-X

17. Deng Y, Li Y, Yang R, Tan W. SARS-CoV-2-specific T cell immunity to structural proteins in inactivated COVID-19 vaccine recipients. *Cell Mol Immunol* (2021) 18(8):2040–1. doi: 10.1038/s41423-021-00730-8

18. Zhao W, Chen W, Li J, Chen M, Li Q, Lv M, et al. Status of humoral and cellular immune responses within 12 months following CoronaVac vaccination against COVID-19. *Mbio* (2022) 13(3):e0018122. doi: 10.1128/mbio.00181-22

19. Jiang Z, Lin H, Zhang H, Shi N, Zheng Z, Dong L, et al. An integrative analysis of the immune features of inactivated SARS-CoV-2 vaccine (CoronaVac). *Vaccines* (2022) 10(6):878. doi: 10.3390/vaccines10060878

20. Long S, Qin Q, Wang Y, Yang Y, Wang Y, Deng A, et al. Nanoporous silica coupled MALDI-TOF MS detection of bence-Jones proteins in human urine for diagnosis of multiple myeloma. *Talanta* (2019) 200:288–92. doi: 10.1016/j.talanta.2019.03.067

21. Park H-G, Jang K-S, Park H-M, Song W-S, Jeong Y-Y, Ahn D-H, et al. MALDI-TOF MS-based total serum protein fingerprinting for liver cancer diagnosis. *Analyst* (2019) 144(7):2231–8. doi: 10.1039/c8an02241k

22. Sun J, Yu G, Yang Y, Qiao L, Xu B, Ding C, et al. Evaluation of prostate cancer based on MALDI-TOF MS fingerprinting of nanoparticle-treated serum proteins/peptides. *Talanta* (2020) 220:121331. doi: 10.1016/j.talanta.2020.121331

23. Liu C, Zhao Z, Fan J, Lyon CJ, Wu H-J, Nedelkov D, et al. Quantification of circulating antigen peptides allows rapid diagnosis of active disease and treatment monitoring. *Proc Natl Acad Sci USA* (2017) 114(15):3969–74. doi: 10.1073/pnas.1621360114

24. Lazari LC, Ghilardi FDR, Rosa-Fernandes L, Assis DM, Nicolau JC, Santiago VF, et al. Prognostic accuracy of MALDI-TOF mass spectrometric analysis of plasma in COVID-19. *Life Sci Alliance* (2021) 4(8):e202000946. doi: 10.26508/lsa.202000946

25. Yan L, Yi J, Huang C, Zhang J, Fu S, Li Z, et al. Rapid detection of COVID-19 using MALDI-TOF-Based serum peptidome profiling. *Anal Chem* (2021) 93(11):4782–7. doi: 10.1021/acs.analchem.0c04590

26. Rocca MF, Zintgraff JC, Dattero ME, Santos LS, Ledesma M, Vay C, et al. A combined approach of MALDI-TOF mass spectrometry and multivariate analysis as a potential tool for the detection of SARS-CoV-2 virus in nasopharyngeal swabs. *J Virol Methods* (2020) 286:113991. doi: 10.1016/j.jviromet.2020.113991

27. Shen B, Yi X, Sun Y, Bi X, Du J, Zhang C, et al. Proteomic and metabolomic characterization of COVID-19 patient sera. *Cell* (2020) 182(1):59–72.e15. doi: 10.1016/j.cell.2020.05.032

28. Gibb S, Strimmer K. MALDIquant: a versatile r package for the analysis of mass spectrometry data. *Bioinformatics* (2012) 28(17):2270–1. doi: 10.1093/bioinformatics/bts447

29. Chong J, Wishart DS, Xia J. Using MetaboAnalyst 4.0 for comprehensive and integrative metabolomics data analysis. *Curr Protoc Bioinf* (2019) 68(1):e86. doi: 10.1002/cpbi.86

30. Zhou Y, Zhou B, Pache L, Chang M, Khodabakhshi AH, Tanaseichuk O, et al. Metascape provides a biologist-oriented resource for the analysis of systems-level datasets. *Nat Commun* (2019) 10(1):1523. doi: 10.1038/s41467-019-09234-6

31. Wu Y, Huang X, Sun J, Xie T, Lei Y, Muhammad J, et al. Clinical characteristics and immune injury mechanisms in 71 patients with COVID-19. *mSphere* (2020) 5(4):e00362–00320. doi: 10.1128/mSphere.00362-20

32. Liao M, Liu Y, Yuan J, Wen Y, Xu G, Zhao J, et al. Single-cell landscape of bronchoalveolar immune cells in patients with COVID-19. *Nat Med* (2020) 26(6):842–4. doi: 10.1038/s41591-020-0901-9

33. Wilk AJ, Rustagi A, Zhao NQ, Roque J, Martínez-Colón GJ, McKechnie JL, et al. A single-cell atlas of the peripheral immune response in patients with severe COVID-19. *Nat Med* (2020) 26(7):1070–6. doi: 10.1038/s41591-020-0944-y

34. Zhou Z, Ren L, Zhang L, Zhong J, Xiao Y, Jia Z, et al. Heightened innate immune responses in the respiratory tract of COVID-19 patients. *Cell Host Microbe* (2020) 27(6):883–890.e2. doi: 10.1016/j.chom.2020.04.017

35. Meizlish ML, Pine AB, Bishai JD, Goshua G, Nadelmann ER, Simonov M, et al. A neutrophil activation signature predicts critical illness and mortality in COVID-19. *Blood Adv* (2021) 5(5):1164–77. doi: 10.1182/bloodadvances.2020003568

36. Yadav PD, Ella R, Kumar S, Patil DR, Mohandas S, Shete AM, et al. Immunogenicity and protective efficacy of inactivated SARS-CoV-2 vaccine candidate, BBV152 in rhesus macaques. *Nat Commun* (2021) 12(1):1386. doi: 10.1038/s41467-021-21639-w

37. Alosaimi B, Mubarak A, Hamed ME, Almutairi AZ, Alrashed AA, AlJuryyan A, et al. Complement anaphylatoxins and inflammatory cytokines as prognostic markers for COVID-19 severity and in-hospital mortality. *Front Immunol* (2021) 12:668725. doi: 10.3389/fimmu.2021.668725

38. Aschenbrenner AC, Mouktaroudi M, Kramer B, Oestreich M, Antonakos N, Nuesch-Germano M, et al. Disease severity-specific neutrophil signatures in blood transcriptomes stratify COVID-19 patients. *Genome Med* (2021) 13(1):7. doi: 10.1186/s13073-020-00823-5

39. Ramlall V, Thangaraj PM, Meydan C, Foox J, Butler D, Kim J, et al. Immune complement and coagulation dysfunction in adverse outcomes of SARS-CoV-2 infection. *Nat Med* (2020) 26(10):1609–15. doi: 10.1038/s41591-020-1021-2

40. D'Alessandro A, Thomas T, Dzieciatkowska M, Hill RC, Francis RO, Hudson KE, et al. Serum proteomics in COVID-19 patients: Altered coagulation and complement status as a function of IL-6 level. *J Proteome Res* (2020) 19(11):4417–27. doi: 10.1021/acs.jproteome.0c00365

41. Mehlhop E, Nelson S, Jost CA, Gorlatov S, Johnson S, Fremont DH, et al. Complement protein C1q reduces the stoichiometric threshold for antibody-mediated neutralization of West Nile virus. *Cell Host Microbe* (2009) 6(4):381–91. doi: 10.1016/j.chom.2009.09.003

42. Mellors J, Tipton T, Longet S, Carroll M. Viral evasion of the complement system and its importance for vaccines and therapeutics. *Front Immunol* (2020) 11:1450. doi: 10.3389/fimmu.2020.01450

43. Kurtovic L, Beeson JG. Complement factors in COVID-19 therapeutics and vaccines. *Trends Immunol* (2021) 42(2):94–103. doi: 10.1016/j.it.2020.12.002

44. Zimmer J, Hobkirk J, Mohamed F, Browning MJ, Stover CM. On the functional overlap between complement and anti-microbial peptides. *Front Immunol* (2014) 5:689. doi: 10.3389/fimmu.2014.00689

45. Ip WKE, Chan KH, Law HKW, Tso GHW, Kong EKP, Wong WHS, et al. Mannose-binding lectin in severe acute respiratory syndrome coronavirus infection. *J Infect Dis* (2005) 191(10):1697–704. doi: 10.1086/429631

46. Curran CS, Rivera DR, Kopp JB. COVID-19 usurps host regulatory networks. *Front Pharmacol* (2020) 11:1278. doi: 10.3389/fphar.2020.01278

47. Zhang H, Zhou G, Zhi L, Yang H, Zhai Y, Dong X, et al. Association between mannose-binding lectin gene polymorphisms and susceptibility to severe acute respiratory syndrome coronavirus infection. *J Infect Dis* (2005) 192(8):1355–61. doi: 10.1086/491479

48. Hendaus MA, Jomha FA. From COVID-19 to clot: the involvement of the complement system. *J Biomol Struct Dyn.* (2020) 40(4):1909–14. doi: 10.1080/07391102.2020.1832919

49. Walls AC, Park Y-J, Tortorici MA, Wall A, McGuire AT, Veesler D. Structure, function, and antigenicity of the SARS-CoV-2 spike glycoprotein. *Cell* (2020) 181(2):281–292.e286. doi: 10.1016/j.cell.2020.02.058

50. Yu J, Yuan X, Chen H, Chaturvedi S, Braunstein EM, Brodsky RA. Direct activation of the alternative complement pathway by SARS-CoV-2 spike proteins is blocked by factor d inhibition. *Blood* (2020) 136(18):2080–9. doi: 10.1182/blood.2020008248

51. Chen N, Zhou M, Dong X, Qu J, Gong F, Han Y, et al. Epidemiological and clinical characteristics of 99 cases of 2019 novel coronavirus pneumonia in wuhan, China: a descriptive study. *Lancet* (2020) 395(10223):507–13. doi: 10.1016/S0140-6736(20)30211-7

52. Zhang S, Liu Y, Wang X, Yang L, Li H, Wang Y, et al. SARS-CoV-2 binds platelet ACE2 to enhance thrombosis in COVID-19. *J Hematol Oncol* (2020) 13(1):120. doi: 10.1186/s13045-020-00954-7

53. Chowdhury SF, Anwar S. Management of hemoglobin disorders during the COVID-19 pandemic. *Front Med* (2020) 7:306. doi: 10.3389/fmed.2020.00306

54. Zhang W, Zhang Z, Ye Y, Luo Y, Pan S, Qi H, et al. Lymphocyte percentage and hemoglobin as a joint parameter for the prediction of severe and nonsevere COVID-19: a preliminary study. *Ann Transl Med* (2020) 8(19):1231. doi: 10.21037/atm-20-6001

55. Wenzhong L, Hualan L. (2020). COVID-19:Attacks the 1-beta chain of hemoglobin and captures the porphyrin to inhibit human heme metabolism. *ChemRxiv* [Preprint]. Available at: https://chemrxiv.org (Accessed Mar 24, 2021).

56. Wagener F.A.D.T.G., Pickkers P, Peterson SJ, Immenschuh S, Abraham NG. Targeting the heme-heme oxygenase system to prevent severe complications following COVID-19 infections. *Antioxidants (Basel Switzerland)* (2020) 9 (6):540. doi: 10.3390/antiox9060540

57. Siwy J, Wendt R, Albalat A, He T, Mischak H, Mullen W, et al. CD99 and polymeric immunoglobulin receptor peptides deregulation in critical COVID-19: A potential link to molecular pathophysiology? *Proteomics* (2021) 21(20): e2100133. doi: 10.1002/pmic.202100133

58. Medeiros GX, Sasahara GL, Magawa JY, Nunes JPS, Bruno FR, Kuramoto AC, et al. Reduced T cell and antibody responses to inactivated coronavirus vaccine among individuals above 55 years old. *Front Immunol* (2022) 13:812126. doi: 10.3389/fimmu.2022.812126

59. Martin S, Heslan C, Jégou G, Eriksson LA, Le Gallo M, Thibault V, et al. SARS-CoV-2 integral membrane proteins shape the serological responses of COVID-19 patients. *iScience* (2021) 24(10):103185. doi: 10.1016/j.isci.2021.103185

60. Zaid Y, Puhm F, Allaeys I, Naya A, Oudghiri M, Khalki L, et al. Platelets can associate with SARS-Cov-2 RNA and are hyperactivated in COVID-19. *Circ Res* (2020) 127(11):1404–18. doi: 10.1161/CIRCRESAHA.120.317703

61. Comer SP, Cullivan S, Szklanna PB, Weiss L, Cullen S, Kelliher S, et al. COVID-19 induces a hyperactive phenotype in circulating platelets. *PloS Biol* (2021) 19(2):e3001109. doi: 10.1371/journal.pbio.3001109

62. Cox D. Targeting SARS-CoV-2-Platelet interactions in COVID-19 and vaccine-related thrombosis. *Front Pharmacol* (2021) 12:708665. doi: 10.3389/fphar.2021.708665

63. Yatim N, Boussier J, Chocron R, Hadjadj J, Philippe A, Gendron N, et al. Platelet activation in critically ill COVID-19 patients. *Ann Intensive Care* (2021) 11 (1):113. doi: 10.1186/s13613-021-00899-1

64. Temesgen Z, Assi M, Shweta FNU, Vergidis P, Rizza SA, Bauer PR, et al. GM-CSF neutralization with lenzilumab in severe COVID-19 pneumonia: A case-cohort study. *Mayo Clin Proc* (2020) 95(11):2382–94. doi: 10.1016/j.mayocp.2020.08.038

65. Greinacher A, Selleng K, Palankar R, Wesche J, Handtke S, Wolff M, et al. Insights in ChAdOx1 nCov-19 vaccine-induced immune thrombotic thrombocytopenia (VITT). *Blood* (2021) 138(22):2256–68. doi: 10.1182/blood.2021013231

66. Ma J, Chen T, Wu S, Yang C, Bai M, Shu K, et al. iProX: an integrated proteome resource. *Nucleic Acids Res* (2019) 47:D1211-D1217.

frontiers | Frontiers in Immunology

TYPE Original Research
PUBLISHED 25 August 2022
DOI 10.3389/fimmu.2022.958418

OPEN ACCESS

EDITED BY
Nicasio Mancini,
Vita-Salute San Raffaele University, Italy

REVIEWED BY
Wondwossen Amogne Degu,
Addis Ababa University, Ethiopia
Tatsuo Shimosawa,
International University of Health and Welfare (IUHW), Japan

*CORRESPONDENCE
Adriana Albini,
adriana.albini@ieo.it

SPECIALTY SECTION
This article was submitted to Vaccines and Molecular Therapeutics, a section of the journal Frontiers in Immunology

RECEIVED 31 May 2022
ACCEPTED 04 August 2022
PUBLISHED 25 August 2022

CITATION
Sonaglioni A, Lombardo M, Albini A, Noonan DM, Re M, Cassandro R, Elia D, Caminati A, Nicolosi GL and Harari S (2022) Charlson comorbidity index, neutrophil-to-lymphocyte ratio and undertreatment with renin-angiotensin-aldosterone system inhibitors predict in-hospital mortality of hospitalized COVID-19 patients during the omicron dominant period. *Front. Immunol.* 13:958418. doi: 10.3389/fimmu.2022.958418

Charlson comorbidity index, neutrophil-to-lymphocyte ratio and undertreatment with renin-angiotensin-aldosterone system inhibitors predict in-hospital mortality of hospitalized COVID-19 patients during the omicron dominant period

Andrea Sonaglioni[1], Michele Lombardo[1], Adriana Albini[2]*, Douglas M. Noonan[3,4], Margherita Re[5], Roberto Cassandro[6], Davide Elia[6], Antonella Caminati[6], Gian Luigi Nicolosi[7] and Sergio Harari[6,8]

[1]Division of Cardiology, Istituto di Ricovero e Cura a Carattere Scientifico (IRCCS) MultiMedica, Milan, Italy, [2]European Institute of Oncology (IEO) Istituto di Ricovero e Cura a Carattere Scientifico (IRCCS), Milan, Italy, [3]Immunology and General Pathology Laboratory, Department of Biotechnology and Life Sciences, University of Insubria, Varese, Italy, [4]Unit of Molecular Pathology, Immunology and Biochemistry, Istituto di Ricovero e Cura a Carattere Scientifico (IRCCS) MultiMedica, Milan, Italy, [5]Division of Internal Medicine, Istituto di Ricovero e Cura a Carattere Scientifico (IRCCS) MultiMedica, Milan, Italy, [6]Division of Pneumology, Semi Intensive Care Unit, Istituto di Ricovero e Cura a Carattere Scientifico (IRCCS) MultiMedica, Milan, Italy, [7]Division of Cardiology, Policlinico San Giorgio, Pordenone, Italy, [8]Department of Clinical Sciences and Community Health, Università Di Milano, Milan, Italy

Purpose: To investigate the clinical predictors of in-hospital mortality in hospitalized patients with Coronavirus disease 2019 (COVID-19) infection during the Omicron period.

Methods: All consecutive hospitalized laboratory-confirmed COVID-19 patients between January and May 2022 were retrospectively analyzed. All patients underwent accurate physical, laboratory, radiographic and echocardiographic examination. Primary endpoint was in-hospital mortality.

Results: 74 consecutive COVID-19 patients (80.0 ± 12.6 yrs, 45.9% males) were included. Patients who died during hospitalization (27%) and those who were discharged alive (73%) were separately analyzed. Compared to patients discharged alive, those who died were significantly older, with higher comorbidity burden and greater prevalence of laboratory, radiographic and echographic signs of pulmonary and systemic congestion. Charlson comorbidity index (CCI) (OR 1.76, 95%CI 1.07-2.92), neutrophil-to-lymphocyte ratio (NLR) (OR 1.24, 95%CI 1.10-1.39) and absence of angiotensin-converting enzyme inhibitors (ACEI)/

angiotensin II receptor blockers (ARBs) therapy (OR 0.01, 95%CI 0.00-0.22) independently predicted the primary endpoint. CCI ≥7 and NLR ≥9 were the best cut-off values for predicting mortality. The mortality risk for patients with CCI ≥7, NLR ≥9 and not in ACEI/ARBs therapy was high (86%); for patients with CCI <7, NLR ≥9, with (16.6%) or without (25%) ACEI/ARBs therapy was intermediate; for patients with CCI <7, NLR <9 and in ACEI/ARBs therapy was of 0%.

Conclusions: High comorbidity burden, high levels of NLR and the undertreatment with ACEI/ARBs were the main prognostic indicators of in-hospital mortality. The risk stratification of COVID-19 patients at hospital admission would help the clinicians to take care of the high-risk patients and reduce the mortality.

KEYWORDS

COVID-19, Charlson comobidity index, neutrophil-to-lymphocyte ratio, angiotensin-converting enzyme inhibitors/angiotensin II receptor blockers, mortality

Introduction

The novel B.1.1.529 severe acute respiratory syndrome coronavirus-2 (SARS-CoV-2) variant was first detected in South Africa and was named Omicron by WHO on Nov 26, 2021 (1).

This variant has many mutations in the spike gene, which may reduce the effectiveness of available vaccines and antibody therapeutics (2).

Due to the variant's increased transmissibility (3) and ability to evade immunity conferred by previous infection or vaccination (4), a rapid increase in SARS-CoV-2 infections was observed in all WHO regions (5), and at the beginning of 2022 Omicron accounted for more than 89% of sequenced samples globally (6).

With the pandemic still growing worldwide and with the limited healthcare capacity, early prediction of COVID-19 severity and mortality is crucial for improving management and treatment of infected patients (7).

Abbreviations: 2D, two-dimensional, ACEI, angiotensin-converting-enzyme inhibitors, ARBs, angiotensin receptor blockers, BMI, body mass index, BSA, body surface area, CAD, coronary artery disease, CCI, charlson comorbidity index, Cis, confidence intervals, CRP, C-reactive protein, CKD, chronic kidney disease, COPD, chronic obstructive pulmonary disease, COVID-19, Coronavirus disease 2019, CT, computed tomography, CXR, chest X-rays, ECG, electrocardiography, eGFR, estimated glomerular filtration rate, Hb, hemoglobin, HS, high-sensitivity, LVEF, left ventricular ejection fraction, NLR, neutrophil-to-lymphocyte ratio, NT-proBNP, N-terminal pro-B-type natriuretic peptide, ROC, receiver operating characteristic curve, RT-PCR, reverse-transcriptase polymerase chain reaction, SARS-CoV-2, severe acute respiratory syndrome coronavirus-2, SPAP, systolic pulmonary artery pressure, TIA, transient ischemic attack, TTE, transthoracic echocardiography, WBCs, white blood cells.

Population studies (8) suggest that the risk of severe outcomes following infection with Omicron might be lower than that observed for previous variants such as Delta, and this risk is attenuated further in those who have received a booster vaccination (9).

However, the total number of hospital admissions and deaths due to Omicron might still be substantial, depending on the role exerted by age and comorbidities in influencing disease severity.

As far as we know, data on outcomes following Omicron infection in older populations with high rates of comorbidity are scanty.

Given the large number of elderly patients with multiple comorbidities who were referred to the Pneumology Division of our Institution during the last few months, we hypothesized that clinical factors as the number of comorbidities, the inflammatory status and the current medical treatment could have contributed to different outcomes.

Accordingly, the present study was primarily designed to investigate the main independent predictors of in-hospital mortality in a retrospective cohort of COVID-19 patients admitted to the Pneumology Division during the Omicron dominant period.

Methods

Study population

All consecutive COVID-19 patients who were admitted to the Pneumology Division of the MultiMedica IRCCS (Milano, Italy) from January 1 to May 15, 2022 (the Omicron dominant period), entered this retrospective observational study.

The inclusion criteria were: 1) confirmed SARS-CoV-2 infection by reverse-transcriptase polymerase chain reaction (RT-PCR) assays on material collected by a nasopharyngeal and oropharyngeal swab; 2) patients who were hospitalized; 3) patients who underwent chest X-rays (CXR) on the day of hospital admission.

Patients with negative results for SARS-CoV-2 infection by RT-PCR, patients who died on admission, patients without baseline data or transferred to other designated hospitals during hospitalization were excluded from the analysis.

Following patients' characteristics were collected from the medical records: age; gender; body surface area (BSA); body mass index (BMI); information about COVID-19 vaccination (subjects vaccinated with 3 doses, with 2 doses, with 1 dose or unvaccinated, respectively); relevant cardiovascular risk factors (hypertension, type 2 diabetes mellitus, smoking, dyslipidemia); electrocardiographic (ECG) data (cardiac rhythm and heart rate); main comorbidities, such as chronic obstructive pulmonary disease (COPD), history of coronary artery disease (CAD), previous stroke/transient ischemic attack (TIA), peripheral vascular disease, chronic kidney disease (CKD), cancer, chronic cognitive deficit; blood tests comprehensive of complete blood count for determining hemoglobin concentration, white blood cells (WBCs) count and neutrophil-to-lymphocyte ratio (NLR), serum levels of creatinine and estimated glomerular filtration rate (eGFR) (10), serum levels of C-reactive protein (CRP), procalcitonin, D-dimer, high-sensitivity (HS) troponine I and N-terminal pro-B-type natriuretic peptide (NT-proBNP); the medical treatment at hospital admission and the COVID-19 in-hospital treatment; finally, the length of hospitalization or days until hospital death.

All hospitalized COVID-19 patients included in the present study underwent accurate anamnesis, objective examination, CXR and/or CT scan, ECG and conventional two-dimensional (2D) transthoracic echocardiography (TTE). COVID-19 patients who died during the hospitalization and those who were discharged alive were separately analyzed. The study design flowchart is depicted in Figure 1.

All procedures were performed according to the ethical standards of the institutional research committee and to the Declaration of Helsinki (1964) and its subsequent amendments or equivalent ethical standards. The study protocol was authorized by the local Ethics Committee (Committee's reference number 436.2020) and the need for informed consent was not required due to the retrospective nature of the study.

Comorbidity assessment

To assess the comorbidity burden, the Charlson comorbidity index (CCI) was retrospectively calculated for each COVID-19 patient. The CCI assigned 1 point for each of the following comorbidities: previous or actual myocardial infarction, history of congestive heart failure, peripheral vascular disease, dementia, cerebrovascular disease, chronic lung disease, connective tissue disease, ulcer, chronic liver disease, diabetes; 2 points for each of hemiplegia, moderate or severe kidney disease, diabetes with end-organ damage, tumor, leukemia, lymphoma; 3 points for moderate or severe liver disease; and 6 points for tumor metastasis or AIDS (11).

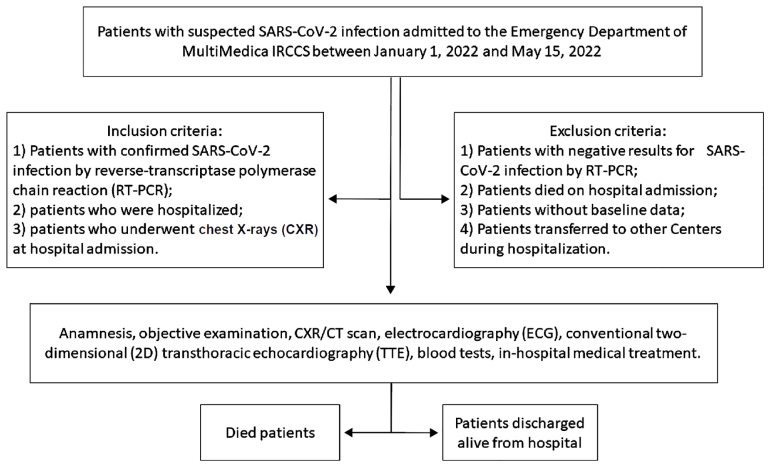

FIGURE 1
The study design flowchart. 2D, two-dimensional; CXR, chest X-rays; CT, computed tomography; ECG, electrocardiography; RT-PCR, reverse-transcriptase polymerase chain reaction; TTE, transthoracic echocardiography.

Radiographic examinations

Radiology data were collected from the Radiology department of our Institution. All COVID-19 patients underwent CXR at hospital admission, and were evaluated for the presence of unilateral or bilateral pneumonia, pulmonary hilar congestion, unilateral or bilateral pleural effusion, or for the absence of pulmonary alterations (negative examination). Computed tomography (CT) pulmonary angiography was performed only in patients with clinical or laboratory suspicion of pulmonary embolism complicating COVID-19 pneumonia. In selected cases, high resolution computed tomography (HRCT) was also performed.

Conventional transthoracic echocardiography and lung ultrasound

Echocardiograhic examinations were performed by two sonographers and by an expert cardiologist (AS) by using Philips Sparq ultrasound machine (Philips, Andover, Massachusetts, USA) with a 2.5 MHz transducer.

Following 2D echocardiographic parameters were retrospectively recorded: left ventricular ejection fraction (LVEF) estimated with the biplane modified Simpson's method (12); average E/e' ratio, as index of left ventricular diastolic function (13); systolic pulmonary artery pressure (SPAP), derived by the modified Bernoulli equation, where SPAP = 4 x (tricuspid regurgitation velocity)^2 + right atrial pressure (14). The latter was estimated from inferior vena cava diameter and collapsibility.

Finally, the presence of multiple B-lines, which are the sonographic sign of lung interstitial syndrome (15), was researched from the anterior, lateral and posterior chest, by using Philips Sparq ultrasound machine (Philips, Andover, Massachusetts, USA) with a 12-4 MHz linear transducer. A number of three or more B lines in any given region was considered a pathological finding.

Primary endpoint

The present study was primarily designed to identify the independent predictors of "in-hospital mortality" in a retrospective cohort of COVID-19 patients.

Details concerning the causes of death of COVID-19 patients were determined by accessing medical records available in the hospital archive and/or from telephone interviews.

Statistical analysis

To calculate the sample size of COVID-19 patients included in the present study, we hypothesized that COVID-19 patients with higher comorbidity burden (as expressed by CCI) might have a significantly increased risk of "in-hospital mortality" than those with lower comorbidity burden. Statistical power analysis revealed that a sample size of 20 COVID-19 patients who died in hospital and 54 COVID-19 patients discharged alive from hospital reached 80% of statistical power to detect a 3 points difference in the CCI between the two groups of patients with a standard deviation (SD) of 3.0 for each parameter, using a two-sided equal-variance t-test with a level of significance (alpha) of 5%.

For the whole cohort of COVID-19 patients and for the two groups of dead and alive patients, continuous data were summarized as mean ± SD, while categorical data were presented as number (%).

The correlation between CCI and NLR in the whole study population was assessed by Spearman Correlation Coefficient.

Univariate logistic regression analysis was performed to evaluate the effect of the main demographic, clinical, biochemical, and instrumental variables, on the occurrence of the primary endpoint, in our cohort of COVID-19 patients. For each variable investigated, correspondent odds ratios with 95% confidence intervals (CIs) were calculated. Only the variables with statistically significant association on univariate analysis (p value <0.05) were thereafter included in the multivariate logistic regression model.

The receiver operating characteristics (ROC) curve analysis was performed to establish the sensitivity and the specificity of the continuous variables that resulted independently associated with the above-mentioned endpoint. Area under curve (AUC) was estimated. The optimal cutoff of these predictors was calculated using the maximum value of the Youden Index (determined as sensitivity + [1-specificity]).

Statistical analysis was performed with SPSS version 26 (SPSS Inc., Chicago, Illinois, USA), with two-tailed p values below 0.05 deemed statistically significant.

Results

Between January 1 and May 15, 2022, a total of 74 consecutive laboratory-confirmed COVID-19 patients (mean age 80.0 ± 12.6 yrs, 45.9% males) were retrospectively analyzed.

Twenty COVID-19 patients (27% of total) died during the hospitalization, whereas the remaining 54 patients (73% of total) were discharged alive.

Table 1 summarizes baseline clinical characteristics of the whole study population and of the two groups of COVID-19 patients.

Overall, our series of hospitalized COVID-19 patients had advanced age, normal BMI (24.5 ± 4.8 Kg/m^2), mild-to-moderate prevalence of the most common cardiovascular risk factors and high comorbidity burden, as assessed by CCI (7.4 ± 3.1). Approximately one-third of COVID-19 patients (35.1%)

10.3389/fimmu.2022.958418

TABLE 1 Baseline clinical characteristics of the whole study population and of the two groups of COVID-19 patients.

	All patients (n = 74)	Dead (n = 20)	Alive (n = 54)	P value
Demographics and anthropometrics				
Age (yrs)	80.0 ± 12.6	85.1 ± 10.6	78.1 ± 13.1	**0.03**
Male sex (%)	34 (45.9)	14 (70.0)	20 (37.0)	**0.01**
BSA (m^2)	1.79 ± 0.25	1.74 ± 0.24	1.80 ± 0.24	0.34
BMI (Kg/m^2)	24.5 ± 4.8	23.7 ± 5.6	24.8 ± 4.5	0.38
Anti-COVID-19 vaccination				
Vaccination with 3 doses of COVID-19 vaccine (%)	26 (35.1)	2 (10.0)	24 (44.4)	**0.006**
Vaccination with 2 doses of COVID-19 vaccine (%)	20 (27.0)	8 (40.0)	12 (22.2)	0.13
Vaccination with 1 dose of COVID-19 vaccine (%)	11 (14.9)	2 (10.0)	9 (16.7)	0.47
Unvaccinated (%)	17 (23.0)	8 (40.0)	9 (16.7)	**0.03**
Cardiovascular risk factors				
Hypertension (%)	46 (62.2)	15 (75.0)	31 (57.4)	0.16
Type 2 diabetes mellitus (%)	22 (29.7)	4 (20.0)	18 (33.3)	0.26
Current or ex-smokers (%)	21 (28.4)	7 (35.0)	14 (25.9)	0.44
Dyslipidemia (%)	21 (28.4)	5 (25.0)	16 (29.6)	0.69
Obesity (%)	11 (14.9)	3 (15.0)	8 (14.8)	0.98
Relevant comorbidities				
COPD (%)	20 (27.0)	6 (30.0)	14 (25.9)	0.72
History of CAD (%)	16 (21.6)	9 (45.0)	7 (13.0)	**0.003**
Previous stroke/TIA (%)	6 (8.1)	3 (15.0)	3 (5.5)	0.19
Peripheral vascular disease (%)	22 (29.7)	10 (50.0)	12 (22.2)	**0.02**
CKD (%)	33 (44.6)	13 (65.0)	20 (37.0)	**0.03**
Cancer (%)	16 (21.6)	6 (30.0)	10 (18.5)	0.29
Chronic cognitive deficit (%)	18 (24.3)	7 (35.0)	11 (20.4)	0.19
CCI	7.4 ± 3.1	9.8 ± 2.7	6.5 ± 2.8	**<0.001**
Medical treatment at hospital admission				
Antiplatelets (%)	20 (27.0)	7 (35.0)	13 (24.1)	0.35
Anticoagulants (%)	16 (21.6)	5 (25.0)	11 (20.4)	0.67
Beta blockers (%)	29 (39.2)	4 (20.0)	25 (46.3)	**0.03**
ACE-i/ARBs (%)	33 (44.6)	1 (5.0)	32 (61.1)	**<0.001**
Calcium channel blockers (%)	15 (20.3)	4 (20.0)	11 (20.4)	0.97
Diuretics (%)	18 (24.3)	5 (25.0)	13 (24.1)	0.93
Statins (%)	21 (28.4)	2 (10.0)	19 (35.2)	**0.03**
Oral antidiabetics (%)	11 (14.9)	3 (15.0)	8 (14.8)	0.98
Insulin (%)	11 (14.9)	1 (5.0)	10 (18.5)	0.15

ACEI, angiotensin-converting-enzyme inhibitors; ARBs, angiotensin receptor blockers; BMI, body mass index; BSA, body surface area; CAD, coronary artery disease; CCI, Charlson comorbidity index; CKD, chronic kidney disease; COPD, chronic obstructive pulmonary disease; COVID-19, Coronavirus disease 2019; TIA, transient ischemic attack.
Significant P values are in bold.

completed the vaccination cycle, 27% of total received 2 doses of COVID-19 vaccine, 14,9% of total received 1 dose of COVID-19 vaccine and the remaining 23% were unvaccinated. As expected, the prevalence of unvaccinated subjects was significantly higher among dead patients in comparison to those discharged alive (40.0 vs 16.7%, p = 0.03).

Compared to COVID-19 patients discharged alive from hospital, those who died in hospital were significantly older (85.1 ± 10.6 vs 78.1 ± 13.1 yrs, p = 0.03) and with a predominance of males (70.0 vs 37.0%, p = 0.01). Distribution of the common cardiovascular risk factors was similar in the two groups of patients. Analysis of comorbidities revealed that patients who died had a significantly greater comorbidity burden than those discharged alive (CCI 9.8 ± 2.7 vs 6.5 ± 2.8, p <0.001). Notably, dead patients showed a significantly increased prevalence of history of CAD, peripheral vascular disease and chronic kidney disease.

Concerning medical treatment at hospital admission, a general underprescription of cardioprotective drugs was observed in COVID-19 patients. Indeed, less than half of patients were regularly treated with beta blockers (39.2%) and angiotensin-converting-enzyme inhibitors (ACEI)/angiotensin receptor blockers (ARBs) (44.6%), and less than one third of patients received antiplatelets (27%), anticoagulants (21.6%),

calcium channel blockers (20.3%) and statins (28.4%). The underprescription of cardioprotective drugs was particularly evident among patients who died. Only 5%, 10% and 20% of them did regular use of ACEI/ARBs, statins and beta blockers respectively, at hospital admission.

Symptoms and signs at hospital admission, biochemical parameters, main instrumental findings, and finally details regarding the in-hospital medical treatment of COVID-19 infection, are listed in Table 2.

Main symptoms detected in COVID-19 patients at hospital admission were dyspnea (63.5%) and dry cough (47.3%); 45.9% of patients had fever. The prevalence of asymptomatic patients was significantly greater among those patients who were discharged alive (31.5 vs 5.0%, p = 0.01), whereas the dyspnea was much more commonly observed among those patients who died during hospitalization (85.0 vs 55.5%, p = 0.02). Blood pressure values were similar in the two groups of COVID-19 patients and only two cases of arterial hypotension (systolic blood pressure <100 mmHg) were reported.

As regards blood tests results, our study group was found with a significant increase in serum levels of inflammatory biomarkers, as WBCs, NLR, CRP, procalcitonin, with a mild chronic renal failure, and finally with a marked increase in serum levels of D-dimer and NT-proBNP. In comparison to COVID-19 patients who were discharged alive, those who died had significantly higher serum levels of WBCs (12.6 ± 5.9 vs 9.7 ± 4.7 × 10^9/L, p = 0.03), NLR (23.6 ± 14.8 vs 7.0 ± 6.6, p <0.001) and NT-proBNP (2915.7 ± 4356.6 vs 1120.6 ± 2553.0 pg/ml, p = 0.03) and significantly impaired renal function (eGFR 48.0 ± 34.9 vs 69.6 ± 27.0 ml/min/m^2, p = 0.006). On the other hand, serum levels of CRP, procalcitonin, HS troponin and D-dimer were similar in the two groups of patients.

On CXR/CT scan, 37.8% of the whole study population was diagnosed with bilateral pneumonia, whereas an acute pulmonary embolism was diagnosed in only 4% of COVID-19 patients, probably due to an extensive prophylactic anticoagulation regimen. The prevalence of bilateral and/or unilateral pneumonia did not differ between dead and alive COVID-19 patients. The latter were more frequently diagnosed with unilateral and/or bilateral pleural effusion. Radiological examinations were totally normal in approximately one-third of alive COVID-19 patients.

The prevalence of atrial fibrillation on ECG was 18.9% of the entire cohort of patients, without statistically significant difference between the two groups of patients (30 vs 14.8%, p = 0.14). However, Group 1 patients had significantly higher heart rate (93.4 ± 20.7 vs 82.2 ± 18.1 bpm, p = 0.02) than Group 2 patients.

On 2D-TTE, LVEF (52.5 ± 12.3%) was substantially preserved in the entire study group and a mild increase in left ventricular filling pressures (LVFP), expressed by the average E/e' ratio (13.4 ± 5.2), and SPAP (39.5 ± 10.6 mmHg) was observed. COVID-19 patients who died during the hospitalization were diagnosed with significantly lower LVEF (41.7 ± 14.0 vs 56.5 ± 8.8%, p <0.001), significantly higher average E/e' ratio (15.9 ± 5.0 vs 12.6 ± 5.1, p = 0.02) and significantly increased SPAP (47.7 ± 13.2 vs 36.5 ± 7.7 mmHg, p <0.001), in comparison to COVID-19 patients discharged alive. On lung ultrasound, three or more B-lines were detected in 28.4% of the whole study group, with significantly increased prevalence in patients who died in comparison to those who were discharged alive (50 vs 20.4%, p = 0.01).

Concerning COVID-19 in-hospital treatment, great majority of patients were treated with subcutaneous enoxaparin (82.4%), intravenous dexamethasone (75.7%), intravenous antibiotics (75.7%) and intravenous diuretics (67.6%). Those patients who died were more commonly treated with high-flow oxygen therapy (60.0 vs 22.2%, p = 0.002), intravenous dexamethasone (95.0 vs 68.5%, p = 0.02), intravenous antibiotics (95.0 vs 68.5%, p = 0.02) and intravenous diuretics (90.0 vs 59.2%, p = 0.01) than those who were discharged alive.

Finally, the length of hospital stay was not significantly different in the two groups of patients (10.5 ± 6.2 vs 12.7 ± 10.3 days, p = 0.37).

Figure 2 illustrates the strong correlation between CCI score and NLR (r = 0.85) observed in the whole study population.

On univariate logistic regression analysis (Table 3), following variables were independently correlated with the primary endpoint "in-hospital mortality": vaccination with 3 doses (OR 0.14, 95%CI 0.03-0.66, p = 0.01); CCI (OR 1.57, 95%CI 1-22-2.03, p <0.001); NLR (OR 1.19, 95%CI 1.09-1.29, p <0.001); eGFR (OR 0.97, 95%CI 0.95-0.99, p = 0.009); LVEF (OR 0.89, 95%CI 0.84-0.94, p <0.001); SPAP (OR 1.11, 95%CI 1.05-1.18, p <0.001); ACEI/ARBs therapy (OR 0.03, 95%CI 0.01-0.27, p = 0.001); finally, high-flow oxygen therapy (OR 3.56, 95%CI 1.22-10.4, p = 0.02).

On multivariate logistic regression analysis (Table 3), CCI (OR 1.76, 95%CI 1.07-2.92, p = 0.02) and NLR (OR 1.24, 95%CI 1.10-1.39, p = 0.001) were linearly correlated with the outcome "in-hospital mortality", whereas ACEI/ARBs therapy (OR 0.01, 95%CI 0.00-0.22, p = 0.006) showed a strong inverse correlation with the primary endpoint.

ROC curve analysis highlighted following cut-off values for CCI (≥7; 95% sensitivity and 67% specificity; AUC = 0.81) and NLR (≥9; 100% sensitivity and 78% specificity; AUC = 0.91), as the cut-off values with the best sensitivity and specificity for predicting the outcome "in-hospital mortality" in our study population (Figure 3).

A chart of risk stratification of in-hospital mortality drawn for our series of hospitalized COVID-19 patients by using CCI, NLR and ACEI/ARBs therapy, is illustrated in Figure 4. The mortality risk for patients with CCI ≥7, NLR ≥9 and without ACEI/ARBs therapy was very high (86%); for patients with CCI <7, NLR ≥9, with (16.6%) or without (25%) ACEI/ARBs therapy was intermediate; for patients with CCI <7, NLR <9 and with ACEI/ARBs therapy was of 0%.

TABLE 2 Symptoms and signs at hospital admission, blood tests, radiographic, ECG and echographic data, and details concerning the in-hospital treatment of COVID-19 infection detected in the whole study population and in the two groups of COVID-19 patients.

	All patients (n = 74)	Dead (n = 20)	Alive (n = 54)	P value
Symptoms and physical examination at hospital admission				
Dry cough (%)	35 (47.3)	10 (50.0)	25 (46.3)	0.77
Dyspnea (%)	47 (63.5)	17 (85.0)	30 (55.5)	**0.02**
No symptoms (%)	18 (24.3)	1 (5.0)	17 (31.5)	**0.01**
BT >37.3°C (%)	34 (45.9)	10 (50.0)	24 (44.4)	0.67
SBP (mmHg)	125.9 ± 20.7	127.9 ± 17.9	125.1 ± 21.7	0.60
DBP (mmHg)	74.8 ± 10.3	76.1 ± 8.8	74.3 ± 10.9	0.51
Blood tests				
Hb (g/dl)	12.8 ± 2.2	13.3 ± 2.4	12.6 ± 1.8	0.18
WBCs ($\times 10^9$/L)	10.5 ± 5.2	12.6 ± 5.9	9.7 ± 4.7	**0.03**
NLR	11.5 ± 11.9	23.6 ± 14.8	7.0 ± 6.6	**<0.001**
CRP (mg/dl)	8.6 ± 7.3	10.1 ± 9.5	8.0 ± 6.4	0.28
Procalcitonin (ng/ml)	0.97 ± 2.42	1.13 ± 1.03	0.9 ± 2.8	0.72
Creatinine	1.26 ± 1.00	1.78 ± 1.14	1.07 ± 0.87	**0.006**
eGFR (ml/min/m^2)	63.7 ± 30.7	48.0 ± 34.9	69.6 ± 27.0	**0.006**
HS troponine I (ng/L)	31.3 ± 75.3	52.3 ± 63.8	23.5 ± 78.2	0.14
D-dimer (ng/ml)	3522.6 ± 6054.8	3661.0 ± 8161.1	3471.4 ± 5158.3	0.90
NT-proBNP (pg/ml)	1605.7 ± 3211.9	2915.7 ± 4356.6	1120.6 ± 2553.0	**0.03**
Radiographic findings on CXR/CT scan				
Unilateral pneumonia (%)	12 (16.2)	4 (20.0)	8 (14.8)	0.59
Bilateral pneumonia (%)	28 (37.8)	8 (40.0)	20 (37.0)	0.81
Pulmonary hilar congestion (%)	10 (13.5)	7 (35.0)	3 (5.5)	**0.001**
Unilateral pleural effusion (%)	6 (8.1)	4 (20.0)	2 (3.7)	**0.02**
Bilateral pleural effusion (%)	6 (8.1)	4 (20.0)	2 (3.7)	**0.02**
Pneumonia + PE (%)	3 (4.0)	1 (5.0)	2 (3.7)	0.80
Negative CXR/CT scan (%)	18 (24.3)	1 (5.0)	17 (31.5)	**0.01**
ECG data				
Heart rate (bpm)	85.2 ± 19.3	93.4 ± 20.7	82.2 ± 18.1	**0.02**
AF (%)	11 (14.9)	8 (40.0)	3 (5.5)	**<0.001**
Main echographic variables				
LVEF (%)	52.5 ± 12.3	41.7 ± 14.0	56.5 ± 8.8	**<0.001**
Average E/e' ratio	13.4 ± 5.2	15.9 ± 5.0	12.6 ± 5.1	**0.02**
SPAP (mmHg)	39.5 ± 10.6	47.7 ± 13.2	36.5 ± 7.7	**<0.001**
≥3 B-lines on lung ultrasound	21 (28.4)	10 (50.0)	11 (20.4)	**0.01**
COVID-19 in-hospital treatment				
No oxygen therapy (%)	25 (33.8)	1 (5.0)	24 (44.4)	**0.001**
Low-flow oxygen therapy (%)	25 (33.8)	7 (35.0)	18 (33.3)	0.89
High-flow oxygen therapy (%)	24 (32.4)	12 (60.0)	12 (22.2)	**0.002**
Subcutaneous enoxaparin (%)	61 (82.4)	19 (95.0)	42 (77.7)	0.08
Intravenous dexamethasone (%)	56 (75.7)	19 (95.0)	37 (68.5)	**0.02**
Intravenous antibiotics (%)	56 (75.7)	19 (95.0)	37 (68.5)	**0.02**
Intravenous diuretics (%)	50 (67.6)	18 (90.0)	32 (59.2)	**0.01**
Intravenous remdesivir (%)	3 (4.0)	0 (0.0)	3 (5.5)	0.56
Length of hospital stay (days)	12.1 ± 9.3	10.5 ± 6.2	12.7 ± 10.3	0.37

AF, atrial fibrillation; BT, body temperature; CRP, C-reactive protein; CT, computed tomography; CXR, chest X-rays; COVID-19, Coronavirus disease 2019; DBP, diastolic blood pressure; ECG, electrocardiographic; eGFR, estimated glomerular filtration rate; Hb, hemoglobin; HS, high-sensitivity; LVEF, left ventricular ejection fraction; NLR, neutrophil-to-lymphocyte ratio; NT-proBNP, N-terminal pro-B-type natriuretic peptide; SBP, systolic blood pressure; SPAP, systolic pulmonary artery pressure; WBCs, whilte blood cells.
Significant P values are in bold.

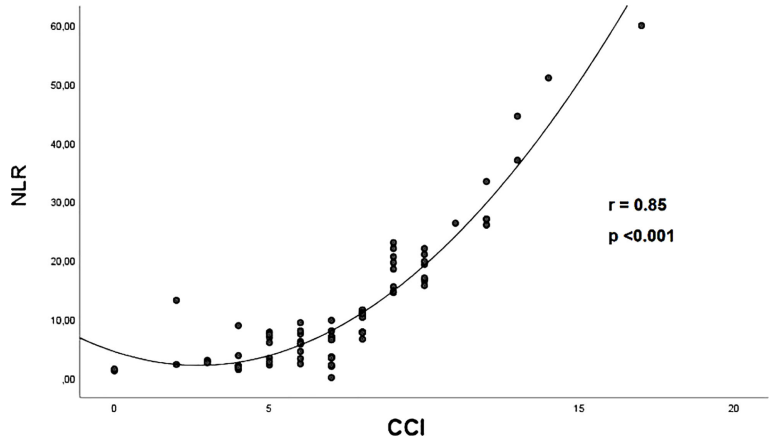

FIGURE 2
The correlation between CCI score and NLR in the whole study population, assessed by Spearman Correlation Coefficient. CCI, Charlson comorbidity index; NLR, neutrophil-to-lymphocyte ratio.

Discussion

The present study carried out on a retrospective cohort of 74 hospitalized COVID-19 patients during the Omicron dominant period revealed that: 1) the in-hospital mortality rate was 27% for the overall sample (20 of 74 patients); 2) compared to patients who were discharged alive, those who died during hospitalization were significantly older, had significantly greater prevalence of incomplete anti-COVID-19 vaccination, showed significantly higher comorbidity burden (as expressed by CCI), increased inflammatory biomarkers (especially WBCs and NLR), marked radiographic and echographic congestive signs, and were generally underprescribed with cardioprotective drugs (especially ACEI/ARBs) at hospital admission; 3) the baseline CCI and NLR were strongly correlated each other in the whole study group; 4) the main independent predictors of "in-hospital mortality" were the CCI, the baseline NLR and the undertreatment with ACEI/ARBs at hospital admission; notably, a CCI score ≥7 and a NLR ≥9 were the best cut-off values for predicting the outcome.

The overall in-hospital mortality rate detected in our series of COVID-19 patients was higher than that observed in previous studies which included younger patients (16, 17) and similar to that observed in other studies which enrolled geriatric patients with several comorbid conditions (18, 19).

During the last two years, a great number of studies reported that advanced age, male sex and multiple comorbidities, such as diabetes, cardiovascular, cerebrovascular, and respiratory diseases, are independent risk factors of mortality for COVID-19 patients (20–30). On the other hand, other studies showed that comorbidities were not effective predictors of mortality in these patients (31, 32). These different findings were likely related to different study designs and/or populations, or to the influence of confounding factors.

In the present study, to evaluate the influence of comorbidities on the patients' outcome we employed the Charlson Comorbidity Index (CCI) score, a well-validated, simple and valid method for estimating risk of death from comorbid disease (11). It summarizes a number of comorbidities, each given a weighted integer from one to six depending on the severity of the morbidity. Consistent with previous studies (7, 33–36), we demonstrated that a higher CCI is strongly associated with increased mortality in COVID-19 patients. In our findings, the ROC curve analysis showed that a CCI threshold ≥7 yielded the best cut-off point for predicting mortality in COVID-19 patients.

Our results also revealed that various inflammatory biomarkers, such as WBCs, NLR, CRP, and procalcitonin, were elevated in the great majority of hospitalized COVID-19 patients. However, logistic regression analysis highlighted that, among these inflammatory biomarkers, only the NLR was independently associated with the primary endpoint in our retrospective cohort of patients.

The NLR, easily calculated from a routinely blood test by dividing absolute neutrophil count by absolute lymphocyte count, is a biomarker of systemic inflammation (37). The high NLR results from increased neutrophil count and decreased lymphocyte count. It's related to the inflammatory response which stimulates the production of neutrophils and speed up the apoptosis of lymphocytes (38).

NLR has been widely used for predicting in-hospital mortality not only in infectious diseases but also in malignancy, cardiovascular diseases, intracerebral hemorrhage, polymyositis and dermatomyostis (39–43).

10.3389/fimmu.2022.958418

TABLE 3 Univariate and multivariate logistic regression analysis performed for identifying the main independent predictors of in-hospital mortality in our cohort of hospitalized COVID-19 patients.

VARIABLES	UNIVARIATE LOGISTIC REGRESSION ANALYSIS			MULTIVARIATE LOGISTIC REGRESSION ANALYSIS		
	OR	95% CI	P value	OR	95% CI	P value
Demographics						
Age (yrs)	1.05	0.99-1.11	0.08			
Male sex	2.32	0.80-6.73	0.12			
Anti-COVID-19 vaccination						
Vaccination with 3 doses	0.14	0.03-0.66	**0.01**	0.25	0.01-4.42	0.34
Cardiovascular risk factors						
Hypertension	2.22	0.71-7.01	0.17			
Type 2 diabetes mellitus	1.08	0.36-3.17	0.89			
Obesity	1.01	0.24-4.28	0.98			
Smoking	1.54	0.51-4.63	0.44			
Dyslipidemia	1.05	0.32-3.45	0.93			
Clinical comorbidity index						
CCI	1.57	1-22-2.03	**<0.001**	1.76	1.07-2.92	**0.02**
Blood tests						
NLR	1.19	1.09-1.29	**<0.001**	1.24	1.10-1.39	**0.001**
CRP (mg/dl)	1.04	0.97-1.11	0.29			
Procalcitonin (ng/ml)	1.04	0.85-1.26	0.72			
eGFR (ml/min/m^2)	0.97	0.95-0.99	**0.009**	0.98	0.95-1.03	0.46
HS troponine I (ng/L)	1.00	0.99-1.01	0.19			
D-dimer (ng/ml)	1.00	0.92-1.09	0.90			
NT-proBNP (pg/ml)	1.00	0.87-1.15	0.95			
Instrumental findings						
Bilateral pneumonia on CXR/CT scan	1.13	0.39-3.24	0.82			
AF	1.22	0.39-3.80	0.72			
LVEF (%)	0.89	0.84-0.94	**<0.001**	0.93	0.80-1.07	0.31
Average E/e' ratio	1.07	0.96-1.19	0.24			
SPAP (mmHg)	1.11	1.05-1.18	**<0.001**	1.07	0.92-1.24	0.36
Medical treatment at hospital admission						
Antiplatelets	1.69	0.56-5.16	0.35			
Anticoagulants	1.31	0.39-4.37	0.67			
Beta blockers	0.58	0.19-1.73	0.33			
ACEi-ARBs	0.03	0.01-0.27	**0.001**	0.01	0.00-0.22	**0.006**
Statins	0.79	0.25-2.55	0.69			
In-hospital treatment of COVID-19 infection						
High-flow oxygen therapy	3.56	1.22-10.4	**0.02**	2.28	0.69-7.50	0.17
Subcutaneous enoxaparin (%)	1.14	0.32-4.07	0.84			
Intravenous dexamethasone (%)	1.38	0.43-4.41	0.59			
Intravenous antibiotics (%)	1.84	0.53-6.33	0.33			
Intravenous diuretics (%)	1.60	0.53-4.82	0.40			

ACEI, angiotensin-converting-enzyme inhibitors; AF, atrial fibrillation; ARBs, angiotensin receptor blockers; CCI, Charlson comorbidity index; COVID-19, Coronavirus disease 2019; CRP, C-reactive protein; CT, computed tomography; CXR, chest X-rays; eGFR, estimated glomerular filtration rate; HS, high-sensitivity; LVEF, left ventricular ejection fraction; NLR, neutrophil-to-lymphocyte ratio; NT-proBNP, N-terminal pro-B-type natriuretic peptide; SPAP, systolic pulmonary artery pressure.
Significant P values are in bold.

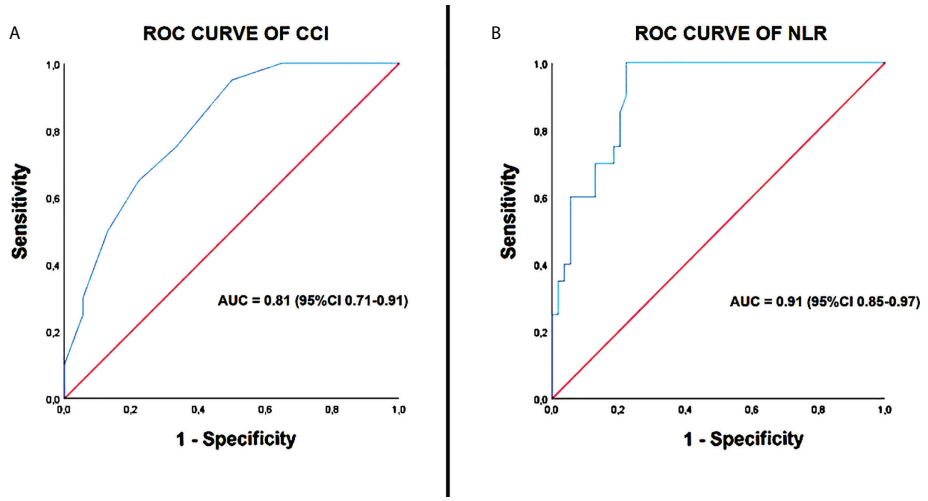

FIGURE 3
ROC curve analysis of CCI **(A)** and NLR **(B)**. CCI, Charlson comorbidity index; NLR, neutrophil-to-lymphocyte ratio; ROC, receiver operating characteristic curve.

Concerning COVID-19 patients, several studies demonstrated that higher NLR levels on admission were associated with severe COVID-19 and mortality (16, 44–46).

In determining the optimal cut-off value of NLR for predicting outcome in COVID-19 patients, NLR values ranging from 3.3 to 5.9 predicted severity in some studies (47, 48), whereas higher NLR values ranging from 7.9 and 11.8 predicted mortality in other studies (49, 50). In our findings, a cut-off value of NLR ≥9 was the best cut-off value for predicting mortality.

The increase in serum levels of NLR indicates an imbalance in the inflammatory response where inflammatory factors related to viral infection, such as interleukin-6, interleukin-8, and granulocyte colony-stimulating factor, stimulate neutrophil production (47) and, in contrast, systemic inflammation accelerates lymphocyte apoptosis, depresses cellular immunity, decreases CD4+, and increases CD8+ suppressor T-lymphocytes (51, 52).

Bacterial co-infections due to low immune functions would be another possible reason for explaining the increased levels of NLR and other inflammatory biomarkers, such as CRP and procalcitonin, in COVID-19 patients with severe disease manifestation.

High levels of NLR may also be related to different combinations of comorbidities, as detected in our study population. Interestingly, we observed a strong correlation

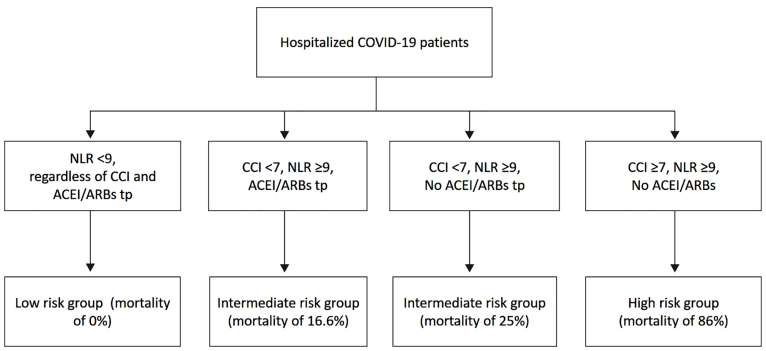

FIGURE 4
Chart of risk stratification of in-hospital mortality for our series of hospitalized COVID-19 patients by using CCI, NLR and ACEI/ARBs therapy. ACEI, angiotensin-converting-enzyme inhibitors; ARBs, angiotensin receptor blockers; CCI, Charlson comorbidity index; NLR, neutrophil-to-lymphocyte ratio.

between NLR and CCI in hospitalized COVID-19 patients, suggesting that aging and comorbidities sinergically contribute to a higher basal proinflammatory status (53). It's known that, at baseline state, the lungs of old individuals show increase in levels of complement and surfactant proteins and pro-inflammatory cytokines (54, 55). These factors can contribute to both pulmonary and systemic exacerbated inflammatory response in older individuals and seem to play a role in increasing susceptibility to respiratory infections (53).

Another important prognostic indicator assessed by our logistic regression analysis was the undertreatment with ACEI/ARBs at hospital admission in COVID-19 patients. Indeed, the mortality rate was significantly lower in patients chronically treated with ACEI/ARBs in comparison to patients not treated with ACEI or ARBs. Our findings would support the assumption that the up-regulation of angiotensin-converting enzyme (ACE)-2, a carboxypeptidase that cleaves angiotensin II into angiotensin- (1–7, 56, 57), induced by both ACEIs (58–60) and ARBs (61), could be potentially useful in the clinical course of SARS-CoV-2-infected patients, due to the cardiovascular protection elicited by the increased activity of angiotensin (1–7), thereby attenuating angiotensin II effects on vasoconstriction and sodium retention (57, 59). Therefore, our results are in alignment with previous studies that demonstrated a significantly lower mortality rate in hospitalized COVID-19 patients treated with ACEI/ARB therapy (62–67).

A possible explanation for the undertreatment with cardioprotective drug, especially ACEI/ARBs and beta blockers, observed in our cohort of COVID-19 patients at hospital admission, might be ascribable to the increased prevalence of comorbid conditions such as CKD and COPD; we believe that the clinicians were reluctant to prescribe ACEI/ARBs to older patients with impaired renal function and increased risk of hyperkalemia and/or to administer beta blockers to patients with COPD and increased risk of bronchospasm, hypotension or bradicardia.

To sum up, the results of the present study may help the clinicians to identify, among the hospitalized patients with COVID-19 infection, those with increased risk of in-hospital mortality. Those patients who are found with CCI ≥9, NLR ≥7 and who are not treated with ACEI/ARBs at hospital admission have a significantly increased risk of in-hospital mortality during COVID-19 infection. In other terms, those patients who are elderly, frail and with multiple comorbidities, who are found with increased inflammatory biomarkers at hospital admission, and who are not adequately treated with cardioprotective drugs, should be considered high-risk patients with more severe clinical presentation of SARS-CoV2 infection and significantly reduced survival probability. On the other hand, COVID-19 patients with CCI <9, NLR <7 and chronically treated with cardioprotective drugs have a significantly increased probability to be discharged alive from hospital.

Main limitation of the present study were the monocentric design of the study, its retrospective nature and the limited sample size of hospitalized COVID-19 patients analyzed. In the present study, Omicron was not confirmed through whole genome sequencing of SARS-CoV-2, which is the gold standard for genomic surveillance (68), not available at our Institution. However, the cases of COVID-19 patients included in this retrospective analysis were primarily attributed to Omicron, based on the global epidemiological temporal updates. In addition, blood tests did not include inflammatory biomarkers such as IL-6 and TNF-alfa, not assessed for the routinely evaluation of COVID-19 patients at our Center. Although a general undertreatment with cardioprotective drugs at hospital admission might have been the main factor responsible for a poor prognosis in our study group, the logistic regression analysis highlighted the independent prognostic role of ACEI/ARBs, only. An external validation cohort and adequately powered, prospective studies are needed to strengthen our results. A further study could be performed to investigate the composite of mortality and rehospitalization for all-causes in the same study population over a 6 and/or 12 months follow-up and/or to evaluate if the introduction and/or uptitration of cardioprotective drugs might improve the prognosis of these patients.

Conclusions

The hospitalized COVID-19 patients included in this retrospective analysis showed a 27% of in-hospital mortality rate.

A high comorbidity burden, high levels of NLR and the undertreatment with ACEI/ARBs at hospital admission were the main independent prognostic indicators of in-hospital mortality in our series of patients.

The risk stratification of COVID-19 patients at hospital admission would help the clinicians to take care of the high-risk patients and reduce the mortality.

Data availability statement

The datasets presented in this study can be found in online repositories. The names of the repository/repositories and accession number(s) can be found below: https://zenodo.org/record/7015021.

Ethics statement

The studies involving human participants were reviewed and approved by Comitato Etico Indipendente IRCCS MultiMedica. Written informed consent for participation was not required for

this study in accordance with the national legislation and the institutional requirements.

Authors contributions

AS, MR, RC, DE, and AC, conceptualization, data curation, investigation, methodology, software, visualization, and writing—original draft. AA and DN, data curation, methodology, writing—review and editing. GN, ML, SH, conceptualization, supervision, validation, writing—review and editing. All authors contributed to the article and approved the submitted version.

Funding

This research was supported by a grant from the Ministero della Salute COVID-2020-12371849 to DN and progetto RCR-2021-23671212. DN is also the recipient of a grant from Programmi di Ricerca Scientifica di Rilevante Interesse Nazionale (PRIN) Grant 2010 NECHBX_003 (to DN). Studies are partially funded by the Italian Ministry of Health Ricerca Corrente-IRCCS MultiMedica.

Conflict of interest

The authors declare that the research was conducted in the absence of any commercial or financial relationships that could be construed as a potential conflict of interest.

Publisher's note

References

1. Ingraham NE, Ingbar DH. The omicron variant of SARS-CoV-2: Understanding the known and living with unknowns. *Clin Transl Med* (2021) 11:e685. doi: 10.1002/ctm2.685

2. Chen J, Wang R, Gilby NB, Wei GW. Omicron (B.1.1.529): Infectivity, vaccine breakthrough, and antibody resistance. *J Chem Inf Model* (2022) 62:412–22. doi: 10.1021/acs.jcim.1c01451

3. Nyberg T, Ferguson NM, Nash SG, Webster HH, Flaxman S, Andrews N, et al. Comparative analysis of the risks of hospitalisation and death associated with SARS-CoV-2 omicron (B.1.1.529) and delta (B.1.617.2) variants in England: a cohort study. *Lancet* (2022) 399:1303–12. doi: 10.1016/S0140-6736(22)00462-7

4. Araf Y, Akter F, Tang YD, Fatemi R, Parvez MSA, Zheng C, et al. Omicron variant of SARS-CoV-2: Genomics, transmissibility, and responses to current COVID-19 vaccines. *J Med Virol* (2022) 94:1825–32. doi: 10.1002/jmv.27588

5. Lambrou AS, Shirk P, Steele MK, Paul P, Paden CR, Cadwell B, et al. Genomic surveillance for SARS-CoV-2 variants: Predominance of the delta (B.1.617.2) and omicron (B.1.1.529) variants - united states, June 2021-January 2022. *MMWR Morb Mortal Wkly Rep* (2022) 71:206–11. doi: 10.15585/mmwr.mm7106a4

6. Flores-Vega VR, Monroy-Molina JV, Jiménez-Hernández LE, Torres AG, Santos-Preciado JI, Rosales-Reyes R. SARS-CoV-2: Evolution and emergence of new viral variants. *Viruses.* (2022) 14:653. doi: 10.3390/v14040653

7. Iaccarino G, Grassi G, Borghi C, Ferri C, Salvetti M, Volpe M, et al. Age and multimorbidity predict death among COVID-19 patients: Results of the SARS-RAS study of the Italian society of hypertension. *Hypertension* (2020) 76:366–72. doi: 10.1161/HYPERTENSIONAHA.120.15324

8. Wolter N, Jassat W, Walaza S, Welch R, Moultrie H, Groome M, et al. Early assessment of the clinical severity of the SARS-CoV-2 omicron variant in south Africa: a data linkage study. *Lancet* (2022) 399:437–46. doi: 10.1016/S0140-6736(22)00017-4

9. Meo SA, Meo AS, Al-Jassir FF, Klonoff DC. Omicron SARS-CoV-2 new variant: global prevalence and biological and clinical characteristics. *Eur Rev Med Pharmacol Sci* (2021) 25:8012–8. doi: 10.26355/eurrev_202112_27652

10. Levey AS, Bosch JP, Lewis JB, Greene T, Rogers N, Roth D. A more accurate method to estimate glomerular filtration rate from serum creatinine: a new prediction equation. *Modification Diet Renal Dis Study Group Ann Intern Med* (1999) 130:461–70. doi: 10.7326/0003-4819-130-6-199903160-00002

11. Charlson ME, Pompei P, Ales KL, MacKenzie CR. A new method of classifying prognostic comorbidity in longitudinal studies: development and validation. *J Chronic Dis* (1987) 40:373–8. doi: 10.1016/0021-9681(87)90171-8

12. Lang RM, Badano LP, Mor-Avi V, Afilalo J, Armstrong A, Ernande L, et al. Recommendations for cardiac chamber quantification by echocardiography in adults: an update from the American society of echocardiography and the European association of cardiovascular imaging. *J Am Soc Echocardiogr* (2015) 28:1–39.e14. doi: 10.1016/j.echo.2014.10.003

13. Nagueh SF, Smiseth OA, Appleton CP, Byrd BF3rd, Dokainish H, Edvardsen T, et al. Recommendations for the evaluation of left ventricular diastolic function by echocardiography: An update from the American society of echocardiography and the European association of cardiovascular imaging. *J Am Soc Echocardiogr* (2016) 29:277–314. doi: 10.1016/j.echo.2016.01.011

14. Rudski LG, WW L, Afilalo J, Hua L, Handschumacher MD, Chandrasekaran K, et al. Guidelines for the echocardiographic assessment of the right heart in adults: a report from the American society of echocardiography endorsed by the European association of echocardiography, a registered branch of the European society of cardiology, and the Canadian society of echocardiography. *J Am Soc Echocardiogr* (2010) 23:685–713. doi: 10.1016/j.echo.2010.05.010

15. Allinovi M, Parise A, Giacalone M, Amerio A, Delsante M, Odone A, et al. Lung ultrasound may support diagnosis and monitoring of COVID-19 pneumonia. *Ultrasound Med Biol* (2020) 46:2908–17. doi: 10.1016/j.ultrasmedbio.2020.07.018

16. Liu Y, Du X, Chen J, Jin Y, Peng L, Wang HHX, et al. Neutrophil-to-lymphocyte ratio as an independent risk factor for mortality in hospitalized patients with COVID-19. *J Infect* (2020) 81:e6–e12. doi: 10.1016/j.jinf.2020.04.002

17. González FJ, Miranda FA, Chávez SM, Gajardo AI, Hernández AR, Guiñez DV, et al. Clinical characteristics and in-hospital mortality of patients with COVID-19 in Chile: A prospective cohort study. *Int J Clin Pract* (2021) 75:e14919. doi: 10.1111/ijcp.14919

18. Trecarichi EM, Mazzitelli M, Serapide F, MC P, Tassone B, Arrighi E, et al. Clinical characteristics and predictors of mortality associated with COVID-19 in elderly patients from a long-term care facility. *Sci Rep* (2020) 10:20834. doi: 10.1038/s41598-020-77641-7

19. Mendes A, Serratrice C, Herrmann FR, Genton L, Périvier S, Scheffler M, et al. Predictors of in-hospital mortality in older patients with COVID-19: The COVIDAge study. *J Am Med Dir Assoc* (2020) 21:1546–1554.e3. doi: 10.1016/j.jamda.2020.09.014

20. Pranata R, Huang I, Lim MA, Wahjoepramono EJ, July J. Impact of cerebrovascular and cardiovascular diseases on mortality and severity of COVID-19-systematic review, meta-analysis, and meta-regression. *J Stroke Cerebrovasc Dis* (2020) 29:104949. doi: 10.1016/j.jstrokecerebrovasdis.2020.104949

21. Yonas E, Alwi I, Pranata R, Huang I, Lim MA, Gutierrez EJ, et al. Effect of heart failure on the outcome of COVID-19 - a meta analysis and systematic review. *Am J Emerg Med* (2021) 46:204–11. doi: 10.1016/j.ajem.2020.07.009

22. Lim MA, Huang I, Yonas E, Vania R, Pranata R. A wave of non-communicable diseases following the COVID-19 pandemic. *Diabetes Metab Syndr* (2020) 14:979–80. doi: 10.1016/j.dsx.2020.06.050

23. Pranata R, Soeroto AY, Huang I, Lim MA, Santoso P, Permana H, et al. Effect of chronic obstructive pulmonary disease and smoking on the outcome of COVID-19. *Int J Tuberc Lung Dis* (2020) 24:838–43. doi: 10.5588/ijtld.20.0278

24. Pranata R, Lim MA, Yonas E, Vania R, Lukito AA, Siswanto BB, et al. Body mass index and outcome in patients with COVID-19: A dose-response meta-analysis. *Diabetes Metab* (2021) 47:101178. doi: 10.1016/j.diabet.2020.07.005

25. Lim MA, Pranata R. Coronavirus disease 2019 (COVID-19) markedly increased mortality in patients with hip fracture - a systematic review and meta-analysis. *J Clin Orthop Trauma.* (2021) 12:187–93. doi: 10.1016/j.jcot.2020.09.015

26. Imam Z, Odish F, Gill I, O'Connor D, Armstrong J, Vanood A, et al. Older age and comorbidity are independent mortality predictors in a large cohort of 1305 COVID-19 patients in Michigan, united states. *J Intern Med* (2020) 288:469–76. doi: 10.1111/joim.13119

27. Argun Barış S, Boyacı H, Akhan S, Mutlu B, Deniz M, Başyiğit İ. Charlson comorbidity index in predicting poor clinical outcomes and mortality in patients with COVID-19. *Turk Thorac J* (2022) 23:145–53. doi: 10.5152/TurkThoracJ.2022.21076

28. Guan WJ, Liang WH, Zhao Y, Liang HR, Chen ZS, Li YM, et al. Comorbidity and its impact on 1590 patients with COVID-19 in China: a nationwide analysis. *Eur Respir J* (2020) 55:2000547. doi: 10.1183/13993003.00547-2020

29. Huang C, Wang Y, Li X, Ren L, Zhao J, Hu Y, et al. Clinical features of patients infected with 2019 novel coronavirus in wuhan, China. *Lancet.* (2020) 395:497–506. doi: 10.1016/S0140-6736(20)30183-5

30. Barek MA, Aziz MA, Islam MS. Impact of age, sex, comorbidities and clinical symptoms on the severity of COVID-19 cases: A meta-analysis with 55 studies and 10014 cases. *Heliyon* (2020) 6:e05684. doi: 10.1016/j.heliyon.2020.e05684

31. Novelli L, Raimondi F, Ghirardi A, Pellegrini D, Capodanno D, Sotgiu G, et al. At The peak of COVID-19 age and disease severity but not comorbidities are predictors of mortality: COVID-19 burden in bergamo, Italy. *Panminerva Med* (2021) 63:51–61. doi: 10.23736/S0031-0808.20.04063-X

32. Xue QL. Frailty as an integrative marker of physiological vulnerability in the era of COVID-19. *BMC Med* (2020) 18:333. doi: 10.1186/s12916-020-01809-1

33. Kim DH, Park HC, Cho A, Kim J, Yun KS, Kim J, et al. Age-adjusted charlson comorbidity index score is the best predictor for severe clinical outcome in the hospitalized patients with COVID-19 infection. *Med (Baltimore).* (2021) 100: e25900. doi: 10.1097/MD.0000000000025900

34. Elia D, Mozzanica F, Caminati A, Giana I, Carli L, Ambrogi F, et al. Prognostic value of radiological index and clinical data in patients with COVID-19 infection. *Intern Emerg Med* (2022) 20:1–9. doi: 10.1007/s11739-022-02985-z

35. Ahmed J, Avendaño Capriles CA, Avendaño Capriles NM, Mehta SM, Khan N, Tariq S, et al. The impact of charlson comorbidity index on mortality from SARS-CoV-2 virus infection. *Cureus.* (2021) 13:e19937. doi: 10.7759/cureus.19937

36. Cho SI, Yoon S, Lee HJ. Impact of comorbidity burden on mortality in patients with COVID-19 using the Korean health insurance database. *Sci Rep* (2021) 11:6375. doi: 10.1038/s41598-021-85813-2

37. Zahorec R. Neutrophil-to-lymphocyte ratio, past, present and future perspectives. *Bratisl Lek Listy* (2021) 122:474–88. doi: 10.4149/BLL_2021_078

38. Faria SS, Fernandes PCJr, Silva MJ, Lima VC, Fontes W, Freitas-Junior R, et al. The neutrophil-to-lymphocyte ratio: a narrative review. *Ecancermedicalscience.* (2016) 10:702. doi: 10.3332/ecancer.2016.702

39. Azab B, Zaher M, Weiserbs KF, Torbey E, Lacossiere K, Gaddam S, et al. Usefulness of neutrophil to lymphocyte ratio in predicting short- and long-term mortality after non-ST-elevation myocardial infarction. *Am J Cardiol* (2010) 106:470–6. doi: 10.1016/j.amjcard.2010.03.062

40. Bhat T, Teli S, Rijal J, Bhat H, Raza M, Khoueiry G, et al. Neutrophil to lymphocyte ratio and cardiovascular diseases: a review. *Expert Rev Cardiovasc Ther* (2013) 11:55–9. doi: 10.1586/erc.12.159

41. Guthrie GJ, Charles KA, Roxburgh CS, Horgan PG, McMillan DC, Clarke SJ. The systemic inflammation-based neutrophil-lymphocyte ratio: experience in patients with cancer. *Crit Rev Oncol Hematol* (2013) 88:218–30. doi: 10.1016/j.critrevonc.2013.03.010

42. Giede-Jeppe A, Bobinger T, Gerner ST, Sembill JA, Sprügel MI, Beuscher VD, et al. Neutrophil-to-Lymphocyte ratio is an independent predictor for in-hospital mortality in spontaneous intracerebral hemorrhage. *Cerebrovasc Dis* (2017) 44:26–34. doi: 10.1159/000468996

43. Ha YJ, Hur J, Go DJ, Kang EH, Park JK, Lee EY, et al. Baseline peripheral blood neutrophil-to-lymphocyte ratio could predict survival in patients with adult polymyositis and dermatomyositis: A retrospective observational study. *PloS One* (2018) 13:e0190411. doi: 10.1371/journal.pone.0190411

44. Qin C, Zhou L, Hu Z, Zhang S, Yang S, Tao Y, et al. Dysregulation of immune response in patients with coronavirus 2019 (COVID-19) in wuhan, China. *Clin Infect Dis* (2020) 71:762–8. doi: 10.1093/cid/ciaa248

45. Yildiz H, Castanares-Zapatero D, Pierman G, Pothen L, De Greef J, Aboubakar Nana F, et al. Validation of neutrophil-to-Lymphocyte ratio cut-off value associated with high in-hospital mortality in COVID-19 patients. *Int J Gen Med* (2021) 14:5111–7. doi: 10.2147/IJGM.S326666

46. Simadibrata DM, Calvin J, Wijaya AD, Ibrahim NAA. Neutrophil-to-lymphocyte ratio on admission to predict the severity and mortality of COVID-19 patients: A meta-analysis. *Am J Emerg Med* (2021) 42:60–9. doi: 10.1016/j.ajem.2021.01.006

47. Yang AP, Liu JP, Tao WQ, Li HM. The diagnostic and predictive role of NLR, d-NLR and PLR in COVID-19 patients. *Int Immunopharmacol.* (2020) 84:106504. doi: 10.1016/j.intimp.2020.106504

48. Sun S, Cai X, Wang H, He G, Lin Y, Lu B, et al. Abnormalities of peripheral blood system in patients with COVID-19 in wenzhou, China. *Clin Chim Acta* (2020) 507:174–80. doi: 10.1016/j.cca.2020.04.024

49. Yan X, Li F, Wang X, Yan J, Zhu F, Tang S, et al. Neutrophil to lymphocyte ratio as prognostic and predictive factor in patients with coronavirus disease 2019: A retrospective cross-sectional study. *J Med Virol* (2020) 92:2573–81. doi: 10.1002/jmv.26061

50. Zhou J, Huang L, Chen J, Yuan X, Shen Q, Dong S, et al. Clinical features predicting mortality risk in older patients with COVID-19. *Curr Med Res Opin* (2020) 36:1753–9. doi: 10.1080/03007995.2020.1825365

51. Menges T, Engel J, Welters I, Wagner RM, Little S, Ruwoldt R, et al. Changes in blood lymphocyte populations after multiple trauma: association with posttraumatic complications. *Crit Care Med* (1999) 27:733–40. doi: 10.1097/00003246-199904000-00026

52. Channappanavar R, Perlman S. Pathogenic human coronavirus infections: causes and consequences of cytokine storm and immunopathology. *Semin Immunopathol* (2017) 39:529–39. doi: 10.1007/s00281-017-0629-x

53. Pietrobon AJ, Teixeira FME, Sato MN. I Mmunosenescence and inflammaging: Risk factors of severe COVID-19 in older people. *Front Immunol* (2020) 11:579220. doi: 10.3389/fimmu.2020.579220

54. Kovacs EJ, Boe DM, Boule LA, Curtis BJ. Inflammaging and the lung. *Clin Geriatr Med* (2017) 33:459–71. doi: 10.1016/j.cger.2017.06.002

55. Canan CH, Gokhale NS, Carruthers B, Lafuse WP, Schlesinger LS, Torrelles JB, et al. Characterization of lung inflammation and its impact on macrophage function in aging. *J Leukoc Biol* (2014) 96:473–80. doi: 10.1189/jlb.4A0214-093RR

56. Crackower MA, Sarao R, Oudit GY, Yagil C, Kozieradzki I, Scanga SE, et al. Angiotensin-converting enzyme 2 is an essential regulator of heart function. *Nature.* (2002) 417:822–8. doi: 10.1038/nature00786

57. Forrester SJ, Booz GW, Sigmund CD, Coffman TM, Kawai T, Rizzo V, et al. Angiotensin II signal transduction: An update on mechanisms of physiology and pathophysiology. *Physiol Rev* (2018) 98:1627–738. doi: 10.1152/physrev.00038.2017

58. Vaduganathan M, Vardeny O, Michel T, McMurray JJV, Pfeffer MA, Solomon SD. Renin-Angiotensin-Aldosterone system inhibitors in patients with covid-19. *N Engl J Med* (2020) 382:1653–9. doi: 10.1056/NEJMsr2005760

59. Gheblawi M, Wang K, Viveiros A, Nguyen Q, Zhong JC, Turner AJ, et al. Angiotensin-converting enzyme 2: SARS-CoV-2 receptor and regulator of the renin-angiotensin system: Celebrating the 20th anniversary of the discovery of ACE2. *Circ Res* (2020) 126:1456–74. doi: 10.1161/CIRCRESAHA.120.317015

60. Albini A, Di Guardo G, Noonan DM, Lombardo M. The SARS-CoV-2 receptor, ACE-2, is expressed on many different cell types: implications for ACE-inhibitor- and angiotensin II receptor blocker-based cardiovascular therapies. *Intern Emerg Med* (2020) 15:759–66. doi: 10.1007/s11739-020-02364-6

61. Gurwitz D. Angiotensin receptor blockers as tentative SARS-CoV-2 therapeutics. *Drug Dev Res* (2020) 81:537–40. doi: 10.1002/ddr.21656

62. Genet B, Vidal JS, Cohen A, Boully C, Beunardeau M, Marine Harlé L, et al. COVID-19 in-hospital mortality and use of renin-angiotensin system blockers in geriatrics patients. *J Am Med Dir Assoc* (2020) 21:1539–45. doi: 10.1016/j.jamda.2020.09.004

63. Shibata S, Arima H, Asayama K, Hoshide S, Ichihara A, Ishimitsu T, et al. Hypertension and related diseases in the era of COVID-19: a report from the Japanese society of hypertension task force on COVID-19. *Hypertens Res* (2020) 43:1028–46. doi: 10.1038/s41440-020-0515-0

64. Kai H, Kai M. Interactions of coronaviruses with ACE2, angiotensin II, and RAS inhibitors-lessons from available evidence and insights into COVID-19. *Hypertens Res* (2020) 43:648–54. doi: 10.1038/s41440-020-0455-8

65. Baral R, Tsampasian V, Debski M, Moran B, Garg P, Clark A, et al. Association between renin-Angiotensin-Aldosterone system inhibitors and clinical outcomes in patients with COVID-19: A systematic review and meta-analysis. *JAMA Netw Open* (2021) 4:e213594. doi: 10.1001/jamanetworkopen.2021.3594

66. Angeli F, Verdecchia P, Balestrino A, Bruschi C, Ceriana P, Chiovato L, et al. Renin angiotensin system blockers and risk of mortality in hypertensive patients hospitalized for COVID-19: An Italian registry. *J Cardiovasc Dev Dis* (2022) 9:15. doi: 10.3390/jcdd9010015

67. Smith SM, Desai RA, Walsh MG, Nilles EK, Shaw K, Smith M, et al. Angiotensin-converting enzyme inhibitors, angiotensin receptor blockers, and COVID-19-related outcomes: A patient-level analysis of the PCORnet blood pressure control lab. *Am Heart J Plus*. (2022) 13:100112. doi: 10.1016/j.ahjo.2022.100112

68. Liu T, Chen Z, Chen W, Chen X, Hosseini M, Yang Z, et al. A benchmarking study of SARS-CoV-2 whole-genome sequencing protocols using COVID-19 patient samples. *iScience* (2021) 24:102892. doi: 10.1016/j.isci.2021.102892

Frontiers in Immunology

Explores novel approaches and diagnoses to treat immune disorders.

The official journal of the International Union of Immunological Societies (IUIS) and the most cited in its field, leading the way for research across basic, translational and clinical immunology.

Discover the latest Research Topics

See more →

Frontiers

Avenue du Tribunal-Fédéral 34
1005 Lausanne, Switzerland
frontiersin.org

Contact us

+41 (0)21 510 17 00
frontiersin.org/about/contact